



ISSN 2255-7776

E-ISSN 2255-8861



**LATVIA UNIVERSITY OF AGRICULTURE
FACULTY OF RURAL ENGINEERING**

Department of Architecture and Building
Departments of Structural Engineering

CIVIL ENGINEERING '11
3rd International Scientific Conference
PROCEEDINGS

Volume 3

Jelgava 2011

Civil Engineering` 11

3rd International Scientific Conference Proceedings, Vol. 3

Jelgava, Latvia University of Agriculture, 2011, 271 pages

ISSN 2255-7776

SCIENTIFIC COMMITTEE

Chairman

Anris Šteinerts, Professor, Dr.sc.ing.

Members

Juris Skujāns, Dr.sc.ing., Latvia University of Agriculture, Latvia
Arturs Lešinskis, Dr.sc.ing., Latvia University of Agriculture, Latvia
Ēriks Tilgalis, Dr.sc.ing., Latvia University of Agriculture, Latvia
Feliksas Mikuckis, Dr.sc.ing., Lithuania University of Agriculture, Lithuania
Gintaras Stauskis, Dr., Vilnius Gediminas Technical University, Lithuania
Jaan Miljan, Dr.sc.ing., Estonian Agricultural University, Estonia
Jānis Brauns, Dr.habil.sc.ing., Latvia University of Agriculture, Latvia
Jānis Kreilis, Dr.sc.ing., Latvia University of Agriculture, Latvia
Jaroslav Zapomel, Dr.sc.ing., Academy of Sciences of the Czech Republic, Czech Republic
Lilita Ozola, Dr.sc.ing., Latvia University of Agriculture, Latvia
Pentti Mäkeläinen, Dr.sc.ing., Helsinki University of Technology, Finland
Simon Bell, Dr., Estonian University of Life Science, Estonia
Daiga Zigmunde, Dr.arch., Latvia University of Agriculture, Latvia
Ralejs Tepfers, Dr.sc.ing., Chalmers University of Technology, Sweden
Uģis Bratuškins, Dr.arch., Riga Technical University, Latvia
Uldis Iljins, Dr.habil.sc.ing., Latvia University of Agriculture, Latvia

REVIEWERS

J.Skujāns, A. Lešinskis, Ē. Tilgalis, F. Mikuckis, G. Stauskis, J. Miljan, J. Brauns, J. Kreilis, J. Zapomel, L. Ozola, M. Urtāne, P. Mäkeläinen, S. Bell, D. Zigmunde, R. Tepfers, U. Bratuškins, U. Iljins, S. Štrausa, G. Andersons, S.Gusta

Every scientific paper was reviewed by two independent reviewers.

Published scientific papers will be submitted in Agris, CAB Abstracts and EBSCO Academic Search Complete databases. The data bases select the articles from the proceedings for including them in their data bases after individual qualitative and thematic examination. Every author is responsible for the quality and the information of his article.

EDITORS

Editor of language

Larisa Malinovska, Asoc.prof.

Technical editor

Daiga Zigmunde, Dr.arch.

© Latvia University of Agriculture

Printed in SIA Drukātava

THE CONFERENCE PROCEEDINGS IS SUPPORTED BY



CONTENT

I Building Materials	7
Olga Finoženok, Ramunė Žurauskienė, Rimvydas Žurauskas. THE INFLUENCE OF VARIOUS SIZE CRUSHED CONCRETE WASTE.....	7
Viktors Mironovs, Jānis Bronka, Aleksandrs Korjamins, Jānis Kazjanovs. IRON CONTAINING WASTE MATERIALS AND POSSIBILITIES OF THEIR APPLICATION IN MANUFACTURING THE HEAVY CONCRETE.....	14
Andina Sprince, Leonīds Pakrašiņš, Aleksandrs Korjamins. EXPERIMENTAL STUDY CREEP OF NEW CONCRETE MIXTURES	20
Diāna Bajāre, Aleksandrs Korjamins, Jānis Kazjanovs. APPLICATION OF ALUMINIUM DROSS AND GLASS WASTE FOR THE PRODUCTION OF EXPANDED CLAY AGGREGATE	27
Raitis Brencis, Juris Skujāns, Uldis Iljins, Ilmārs Preikšs. RESEARCH OF HEMP'S FIBROUS REINFORCEMENT EFFECT TO BENDING STRENGTH AND SOUND ABSORPTION OF FOAM GYPSUM	32
Jānis Justs, Diāna Bajāre, Genādijs Šahmenko, Aleksandrs Korjamins. ULTRA HIGH PERFORMANCE CONCRETE HARDENING UNDER PRESSURE	38
Raimondas Sadzevicius, Feliksas Mikuckis, Dainius Ramukevicius. DEFECTS' ANALYSIS OF REINFORCED CONCRETE SLABS FOR EARTH DAM SLOPE PROTECTION.....	44
Diāna Bajāre, Jānis Justs, Ģirts Baumanis. OBTAINING COMPOSITION OF GEOPOLYMERS FROM LOCAL INDUSTRIAL WASTES	50
Mārtiņš Zaumanis, Juris Smirnovs. ANALYSIS OF THE POSSIBILITIES FOR THE USE OF WARM MIX ASPHALT IN LATVIA	57
Vincas Gurskis, Karolis Bunevicius, Rytis Skominas. RESEARCH OF THE TRADITIONAL AND NONTRADITIONAL ADMIXTURES ON MORTAR AND CONCRETE	65
Pēteris Šķēls, Edmunds Šķēle, Kaspars Bondars, Thomas Ingeman-Nielsen, Anders Stuhr Jørgensen. QUICKLIME (CaO) STABILIZATION OF FINE-GRAINED MARINE SEDIMENTS IN LOW TEMPERATURE AREAS	71
Ilmārs Preikšs, Juris Skujāns, Uldis Iljins. POSSIBILITIES OF SILICA AEROGEL USEFULNESS FOR FOAM GYPSUM COMPOSITIONS.....	78

Māris Strozis, Genādijs Šahmenko. THE USE OF STRAW-CLAY MATERIAL IN WALLS	84
Regino Kask, Harri Lille, Kristjan Siim, Peeter Paabo, Kuldar Sillaste. STUDY OF PHYSICAL AND MECHANICAL PROPERTIES OF ORIENTED STRAND BOARD DEPENDING ON MOISTURE CONTENT	91
Viktors Mironovs, Mihails Lisicins, Genādijs Šahmenko, Lāsma Kaļva. ANALYSIS OF APPLICATION OF PERFORATED STEEL BAND IN BUILDING CONSTRUCTION	95
II Materials and Structures	103
Jānis Brauns, Kārlis Rocens. TOPOLOGY OPTIMIZATION OF MULTI-LAYERED COMPOSITE STRUCTURES.....	103
Ulvis Skadiņš, Jānis Brauns. MODELING OF FIBRE BRIDGING BEHAVIOUR IN SFRC	109
Kauni Kiviste, Alexander Ryabchikov, Harri Lille. DETERMINATION OF SHRINKAGE OF FIBRE REINFORCED CONCRETE	113
R. Tepfers, G.O. Sjöström, J. I. Svensson. DEVELOPMENT OF METHOD FOR MEASURING DESTRUCTION ENERGY AND GENERATED HEAT AT FATIGUE OF CONCRETE	117
Sanita Ziķe, Kaspars Kalniņš. ENHANCED IMPACT PROPERTIES OF PLYWOOD LAMINATES	125
Jānis Šliseris, Kārlis Rocens. INFLUENCE OF TECHNOLOGICAL AND STRUCTURE PROPERTIES ON SHAPE OF ASYMMETRIC PLYWOOD SHEET	131
Marko Teder, Kalle Pilt, Matis Miljan, Martti Lainurm, Ragnar Kruuda. OVERVIEW OF SOME NON-DESTRUCTIVE METHODS FOR IN SITU ASSESSMENT OF STRUCTURAL TIMBER	137
Līga Gaile, Ivars Radiņš. TIME DEPENDING SERVICE LOAD INFLUENCE ON STEEL TOWER VIBRATIONS	144
Andris Šteinerts, Leonīds Pakrastiņš, Līga Gaile. IMPLEMENTATION OF EUROCODE STANDARDS IN LATVIA	150
Wei Lu, Pentti Mäkeläinen, Jyri Outinen. BEHAVIOUR OF COLD-FORMED Z-SHAPED STEEL PURLIN AT ELEVATED TEMPERATURES.....	154

Edgars Labans, Kaspars Kalniņš. NUMERICAL VERSUS EXPERIMENTAL INVESTIGATION OF PLYWOOD SANDWICH PANELS WITH CORRUGATED CORE	159
Artis Dandens, Jānis Kreilis, Guntis Andersons. PROPERTIES OF COLD-FORMED STEEL SECTIONS	166
III Landscape and Environment	171
Peter Kurz. “CLIMATE-ENERGY-AND CULTURAL LANDSCAPE MODEL SAUWALD DONAUTAL” INTRODUCING A PILOT PROJECT ON INTEGRATED REGIONAL RESOURCE MANAGEMENT BASED ON A NEW BIOGAS TECHNOLOGY	171
Aija Ziemeļniece. INTEGRATION OF RURAL POPULATED AREAS WITHIN ARCHITECTURAL SPATIAL SYSTEM OF THE REGION	178
Natālija Nitavska, Daiga Zigmunde, Raimonda Lineja. THE FORMING ELEMENTS OF THE BALTIC SEA COASTAL LANDSCAPE IDENTITY FROM THE TOWN OF AINAŽI TO THE ESTUARY OF THE RIVER SALACA	182
Una Īle. DEVELOPMENT TENDENCIES OF LANDSCAPE COMPOSITION IN THE URBAN RESIDENTIAL AREAS OF LATVIA	193
Maija Jankevica. THE POSSIBILITIES OF UNIFIED LANDSCAPE DEVELOPMENT IN TRANSNATIONAL BORDERLAND. VALKA-VALGA EXAMPLE	202
IV Engineering of Environmental Energy	209
Leonīds Ribickis, Ansis Avotiņš. ANALYSIS OF GHG REDUCTION POSSIBILITIES IN LATVIA BY IMPLEMENTING LED STREET LIGHTING TECHNOLOGIES	209
Uldis Iljins, Uldis Gross, Juris Skujāns. PECULIARITIES OF HEAT FLOWS OF INSULATION CONSTRUCTIONS IN BUILDINGS WITH COLD UNDERGROUND	215
Sandris Liepiņš, Silvija Štrausa, Uldis Iljins, Uldis Gross. THERMAL ANALYSIS OF OVERGROUND BOUND CONSTRUCTIONS	221
Ēriks Krūmiņš, Arturs Lešinskis, Ilze Dimdiņa. HEAT ENERGY CONSUMPTION IN NOT RENOVATED BUILDINGS AND IN BUILDINGS AFTER A PARTIAL RENOVATION	227

Ilze Dimdiņa, Arturs Lešinskis, Ēriks Krūmiņš, Vilis Krūmiņš, Laimdota Šnīdere. INDOOR AIR QUALITY AND ENERGY EFFICIENCY IN MULTI-APARTMENT BUILDINGS BEFOR AND AFTER RENOVATION: A CASE STUDY OF TWO BUILDINGS IN RIGA.....	236
Gaļina Stankeviča. INDOOR AIR QUALITY AND THERMAL COMFORT EVALUATION IN LATVIAN DAYCARE CENTERS WITH CARBON DIOXIDE, TEMPERATURE AND HUMIDITY AS INDICATORS.....	242
V Environmental Engineering.....	247
Zydrunas Vycius, Tatjana Sankauskiene, Petras Milius. ANTI-SEEPAGE MEANS FOR THE PROTECTIVE EMBANKMENT OF THE KARIOTIŠKĒS SEWAGE SLUDGE DUMP	247
Meeli Kams. THE THERMAL CONDUCTIVITY OF THATCHED (REED) ROOF INSULATED WITH SAW DUST IN DWELLING HOUSE.....	253
Sandra Gusta. BUILDING AS A LONG-TERM ENVIRONMENTAL DEVELOPMENT AND PRESERVATION CONDITION	256
Ēriks Tilgalis, Linda Grīnberga. THE ENERGY – EFFICIENT WASTEWATER TREATMENT TECHNOLOGIES IN CONSTRUCTED WETLANDS	263
Reinis Ziemeļnieks, Ēriks Tilgalis. CALCULATION METHOD OF RAINWATER DISCHARGE.....	267

I BUILDING MATERIALS

INFLUENCE OF VARIOUS SIZE CRUSHED CONCRETE WASTE AGGREGATES ON CHARACTERISTICS OF HARDENED CONCRETE

Olga Finoženok*, Ramunė Žurauskienė**, Rimvydas Žurauskas***

Vilnius Gediminas Technical University

Department of Building Materials

*olga.finozenok@yahoo.com; **ramune.zurauskiene@vgtu.lt; ***rzuster@gmail.com.

ABSTRACT

The characteristics of hardened concrete depend on the raw materials used for the concrete mixture, their characteristics. Therefore, in the research, the variation of characteristics of concrete samples with concrete waste materials was analysed. During the analysis, concrete waste of different fractions was used as coarse and fine aggregate, as well as filler aggregate of crushed concrete waste was used. The research covers the implementation of X-ray analysis of the filler aggregate and identification of the main minerals of the aggregates produced from the concrete waste. The main physical and mechanical characteristics of the samples were determined through the implementation of the standard methodologies: the density of the samples was determined by following the standard LST EN 12390-7, compressive strength – LST EN 12390-3; impregnation – LST 1428.18:1997. It was found that the physical and mechanical characteristics of the concrete, produced by using crushed concrete waste with different particle size, differ from the characteristics of the reference samples. However, these characteristics satisfy the requirements of the designed concrete class C30/37. The obtained results show that crushed concrete waste can be utilised as coarse and fine aggregates for the production of new concrete products.

Keywords: demolition waste, concrete waste, recycled aggregate, filler aggregate, strength

INTRODUCTION

Concrete is one of the oldest and universal construction materials, and is suitable for the production of wide range of products and constructions both, at construction sites and factories. However, the concrete is a multicomponent material of complex structure, and this material consists of different components. These are coarse and fine aggregates with the size of up to few centimetres, binding material with the size of few micrometres, additives and water. Still, the origin of coarse and fine aggregates, used in concrete production, might be different. These can consist of concrete, ceramics and silicate waste, scrap glass, wood waste, pumice of blast-furnaces, volcanic ash, granulated tire rubber and other materials. These materials can substitute the natural aggregates and contribute to the production of the concrete with desirable and specific characteristics. Concrete waste can be utilised as cheap coarse and fine concrete aggregate. However, special attention should be paid to the production of this aggregate, because after building (when their lifetime ends) demolition, such demolition waste can consist of concrete, silicate or ceramic bricks, wood, roof material, metals, plastic, cardboard and other materials (Fig. 1).

Therefore, it is necessary to carry out the initial sorting of the materials produced during the

building demolition, separation of concrete and reinforced concrete products from other materials. Only after the sorting the reprocessing works of reinforced concrete can be implemented: reinforcement separation, shredding of large pieces, crushing and grain sorting into fractions. In this way the coarse, fine and filler aggregate is produced from the concrete waste.



Figure 1. Demolition work of commissioned buildings.

The quality and characteristics of the manufactured production must be constantly monitored, because the crushed constructions may have different strength characteristics. For instance, when ceiling

slabs, columns, as well as partition constructions, are crushed. The aggregate mixture, produced from the crushed concrete waste, consists of the particles of cement stone, particles of rock with the cement stone plastered to, and the particles of rock separated during the crushing. In these aggregate particles the pores and micro-cracks, formed during the crushing, dominate. During the analysis, it was determined that the porosity of such aggregate varies and ranges from 5.8 % to 12.5 % (Tam et al., 2008; Zaharieva et al., 2003). As indicated by the researchers (Мырзаев et al., 2008), water absorption of the aggregates increases due to the porous structure of the aggregate produced from concrete waste. As a result, when aggregates of concrete waste are used during the preparation of concrete mixture, the amount of water, necessary to prepare the concrete mixture of the required consistence, increases. (Мырзаев et al., 2008) states that the required amount of water can increase even up to 15 %.

When coarse aggregate, produced from the strong concrete waste, is used, it is possible to produce the concrete the class thereof would satisfy the strength class requirements of the typical concrete (Бибиќ, 2010). Scientists (Evangelista et al., 2010) state that the compressive strength of the concrete, produced from concrete waste is close to the strength of the concrete produced from natural materials. These scientists determined that after the substitution of 30 % of coarse aggregate by concrete waste, the strength of hardened concrete decreases only by 3.6 %. In addition, the scientists also determined that, when 100 % of coarse aggregate was substituted by the aggregate, produced from the concrete waste, the compressive strength decreases by 7.6 %.

Concrete waste can be also used for the production of fine aggregate, which can replace a part or whole amount of sand required for concrete production. Scientists (Kou et al., 2009) analysed the utilisation of fine aggregate, produced from concrete and reinforced concrete waste, for the concrete production. During the investigation 25 % and 100 % amount of sand was replaced by concrete waste. After 28 days of hardening the strength of concrete decreased by 3.2 % and 8.4 %, comparing to the strength of the reference concrete samples. After proper reprocessing of concrete and reinforced concrete waste, it can be utilised for manufacturing of products of the required quality. Large amounts of construction waste occupy a lot of space in dump areas. During the past decades, the problems of reprocessing and utilisation of concrete waste are being resolved intensively, because every year huge amounts of construction waste are accumulated in the world, and this waste does not fragment and contaminate the environment in the course of time.

In Finland strict laws are employed to ensure that all demolition waste is recycled. In Japan, almost all reprocessed concrete and reinforced concrete waste

is utilised for road construction. In Germany, in 2004 89 % of concrete and reinforced concrete waste was returned to the production line of new products (Klee, 2009).

In Lithuania, according to the waste records of 2007, 67 % of construction waste was reprocessed. On 19-11-2008 the directive 2008/98/EB of the European Parliament and Board was confirmed. In this directive it is stated that till 2020 at least 70 % of non-hazardous construction and demolition waste must be prepared for recycling and reprocessing.

Hence, the target of the research is to investigate the possibilities of secondary utilisation of concrete waste in concrete mixtures, and analyse the variation of characteristics of hardened concrete, for the production thereof the concrete waste aggregates with different particle sizes were utilised.

MATERIALS AND METHODS

Research materials

The following raw materials were utilised in the research:

Coarse aggregate: gravel breakstone and crushed concrete waste.

Fine aggregate: natural sand and crushed concrete waste. The main characteristics of coarse and fine aggregates are shown in Table 1.

Table 1

Characteristics of coarse aggregate

Coarse aggregate	Parameter and its value		
	Bulk density, g/cm ³	Particle density, g/cm ³	Hollowness, %
Crushed gravel 4/16 mm	1.44	2.45	41
Concrete waste 4/16 mm	1.16	2.10	45
Crushed gravel 0.125/4 mm	1.64	2.41	32
Concrete waste 0.125/4 mm	1.21	2.30	47

Filler aggregate: crushed concrete waste, the particle size of which is smaller than 0.125 mm. The main characteristics of the filler aggregate are shown in Table 2.

Cement: Composite Portland limestone cement CEM II/A-L 42.5 N, satisfying the requirements of the standard LST EN 197-1. The chemical composition of this cement is provided in Table 3, and mineral composition – in Table 4. The physical-mechanical characteristics of the utilised cement are shown in Table 5.

Table 2 Composition of the mixtures analysed

Characteristics of filler aggregate			
Filler aggregate	Parameter and its value		
	Bulk density, g/cm ³	Particle density, g/cm ³	Specific surface, cm ² /g
Crushed concrete waste 0/0.125mm	0.95	2.50	2904

Table 3

Chemical composition of the cement						
Chemical composition, %						
SiO ₂	CaO	Al ₂ O ₃	Fe ₂ O ₃	MgO	SO ₃	Other
20.6	63.4	5.45	3.36	3.84	0.80	0.34

Table 4

Mineral composition of the cement			
Mineral composition, %			
C ₃ S	C ₂ S	C ₃ A	C ₄ AF
57.26	15.41	8.68	10.15

Table 5

Physical-mechanical characteristics of the cement	
Parameter	Value
Size of particles	5–30 μm
Early compressive strength after 2 days, N/mm ²	21
Standard compressive strength after 28 days, N/mm ²	47
Initial set, min.	190
Final set, min	230
Specific surface, cm ² /g	3950
Specific particle density, g/cm ³	2.75
Bulk density, g/cm ³	1.02

Four concrete mixtures were prepared during the research. Their compositions are provided in Table 6. Concrete compositions K, C1, C2, C3 were selected depending on the characteristics of raw materials, by implementing computational - experimental methodology and by using tables, diagrams and nomograms. The selected class of the concrete compressive strength was C30/37, mobility – 3 cm.

An equal ratio of water and binding materials W/B – 0.43 was used in all concrete mixtures. This ratio influences the structure, strength, durability and quality of the hardened concrete. The water amount selection is a very important stage, because this amount is related to the concrete composition, characteristics of its components. Minimal amount of water shall ensure the production of the concrete mixture of the required consistence.

During the research natural coarse aggregate, the particle size of which was 4/16 mm, was used. Only in C2 mixture the coarse aggregate, produced from crushed concrete waste, was utilised. The size of the particles of this aggregate was 4/16 mm. The aggregate, produced from concrete waste, replaced the overall amount of coarse aggregate. The amount of fine aggregate in this mixture was increased, because the selection of the concrete mixture composition, where the overall amount of coarse aggregate is replaced by crushed concrete waste, results in the lack of fine fraction aggregate. In mixture C3 the overall natural fine aggregate was replaced by concrete waste.

During the selection of concrete compositions, the cement part in C1 mixture was replaced by filler aggregate. In accordance with the standard LST 1577:1999, the mass ratio between the filler aggregate and Portland cement CEM II A cannot exceed 15 %. After the designing of the concrete composition, it was decided to add a half of this amount and 8 % of cement mass was replaced by the filler aggregate.

Table 6

Concrete marking	Compositions of concrete mixtures							
	Composition							
	Cement, kg/m ³	Coarse aggregate, kg/m ³		Fine aggregate, kg/m ³		Filler aggregate, kg/m ³	Water, l/m ³	W/B
		Crushed gravel	Concrete waste	Sand	Concrete waste			
K	395	1277	–	372	–	–	170	0.43
C1	363	1277	–	372	–	32	170	0.43
C2	410	–	930	690	–	–	180	0.43
C3	415	1280	–	–	420	–	180	0.43

The filler aggregate was produced by crushing concrete waste with alligator and by sifting out the produced material with laboratory separators into fractions belonging to coarse aggregates, fine aggregates and filler aggregates.

All concrete mixtures were prepared manually in the laboratory. The prepared concrete mixture of the required consistence was poured to 100×100×100 mm size moulds. The samples were thickened by vibration on the laboratory vibrating platform for approximately 1 min. The samples were hardened in the moulds for 24 hours, and then stored in 20°C±2°C temperature water (according to LST EN 12390-2) until the tests for the assessment of the characteristics were performed. Five samples were chosen from three concrete lots produced in laboratory conditions.

Research methodology

After 28 days of hardening in water, the density of the concrete cubes was estimated in accordance with the standard LST EN 12390-7, impregnation – in accordance with LST 1428.18:1997 and the compressive strength of the concrete – in accordance with LST EN 12390-3. The samples were compressed by using the press “ALPHA 3-3000”, complying with the requirements of the standard LST EN 12390-4.

The concrete compressive strength was calculated by employing formula (1).

$$f_{cm} = \frac{F_b}{A_b}, \quad (1)$$

where : F_b – fragmenting compressive force, kN;
 A_b – sample cross-section area, mm².

During the investigation the mineral composition of the filler aggregate X-ray analysis of the filler aggregate was implemented by using the diffraction meter DRON-2 (Cu anode, Ni filter, monochromator, cracks with the size of 1:8:0.5 mm). The operation mode of the tube of diffractometer: U=30 kV, I=10 mA. The recorded diffractogram was decoded by comparing the obtained experimental values of multilayer distances d and specific integral intensity I/I_0 values of the lines with the corresponding values in ASTM file.

RESULTS AND DISCUSSION

After the X-ray analysis of the filler aggregate implemented during the research, its mineral composition was determined. The X-ray pattern is shown in Fig. 2. We can notice that the main minerals of this raw material are as follows: silica Q (0.137, 0.138, 0.145, 0.154, 0.167, 0.182, 0.197, 0.213, 0.223, 0.228, 0.246, 0.335, 0.425 nm), calcite K (0.152, 0.160, 0.187, 0.198, 0.209, 0.250, 0.304, 0.385 nm), dolomite D (0.180, 0.201, 0.219, 0.240, 0.269, 0.402 nm), feldspars F (0.319 0.324 nm), portlandite P Ca(OH)₂ (0.491) dominates as well, illite I (0.100 nm).

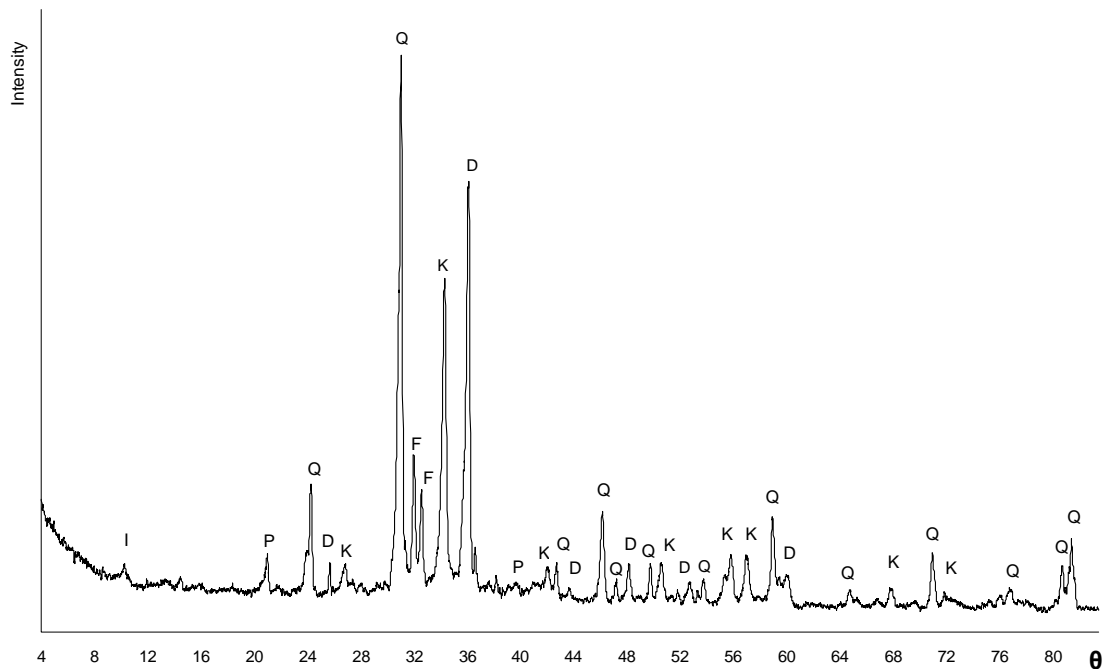


Figure 2. X-ray pattern of filler aggregate: Q – quartz; K – calcite; D – dolomite; F – feldspars; P – portlandite; I – illite.

Considering the results of the X-ray analysis of the filler aggregate, it can be assumed that its mineral composition is related to the initial material used for the crushing.

80 % of the concrete volume is occupied by concrete aggregates. They have a large influence on the concrete characteristics and durability, and the strength of the concrete depends very much on the mineral composition, quality, strength, hollowness, cleanness and granulometric composition of the aggregates.

During the research the compressive strength values of the concrete samples were estimated. It was noticed that the compressive strength depends on the size of the particles of the aggregate utilised. As scientists assume (Naujokaitis, 2007) strength of the concrete depends on the characteristics of the coarse aggregates, because their particles form the concrete framework and have an influence on the nature of the distribution of the concrete stresses, deformations, as well as on the formation of cracks due to various loads applied. The amount of water required for the preparation of the concrete mixture is related to the fine aggregates. In addition, the granulometric composition of the fine aggregate, characteristics, shape and amount of the particles influence the concrete macrostructure, and this is the structure of cement grout (with sand aggregate) existing in the concrete.

The results of the estimation of the compressive strength of hardened concrete are provided in Fig. 3.

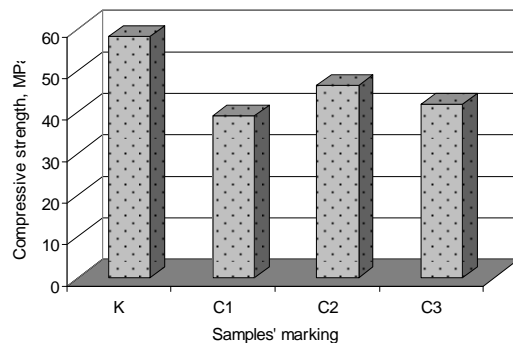


Figure 3. Results of estimation of compressive strength of concrete samples.

Fig. 3 shows that the compressive strength of the concrete samples with concrete waste aggregates with the particles of different sizes reaches 67–80 % of the strength of the reference samples (K). The lowest strength was achieved when a part of the cement of concrete mixture was replaced by the filler aggregate produced from crushed concrete waste. The compressive strength of the concrete samples, where 100 % of natural coarse or fine aggregates were replaced by the aggregate produced from concrete waste, varies depending on the size

of the particles of the new aggregate. The compressive strength of the sample C2, where the coarse aggregate was replaced by crushed concrete waste, decreased by 20 %, and, when natural sand was replaced (sample C3), the compressive strength decreased by 28 %. However, the strengths of the concrete samples C2 and C3 reach their compression class requirements. As scientists (Evangelista et al., 2010) state, when concrete waste is utilised as fine aggregate, the strength of the newly hardened concrete can decrease by up to 30 %.

The compressive strength is a very important characteristic of concrete. In addition to this, concrete is the most resistant to the compression stresses. As it is stated by (Naujokaitis, 2007), concrete, that is influenced by compression loads, disintegrates according to three models: the first – when disintegration occurs through the cement stone, the second – when disintegration occurs through the aggregate and the third – when concrete disintegrates through both, cement stone and aggregate. It was noticed that during the compression process, when the concrete samples were disintegrating, the disintegration occurred not only through the cement stone, but also through the aggregates produced from concrete waste.

In Fig. 4 a view of a cut concrete sample, in the production thereof the concrete waste was used as the coarse aggregate, is showed.

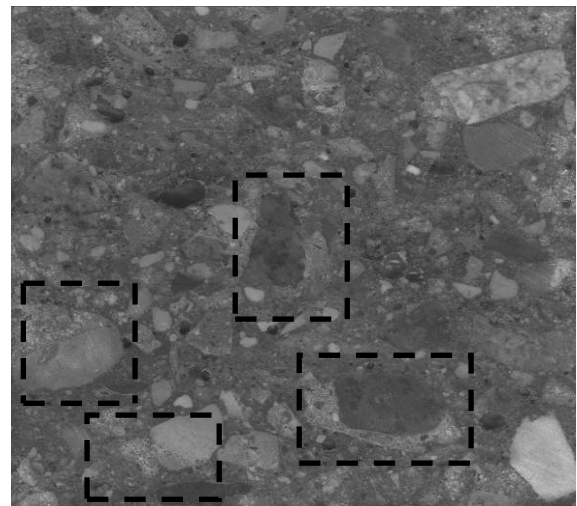


Figure 4. View of cut concrete sample.

Newly created cement stone, coarse and fine aggregates can be noticed in this view. Newly created aggregate from the concrete waste is marked in the figure, and it is clear that this aggregate is formed from the natural aggregate and the adhered cement stone, which remained uncrushed during the crushing process. In addition, it can be seen how this aggregate adheres to the newly formed cement stone.

The concrete density, as well as the compressive strength, are one of the main quality parameters of hardened concrete. The variation of the density of hardened concrete, depending on concrete composition, is shown in Fig. 5.

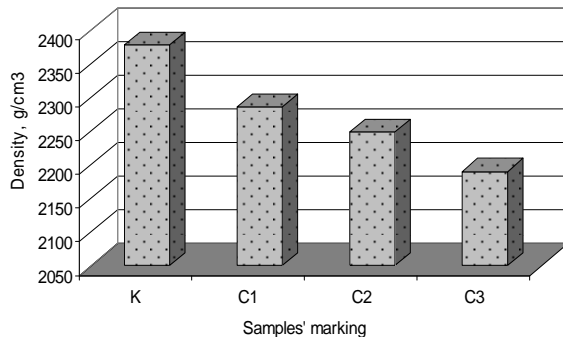


Figure 5. Results of density estimation of concrete samples.

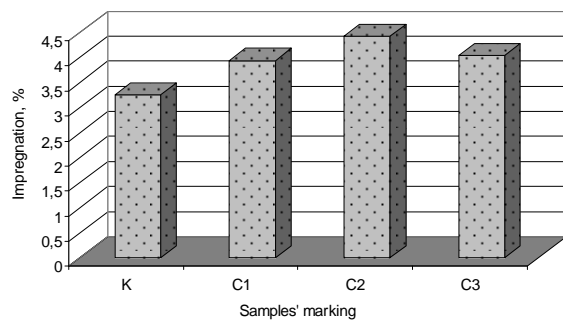


Figure 6. Results of the estimation of sample impregnation.

It can be noticed that concrete C1, where only natural aggregates were used and 8 % part of the cement was replaced by the filler aggregate produced during the crushing of the building concrete constructions, density reached the highest value – 2286 kg/m³. Comparing with the reference concrete samples, the density decreased by only 4 %, even though the concrete strength decreased by 33 %. The density decreases when concrete waste replaces coarse or fine aggregates. The density of the concrete, produced by utilising coarse aggregates from crushed concrete waste, is 2249 kg/m³, i.e., this value is by 3 % higher than the one of concrete, produced by utilising concrete waste instead of fine aggregate. However, the density of all samples satisfies the density requirements applicable for normal concrete, the density of which after 28 days of hardening and drying must be in the range of 2000–2600 kg/m³.

The concrete density is not fixed, and it depends on the characteristics of the raw materials utilised. Therefore, it is necessary to constantly analyse the

main characteristics of the aggregates produced from concrete and reinforced concrete waste, because these characteristics influence the properties of the hardened concrete.

Water impregnation of the hardened concrete samples was estimated after 72 hours of soaking. The results of impregnation are shown in Fig. 6.

CONCLUSIONS

- 1) Waste reprocessing problems are very important in the world and are being resolved intensively, because more and more new buildings are built and old, unused constructions are demolished. In respect to the ecological safety and in order to save natural resources, concrete waste can be utilised for the production of high quality products by returning this waste to the production technological cycle.
- 2) After analysis of the influence of the size of particles of the aggregates utilised in concrete production, it was noticed that the compressive strength values vary. The compressive strength decreases by 20 % when coarse aggregates are replaced by concrete waste, and, after fine aggregate is replaced by the crushed concrete waste, the concrete compressive strength decreased by 28 %. However, when natural aggregates are replaced by concrete waste, the strengths of the newly produced hardened concrete samples reach the compression strength value of the class C30/37 of the designed concrete.
- 3) The results of the analysis show that, when natural coarse and fine aggregates are utilised and 8 % of the amount of cement is decreased by replacing it with the filler aggregate from crushed concrete waste, the compressive strength decreases significantly, density increases by 21 % and impregnation decreases only by 4 %.
- 4) According to the density results of the concrete samples it can be assumed that the density values of the produced concrete samples satisfy the requirements applicable for normal concrete, because the obtained values vary from 2190 to 2286 kg/m³.
- 5) The results of the analysis showed that, when crushed concrete waste is used for the concrete, the characteristics of the hardened concrete worsen, comparing to the reference concrete sample where waste was not utilised. However, during further analysis it is possible to estimate the optimal compositions of concrete mixtures and to monitor the characteristics of the produced products.

REFERENCES

- Evangelista L., de Brito J. (2010) Durability performance of concrete made with fine recycled concrete aggregates. *Cement & Concrete Composites*, Vol. 32, No. 1, p. 9-14.
- Klee H. (2009) The cement sustainability initiative. Recycling Concrete [online] [accessed on 11.01.2010]. Available: <http://www.wbcdcement.org/pdf/CSI-RecyclingConcrete-FullReport.pdf>
- Kou S.C., Poon C.S. (2009) Properties of self-compacting concrete prepared with coarse and fine recycled concrete aggregates. *Cement & Concrete Composites*, Vol. 31, No. 9, p. 622-627.
- LST 1428.18:1997 Concrete. Testing methods. Determination of water absorbability. Lithuanian Standards Board. Vilnius, 1997. 4 p.
- LST 1577 Concrete and mortar fillers. Technical requirements. Lithuanian Standards Board. Vilnius, 1999. 6 p.
- LST EN 12390-2 Testing hardened concrete - Part 2: Making and curing specimens for strength tests. Lithuanian Standards Board. Vilnius, 2009. 8 p.
- LST EN 12390-3 Testing hardened concrete - Part 3: Compressive strength of test specimens. Lithuanian Standards Board. Vilnius, 2009. 18 p.
- LST EN 12390-4 Testing hardened concrete. Compressive strength. Specification for testing machines. Lithuanian Standards Board. Vilnius, 2003. 15 p.
- LST EN 12390-7 Testing hardened concrete - Part 7: Density of hardened concrete. Lithuanian Standards Board. Vilnius, 2009. 10 p.
- LST EN 197-1:2001/A1:2004 Cement – Part 1: Composition, specifications and conformity criteria for common cements. Lithuanian Standards Board. Vilnius, 2006. 9 p.
- Naujokaitis A. (2007) *Statybinės medžiagos. Betonai* [Building materials. Concrete]. Vilnius: Technika. 355 p.
- Tam V. W. Y., Wang K., Tam C. M. (2008) Assessing relationship among properties of demolished concrete, recycled aggregate and recycled aggregate concrete using regression analysis. *Journal of Hazardous Materials*, Vol.152, No. 2, p. 703-714.
- Uselytė R; Silvestravičiūtė I.; Šleinotaitė-Budrienė L. (2008) Antrinių žaliavų perdirbimo plėtros prioritetų ir priemonių 2009-2013 metams studija [Recycling development priorities and measures in 2009-2013 year study] [online] [accessed on 22.03.2010] Available: http://www.ukmin.lt/lt/veikla/veiklos_sritys/pramone_ir_verslas/reglamentavimas/mokslo%20studijos/AZPP_studijos_ataskaita_Ekokonsultacijos_12_31.pdf
- Zaharieva R., Buyle-Bodin F., Skoczylas F., Wirquin E. (2003) Assessment of the surface permeation properties of recycled aggregate concrete. *Cement & Concrete Composites*, Vol. 25, No.2, p. 223-232.
- Бибик М. С. (2010) Исследование влияния физико-механических характеристик щебня из дробленого бетона различных классов по прочности на сжатие на свойства бетонной смеси и бетона [The research of influence on physical and mechanical characteristics of crushed stone from concrete waste of different compressive strength classes on the properties of concrete compound and concrete]. *Строительная наука и техника*, № 1–2, с. 55–59.
- Муртазаев С-А. Ю., Саламанова М. Ш., Гишлакаева М. И. (2008) Формирование структуры и свойств бетонов на заполнителе из бетонного лома [The formation of structure and properties of concrete on the aggregate of the concrete waste]. *Бетон и железобетон*, № 5, с. 25-28.

POSSIBILITIES OF APPLICATION IRON CONTAINING WASTE MATERIALS IN MANUFACTURING OF HEAVY CONCRETE

Viktors Mironovs*, Jānis Bronka**, Aleksandrs Korjakins***, Jānis Kazjonovs****

*Riga Technical University,

Institute of Building Production, Faculty of Transport and Mechanical Engineering

viktors.mironovs@gmail.com

**Riga Technical University, Faculty of Civil Engineering

janis.bronka@gmail.com

***Riga Technical University,

Institute of Materials and Structure, Faculty of Building Materials and Units

aleks@latnet.lv

****Riga Technical University, Faculty of Civil Engineering

janis.kazjonovs@rtu.lv

ABSTRACT

Rational use of highly dispersed metal waste is an important issue of material science and environment protection. The quantity of the powdered metallic materials used in industry is steadily increasing; they are especially widely used in the enterprises producing iron powders, in metal sheet production, as well as in abrasive machining. This paper presents an analysis of several kinds of metal waste such as iron and steel powders, mill scales, steel punching, metal shavings and other iron-containing waste from mechanical engineering and metallurgy industries, and the possibility of their use in the manufacturing of concrete products like fillers. This study investigates properties of the samples of the concrete manufactured using highly dispersed metallic fillers. The highest density obtained is in the range of 4000 - 4500 kg/m³. The common characteristics of the aforementioned materials are their low cost, availability and thus the potential for large production volumes, need for recycling, and tendency to further oxidation and corrosion.

Key words: metal fillers, heavy concrete, metal powders, metal dust, mill scale, steel punching

INTRODUCTION

A broad study of heavy concrete manufactured with iron inclusions commenced after the scientific publication "Strength and Fracture Toughness of Heavy Concrete with Various Iron Aggregate Inclusions" published in 2004 (Kan, Pie, Chang, 2004). The research in Latvia was launched in 2009 at the Riga Technical University and still is in progress. The result of the investigation at the Institute of Building Production is a patent of the Republic of Latvia LV 14019 B (V. Mironovs, Zemčenkovs, Korjakins, Šahmenko, 2010).

Heavy concrete materials are those with the density greater than 2600 kg/m³. In order to achieve higher density traditional fillers of concrete (sand, gravel, crushed rocks) are entirely or partially replaced with other materials with larger specific gravity - e.g., magnetite, hematite, barite, iron and steel powders, mill scales, steel punchings, metal shavings etc. For manufacturing heavy and extra heavy concrete the most commonly used material is either Portland cement or alumina cement (Chundelly, Geeno, 2001). Heavy concrete is used for the manufacturing of anchors, pontoons and contra weights, as well as in hydro technical structures and radiation shielding and storage.

In the production of metal powders and their manufactures the waste is generated in different

stages – dust particles on the filters, waste on sieves, powders from setting up equipment etc. (Дьячкова, Керженцева, Маркова, 2004).

Rational use of highly dispersed metal waste is an important issue of material science and environment protection. The quantity of the powdered metallic materials used in industry is steadily increasing; they are especially widely used in the enterprises producing powders, in metal sheet production, as well as in abrasive machining (Делюсто, 2002).

The common characteristics of the aforementioned materials are their low cost, availability and thus the potential for large production volumes, need for recycling, and tendency of further oxidation and corrosion. Considering the current economic situation in the construction industry in Latvia, economy of resources, reducing consumption of materials, and development of new materials with special properties such as high density and durability are the tasks of major importance.

1. PROPERTIES OF IRON CONTAINING CONCRETE FILLERS

1.1. Metal powders

This study analysed powders SC100.26 (Fig. 1), MH.80.23 and ASC.100.29 from the Swedish Company Höganäs AB.

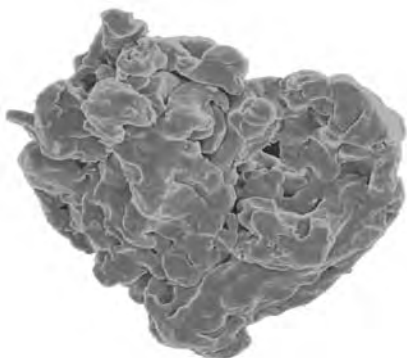


Figure 1. Powder SC100.26 microstructure (average particles size is 45 – 150 μm).

The metal powder SC100.26 has the best compressibility of all Höganäs sponge iron powder grades. The green strength is also high. It should be used particularly if high density after single pressing and sintering is desirable. MH80.23 is specially designed to match the requirements for self-lubricating bearings. Its range of the particle size is chosen to give an optimum pore structure for this application. The metal powder MH80.23 can also be added to powder mixes in small quantities to substantially improve green strength. The metal powder ASC100.29 is an atomised iron powder with a very high compressibility, which makes it possible to single press compacts with densities of up to 7.2 g/cm³. ASC100.29 is particularly suited for high density structural parts and as a base material for soft magnetic applications (Höganäs AB, 2010).

The iron content in powders is greater than 95%. The sieve analysis is shown in Fig. 2.

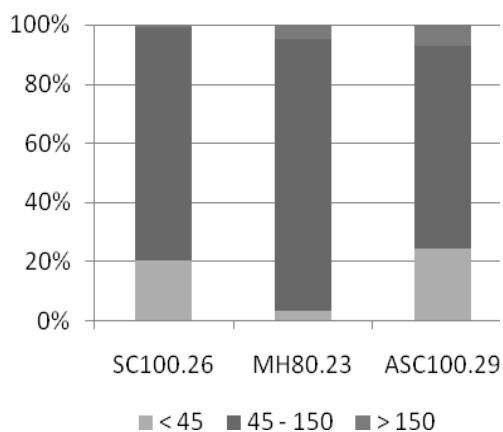


Figure 2. Sieve analysis, μm.

Table 1
Apparent density and flow of metal powders

Metal powder	AD, g/cm ³	Flow, s/50 g
SC100.26	2.68	29
MH80.23	2.30	34
ASC 100.29	2.98	24

The apparent density and flow of the aforementioned powders are shown in Table 1.

1.2. Metal dust

Air filters in manufacturing enterprises collect large amounts of dust. The Swedish company Höganäs AB delivers this waste material to consumers under the brand CMS (Fig. 3).

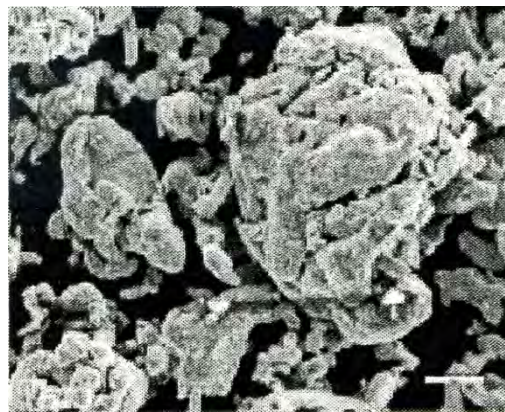


Figure 3. Microstructure of CMS.

Table 2
Sieve analysis of powder CMS 95

	<45, μm	45<212, μm	>212, μm
Test results	56.8%	43.2%	0.0%
Min	35.0%		
Max			1.5%

The product has high iron content (guaranteed over 90%), and its sieve analysis is shown in Table 2.

1.3. Mill scales

Mill scale is flaky dross obtained in rolling red hot steel or in steel mills. The thickness of the dross layer is approximately 10 – 15 microns.

The main components of iron dross are Fe₂O₃ (hematite), Fe₃O₄ (magnetite) and FeO. The properties of iron oxides are shown in Table 3.

Table 3
Properties of iron oxides

	FeO	Fe ₃ O ₄	Fe ₂ O ₃
Molar mass, g/mol	71.84	231.52	159.68
Specific gravity, g/cm ³	5.28	5.20	5.12
Hardness, HV	270 – 350	420 – 500	1030
Part of mass in mill scale	50%	40%	10%

The study used mill scale from the rolling of steel reinforcement supplied by “Liepajas Metalurģs” (Latvia). The particles of raw mill scale are shown in Fig. 4.

The iron content in the mill scale is greater than 70%, humidity from 1 to 5 % and specific gravity of the material is $5.2 \div 5.5 \text{ g/cm}^3$.



Figure 4. Raw mill scale from JSC “Liepajas Metalurgs”.

The mill scale had an apparent density of $1.9 \div 2.1 \text{ g/cm}^3$ and hardness from 200 to 500 HB. The sieve analysis of the mill scale is shown in Table 4.

Table 4
Sieve analysis of raw mill scale

<150, μm	150 – 300, μm	300 – 600, μm	> 600, μm
34.73%	25.25%	10.82%	29.20%

In order to decrease the size of the particles, it is possible to process the raw mill scale. One of the methods is grinding.

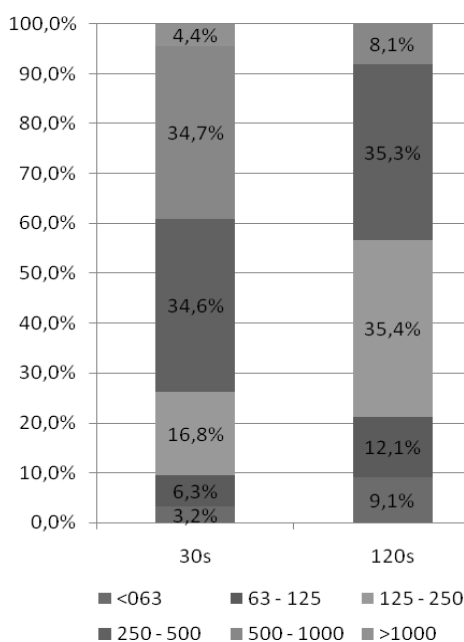


Figure 5. Sieve analysis of grinded mill scale, μm.

Table 5
Sieve analysis of grinded mill scale

Particle size, μm	Grinded mill scale	
	30 s	120 s
<063	3.2%	9.1%
63 – 125	6.3%	12.1%
125 – 250	16.8%	35.4%
250 – 500	34.6%	35.3%
500 – 1000	34.7%	8.1%
>1000	4.4%	0.0%

Fig. 5 and Table 5 present the sieve analysis of 30 s and 120 s grinded mill scales. It was ground in planetary ball mills with nominal speed of 300 rpm (Kazjonovs, Bajare and Korjakins, 2010).

1.4. Steel punching

One kind of steel scrap is steel punching, which is formed by cutting sheet materials (Fig. 6).



Figure 6. Steel punching from JSC “DITTON Driving Chain Factory” (Latvia). Diameter $3.0 \div 10.8 \text{ mm}$, height $0.5 \div 3.3 \text{ mm}$. The specific gravity of steel punching is 7800 kg/m^3 .

This research used punching formed by the stamping of circuit elements supplied by the enterprise JSC “DITTON Driving Chain Factory” (Latvia). The cuttings have a round shape and various geometric dimensions, the diameter and thickness of the samples are shown in Table 6. The specific gravity of steel punching is 7800 kg/m^3 .

Table 6
The size of steel punching

	Steel punching types							
	D, mm	3.0	3.9	4.6	5.8	6.4	7.1	10.8
H, mm	0.7	0.8	0.5	1.0	1.0	2.3	3.3	

The investigation of the properties reveals that hardness of the elements is up to 100 HB.

2. HEAVY CONCRETE COMPOSITIONS AND PROPERTIES

2.1. Mixture proportioning and preparation

This study analysed prepared types of heavy concrete S1 and S2 that are patented in Latvia (Mironovs, Zemčenkovs, Korjakins, Šahmenko, 2010). The components used in manufacturing heavy concrete and their part of mass are shown in Table 7.

Table 7
Heavy concrete compositions (by weight)

Component	Mix	
	S1	S2
Cement CEM I 42.5N	1.00	1.00
Mill scale	3.95	3.49
Sand	0.65	0.00
Steel punchings	0.00	2.69
Metal powder	0.00	1.62
Superplasticizer	0.015	0.016
W/C ratio	0.55	0.62

Several ingredients are prepared before application, e.g., the steel punching is cleaned of oil that is applied in the manufacturing process. The traditional concrete component sand is applied as fine filler in the mix S1. In the second mix S2 all traditional concrete components are replaced with iron containing waste materials.

In order to improve the workability of the mix and reduce W/C ratio, a superplasticizer is added in both mixtures. Optimisation of packing is applied to decrease W/C ratio of the concrete and enlarge its density. Vibration of the concrete is used briefly to avoid the segregation as a result may be issued of metal filler higher specific gravity. Three specimens have been prepared as for compression tests as well for tensile test using each concrete composition S1 and S2. To provide detailed properties of the concrete, this study also discusses two heavy concrete types S50 and S100 from the scientific publication “Designing of High Density Concrete by Using Steel Treatment Waste”.

Table 8
Details about aggregate proportions

Concrete mix	S50	S100
	% aggregate	
High-weight waste aggregate:	50	100
Iron dross:		
Grinded 30 s	5	20
Grinded 2 min	15	20
Mix of steel punching	30	60
Natural aggregate:	50	-
Gravel	35	-
Sand	15	-

The heavy concrete S50 and S100 and their aggregate proportions are shown in Table 8, the mechanical and physical properties in Table 9 and Table 10 respectively (Kazjonovs, Bajare, Korjakins, 2010).

2.2. Properties of mix

The physical properties of the heavy concrete samples are shown in Table 9. As expected, the iron containing waste materials heighten the density of the product.

Table 9
Physical properties

Concrete type	Density, kg/m ³
S1	3200
S2	4300
S50	3500
S100	4600

The highest density obtained in this study is in the range 4000 – 4500 kg/m³. Also, approximate expenses were estimated for heavy concrete mixtures. The higher density sample had greater expenses mainly due to the metal powder used as fine filler. After 28 days the samples were tested in compression and tension. The results are shown in Table 10.

Table 10
Mechanical properties (after 28 days)

Concrete type	Compressive strength, MPa	Tensile strength, MPa
S1	50.7	7.15
S2	43.1	6.32
S50	40.7	4.10
S100	36.6	4.15

The results show that S2 mixture has lower strength in compression and tension than S1 mixture. The structure of a split S2 sample is shown in Fig. 7. Another potential drawback of steel punching is corrosion that should be tested in further researches.

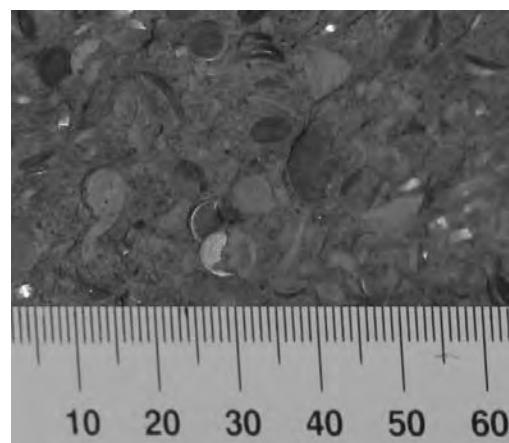


Figure 7. Structure of S2 mixture sample.

The research by Kan, Pie and Chang (2004) reveals that the elastic modulus of heavy concrete is higher than for the regular concrete mortar. Moreover, it is increasing with the increase of iron ore. As shown in Fig. 8, heavy aggregate inclusion of 48.8% in the volume makes the elastic modulus of concrete raise approximately 1.5 times that of regular mortar.

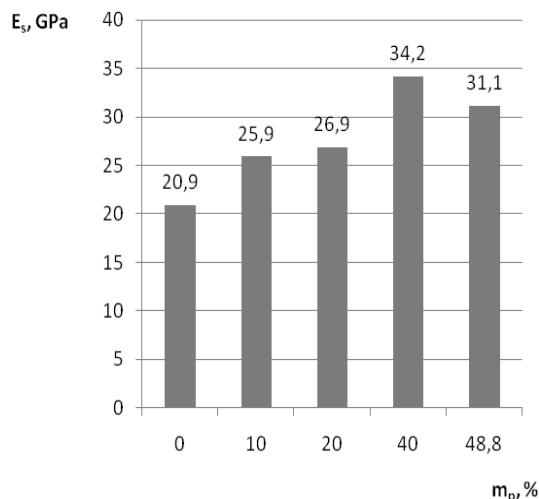


Figure 8. Modulus of elasticity for concrete with various metallic aggregates.

However, it does not make the compressive strengths too much difference as previously mentioned (Kan, Pie and Chang, 2004).

3. APPLICATION POSSIBILITIES OF HEAVY CONCRETE

Heavy concrete has high application possibilities in the field of contra weights. The main contra weight material properties are their high density, fine resistance to external environment impacts and low production cost.

Contra weights are used to ensure stability of enginery – e.g., machinery, lifts, bridges, floodgates, cranes etc. (Mehta and Monteiro, 2006)

It is also effective to use heavy concrete in underwater constructions due to its high density that is more notable because of the buoyant force (1), namely, the weight in the water depends on the material mass and density.

$$P = mg \left(1 - \frac{\rho_w}{\rho_m}\right) \quad (1)$$

where P – weight in water, N;
m – mass of manufacture, kg;
g – gravitational acceleration, m/s²;
 ρ_w – density of water, kg/m³;
 ρ_m – density of material, kg/m³.

Heavy concrete can be used to manufacture the substructure of breakwaters. Another perspective

product category includes anchors which would be suitable in fast currents or rocky seafloor. The Institute of Building Production has developed the construction scheme of such anchor that is shown in Fig. 9.

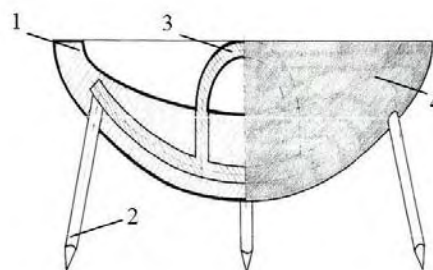


Figure 9. Construction scheme of anchor (1 – heavy concrete body, 2 – metal pine, 3 – metal ring, 4 – rubber cover).

The rubber cover is used to avoid unfavourable impacts of sea water and possible corrosion. In this study were produced anchor model made of heavy concrete with the density approximately 4300 kg/m³ (Fig. 10).



Figure 10. Anchor model.

Heavy concrete could also be used as a radiation shielding material in nuclear stations and buildings with heightened radiation level. There are two types of radiation:

1. X-rays and gamma rays. According to the Compton scattering effect, the attenuation efficiency is approximately proportional to the mass of the material used in the shield of radiation (Mehta and Monteiro, 2006). Also, researches confirm that the attenuation coefficient depends on the density of the concrete (Ismail and Al-Hashmi, 2008).
2. Neutrons. An efficient neutron-occluding material consists of heavy elements such as iron the atomic mass of which is 56 and light elements, preferably, hydrogen (Mehta and Monteiro, 2006).

The structure of heavy concrete conforms to both types of radiation attenuation requirements. In addition, heavy concrete has a decent compressive strength, and thus it is usable as a supporting structure. Bore could be used as filler in concrete in order to better attenuate the radiation.

CONCLUSIONS

1. As planned, the iron containing waste materials heighten the density of product. The highest density obtained in this study is in range 4000 – 4500 kg/m³, though higher density concrete also had greater expenses per mass unit.

2. Elastic modulus of heavy concrete is higher than regular concrete mortar and is increasing with the increase of metallic aggregates .
3. Optimization of packing was applied to decrease concrete W/C ratio and enlarge density.
4. Vibration of concrete was used briefly for avoiding of segregation as a result may be issued of metal filler higher specific gravity.
5. Potential drawback of steel punching is corrosion that should be tested in further researches.

REFERENCES

- Basyigit C. (2006) The Physical and Mechanical Properties of Heavyweight Concretes Used in Radiation Shielding. *Journal of Applied Sciences*, Vol. 6, Issue 4, p. 762. – 766.
- Chundelly R., Greeno R. (2001) *Building Construction Handbook*. British Library Catalogue in Publication Data. 347 p.
- Höganäs AB (2010) Iron Powders for Sintered Components [online] [accessed on 30.04.2011.]. Available: http://www.hoganas.com/Documents/Brochures/Iron_Powders_for_Sintered_Components_November_2010_web.pdf
- Höganäs AB (2010) Overview of Powder Grades [online] [accessed on 30.04.2011.]. Available: http://www.hipih.com/cgi-shl/DC_Show_File.exe?fileId=2257&btnId=50&isWebSiteItem=1&save=0
- Ismail ZZ, Al-Hashmi EA. (2008) Reuse of waste iron as a partial replacement of sand in concrete. *Waste Management*, Vol. 28, Issue 11, p. 2048. – 2053.
- Kan Y.C., Pie K.C., Chang C.L. (2004) Strength and Fracture Toughness of Heavy Concrete with Various Iron Aggregate Inclusions. *Nuclear Engineering and Design*, Vol. 228, Issues 1-3, p. 119 – 127.
- Kazjonovs J., Bajare D., Korjakins A. (2010) Designing of High Density Concrete by Using Steel Treatment Waste. The 10th international Conference Modern building materials, structures and techniques, Lithuania, Vilnius, p. 138 – 142.
- Lorente A., Gallegoa E., Vega - Carrillo H. R., Mendez R. (2008) Neutron Shielding Properties of a New High - Density Concrete. 12th International Congress of the International Radiation Protection Association, IRPA-12, Buenos Aires, Argentina, p. 1 – 10.
- Mehta P., Monteiro P. (2005) *Concrete Microstructure, Properties, and Materials*. New York: McGraw - Hill Professional. 261 – 262 p., 528 – 530 p.
- Mironovs V., Zemcenkovs V., Korjakins A., Sahmenko G. (20.01.2010.) *Heavy concrete*. LR patent LV 14019B, Int. Cl. C04B18/04 (C04B28/00).
- Делюсто Л.Г. (2002) *Абразивно-порошковая очистка проката от окалины*. М:Машиностроение. 460 с.
- Дьячкова Л.Н., Керженцева Л.Ф., Маркова Л.В. (2004) *Порошковые материалы на основе железа*. Минск: Тонник. 226 с.

EXPERIMENTAL STUDY ON CREEP OF NEW CONCRETE MIXTURES

Andina Sprince*, Leonids Pakrastinsh, Aleksandrs Korjakins*****

*Riga Technical University, Department of Structural Engineering
andina.sprince@rtu.lv

**Riga Technical University, Department of Structural Engineering
leonids.pakrastins@rtu.lv

***Riga Technical University, Institute of Materials and Structures
aleksandrs.korjakins@rtu.lv

ABSTRACT

The aim of this study was to experimentally investigate the creep behavior of developed concrete compositions in order to evaluate the possibility of using glass powder and small clay particles as active additives in concrete by replacing cement. Several concrete mixes were designed and prepared, then 160x40x40mm specimens of each batch were made and tested. The specimens were subjected to a uniform compression load kept constant over a long period of time in a constant room temperature and with a constant level of moisture. The specimens were hardened in two extreme environments: in one case there was 100% humidity provided by protecting the specimens from desiccation and in the other case the specimens were air-dried and protected from any moisture. The compression strength and modulus of elasticity of the developed concrete mixes were determined and compared with those of the reference concrete.

Keywords: creep, lamp glass powder, small clay particles, compression strength, modulus of elasticity

INTRODUCTION

In the design of concrete structures, the two main design objectives are strength and serviceability. A structure must be strong enough and sufficiently ductile to resist, without collapsing, the overloads and environmental extremes that may be imposed on it. It must also perform satisfactorily under the day-to-day service loads without deforming, cracking or vibrating excessively (Gilbert et al., 2011). Formulation of creep and relaxation models has been ongoing from more than hundred years. In the case of concrete, elastic behaviour of concrete was taken for granted for a long time. However, in 1907 Hatt wrote an article on a test performed on reinforced concrete beams subjected to constant load. Hatt discovered that the deflection increased significantly with time (Westman, 1999).

Creep of concrete originates in the hardened cement paste that consists of solid cement gel containing numerous capillary pores. The cement gel is made up of colloidal sheets of calcium silicate hydrates separated by spaces containing absorbed water. Creep is thought to be caused by several different and complex mechanisms not yet fully understood. (Neville et al., 1983) identified the mechanisms for creep. Recent research relates the creep response to the packaging density distributions of calcium-silicate-hydrates. At high stress levels, additional deformation occurs due to the breakdown of the bond between the cement paste and aggregate particles. (Gilbert et al., 2011; ACI Committee 209, 2008; Neville, 1995; Neville, 1970; Neville et al., 1983; Bazant et al., 1983; Gilbert, 1988; Vandamme et al., 2009).

Therefore, designers and engineers need to know the creep properties of concrete and must be able to take them into account in the structure analysis. After all, the end product of an engineer's endeavours is a structure the strength of which is adequate, but not wastefully excessive, the durability is commensurate with the conditions of exposure, and serviceability ensures fitness for the purpose. Consideration of creep is a part of a rational approach to satisfying these criteria. Deformation characteristics of materials are an essential feature of their properties, and a vital element in the knowledge of their behaviour. After all, it is the subject that matters: creep is important if its deformation increases with time under a constant stress (Neville et al., 1983).

In the last few years it has been recognized that one of the main sources of environmental pollution is waste. It has become a major environmental problem because many types of waste do not break down, that is, essential physical, biological and chemical changes do not take place. One of the possibilities of utilizing waste is recycling, which would not only save natural resources, but also decrease the amount of deposited waste. Glass waste requires recycling. Since there are different types of glass with different chemical compositions, there are also different possibilities of its use.

In accordance with the decision of the European Committee, all simple incandescent lamps are to be replaced by fluorescent lamps until 2012, therefore, after a couple of years the problem of their recycling and utilization will become more severe (Korjakins et al., 2010).

One of the solutions would be to recycle the lamp glass by using it in concrete production, where it can partly replace fine sand or cement and thus help create a new construction material. Using lamp glass powder (LGP) in concrete is an interesting possibility for economy on waste disposal sites and conservation of natural resources (Mageswari et al., 2010).

One of the main constituents of the reference concrete is cement. Every year approximately 2.35 billion tons of cement are produced — that is almost 1 m³ of cement for every person in the world. The carbon dioxide released into the atmosphere during the cement production process accounts for approximately 5-10% of the overall CO₂ production in the world. Its release into the atmosphere contributes to the global warming and the development of holes in the ozone layer. If the CO₂ production in cement factories could be decreased by 10%, the overall release into the atmosphere would decrease by 5.2%.

The use of waste glass and small clay particles in concrete production can make the construction industry more environmentally friendly.

MATERIALS AND METHODS

One of the goals of the experiment was to find out whether the new concrete composition can be competitive and whether its physical and mechanical properties are equivalent to those of the reference concrete. The object of this experimental study was concrete made with lamp glass powder (LGP) obtained from fluorescent lamp waste and concrete made with small clay particles (SCP) partially replacing cement. The other raw materials used for this study were natural coarse aggregate, fine aggregate and normal cement CEM I 42.5 N (Kunda).

The experiment consisted of replacing cement with lamp glass powder (LGP) in amounts of 0, 20 and 40 per cent and small clay particles (SCP) in amounts of 1 per cent of the total cement volume. Standard sample cubes of 100x100x100 mm were produced in order to investigate the mechanical characteristics of the material. Concrete mixtures were cast into oiled steel moulds and compacted at the vibrating table. After two days the moulds were removed. Standard hardening conditions (temperature +20 ± 2 °C, RH > 95%) were provided. After the hardening period, the specimens were measured and tested in standard conditions. Their compression strength was determined in conformity with LVS EN 12390-3:2002. A testing machine with accuracy +1% was used, and the rate of loading was 0.7 MPa/sec.

Creep experiments were carried out on prismatic 40x40x160 mm specimens that had been weighted both before and after the test.

The creep (time-dependent strain) was measured in hardened concrete specimens.

Consider a point in a concrete specimen subjected to a constant, sustained compressive stress σ_{c0} applied at time τ_0 and equal to 40 per cent of the characteristic compressive strength of concrete, i.e. $\sigma_{c0} = 0.4 f_c$. The load was applied gradually in 4 steps and as quickly as possible.

The instantaneous strain that occurs immediately upon application of the stress may be considered to be elastic at low stress levels, and therefore:

$$\varepsilon_{e(t)} = \sigma_{c0} / E_{c(\tau_0)} \quad (1)$$

where $E_{c(\tau_0)}$ is the elastic modulus at time τ_0 , $\varepsilon_{e(t)}$ is the instantaneous strain, σ_{c0} is the compressive stress.

The capacity of concrete to creep is usually measured in terms of the creep coefficient, $\square_{(t,\tau)}$. In a concrete specimen subjected to a constant sustained compressive stress, $\sigma_{c(\tau)}$, first applied at age τ , the creep coefficient at time t is the ratio of the creep strain to the instantaneous strain and is given by:

$$\square_{(t,\tau)} = \varepsilon_{cr(t,\tau)} / \varepsilon_{e(\tau)} \quad (2)$$

where $\square_{(t,\tau)}$ is the creep coefficient, $\varepsilon_{cr(t,\tau)}$ is the creep strain, $\varepsilon_{e(\tau)}$ is the instantaneous strain (Gilbert *et al.*, 2011).

At the beginning of the test, the specimens were 51 and 57 days old. They were kept under constant load for 90 days. The tests were conducted in two extreme conditions. In one case no moisture exchange with the environment was permitted, which was ensured by protecting the specimens against desiccation, and in the other case drying was permitted under conventional conditions, by protecting the specimens against moisture (Rilem TC 107-CSP, 1998).

In this paper these batches shall be called Reference (dry), Reference (moist), 20% LGP (dry), 20% LGP (moist), 40% LGP (dry), 40% LGP (moist), SCP (dry) and SCP (moist)". In order to prevent humidity exchange between the specimen and the environment, the surface of the specimens was coated with two protective silicone layers.



Figure 2. Specimens with aluminium plates.

Before this sealing, four steel plates were centrally and symmetrically glued onto two sides of the test prism in order to provide a basis for the strain gauges (see Fig. 2).

The distance between two plates was 50 mm. Two ± 0.01 mm precision strain gauges were symmetrically connected to each specimen, and then the specimens were put into a creep lever test stand and loaded (see Fig. 3).



Figure 3. Specimens in the creep lever test stand

They were kept in dry atmosphere of controlled relative humidity in standard conditions: temperature $23 \pm 1^\circ\text{C}$ and relative humidity $25 \pm 3\%$.

RESULTS AND DISCUSSION

Strength tests were carried out on the cubes after 7, 28, 42 and 58 days (see Table 1) of hardening in standard conditions. The various compression strengths of concrete specimens in different ages containing LGP and SCP were then compared to those of the reference concrete specimens.

Table 1

Compression strength of concrete compositions

Specimen	Age, days	Compression strength, MPa
Reference	7	55
Reference	28	63
Reference	58	71
20% LGP	7	42
20% LGP	28	60
20% LGP	58	70
40% LGP	7	32
40% LGP	28	55
40% LGP	58	65
Reference	7	59
Reference	42	40
SCP	7	89
SCP	42	60

The concrete containing a LGP showed lower strength in the first 7 days, but on the 28th and 58th day the strength increased and was very similar to that of the reference concrete. The specimens with

40% LGP showed 103% increase of the compression strength, while the specimens with 20% LGP showed 66% increase of the compression strength. The reference specimens, however, showed only 30% increase of the compression strength. Fine lamp glass powder caused a long-term hardening effect (see Fig. 4).

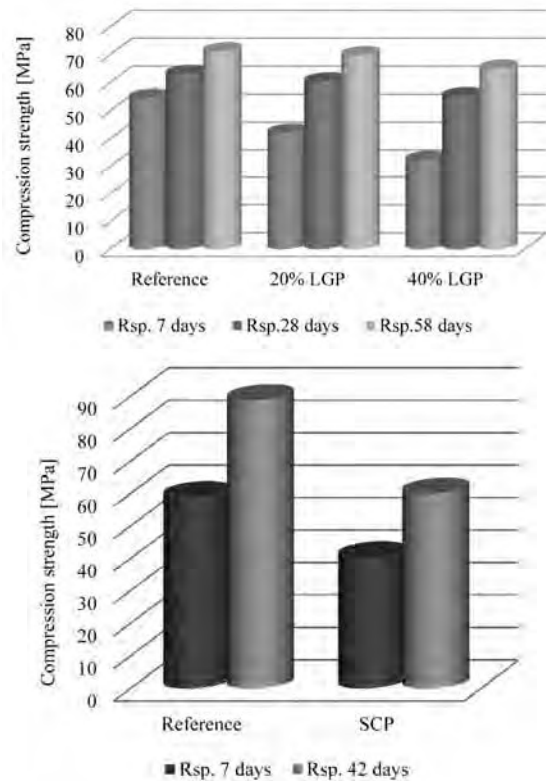


Figure 4. Compressive strength of new concrete mixtures at different ages [MPa].

In the first 7 days, the strength showed by concrete containing SCP was lower than the reference concrete strength by 31.4% and on the 42nd day the strength was lower by about 32.4%. The specimens with SCP showed 48.5% increase of the compression strength, but the reference specimens showed 50.8% increase of the compression strength (see Fig. 4).

The modulus of elasticity (see Fig. 5) was determined by measuring the deformations on the sides of the specimens according to Hooke's law. For the reference concrete the difference between the specimens hardened in moist and dry conditions is approximately 2.8%. For the specimens with 20% LGP this difference is approximately 12.4% and for the specimens with 40% LGP it is 27.4%. The comparison of the modulus of elasticity of the reference concrete specimens and the specimens with 40% LGP shows that for the specimens hardened in moist conditions this difference is 11.7%, while for the specimens hardened in dry conditions it is 32.6%.

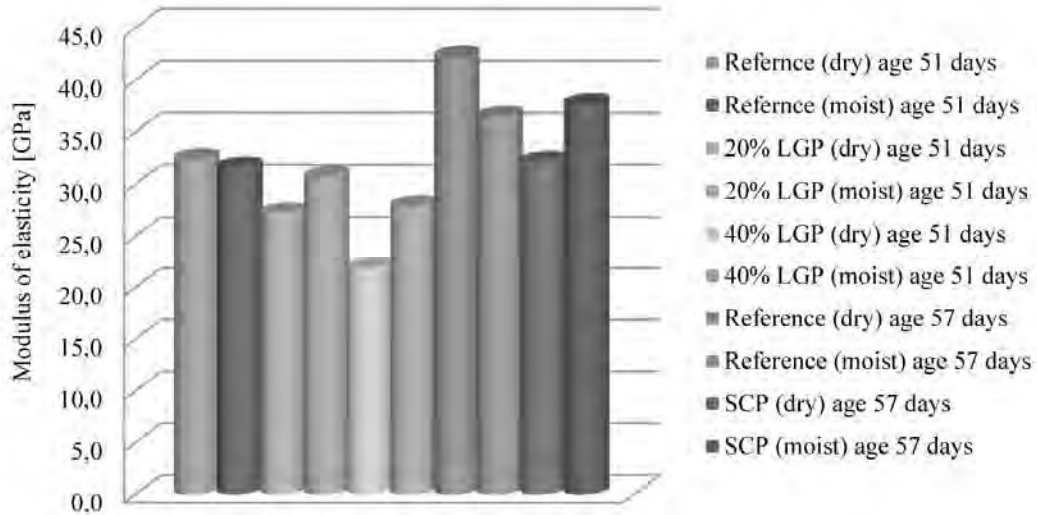


Figure 5. Elasticity modulus of different concrete.

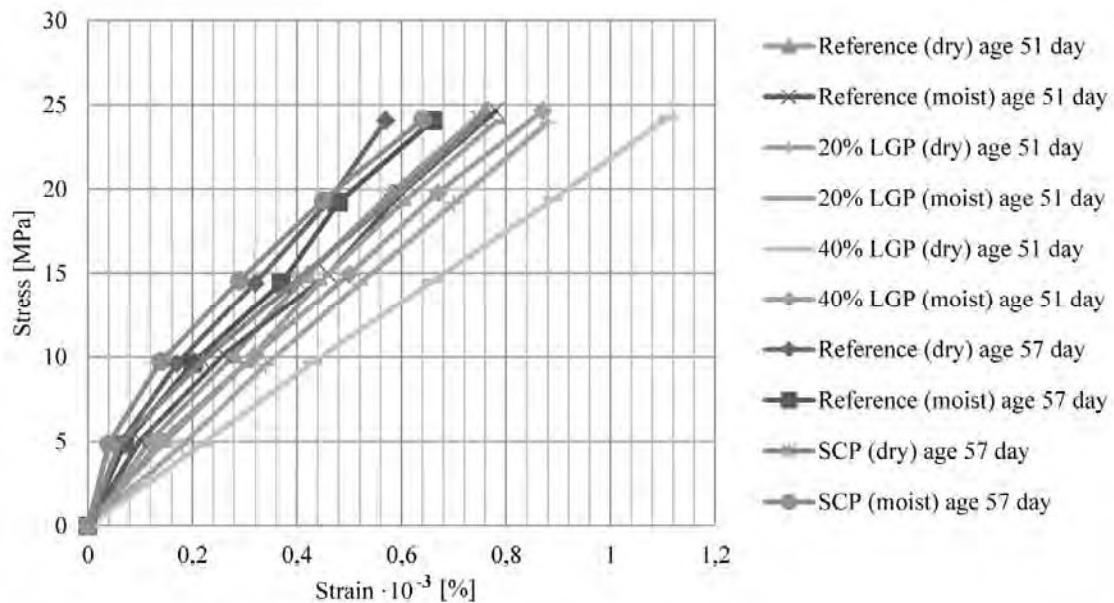


Figure 6. Relation between stress and strain..

The corresponding differences between the reference concrete specimens and the specimens with 20% LGP is 2.9% and 16.3% respectively. For the reference concrete and the specimens with SCP this difference between the specimens hardened in moist and dry conditions is approximately 17% and 16% respectively (see Fig. 5). The comparison of the modulus of elasticity of the reference concrete specimens and the specimens with SCP shows that for the specimens hardened in moist conditions this difference is 3.3%, while for the specimens hardened in dry conditions it is 24%. The same tendency can also be seen from the stress-strain relation (see Fig. 6). When concrete is subjected to a sustained stress, creep strain develops gradually in time as shown in Fig. 7. Creep increases with time at a decreasing

rate. In the period immediately after initial loading, creep develops rapidly, but with time the rate of the increase slows considerably. In a loaded specimen that is in hygral equilibrium with the ambient medium (i.e., no drying), the time-dependent deformation caused by stress is known as *basic creep* (Neville et al., 1983). The graph in Figure 7 shows elastic strain plus linear basic creep and shrinkage. From the gathered data it is evident that the smallest creep is exhibited by the concrete specimens with 40% LGP (dry). The average difference between basic creep of the reference concrete specimens hardened in moist and in dry conditions is approximately 47.4%. For the specimens with 20% LGP this difference is approximately 52.4% and for the specimens with 40% LGP it is 12%.

Table 2

Mechanical properties of concrete compositions

Specimen	Age, days	Modulus of elasticity, GPa	Elastic strain ϵ ($\cdot 10^{-3}$)	Basic creep ϵ ($\cdot 10^{-3}$)	Creep coefficient (90 days)
Reference	51	32,5 (dry)	0,8 (dry)	2,0 (dry)	2,7 (dry)
Reference	51	31,6 (moist)	0,8 (moist)	3,9 (moist)	5,0 (moist)
20% LGP	51	21,9 (dry)	0,9 (dry)	3,5 (dry)	4,0 (dry)
20% LGP	51	27,9 (moist)	0,8 (moist)	2,3 (moist)	2,9 (moist)
40% LGP	51	27,2 (dry)	1,1 (dry)	2,1 (dry)	2,8 (dry)
40% LGP	51	30,7 (moist)	0,9 (moist)	2,4 (moist)	2,8 (moist)
Reference	57	42,3 (dry)	0,6 (dry)	2,4 (dry)	4,2 (dry)
Reference	57	36,5 (moist)	0,7 (moist)	3,0 (moist)	4,6 (moist)
SCP	57	32,2 (dry)	0,8 (dry)	2,9 (dry)	3,9 (dry)
SCP	57	37,7 (moist)	0,6 (moist)	3,4 (moist)	5,3 (moist)

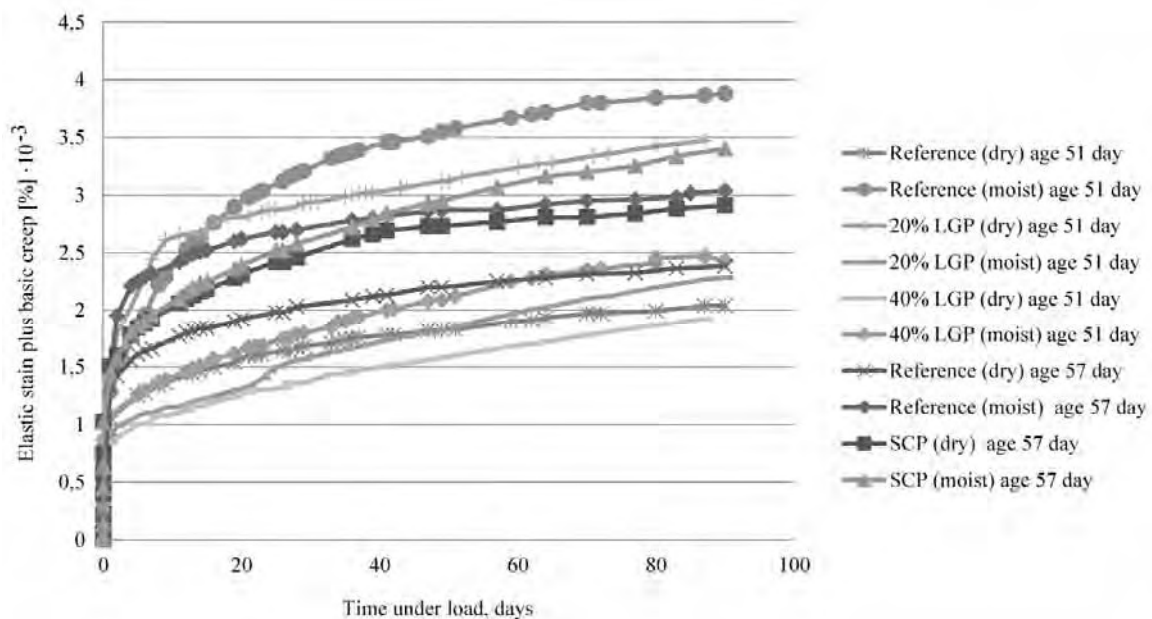


Figure 7. Elastic strain and basic creep of new concrete mixtures.

By comparing the average difference between the reference concrete specimens and the 20% LGP it can be seen that for the specimens hardened in moist conditions this difference is 41%, and for the specimens hardened in dry conditions it is 71%. In comparison with the 40% LGP specimens, the difference is 37.4% and 4.7% respectively. The results of the experiments are presented in Table 2. In the graph in Figure 7 it is evident that the smallest creep is exhibited by the reference concrete specimens in dry conditions. The average difference between basic creep of the reference concrete specimens hardened in moist and in dry conditions is approximately 21%. For the specimens containing SCP this difference is approximately 14.5%. By comparing the average difference between the reference concrete specimens and the SCP, it can be seen that for the

specimens hardened in moist conditions this difference is 12.8%, and for the specimens hardened in dry conditions it is 22%. The results of the experiments are presented in Table 2.

Under constant mechanical loading, the strain of the reference concrete increases significantly with the loading duration, the increase reaching 2.68 to 4.97 times the value of the instantaneous strain. The strain increase of the concrete specimens with 20% LGP reaches 2.93 to 3.95 times the value of the instantaneous strain and for the specimens with 40% LGP it reaches 2.79 to 2.84 times.

The strain of the reference concrete increases significantly, the increase reaching 4.15 to 4.61 times the value of the instantaneous strain, and for the specimens containing SCP it reaches 3.88 to 5.32 times. The creep coefficient increases with time at an ever-decreasing rate.

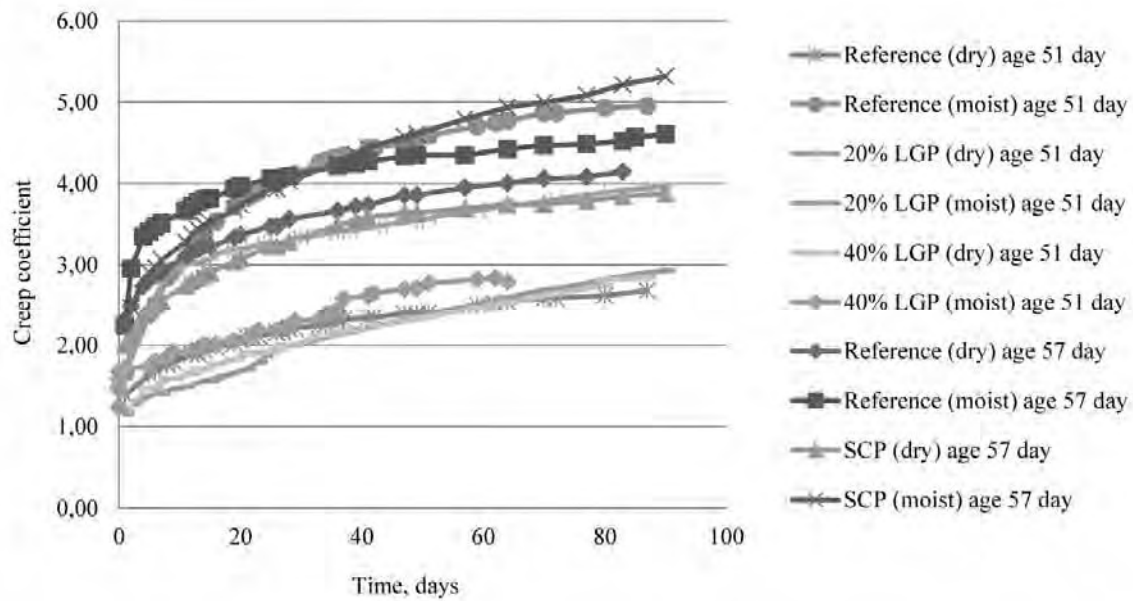


Figure 8. Creep coefficient of high strength concrete mixtures.

The final creep coefficient is a useful measure of the creeping capacity of concrete.

The graph in Figure 8 shows the increase of the creep coefficient in time. The comparison of the creep coefficients of the reference concrete specimens and 20% of LGP specimens shows that the creep coefficient for the reference concrete specimens in dry conditions is smaller, but for the reference specimens in moist conditions it is larger than for the specimens with 20% and 40% of LGP. The average difference between the reference concrete specimens in moist and in dry conditions is approximately 46%, but for the specimens containing 20% of LGP this difference is approximately 35%. For the specimens containing 40% of LGP this difference is approximately 2%. If we compare the average difference between the reference concrete specimens and the ones containing 20% of LGP we can see that for the specimens hardened in moist conditions this difference is 41%, and for the specimens hardened in dry conditions it is 47.4%, while for the specimens containing 40% of LGP this difference is 44% and 6% respectively. The comparison of the creep coefficients of the reference concrete specimens and SCP specimens shows that the creep coefficient of the specimens containing clay particles and hardened in dry conditions is larger but in the moist conditions the creep coefficients are larger than the reference concrete. The average difference between the reference concrete specimens in moist and in dry conditions is approximately 10%, but for the SCP specimens this difference is approximately 27%. If we compare the average difference between the reference concrete specimens and the ones containing SCP we can see that for the specimens

hardened in moist conditions this difference is 15.4%, and for the specimens hardened in dry conditions it is 6.5%.

CONCLUSIONS

This experimental study proves that lamp glass powder and small clay particles can be successfully used in the production of concrete, thus potentially decreasing the amount of deposited waste and the use of cement, which would lead to a reduction of carbon dioxide release into the atmosphere. In order to decrease the dispersion of the results, the number of specimens and tests should be increased.

In the future, the physical and mechanical properties of this new concrete containing lamp glass powder and small clay particles should be investigated in a more detailed way. The results of this experiment can be used to predict creep deformations.

Long-term deformations testing was carried out, and the modulus of elasticity, the compression strength of ordinary concrete and of concrete containing lamp glass powder and small clay particles were determined. The basic creep test results were summarized on the 90th day.

Lamp glass powder caused a long-term hardening effect. The specimens in which cement was partially replaced by lamp glass powder showed a larger increase of the compression strength than the reference concrete specimens, and the compression strength of 58 days old concrete specimens containing LGP was larger than that of the reference concrete specimens.

The reference concrete specimens and specimens containing SCP showed a similar increase of the compression strength at both ages.

The modulus of elasticity in dry conditions was

larger for the reference concrete specimens. For the specimens containing LGP the larger modulus of elasticity was achieved by hardening in moist conditions.

The modulus of elasticity in dry conditions was larger for the reference concrete specimens but in moist conditions the larger modulus of elasticity was for the specimens containing SCP.

Creep strain increases with time at a decreasing rate. In the period immediately after initial loading, creep develops rapidly, but with time the rate of increase

slows significantly. The concrete specimens cured in moist conditions showed larger increase of basic creep deformations.

Under constant mechanical loading, the strain of concrete increases significantly with the loading duration. The creep coefficient increases with time at an ever-decreasing rate. The final creep coefficient is a useful measure of the creep capacity of concrete. On the 90th day of testing the value of the basic creep coefficient reaches 2.68 to 5.32 times the value of the instantaneous strain.

ACKNOWLEDGEMENT

This work has been supported by the European Social Fund within the scope of the project "Support for the Implementation of Doctoral Studies at Riga Technical University".

REFERENCES

ACI Committee 209 (2008) *Guide for modeling and calculating shrinkage and creep in hardened concrete* (ACI 209.2R-8). Michigan: American Concrete Institute.

ACI Committee 209 (2005) *Report on factors affecting shrinkage and creep of hardened concrete* (ACI 209.1R-05). Michigan: American Concrete Institute.

Bazant, Z.P., Wittmann, F.H. (eds) (1983) *Creep and Shrinkage in Concrete Structures*. John Wiley and Sons Ltd.

Gilbert R.I., Ranzi G. (2011) *Time-Dependent Behaviour of Concrete Structures*. London and New York: Span Press, p.11, 25- 27,29,30.

Gilbert, R.I. (1988) *Time Effects in Concrete Structures*. Amsterdam: Elsevier Science Publishers.

Korjakins A., Shakhmenko G., Bumanis G. (2010) The Use of Borosilicate Glass Waste as Concrete Micro-Filler. *Proceeding of 2nd International Conference of Advanced Construction*, Kaunas, Lithuania, p. 129-134.

Mageswari M. and Vidivelli B. (2010) The Use of Sheet Glass Powder as Fine Aggregate Replacement in Concrete. *The Open Civil Engineering Journal*, 4, p. 65-71.

Neville, A.M. (1995) *Properties of Concrete*. 4th Edition. UK: Pearson Education Limited.

Neville, A.M. (1970) *Creep of Concrete: Plain, Reinforced and Prestressed*. Amsterdam: North Holland Publishing Co.

Neville, A.M., Dilger, W.H., Brooks, J.J. (1983) *Creep of Plain and Structural Concrete*. London and New York: Construction Press.

Rilem TC 107-CSP (1998): *Creep and shrinkage prediction models: principles of their formation*. Measurement of time-dependent strains of concrete. *Materials and Structure*, Vol. 31, p. 507-512.

Vandamme, M., Ulm, F.-J. (2009) Nanogranular origin of concrete creep. *Proceedings of the National Academy of Sciences*, Vol. 106, No. 26, p. 10552–10557.

Westman G. (1999) *Concrete creep and thermal stresses*. Doctoral thesis. Lulea, Sweden, p.7.

APPLICATION OF ALUMINIUM DROSS AND GLASS WASTE FOR PRODUCTION OF EXPANDED CLAY AGGREGATE

Diana Bajare, Aleksandrs Korjakins, Janis Kazjonovs

Riga Technical University, Faculty of Civil Engineering, Department of Building Materials and Construction, Institute of Materials and Structures,
diana.bajare@rtu.lv

ABSTRACT

This research provides possibilities to reuse solid waste from aluminium scrap recycling factories and municipal solid waste (MSW) container glass for the production of lightweight aggregates. The aluminium dross residue is increasing along with the increase in the aluminum production. Similarly the problem of container glass rational utilization is a topical problem over the world. The presented research is focused to solve problems concerning to both industrial and municipal waste collection.

The production of expanded clay aggregate was simulated in the laboratory with pilot rotary furnace and electric furnace. Expanded clay aggregate was produced with different glass waste: aluminium dross: clay mix ratios, where aluminium dross acted as an extra pore-forming agent and glass waste as a fluxing agent. Pore structure was abundant ranging from irregular to spherical, resulting in low apparent density values, which directly was affected with the firing temperature up to 1200 °C and time, controlled with the rotation velocity and furnace incline.

The main objectives of this experimental study are to examine the effects of aluminium dross and glass waste addition to the physical and microstructure properties of expanded clay aggregate sintered on a laboratory scale.

Key words: expanded clay aggregate, glass waste, aluminium dross

INTRODUCTION

Expanded clay aggregates (ECA) occur in nature (pumice, volcanic tuffs, etc.) or they can be industrially manufactured. For their production two mechanisms are necessary to occur simultaneously during firing (Ehlers, 1958): first, the development of a highly viscous glassy phase, able to entrap the formed gases, and second, the production of gases. At this temperature, the material is in pyroplastic condition and the gases do not escape readily, allowing the aggregate to expand. The result is a cellular structure comprised of pores distributed within the mass.

The consumption of aluminium recycling waste has been rising continuously worldwide, which is great stimulus for developing a non-waste technology (Shinzato and Hypolito 2005; Shen and Forsberg 2003; Lucheva et al. 2005). Aluminium dross represents residue from primary and secondary aluminium production. Drosses are classified according to the aluminium metal content into white and black dross. White dross has a higher metal aluminium content and it is produced from primary and secondary aluminium smelters, whereas black dross has a lower metal content and is generated during aluminium recycling (secondary industry sector). Black dross typically contains a mixture of aluminium oxides and slag with recoverable aluminium content ranging between 12–18% (Gil, 2005; Shen and Forsberg, 2003; Lucheva et al., 2005). The conventional rotary furnaces heated with

a fuel or a gas burner are used to recover the extra aluminium from black or white dross. This treatment process produces the non-metal product called aluminium recycling waste containing alumina, salts, impurities and a little amount (3–5%) of metallic aluminium. There have been previous research studies which investigate the use of aluminium recycling waste (non-metal product NMP) generated from dross processing (Bajare et al., 2008; 2010; Bajare and Korjakins, 2009). NMP was used as a pore formatting agent. It was concluded that NMP is suitable for production of ECA with the density from 0.4 to 0.7 g/m³. The density of ECA noticeable depends on two factors: the amount of added aluminium recycling waste and sintering temperature.

A major component in municipal solid waste (MSW) is container glass, even though it is relatively easy to separate (Karamberi and Moutsatsou, 2005). Glass is included in the EU Thematic Strategy on the Prevention and Recycling of Waste rates set for the Member States. By 2020, 50% by weight of glass will have to be recycled in Latvia. In 2007 the rate was 34.5% (EUROPA, 2007).

Glass has been successfully used as a binder and fluxing agent in ceramics and bricks, as it lowers the softening temperature, firing time and energy consumption (Barbieri et al., 1997, 2000; Nagaraj and Ishikawa, 1999; Ducman et al., 2002; Karamberi and Moutsatsou, 2005).

The main objective of this experimental study is to examine the effects of the waste glass usage as a fluxing agent which lowers the sintering temperature on the physical and microstructural properties of ECA.

MATERIALS AND METHODS

In the current study, ECA were produced from clays with high content of carbonates, aluminium dross and glass waste in different compositions.

Clay

The clay used in the experiments is a natural raw material. It is plastic clay composed of quartz, calcite, dolomite, illite, kaolinite and anorthoclase, according to the X-ray diffraction (XRD) analysis. Dolomite, as a mineral, has been determined in the average proportion of 21.6 % in the clay composition. The chemical composition of clay is given in Table 1. According to the analysis, the clay used in the experimental studies is typical carbonate clay.

Aluminium dross (NMP)

According to the element analysis resulted from inductive coupled plasma optical spectrometry (ICP-OES), atomic absorption spectroscopy (AAS) and potentiometer titration analyses, the NMP contains: aluminium (Al) – 34.4%, silicon (Si) – 4.4% magnesium (Mg) – 2.4%, calcium (Ca) – 1.32%, sodium (Na) – 1.69%, potassium (K) – 2.31%, sulphur (S) – 0.07%, chlorine (Cl) – 4.23, ferric (Fe) – 3.6%, copper (Cu) – 0.99%, zinc (Zn) – 0.6%.

These data correspond to the chemical composition of aluminium recycling waste, which is given in Table 1. From the point of the chemical composition the analyzed wastes contain also aluminium nitride (AlN) - on average 5%, aluminium chloride – (AlCl₃) - on average 3%, potassium and sodium chloride (KCl +NaCl) – totally 5% and ferric sulphide (FeSO₃) - on average 1%.

The mineralogical composition of the NMP is determined by using the XRD analysis. According to the analysis data, the NMP contains corundum (Al₂O₃), silica (SiO₂), ferric sulphite (FeSO₃), aluminium chloride (AlCl₃), calcium ferric oxide (Ca(FeO₃)), calcium, magnesium or ferric carbonate (Ca(Mg,Fe)(CO₃)₂), gibbsite (Al(OH)₃), spinel (FeAl₂O₄) or (MgAl₂O₄) and aluminium nitride (AlN).

Waste glass

Waste glass derived from bottles and window glass was crushed and ground to a fineness of less than 100 µm. Its chemical composition is given in Table 1.

Table 1
Basic chemical composition of clay and NPM and waste glass (amount %)

	Clay	NMP	Waste glass
Al ₂ O ₃	14.34	63.19	1-3
SiO ₂	50.22	7.92	70-74
CaO	8.54	2.57	5-11
SO ₃	0.07	0.36	-
TiO ₂	0.56	0.53	-
Na ₂ O	0.43	3.84	12-16
K ₂ O	3.09	3.81	-
MgO	3.07	4.43	1-3
Fe ₂ O ₃	5.74	4.54	-

It is clear from the chemical analysis that this waste consists of high amounts of fluxing oxides such as Na₂O and CaO.

Preparation and synthesis of lightweight expanded clay aggregates (ECA)

Clay was mixed with NMP and glass waste in different ratios. The glass waste mass ratio in the composition was from 5-14%, NMP mass ratio was 14-35%. The raw materials were ground and mixed together in the planetary ball mills. The average particle size of the mixes was 54 µm. Plastic mass was prepared by adding 20–25% water and rounded by shaping operation. The prepared aggregates were dried in an oven at 105°C to avoid reaction between aluminium recycling waste and water used for preparation of the plastic mass. Green aggregates were treated at sintering temperatures from 1110 to 1250°C in an electrical furnace. The rate of temperature increase in the furnace was kept constant as 15°C/min. The gasiform substances and new minerals from NMP like spinel and alumina are originated during the heat treatment process of NMP. The phenomena of origination of gasiform substances during the heat treatment of NMP should be used as a pore creator for obtaining a porous structure of lightweight ceramic aggregates (ECA). As the hazardous compounds of NMP are transformed into new ones, non-hazardous compounds, NMP does not have the toxic nature anymore and it becomes environmental friendly and it can be a constituent part of a new, environmental friendly material (Bajare et al., 2009). Meanwhile, waste glass is used as a fluxing agent lowering the sintering temperature. After production the physical property, like water absorption after 24 h, open porosity and bulk density tests were conducted on the aggregate samples. The microstructure of the lightweight aggregates produced at different temperatures was observed by an optical microscope.

RESULTS AND DISCUSSION

The physical properties of ECA granules produced in the present study are shown in Table 2. According to the test results, the sintering temperature decreased with the increase in the

waste glass amount in the composition.

One of the most important properties of ECA granules is the bulk density which in this present study is between 0,465 and 1,090 g/cm³.

Table 2.

Physical properties of ECA sintered at different temperatures

Composition ratio (waste glass:NMP: clay)	Sintering temperature (°C)	Bulk density (g/cm ³)	Water absorption (%)	Open porosity (%)
0:2:10	1160	0,47	4,0	1,9
0:4:10	1230	0,50	14,0	7,0
0:6:10	1260	0,76	12,0	9,2
1:2:10	1130	0,57	2,4	1,4
	1140	0,59	2,7	1,6
	1150	0,59	2,4	1,4
1:4:10	1170	0,90	6,5	5,9
	1180	0,68	6,4	4,4
	1190	0,58	5,7	3,3
1:6:10	1230	0,71	11,5	8,2
	1240	0,56	10,5	5,8
	1250	0,54	9,2	4,9
2:2:10	1110	0,49	4,0	2,0
	1120	0,51	3,0	1,5
	1130	0,49	3,8	1,9
2:4:10	1120	0,64	6,3	4,0
	1130	0,53	5,7	3,0
	1140	0,46	3,0	1,4
2:6:10	1170	1,09	5,5	6,0
	1180	1,01	5,5	5,6
	1190	0,70	5,6	3,9

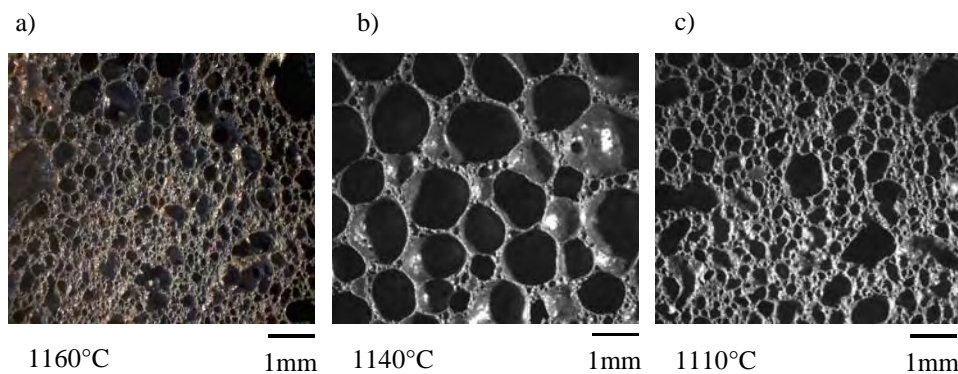


Figure 1. Pore structure of aggregates sintered at different temperatures:

- a) Composition 0:2:10 sintered at 1160°C
- b) Composition 1:2:10 sintered at 1140°C
- c) Composition 2:2:10 sintered at 1110°C

It is clear that in the same temperature and the same NMP and clay content in the composition the lowest density is for the aggregate where the waste glass amount is higher.

Waste glass reacts as a fluxing agent and melts earlier and makes the aggregate structure softer allowing the gases to expand and develop a larger pore structure.

The surface properties of the aggregates are important for water absorption and open porosity. The results show a trend that the added glass waste lowers the water absorption and open porosity. Additional glass creates a compact and homogenous outer glassy film that makes them impervious to water. It is seen that the lowest open porosity 1,4-1,6% and water absorption 2,4-2,7% is for the composition 1:2:10 (glass waste:NMP:clay).

It is clear that the pore structure and surface properties of the aggregates are significantly affected by NMP.

The pore structures and surface textures of some aggregates composition of 2 mass ratio of NMP addition are illustrated in Fig. 1. It is seen that the sintering temperature decreases for 50°C compared to the reference composition 0:2:10 sintered at 1160°C and the 2:2:10 sintered at 1110°C.

Both compositions have a similar bulk density 0,47 and 0,49 g/cm³, respectively, water absorption 4% and open porosity 1,9 and 2,0%, respectively.

The data in Table 1 show that for 2:2:10 in sintering range from 1110°C to 1130°C, the physical properties are similar; bulk density from 0,49 to 0,51 g/cm³, water absorption from 3,8 to 4,0% and open porosity from 1,5 to 2,0%. For 1:2:10 composition the sintering temperature in the range from 1130 to 1150°C seems to be too high, because there are melting signs, which result in large pore structure and increased bulk density (0,57 to 0,59 g/cm³).

The pore structures and surface textures of some aggregates composition of 4 mass ratio of NMP addition are illustrated in Fig. 2. The more NMP in the composition, the higher the sintering temperature is (Bajare et al., 2010). These structure photos present a slight increase in the pore size and a decrease in the sintering temperature, bulk density, water absorption and open porosity. The decrease in the sintering temperature compared to 0:4:10 and 2:4:10 compositions is 90°C and the decrease for the bulk density is from 0,5 to 0,46 g/cm³.

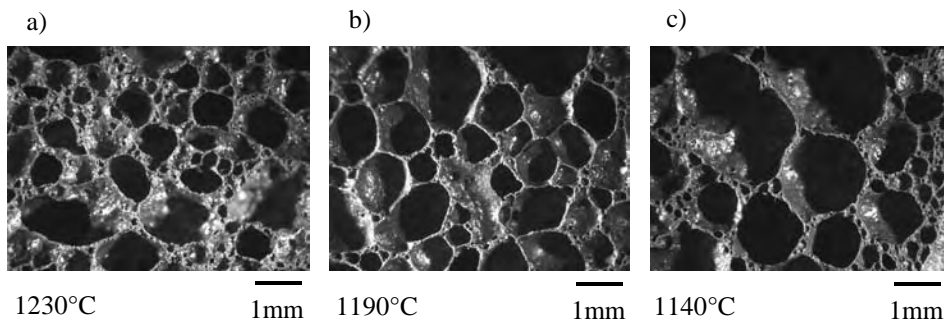


Figure 2. Pore structure of aggregates sintered at different temperatures

- a) Composition 0:4:10 sintered at 1230°C
- b) Composition 1:4:10 sintered at 1190°C
- c) Composition 2:4:10 sintered at 1140°C

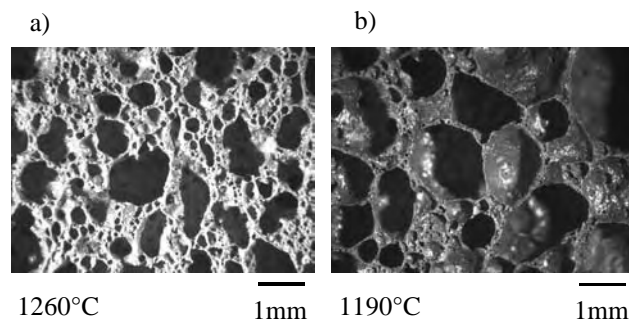


Figure 3. Pore structure of aggregates sintered at different temperatures

- a) Composition 0:6:10 sintered at 1260°C
- b) Composition 2:6:10 sintered at 1190°C

From the data in Table 1 it can be seen that for 1:4:10 sintered at 1180°C and 2:4:10 sintered at 1120°C the physical properties are similar; the bulk density from 0,64 to 0,68 g/cm³, water absorption from 6,3 to 6,4% and open porosity from 4,0 to 4,4%, resulting in 60°C decrease in the sintering temperature. A similar situation is for compositions 1:4:10 sintered at 1190°C and 2:4:10 sintered at 1130, resulting also in 60°C decrease.

The pore structures and surface textures of some aggregates composition of 6 mass ratio of NMP addition are illustrated in Fig. 3. 0:6:10 and 2:6:10 compositions have a similar bulk density of 0,76 and 0,70g/cm³, but a different pore structure with more voids. That might be explained by higher density of NMP than clay. The values of water

absorption and open porosity decreased from 12 to 5,6% and 9,2 to 3,9%, respectively.

CONCLUSIONS

It was feasible to produce ECA from clay, NMP and waste glass with the characterized properties. Waste glass acted as a fluxing agent and lowered the sintering temperature, consuming a smaller amount of energy in the production process. The sintering temperature of ECA can be lowered for up to 60°C remaining the same pore structure and physical properties.

With increasing the sintering temperature the material is more effectively sintered but with a bubbled microstructure containing larger voids.

REFERENCES

- Bajare D., Berzina - Cimdina L., Stunda A., Rozenstrauha I., Korjakins A. (2008) Characterisation and application of the mix of oxides from secondary aluminium industry. *2nd International congress on ceramics (ICC2)*, Verona, Italy, 7 p.
- Bajare D., Korjakins A. (2009) Production of Porous Building Ceramic by Using Waste from the Aluminium Scrap Recycling Factories. *17. Internationale Baustofftagung IBAUSIL : Tagungsbericht*, Vol. 2, p. 1175-1180.
- Bajare D., Korjakins A., Zakutajevs M., Voronenko F. (2010) Applying of aluminium scrap recycling waste (Non-Metal Product, NMP) for production environmental friendly building materials. *The 10th International Conference Modern Building Materials, Structures and Techniques*, p. 13-17.
- Barbieri L., Corradi A, Lancellotti I. (2000) Bulk and sintered glass-ceramics by recycling municipal incinerator bottom ash. *Journal of the European Ceramic Society*, No. 20, p. 1637-1643.
- Barbieri L, Manfredini T, Queralt I, Rincon JM, Romero M. (1997) Vitrification of fly ash from thermal power stations. *Glass Technology*, No. 38, p. 165-170.
- Ducman V, Mladenovic A, Suput JS. (2002) Lightweight aggregate based on waste glass and its alkali-silica reactivity. *Cement and Concrete Research*, No. 32, p. 223-226.
- Ehlers E. G. (1958) The mechanism of lightweight aggregate formation. *Am. Ceram. Soc. Bull.*, p. 95-99.
- EUROPA. (2007) *Packaging and packaging waste*. Available: <http://ec.europa.eu/environment/waste/packaging/data.htm>
- Karamberi A, Moutsatsou A. (2005) Participation of coloured glass cullet in cementitious materials. *Cement and Concrete Composites*, No. 27, p. 319-327.
- Lucheva B., Tsonev Ts., Petkov R. (2005) Non-waste Aluminium Dross Recycling. *Journal of the University of Chemical Technology and Metallurgy*, Vol. 40, No.4, p. 335-338.
- Nagaraj TS, Ishikawa T. (1999) Structural lightweight concretes with fly ash pelletized coarse aggregate-mix proportioning. *Exploiting wastes in concrete: Proceedings of the international seminar held at the University of Dundee*. London, United Kingdom: Thomas Telford Publishing.
- Shen H., Forssberg E. (2003) An overview of recovery of metals from slags. *Waste Management*, No. 23. p. 933-949.
- Shinzato M.C., Hypolito R. (2005) Solid Waste from Aluminium Resycling Process, Characterization and reuse of its Economically valuable Constituents. *Waste Management*, No. 25, p. 37-46.

RESEARCH OF HEMP FIBROUS REINFORCEMENT EFFECT TO BENDING STRENGTH AND SOUND ABSORPTION OF FOAM GYPSUM

Raitis Brencis, Juris Skujans, Uldis Iljins*, Ilmars Preikss

Latvia University of Agriculture, Faculty of Rural Engineering,

Latvia University of Agriculture, *Faculty of Information Technologies

raitis.brencis@llu.lv, juris.skujans@llu.lv, uldis.iljins@llu.lv, ilmars.preikss@gmail.com

ABSTRACT

Natural resources have been widely used for production of building materials in many countries in the entire world. Use of local minerals, such as materials on foam gypsum basis, in construction material production and usage in sound and heat isolation in building structures, is a significant benefit in national economy. The current research in foam gypsum shows that such possibilities exist (Skujans et al., 2010). Varying at the process of manufacturing with the ratio of gypsum and water, as well as the volume of the surface active stuff, foam gypsum of different volume density can be obtained but it has to be noted that the low bending strength of foam gypsum is a disadvantage. Material modification with fibrous reinforcement (hemp reinforcement) can serve as improvement of foam gypsum bending strength but it depends on the measure and amount of hemp reinforcement. Shorter fibers of hems increase the material strength but longer fibers increase the sound absorption coefficient. Both fiber types have an impact on the pore structure of foam gypsum as it is on foam gypsum without fibrous reinforcement manufactured with the same technology.

Key words: foam gypsum, hemp reinforcement, pore structure.

INTRODUCTION

The authors research in the qualities of foam gypsum and hemp reinforcement and its usage as a heat and sound isolation material in building structures. Hems as a building material are used in lot of building structures in Europe countries (Allin, 2005; Kymalainen et al., 2008). Fibrous plants are relatively widely used in building, production of industrial products, in vehicle production sphere, agriculture and others. Special attention is paid to the use of fibrous hemp in various sectors of the national economy. The research in this topic is developed in Germany, France, Great Britain (Ulme and Freivalde, 2009).

Hemps as fibers have been used (Madsen et al., 2007) in a lot of composite materials, for example, in composition with lime and mortar (Elfordy et al., 2008). At present the usage of various fibrous plants in foam gypsum production, as well as the production costs and ecological efficiency have not been evaluated. Hems as heat insulation are similar with rock wool (Timber... 2010) and hemp fibers increase the bending strength and sound absorption of foam gypsum (Brencis, 2011).

The foam gypsum pore structure has influence on the material volume density and its physical and mechanical properties (Skujans et al., 2010). The hemp reinforcement influence on the foam gypsum pore structure has not been investigated. The purpose of the research is to develop the technology of production of new energy resources saving the composite building material – foam gypsum with fibrous hemp reinforcement, as well as research in

the mechanical and sound absorption qualities of this material. The research coincides with the EU objectives of environment protection and is directed to construction of ecological dwelling houses in the future.

MATERIALS AND METHODS

Production technology of the foam gypsum sample

The foam gypsum was produced using the dry mineralization method (Skujans et al., 2007), mixing water, gypsum, surface active stuff (SAS), and adding hemp reinforcement. The concentration of hemp fiber is the amount of fiber in grams per 1 kg dry gypsum raw material (c, g/kg). The hemp fiber concentration was varied within the limits of 15÷50 g/kg.

Fibers of two lengths were used in sample production, and they were added to the foam gypsum during its production process. The fibers were prepared by chopping and sifting in order to get two different lengths - 2.5÷5.0 mm (hereinafter – short fibers) and with the length 5÷10 mm (hereinafter – long fibers).

Beams of size 40x40x160 mm were produced from the foam gypsum, which were further used for testing the bending and pressure resistance, by pressing the material to the utter rupture. The foam gypsum beams were processed using a round shape knife, and a cylinder type sample with Ø 40 mm and the length 160 mm was produced for tests in acoustic tube.

Methodology of the foam gypsum sound absorption properties

The sound absorption measurements were carried out using the company “Sinus” produced impedance tube (Fig. 1). With the tube it was possible to measure the sound absorption coefficient in the range of frequencies from 250 Hz up to 4000 Hz, when the sound reflects from the sample. The impedance tube has two different diameters Ø100 mm and Ø40 mm. In the tube part of Ø100 mm the sound source was placed, but in the part of Ø40 mm, two measure-microphones and a sample of Ø40 mm, to be measured, were located.

$$\alpha = \frac{I_{abs}}{I_{fal}} \quad (1)$$

where I_{abs} – intensity of absorbed sound;
 I_{fal} – sound intensity falling on the sample.

For all range of frequencies the mean value of the absorption coefficient was determined according to the standard (EN ISO 11654:1997).

Research methodology of the foam gypsum bending and pressure resistance

The research in the bending and pressure resistance of the composite material (foam gypsum + hemp fiber) was carried out by the device Zwick Roell 2.5 TS (Fig. 2.).

Investigation methodology of foam gypsum pores

The structure of pores was investigated by the digital microscope VNX-100. Before the investigation of the pores under the microscope, the samples have been grinded with following cleaning of the surfaces from the dust.

The measurements of the pores for each of the samples were done in five places with 50 times magnification. The disposition of the spots of the measurements made a cross on the sample surface. In each of 5 positions the picture, seen in the object-glass, has been divided in 1x1 mm squares. From this three regions were chosen. Each sample at 15 reiterations was measured. The pores making the porous structure of the samples do not have ideally round shape.

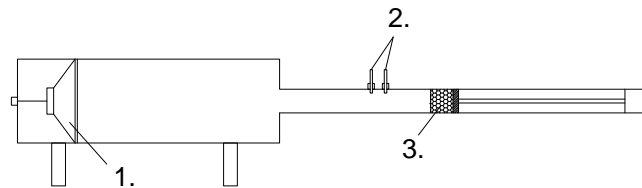


Figure 1. Device produced by the company “Sinus” for measuring sound absorption: 1-sound source, 2-measuring microphones, 3-measurable sample.

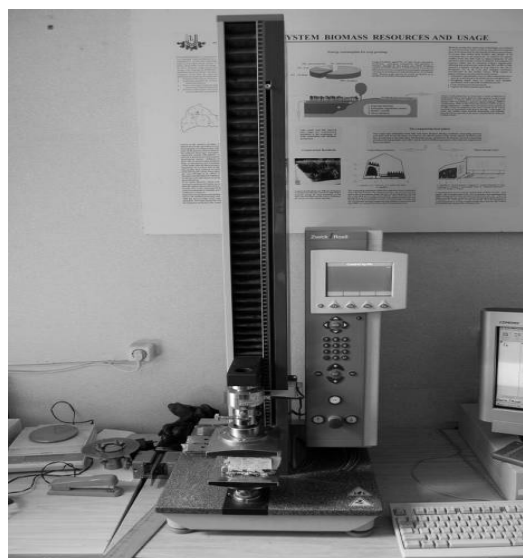


Figure 2. Company „Zwick” device for testing bending and pressure resistance.

Therefore, the area of pores per 1 mm² instead of its diameter has been determined. A large amount of pores are linked with adjacent ones. The cross-sectional area of these joint pores is distinctive for different samples and depends on its volume density, amount of the surface active stuff, added during the production process of the sample, as well as other reasons related with the technology used in production of foam gypsum.

RESULTS AND DISCUSSION

Varying at the process of manufacturing with the gypsum - water ratio, as well as the volume of the surface active stuff (SAS) and concentration of hemp fibers, samples of volume density from 380 kg/m³ to 1000 kg/m³ have been obtained. In further investigations samples with the volume density range from 380 kg/m³ to 500 kg/m³ were chosen. It

was found that the sound absorption coefficient (α) increases with decrease of the volume density of the foam gypsum (Skujans et al., 2010). This tendency was observed also when the foam gypsum was modified with hemp reinforcement. It is possible to obtain a better sound absorption coefficient of the material at equal foam gypsum volume density (Fig. 3). By increasing the short fiber concentration in the foam gypsum, its volume density value increases, but this coherence is in the opposite when producing foam gypsum with long fiber reinforcement (Fig. 4). Fig. 5 reflects the dependence of the bending stresses of the samples with long and short fibers. Increasing of the short fiber concentration, the bending stresses prevalently increase. By increasing the concentration of long fibers, the bending stresses decrease.

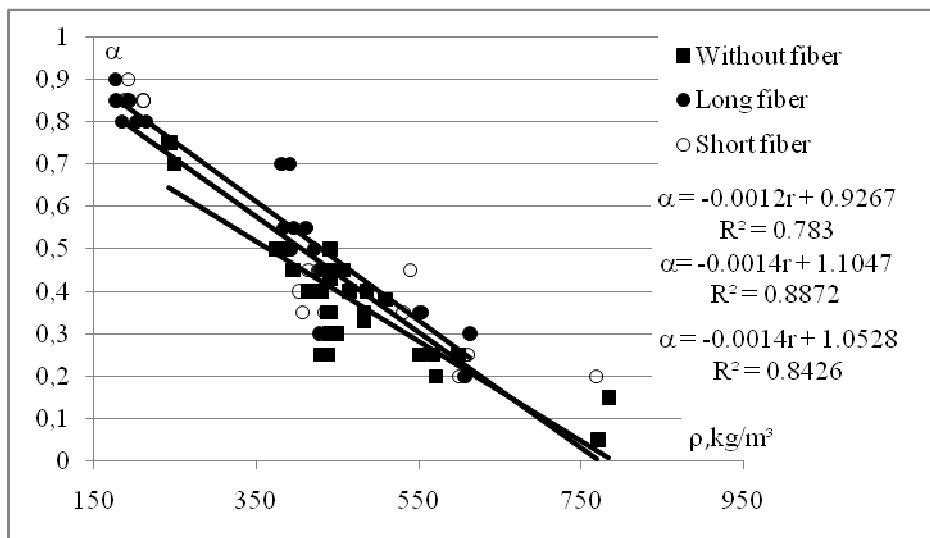


Figure 3. Value of sound absorption depending on volume density (Brencis, 2011).

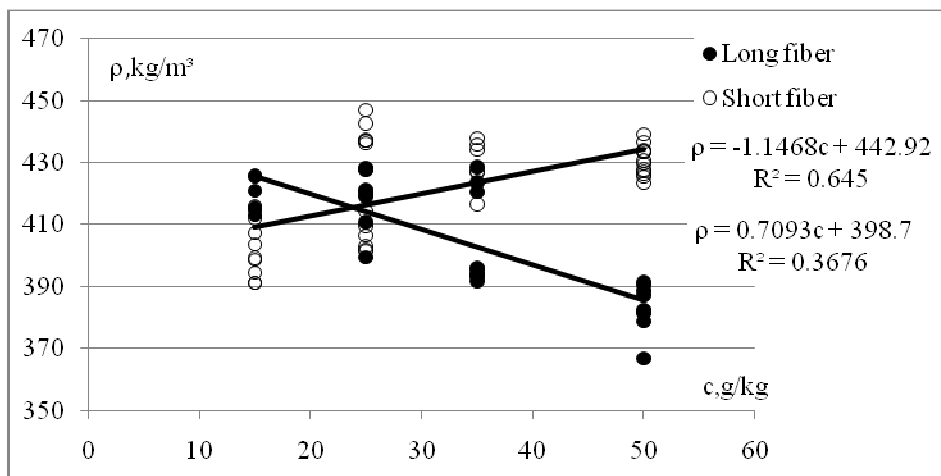


Figure 4. Volume density of composite material depending on short and long fibers (Brencis, 2011).

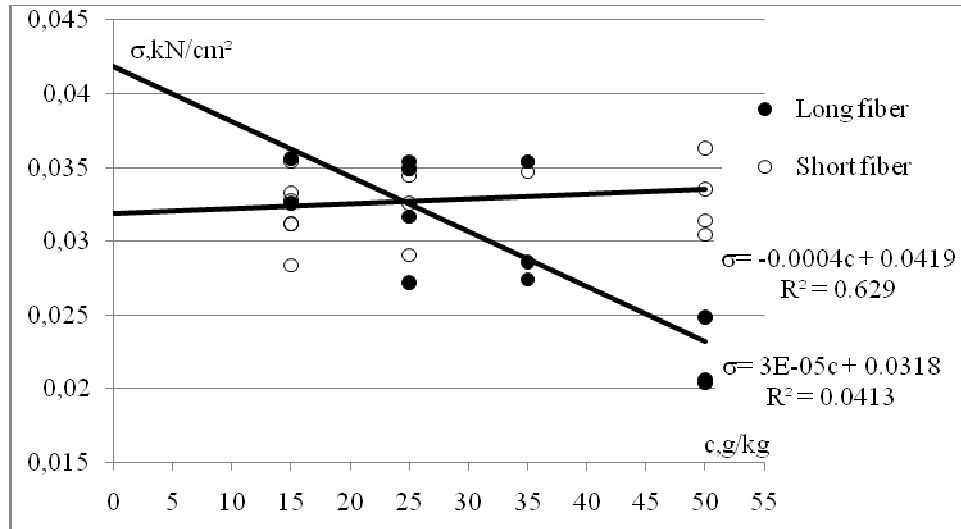


Figure 5. Value of bending stresses in composite material depending on concentration of long and short fibers (Brencis, 2011).

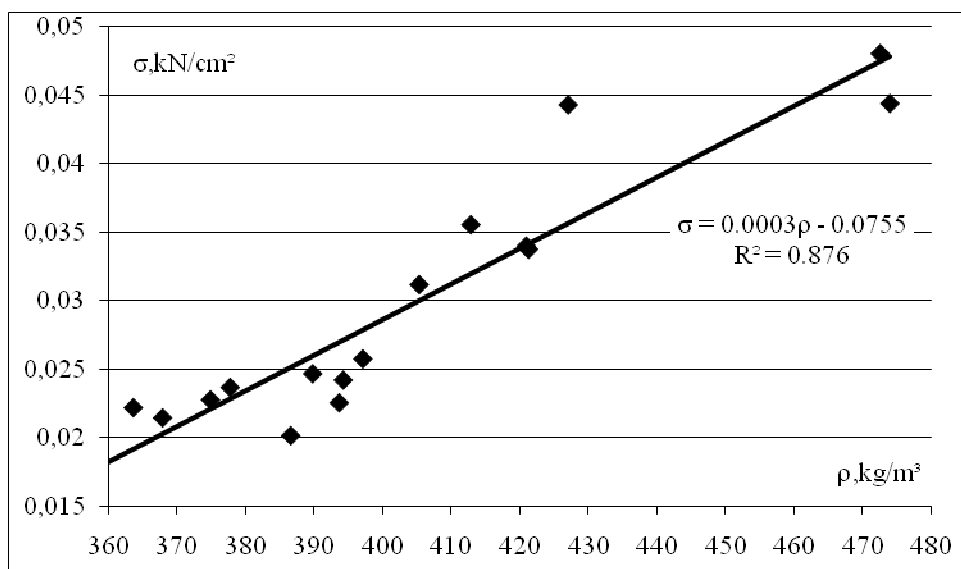


Figure 6. Value of bending stresses in foam gypsum without fibers depending on its volume density.

This coherence correlates with the volume density influence on the material strength (Fig. 4), where increasing the short fibers concentration, the volume density increases, but for the foam gypsum with long fibers, the volume density value decreases.

The values of the bending resistance of foam gypsum without fibers are shown in Fig. 6. The volume density of foam gypsum increase correlates with the bending resistance. In the volume density range between 360 - 450 kg/m^3 the bending

resistance is 0.02-0.045 kN/cm^2 .

Fig. 7 shows the porous structure of foam gypsum with hemp reinforcement. Pores have not ideal round shape and some of them are linked with the adjacent ones. Around the hemp reinforcement the amount of pores is higher. In foam gypsum modified with hems the amount of pores decreases (Fig. 8), but the fiber influence on the pores is not so relevant (Fig. 9). Joint pores and normal pores have the same inherence with different concentration of hemp fibers.

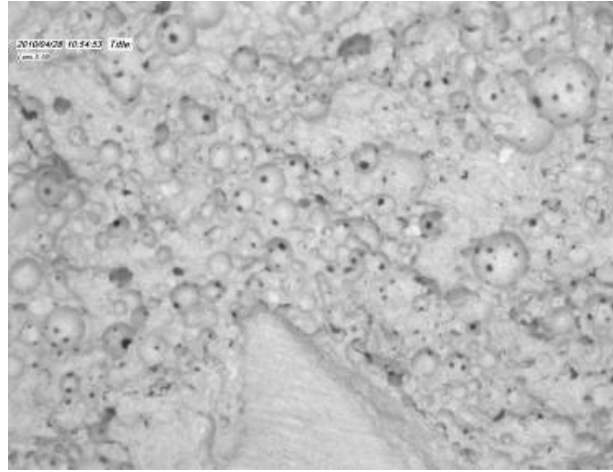


Figure 7. Foam gypsum porous structure with hemp reinforcement at 50 times magnification.

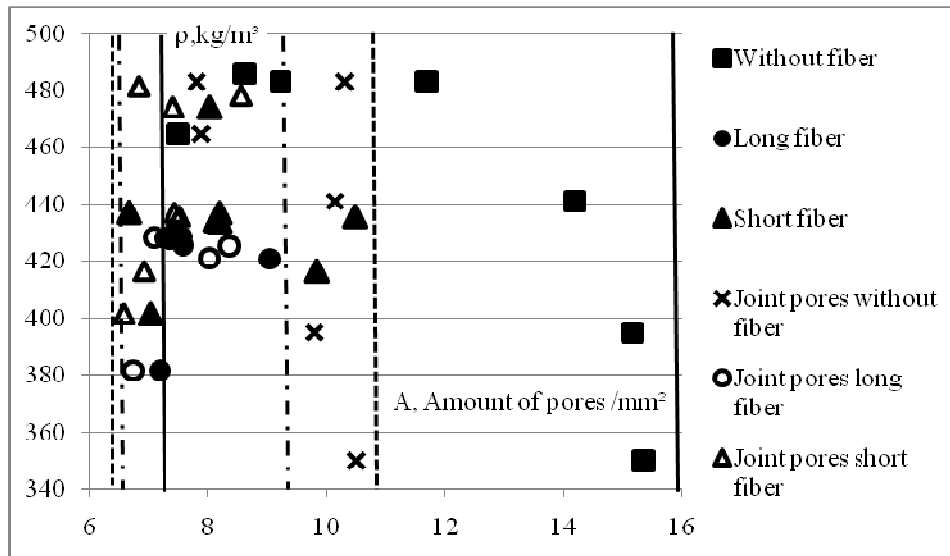


Figure 8. Volume density of reinforced foam gypsum depending on amount of pores in 1mm².

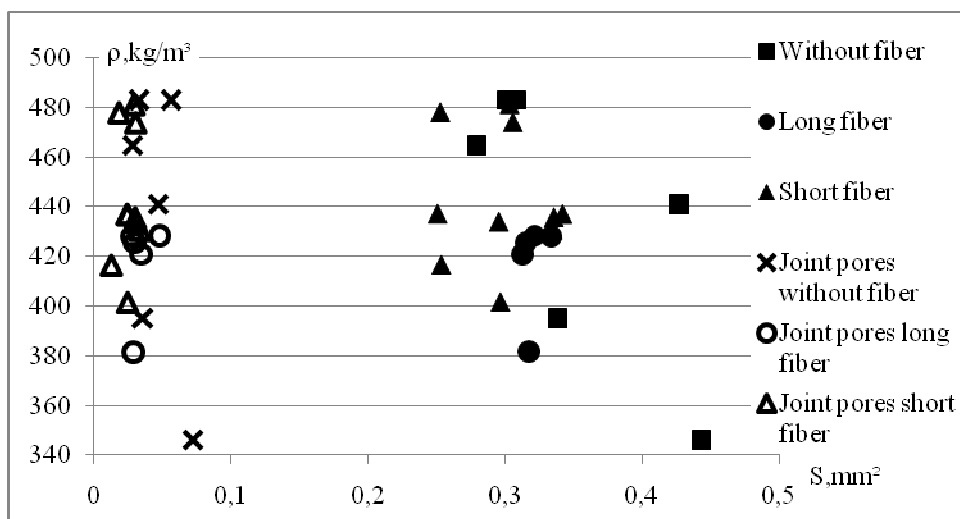


Figure 9. Volume density of reinforced foam gypsum depending on pore area in 1mm².

CONCLUSIONS

1. The results of the reported research demonstrate that hemp fiber reinforcement is affecting the macrostructure and bending strength, as well as the sound absorption characteristics of foam gypsum.
2. Applying of long hemp fibers of the length 5...10 mm and short fibers (2,5...5,0 mm) as reinforcement of foam gypsum, the amount of the pores of 1 mm² is decreasing but their size is increasing. The volume density of the material remains the same as the hemp fibres are substituting the volume of the pores..
3. Hemp reinforcement increases the sound absorption coefficient of foam gypsum in the range of the volume density form 340 to 500 kg per m³.
4. Increasing of the concentration of short fibers increases the volume density of foam gypsum, but increasing of the concentration of long fibers very opposite – decreases the volume density. Alteration of the volume density in its turn determines the bending resistance of foam gypsum.

ACKNOWLEDGEMENTS

The work was supported by European Social Fund project „Realization assistance of LLU doctoral studies”. Contract No. 2009/0180/1DP/1.1.2.1.2/09/IPIA/VIAA/017 and ERAF Project No. 2010/0320/2DP/2.1.1.1.0/APIA/VIAA/107.

REFERENCES

- Allin S. (2005) *Building with Hemp.*, Ireland: Seed Press Rusheens, Kenmare, Co. Kerry. 192 p.
- Brencis, R., Skujans, J., Iljins, U., Ziemelis, I., Osits, N. (2011) Research on foam gypsum with hemp fibrous reinforcement. *Chemical Engineering Transactions*, No. 25, p. 159-164.
- Kymalainen H.R., Sjoberg A.M. (2008) Flax and hemp fibres as raw materials for thermal insulation. *Building and Environmental*, 43, pp. 1261-1269.
- Skujans J., Iljins U., Ziemelis I., Gross U., Ositis N., Brencis R., Veinbergs A. and Kukuts O. (2010) Experimental research of foam gypsum acoustic absorption and heat flow. *Chemical Engineering Transactions*, No. 19, p. 79 – 84.
- Skujans J., Vulans A., Iljins U. and Aboltins A. (2007) Measurements of heat transfer of multi-layered wall construction with foam gypsum. *Applied Thermal Engineering*, Vol. 27, No.7, p. 1219-1224.
- Ulme A. and Freivalde L. (2009) Renewable material development in area of Latvia. *Scientific Journal of Riga Technical University. Material Science*, Vol. 9, No. 4, p. 63-67.
- Timber buildings. Low-energy constructions* (2010). C.Bene (ed.). Bozen: Bolzano University Press. 175 p.
- Elfordy S., Lucas F., Tancret F., Scudeller Y., Goudet L. (2008) Mechanical and thermal properties of lime and hemp concrete (“hempcrete”) manufactured by a projection process. *Construction and building materials*, No. 22, p. 2116-2123.
- Madsen B., Hoffmeyer P., Thomasen A.B., Lilhalt H. (2007) Hemp yarn reinforced composites. *Composites: Part A*, p. 2194-2203.

ULTRA HIGH PERFORMANCE CONCRETE HARDENING UNDER PRESSURE

Janis Justs, Diana Bajare, Genadij Shakhmenko, Aleksandrs Korjakins
Riga Technical University, Institute of Materials and Structures,
Professor's Group of Building Materials and Units
janis.justs@rtu.lv

ABSTRACT

In this study effect of pressure application to a fresh concrete right after casting and during the first 24 hours of hardening has been examined. Ordinary concrete can be defined as a porous media with high capillary porosity, especially in the aggregate–hydrated cement paste transition zone. The aim of pressure application is to maximally eliminate pores, to remove excess capillary water, and to improve density of the concrete matrix. By the pressure application it is possible to considerably reduce an amount of pores (>20 nm), to make concrete matrix denser and significantly increase its compressive strength. In this study concrete was cast in a specially designed cylindrical mould with an option to apply pressure. Pressure of 0 – 50 MPa has been applied. Cylindrical samples with a diameter of 50 mm and a diameter to height ratio 1:2 have been prepared. The concrete mix, incorporating silica fume and nanosilica particles has been prepared.

Keywords: High performance concrete, pressure application, compressive strength

INTRODUCTION

Ultra high performance concrete (UHPC) is a modern building material with superior properties such as high compressive strength, high modulus of elasticity, low permeability, excellent durability and high fluidity. All these properties can be achieved taking into account some basic principles and processing methods, that can be listed as follows: (i) minimising defect occurrence in concrete matrix and obtaining maximum density by optimizing particle size distribution (ii) minimising water/cement ratio by using high range water reducing admixtures which are compatible with the cement (iii) using pozzolanic materials such as silica fume to fill voids between larger particles, improve rheological properties and enhance secondary calcium silicate hydrate formation (iv) incorporation of steel fibers to prevent brittle failure and polypropylene fibers to increase UHPC fire resistance (Aitcin, 1998; Jain, 2003; Khurana, 1998; Khayat et al., 1996; Richard et al., 1996)

In 1994 Richard and Cheyrezy (Richard et al., 1994) produced reactive powder concrete (RPC) with compressive strength of 800 MPa. RPC is a type of UHPC which is characterized by very fine particles, no coarse aggregate is present. Production technology includes pressure application and heat treatment.

First demonstrations of UHPC outside laboratory were in footbridges. These structures appeared in the end of 1990ties. Some of the most well-known examples are in Sherbrook (1997), Seoul (2002) and Kassel (2007) (Tang, 2004; Fehling et al., 2004). First two road bridges using UHPC with a compressive strength more than 170 MPa were built in France in 2001 (Bourg-lès-Valence bypass) (Hajar et al., 2004). Initially structures were

designed basing on the experimental data of particular concrete as there were no building codes for UHPC present. However, first guidelines for UHPC appeared in 2002 in France.

UHPC is one of the most promising types of concrete in 21st century. Although efforts in developing the UHPC started in the last century, it is most probable that 21st century will benefit more from UHPC technology and more slender and aesthetical structures will be designed by architects who have acquired knowledge about UHPC. One of the factors of wider UHPC application will also be cost reduction as technology will be improved. There are already examples of commercially available UHPC that is used in the construction industry today. One such example is Ductal[®]. The Ductal[®] technology was developed by the combined efforts of three companies, Lafarge, the construction materials manufacturer, Bouygues, contractor in civil and structural engineering and Rhodia, chemical materials manufacturer (Acker et al., 2004).

The aim of this study is to investigate influence of different pressure applied during sample hardening process. Concrete mix composition with compressive strength of approximately 100 MPa was selected as basic mix. Pressure has been applied right after casting in order to improve concrete properties, mechanical strength of prepared samples was compared. By pressing concrete in the fresh state, most of entrapped air and excess capillary water can be eliminated, pore diameters reduced and some chemical adverse effects coming with cement hydration, for example autogenous shrinkage, eliminated. Distance between particles determines most of the concrete properties, eliminating of voids and reducing pore diameters would result in enhancement of concrete performance (Neville, 1995; Freyssinet, 1936).

As the macroscopic properties of UHPC are related to its microstructure - porosity, pore-size distribution as well as morphology of hydration products, concrete has been observed using scanning electron microscope (SEM) and very few pores with diameters >50nm have been found. Ultra high performance concrete border of 150 MPa has been reached by 50 MPa pressure application.

MATERIALS AND METHODS

The materials used in this study were commercially available raw materials, cementitious materials and admixtures. UHPC is characterised by very high content of high performance cement and silica fume. In this study concrete mix has been designed to reach approximately 100 MPa without pressure application at the age of 28 days and by pressure application right after casting make concrete matrix denser to achieve UHPC compressive strength border (150 MPa) at the age of 28 days.

Table 1

Concrete mix composition

Material	Quantity, kg/m ³
Cement CEM I 42,5 N	800
Sand 0.3-2.5 mm	510
Sand 0-1.0 mm	480
Ground quartz sand	200
Silica fume	100
Nanosilica	20
Superplasticizer	20
Water	200

Relatively high amount of ordinary type CEM I 42.5 N portlandcement was used. The amount of silica fume and nanosilica was 12.5% and 2.5% of cement mass respectively. Both silicas were made by Elkem (Norway). Polycarboxilate based superplasticizer has been used. The W/C ratio was 0.25. Basic concrete mix has been designed in order to provide 28 day compressive strength in the range of 100 MPa. Mix composition is given in the Table 1.

Particle size distribution

To produce UHPC, well grading of materials is essential. Particle size distribution curve of selected mix is given in Figure 1.

Optimal packing of available materials for the mix was obtained via computer programm EMMA by Elkem materials. To determine particle packing down to nano-scale, modified Andreassen particle packing model was employed (curve parameters $q=0.25$, $D_{max} = 2.5$ mm and $D_{min} = 0.0001$ mm was selected).

Mixing procedure

The mixing procedure of materials was the following: all dry materials were mixed till a homogenous mixture formed (approximately for 1.5 min). Then water and superplasticizer was added in two steps. During the first step approximately 70% of water was added. During the second step the rest of the water and the full amount of superplasticizer were added. Total mixing time was approximately 6 minutes. Mix with the cone slump of class S2 has been obtained after finishing mixing.

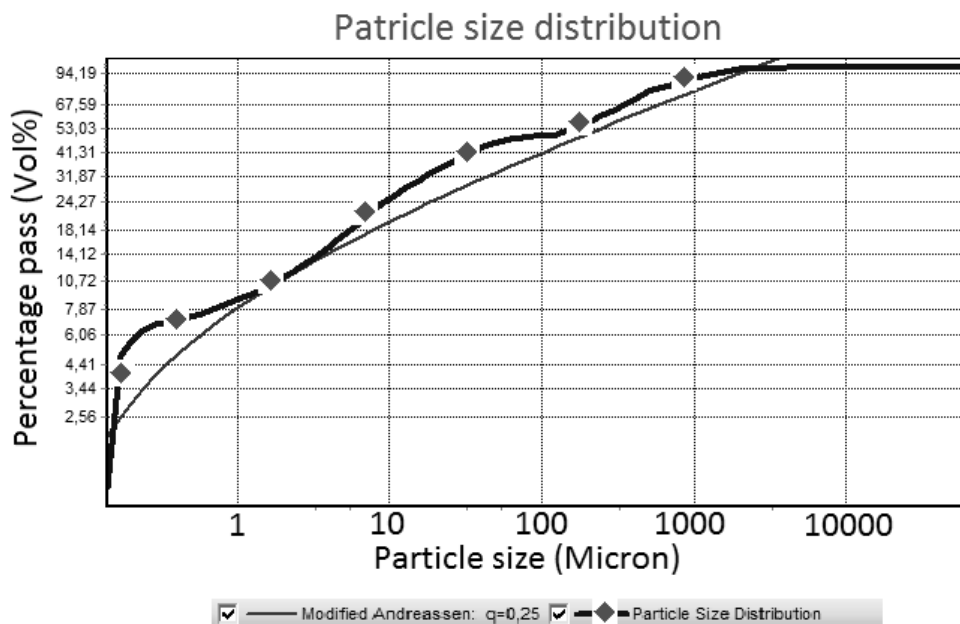


Figure 1. Particle size distribution of the selected concrete mix.

Experimental setup

Special cylindrical mould with inner diameter of 50 mm and varying height was designed and produced for this study. The mould consisted of 3 high precision details: central cylinder and two pistons closing cylinder from both ends. Pressure was applied by a manual hydraulic press. Pressure readings were taken from the manometer installed on the press. The experimental setup for pressure application is shown in Figure 2.



Figure 2. Experimental setup for pressure application to the specimens.

Right after casting pressure was applied to the concrete and retained for 24 hours.

Cylindrical specimens with a diameter 50 mm and height 100 mm were prepared. Pressures of magnitude 0, 10, 20, 30, 40 and 50 MPa were applied to the specimens during initial hardening in order to remove the entrapped air and excess water. After 24 hours the specimens were demoulded and cured in the water at the temperature of 20 °C until the age of 28 days was reached. At the age of 28 days compressive strength was determined.

RESULTS AND DISCUSSION

Quite stable pressure value has been kept up during pressure application, only minor corrections in first 20 minutes were necessary. Due to relatively low W/C ratio (0.25), little excess water was observed.

Macroscopic observations

As the macroscopic properties of UHPC are closely related to its microstructure, right after demoulding all specimens were evaluated visually. Macroscopic observations revealed that the samples hardened under higher pressure had significantly less porous structure. If there were clearly visible pores for samples hardened without pressure, completely opposite situation was for samples hardened under 50 MPa pressure, where no pores in macroscopic level could be discovered. Even for the specimens hardened under 10 MPa pressure very few macroscopic defects were noticed (Figure 3).



Figure 3. The specimens prepared by 10 MPa pressure application.

Material density

Densities of the specimens were observed carefully in order to control pressure application process. Theoretically there could be situation that side wall friction between cylinder and piston increases significantly if fine concrete particles are entrapped between the two details and consequently lower pressure is applied to the sample. However, due to the high precision of cylinder and piston details and careful concrete casting such negative situation was not experienced. Measured densities for samples with different pressure levels are shown in Figure 4. In figure 4 two different regions can be clearly divided pressure 0 -10 MPa and pressure 10 – 50 MPa. Figure 4 show that the most significant increase of density is observed, when pressure is increased from 0 to 10 MPa. In next intervals density increases almost linear, but the increase rate is in average only 7.6% of that observed in first interval. Conclusion can be drawn that for concrete with cone slump class S2, 10 MPa pressure is sufficient to eliminate most of entrapped air and excess water. By increasing pressure above 10 MPa, further micro and nano scale pore diameters are decreased.

Porosity

Porosity percentage of specimens was calculated taking into account material density and specific gravity of the concrete samples.

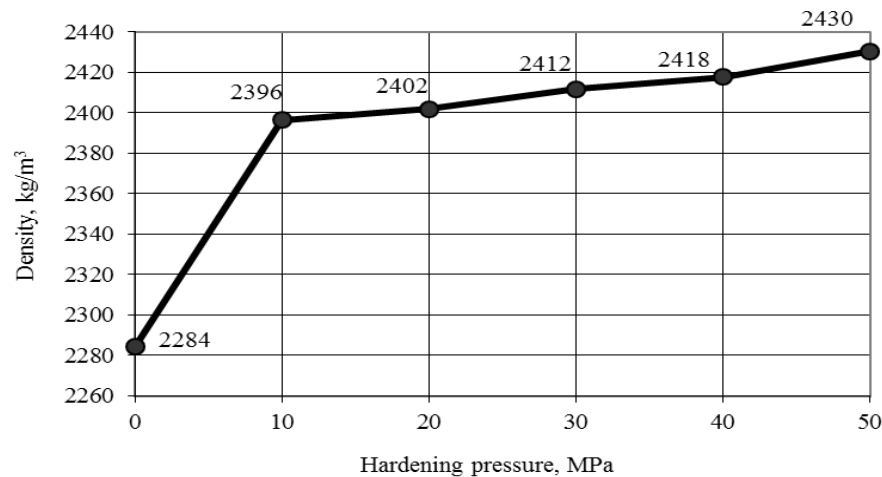


Figure 4. Density of the specimens depending on hardening pressure applied

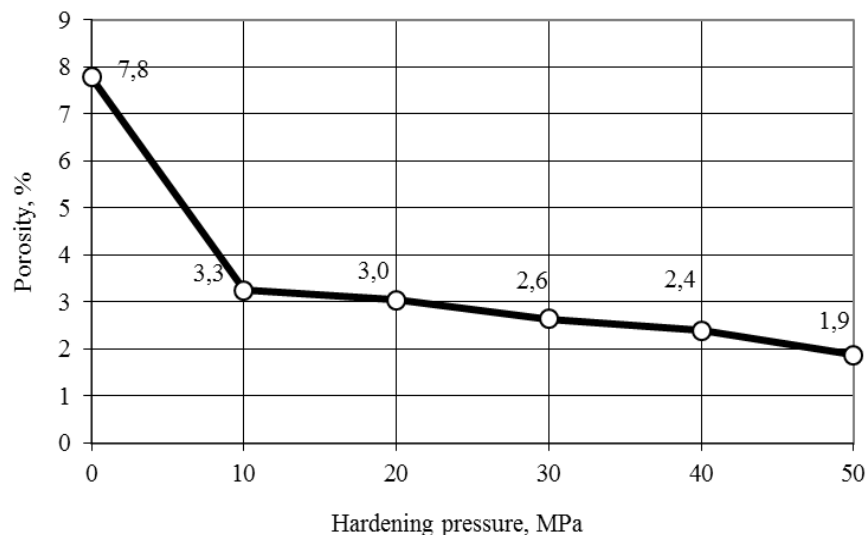


Figure 5. Porosity of the specimens depending on hardening pressure applied

Specific gravity was determined by pycnometer method (the sample was ground before test) and porosity was calculated using previously obtained sample densities. Results are displayed in Figure 5.

In Figure 5 two different regions can be divided identically as in case of density. By increasing pressure from 0 MPa – 10 MPa, porosity rapidly decreases from 7.8% – 3.3%. By increasing pressure from 10 MPa – 50 MPa porosity decreases with the average rate of 7.8% of that observed in the first interval. Rapid porosity decrease in the first pressure interval can be explained by the fact that calculated porosity results also include macroscopic defects and relatively small pressure is necessary to eliminate macroscopic air voids. However, significantly higher pressure is required to reduce the micro and nano-scale pore size diameters. The lowest porosity value acquired in this study by 50 MPa pressure application was 1.9%.

Compressive strength

Samples without pressure application reached compressive strength of 103.9 MPa. Samples with 50 MPa pressure application reached compressive strength of 153.6 MPa, which corresponds to the strength increase of 48%. Every 1 MPa of pressure applied to sample in the first 24 hours gave in average an extra 1 MPa of compressive strength after 28 day hardening. In the interval of first 10 MPa pressure application this rate was three times higher. This pressure interval may be practically applied in the pre-cast concrete industry, although higher pressure value is technologically difficult to achieve for the real concrete elements. The smaller the distance between concrete particles, the lower porosity, the higher density and higher final compressive strength was reached. The compressive strength results are given in the Figure 6.

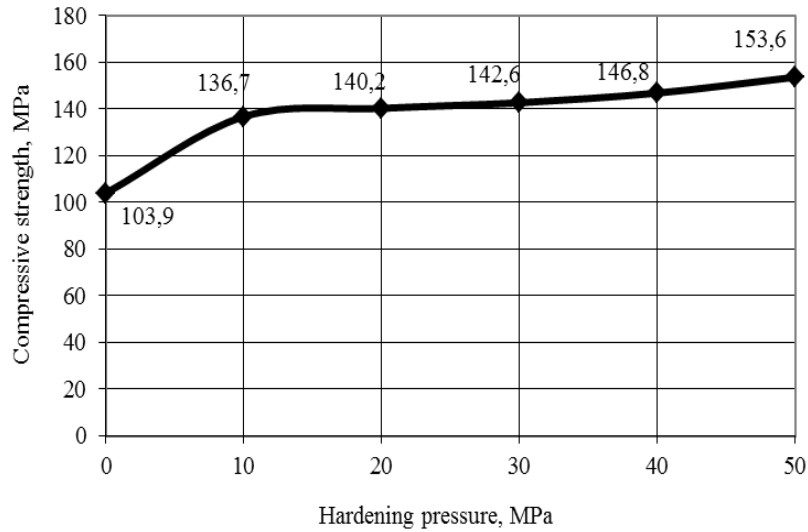


Figure 6. Compressive strength of the specimens depending on hardening pressure applied

Microscopic (SEM) observations

Figure 7 shows destroyed concrete surface at the magnitude of 100 times. The concrete specimens with highest compressive strength (153.6 MPa) were observed by SEM. Samples were taken from the middle of destroyed specimens to observe microstructure of the concrete. Dense concrete matrix and destroyed aggregates are visible in Figure 7. Magnitude of 1000 times (Figure 8) reveals dense structure of calcium silicate hydrates. Pore diameters were evaluated graphically from SEM micrographs. Very few pores with diameters larger than 200 nm were determined, however, there are some examples of pores with diameter approximately 200 nm (Figure 9).

In terms of the different effect of pore size on concrete performance, the pores in concrete can be classified as follows: harmless pores (<20 nm), few-harm pores (20–50 nm), harmful pores (50–200 nm) and multi-harm pores (>200 nm) (Ye, 2001).

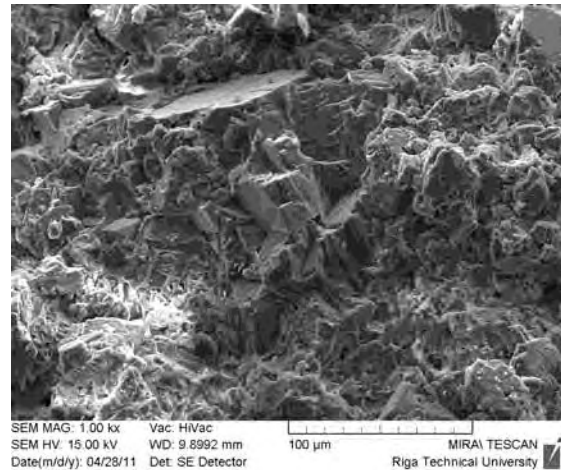


Figure 8. Concrete at the magnitude of 1000 times

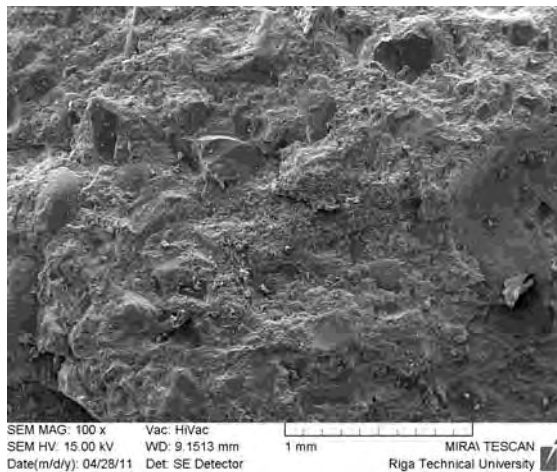


Figure 7. Concrete at the magnitude of 100 times

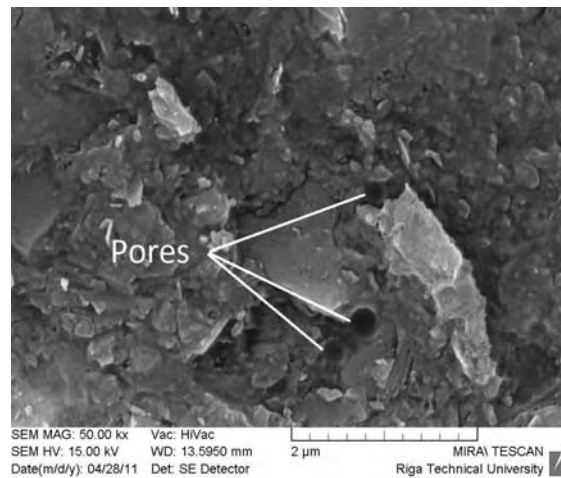


Figure 9. Concrete at the magnitude of 50 000 times

CONCLUSIONS

Pressure of 10, 20, 30, 40 and 50 MPa was applied to the concrete specimens during initial hardening (24 hours) in order to improve physical and mechanical properties of the materials. Compressive strength, density and microstructure were investigated. Following conclusions can be drawn from this study.

Applying pressure in concrete initial hardening phase it is possible to achieve UHPC compressive strength border (150 MPa) for the concrete mixes, which normally at the age of 28 days achieve only 100 MPa.

The greatest gain in concrete performance characteristics was observed by applying pressure at the rate of 10 MPa (strength increase in 31.5 %). By increasing pressure further to 50 MPa slower enhancement of the concrete properties was noticed.

Due to 50 MPa pressure application density of samples increased from 2284 kg/m³ to 2430 kg/m³, porosity decreased from 7,8% to 1,9%, excess capillary water was removed. Significant gain of compressive strength of 48% (103,9 to 153,6 MPa) was observed for samples pressed with 50 MPa.

Pressure application during the concrete setting can be used in precast element fabrication. For real concrete elements pressure up to 10 MPa may be practically applied in pre-cast plants, higher pressure technologically is difficult to achieve. Results of this study indicate that even relatively small pressure gives significant positive effect in enhancement of concrete properties. Influence of pre-set pressure in range of 0 – 10 MPa must be investigated in future in details.

Summarizing the results it can be concluded, that pressure is an effective instrument to achieve high mechanical strength and high performance characteristics of concrete.

ACKNOWLEDGEMENT

The financial support of the ERAF project Nr. 2010/0286/2DP/2.1.1.1.0/10/APIA/VIAA/033 „High efficiency nanoconcretes” is acknowledged.

REFERENCES

- Acker P., Behloul M. (2004) Ductal® Technology: a Large Spectrum of Properties, a Wide Range of Applications. *Proceedings of the International Symposium on Ultra High Performance Concrete*, Kassel, p. 9-23.
- Aitcin, P.C. (1998) *High Performance Concrete*. London: E and FN. Spon.
- Fehling E., Bunje K., Schmidt M., Schreiber W. (2004) Ultra High Performance Composite Bridge across the River Fulda in Kassel– Conceptual Design, Design Calculations and Invitation to Tender. *Proceedings of the International Symposium on Ultra High Performance Concrete*, Kassel, p. 69-75.
- Freyssinet M.E. (1936) *Cement and Concrete Manufacture*. Vol. 9, p. 71.
- Hajar Z., Lecointre D., Simon A., Petitjean J. (2004) Design and Construction of the world first Ultra-High Performance Concrete road Bridges. *Proceedings of the International Symposium on Ultra High Performance Concrete*, Kassel, p. 39-48.
- Jain, A (2003) High Performance Concrete Research and Practice. *Proceedings of Construction Management and Materials*, Kharagpur, p. 450-560
- Khayat K.H., Aitcin P.C., (1996) Silica fume in concrete: an overview. Fourth CANMET/ACI International Conference on Fly ash, Silica fume, slag and natural pozzolans in concrete, SP-132, V.2 (1992), 835. Guide for use of silica fume, 234R-96 ACI Publications
- Khurana R. (1998) Admixtures for ready mixed high strength and durable concrete. *ERMCO, 12th European Congress*.
- Neville A. M. (1995) *Properties of concrete*. 4th ed. England: Longman group limited.
- Richard P., Cheyrezy M. H., (1994) Reactive powder concretes with high ductility and 200-800 N/mm² compressive strength. P.K. Metha (ed.). *Concrete Technology: Past, Present and Future*, p. 507-517
- Richard P, Cheyrezy M. (1995) Composition of reactive powder concretes. *Cement and Concrete Research*, Vol. 25, No. 7, p. 1501-1511.
- Tang M.-C. (2004) High Performance Concrete – Past, Present and Future. *Proceedings of the International Symposium on Ultra High Performance Concrete*, Kassel, p. 3-9.
- Ye Q. (2001) *New Build. Mater.* p. 4–6.

DEFECT ANALYSIS OF REINFORCED CONCRETE SLABS FOR EARTH DAM SLOPE PROTECTION

Raimondas Sadzevicius, Feliksas Mikuckis, Dainius Ramukevicius
Lithuanian University of Agriculture,
Department of Building Constructions
raimondas.sadzevicius@lzuu.lt; sk@lzuu.lt; dainius.ramukevicius@lzuu.lt

ABSTRACT

Many of hydraulic structures on Lithuania hydroschemes are older than 30 years; therefore, the ageing of building materials causes greater probability of deterioration and even failure. Every reinforced concrete construction of hydraulic structures is getting worse with time, but especially often there are deteriorated reinforced concrete slabs for earth dam slope protection. Due to environmental impacts some deteriorations of the slabs take place, which influence negatively not only some slabs, but after their failure the danger arises for the whole slope protection, for the reliability, durability and safety of the hydraulic structure in general. If dangerous defects and deteriorations are not repaired in time, big technical and ecological loss may occur. From the economic point of view execution of new slope protection is more expensive; therefore, a more topical problem is to preserve the present reinforced concrete slabs by means of restoration and/or reconstruction. The main defects and deterioration of reinforced concrete slabs for earth dam slope protection, the character and causes of ones are described in the article; the technical state of strengthening slabs was estimated by points. It is established that rupture of slabs of hydroschemes in the time being was caused in many cases by unfit manufactured concrete, which properties do not satisfy the requirements of usage; the influence of aggressive environments, unfit exploitation. The data of the investigations published in the article are given for improvement in designing new strengthening slabs, repairing the damaged part of the construction timely.

Key words. Defects, reinforced concrete slabs, technical state.

INTRODUCTION

The slopes of earth dams are effected by external climatic and other factors (Building standards STR 2.05.15:2004): water, waves, ice, wind, atmospheric conditions (high and low temperature, solar radiation, humidity, frost cycles, etc.), ground, vegetation and even burrow animals, livestock and so on.

Earth dam slopes protection methods involve such structural approaches as rip-rap, stone pitching, concrete (slabs, concrete filled bags), dikes, fences, asphalt, gabions, matting, bulkheads, geosynthetic lining systems etc. Reinforced concrete strengthening slabs are the most popular coverage of earth dam slopes in Lithuania. The covering of earth dam slopes were constructed and arranged in accordance with the building standards and regulations (STR 2.05.17:2005; ST 2079337.09:2000).

The main slope coverage is in the most intensive ice and water wave impact zone. The monolithic, precast or combine (cast in place - precast) reinforced concrete slabs were used. The reinforced concrete coverage of earth dams was divided in separate sections by contraction joints (Webber et al., 1987). At present the state of every reinforced concrete strengthening slab in functioning hydraulic structure (here and after HS) is unequal. There is a

number of strengthening slabs functioning almost well, others are more or less deteriorated (Damulevicius et al., 2001; Damulevicius, Vycius, 2007; Sadzevicius, 2002). The regulations (Building standards STR.1.12.03:2006) briefly describe the state of upstream slopes and discount the condition of reinforced structures. In order to evaluate the type of physical deterioration and the technical state of strengthening slabs, a mass of initial data must be collected. Reinforced concrete is a durable material, but like any other it is deteriorated in time. Deteriorations of constructions create not only favorable conditions for rapid destruction of the structure, but can cause crash of the whole construction as well (Vaišvila, Vilkas, 1998; Vaisvila et al., 1999).

The purpose of these investigations, based on the research in the field, is to identify the shortcomings during the construction aging, to clarify characteristic breakdowns, failures, to establish the character and causes of the main defects in the reinforced concrete strengthening slabs.

MATERIALS AND METHODS

In 1998-2011 the reinforced concrete strengthening slabs of 30 HS were investigated in the field. The actual quantities of the main physical-mechanical properties of concrete, defects and deteriorations of

the structures were established. The principal attention was located to establish the actual quantities of the compressive strength, main deteriorations and ruptures in reinforced concrete strengthening slabs.

The compressive strength of concrete of the structures was estimated by nondestructive methods in accordance with the Standard and instructional manual of instrument devices requirements (Building standards LST ISO 4012:1995; LST 1428.11.1996; LST 1428.14:1997).

The concrete compressive strength of strengthening slabs evaluation was performed by using the standard Schmidt E. – hammer apparatus (Building standards LST 1428.11.1996). The sufficiency of quantity impact produced with nondestructive apparatus was controlled in accordance with the manual requirements. The calibration curves of the mentioned apparatus to calculate the strength of the tested concrete were used. We prepared split concrete pieces from the structure for testing the compressive strength of concrete by the destructive method. The split concrete pieces were placed in hermetically sealed polythene sacks and carried to the laboratory for tests. The structures on location were visually examined and their most deteriorated places, the character of defects, area and the depth of cracks and deteriorations were established.

On the basis of the field investigations the main deterioration and rupture of reinforced concrete strengthening slabs character and causes of ones are described, the technical state of the strengthening slabs was evaluated by defectiveness points (B_u) in the ten point criterion system by the standing construction regulations STR 1.12.03:2006: 0 points – ideal condition, 10 points – emergency condition. The detailed point determination is presented below:

- element condition meets the requirements of the construction regulations, irregularity is small — 0

$< B_u \leq 2.0$ points (good condition);

- deterioration of the element has no influence to the strength and normal maintenance of the dam, small deteriorations are recorded – $2.1 < B_u \leq 4.0$ points (moderate condition);
- deterioration of the element does not have important influence to the strength, reliability and the actual service life of the element, some defects and deteriorations are significant – $4.1 < B_u \leq 6.0$ points (satisfactory condition), the technical state can be improved by repairing;
- deterioration reduces the strength and reliability of the element very much, defects and deteriorations are significant – $6.1 < B_u \leq 8.0$ points (unsatisfactory condition), big repair needed;
- remarkable deterioration and maintenance of the element is impossible – $8.1 < B_u \leq 10.0$ points (critical condition), the dam should be reconstructed.

RESULTS AND DISCUSSION

In the paper the data and analysis of reinforced concrete strengthening slabs of 30 functioning HS are presented. The investigations were performed in 1998-2011.

For investigations hydraulic structures were selected in various regions of Lithuania. The investigated structures were built in different time. The selected ones are located in Alytus, Anyksciai, Birzai, Kaunas, Kedainiai, Marijampole, Joniskis, Pasvalys, Raseiniai, Ukmerge and Utena districts (Tvenkiniu katalogas, 1998).

The data of the investigated HS: the actual service life, the average compressive strength of concrete, deterioration and defects of reinforced concrete strengthening slabs, conditions of them in points are given in Table 1.

Table 1

Data of investigated strengthening slabs

No	HS, Age of constr., years	Compressive strength, MPa	Character of deterioration and defects	Causes of deterioration rising	Condition, points
1	2	3	4	5	6
Alytus district					
1.	Krokia-laukis 26	14.7±1.4	Scour, deformation of dam slope protection slabs, collapsing of joints	Mounting inaccuracy, damaged joints, wave blows	8.7
Anyksciai district					
2.	Elmininkai 24	16.0±0.8	Scour, deformation of dam slope protection slabs	Damaged joints by grass, bushes roots, wave blows	8.5
3.	Leliunai 11	19.8±1.0	Deformation of dam slope protection slabs	Damaged joints, wave blows	6.0

Continuation of the Table 1					
1	2	3	4	5	6
4.	Pagoje 10	12.7±0.6	Damaged joints, deteriorated surfaces	Concrete, which properties do not satisfy requirements of usage (weak concrete), damaged joints	5.0
Birzai district					
5.	Ageniskis 32	11.8±0.4	Damaged joints	Damaged joints by grass	7.0
6.	Gulbinai 32	24.3±1.2	Damaged joints, corrosion of reinforcement and concrete,	Damaged joints by grass	7.0
Kaunas district					
7.	Gailiusiai 29	9.1±0.4	Damaged joints, damaged surfaces	Weak concrete, damaged joints	5.9
8.	Grauze III 37	7.1±0.4	Damaged joints, damaged surfaces, corrosion of reinforcement and concrete,	Weak concrete, damaged joints by grass, bushes roots, thin covering layer	7.7
9.	Muniskiai 24	8.3±0.7	Deteriorated surfaces	Weak concrete, frost cycles	7.2
Kedainiai district					
10.	Angiriai 34	7.9±0.6	Light irregularity		4.2
11.	Kruostas HPS 49	5.5±0.2	Damaged joints, deteriorated surfaces	Concrete, which properties do not satisfy requirements of usage (weak concrete), damaged joints, frost cycles	6.1
Marijampole district					
12.	Antanavas HPS 51	6.0±0.4	Biocorrosion, deformation of dam slope protection slabs	Exploitation denormalization	8.6
13.	Marijampole 67	6.0±0.9	Damaged joints, deteriorated surfaces	Mechanical rupture	7.8
14.	Jure 23	9.8±0.5	Defects of surface, pittings, corrosion of reinforcement and concrete, damaged joints	Weak concrete, damaged joints, exploitation denormalization, thin covering layer	7.9
15.	Kazlai 18	7.7±0.4	Light irregularity		3.0
16.	Pilve-Vabalksnis 45	9.6±1.4	Unallowable strain of elements, scour	Undercut basis of slabs, weak concrete	9.0
Joniskis district					
17.	Berzenai	13.3±1.0	Damaged joints, deteriorated surfaces	Seepage, damaged joints by grass, frost cycles	5.1
18.	Linkaiciai	15.3±0.6	Deteriorated surfaces	Weak concrete, frost cycles	4.3
Pasvalys district					
19.	Smilgiai 33	20.0±0.6	Biocorrosion, damaged joints	Damaged joints by grass	5.0

Continuation of the Table 1					
1	2	3	4	5	6
20.	Svobiskis 89	29.3±1.2	Biocorrosion, damaged joints	Damaged joints by grass	4.0
21.	Paiesmenys 36	24.0±0.8	Biocorrosion, damaged joints	Damaged joints by grass	6.0
Raseiniai district					
22.	Anulynas 20	6.2±0.7	Defects of surface, pittings, corrosion of reinforce and concrete, damaged joints	Weak concrete, damaged joints, exploitation denormalization, thin covering layer	8.1
23.	Kaulakiai 19	15.0±1.2	Damaged joints, deteriorated surfaces	Weak concrete damaged joints by grass, frost cycles	6.8
24.	Musia 17	23.1±1.2	Light irregularity		3.0
Ukmerge district					
25.	Ukmerge 29	29.3±0.8	Damaged joints, deformation of dam slope protection slabs, deteriorated surfaces	Damaged joints by grass, wave blows, weak concrete	4.0
26.	Virksčiai 33	13.8±0.7	Damaged joints	Damaged joints by grass	5.0
Utena district					
27.	Utena 34	20.2±0.6	Damaged joints, deformation of dam slope protection slabs	Damaged joints by grass, wave blows	4.0
28.	Nemėi- kščiai 28	22.9±0.9	Damaged joints	Damaged joints by grass	4.0
29.	Biliakiemis 29	17.1±0.6	Damaged joints	Moss, grass, bushes roots	7.0
30.	Packėnai 34	22.9±0.6	Damaged joints	Moss, bushes roots	7.0

The most damaged reinforced concrete strengthening slabs (in critical condition) are in Krokialaukis, Elmininkai, Antanavas, Anulynas, Pilve –Vabalksnis hydroschemes. Rehabilitation of these hydroschemes is necessary.

The actual service life of the oldest hydraulic structure is 89 years and 10 years of the last one. The strongest concrete with average compressive strength 29.3 MPa was established in the slabs of Ukmerge HS, the weakest one – 5.5 MPa in the structures of Kruostas HPS. The surfaces of the structures manufactured with stronger concrete were less damaged. Concrete is affected in the changing water level most intensively. Pittings on the surface of the structures proceed rapidly in this zone. The possibility of damages of the covering layer is created by sufficient conditions for corrosion of reinforcement. Defects are in progress then joints are damaged (25 from 30 investigated objects). The bad exploited joints were damaged by the weeds or even scrubs. Roots of scrubs can break reinforced concrete strengthening slabs (Fig.1).

It was noticed during the expedition, that all the investigated surfaces of the earth dam slopes slabs in the zone of the changing water level are more or less deteriorated in form of pitting. There are

several reasons of forming pitting, but the main is–erosion of concrete by the influence of frost cycles (Fig. 2). The surface of the structures on the changing water level zone is touched by ice, swimming solids or sediments (especially gravel) abrasive impact. After establishment, which impact is the most actual in separate ponds, there is a need to explore in more detail the pitting appearance reasons. Other reasons of concrete erosion presented in literature, for instance, cavitations, are less found in our researched structures, because in the researched ponds, the water flow pulsation speeds are small (<2m/s).

It was established, that the cover layer and junctures defects are caused by environmental (frost cycles; ice, wave blows; moss, grass, bushes roots, collapsing impacts; periodical wetting etc.) impacts, appearing in degradation processes (concrete and reinforcement corrosion, erosion, biological actions). Deterioration processes mostly break badly made covering layer (small concrete strength and frost resistance), which being under the influence of frost cycles crumbles, its physical–mechanical properties change, forms deterioration – pitting. Most intensively concrete is destroyed in ice and wave impact (changing water level) zone.

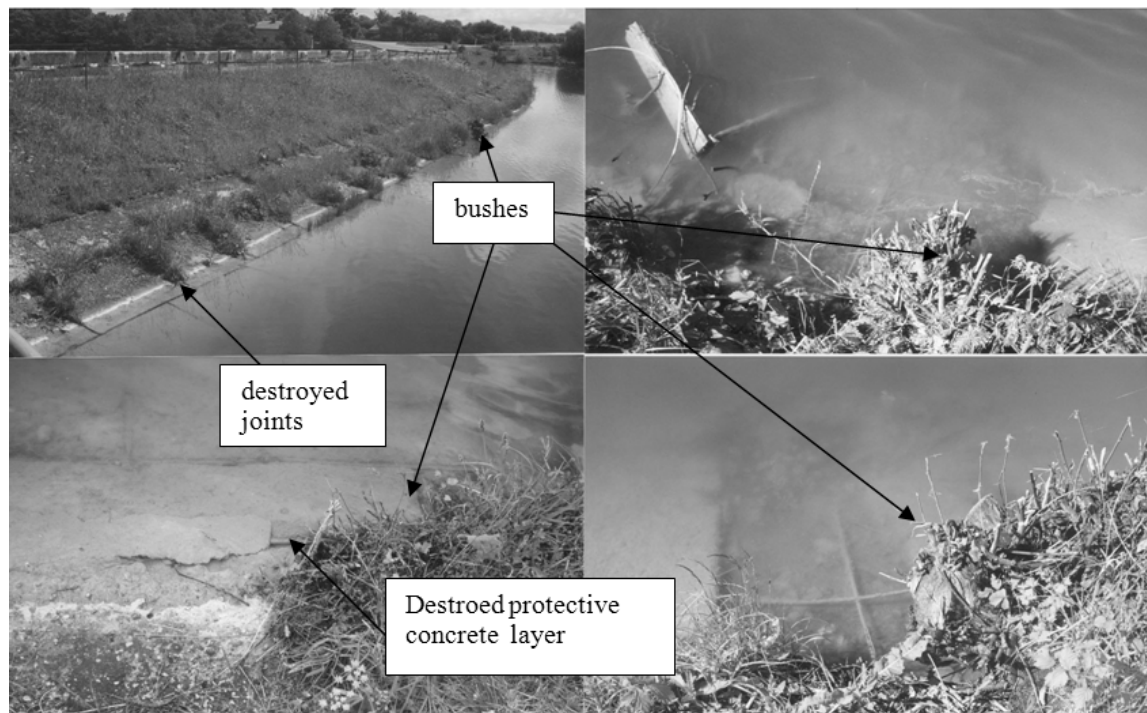


Figure 1. Destroyed joints by grass, bushes roots in Grauze pond (Kaunas district).



Figure 2. Erosion of surface on concrete slabs (Ageniskis pond) by influence of frost cycles.

The main attention should be paid to the zones where deterioration and defects are often formed – pitting is formed in the changing water level in the flow compression zone – in slabs, which are not far from the inflow part of shaft spillways or in the flow parts of overflow spillways.

REFERENCES

Building standards. LST ISO 4012:1995 (1995) Concrete determination of compressive strength of test specimens. Vilnius: Lietuvos standartizacijos dep. [Lithuanian Standards Board]. 5 p.

Building standards. LST 1428.14:1997 (1997) Concrete. Testing methods. Cored specimens, taking, examination and testing in compression.. Vilnius: Lietuvos standartizacijos dep. [Lithuanian Standards Board]. 7 p.

CONCLUSIONS

1. The results of 30 earth dam slope protection slabs field investigations show, that mostly occurred defects and deteriorations of slab are: deterioration of the cover layer (12 from 30 objects) and collapsing of joints (25 from 30 objects), accordingly 40 % and 83 % of the researched objects.
2. The rupture and deterioration of the cover layer of reinforced concrete slabs in the time being were caused in many cases by unfit manufactured concrete, which properties do not satisfy the requirements of usage (weak concrete); unfit exploitation- bad exploited joints were damaged by the weeds or even scrubs.
3. The reinforced concrete strengthening slabs in Krokialaukis, Elmininkai, Antanavas, Anulynas, Pilve –Vabalksnis hydroschemes are in critical condition and should be repaired immediately.

- Building standards. LST 1428.11.1996 (1996) Concrete. Testing methods. Non-destructive testing. Determination of rebounding number. Vilnius: Lietuvos standartizacijos dep. [Lithuanian Standards Board]. 7 p.
- Building standards. STR.1.12.03:2006 (2007) Regulations of maintenance of hydraulic structures. Vilnius. *Valstybės žinios [Official Gazette]*. 33 p.
- Building standards. STR 2.05.15:2004 (2004) Hidrotechnikos statinių poveikiai ir apkrovos [The impacts and loads on hydraulic Structures]. *Valstybės žinios [Official Gazette]*, Nr. 130–4681.
- Building standards. STR 2.05.17:2005 (2006) Gruntinių medžiagų užtvankos [Ground material dams]. *Valstybės žinios [Official Gazette]*, Nr. 19–664.
- Building regulations. ST 2079337.09:2000 (2000) Requirements for built performance of hydrotechnical building. Vilnius: Lietuvos melioracijos įmonių asociacija [Association of Lithuanian Companies for Melioration], 148 p.
- Damulevičius, V.; Rimkus, Z.; Vyčius, J. (2001) Investigation of the technical state of hydraulic structures in Lithuania. *Water management engineering*, Vol. 15, No. 37, p. 81–89.
- Damulevičius, V.; Vyčius, J. (2007) Gruntinių statinių šlaitų tvirtinimo priemonių techninės būklės analizė [Analysis of the technical state of the ground slopes lining]. *Vandens ūkio inžinerija [Water management engineering]*, Vol. 32, No. 52, p. 108–116.
- Lindišas L., Vaišvila K.A., Žekevičius R. (1999) Investigation of physical- mechanical properties of damaged concrete structures in exploited WEC. *Water management engineering*, T.6,(28), p. 42 – 48.
- Šadzevicius, R.; Vaišvila, K. A.; Lindišas, L. (2001) The research of deterioration of reinforced concrete structures functioning in the alternative level of water engineering constructions. *Vandens ūkio inžinerija [Water management engineering]*, Vol. 18, No. 40, p. 47–52.
- Šadzevicius, R. (2002) Tvenkinių hidromazgų šlaitų tvirtinimo gelžbetoninėmis plokštėmis techninės būklės vertinimas [Evaluation of technical status of reinforced concrete strengthening slabs of ponds embankments]. *Vandens ūkio inžinerija [Water management engineering]*, Vol.20, No.42, p. 88–93.
- Tvenkinių katalogas [Catalog of ponds]* (1998) Aplinkos apsaugos ministerija, Hidrografinio tinklo tarnyba [Dept. Of Hydrographic System, Ministry of Environment of the Republic of Lithuania]. Kaunas. 68 p.
- Vaišvila K.A., Vilkas V. (1998) Approximate estimation of deterioration in exploited WEC concrete structures. *Water management engineering*, T.4,(26), p. 158 – 164.
- Webber D., Parrett N., Blair H. K. and others (1987) *Design of Small dams. Manual*. US Department of the Interior Bureau of Reclamation. Washington. A Water Resources Technical Publication. 860 p.

OBTAINING COMPOSITION OF GEOPOLYMERS (ALKALI ACTIVATED BINDERS) FROM LOCAL INDUSTRIAL WASTES

Diana Bajare, Girts Bumanis, Genadij Shakhmenko, Janis Justs

Riga Technical University,
Institute of Materials and Constructions,
Professor's Group of Building Materials and Wares
diana.bajare@rtu.lv

ABSTRACT

The aim of the research is development of geopolymers – the new, knowledge-based, multi-functional materials with high performance, reduced environmental impact and adjustable to customer needs. Depending on selection of the raw material and processing conditions, geopolymers can exhibit a wide variety of properties and characteristics, including high compressive strength, low shrinkage, fast or slow setting, acid resistance, fire resistance and low thermal conductivity. Materials used in preparation of geopolymers are local industrial waste and by-products such as ashes obtained from burning grasses, glass powder recycled from lamp demercuration facility in Liepaja and calcined clay minerals. Raw materials were investigated and treated by using calcination and grinding methods to increase their activity. Mechanical and physical properties of obtained geopolymers were tested. A variety of results were observed. Depending on the used waste materials in geopolymer composition and curing conditions hardened geopolymer samples possessed either good compressive strength results and waterproof or marginally low compressive strength and weak waterproof.

Key words: geopolymers, local industrial waste, construction material, compressive strength

INTRODUCTION

Ordinary Portland cement is the most commonly used cementitious material nowadays. During production of one ton of cement 0.65-0.92 tons of CO₂ gasses are released in the atmosphere. This is a significant degree of pollution, which enhances greenhouse effect. To avoid further pollution and CO₂ emission, new cementitious materials are created (Davidovits, 2008; Juenger et al., 2010). Geopolymers are among the most efficient. Glukhovsky first introduced a general conceptual model for the alkali activation of the aluminosilicate materials in 1950s (Glukhovsky, 1959). However the term “geopolymer” was introduced by J. Davidovits (Davidovits, 1991) to describe mineral binders closely related to artificial zeolites. Development of geopolymers – a new generation of cementitious materials being an alternative to traditional cement and concretes through alkali activation of industrial waste is a relatively new area and research topic for the scientific community. The alkali activation of materials is a chemical process that ensures rapid transformation of some specific phases (partially or totally amorphous) into compact cemented frameworks. To obtain alkali-activated binder the source materials must be rich with alumina and silicate. Such elements are widely spread in different types of ashes, glass and clay minerals.

Development of geopolymer technology is in accordance with the requirements of sustainable development, because in this way significant

amounts of industrial waste materials are not only used as a secondary raw material, but are converted to a new product. Creation of a new material from different industrial by-products might result in reduced energy consumption, reduction of waste production, reduction of global CO₂ emissions, as well as in the reduction of exploitation of natural resources, which are commonly used for production of Portland cement. The production of geopolymers could reduce 80% of those CO₂ emissions, which are released during ordinary Portland cement production (Duxson et al., 2007; Gartner, 2004).

The aim of this work is to obtain geopolymer binder material with proper mechanical and physical properties from local industrial waste and by-products. In mix design either single by-product material like ashes or combination of waste materials are used in order to improve chemical composition and obtain higher mechanical properties. In this work six different geopolymer mortars have been created.

MATERIALS AND METHODS

The materials used in geopolymer composition are mainly by-products and industrial wastes. The bottom ashes used in geopolymer compositions were taken from local heating plant furnaces. Wood bottom ashes and barley bottom ashes were tested as potential geopolymer compounding material. Ashes were ground in a planetary ball mill to obtain powder particle material, to ensure material homogeneity and enlarge specific surface area in

order to make material more reactive. Chemical compositions of ground bottom ashes were determined.

The other raw material used in investigations was taken from the local fluorescent lamps utilisation plant. Glass is rich with siliceous dioxide and it is an excellent source for amorphous siliceous in geopolymer composition. Glass from fluorescent lamps is not possible to recast in the traditional way due to unacceptable and toxic impurities. Landfill disposal of the glass waste is common solution until now. The utilisation of this type of glass as a raw material in geopolymer composition will make unequivocal positive impact to environment. Fluorescent lamp glass normally is roughly grounded in the plant during recycling process. Roughly grounded and additionally grounded glass was used in the investigations.

Another important component in geopolymers is alumina. Alumina is needed to form aluminosilicate, which is the compound that gives strength and other physical and mechanical properties to the obtained material.

Most common alumina containing material used in geopolymers is metakaolin. Since metakaolin is not the local raw material, calcined clay with low content of carbonates was used as alumina source in geopolymer composition. Calcined clay was obtained from producer of ceramic building materials JSC Lode or made in laboratory by treatment of clay in the furnace under 700°C for 3 hours.

In the experimental work activation solution (6M NaOH) was used.

Chemical composition of raw materials

Preliminary investigation of chemical and mineralogical composition of geopolymer raw materials was carried out. Chemical analysis results

for ashes, waste glass and calcined clay are summarized in Table 1.

Table 1

Chemical composition of raw materials

	Barley ash	Wood ash	Waste glass	Calcinated Clay
Loss of ignition	0.49	0.64	0.5	0.1
SiO ₂	66.07	59.92	74.25	68.41
CaO	6.06	19.89	2.09	0.91
MgO	1.68	2.32	0	1.41
Al ₂ O ₃	5.38	4.3	1.65	14.01
Fe ₂ O ₃	1.78	1.6	0.16	5.55
Na ₂ O	0.24	0.37	3.82	0.29
K ₂ O	7.14	3.59	0.93	3.48
B ₂ O ₃	0	0	16.63	0

As it seen in the Table 1, materials used in geopolymer composition are rich with silica dioxide SiO₂ – from 59.92% to 74.25%. The other important element is Al₂O₃. Clay contains 14.01% of Al₂O₃, while ashes contain only 4.3-5.38% of Al₂O₃. Barley ashes contain the highest alkali content – 7.38% K₂O+Na₂O.

The geopolymerisation process involves the dissolution, migration and polymerization of Al and Si elements. The presence of cat ions (Na, K and Ca) in the composition is very important, because they provide balancing and catalytic properties (Luna et al., 2007)

The results of XRD analysis for wood ash are given in Figure 1.

As it is seen, wood ashes are very rich with crystalline quartz (SiO₂). Also wollastonite (CaSiO₃) and akermanite (Ca₂MgSi₂O₇) are found as most common minerals. Small amount of potassium calcium silicate (K₄CaSi₃O₃) as well as cristobalite (SiO₂) were determined in the wood ash. Mineralogical composition of wood ashes corresponds to the results from chemical analysis.

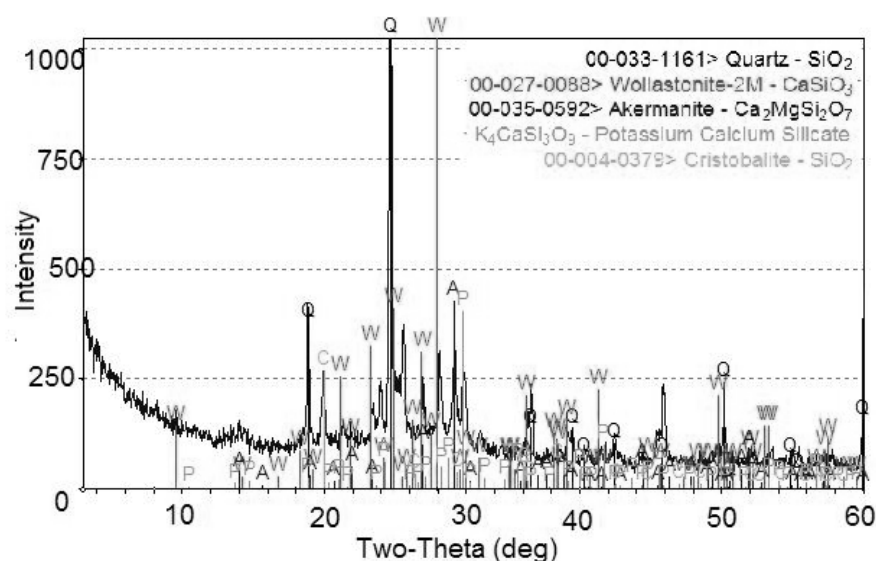


Figure 1. XRD analysis of wood ash.

Grading analysis of raw materials

Particle size and particle size distribution of raw materials also was obtained. Materials used in geopolymer composition were finely ground in the planetary ball mill to improve the homogeneity and reactivity of them.

Barley ashes were ground for 4 minutes, but wood ashes were ground for 10 min. Particle size distribution of wood and barley ashes was smaller than 63µm.

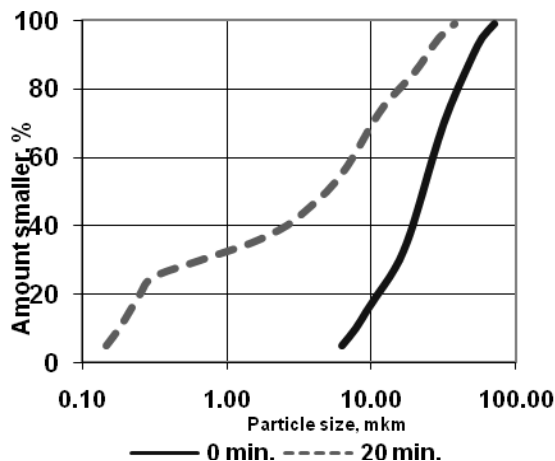


Figure 2. Roughly ground waste glass and additionally ground waste glass particle size distribution curves.

Waste glass was already roughly ground during the recycling process. Part of glass was additionally ground for 20 min to enlarge fineness of glass particles and increase glass reactivity. The particle size distribution curves of the roughly ground waste glass and additionally ground waste glass are summarised in Figure 2.

Calcined clay particle size used in geopolymer composition was smaller than 0.315mm.

Geopolymer composition

Different potential geopolymer compositions were created from alumina and silicate rich industrial waste materials and by-products. Proper chemical and mineralogical composition as well as particle size distribution is common requirements for raw materials used in the production of geopolymers.

The curing temperature of geopolymers is another important aspect. Geopolymerisation process is less active at the ambient temperature, but using higher curing temperature should accelerate it. In finally solid material can be marked with higher mechanical properties.

Six different geopolymer compositions were obtained and tested. Barley ash (BA) and wood ash (WA) were activated by adding 6M NaOH solution. Certain amount of NaOH solution was added to

ashes to achieve the optimal consistence of binder and to ensure proper moulding properties. The other two mixes were obtained from waste glass and calcined clay. The ratio of calcined clay and glass was kept constant at ratio 1:3. In the first mix the original roughly ground glass (ORG) was used, but in the second - additionally ground waste glass (AGW) was used. The last two mixes were combinations of both barley (BTG) or wood ashes (WTG) and calcined clay. Mix compositions are shown in Table 2.

Table 2

Geopolymer composition material ratios

Material	Material ratios in composition					
	WA	BA	OWG	AGW	BTG	WTG
Wood ash	1	-	-	-	-	1
Barley ash	-	1	-	-	3	-
Rough Ground Glass	-	-	1	-	-	-
Additionally ground glass	-	-	-	1	-	-
Teniside	-	-	3	3	1	3
Burned clay	-	-	-	-	-	-
6M NaOH	0.407	0.405	2.08	1.65	1.9	1.41

Mixed geopolymer binder mortar was cast in 40x40x160mm bar moulds and the curing conditions were kept constant at the two different temperature regimes: at ambient temperature of 20°C±2°C and 75°C for 24h to improve the process of geopolymerisation.

Physical and mechanical properties of hardened geopolymer mortar bars were tested. Mineralogical composition of specimens was determined by using X-ray diffraction spectroscopy, but scanning electron microscopy (SEM) was used to examine structure of obtained geopolymers.

RESULTS

Samples, which were cured at elevated temperatures, were fully hardened after 24h at 75°C. Samples which were cured at ambient temperature after 24h were still soft and not solid. Samples were held in moulds for 72h to ensure mortar bar safe remoulding without damaging the sample.

It is important to note that some samples cured at elevated temperature showed high shrinkage (mix OWG) and minor cracks (WA). The reason of shrinking and cracking of specimens should be resulted by thermal shock or rapid reaction progress.

Water absorption

Water absorption of geopolymer specimens hardened in the different temperatures was tested. Water absorption of geopolymer specimens is shown in Table 3.

Table 3

Geopolymer water absorption

Composition	Water absorption, %	
	20°C	75°C
WA	13.2	12.7
BA	12.4	11.9
OWG	9.7	7.9
AGW	9.5	8.2
BTG	12.5	12.4
WTG	11.7	11.9

Specimens cured at temperature 75°C demonstrated lower water absorption compare with specimens cured at the ambient temperature. It is explained by geopolymerisation process, which is more active at elevated temperature.

The specimens made from waste glass and calcined clay (AGW and OWG), cured at elevated temperature, demonstrated lowest water absorption 8.2% and 7.9% respectively, but specimens with same composition, cured at ambient temperature showed water absorption 9.5% and 9.7%. Geopolymers containing ashes showed the highest water absorption ranging between 11.9-13.2%. Similar results showed specimens made from ashes and calcined clay (11.4-12.5%).

Compression strength

Compression strength of hardened geopolymer samples was determined. Results of compression strength are given in Figure 3. As seen in the Figure 3, the curing temperature is the key determinant factor, which divides the samples into two large groups with diverse compressive strength. Samples cured at 75°C for 24h show from 6.46-

16.36 MPa, i.e., better compressive strength results than the samples cured at ambient temperatures. The elevated temperature provides reaction or geopolymerisation process and at higher temperatures geopolymers originates much faster.

The specimens cured at ambient temperature provided compression strength from 2.7-6.8MPa. The best results were demonstrated by the geopolymers with composition OWG and AGW (6.6 and 6.8 MPa), but geopolymers which are containing ashes showed on average a 50% less compressive strength results compared to the samples with glass and calcined clay.

At the curing temperature of 75°C the compression strength for geopolymer mixes demonstrated larger variety of results. The best strength gain was demonstrated by the AWG mix which is 23.16MPa. Barley ash geopolymer composition strength grew to 13.5MPa and wood ash geopolymer strength – 9.8MPa.

Geopolymer containing ashes in the composition with calcined clay provided strength results similar to the specimen without clay minerals. In the mix with wood ashes the compression strength was 9.16MPa and the mix with barley ash - 13.7MPa.

XRD analysis

Mortar bars were tested with X-ray laser diffraction spectroscopy to characterize geopolymer mineralogical composition.

Geopolymers are often described as ‘X-ray amorphous’ (Duxon et al., 2006). Although this material appears amorphous to XRD initially, evidence of crystalline phase can be observed. XRD results are given in Figure 4 and 5.

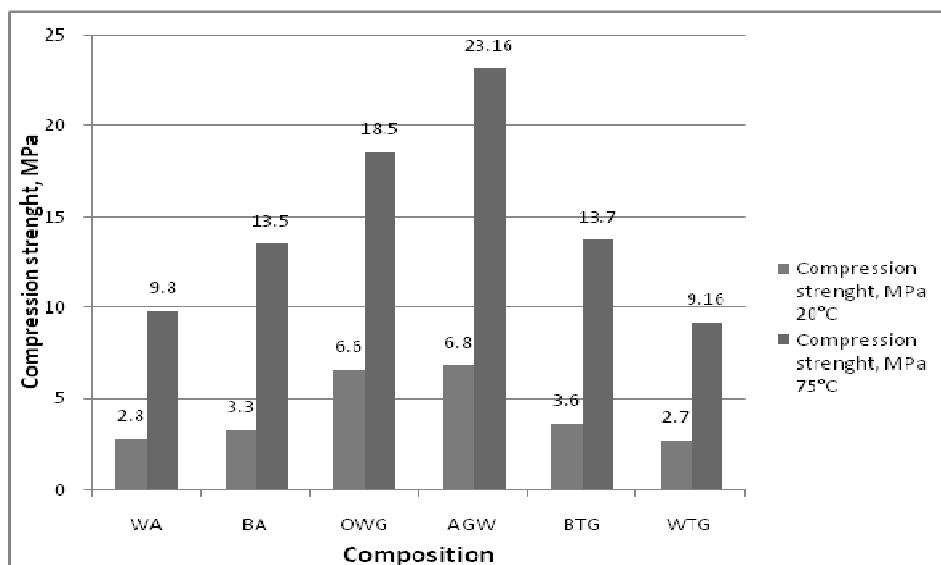


Figure 3. Compression strength results for geopolymer specimen cured at ambient temperature and 75°C.

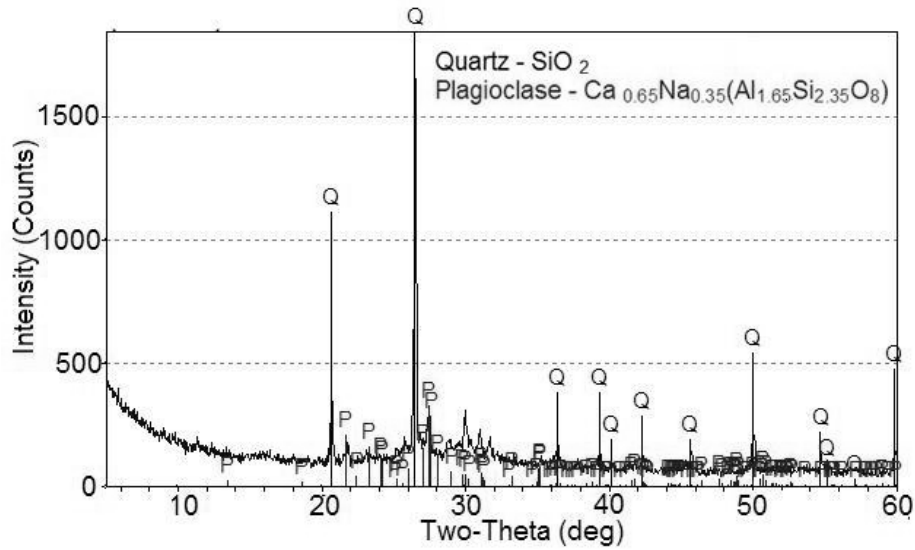


Figure 4. XRD diffractogram of hardened specimen contained wood ash (WA)

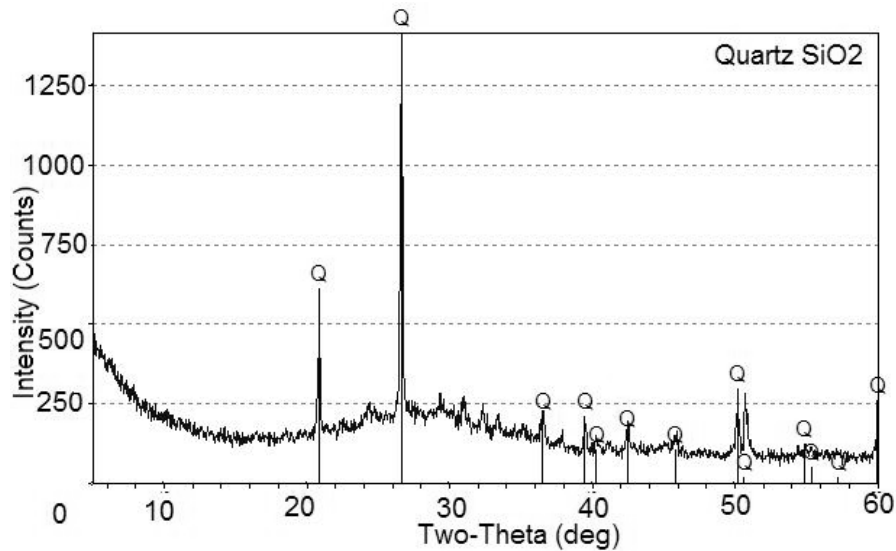


Figure 5. XRD diffractogram of hardened specimen contained additional ground glass waste (AGW)

Amorphous and crystalline quartz phases appear in all geopolymer mix compositions. Presence of plagioclase minerals was characteristic only to geopolymers containing wood ash. Quartz minerals are typical for geopolymers containing waste glass and calcined clay.

Scanning electron microscope analysis

Scanning electron microscope (SEM) analysis was performed in order to study the microstructure and to view the reacted and unreacted region of the geopolymer's samples. SEM analysis results of specimen with additional ground glass and calcined clay are given in Figure 6, but in the Figure 7 is shown microstructure of geopolymer specimen made from wood ash.

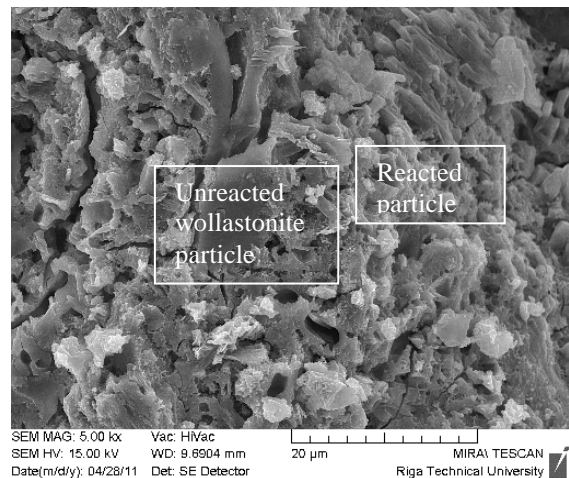


Figure 6. SEM image of hardened geopolymer contained additional ground glass (AGW).

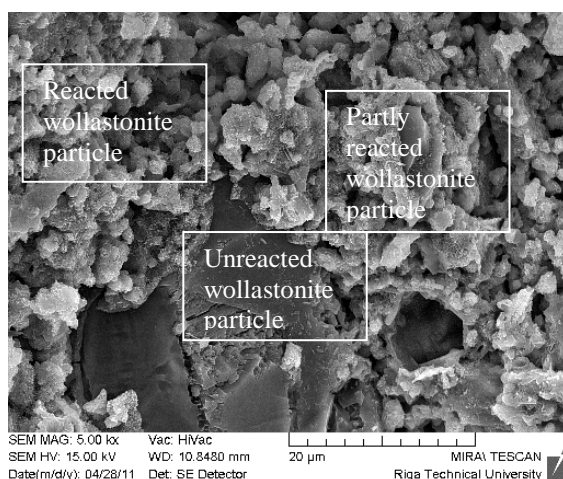


Figure 7. SEM image of hardened geopolymer contained wood ash (WA).

Annotated SEM micrographs of geopolymer show a highly complex product morphology that consists of unreacted, partially reacted, and completely reacted materials. The geopolymer matrix also includes quartz crystals and mullite needles.

Unreacted wollastonite minerals can be observed in the both figures. Typical pore structure for a geopolymer is nonuniform with a wide size distribution (Figure 6 and 7). It is confirmed also by Waltrud (2008).

DISCUSSION

Waste materials examined in this work proved to be an appropriate material for development of geopolymers. Industrial waste and by-products like different types of ashes obtained as bottom ash from thermal furnaces could be used in geopolymer composition as a secondary raw material when the bottom ashes are ground to fine particles.

Additional grinding of the glass made the material more reactive thus accelerating the reaction process and gaining additional strength.

Mixes with ashes and composition with ashes and calcined clay did not demonstrate as high result as the samples with glass and calcined clay composition. However an increase in strength is considerable from the temperature regime aspect.

REFERENCES

- Davidovits J. (2008) *Geopolymer Chemistry and Applications*. Saint-Quentin: Institut Géopolymère.
- Davidovits J. (1991) Geopolymers — inorganic polymeric new materials. *J. Therm. Anal.*, Vol. 37, No. 8, p. 1633–1656.
- Duxson P., Fernandez-Jimenez A. Provis J.L. Lukey G.C. Palomo A. Van Deventer J.S.J. (2007) Geopolymer technology: the current state of the art. Springer, *Advances in geopolymer science & technology. J Mater Sci*, No. 42, p. 2917-2933.

This work proved the importance of the temperature level. After 24h curing at ambient temperature geopolymer specimen were slightly hardened. Samples cured at 75°C for 24h were completely hardened and showed good compression strength results.

To reduce thermal shock during curing at elevated temperature, the temperature regime should be better studied in order to reduce geopolymers shrinkage and cracking.

A lot of research is still required to further investigate geopolymer binder properties and material characteristics. The economic aspect must be taken into account as well as mix design optimisation should be carried out.

Lack of appropriate standards and test procedures prevents geopolymer binders from wider application therefore in order to test new material samples mortar and concrete standards and methods should be developed.

Further investigations should include geopolymer-sand mortar tests at different curing temperature regimes and mix designs.

CONCLUSIONS

Water absorption for obtained geopolymers varied from 7.9-13.2% where the lowest water absorption value was for heat cured OWG specimens.

Geopolymers cured at ambient temperature showed compressive strength in the range 2.7-6.8 MPa. This proves that ambient temperature does not provide the rapid geopolymerisation process.

Specimens cured at elevated temperature showed significant increase of the compression strength. It varied from 9.16 to 23.16MPa. The best compressive strength results were achieved by mixes containing rough ground (OWG) and additional ground glass (AGW): 18.5 MPa and 23.16 MPa.

According to XRD amorphous and crystalline quartz phases appear in all compositions of geopolymers.

SEM micrographs of geopolymers show a highly complex morphology of microstructure which consists of unreacted, partially reacted, and completely reacted materials.

Duxson P., Provis J.L., Lukey G.C., J.S.J. van Deventer. The role of inorganic polymer technology in the development of 'Green concrete'. *Cem. Concr. Res.* , Vol. 37, No. 12, p. 1590–1597.

Gartner E. (2004) *Cem Conc Res*, No. 34, p. 1489.

Glukhovskiy V.D. (1959) *Soil silicates*. Kiev: Gosstroyizdat. 154 p.

Juenger M.C.G., Winnefeld F., Provis J.L., Ideker J., Advances in alternative cementitious binders. *Cem Concr Res* (in press), DOI 10.1016/j.cemconres.2010.11.012.

Luna Y., Querol X., Antenucci D., Jdid El-Aid, Fernandez Pereira C., Vale J. (2007) Immobilization of a metallurgical waste using fly ash-based geopolymers. 2007 World of Coal Ash, May 7-10, 2007, Covington, Kentucky, USA.

Waltrud M., Kriven, Bell J.L. (2008) Effect of alkali choice on geopolymer properties. *28th International Conference on Advanced Ceramics and Composites B: Ceramic Engineering and Science Proceedings*, Vol. 25, No. 4.

ANALYSIS OF POSSIBILITIES FOR USE OF WARM MIX ASPHALT IN LATVIA

Martins Zaumanis, Juris Smirnovs
Riga Technical University, Faculty of Civil Engineering
jeckabs@gmail.com

ABSTRACT

Warm Mix Asphalt (WMA) production technologies allow lowering the production and paving temperature of the conventional Hot Mix Asphalt (HMA) by at least 20°C without compromising the performance of asphalt. This promises various benefits over HMA, for example, allows to reduce the energy consumption, thus lowering the greenhouse gas emissions, permits to extend the paving season, attain better compaction, provides longer haul distances etc. However, in order to reach widespread implementation of WMA, it is necessary to provide enough information to the decision makers on the benefits of this technology. The article presents an overview of different WMA products and production principles, benefits and drawbacks associated with the technologies. A total of fifteen products that were found to be used in Europe are reported in the paper. However, not all of the technologies are suitable for Latvia, because of the necessary economical investments, climate, local legal provisions and the industry traditions. Potentially most favourable technologies for Latvian circumstances are analysed with the reference to local road specifications.

Key words: Warm Mix Asphalt (WMA), greenhouse gases

INTRODUCTION

WMA is a relatively new technology that allows significant lowering of the production and pavement temperature of conventional hot mix asphalt (HMA) without compromising the performance of the pavement. The temperature reduction range varies depending on what WMA product is used, but the common classification of asphalt by the production temperature is presented in Figure 1.

WMA promises various benefits, e.g., reduced greenhouse gas emissions, lower energy consumption, improved working conditions, lower binder viscosity, better compaction, etc. These

technological advantages of WMA allow using it not only as a substitute for conventional HMA by applying the same asphalt specifications, but also to use it in circumstances, where the usage of HMA would not be eligible. However, in order to reach widespread implementation of WMA, it is necessary to provide enough information to the decision makers on the benefits of this technology and ensure that the asphalt has the same or better mechanical characteristics and long-term performance as HMA.

The article is based on the Master thesis by Martins Zaumanis at the Danish Technical University, published as a monograph (Zaumanis, 2011).

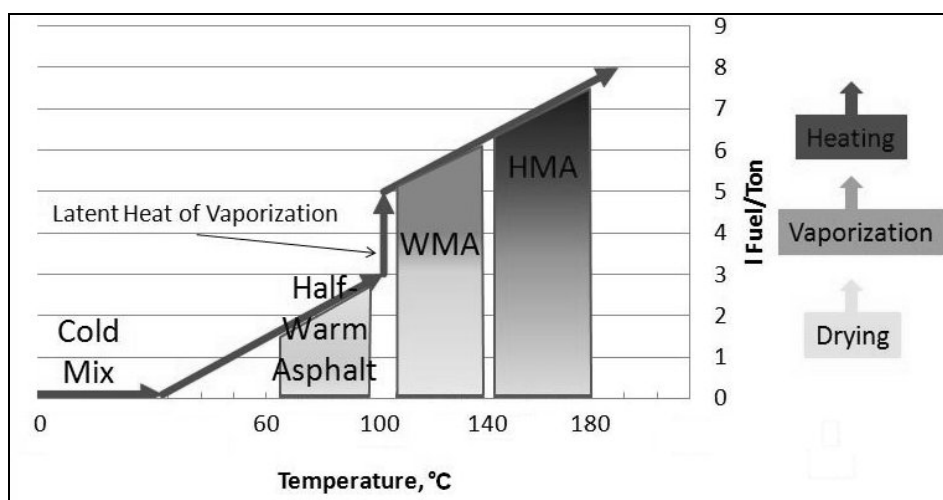


Figure 1. Asphalt classification by production temperature.

WMA PRODUCTION TECHNOLOGIES

The existing WMA production technologies can be categorised in three groups:

1. Foaming technologies;
2. Organic or wax technologies;
3. Chemical additives.

The most widely used products available in the European market and their descriptions are listed in Table 1. The reported values of the production temperatures were not the same in all the literature

reports, therefore the most commonly reported data or data supported by the production company are listed first and the data from a different research - afterwards. Differences in the reports may be caused by different factors, such as the production technology, type and the amount of additives used, mix design methods, climatic conditions, material use, etc. The amount of WMA additive usually depends on the materials used, their proportion and especially the grade and type of the bitumen used.

Table 1

Common WMA Technologies in Europe

Product	Company	Description	Reports from countries	Additive	Production temperature [or reduction ranges]
FOAMING TECHNOLOGY					
Low Energy Asphalt	LEACO	Water based Hot coarse aggregate mixed with wet sand	US; France, Spain, Italy	Yes, $\pm 0.5\%$ of bitumen weight of coating and adhesion additive	$\leq 100^{\circ}\text{C}^*$ 105-124°C
WAM-Foam	Shell and Kolo- Veidekke	Foaming process using two binder grades	US, Norway	Antistripping agents could be added to soften binder	110-120°C* 100-120°C. 62°C
LEAB	BAM	Water based Mixing of aggregates below water vaporization	Netherlands	0.1% of bitumen weight of coating and adhesion additive	90°C
LT Asphalt	Nynas	Water based Binder foaming + hydrophilic filler	Italy, Netherlands	0.5-1.0% of hygroscopic filler by mixture weight	90°C
Aspha-Min	Eurovia	Water containing Zeolite	US; France, Germany	0.3% by mixture weight	[30°C]* [12°C] [20-30°C]
ORGANIC TECHNOLOGY					
Sasobit	Sasol	Fischer-Tropsch wax	US, EU, worldwide	2.5-3.0% of bitumen weight in Germany 1-1.5% of bitumen weight in US	[10-30]* [20-30°C] [18-54°C] 130-150°C
Asphaltan A Romonta N	Romonta GmbH	Montan wax for mastic asphalt	Germany	1.5-2.0% of bitumen weight	[20°C]
Asphaltan B	Romonta GmbH	Rafined Montan wax with fatty acide amide for rolled asphalt	Germany	2-4% by mixture weight 2.5% by mixture weight	[20-30°C]
Licomont BS 100	Clariant	Fatty acid amide	Germany	3% of bitumen weight	[20-30°C]

Product	Company	Description	Reports from countries	Additive	Production temperature [or reduction ranges]
3E LT or Ecoflex	Colas	proprietary	France	Yes, not specified	[30-40°C]
CHEMICAL TECHNOLOGY					
Evothem ET	Mead-Westvaco	Chemical bitumen emulsion	US, France, worldwide	In form of bitumen emulsion	[50-75°C]* [37-54°C] >93°C. 85-115°C
Evothem DAT	Mead-Westvaco	Chemical package plus water	US, France, worldwide	30% by weight of binder	[45-55°C]* >93°C. 85-115°C
CECABAS E RT	CECA Arkema group	Chemical package	US, France	0.2-0.4% by mixture weight	120°C* 101°C
Rediset WMX	Akzo Nobel	Cationic surfactants and organic additive	US, Norway	1.5-2% of bitumen weight	[≥30°C]* [16°C] 126°C
Warmmix L	Star Asphalt	Amide based chemical package	France, Italy, East. Europe	0,5% of bitumen weight	[30 °C]*

*Temperature range from the product supplier

Foaming technology

Foaming technologies use small amounts of cold water injected into the hot binder or directly in the asphalt mixing chamber. The water rapidly evaporates and is encapsulated in the binder, producing a large volume of foam. The foaming action in the binder temporally increases the volume of the binder and lowers the viscosity, which improves the coating and workability. In the foaming processes enough water must be added to cause the foaming action without adding too much, so that stripping problems arise. To ensure this, most of the producers advise to use antistripping (adhesion, coating) additives to ensure that moisture susceptibility of an asphalt mixture is minimized. Liquid antistripping additives are recommended for WMA production processes (D'Angelo et al, 2008; Chuwdhury et al., 2008). They are added to the binder just before mixing with aggregates, typically 0.5% by the weight of the binder.

There are several foaming technologies available that could be sub-categorised into two groups: water based and water containing (Asphalt Institute, 2007; Perkins, 2009).

The water containing technology uses finely powdered synthetic zeolite that has been hydrothermally crystallized. It contains about 21 percent water of crystallization which is released when temperature is increased above 85°C. When the additive is added to the mixture simultaneously with the binder, water is released as fine mist, which

foams the binder. Controlled foaming effect of 6 to 7 hours of increased workability is reported (Chuwdhury et al., 2008; D'Angelo et al., 2008; Drüschner, 2009).

Water based technologies use a foaming process which is created by injecting cold water into hot asphalt binder using special equipment or technology. The water rapidly evaporates, producing a large volume of foam, which slowly collapses (Asphalt Institute, 2007; Perkins, 2009).

It is considered that these technologies are the most technically complex and require relatively large financial investments for plant modification. There are also some concerns on the moisture susceptibility and permanent rutting of asphalt produced by these technologies. These are pressing problems in Latvia even for HMA, therefore, it is considered that thorough research and laboratory testing is necessary before implementing these technologies in Latvia.

Organic technology

Organic or wax additives are used to achieve the temperature reduction by reducing the viscosity of the binder at the production temperature. The processes show the decrease of viscosity above the melting point of wax, making it possible to produce asphalt mixes at lower temperatures. After crystallisation, waxes tend to increase the stiffness of the binder and the resistance of asphalt to deformation. The type of wax must be selected

carefully so that the melting point of the wax is higher than expected in service temperatures and to minimize embrittlement of the asphalt at low temperatures (D'Angelo et al., 2008; Perkins, 2009).

Different researches (for example (Zaumanis et al., 2010; Hurley et al., 2006)) show that WMA that is produced using waxes often has better resistance to plastic deformation than the traditional HMA. This performance can be explained by forming of the lattice structure in bitumen below the crystallisation point of wax. This process stiffens the binder and increases the resistance to permanent deformations of asphalt.

Waxes are also often used as additives to improve the resistance to deformation and to improve the workability of the mixture for the traditional HMA. Keeping in mind that there are considerable problems with the resistance to permanent deformations in Latvia it is considered that waxes may be successfully used for the production of WMA here.

Chemical additives

A variety of chemical packages are used for different products. They usually include a combination of emulsification agents, surfactants, polymers and additives to improve the coating, mixture workability, and compaction, as well as adhesion promoters (antistripping agents). The added amount and temperature reduction depends on the specific product used. The chemical additive package is used either in the form of an emulsion or added to bitumen in the mix production process. This results in relatively minor modifications needed to the asphalt plant or to the mix design process (Chuwadhury et al., 2008; Perkins, 2009).

BENEFITS AND DRAWBACKS OF WMA

WMA technologies promise a number of benefits, when used. They can vary depending upon which specific WMA technology is used. However, generally the benefits can be categorized in four groups:

- Environmental;
- Production;
- Paving;
- Economic.

The concerns are mostly subjected to a relatively short WMA implementation period and insufficient accessibility of in-situ performance results. The test results in laboratory show some potential problem areas that should be given care to when designing and using WMA. They will be discussed later.

Environment and production

The most important benefit of WMA is the possibility to reduce the greenhouse gases in the

atmosphere. This is realized through reduced temperature for production and paving of asphalt. The ranges of possible energy reduction in the production process reported in the research (Kristjansdottir, 2007) are:

- WAM Foam – 30% to 40%;
- Aspha-Min – 30%;
- Sasobit – 20%;
- Evotherm – 50% to 70%.

According to the research (D'Angelo et al., 2008), this gives a plant stack emission reduction of:

- CO₂ in the range of 15% to 40%;
- SO₂ – 20% to 35%;
- volatile organic compounds (VOC) up to 50%;
- carbon monoxide (CO) – 10% to 30%;
- nitrous oxides (NO_x) – 60% to 70%.

The reduction of aerosols, fumes and dust is also beneficial to the worker health and to the people in the surrounding territories of production and paving sites. This may mean easier permission for a plant site in urban areas. The actual reduction in each specific case depends primarily on the temperature reduction rate and according to (Brosseaud et al., 2008) greenhouse gases (CO₂, N₂O, and CH₄) are reduced in the same proportion as the energy gain, which is illustrated in Figure 1. Reduction of fuel used for asphalt production results also in reducing the demand of non-renewable fuel extraction and dropping the carbon footprint of fuel production and transportation.

Because of the different production technology for WMA, it promises several benefits that are indirectly related to the reduction of atmospheric pollution. Lower mixing temperatures and the modification of bitumen results in different visco-elastic behaviour of the binder in the WMA technology pavements. Less aging during the production and paving process tends to improve the pavement flexibility, which reduces susceptibility to fatigue and temperature cracking. This results in the improvement of the pavement longevity (life cycle), further reducing the potential costs for restoring the asphalt overlay (Perkins, 2009). Lowering of bitumen viscosity in the production process allows incorporating a higher percentage of reclaimed asphalt pavements (RAP). Even up to 90% of RAP is reported in the research (Drüschner, 2009) and WMA still results in less effort needed for compaction, which means additional energy saving realized in the paving process. The overall benefit of RAP usage is the resolving of the problem of RAP utilisation, saving of landfill space, reduction of virgin aggregates and energy used for mining.

It must be noted that some of the environmental benefits may be offset with the carbon footprint embodied for producing additives and/or any additional equipment supporting the production of WMA. The producers of two WMA additives were contacted. None of them were able to provide the

necessary information of the amount and types of energy used in the production of these products or the amount of the greenhouse gases produced.

Paving

Improved workability and compaction are attained when using WMA. Lower paving temperature enhances the working conditions for the paving crew, which means enhanced productivity and improved quality. The reduced viscosity decreases the risks of ensuring the necessary compaction, especially when working in cold weather and, because the difference between the mix and ambient temperature is smaller than for HMA, a longer compaction window is provided. It may permit a longer paving season and/or paving during nights. Additionally, producing WMA at HMA temperatures will permit even longer compaction time. The Latvian road specifications (LVC, 2009) permit paving of asphalt wearing course only when the temperature is higher than 10°C (for layers between 40-60mm) or higher than 15°C (for layers <40mm). These temperatures are usual for Latvia only from April to September (Latvijas vides, ģeoloģijas un meteoroloģijas centrs, 2011). Use of WMA additives could allow extending the paving season by several months thus ensuring a significant economical effect for contractors. It is reported (D'Angelo et al., 2008) that field trials were conducted in Germany with Sasobit at ambient temperatures ranging from +1°C to +3°C and better density was achieved if compared to HMA mixture. Similarly to cold weather paving, because of the possibility to compact the mixture in lower temperature, longer haul distances are promised for WMA. Therefore, producing WMA technology mixtures at the temperatures traditional for HMA, more distant sites and large urban areas like Riga can be served from large distances without losing workability. This means expanded market areas and

a reduced asphalt cost due to the decrease in the mobilisation expenses. Another benefit for the city or high maintenance roads that need to be opened for traffic as soon as possible is that faster putting into operation times can be achieved. Since the initial temperature is significantly lower, less time is necessary for cooling the mixture. This can also be important for expanding airports, like the International Airport of Riga, where the stretch of time for construction can be very tight.

Economical

Different techniques of producing Warm Mix Asphalt (WMA) promise various energy savings for the production - this mostly depends on how much the production temperature was lowered and what kind of fuel is used. The economical benefit from the energy savings should be discussed together with the cost and type of the energy used, as higher energy prices promise greater savings. Indirect economical effects can be realized through the reduction of the mobilization costs and longer paving season. Another indirect benefit is less wear on the asphalt plant due to the reduced temperature. Economical benefits should be evaluated together with environmental benefits. If stricter emission standards are implemented, there may be higher economical potential for WMA. In this case the potential benefits may not be completely economically quantifiable and should be evaluated together with environmental regulations. The savings with reduced energy consumption may be offset by the additional costs of WMA production technologies. It must be established if the reduced energy consumption reduces the overall costs of WMA production in each specific case. If no proof on production cost lowering is established, it may be possible that contractors will not choose this technology for the other benefits alone.

Table 2

Additional costs for some of WMA products

Parameter	WAM Foam	Aspha-min	Sasobit	Evotherm
Equipment modification or installation costs	\$30,000-\$70,000	\$0-\$40,000	\$0-\$40,000	Minimal
Royalties	\$15,000 first yr \$5,000 plant/yr 0.30/ton	None	None	None
Cost of material	N/A	\$1.3/kg	\$1.7/kg	7-10% more than asphalt binder
Recommended dosage rate	N/A	0.3% by weight of mix	1.5 to 3.0% by weight of binder	Use in place of bitumen
Approximate cost per ton of mix	\$0.30 (not incl. royalties)	\$3.60	\$1.30-\$2.60	\$3.50-\$4.00

Potential increases depend on production techniques as different WMA technologies require different additional costs. Increase in costs may arise from:

- the investment and the depreciation of plant modification;
- the costs of the additives;
- possible costs for technology licensing.

The research (Kristjansdottir, 2007) involves comparison of possible additional expenses for WMA production (Table 2).

The data are gathered from different research and therefore using different production plants and other specific conditions. However, it gives a good impression on the additional costs of different WMA technologies.

CONCERNS ON WMA PERFORMANCE

In order to reach widespread implementation of WMA, it is necessary to ensure that the asphalt has the same or better mechanical characteristics and long-term performance as HMA. WMA has been used in all types of bituminous mixtures, including dense graded, stone mastic, porous, and mastic asphalt. It has been used with different aggregates and all grades of binder as well as polymer modified bitumen and Reclaimed Asphalt Pavement (RAP), and a variety of layer thicknesses and traffic levels have been applied for WMA. Based on these findings, there are generally no restrictions on WMA implementation. However, there is some concern about some mechanical properties and longevity of WMA.

Permanent deformations

There is a general concern for WMA rutting performance that is connected with the decreased mixing temperature which may lead to incomplete drying of aggregates and insufficient coating with bitumen.

Another aspect that may influence decreased resistance to permanent deformations is the decreased oxidative hardening of bitumen due to the lower production and compaction temperature. These problems might be treated with adding active adhesion agents or initially choosing a harder bitumen grade.

Potential rutting problems require careful evaluation of asphalt in laboratory. Care should be given to preparation of the testing samples, because there might be a necessity for mixture aging before compaction to ensure proper correlation with the actual production process. The choice of the right compaction method might also be a problem, because some methods might not be sensitive enough to temperature changes.

The WMA that is produced by treating bitumen with wax usually shows better resistance to deformations than the reference HMA. This can be explained by forming of the lattice structure in

bitumen below the crystallisation point of wax, which stiffens the asphalt at in-service temperatures.

Moisture sensitivity

Due to low mixing temperatures, the moisture contained in the aggregate may not completely evaporate during mixing and the retained water in the aggregates could lead to increased susceptibility to moisture damage. Because of residual moisture left behind by the microscopic foaming process, this is even more critical for WMA technologies that involve foaming as a binder viscosity lowering action. These problems, if they occur, may be successfully treated with active adhesion agents.

Low temperature behaviour

It is reported in several researches from the U.S (Wanger et al., 2008; Hurley et al., 2006; Chowdhury et al., 2008) that the use of waxes for tests with the Bending Beam Rheometer (BBR) increases the bitumen stiffness and reduces the relaxing abilities at low temperature regimes. Accordingly, wax modification leads to worsening of the low temperature behaviour and it has been determined that the threshold of SUPERPAVE concept PG bitumen leads to worsening of low temperature grade of 2-3°C and the bitumen ability to creep is worsened by 6-9°C.

Compaction

WMA is reported to have better compaction potential due to decreased viscosity and less bitumen ageing in the production process. This can allow to save the compaction energy and to reduce the time necessary for compaction which may be especially important at low temperature paving. The reduced compaction risks, if realized, carry the cost that can far exceed the additional costs for WMA production.

However, wax technologies require additional attention regarding the temperature conditions for rolling. The compaction must be finished before the wax starts to crystallize; after this temperature the wax forms a lattice structure in the asphalt that may be damaged if the compaction is continued. This means that the compaction window is shorter than for HMA and additional rollers may be required to reach the necessary density in the given time window.

WMA AND NORMATIVE

The European standards for bituminous mixtures (EN 13108-1 to -7) do not preclude the use of WMA. The standards include maximum temperatures for particular mixtures, but there are no minimum requirements. The minimum temperature of asphalt mix is declared by the

manufacturer. The standards also allow usage of additives if the performance of asphalt is equivalent to the reference mixture. Thus the European standards are not a barrier for introduction of WMA.

The Latvian Road Specifications 2010 (LVC, 2009) also allow introduction of different chemical additives, if the asphalt manufacturer can ensure the required asphalt performance and a test section of 2 lanes in 50 m length to prove this has been built. The production temperature is precluded and depends on the bitumen type. For example, for 70/100 bitumen it is 140°C-180°C. At the moment only for asphalt with polymer modified bitumen it is allowed to define different temperature. However, the work group that develops the newest redaction of the Latvian Road Specifications has proposed to remove this provision, therefore, this will no longer be an obstacle when the new document is approved.

CONCLUSIONS

The most significant advantage of the use of WMA is, of course, the possibility to reduce the use of fuel and thus cut the carbon footprint of the asphalt industry. The results show, for example, the possible direct savings of CO₂ in the range from 15% to 40% and other indirect environmental benefits. The mechanical properties of WMA show that it has a potential to replace the conventional HMA and in special circumstances it even has advantages over HMA. However, despite the promising performance in comparison with HMA, this technology has not yet gained acceptance in the asphalt industry, mostly because of the lack of information on the testing results. More data and in-situ case study examples that compare WMA and HMA technologies would help to overcome the caution in the road building industry for implementation of WMA. Introduction of the EN standards for WMA and national specifications that would allow adequate evaluation of WMA would

also stimulate the usage of WMA technologies.

Environmental and other benefits alone are not sufficient for widespread implementation of this technology. It must be established whether the reduced energy consumption also reduces the overall costs of WMA production. If no proof of lower production costs is established, it is most likely that contractors will not choose this technology for its other benefits alone, and WMA may not become widespread. However, the economical benefit from energy savings should be discussed together with the cost and type of the energy used, because higher energy prices promise greater savings when temperature is reduced. The prices of additives may also change when the technology becomes more widespread and finally, application of stronger environmental regulations and additional taxes for carbon footprint will also stimulate faster development of WMA technologies and usage in actual commercial projects.

The most promising specialization for WMA in Latvia at the moment is the reduced pavement compaction risks in cold weather. This could allow to extend the paving season and thus ensure decreased due dates of construction objects and additional turnover for contractors.

There are some considerations on the physically-mechanical characteristics of asphalt that have to be taken into account before switching from production of WMA to HMA. The research results show varying performance for different WMA products; therefore careful examination should be performed with the local materials and in the given climatic conditions the characteristics of a particular WMA product before implementing it into regular practice should be examined. Performance based tests are considered to be most useful for the evaluation of WMA at the desired temperature and special care should be given to the evaluation of the moisture sensitivity, permanent deformation, low temperature properties (for waxes) and stiffness.

REFERENCES

- Akzo nobel N.V. Akzo Nobel Asphalt Applications. [online] [accessed 03.03.2010]. Available: <http://www.surfactants.akzonobel.com/asphalt/newwarmmixsystem.cfm>.
- Star Asphalt S.p.A. Technical data sheet Warm-Mix L. [online] [accessed 30.03.2011]. Available: <http://www.starasphalt.com>.
- Aspha-Min GmbH. Aspha-min – The high performacne additive. [online] [accessed 05.04.2010]. Available: <http://www.aspha-min.com/asphamin-en.html>.
- Brosseaud, Y., Saint Jacques, M. (2008) Warm asphalt mixes: overview of this new technology in France. *Transport Research Arena Europe*, Paper 0309.
- CECE Arkema group. Green Road Formulation – Warm Mix Asphalt. [online] [accessed 05.04.2011]. Available: http://www.cecachemicals.com/sites/ceca/en/business/bitumen_additives/warm_coated_material/warm_coated_material.page.

Chowdhury, A., Button, J. (2008) *A Review of Warm Mix Asphalt*. Springfield, Virginia: National Technical Information Service. 75 p.

Damm, K.-W., Abraham, J., Butz, T., Hildebrand, G., Riebesehl, G. (2002) Asphalt Flow Improvers As 'Intelligent Fillers' For Hot Asphalts - A New Chapter In Asphalt Technology. *Journal of Applied Asphalt Binder Technology*, p. 36–69.

D'Angelo, John; Harm, Eric; Bartoszek, John; Baumgardner, Gaylon; Corrigan, Matthew; Cowsert, Jack; Harman, Thomas; Jamsihidi, Mostafa; Jones, Wayne; Newcomb, Dave; Prowell, Brian; Sines, Ron; Yeaton, Bruce. (2008). *Warm-Mix Asphalt: European Practise*. American Trade Initiatives. Washington, DC: U.S. Department of Transportation. 72 p.

Drüschner, L. (2009) *Experience with Warm Mix Asphalt in Germany*. Sønderborg: NVF-rapporter. p. 11-58

WeadWestvaco. Evotherm warm mix asphalt. [online] [accessed 05.04.2011]. Available: <http://www.meadwestvaco.com/SpecialtyChemicals/AsphaltAdditives/MWV002106>.

Hrley, G., Browell, B. (2005) *Evaluation of Sasobit for use in warm mix asphalt*. Auburn: National Center for Asphalt Technology. 32 p.

Hurley, G., Prowell, B. (2005) *Evaluation of Aspha-Min zeolite for use in warm mix asphalt*. Auburn: National Center for Asphalt Technology. 35 p.

Hurley, G., Prowell, B. (2006) *Evaluation of Potential Processes for Use in Warm Mix Asphalt*. Alabama: National Center for Asphalt Technology, Auburn University. 46 p.

Asphalt handbook MS-4 7th edition (2007) USA: Asphalt Institute. 358 p.

Kristjansdottir, O. (2007) Warm Mix Asphalt Technology Adoption. *NVF 33 Annual Meeting*.

Latvijas vides, geoloģijas un meteoroloģijas centrs. Meteoroloģiskie apstākļi Latvijā. [online] [accessed 02.02.2011]. Available:<http://www.meteo.lv/public/29591.html>.

LEA-CO. Low Energy Asphalt. [online] [accessed 05.04.2010]. Available: http://www.lea-co.com/lea_co/index2.php?lang=en.

LVC. *Celu specifkacijas 2010* (2009) Riga: Latvijas Valsts Celi. 239 p.

Olar, Olard, F., Heriter, B., Beduneau, E. (2008). Low energy asphalt LEA: new half-warm mix asphalt for minimizing impacts from asphalt plant to job site. *Asphalt Pavements and Environment*, p. 207-230.

Perkins, S. (2009) *Synthesis of warm mix asphalt paving strategies for use in Montana highway construction*. Montana: The state of Montana, department of transportation. 212 p.

Sasol-wax. Sasobit. [online] [accessed 08.03.2010]. Available:http://www.sasolwax.com/sasolwaxmedia/Downloads/Bitumen_Modification-p-409/Sasobit_since_1997.pdf.

U.S.Department of Transportation, Federal Highway Administration. Warm Mix Asphalt Technologies and Research. [online] [accessed 03.03.2010]. Available: <http://www.fhwa.dot.gov/pavement/asphalt/wma.cfm>.

Shell bitumen. Shell WAM Foam process. For reducing energy consumption and emissions. [online] [accessed 05.04.2010].

Available: http://www-static.shell.com/static/bitumen/downloads/business/shell_wamfoam_brochure.pdf.

Wanger, M., Stangl, K., Blab, R. (2008) Fischer-Tropsch paraffin modified bitumen - performance parameter and reduction of energy consumption. *Asphalt pavements and environment*, p. 197-206.

Zaumanis, M. (2011) *Asphalt is Going Green*. Saarbrücken: LAP LAMBERT Academic Publishing GmbH & CO. 101 p.

Zaumanis, M., Haritonovs, V. (2010) Research on Properties of Warm Mix Asphalt. *Scientific Journal of Riga Technical University, Construction Science*. p. 77-84.

RESEARCH OF INFLUENCE OF TRADITIONAL AND NONTRADITIONAL ADMIXTURES ON MORTAR AND CONCRETE

Vincas Gurskis, Karolis Bunevičius, Rytis Skominas

Lithuanian University of Agriculture,
Department of Building Construction
vgurskis@hidro.lzuu.lt; rytis.skominas@lzuu.lt

ABSTRACT

During the research the influence of several traditional and nontraditional admixtures on mortar/concrete was investigated. Plasticizers were used as traditional admixtures and dishwashing liquids – as nontraditional ones. The influence of admixtures was established according to the properties of cement paste, fresh mortar /concrete, hardened mortar/concrete. The results show that all analyzed additives are plasticizing but the nontraditional admixtures have the side-effect (air entraining effect). Due to this effect the water absorbability of mortar/concrete increased; the density and strength of mortar/concrete decreased.

Keywords: concrete/mortar, plasticizer, dishwashing liquid

INTRODUCTION

Nowadays, ninety-nine of hundred concretes and mortars are made using admixtures (Hewlett, 1989). Admixtures are mineral or organic materials, which are used for the preparation of concrete or mortar. The purpose of these materials is the regulation of solidification and technological properties of concrete/mortar. Admixtures can increase the workability, reduce the water content of fresh concrete/mortar, speed up or speed down the hydration of the concrete/mortar, increase the strength and durability, reduce damage during freeze-thaw cycles of hardened concrete/mortar.

Generally, admixtures are aqueous solutions made from mineral or organic materials. There are two types of admixtures which are used for mixtures with mineral binder (cement, lime, gypsum): mineral and chemical. Mineral admixtures are materials in the form of powder, which are added to the mix to improve the properties of the mixture or as a replacement for binder. Chemical admixtures are chemical materials that are added to mixtures in negligible quantity and which have special effectiveness. The effectiveness of admixture is characterizing the ability to change the properties of the mixture or hardened material without harmful effects. Mostly chemical admixtures are materials in the form of fluid but sometimes they can be in the form of powder. The concentration of admixtures in the fluid form describes the quantity of the active substance, which determines the effectiveness. The effectiveness can be evaluated in various values. For example, the effectiveness of plasticizers is evaluated by the reduction of the water amount for mixture in percents.

Chemical admixtures can bring a harmful effect (retard the solidification and hardening, cause the corrosion of concrete or reinforcement, reduce the strength) in mixtures. Due to this effect chemical

admixtures are used only under the recommended proportions of the producers.

Admixtures of analogical purpose are produced in many countries with different branded titles. These materials are relatively expensive, therefore, sometimes cheaper nontraditional materials (dishwasher liquids), which have a plasticizing effect on concrete/mortar, are used in local building as well. A lot of experimental researches concerning traditional plasticizers (Alsayed, 1998; Green et al., 1999; Paivaa et al., 2009) were carried out, but the influence of nontraditional materials on the properties of fresh and hardened concrete/mortar was not investigated.

The aim of the present work is to research and compare the influence of traditional and nontraditional admixtures on concrete and mortar.

MATERIALS

During the research plasticizers STACHEPLAST 125 (based on lignosulfonates) and Glenium ACE 430 (based on polycarboxylic ethers) were used as traditional admixtures and dishwashing liquids BANGA, TOMIK and FAIRY were used as nontraditional admixtures. The latter admixtures are often used by Lithuanian builders, which work by business license.

Mortar was prepared using the Portland cement CEM II/A-LL-42,5N, natural sand (fraction 0...4 mm) and water. Sand and water meet the requirements described in the European standards EN 13139:2002 and EN 1008:2002.

Concrete was prepared using the Portland cement CEM II/A-LL-42,5N, natural gravel (fraction 4...16 mm), natural sand (fraction 0...4 mm) and water. Gravel, sand and water meet the requirements described in the European standards EN 12620:2002+A1:2008 and EN 1008:2002.

TEST METHODS

In order to compare the effectiveness of admixtures the concentration was estimated by the desiccation method according to the European standard EN 480-8:1996.

The admixtures were dozed under dry material up to 2 % (from cement mass). The amount of water (for the achievement of the normal consistency of cement paste) was estimated according to the European standard EN 197-2:2000.

The consistency of fresh concrete was estimated according to two methods: Slump-test (EN 12350-2:2009) and Flow table test (EN 12350-5:2009). The consistency of fresh mortar was evaluated by the embed depth of standard cone (height 150 mm, angle of spike 30°, mass with stick attached to base 300±2 g), according to LST L 1346:2005.

The density, compression strength and water absorbability of hardened concrete were established

according to standard methods (EN 12390-7:2009, EN 12390-3:2009, EN 13369:2004). The size of the tested concrete specimens was 100×100×100 mm with the age of 28 days. In order to evaluate the water absorbability, compression and flexural strength of mortar, the specimens (40×40×160 mm) were prepared and tested after 28 days by standard test methods (EN 196-1:2007).

RESULTS AND DISCUSSION

The concentration (amount of dry materials) test results (Table 1) show us, that the differences between the used admixtures are more than 3 times. The effectiveness of admixtures was established according to the amount of water necessary for normal consistency of cement paste (Table 2). The paste was prepared using only water and water with 0.5; 1.0; 2.0 % (from cement mass) of admixtures.

Concentration of admixtures

Table 1

Admixture	Concentration %
STACHEPLAST 125	37.9
Glenium ACE 430	27.7
BANGA	8.9
TOMIK	10.7
FAIRY	11.4

Amount of water necessary for normal consistency of cement paste

Table 2

Admixture/Amount of admixture, %	Amount of water, %	Coefficient of effectiveness
Without admixture	29.00	1.00
Glenium ACE 430	0.5	0.84
	1.0	0.78
	2.0	0.69
BANGA	0.5	1.05
	1.0	0.92
	2.0	0.84
TOMIK	0.5	0.96
	1.0	0.88
	2.0	0.76
FAIRY	0.5	0.96
	1.0	0.88
	2.0	0.89

Slump and flow table test results

Table 3

Admixture used	Slump, mm	Coefficient of effectiveness	Slump class	Flow, mm	Coefficient of effectiveness	Flow class
Without admixture	16	1.00	S1	378	1.00	F2
Glenium ACE 430	205	12.81	S4	510	1.35	F4
BANGA	62	3.88	S2	425	1.12	F3
TOMIK	49	3.06	S2	398	1.05	F2
FAIRY	185	11.56	S4	425	1.12	F3

Table 4

Test results of fresh concrete density

Admixture used	Density of fresh concrete kg/m ³	Coefficient of effectiveness
Without admixture	2374	1.00
Glenium ACE 430	2380	1.00
BANGA	2185	0.92
TOMIK	2120	0.89
FAIRY	2110	0.89

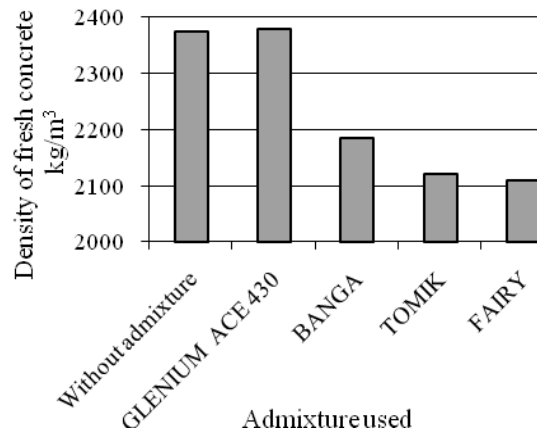


Figure 1. Dependency of used admixtures (0.5 % from cement mass) on density of fresh concrete.

The test results confirm the effectiveness of the traditional admixtures Glenium ACE 430 and STACHEPLAST 125. These materials reduced the amount of water most of all (18-31 %). The effect of the nontraditional admixtures is less: the dishwashing liquid BANGA reduced the amount of water by 16 %, TOMIK – by 24 % and FAIRY – by 11 %.

Test results of fresh concrete

In practice it was confirmed that nontraditional admixtures increase the plasticity of concrete/mortar. It is the main reason for the use of admixtures in building. The effect of admixtures on the properties of fresh and hardened concrete was estimated on mixture made from cement ($c=380$ kg/m³), water ($w = 180$ kg/m³), natural gravel (940 kg/m³) and sand (900 kg/m³). The ratio of cement and water was $w/c=0.47$. The consistency of fresh concrete was estimated by slump and flow table test methods using 0.5 % (from cement mass) of the admixture (Table 3).

The test results show that all admixtures increase the plasticity of fresh concrete. The most effective admixtures are GLENIUM ACE 430 and FAIRY, which increased the slump more than 10 times.

The effect of admixtures to the flow of fresh concrete is less expressed in comparison with the slump. Glenium ACE 430 increased the flow most of all (35 %). According to the test results of fresh concrete density it is seen that some admixtures (especially nontraditional) decreased this parameter

(Table 4, Fig. 1). The admixtures BANGA and FAIRY decreased the density of fresh concrete most of all (11 %). Such change is connected with the air-entraining effect.

Test results of hardened concrete

With the decrease of the density of fresh concrete, which was modified with nontraditional admixtures, let us assume that these admixtures will have a negative effect on the properties of hardened concrete. In order to approve this assumption the density, compression strength and water absorbability of hardened concrete with different admixture were established (Table 5, Fig. 2, 3).

The results show us that all nontraditional admixtures reduced the density of hardened concrete by 6÷9 % and compression strength by – 38÷53 %. We can see an opposite effect with the traditional admixture Glenium ACE 430. This admixture increased the density by 2 %, compression strength by 1 % and water absorbability decreased by 20 %. The nontraditional admixtures had a negative effect on water absorbability too. FAIRY increased it by 16 % and TOMIK – by 8 %. Such decrease of the density and compression strength of concrete modified with nontraditional admixtures is connected with the air-entraining effect, because every percent of entrained air decreases the compression strength of concrete by 6 %. The linear dependency of the concrete density on the compression strength was estimated (Figure 3).

Table 5

Test results of density, compression strength and water absorbability of hardened concrete modified with traditional and nontraditional admixtures (0.5 % from cement mass)

Admixture used	Compression strength $f_c = \beta \cdot F/A$ N/mm ² ; $\beta = 0.95$	Density kg/m ³	Water absorbability %	Coefficient of effectiveness		
				For density	For compression strength	For water absorbability
Without admixture	38.0	2380	6.21	1.0	1.0	1.0
Glenium ACE 430	38.4	2426	4.97	1.02	1.01	0.80
BANGA	22.5	2204	6.16	0.93	0.59	0.99
TOMIK	23.5	2244	6.68	0.94	0.62	1.08
FAIRY	17.7	2163	7.20	0.91	0.47	1.16

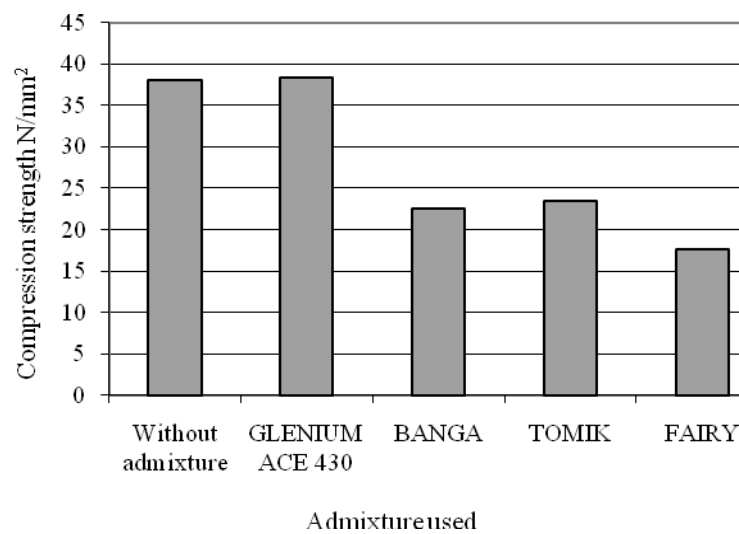


Figure 2. Dependency of used admixtures (0.5 % from cement mass) on density of hardened concrete.

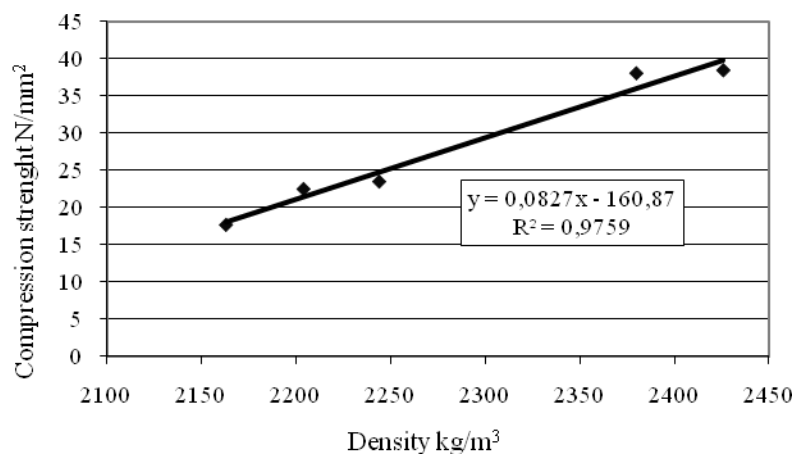


Figure 3. Dependency of concrete density on compression strength.

The test results of concrete water absorbability show us, that these nontraditional admixtures form the open pore structure of concrete, which notes

enlarged water absorbability. Therefore, the concrete will be less frost resistant.

Table 6

Test results of consistency of fresh mortar

Admixture used (0.5 % from cement mass)	Embed depth of cone, mm	Coefficient of effectiveness
Without admixture	41	1.00
STACHEPLAST 125	105	2.56
FAIRY	114	2.78
BANGA	103	2.51
TOMIK	110	2.68

Table 7

Test results of water absorbability, flexure and compression strength of hardened mortar modified with traditional and nontraditional admixtures (0.5 % from cement mass)

Admixture used	Compression strength, N/mm ²	Flexure strength, N/mm ²	Water absorbability, %	Coefficient of effectiveness		
				For compression strength	For flexure strength	For water absorbability
Without admixture	44.7	6.93	9.22	1.00	1.00	1.00
STACHEPLAST 125	36.0	6.03	8.04	0.80	0.87	0.87
BANGA	19.1	4.63	9.62	0.43	0.67	1.04
TOMIK	22.2	4.41	10.64	0.50	0.64	1.15
FAIRY	15.6	4.01	10.22	0.35	0.58	1.11

Test results of mortar

In order to estimate the influence of traditional and nontraditional admixtures on fresh and hardened mortar the mixture (1 part of cement, 3 parts of natural sand and 0.44 part of water) was made. The ratio of cement and water was $w/c=0.44$. The amount of admixtures made 0.5 % from the cement mass. The test results (Table 6) of the consistency of fresh mortar evaluated by embed depth of standard cone show us that all admixtures increased the plasticity of mortar. The nontraditional admixture FAIRY had the best effect on this parameter (increased it by 178 %).

In order to evaluate the influence of admixtures on the properties of hardened mortar specimens (40×40×160 mm) with different admixture were made and they were tested after 28 days of solidification (1 day in the form and 27 days in water). The test results of the water absorbability, flexure and compression strength are presented in Table 7. The test results show us that nontraditional admixtures have a negative effect on the mechanical properties of mortar. The compression strength of mortar has decreased by 20÷65 % and flexure strength – by 13÷40 %. This negative effect is higher than that with hardened concrete, which is maybe connected with the different condition of solidification (mortar specimens were solidified in water and concrete specimens – in moist air). Like in concrete specimens the nontraditional admixtures increased the water absorbability of the mortar

specimens, too. This effect confirms the existence of the open pore structure. Besides, it is not advisable to solidify mortar or concrete in water using air-entraining admixtures, because in the length of time the air pores of mortar or concrete fill with water to a higher degree and raise the negative water effect on the strength of the material.

CONCLUSIONS

1. According to the amount of water necessary for normal consistency of cement paste (with traditional and nontraditional admixtures) all admixtures have a plasticizing and water reducing effect. Using 2 % (from cement mass) of nontraditional admixtures to prepare normal consistency of cement paste the amount of water reduces by 11–24 %.
2. Traditional and nontraditional admixtures increased the slump class of concrete from S1 to S4 and the flow class – from F2 to F4. The traditional admixture Glenium ACE 430 has the best effect.
3. All admixtures used in the research increased the plasticity of mortar evaluated by embed depth of standard cone up to 2.8 times.
4. Nontraditional admixtures have an air-entraining effect. Due to this the density, compression and flexure strength of concrete and mortar decreased.
5. According to the test results nontraditional admixtures are not suitable to concrete and masonry mortar for load-bearing structures due to the decreasing strength.

REFERENCES

- Alsayed S. H. (1998) Influence of superplasticizer, plasticizer, and silica fume on the drying shrinkage of high-strength concrete subjected to hot-dry field conditions. *Cement and Concrete Research*, Vol. 28, No. 10, p. 1405-1415.
- EN 197-2:2000 Cement - Part 2: Conformity evaluation.
- EN 197-1:2000/A1:2004 Cement - Part 1: Composition, specifications and conformity criteria for common cements.
- EN 480-8:1996 Admixtures for concrete, mortar and grout - Test methods - Part 8: Determination of the conventional dry material content).
- EN 1008:2002 Mixing water for concrete - Specification for sampling, testing and assessing the suitability of water, including water recovered from processes in the concrete industry, as mixing water for concrete.
- EN 12350-2:2009 Testing fresh concrete - Part 2: Slump-test.
- EN 12350-5:2009 Testing fresh concrete - Part 5: Flow table test.
- EN 12350-6:2009 Testing fresh concrete - Part 6: Density.
- EN 12390-2:2009 Testing hardened concrete - Part 2: Making and curing specimens for strength tests.
- EN 12390-3:2009 Testing hardened concrete - Part 3: Compressive strength of test specimens.
- EN 12390-7:2009 Testing hardened concrete - Part 7: Density of hardened concrete.
- EN 12620:2002+A1:2008 Aggregates for concrete.
- EN 13139-2:2002 Aggregates for mortar.
- EN 13369:2004 Common rules for precast concrete products.
- EN 13369:2004 Common rules for precast concrete products.
- Green K.M., Carter M.A., Hoff W.D. (1999) The effects of lime and admixtures on the water-retaining properties of cement mortars. *Cement and Concrete Research*, Vol. 29, No. 11, p. 1743-1747.
- Hewlett P.C. (1989) Cement admixtures market and usage trends. *Construction and Building Materials*, Vol. 3, No. 2, p. 92-99.
- LST L 1346:2005 Mortars for construction. Classification and specifications. (In Lithuanian).
- Paivaa H., Esteves L.P., Cachim P.B., Ferreira V.M. (2009) Rheology and hardened properties of single-coat render mortars with different types of water retaining agents. *Construction and Building Materials*, Vol. 23, No. 2, p. 1141-1146.

QUICKLIME (CaO) STABILIZATION OF FINE-GRAINED MARINE SEDIMENTS IN LOW TEMPERATURE AREAS

Peteris Skels

Department of Civil Engineering, Technical University of Riga,
peteris.skels@gmail.com

Thomas Ingeman-Nielsen, Anders Stuhr Jørgensen

Department of Civil Engineering, Technical University of Denmark,
tin@byg.dtu.dk; asj@byg.dtu.dk

Kaspars Bondars, Edmunds Skele

Department of Civil Engineering, Technical University of Riga,
kaspars.bondars@j-a.lv; edmunds.skele@rtu.lv

ABSTRACT

This study presents laboratory testing on quicklime (CaO) stabilization of fine-grained marine sediments in low temperature areas. The soil was sampled on the Fossil Plain in Kangerlussuaq, Greenland, and analyzed in the laboratory at the Technical University of Denmark (DTU). The optimum CaO content in a soil-CaO mixture was determined using a number of laboratory methods, such as pH test, consistency limit analysis, degree of compaction, and short term California Bearing Ratio (CBR) values. The study also numerically demonstrates a long term strength development of the soil-CaO mixture at 1°C and 10°C curing temperatures, comparing stabilization effectiveness between low and normal soil temperature conditions.

Key words: quicklime stabilization, pH test, CBR, soil compaction, temperature

INTRODUCTION

During the construction phase of a civil engineering project, it is of critical importance to ensure the accessibility of the heavy vehicles and equipment used on a construction site. In areas with fine-grained materials, the accessibility may be greatly reduced due to large water contents in the sediments. Furthermore, the ability to compact the material to get an optimal bearing capacity may be reduced as well, with the consequence that one may have to choose between expensive material substitution and higher maintenance costs due to subsequent settlements, structural and pavement damage.

These problems are enhanced in areas with permafrost, especially where the deposits are ice-rich and under warming. The summer thaw layer (the active layer, typically up to 3 m thick) often becomes water logged from the thaw process, and may suffer severe loss in the bearing capacity.

Thick deposits of fine-grained marine sediments exist in large areas of western Greenland. The sediments have been transported by melt-water rivers from the Greenlandic ice sheet to the fiords and sea, where it was deposited in thick sequences of silts and clays. As a consequence of the glacial retreat, the sediments were uplifted due to the isostatic rebound. Today, many of the fine-grained sediments are located above the sea-level, and now complicate construction projects in developing areas.

Most of the housing in Greenland is built directly on the bedrock or founded on point-loaded piles directly to bedrock. However, it is difficult to avoid

the mentioned soil stability problems when roads and other linear infrastructure are constructed. It is therefore of great economic and societal interest to develop methods to improve the stability of fine-grained sediments in Greenland.

There are different soil modification/stabilization methods and modifier/stabilizer types available. Lime is one of the chemical modification/stabilization agents in the form of quicklime (calcium oxide- CaO), hydrated lime (calcium hydroxide- Ca(OH)₂), or lime slurry (a suspension of hydrated lime in water, can be made from either hydrated lime or quicklime). The previous experience has shown that lime reacts with medium-, moderately fine-, and fine-grained soils to produce decreased plasticity, increased workability and strength, and reduced swell.

Lime stabilization, having started as an aid in maintenance work in temperate areas, now covers most fields in construction. This includes highways, farm-to-market roads, shoulders and parking lots as well as non-highway uses such as airport runways, building foundations, and railroad subgrades (Eades et al., 1966). Lime can be used either to modify some of the physical properties and thereby improve the quality of the soil or to transform the soil into a stabilized mass, which increases its strength and durability (*Military Soil Engineering*, 1992). The reaction between lime and soil can be described as a series of chemical reactions. When lime is added to a clayey soil, it must first satisfy the affinity of the soil for lime, i.e., ions are absorbed by clay minerals and are not available to the stabilizing reactions until the affinity is satisfied

(Bell, 1996). Thus, more lime is normally needed for soil stabilization, than for soil modification.

The optimal lime amount is determined by several measuring procedures such as pH test, degree of plasticity, soil compaction properties. Soil compaction is one of the most critical components in the construction of roads, airfields, embankments, and foundations. The durability and stability of a structure are related to the realization of proper soil compaction, thus the optimal lime amount in this study is also estimated in relation to the compaction optima at natural water content in the field. Additionally, there are well defined the minimal requirements for improved and stabilized soil in EN 14227-11 (EN 14227-11:2006...). However, the choice of the stabilization/modification method is ultimately an economical trade-off.

The objective of this survey is to study the effect of temperature on the optimal CaO content and evaluate the long term strength development, California bearing ratio (CBR), in time for a fine-grained soil from Kangerlussuaq, Greenland.

MATERIALS AND METHODS

A lime stabilization application was tested to the fine-grained soil from Kangerlussuaq, Greenland, at the laboratories of the Arctic Technology Center at the Technical University of Denmark (DTU).

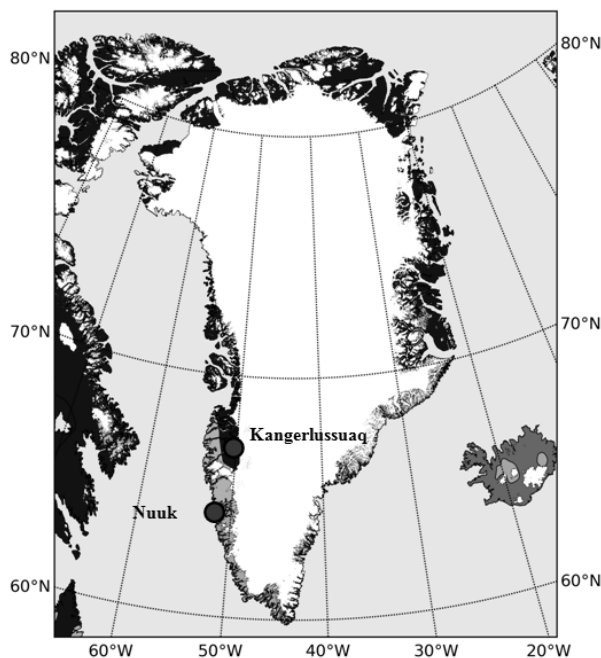


Figure 1. Map of Greenland with the capital, Nuuk, indicated as well as the field site location at Kangerlussuaq. The map also shows the permafrost distribution in Greenland, sporadic (green), discontinuous (orange) and continuous permafrost (blue), according to the classification of (Brown et al., 1998).

The material was sampled close to the Kangerlussuaq International Airport, which is located in an area with continuous permafrost, see Figure 1.

The sieve analysis, hydrometer method (ISO/TS 17892-4:2004...), consistency limits analysis (ISO/TS 17892-12:2004...), pH test, Proctor compaction experiments (EN 13286-2...) and CBR tests (EN 13286-47...) were performed to determine the geotechnical properties of the natural and lime-treated material.

The optimum CaO content was determined in a series of measurements of the soil compaction, pH, and changes in plasticity. In order to achieve the soil compaction optima under the given compaction rate, it is necessary to accomplish the maximum dry density at the natural water content, assuming that extra water is not added. It can be easily evaluated from the Proctor compaction curves for the different soil-lime mixtures. However, it is time consuming to make all these Proctor curves for many different soil-lime mixtures; furthermore, there can be mistakes in the measuring process, because of problems compacting soil properly at very low and very high water contents. Therefore, a new method of determining the optimum lime content for the compaction optima under the given compaction effort and at the natural water content is introduced. The same batch is decided to be reused, adding quicklime (CaO) in portions, mixing it, doing the Proctor compaction test, remolding, and again adding a new portion of CaO. The portions are decided to be small, so that the maximum dry density is expected to match with the 100% dry density or close to that.

The pH of soil-lime mixture is evaluated to be approximately 12.4, the pH of saturated lime water (Eades et al., 1966). The activity of the clay and other minerals in the material mainly affects the plasticity of fine-grained sediments (Bell, 1996). A previous survey by L. Bjerrum on geotechnical properties of Norwegian marine clays showed that the high sensitivity of marine clay is a result of the leaching of salts (Brown et al., 1998), and thus the salinity of the soils should be taken into account as well.

Soil-lime mixtures molded in the large Proctor compaction molds and raw mixtures in sealed plastic bags were stored at 1°C and 10°C curing temperatures for 28-day and 56-day time periods, respectively. The tests were carried out during the curing period after approximately 7, 14, 28 and 56 days. The Proctor tests were performed using a 2.5 kg rammer in the large Proctor mold according to EN 13286-2 point No 7.2 (EN 13286-2...). The Proctor compacted elements were afterwards used in the California bearing ratio (CBR) test, according to EN 13286-47 (EN 13286-47...). pH measurements were conducted at the same time to define how much residual CaO has left for

pozzolanic reactions. The two curing temperatures were chosen in order to compare the soil stabilization effectiveness between low and normal soil temperature conditions.

Raw mixtures were chosen, because it is common that mixing and storing of soil-lime is performed away from the construction field. On the other hand, the molded samples correspond to the mixing, compacting, and curing in situ.

Physical and chemical properties of soil used in the study

The geotechnical properties and semi-quantified mineralogy of the soil used in the study are given in Table 1 and Table 2, respectively.

Table 1
Geotechnical properties of fine-grained sediments

		Marine sediments from Kangerlussuaq
Soil classification		SILT, clayey
Particle size distribution:		
<2µm (%)		57
<5µm (%)		75
<0.01mm (%)		85
<0.1mm (%)		99.8
Average natural water content (%)		24
Average natural salinity (‰)		10
Liquid limit at natural salinity (%)		40.63
Plastic limit at natural salinity (%)		26.50
Plasticity index at natural salinity (%)		14.13
CBR value at average natural water content (%)		3.10
γ (kN/m ³)		1.61
γ _s (kN/m ³)		2.80
pH value		7.4

Table 2
Semi-quantified mineralogy

		Marine sediments from Kangerlussuaq (%)
Quartz		18
Plagioclase (Ca-albite)		36
Amphibole (hornblende)		13
Pyroxene (clinopyroxene)		9
Alkali feldspar (microcline)		17
Chlorite (Clinochlore)		7

The properties of lime used in the study

A/S "Faxe Kalk" quicklime "Proviacal® ST Q" was used for the soil stabilization. The chemical composition, reactivity and fineness of this commercial grade lime material are listed in Table 3.

Table 3
Chemical and physical properties of quicklime

	Mean	Std.dev.
Chemical composition:		
CaO _{total}	95.0%	1.1%
MgO	0.9%	0.1%
SiO ₂	1.6%	0.2%
Al ₂ O ₃	0.25%	0.1%
Fe ₂ O ₃	0.25%	0.1%
P ₂ O ₅	0.15%	0.02%
TiO ₂	0.03%	0.01%
MnO	0.04%	0.01%
CO ₂	1.0%	0.5%
S	0.18%	0.02%
K ₂ O + Na ₂ O	0.07%	0.01%
CaO _{activ}	92.0%	0.7%
Reactivity:		
R (reactivity)	20°C/min	3°C/min
T _{60°C} (time for otaining at temp. 60°C)	2 min	2 min
Fineness of material:		
Material remaining through 1 mm sieve	0%	0%
Material remaining through 0,09 mm sieve	10%	2.5%

RESULTS

Material physical and chemical analysis

The particle size analysis was performed using the hydrometer method according to ISO/TS 17892-4:2004 (*ISO/TS 17892-4:2004...*). 99.8% of the material passed through a 0.063mm sieve, and thus fell in the Silt and Clay fractions. It was estimated, that 57% of the material is in the clay fraction, i.e., the grain size is smaller than 2µm. Additionally, a few gastropod fossils were also present in the soil, but all of them were removed before the particle size analysis. In spite of the observed grain size distribution, the semi-quantitative X-ray diffractometer (XRD) analysis of the bulk sample did not indicate a remarkable clay mineral content. We found mainly silicates (pyroxene, amphibole, and chlorite), quartz and feldspar minerals (microcline, Ca-albite). These minerals, e.g., quartz (mainly consist of SiO₂) in fine state does react with quicklime (Bell, 1996).

Soil compaction

The Proctor compaction experiments according to the previously described method were used for

determining the optimal lime content at the soil natural water content in the field, which in average is 24%. Step by step, the Proctor compaction test was done, the water content was measured, and the dry density was determined for each of the different CaO contents, adding CaO in small portions and reusing the same batch for the next step on the CaO addition.

The dry densities obtained from all the tests have been plotted as a function of CaO content (see Figure 2).

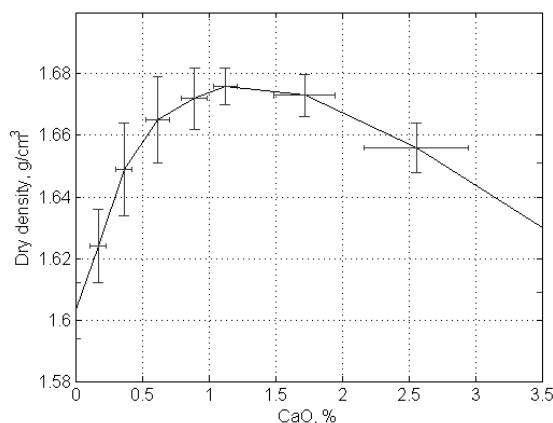


Figure 2. Dry density as a function of CaO content at 24% water content.

Small CaO steps at low CaO contents (from 0%-1.5%), larger CaO steps at higher CaO contents (1.5%-3.5%) account for differences in horizontal errorbars.

Reusing the same material batch, adding CaO in portions, and doing the Proctor compaction testing, the water content is greatly reduced by water evaporation during preparation and testing, especially when there are many measurements and manipulations with the same batch. This results in noticeable dissimilarities in the lime-treated soil dry densities for the same CaO content in vertical direction. Therefore, the soil-lime dry densities are not directly comparable- there are time, reworking, and evaporation factors. Although, the testing procedure described has to be improved, the results presented indicate that the optimal lime amount is 1.2% of CaO for the compaction optima at natural water content.

pH test

The pH values were determined for all the same test samples used in the compaction tests. The soil pH was measured in a suspension of soil and KCl (potassium chloride) of the ratio 1:2.5, determining the pH value with a special pH meter. The pH values from a series of determinations as ordinates against the corresponding CaO as abscissa can be plotted (see Figure 3).

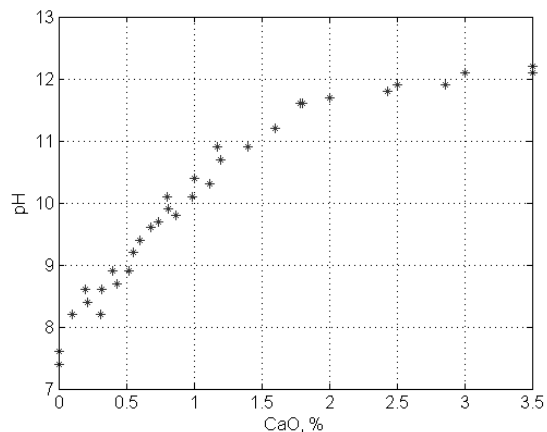


Figure 3 pH values as a function of CaO content.

The pH value is notably rising from 0% to 3% CaO content, after which the increase is slower. Although, the pH for soil solution with 3% CaO content is less than 12.4, it can be estimated as the optimum CaO content, because pH does not increase much more for a higher CaO content.

Changes in plasticity

The soil plasticity properties were measured for 1%; 2%; and 3% lime-treated soil by routine experiments according to ISO/TS 17892-12 (*ISO/TS 17892-12:2004*). The consistency limit values from a series of determinations can be seen in Table 4.

Table 4
Changes in consistency after CaO addition

Lime content (%)	Plastic limit (%)	Liquid limit (%)	Plasticity index (%)
0	26.50	40.63	14.13
1	32.49	52.71	20.22
2	33.25	46.68	13.43
3	33.96	43.94	9.98

The plastic limit sharply rises on addition of 1% CaO, after which it remains more or less steady or rises to a small amount. The liquid limit also rises, but then it slowly decreases. The plasticity index drops below 10% on 3% CaO addition, i.e., corresponding to the plasticity index for a non-plastic soil, so higher CaO content would be illiterate. Therefore, also changes in plasticity indicate that the optimal lime content for the soil stabilization is 3% CaO content.

Determination of optimal lime content

It was proved that the applied methods for determining the optimal soil compaction should be improved in order to get comparable results and to determine the compaction optima and so also to

find the optimal lime amount, however, the method used indicated that the optimal CaO amount is 1.2%. On the other hand, the optimum lime content was assumed to be 3% CaO according to the pH test and changes in plasticity.

In order to evaluate and compare the strength gain in time, the long term measurements were done for both 1.2% and 3% CaO content.

Long term measurements

Strength development at 10°C curing temperature

In the first stage of the long term measurements 1.2% and 3% CaO soil-treated samples were stored at 10°C. The CBR values from this measurement series is plotted as ordinates against the corresponding time step in days in Figure 4.

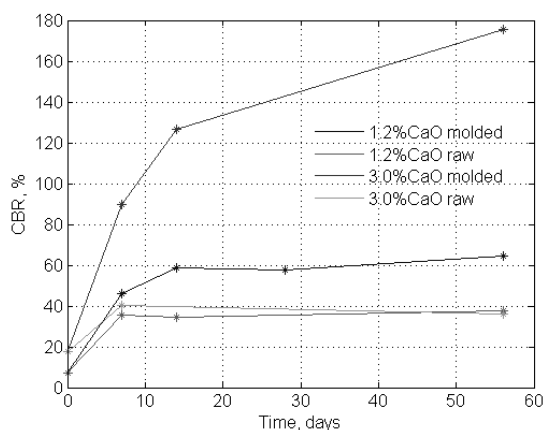


Figure 4 CBR values as a function of time at 10°C curing temperature.

The CBR value after 14 days storing at $t^{\circ}=10^{\circ}\text{C}$ for 3% CaO soil-lime molded samples is 126.83%, while for 1.2% CaO soil-lime molded samples it is 58.49%. After 56 days storing at $t^{\circ}=10^{\circ}\text{C}$ for 3% CaO soil-lime molded samples the CBR value is 175.39%, while for 1.2% CaO soil-lime molded samples it is 64.73%. In general, these results indicate that for 3% CaO content the CBR value increase is greater than for 1.2% CaO content for molded material samples.

Raw soil-lime samples showed similar results both for 3% CaO content and for 1.2% CaO content. It can be seen that the CBR value after 7 days storing at $t^{\circ}=10^{\circ}\text{C}$ for 3% CaO soil-lime raw samples is 40.24%, while for 1.2% CaO soil-lime raw samples it is 35.68%. After 56 days storing at $t^{\circ}=10^{\circ}\text{C}$ for 3% CaO soil-lime raw samples the CBR value is 36.24%, while for 1.2% CaO soil-lime raw samples it is 37.38%.

Strength development at 1°C curing temperature

In the second stage of the long term measurements 1.2% and 3% CaO soil-treated samples were stored

at 1°C. The CBR values from a series of determinations as ordinates against the corresponding time step in days as abscissas are plotted in Figure 5.

The plot shows a great increase in the CBR values for 3% CaO soil-lime molded sample, while the CBR value for 1.2% CaO lime-soil molded sample has increased after 7 days and then the increase has been small. After 28 days storing at $t^{\circ}=1^{\circ}\text{C}$ for 3% CaO soil-lime molded samples the CBR value is 77.00%, while for 1.2% CaO soil-lime molded samples it is 43.53%. In general, these results indicate that for 3% CaO content the CBR value increase is greater than for 1.2% CaO content also at 1°C curing temperature for molded material samples. Raw soil-lime samples showed similar results both for 3% CaO content and for 1.2% CaO content.

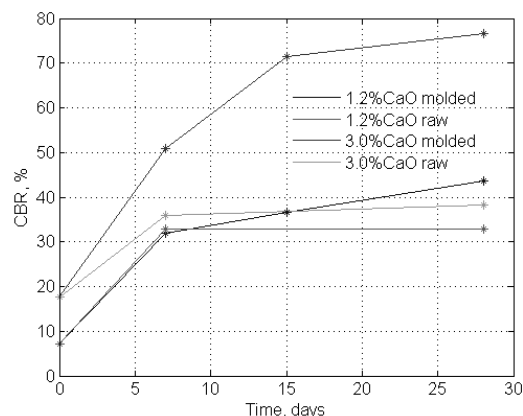


Figure 5 CBR values as a function of time at 1°C curing temperature.

Furthermore, the CBR value after 28 days storing at $t^{\circ}=1^{\circ}\text{C}$ for 3% CaO soil-lime raw samples is 38.22%, while for 1.2% CaO soil-lime raw samples it is 32.80%.

Comparing the CBR values between $t^{\circ}=1^{\circ}\text{C}$ and $t^{\circ}=10^{\circ}\text{C}$ curing temperatures, we observe that the strength increase is greater at $t^{\circ}=10^{\circ}\text{C}$ curing temperatures for the molded material samples, but for the raw material samples it is almost the same.

pH measurements

As it was expected, the pH values decreased in long term soil-lime reactions for both $t^{\circ}=1^{\circ}\text{C}$ and $t^{\circ}=10^{\circ}\text{C}$ curing temperatures. Our measurements showed that the pH values after 14 days curing at $t^{\circ}=10^{\circ}\text{C}$ decreased faster than at $t^{\circ}=1^{\circ}\text{C}$. That means the pozzolanic reactions are retarded at $t^{\circ}=1^{\circ}\text{C}$, which is in agreement with the long term strength development measurements.

Relatively low strength increase for 1.2% CaO soil-lime molded samples after 7 days could be explained by the fact that the pH values decreased below the value of 10.5 at $t^{\circ}=1^{\circ}\text{C}$ or even below the value of 10.0 at $t^{\circ}=10^{\circ}\text{C}$, which are pH values when

solubility of silica and alumina are reduced. For 3% CaO soil-lime molded samples the pH value after 7 days curing is still high enough to maintain solubility of silica and alumina, and ensure the pozzolanic reactions to continue and increase the sample CBR value.

CONCLUSIONS

1. The optimal lime amount was well estimated with the pH test. A CaO content of 3% was evaluated as the optimal lime amount for soil stabilization. The plasticity for 3% soil-CaO mixture dropped below 10%, a value typical of non-plastic material. Therefore, these two methods can be used together for the optimal CaO content evaluation.

In this survey the optimal CaO content was also determined for the compaction optima at the natural water content in the field. We found that 1.2% of CaO is the optimum lime amount for the compaction optima at the natural water content in the field.

2. The CBR values for 1.2% and 3% soil-lime mixtures in time can be seen in Figure 4 and Figure 5.

The long term analysis showed that for 3% of CaO content the CBR value increase is greater than for 1.2% of CaO content at both 10°C and 1°C curing temperatures; therefore, even if the compaction optima is not reached for 3% of CaO content, the strength gain in the soil more than compensate for the changes in the compaction optima, and they should not be regarded as disadvantageous.

The CBR value from 3.10% for natural non-treated soil is increased to 175.39% for 3% lime-treated molded sample after 56 day curing at 10°C temperature and to 77.00% after 28 day curing at 1°C temperature, while it is increased to 64.73% for 1.2% lime-treated molded sample

after 56 day curing at 10°C temperature and to 43.53% after 28 day curing at 1°C temperature. The CBR value increases are remarkable for both 1.2% and 3% lime-soil moulded samples. However, the immediate bearing index (immediate CBR test) for 1.2% of CaO content was only 7.16% while for 3% of CaO content it was 17.63%; therefore, according to EN 14227-11 lime-soil mixture of 1.2% does not fulfil the immediate bearing index value of at least 10% for soil stabilization. Therefore, also according to EN 14227-11 recommendations 3% CaO content is regarded as sufficient for soil stabilization, while 1.2% CaO content is not.

3. The CBR values for raw soil-lime mixture cured in sealed plastic bags remained almost constant after the first time step for both 1.2% and 3% CaO contents curing at 1°C and 10°C temperatures. We consider this effect to be caused by the long term pozzolanic reactions not occurring among particles, as in the case of molded samples; moreover, compaction is less optimal, because of reduced water content in the cured material. In the field it could mean that the greatest compaction and strength effect would be achieved in the case where the material is treated and compacted in situ.

The initial swelling tests showed that the test material does not exhibit notable swelling behaviour. It was therefore decided to exclude swelling from the measuring procedure.

4. All in all, application of the CaO stabilization of the fine-grained marine sediments from Kangerlussuaq, Greenland, is useful both in normal and low temperature soil temperature conditions, although, the stabilization effect is greatly reduced at 1°C temperature. For the future work, it would be essential to evaluate the CaO stabilization effectiveness in the field.

ACKNOWLEDGEMENTS

This study was funded by the Danish Research Council, Commission for Scientific Research in Greenland, under the grant number 2138-09-0011.

REFERENCES

Eades J.L., Grim R.E. (1966), A quick test to determine lime requirements for lime stabilization. University of Illinois, U.S.A: Department of Geology.

Military Soil Engineering (1992), Headquarters. Washington, DC: Department of Army, p. 291-372.

Bell F.G. (1996) *Lime stabilization of clay minerals and soils*. University of Natal, South Africa: Department of Geology and Applied Geology.

Lime-treated soil construction manual. Lime stabilization and lime modification (2004). National Lime Association.

EN 14227-11:2006 Hydraulically bound mixtures- Specifications- Part 11: Soil treatment by lime.

ISO/TS 17892-4:2004 Geotechnical investigations and testing- Laboratory testing of soil- Part 4: Determination of particle size distribution.

ISO/TS 17892-12:2004 Geotechnical investigations and testing- Laboratory testing of soil- Part 12: Determination of Atterberg limits.

EN 13286-2 Unbound and hydraulically bound mixtures- Part 2: Test methods for the determination of the laboratory reference density and water content- Proctor compaction.

EN 13286-47 Unbound and hydraulically bound mixtures- Part 47: Test methods for the determination of California bearing ratio, immediate bearing index and linear swelling.

Bjerrum L. (1956) *Geotechnical properties of Norwegian marine clay.*

Brown J., Ferrians Jr. O.J., Heginbottom J.A., Melnikov E.S. (1998) *Circum-Arctic map of permafrost and ground-ice conditions.* Boulder, CO: National Snow and Ice Data Center/World Data Center for Glaciology. Digital Media.

POSSIBILITIES OF SILICA AEROGEL APPLICATION FOR FOAM GYPSUM COMPOSITIONS

Ilmārs Preikšs, Juris Skujāns, Uldis Iljins*

Latvia University of Agriculture, Faculty of Rural Engineers,
Latvia University of Agriculture, *Faculty of Information Technologies
ilmars.preikss@gmail.com, juris.skujans@llu.lv, uldis.iljins@llu.lv

ABSTRACT

The current situation, when energy rates are increasing constantly and fossil fuel resources are decreasing, furthermore, energy-efficiency and acoustic standards for buildings become increasingly stringent, using a traditional insulation material often means having to accept increasingly thick layers of insulation. The solution to this can be the use of advanced and innovative materials. One of these is silica aerogel. The purpose of this study was to investigate the impact of silica aerogel granules and silica aerogel blanket on the thermal and acoustic properties of foam gypsum. To achieve this, seven different specimen types were prepared. Five specimens of each type were prepared. Summary 35 specimens were tested. The specimen coefficient of thermal conductivity λ was determined by applying specially developed equipment and software. The specimen sound absorption coefficient α was determined by applying the acoustic tube. The results obtained from the tests show that there are some advantages and disadvantages of silica aerogel application. It was discovered that as silica aerogel granules interfere with formation of foam gypsum, a different production technology should be used. However, experiments need to be continued for new results. The authors recommend that further research should be carried out with different types of aerogel and different volumes of aerogel granules. The authors of this study leave the research field open for further investigations.

Keywords: aerogel granules, aerogel blanket, thermal insulation, thermal conductivity, foam gypsum, sound absorption.

INTRODUCTION

Gypsum is a significant local resource of Latvia. Its usage for Latvia's national economy is economically beneficial. Gypsum is the main raw material for foam gypsum, therefore, the foam gypsum usage as presented by researches (Iljins et al., 2009; Skujans et al., 2010), creates additional outlets for gypsum and extends the product assortment of construction industry.

The purpose of this study was to investigate the impact of silica aerogel granules (adding 5%, 15% and 30% of mould capacity) and silica aerogel blanket (attached to one side of the specimens) on the coefficient of thermal conductivity λ and the sound absorption coefficient α of foam gypsum.

It was hypothesized that adding silica aerogel granules, the coefficient of thermal conductivity λ of foam gypsum decreases. The hypothesis was based on the assumption that silica aerogel granules encapsulate in the pore walls of foam gypsum, thereby slowing the flow of heat, which is due to the wall thermal conductivity (coefficient of thermal conductivity of silica aerogel granules is 0.018 W/m.K; coefficient of thermal conductivity of foam gypsum is 0.109 W/m.K at volume density 388.2 kg/m³).

Previous research (Skujans et al., 2007) on foam gypsum showed that foam gypsum could be similar

to other thermal insulation and sound absorption materials.

MATERIALS AND METHODS

The basic materials that were used for preparation of the specimens: water (drinking quality), gypsum (powder), surface active stuff (SAS, liquid), silica aerogel granules (CABOT Nanogel TLD 100, particle size 0.2 to 4.0mm, volume density 90 to 100 kg/m³, Fig. 1), silica aerogel blanket (ASPEN AEROGEL SPACELOFT, thickness=5mm, Fig. 2).

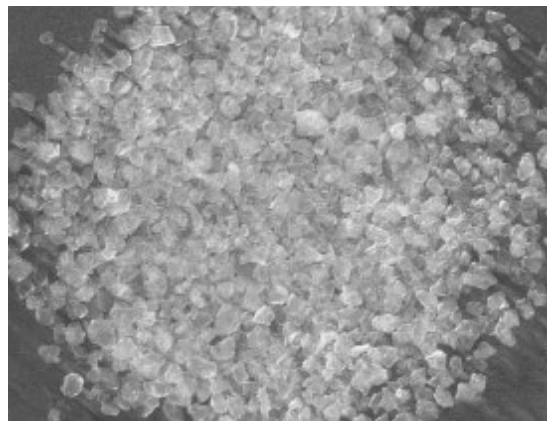


Figure 1. Silica aerogel granules “CABOT Nanogel TLD 100”.

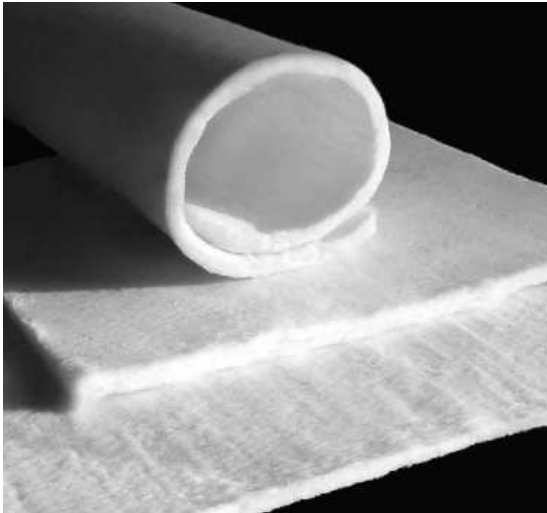


Figure 2. Silica aerogel blanket "ASPEN AEROGEL SPACELOFT".

The specimens were produced using the dry mineralization method (Скрянс, 1984) mixing water, gypsum, surface active stuff and adding silica aerogel granules. Silica aerogel blankets were attached to one side of the specimens.

All specimens were based on the ratio of water and gypsum 0.8. The silica aerogel granules were added at 5%, 15% and 30% of the mould capacity.

The silica aerogel blankets were attached to one side of the specimens. In total 35 specimens were tested to determine the coefficient of thermal conductivity (specimen dimensions were thickness=40mm, width=400mm, length=400mm): 6 solid gypsum specimens (BG), 6 foam gypsum specimens (PG), 5 foam gypsum +5%AG, 6 foam gypsum +15%AG, 6 foam gypsum +30%AG, 2 solid gypsum specimens +P, 4 foam gypsum +P. 93 specimens were tested to determine the sound absorption coefficient (specimen dimensions were thickness=40mm, diameter=39mm): 15 - BG, 15 - PG, 12 - PG+5%AG, 9 - PG+15%AG, 9 - PG+30%AG, 9 - BG+P, 15 - PG+P, 9 - P. The volume density for BG+P and PG+P was calculated by equation:

$$\rho = \frac{m_1 + m_2}{V_1 + V_2} \quad (1)$$

In equation (1) ρ is the volume density for the whole specimen (kg/m^3), m_1 and m_2 are the masses (kg) of each layer, V_1 and V_2 are the volumes of each layer. The test specimens for the determination of the coefficient of thermal conductivity were prepared by pouring gypsum (and other composites) into a mold. The specimens for the determination of the sound absorption coefficient were obtained by cutting the material to specific sizes (cylinders) and then grinding the surface of the materials.

The measurements were carried out using commercially available instruments. All specimens were dried at ambient air pressure and temperature ($\sim 20^\circ\text{C}$) for 1 month before testing to drive off free moisture. Weight invariability was used as control of the specimen dryness (specimens were weighed weekly, but at the fourth week - daily) (Iljins et al., 2009). To gather the data presented in this paper, the following methods and instruments were used. The specimen coefficient of thermal conductivity was determined by applying specially developed equipment and software (k type wires for surface temperature measurements, Ahlborn Heat Flow Plates Type FQ90xxx for heat flow measurements; as a control device LaserComp FOX 600 Heat flow meter was used - the guarded hot plate test, for one correct measurement at each type of specimens). The sound absorption measurements had been carried out using the company "Sinus" impedance tube produced by the industry (device was calibrated before each measurement). The sound absorption measurements were made in the temperature $\sim 23^\circ\text{C}$ (for each measurement determined).

For the materials tested, the following information will be presented in detail:

The graph showing the dependence of the coefficient of thermal conductivity, λ , on the volume density ρ . The coefficient of thermal conductivity, expressed in $\text{W/m}^\circ\text{K}$, is defined as the proportionality constant between the rate of heat transfer and the product of temperature gradient across the solid and the area through which the heat is transferred. The volume density expressed in kg/m^3 . The graph showing the dependence of the coefficient of sound absorption, α , on the volume density ρ .

RESULTS AND DISCUSSION

In the following paragraphs, a brief discussion of the trends in the data obtained in the coefficient of thermal conductivity and coefficient of sound absorption tests is presented. The thermal and acoustic properties are also discussed and compared to each other to show the influence of the type of material. Thermal conductivity is very sensitive to the microstructure of the material. It is strongly influenced by such factors as mineral composition, impurities in the crystal structure, average grain size, grain orientation, and porosity. The sound absorption coefficient is very sensitive to the volume density, type of surface (smooth or rugged) and porosity (also surface porosity) (Горлов, 1989). The different specimens of foam gypsum composites (with and without silica aerogel granules dispersion) were obtained and tested (Fig. 3., 4., 5., 6., 7.). Fig. 5., 6., 7. indicate that adding silica aerogel granules to foam gypsum, the porosity decreases.

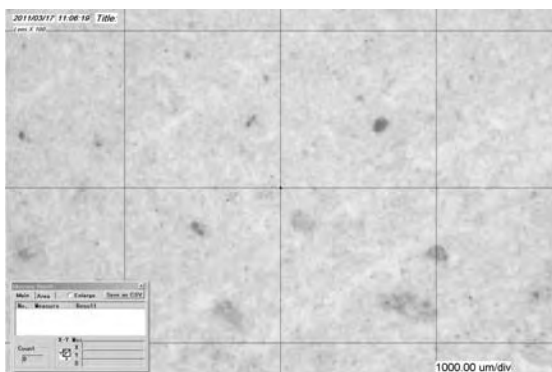


Figure 3. Solid gypsum zoomed 100x, where size of square 1x1mm.

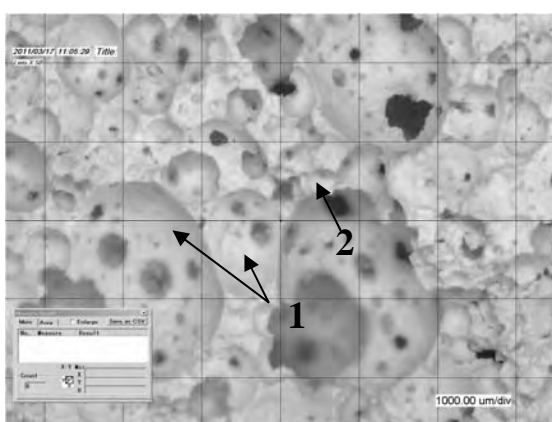


Figure 4. Foam gypsum, zoomed 50x, where size of square 1x1mm, where 1 – pores; 2 – gypsum matrix.

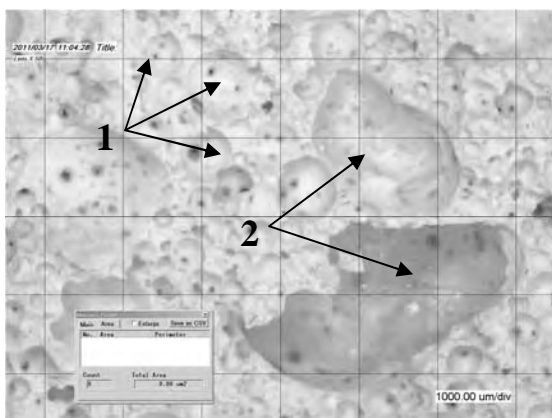


Figure 5. Foam gypsum +5% AG, zoomed 50x, where size of square 1x1mm, where 1 – pores; 2 – silica aerogel granules.

The hypothesis that adding silica aerogel granules to foam gypsum, the coefficient of thermal conductivity decreases, did not prove as it was expected and was not supported by the data. The

tendency of the coefficient of thermal conductivity of foam gypsum is illustrated in Fig. 8 to 9. The tendency of the coefficient of sound absorption is illustrated in Fig. 10 to 11.

Fig. 8 indicates that the coefficient of thermal conductivity of solid gypsum is believable (Otto, 2004). Moreover, Fig. 8 shows that the silica aerogel blanket reduced the greatest part of the coefficient of thermal conductivity by itself.

As we can see in Fig. 10 to 11, adding silica aerogel granules to foam gypsum decreased the coefficient of sound absorption for the both values (1000Hz frequency and rated).

Fig. 10 to 11 show that usage of the silica aerogel blanket for foam gypsum did not increase the value of the coefficient of sound absorption, but it did for solid gypsum.

The results presented that foam gypsum is a sound absorption material of class D (EN ISO 11654), other tested materials are not classified. The data presented in this study can be used for further investigations.

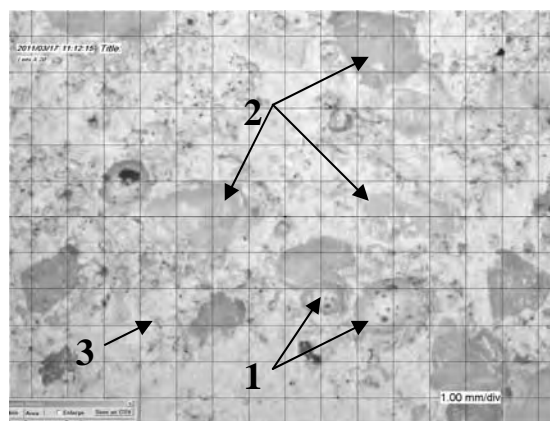


Figure 6. Foam gypsum +15% AG, zoomed 20x, where size of square 1x1mm, where 1 – pores; 2 – silica aerogel granules; 3 - gypsum matrix.

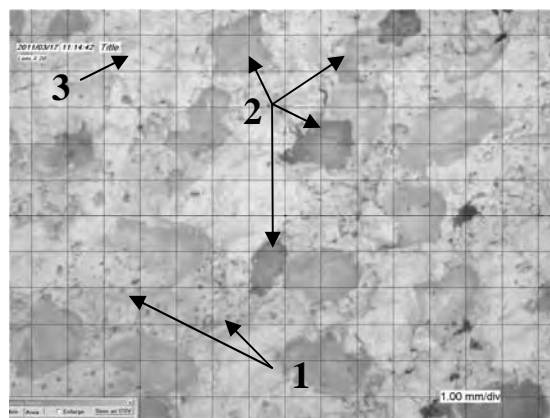


Figure 7. Foam gypsum +30% AG, zoomed 20x, where size of square 1x1mm, where 1 – pores; 2 – silica aerogel granules; 3 - gypsum matrix.

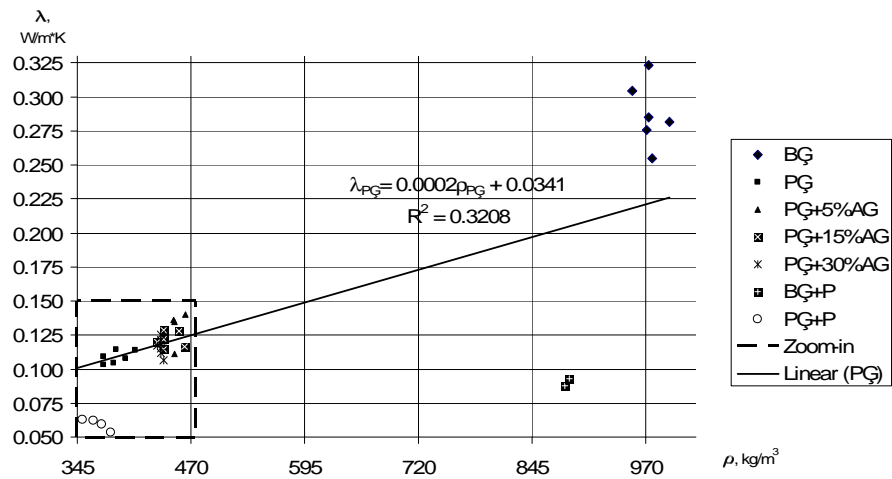


Figure 8. Coefficient of thermal conductivity depending on volume density.

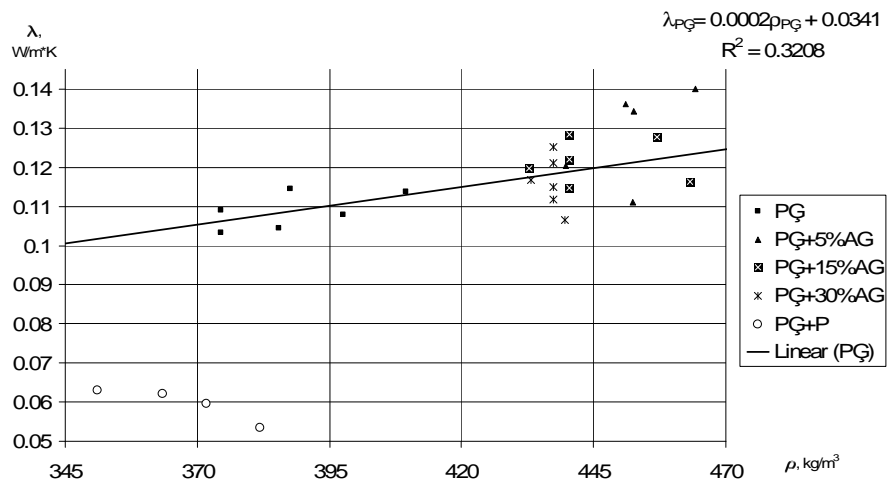


Figure 9. Zoomed. Coefficient of thermal conductivity depending on volume density.

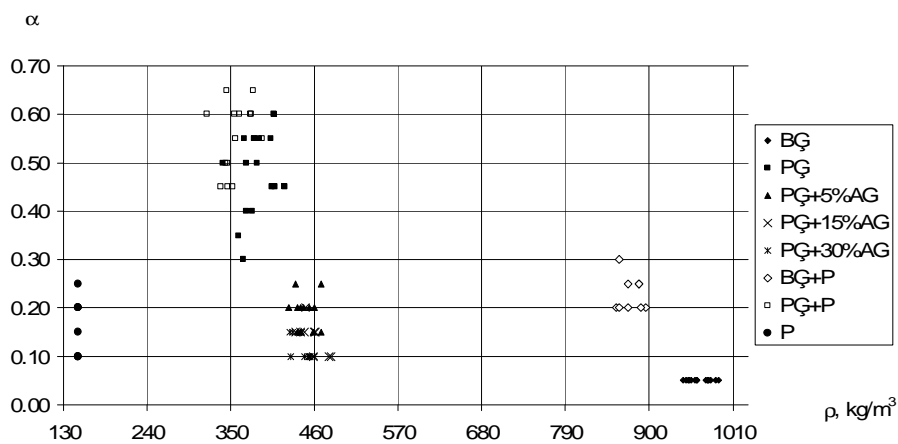


Figure 10. Sound absorption coefficient in one third octave mid band 1000Hz frequency depending on volume density.

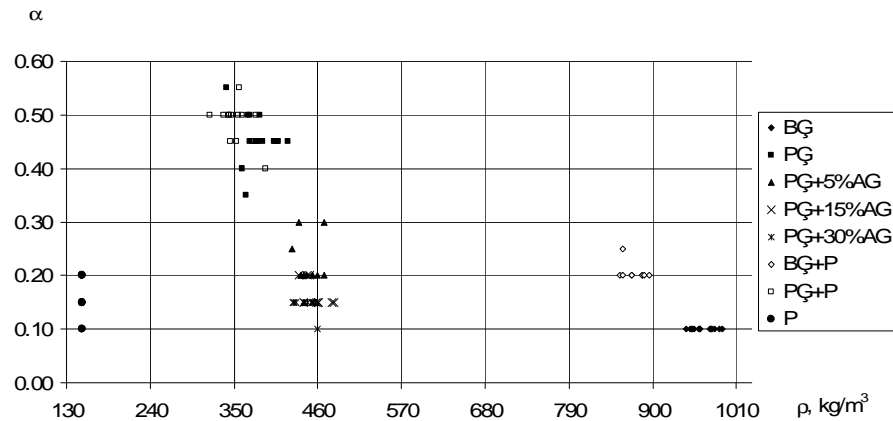


Figure 11. Rated sound absorption coefficient depending on volume density.

CONCLUSIONS

Based on the experimental data presented, the following conclusions can be summarized:

1. Composite materials, which were made by the method of dry mineralization described above, with the concentration of silica aerogel granules as defined, did not decrease the coefficient of thermal conductivity ($\lambda_{PGmin}=0.103$ W/m.K, $\lambda_{PG+30AGmin}=0.106$ W/m.K).
2. The experiments showed that attaching the silica aerogel blanket to one side of the specimen, the coefficient of thermal conductivity of the composite decreases, that indicates on the influence of the silica aerogel blanket on the thermal conductivity (without blanket $\lambda_{PGmin}=0.103$ W/m.K, with blanket $\lambda_{PG+Pmin}=0.054$ W/m.K).

3. Addition of the silica aerogel granules decreases the sound absorption coefficient at the measured frequency range compared to foam gypsum with no additives ($\alpha_{PGmax1000Hz}=0.55$, $\alpha_{PG+30AGmax1000Hz}=0.15$).
4. Attaching of the silica aerogel blanket to one side of the foam gypsum specimen, did not lead to the increase of the sound absorption coefficient.
5. Attaching of the silica aerogel blanket to one side of the solid gypsum specimen leads to the increase of the sound absorption coefficient ($\alpha_{BGmax1000Hz}=0.05$, $\alpha_{BG+Pmax1000Hz}=0.30$).
6. It was observed that silica aerogel granules significantly reduce the amount of persistent foam (Figures 4., 5., 6., 7.), possibly it increases the volume density. Moreover, the volume density increase promotes that the coefficient of thermal conductivity increases and the sound absorption coefficient decreases.

NOMENCLATURE

BG – solid gypsum;

PG – foam gypsum;

PG+5% AG - foam gypsum with silica aerogel granules 5% of mould capacity;

PG+15% AG - foam gypsum with silica aerogel granules 5% of mould capacity;

PG+30% AG - foam gypsum with silica aerogel granules 5% of mould capacity;

BG+P – solid gypsum with silica aerogel blanket;

PG+P – foam gypsum with silica aerogel blanket;

P - silica aerogel blanket (“ASPEN AEROGEL SPACELOFT”, thickness=5mm).

AG - Silica aerogel granules – „CABOT Nanogel TLD 100“

ACKNOWLEDGEMENTS

The work was supported by European Social Fund (agreement No. 2009/0165/1DP/1.1.2.1.1/09/IPIA/VIAA/008)

REFERENCES

Otto W. Wetzell (Hrsg.) (2004) *Wendehorst Bautechnische Zahlentafeln 31.Auflage*. Berlin: Beauth. 1439 p.

Skujans J., Iljins U., Ziemelis I., Gross U., Ositis N., Brencis R., Veinbergs A., Kukuts O. (2010) Experimental research of foam gypsum acoustic absorption and heat flow. *Chemical Engineering transactions*, Vol. 19, p. 79 - 84.

Skujans J., Vulans A., Iljins U., Aboltins A. (2007) Measurements of heat transfer of multi-layered wall construction with foam gypsum. *Applied Thermal Engineering*, Vol. 27, No. 7, p.1219-1224.

Iljins U., Skujāns J., Ziemelis I., Gross U., Veinbergs A. (2009) Theoretical and experimental research on foam gypsum drying process. *Chemical Engineering transactions*, Vol. 17, p.1735-1740.

Горлов Ю.П. (1989) *Технология теплоизоляционных и акустических материалов и изделий*: Учеб. для вузов по спец. „Пр-во строит. изделий и конструкций”. М.: Высш. шк. 384 с.

Скуянс Ю. Р., Штакельберг Д. И., Чучуев А. С. (1984) Технологические аспекты изготовления пеноматериалов. В кн., *Строительные материалы конструкции для сельского строительства*. Елгава: Латв. СХА, 3-8 с.

Silica aerogel granules. Available: <http://www.cabot-corp.com/Aerogel/Building-Insulation/Products/Downloads/DL201005131356PM3125/>

Silica aerogel blanket. Available: http://www.aerogel.com/products/pdf/Spaceloft_DS.pdf

USE OF STRAW-CLAY MATERIAL IN WALLS

Maris Strozs, Genadijs Shakhmenko

*Riga Technical University, Institute of Materials and Structures
maris.strozs@gmail.com; gs@apollo.lv

ABSTRACT

The research aims to investigate the use of straw-clay material in wall construction, its load bearing and heat insulation properties. The main objective of this study is to get optimal straw-clay construction material, which could be used in load bearing external wall constructions of one-storey houses. The effectiveness of different kinds of straw and clay proportions in construction materials is determined by compression and thermal conductivity tests. To show the effectiveness of straw-clay material in load bearing external walls, a specific model of a one-storey house in the finite element analysis program Ansys is created. As a result of this study it is determined that straw-clay block construction material in right proportions can be used in one-storey house load bearing external walls with sufficient compressive strength and thermal resistance.

Key words: straw-clay wall, ecological housing, thermal resistance

INTRODUCTION

The use of straw in construction has had a long history. Initially, it was used for building shelters. The use of straw in a baled form for wall constructions was pioneered by the early settlers in America out of a desperate need to protect their farm animals from winter cold weather, and the practice was later extended to build houses for humans. That was more than a century ago. Recent rediscovery of straw bale construction is largely derived from the realization that our way of living is not sustainable if we keep doing things as we do now. Resources that support our materialistic lifestyle are depleting fast; animal species that are a vital part of our living environment are becoming extinct at an alarming rate. Providing safe shelters has always occupied a position of utmost importance in any culture and in any society, be it simple or complex. Construction activity is the single biggest contributor to global warming. Straw is a renewable resource. Compared with timber, which is regenerated typically every 20 to 30 years, straw is generated once or twice per year. As long as people need grain as a food source, straw will be generated as a by-product. Straw in many parts of the world is still regarded as a waste. Even its disposal has become an environmental issue, like burning in the field. On the other hand, straw has certain excellent properties as a building material, such as its thermal capacity. In baled form, it keeps its integrity reasonably well. Once rendered, straw is durable and strong. Straw bale building has seen a renaissance in recent years. It is spreading fast like a wildfire to every corner of the earth (Hodge, 2006).

Nowadays there is a great interest to develop construction technologies using straw and clay as ecological material in America, Europe, including

the Baltic states. Not only straw bales, but also straw-clay material used in walls is with high potential. Building regulations for load bearing type of this material used in house building still develops and is noticed worldwide (Goodhew, 2005). The use of straw-clay material in construction grows mainly due to its good insulation, natural properties and economical reasons. Comparing with straw bales the straw-clay blocks provide higher fire resistance and smaller deformations.

Straw-clay or straw bale houses are constructed in one of three different methods. The first and oldest method is that of load bearing. The straw bales or blocks of straw-clay material support the roof. The second is infill construction. This has been particularly popular in the revival of straw-clay block building, as it has been easier to convince the regulatory authorities that this is a structurally sound system. This building type has either a steel or timber structure that is totally self-supporting with the blocks fitted between the supports to fill in the gaps (Duan, 2010). The third method is a combination of both of the above, and is referred to as structural infill. The structural infill home has a sub-structure to carry the vertical load of the roof and/or upper floor joists; however it is not self-supporting. As opposed to infill construction, it has no bracing to provide the lateral stability of the structure. This lateral stability is achieved through the installation of blocks into the walls (Hodge, 2006).

There are a lot of houses built using straw-clay material, but it is not researched enough to get convincing arguments for usage as a construction material. That is why it is necessary to investigate this material. The aim of this work is to investigate in the laboratory straw-clay material in order to promote the use of ecologically friendly materials in building construction.

EXPERIMENTAL INVESTIGATION

Material and mix preparation

Six straw–clay compositions were created and tested using different clay and cement proportions. The mix components are summarized in Table 1. The straw–clay cubes are shown in Fig. 1 and the straw–clay plate is shown in Fig. 2.

The mix with number 3 was selected as a compromise variant between strength and density, which could be used as constructive insulating material. That is why the plate was made with the same components and proportions as the third mix sample. The used barley straws were cut into small pieces – the length 30 mm to 40 mm, their diameter 1mm to 3mm. Illite type clay was used as a binding agent in the mix. The clay chemical composition results present the following oxides: SiO₂ 60,72%, Fe₂O₃ 6,08%, Al₂O₃ 18,40%, TiO₂ 0,9%, CaO 1,12%, MgO 3,22%, Na₂O 0,07%, K₂O 4,12%.

Clay was mixed with water in order to obtain plastic consistence (water content 30%). The prepared clay paste was mixed with straw pieces in the laboratory mixer and then placed in forms. The mix with number 6 was prepared using Portland cement addition (type CEM I 42.5 N). All straw–clay test samples were placed in 20°C temperature, humidity 50–60%.



Figure 1. Straw–clay cubes.



Figure 2. Straw–clay plate.

Moisture change measuring

During the drying process the prepared straw–clay samples were weighed and measured with accuracy $\pm 0,1$ mm. The moisture percentage and shrinkage deformation of the material were determined. The diagram of straw–clay cube moisture change in time is shown in Fig. 3.

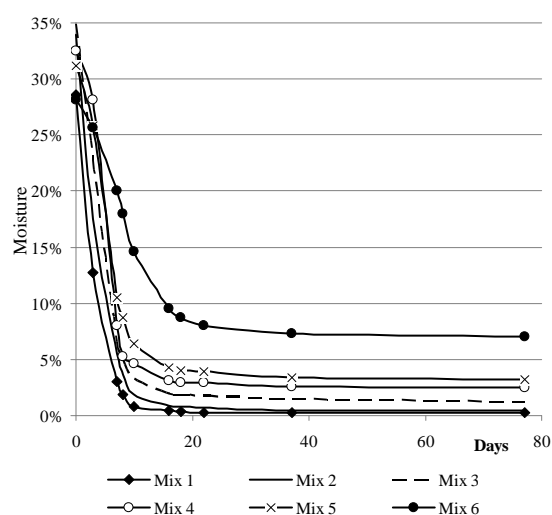


Figure 3. Moisture percentage change in time.

Designed mix compositions in 1m³

Table 1

Mix number	1	2	3	4	5	6
Barley straw, kg	80	80	80	80	80	80
Clay, kg	300	400	500	700	800	400
Portland cement, kg	–	–	–	–	–	75
Water in clay, %	30	30	30	30	30	30
Additional water, kg	50	50	50	50	50	50

The material density was calculated considering the weight and actual dimensions of the sample. The density and shrinkage numerical results are summarized in Table 2.

Table 2

Material density and shrinkage results

Mix number	Density, kg/m ³	Shrinkage of cubes, %
1	345	10.0
2	393	10.1
3	470	10.1
4	638	10.2
5	728	10.2
6	487	4.9

The cubes with less density had some straw drop-outs. After 77 days the cubes with no Portland cement component had 10% shrinkage, the others with Portland cement component had 5% shrinkage.

Compression and thermal conductivity tests

The cubes were tested by the compression test using universal the testing machine Zwick 100 (Fig. 5) till their deformations became too big or the inner structure crushed (force determination accuracy $\pm 10\text{N}$, test speed 1 mm/min). Force–deformation diagrams were obtained. When straw–clay mix is put into moulds, straw fiber orientation becomes parallel to the bottom surface. In the compression test cube samples were placed with straw fibers oriented horizontal (variant 1) and for comparison some cube samples were placed on the edge (variant 2). The sketch is shown in Fig. 4. The numerical results including the gained elastic modulus from the cube compression test stress–strain curve are summarized in Table 3.

The obtained results indicate a significant impact of straw fiber orientation on the compressive strength and modulus of elasticity.

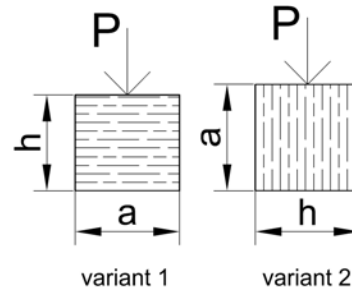


Figure 4. Cube orientation in compression test.

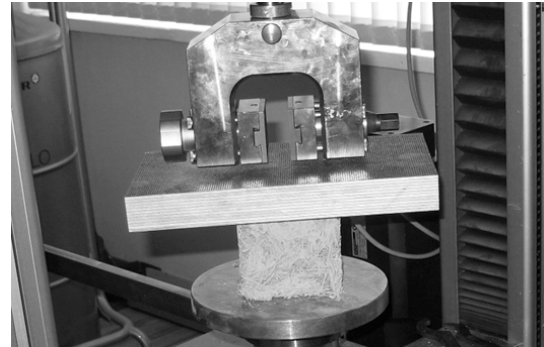


Figure 5. Compression test.



Figure 6. Thermal conductivity test.

Table 3

Mechanical properties of tested cube samples

Mix number	Loading variant (Fig. 4)	Compression strength, MPa	Vertical max. deformations, %	Elastic modulus, MPa	Moisture, %
1	2	0.038	1.9	2.500	0.3
2	2	0.094	3.5	5.200	0.5
3	1	0.499	20.0	3.082	2.4
4	1	0.543	16.3	3.235	2.4
	2	0.222	3.0	7.500	2.4
5	1	0.590	17.7	3.880	3.2
	2	0.289	4.5	11.850	3.2
6	2	0.118	3.0	5.500	7.1

Force added perpendicular to straw fibers gives higher compressive strength, but less modulus of elasticity and higher maximum deformations.

The mix number 1 and 2 having clay/straw proportions 3.75:1 and 5:1 correspondingly indicates low compressive strength. This material may be used only as heat insulating material.

The plate was tested by the thermal conductivity test using the device FOX600 (Fig. 6). The sample was fixed horizontally. During the test the temperature of the lower surface was +20°C and 0°C of the upper surface. The heat transmission coefficient was determined considering constant heat flow between two sides of the sample. The heat transmission test was carried out in different moisture conditions of the straw-clay plate: 43, 12 and 2.5%. The results are summarized in a diagram (Fig. 7).

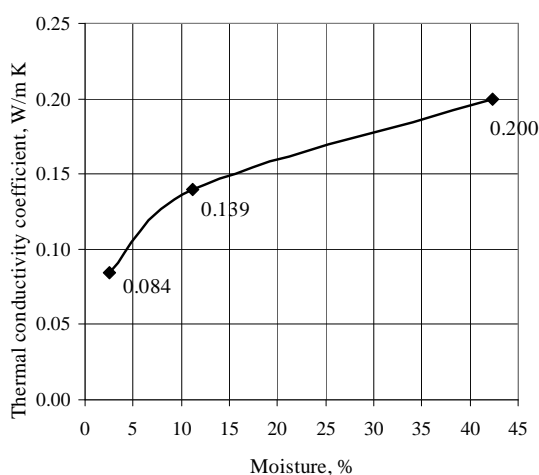


Figure 7. Thermal conductivity coefficient by various moisture.

The range of moisture between 2% and 5% may be considered as the corresponding value for real exploitation conditions of straw-clay walls.

MODEL OF ONE-STOREY HOUSE

External and internal walls of this one-storey house model (Fig. 8) are made from straw-clay blocks (500x240x250mm). In external walls the blocks are placed so that the width of the load bearing wall would be 500 mm.

The block mechanical material properties are taken from the 3 mix sample and the thermal conductivity coefficient is taken from the plate thermal conductivity test. The material density is 500 kg/m³, moisture 2,3% (maximum 5%), the ratio between clay and straw is 1:6. The weight of one block (Fig. 9) is 15kg, which is acceptable from the building technology point of view.

The external wall is rendered with lime 30mm thick on each side. The model of this house is made in the finite element analysis program Ansys.

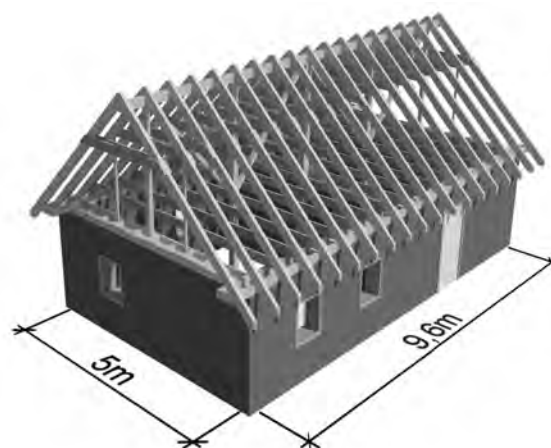


Figure 8. Model of one-storey house.

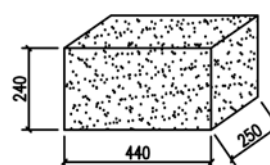


Figure 9. Straw-clay block.

The dimensions between the external walls are chosen 9,6m and 5m – according to the necessary timber element lengths for the roof construction. The height of the walls is 2,5m. In the middle of the building there is an internal wall (width 250mm), which provides total stability. The building stability is increased by the constructed roof construction, which bases on a specially designed wall-plate (Fig. 10, Fig. 11).

The applied normative loads: wind load 0,35kN/m²; snow load 1,25kN/m²; permanent load on the roof construction beams 0,265kN/m²; permanent load on the roof ceiling beams 0,376kN/m². All construction self-weights are considered in the finite element program. The design values are calculated according to the European codes (Eurocode 0, 1996), considering the given partial safety coefficients and design combinations. For snow load the roof slope effect is considered, for wind load the aerodynamic coefficient and coefficient, which considers the height of the wall. For walls in the finite element model the effective width of the load bearing external wall is taken 0,46m instead of real 0,5 m in order to consider imprecision.

The compression stress in the walls from the worst load combinations is shown in Fig. 12, but vertical deformations considering creep from the normative loads is shown in Fig. 13.

The compressive strength variant 1 (Fig. 4) is relative, because the test was stopped due to high vertical deformations. The masonry wall design compressive strength was calculated using the European codes (Eurocode 6, 1996).

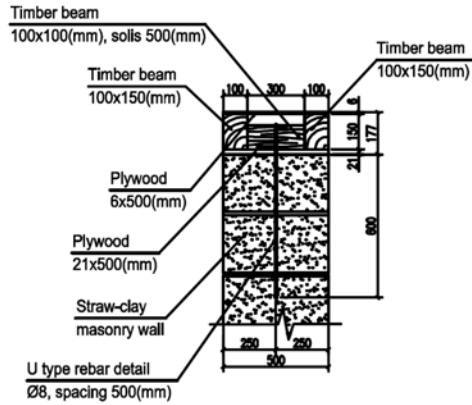


Figure 10. Straw-clay masonry wall connection with wall-plate.

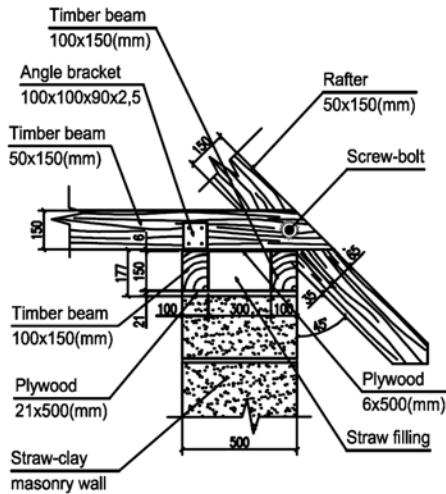


Figure 11. Rafter connection with wall-plate.

The straw-clay masonry wall construction design compressive strength can be calculated as

$$f_d = f_k \cdot \gamma_c \quad (1)$$

where f_d – masonry wall design compressive strength, kN/m^2 ;

f_k – masonry wall characteristic compressive strength, kN/m^2 ;

γ_c – work condition coefficient.

$$f_k = K \cdot f_b^{0,7} \cdot f_m^{0,3} \quad (2)$$

where K – constant, which considers element compressive strength transformation to masonry compressive strength;

f_b – element normalized average compressive strength along added loading, kN/m^2 ;

f_m – used mortar compressive strength, kN/m^2 .

$$f_b = f_k \cdot \gamma_1 \cdot \gamma_2 \cdot \gamma_3 \quad (3)$$

where f_k – experimental cube compressive strength;

γ_1 – constant, which considers tested element number;

γ_2 – constant, which considers cube to block size effect;

γ_3 – constant, which considers long term loading and moisture.

By the made calculations the masonry wall relative design compressive strength is more than $73,54 \text{ kN/m}^2$. The thermal resistance of this one story house external wall is calculated according to the Latvian building standard (LBN 002-01).

$$U_{RN} = 0,3k \quad (4)$$

where U_{RN} – overall normative heat transfer coefficient;

k – temperature factor (dependent on indoor and outdoor air temperature).

$$U = \frac{1}{R_T} \quad (5)$$

where U – overall heat transfer coefficient;

R_T – overall thermal resistance value.

For comparison there are calculated two kinds of straw-clay wall types – one with blocks, other with monolith filling. The thickness of the monolith filling is limited to 300mm because of the slow moisture drying, but the thickness of the masonry wall is taken from the previous calculated load bearing straw-clay wall. The overall heat transfer coefficient of both types is calculated with 2,3% moisture, density 500 kg/m^3 and rendered lime is 30mm thick on each side. In the masonry variant the connection between the blocks is provided by straw-clay mixture (15mm thick) with thermal conductivity $0,4 \text{ W/mK}$. Both variants – the variant with monolith filling between the timber elements and variant with blocks are considered as not homogeneous. The design value of the straw-clay thermal conductivity is gained from the experimental thermal conductivity $0,084 \text{ W/mK}$ summed with correction thermal conductivity coefficient $0,03 \text{ W/mK}$. The calculated overall heat transfer coefficient of the masonry wall is $0,261 \text{ W/m}^2\text{K}$, which is enough for one story house according to the Latvian building standard (with 17,67% reserve).

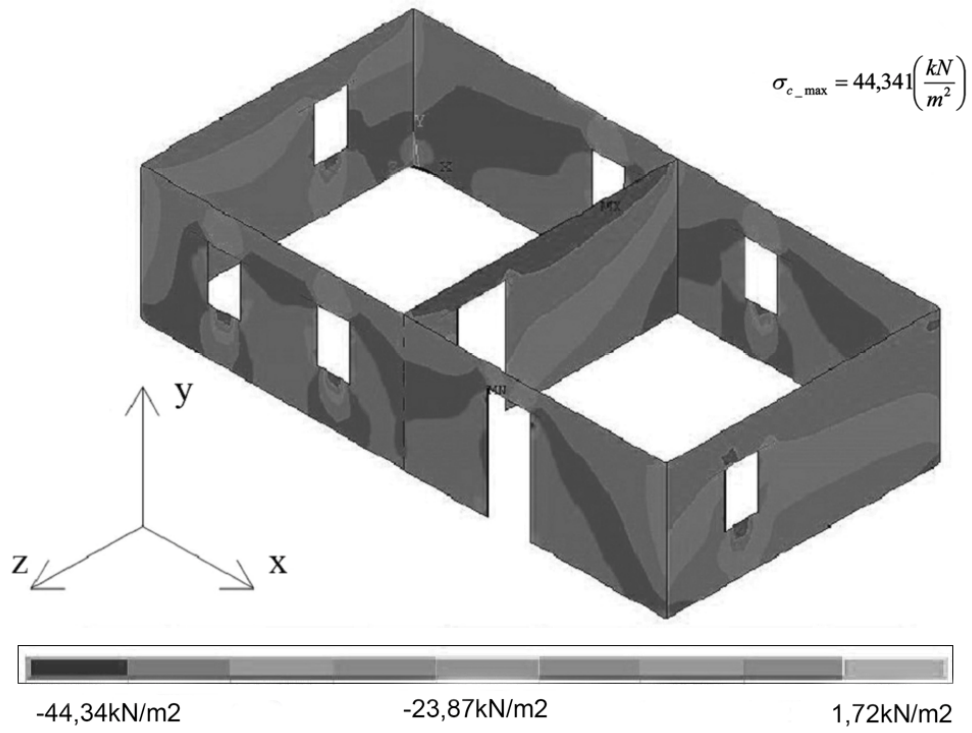


Figure 12. Compression stress distribution in walls, where σ_{c_max} – maximum compression stress value.

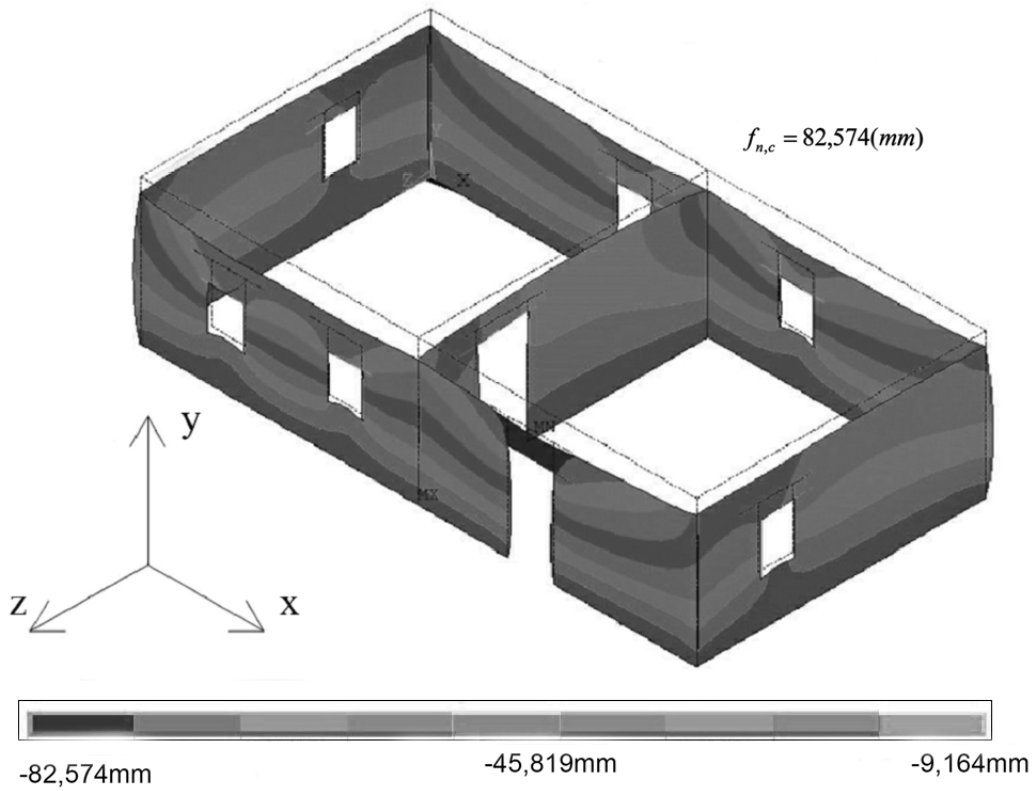


Figure 13. Deformation of walls in y axis direction considering creep, where f_n – maximum vertical deformation value.

According to the data in Fig. 6 the thermal resistance of this masonry wall would be enough even by 6...7% of moisture. The variant with monolith filling would provide the required thermal resistance with thickness more than 340mm, which is more than recommended due to moisture drying. That is why this variant is not recommended for using in external walls as the only heat insulating material.

RESULTS

Physical and mechanical properties of different straw-clay compositions were investigated. It is established that the material is non-homogeneous, its properties depend on the straw fiber direction. Straw-clay compositions have high drying shrinkage (up to 10%). Portland cement admixture in small amounts (75kg in cubic meter) decreases shrinkage to 5%. Use of specially produced precast straw-clay elements (blocks) allow to minimize the negative effect of shrinkage. The residual moisture content is dependent on the straw-clay material density. Portland cement component does not give much positive effect on the element compressive strength or deformation properties.

Heat insulating properties of straw-clay compositions depend on moisture of the material. In order to provide sufficient heat resistance and durability of straw-clay walls, the material must be in air-dry condition (moisture not more than 5%). That is the reason why the wall must be protected against water penetration.

The compression stress in masonry walls, created by the worst load combination of this one-storey house model is 44,34 kN/m², which gives more than 40,5% reserve. Theoretically masonry walls of this block material could be used for bigger vertical loading, but the vertical deformations are quite big (20mm and 83mm considering creep) and therefore the loading is limited. Because of the relative big deformations it is necessary to avoid concentrated load. That is why it is necessary to provide a wall-plate under the roof construction – it evens out the

loading on the wall.

One of the straw-clay material biggest disadvantages is the moisture effect on its longevity as construction material. That is why it is important to investigate some ways to reduce the negative moisture effect and long time creep deformations.

CONCLUSIONS

Straw-clay material with the density 500kg/m³ (weight ratio clay/straw 1:6, moisture 2–5%) used in blocks of the masonry wall with 500 mm load-bearing thickness plus 30mm rendered lime on each side of the wall provides thermal resistance enough for an one-storey house according to the Latvian building standard. The same block material used in load-bearing masonry walls of an one-storey house with overall dimensions 9,6x5x2,5m provides the necessary compressive strength with vertical wall deformations 20mm at first and 83mm considering creep. The thermal resistance will decrease because of the vertical deformation, that is why it is important to make the masonry wall with straw-clay blocks, which have moisture less than 5%.

In load bearing walls straw-clay blocks placed with straw fibers oriented horizontal give bigger vertical deformation, but at the same time bigger compressive strength. Thus, vertical deformation is the aspect which limits the usage of straw-clay blocks in load bearing walls.

Special attention must be paid to protection of straw-clay material against penetration of water, appropriate hydro insulation, drainage system and of course roof construction must be provided. Modifying straw-clay compositions with special mineral or organic admixtures is a way to increase the water resistance and dimensional stability of the material. This is a task for future investigations.

The obtained results of straw-clay compositions allow to conclude: ecologically friendly straw-clay material may be used in wall constructions of single storey buildings and provided investigation in this field must be continued.

REFERENCES

- Goodhew S., Griffiths R. (2005) Sustainable earth walls to meet the building regulations. *Energy and Buildings*, Vol. 37, No. 5, p. 451-459.
- Duan W., Bai A., Cao B. (2010) The possibility analysis on application of new light-weight steel-straw bale thermal insulating dwellings in northeast rural areas of China. *Proceedings of the International Conference on E-Product E-Service and E-Entertainment*, Article number 5660656
- Hodge B. (2006) *Building your straw bale home: from foundations to the roof*. Collingwood: Csiro Publishing. 260 p.
- Eurocode 0. (1996) *Basis of structural design*. ENV 1991-1.
- Eurocode 6. (1996) *Design of masonry structures*. Part 1-1: *General rules for reinforced and unreinforced masonry structures*. ENV 1996-1-1.
- LBN 002-01 (2001) *Heat engineering of buildings and isolation structures*.

STUDY OF PHYSICAL AND MECHANICAL PROPERTIES OF ORIENTED BOARD DEPENDING ON MOISTURE CONTENT

Regino Kask, Harri Lille, Kristjan Siim, Peeter Paabo, Kuldar Sillaste

Estonian University of Life Sciences
Institute of Forestry and Rural Engineering
hlille@emu.ee

ABSTRACT

The goal of this study was to analyze the moisture content of the oriented strand board (Durélis/Populair and OSB 3) representing moisture resistant boards for load-bearing applications in humid conditions. The studied properties are modulus of rupture (MOR), modulus of elasticity (MOE), static hardness, thickness swelling and absorption of water. The moisture content of specimens was altered by soaking during different periods of time (6h, 12h, 18h, 24h, 36h) while one series (24h) was dried out in a climate chamber. An analytical equation was used for approximation of the change of the physical and mechanical properties of the specimens depending on their moisture content. The sensitivity of the measured data has been studied and the expanded uncertainties of the computed mean values are presented. The study reveals that although the boards are moisture resistant, there are some significant differences from the physical and mechanical properties set by the standard, which are caused by their different manufacturing technologies and differences in their structure.

Key words: particleboard, modulus of rupture, modulus of elasticity, static hardness, thickness swelling

INTRODUCTION

Oriented strand board should be moisture resistant in accordance with the standard EVS EN 300 Grade OSB 3. The mechanical properties of OSB generally surpass those of particleboard but it has higher thickness swelling and poorer surface smoothness. Particleboards are used for cladding walls and ceilings indoors or outdoors, as floor decking material and wind barrier. This kind of material is also used in load bearing structures as rigidity material (e.g., OSB 4). The Durélis/Populair and the OSB 3 panel as wood-based sheets are hygroscopic materials and the mechanical and their physical properties are dependent on their moisture content and surrounding temperature.

The goal of this research was to study the changes in the modulus of rupture (MOR), modulus of elasticity (MOE) in bending, static hardness and thickness swelling at different moisture contents.

The main method is to soak specimens in water for a certain period of time or to dry them in a climate chamber; further, to measure the moisture content and to test them with the universal test machine INSTRON 3369. After these procedures they are analyzed.

EXPERIMENTAL PROCEDURE AND METHOD

The MOR and the MOE in bending are found by three-point bending using the test machine INSTRON 3369 (Fig. 1). Deflection for calculating the modulus of elasticity was measured by an optical gauge (Advanced Video Extensometer

2663-821). The experiments were made with three series (the minimum number of specimens in series is eight). The specimens were cut in different directions from a board: one in the longitudinal direction (lengthwise) of the board and another in the transversal direction (crosswise).

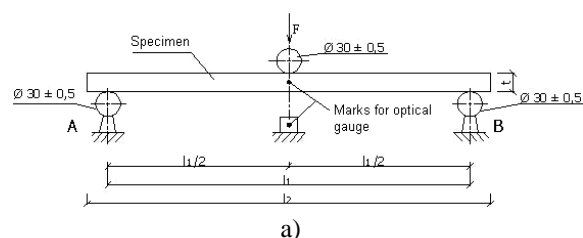


Figure 1. Three-point bending and points of deflection measurement: a) scheme b) photo

Figure 2 presents the MOE obtained by the bending testing and by the approximation of the load-deflection curve with the straight line (Fig. 2).

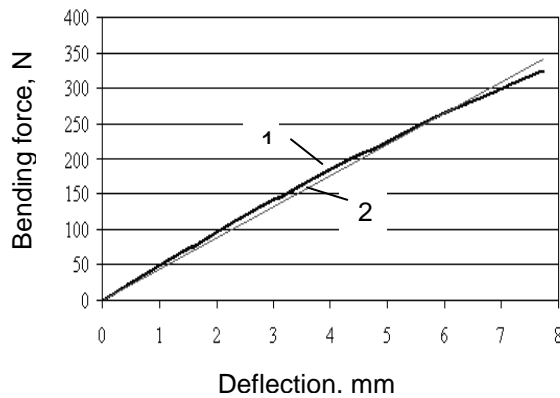


Figure 2. Dependence of deflection on bending force: 1 – real curve; 2 – approximation line.

The MOE was determined by the following formula (see the standard EVS-EN 310:2002)

$$E_m = \frac{l_1^3 (F_2 - F_1)}{4bt^3 (a_2 - a_1)}, \quad (1)$$

where

l_1 is the length between the supports, (240mm);
 b is the width of a specimen, (50±1mm);
 t is the thickness of a specimen, (12mm);
 F_1 and F_2 are 10% and 40% from the maximum bending force, respectively;
 a_1, a_2 are deflections according to the loads F_1, F_2 .

The MOR was calculated by the following formula (see the standard EVS-EN 310:2002)

$$f_m = \frac{3F_{\max} l_1}{2bt^2}, \quad (2)$$

where F_{\max} is the maximum load, N.

Static hardness was determined by the Janka hardness test on the test machine INSTRON 3369 using 50×50 mm specimens.

The following analytical expression was used to approximate the experimental data for the investigated parameters depending on their moisture content

$$Y(x) \equiv Y_0 \times e^{-(cx)^2}, \quad (3)$$

where Y_0 is the value of the investigated properties ($x = 0$), c is a dimensionless parameter.

The purpose was to find unknown constants so that the measured properties can be approximated in the best way. This problem was solved using the mathematical program *Mathcad 2001i Professional*

regression function *genfit* (v_x, v_y, F) (Kir'yanov, 2001).

MEASUREMENT UNCERTAINTIES

In general, the result of a measurement is only an approximation or an estimate of the value of a specific quantity subject to the measurement, and thus the result is complete only when accompanied by a quantitative statement of this uncertainty. This is the amount of doubt in a reported result of a measurement. It is usually described by a parameter that defines the range within which the true value of the quantity to be measured is estimated to fall within a given confidence range – usually 95%. Standard uncertainty can be calculated by the following formula (Laaneots, Mathiesen, 2006).

$$s_{w,j} = \sqrt{\frac{1}{n-1} \sum_{j=1}^n (x_{i,j} - \bar{x}_i)^2}, \quad (4)$$

where n is the amount of specimens, \bar{x}_i is the mean of the input estimates $x_{i,j}$.

$$\bar{x}_i = \frac{1}{n} \sum_{j=1}^n x_{i,j}. \quad (5)$$

Calculation of uncertainty of the measurements is carried out according to the standard EVS-EN 326-1:2002.

The lower confidence level at the significant level 5%

$$L^q_{5\%} = \bar{x} - t_n s_{w,j}, \quad (6)$$

where

t_n is the coverage coefficient.

The upper limit confidence level at the 5% significance

$$U^q_{5\%} = \bar{x} + t_n s_{w,j}. \quad (7)$$

RESULTS AND DISCUSSION

The investigated OSBs are manufactured: Durelis/Populair, Spano Group NV, Belgium; OSB 3, Bolderaja Ltd, Latvija; and Kronopol, Poland, according to the European Union standard EN 312. The water absorption of the test specimens of the investigated materials, depending on the soaking time, is presented in Fig. 3.

The absorption of water in the OSB 3 panels is noticeably higher than in Durelis/Populair. MOR, MOE and static hardness were approximated by the presented logarithm function. The proposed formula approximated the experimental data satisfactorily. Here we present only MOR (see Fig. 4).

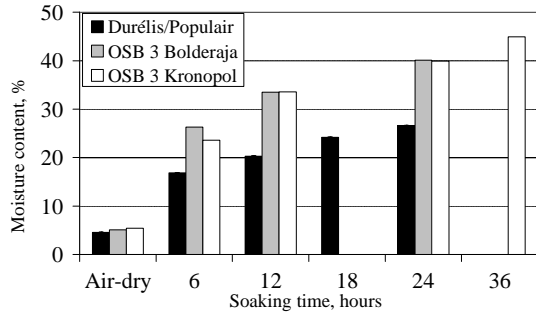


Figure 3. Moisture content depending on soaking time

The decrease in the values of the studied properties (about two times or more) is the largest at the moisture content from air-dry to 40%. For all values of the calculated properties the dimensionless parameter $c \approx -2$ (in the limits of measurement uncertainty). Thus, so we can determine to a certain extent the mechanical and physical properties if the moisture content is known. We can see that the MOR and the MOE are considerably higher for OSB 3 panels than for Durélis/Populair, which are cut lengthwise. The values of these parameters are more similar for the specimens cut crosswise.

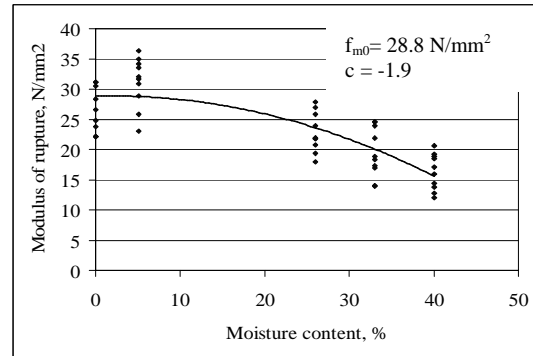
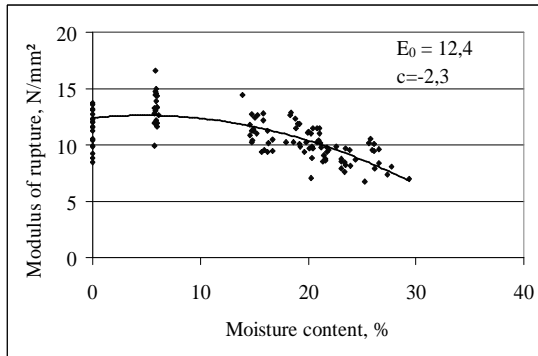


Figure 4. Dependence of modulus of rupture on moisture content (lengthwise):
a) Durélis/Populair; b) OSB 3 panel (Bolderaja)

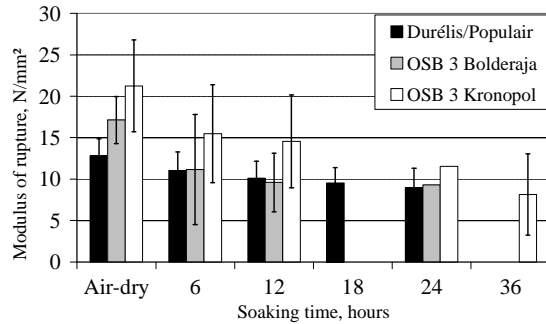
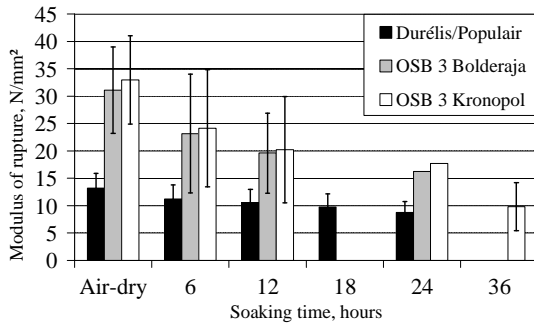


Figure 5. Dependence of modulus of rupture on moisture content:
a) lengthwise, b) crosswise

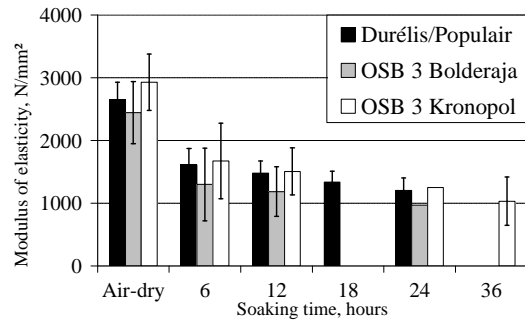
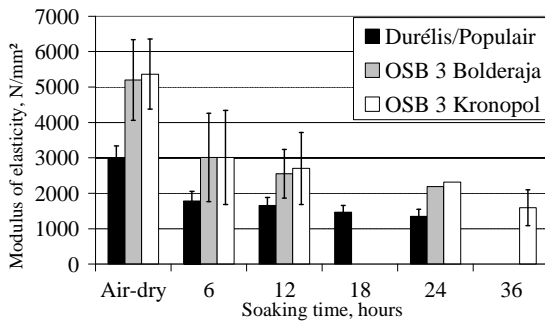


Figure 6. Dependence of modulus of elasticity on moisture content:
a) lengthwise, b) crosswise.

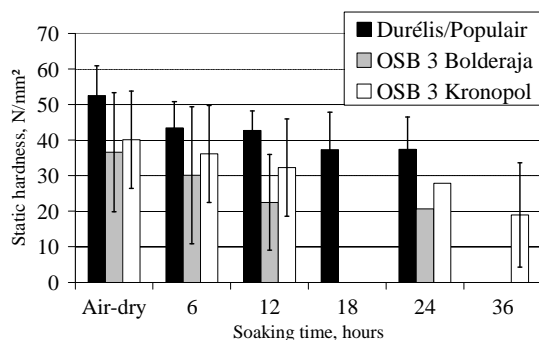


Figure 7. Dependence of static hardness on moisture content.

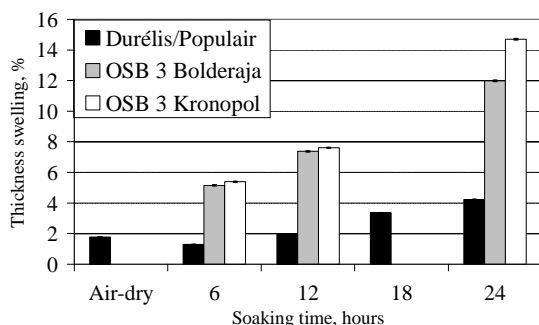


Figure 8. Dependence of thickness swelling on moisture content.

Long-term exposure to high levels of moisture causes reduction in the strength and stiffness. The static hardness of Durélis/Populair panels is higher than that of OSB 3 panels but this property is less affected by the moisture content. The thickness swelling was determined in the middle of the specimens with the dimensions 50× 50 mm.

REFERENCES

- Bolderaja Ltd. Products, OSB chipboard. [<http://www.bolderaja.lv/index.php?act=page&id=12>] (03.05.2011).
- EVS-EN 300:2000: *Oriented Strand Boards (OSB) - Definitions, classification and specifications*. Tallinn. Eesti Standardikeskus.
- EVS-EN 317:2000: *Particleboards and fibreboards - Determination of swelling in thickness after immersion in water*. Tallinn. Eesti Standardikeskus.
- EVS-EN 310:2002. *Wood-based panels - Determination of modulus of elasticity in bending and bending strength*. Tallinn: Eesti Standardikeskus.
- Kir'yanov, D. (2001) *Mathcad 2001. Manual for self-tuition*, Sankt-Petersburg: BHV-Petersburg.
- Kronopol. Products, Construction products, Kronopol OSB 3. [<http://en.mdb.kronopol.pl/OSB-boards/Programme>] (03.05.2011)
- Laaneots R. , Mathiesen O. (2006) *An Introduction to Metrology*. Tallinn: TUT Press. 206 p.
- Paabo, P. (2008) *Study and comparison of oriented strand board (OSB) mechanical and physical values*. M.Eng. Thesis. Tartu: Estonian University of Life Sciences. 113 p.
- Siim, K. (2010) *Study of physical and mechanical properties of Durélis/Populair particleboards depending on moisture content*. M. Eng. Thesis. Tartu: Estonian University of Life Sciences. 87 p.
- Sillaste, K. (2011) *Study and comparison of oriented strand board (OSB) mechanical and physical values*. M. Eng.Thesis. Tartu: Estonian University of Life Sciences. 74 p.
- SpanoGroup – Wood Based Solutions. Durélis/Populair. [<http://www.spano.be/productdetails.aspx?con=238>] (19.04.2010).

The thickness swelling of OSB 3 panels is more than two times larger than that of Durélis/Populair. The uncertainties of the determined properties are lower for Durélis/Populair than for OSB 3 panels. The results of the study show that there are some significant differences from the physical and mechanical properties set by the standard, which are caused by different manufacturing technologies and differences in their structure.

CONCLUSIONS

The investigated properties are affected by the soaking time: 12 hours for OSB 3 (moisture content 33%), 24 hours for Durélis/Populair (moisture content 27%) or higher. In the case of a higher moisture content the values of the properties decrease significantly (about two times) particularly, the values MOE, when the specimens were cut lengthwise from the test board. The results of this study showed that the MOR and the MOE were lower for the specimens that were cut crosswise from the test boards compared with the specimens that were cut lengthwise, at all measured moisture contents.

The specimens cut from OSB 3 (Kronopol) panels after a soaking time of 24 hours were dried out in a climate chamber and they lost about 41% to 47% for MOR and MOE, 20% for the static hardness of their values of the investigated properties obtained at air-dry moisture.

The presented analysis is limited to the data obtained from the above described experiments. A logarithmic function is proposed for approximation of the experimental data.

ANALYSIS OF PERFORATED STEEL TAPE USAGE POSSIBILITY IN CONSTRUCTION

M. Lisicins, V. Mironovs, L. Kalva

Riga Technical University,
Institute of Building Production,
Division of Building Machines and Building Mechanisation
mihails.lisicins@gmail.com; viktors.mironovs@gmail.com

ANNOTATION

This work is devoted for analysis of perforated steel tape, in this case also manufacturing remnant, usage possibility. There are defined physically-mechanical properties and geometrical characteristics for different types of tape. The perforated tape samples tension strength is noticed in the amplitude of 168 to 921 MPa, compressive strength of profiled stands – 350 MPa, but surface hardness in the amplitude of 830 to 3030 MPa. It is proved that tape by its physically – mechanical and esthetical features can be effectively used as a design element, reinforcing and constructive material in the construction processes. Effective solutions for use of perforated steel tape are form elements, reinforcing in reinforced concrete constructions and brick masonry, floor spacers, elements of wall constructions and other construction load-bearing elements.

Key words: perforated steel tape, technological rubbish, reinforced concrete, strength, hardness.

INTRODUCTION

Construction is an area for which fast development, unstoppable searching of new solutions and investigating of new technologies are characteristic. One of the tendencies is usage of light constructions. Light constructions can be made from perforated steel tapes, plates and profiles.

Perforated profiles and tapes using in the construction let to reduce metal usage, make faster preparation and montage of the construction, reduce the amount or necessity of welding works.

However, determined making of perforation visibly make bigger manufacturing costs that is why the biggest meaning is being achieved of perforated tapes as usage of manufacturing waste.

Valuable usage of the materials is one of the significant modern tasks of the material science (Mironovs, Serdjuks, 2003). One of the ways of solution of this task is reiterative manufacturing waste usage. Latvia also has a number of factories, whose production waste can be re-used for different targets. Perforated steel tape as waste material after punching in Latvia is obtained in JSC “Ditton Driving Chain Factory” (*Perforated tape...*). Now as example of successful usage for realization of building solutions perforated steel tape is shown (Миронов, Сердюк, Муктепавела, 2004).

THE ROPERTIES AND EXPERIMENTAL EVALUATION

In the work are researched mechanical and geometric properties of the perforated steel tape which is waste of the manufacturing processes. They differ with the cross-section area, form and size of the perforation and with the amount of it.

Some geometrical characteristics are shown in Table 1.

Samples of perforated tape with the standard method were tested on the tension strength. The test of the tension strength was made with the device INSTRON 8802.

The experimental results showed that the tension strength depending on type of tape changes are in the interval 168 – 921 MPa.

The critical load, tensile extension and tensile strength of samples from Table 1 are shown in Fig. 2 and Table 2. Results were obtained using the weighted average of the 5 test attempts.

With Brinels method a test on hardness at 50 and 300 N big load was made, using a device which allows to make larger load up to 1000 N. In the result of the test was achieved material hardness that was from 830 to 3030 MPa. The results are matching with the steel mark hardness which are shown in Table 2.

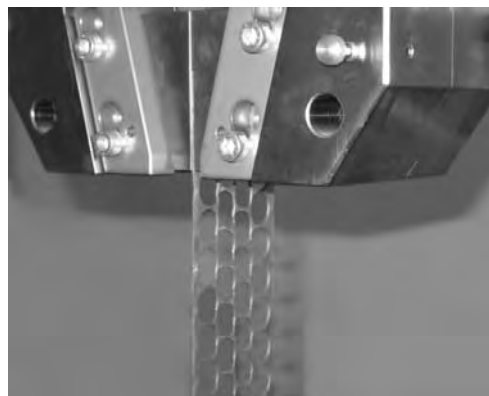


Fig.1 The test of perforated steel tape tension strength.

Table 1

Different types of perforated steel tape and their geometric properties

Type of tape	LM - 1	LM - 2	LM - 3	LM - 4
Width, mm	80,00	77,50	94,00	75,00
Thickness, mm	1,20	1,50	1,00	1,80
Cross-sectional area (Brutto), mm ²	96,00	116,25	94,00	135,00
Cross-sectional area (Netto), mm ²	14,60	24,27	12,35	29,27
Permeable area, %	74	69	67	63

Table 2

The mechanical properties of different types of perforated steel tape

Type of tape	Steel mark, Standard	Max load, N	Max tensile extension (to collapse), mm	Tensile strength, N/mm ²
LM - 1	St 50 ps, AUSS 2284-79 [5.]	13457,63	2,45	921,76
LM - 2	St 08 ps, AUSS 503-81 [4.]	14056,56	2,49	579,17
LM - 3	St 08 ps, AUSS 503-81	5703,45	8,45	461,82
LM - 4	St 08 ps, AUSS 503-81	4944,92	6,21	168,94

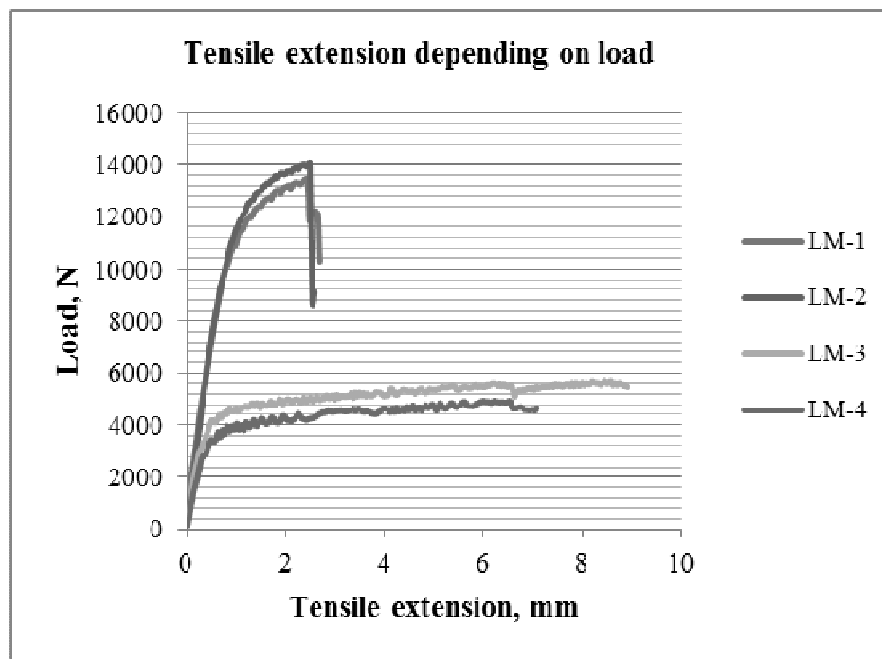


Fig.2. Load - tensile extension curves for 4 types of perforated steel tapes.

The achieved results let us to conclude that the viewed different mechanical features of the perforated tape waste can be equated to these steel tape mechanical features which are now used in the realization of different building targets. For example, steel tape which is used as different type surface load bearing elements strength is in limits of 380 – 900 MPa (Ермолов , 1991).

ANTI CORROSION EVENTS

As with every metal element, including also steel, there is disposition to corrode with the time and with it to lose the initial mechanical features and then there is a necessity to make anti-corrosion events.

One of the protection methods is zincing. As zincing disadvantages we can consider higher process costs and possible material rolling by its dipping in the bath with zinc fusion.

Many samples were overlaid with zinc coat in the density of 30-40 mkm. The hardness measurements using the Brinel method on the most of the surfaces showed relation to the initial values – HB = 1060 – 1200 MPa.

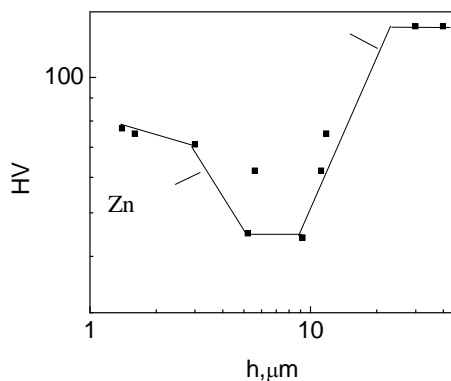


Fig.3. Micro hardness (HV) dependence on ferrule absorption (h) zinc overlay on steel surface.

For notification of micro hardness an accurate measuring device was used [9] that let us to use a load from 3 mN to 2 N. Micro hardness notification relating from the ferrule pressing depth let us evaluate the surface hardness and adhesion with the base. As we can see in Figure 6, micro hardness in dipped diapason up to 10 mkm corresponds to the zincing galvanic overlay with good adhesion. Whereas rising of micro hardness at bigger dipping depth is related with hard steel influence.

As cheaper anti-corrosion way we can mention polymeric overlay which is laid with help of thin disperse powder. For putting thin disperse powder on the perforated tape surface we used a method with putting it in electronic area (Герасименко, 2001).

After putting on 30-40 mkm lay, the tape or construction with its usage was subjected to thermal heating in the term camera till temperature of polymerization of the overlay. But we must notice,

that polymeric overlay adhesion with the steel surface in the given case is not big. It is expediently at first to subject the tape to mechanical cleaning from oil or other dirt and further subject to chemically – thermal processing, for example, phosphoting. In this case the overlay adhesion with the steel tape is higher.

USAGE POSSIBILITIES IN THE CONSTRUCTION

Interior and exterior elements

Perforating tape is possible to use in interior and exterior decorative formatting, this let us find interesting and unusual solutions. For example, it is possible to make decorative sieve wicker works, panels (possible usage area – making of saving elements of blast, fireplace and stove). In Figure 4 a sample of blast panel in which the base is sieve from perforated steel tape is shown. Decorative type is achieved overlaying two layers perpendicular one to another performed tape samples with the same perforation (in the given case on its basics there is round punching).

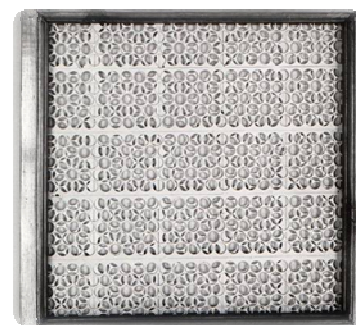


Fig.4. Decorative blast panel from perforated steel bands.

In the same way on the basis of perforated elements it is possible to make different limiting constructions inside and outside (for example, for borders of balconies and loggias).

Without the samples mentioned before, from perforated steel tape it is possible to make lightning systems with unique light separation (Mironovs, Truļins, 2009), different furniture details, for example, table legs (Kaļva, 2010), shelf systems, and perforated benches.

Bricklaying works

It is possible to use perforated tape for reinforcement of bricks and other materials of brick walls (Mironovs, Lapsa, 2006). The reinforcement sieve which is laid in the brick horizontal joints (Figure 5), for manufacturing it is possible to use industrial waste at which belong also in this work overviewed perforated tape and it is considered as a pretty rational approach.

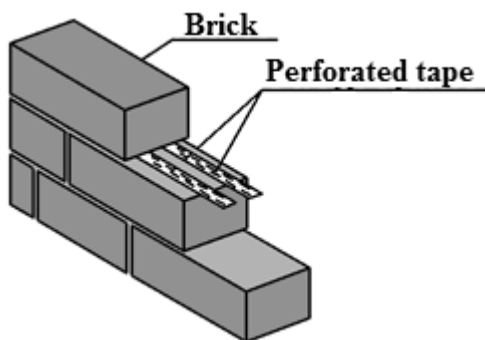


Fig.5. Brick wall reinforcement with perforated tape.

At first, due to brick wall reinforcement, its load-bearing ability is rising (due to this that reinforcement delaying longitudinal tension deformation development in the bricks and delaying vertical cross curve distribution in all height of the bricks) and secondly, expediently raw material waste is used.

For this kind of brick reinforcement technologies establishment also patents are known (Mironovs, Lapsa, 2006).

Reinforcement sieves which are made on the basis of perforated tape (sieve fragment is shown in Figure 6) have high functionality, they have high strength characteristics, the tape sizes are easy comparative with the brick sizes, whereas the perforation curves, which constituting about 60 – 70%, ensure good adhesion with brick java.

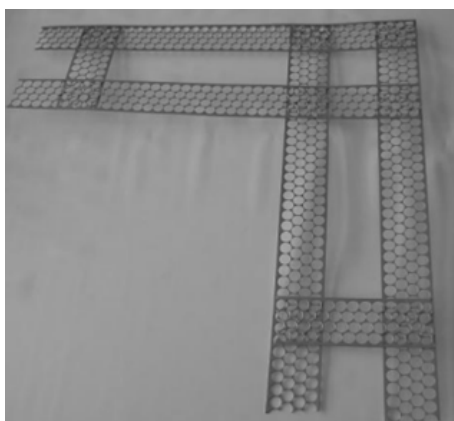


Fig.6. Reinforcement sieve fragment which is made of perforated steel tape.

Perforated tape usage in brick reinforcement already has achieved good references from builders – it is better placed in joint places and easier cut in the necessary pieces.

In addition, worth nothing that perforated waste tape is up to 3 – 4 times cheaper (0,08EUR/m) than special reinforcement (Bi - armature) – 0,28EUR/m (*Steel reinforcement.....*).

Internal and external finishing works

- Perforated steel band and its products in plastering works

Riddles made of perforated steel band rolled with a small thickness, can be successfully used in plastering works for wall surfaces. For this purpose elements of the perforated steel band are first connected by welding in riddles.

Another variant of using perforated steel band in plastering works – profiles made of perforated steel band can be used as guide profiles, finishing profiles and corner profiles. Corner profiles provide a connection between a plaster of two perpendicular walls, so developing of cracks is prevented.

- Using perforated steel band profiles for insulation fixing in wall and ceiling constructions

One of the possible ways for fixing heat insulation using perforated double-T shaped profile is shown in Figure 7. In this case into the hollow space of the double-T profile a heat insulation material has been put in, from outside this construction has been covered with gypsum slabs.

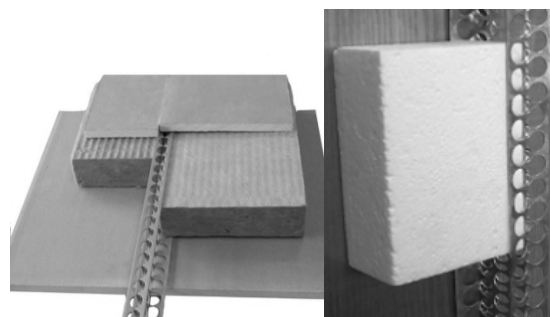


Fig.7. Using of perforated profiles in wall construction solutions..

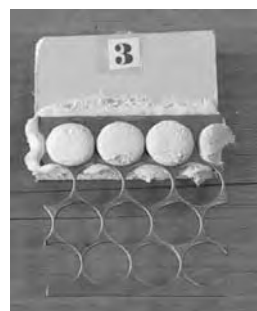


Fig.8. Connection of perforated steel band and gypsum plate with adhesive on gypsum basis.

Road-adherence between perforated steel profile and gypsum plate is possible get by using quick-hardening adhesives on gypsum basis (Fig. 8) (Lapsa, Mironovs, 2005). The strength tests of this kind of joints showed that the shear strength of the joint is from 0.75 to 1.50 MPa. The main characteristics of this method is its simplicity, high

productivity, so this method of joining perforated steel profiles and gypsum plates is advisable in montage of non-responsible building constructions (Mironovs, Boyko, Sedjuks, 2006).

The load carrying capacity of the double-T shaped and U-shaped struts (Li, John, Maricherla, 2006) with a joint support was evaluated as centristpressed elements with constant cross-section.

For example, with the folding methods there were made 2 U-shaped profiles, with the „wall” height $h=53$ mm, these profiles were connected together by using the spot welding method, thus creating a double-T shaped perforated profile.



Fig.9. Perforated struts before pressure strength test

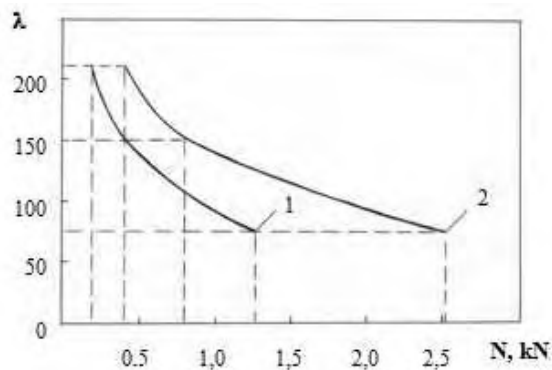


Fig.10. Load bearing capacity N of struts, depending on flexibility λ (1 – strut with U-shaped cross-section; 2 – strut with double-T cross-section).

As a result the max load bearing capacity of the struts was gained, when the flexibility of the struts were $\lambda = 75$. The yield strength was 350 MPa. The load bearing capacity depending on the flexibility of the struts with different cross-section is shown in Figure 10.

- Perforated steel band in suspended ceiling constructions

When making suspended ceiling constructions, there are different ways how to brace the ceiling plates, for example, we can use strands; use hang up elements with a special upper part; it is also possible to fasten the plates directly to the wooden

elements (beams). It is also possible to use perforated steel band as a hang up element, as it is shown in Figure 11.

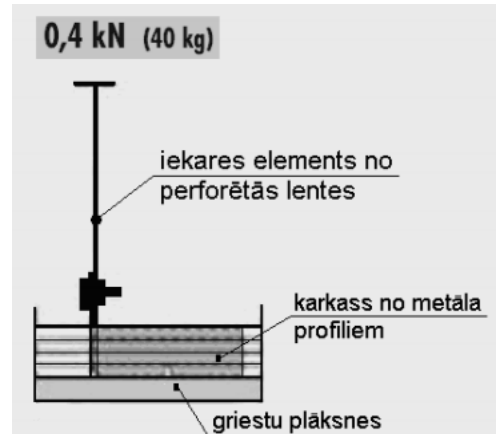


Fig.11. Perforated steel band in suspended ceiling constructions

According to DIN 18 168, the load carrying capacity of the perforated steel band hang up element is 0,4 kN.

Perforated steel band as a reinforcement element

- Perforated steel band reinforcement for sewerage tubes

For this purpose spatial spiral-shaped carcasses have been created, as it is shown in Figure 12. In the manufacturing process this spatial carcass is covered with a rubber layer from both sides and then vulcanization is carried out in special ovens. Thus, we get tubes that are a safe and resistant building material, suitable for non-pressure sewerage networks.

The main physical-mechanical characteristics of the sewerage tubes made in such way meet the requirements set up for sewerage tubes (for example, water absorption less than 8%) (Kaļva, 2010).

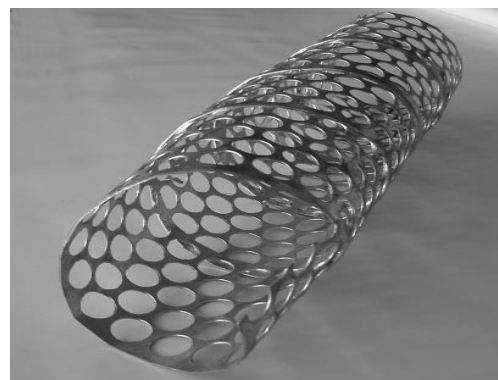


Fig.12. Spatial spiral-shaped carcass for manufacturing of tubes.

- Manufacturing of reinforced rubber

It is rubber that has reinforcement of reinforcement nets, made or perforated steel band elements. Reinforced rubber is used for manufacturing, for example, rugs for vibration smothering. These rugs are used under motors, vibrating-tables, air-pumps and other devices that make noise and vibration.

- Road surfacing with reinforcement from perforated steel band

A fragment of the decorative pedestrian road with reinforcement from perforated steel band is shown in Figure 13. Wide bands of the reinforcement prevent the birth of cracks as a result of concrete compaction.



Fig.13. Fragment of decorative pedestrian road.

Also motorways are made using reinforcement of perforated steel band. Reinforcement nets are made for this purpose and embedded before asphalt is covered.

Concrete works

- Block constructions

Perforated materials can be used also in making block constructions (Figure 14).

Block elements consist of a frame and reinforced-rubber shields. Perforated steel band is used as reinforcement for the shields. Reinforcements can be made of double-T shape perforated profiles as well. The dimensions, thickness of perforated profile depend on the size of the block element. The gain is that by using reinforced-rubber block elements, road adherence between the concrete and block element is minimized.



Fig.14. Shield block made using reinforced-rubber and perforated profiles.

Block elements after removing are very clean, there is no need to clean them. Reinforced-rubber shields also give a possibility to make decorative patterns on the concrete surface. Strong and safe block element construction provides repeated usage of the block element, and because of its small weight it is quick to install.

- Spacers for floor and covering concrete works

One of the most perspective ways how to use perforated steel band in building constructions is manufacturing spacers (Lange, Song, 2004) that can be used in concrete works.

The main tasks of the spacers is to fix reinforcement in stable position while performing concrete works, also to provide the necessary thickness of the concrete layer for anti-corrosion.

Spacers made as concrete prisms (Тепиченко, Лapidус, 2005), plastic spacers (Chudley, Greeno, 2001) and „small-bench” type spacers from reinforcement steel (*Betomax.....*) are already known.

If we compare the spacers mentioned this line above, the spacers made of perforated steel band have the following advantages:

- 1) In comparison with plastic spacers the load (common weight of reinforcement carcasses and workers) bearing capacity is higher;
- 2) Lower manufacturing costs (using perforated steel band which is as a manufacturing waist product);
- 3) Usage of metal working products – thus ecological factors have been taken into consideration (Lapsa, Mironovs, 2006).

The physically-mechanical characteristics of perforated steel band gives a possibility to bend it, also to weld it, so it is possible to make different spacers with a wide range of shapes.

T-shaped spacers can be made by welding, when two L-shaped elements are welded together; another way is bending T-shaped spacer from one element (Figure 15).

Double-T shaped spacers can be with different whatnot width (Figure 16, a), or with similar whatnots (Figure 16, b). This kind of spacers is made of two U-shaped elements

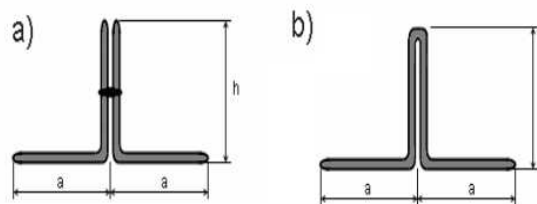


Fig.15. T-shaped spacers (a – welded from two L-shaped elements;
b – curved from one element).

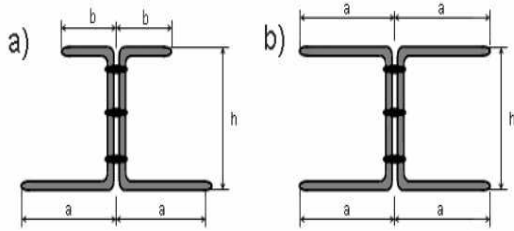


Fig.16. Double-T shaped spacers, weld of two U-shaped elements (a – with different whatnot width; b – with similar whatnots).

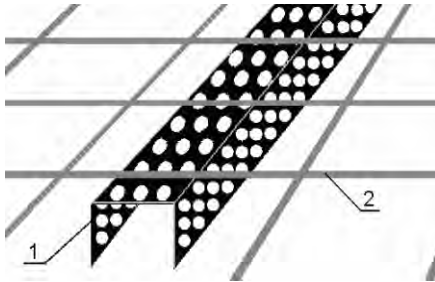


Fig.17. Support of reinforcement on long U-shaped spacer (1 – spacer; 2 – reinforcement).

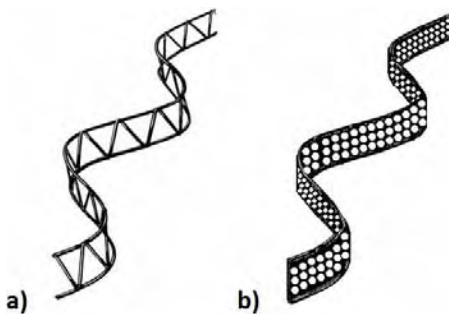


Fig.18. „Serpent-shaped” spacer (a – traditionally known „serpent-shaped” spacer; b – spacer from perforated steel band).

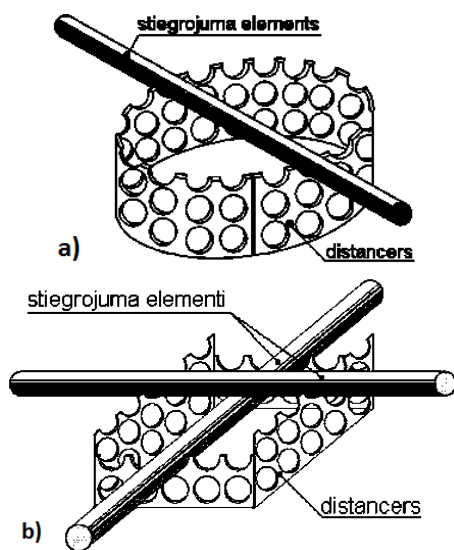


Fig.19. Round (a) and quadrate (b) shape spacers from perforated steel band.

One of the spacer kinds, which is most easy to be made and also most stable in its construction is the U-shaped spacer. U-shaped spacers can be used in two ways – with their whatnot position to top or to bottom.

This kind of spacers can be made short, and then it is suitable for placing reinforcement nets in their cross-points. They can be made also tall, then spacers will be more stable, but in this case the material usage will be larger (Figure 17).

In Figure 18,a a traditional “serpent-shaped” spacer is shown, widely used for upper and lower reinforcement nets upheld. This kind of spacers can be easy made from perforated steel band, by modulating it in the desirable shape (Figure 18,b).

One more very efficient kind of reinforcement spacers is round and quadrate shaped spacers, bended and welded from perforated steel band (Figure 19).

The shape of the spacers gives high stability, but perforation wholes give stability for upheld reinforcement and also a possibility to choose the direction of upheld strands.

Quadrate shaped spacers can be made also with dissimilar height of their sides. In this case it is possible to place oblong-reinforcement and crosswise-reinforcement together.

CONCLUSIONS

On the basis of the test results and analysis of possible usage of perforated steel band in civil engineering, we can conclude that:

- 1) perforated steel tape have very different geometry, area of perforation is not less than 60 % of the total area;
- 2) the tensile strength of different types of tape is noticed in amplitude 168 – 921 MPa, but hardness 830 – 3030 MPa;
- 3) the load bearing capacity of double-T shaped struts is between 0,4-2,6 kN when the flexibility λ is 75-220. The maximal pressure strength is 350 MPa, when the flexibility $\lambda=75$;
- 4) the possibilities to use perforated steel band in civil engineering become wider, if we perform profiling of the band;
- 5) Thus, physically-mechanical characteristics of perforated steel band, also as a manufacturing waist product, allow using it not only for decorative interior and exterior purposes, but also for different kind of constructions. Reinforcement of brick and stone walls, masonries; using of armo-rubber shield blocks and spacers of perforated steel band can be known as most efficient.

REFERENCES

- Betomax, *Abstandtechnik – Abstandhalter – Stahl*. Available: <http://www.betomax.de>
- Bogojavenskij K.N., Neubauer A., Wladimirowitsch Ris V. (1978) *Technologie der Fertigung von Lichtbauprofilen*. Leipzig: WEB Deutscher Verlag für Grundstoffindustrie. 565 p.
- Chudley R., Greeno R. (2001) *Building construction handbook*. Oxford.
- Kaļva L. (2010) *Metallic Perforated Materials In Concrete Works*. Riga Technical University, p. 29, 38.
- Lange J., Song J. (2004) *Untersuchung der Anrißlebensdauer von Betondübeln mit Hilfe des Örtlichen Konzepts*.
- Lapsa V-A., Mironovs V. (2005) *Sienas konstrukcija*. Latvijas patents Nr. 13363B, Cl. E04C5/03, iesn. 31.03.2004, iesn. Nr. P-04-38, publ. 01.12.2005.
- Lapsa V-A., Mironovs V. (2006) *Dzelzsbetona konstrukciju stiegrojuma distanceri*. Latvijas patents Nr. 13404B, Cl. E04C5/01, iesn. 16.08.2004, iesn. Nr. P-04-98, publ. 20.08.2006.
- Li G., John M., Maricherla D. (2006) *Experimental study of hybrid composite beams*.
- Manika A., Muktepavela F. (1998) Microhardness and adhesion of TIN/AIN multilayer coatings. *Surface & Coatings Technology*, p. 333-357.
- Mironovs V., Truļins A. (2009) *Apgaismes ierīce*. Latvijas patents Nr. LV13818B, Cl. F21V1/00, iesn. 16.09.2008, iesn. Nr. P-08-162, publ. 20.01.2009
- Mironov V., Boyko I., Serdjuk. D. (2006) Recycling and application of perforated steel band and profiles. In *proceeding of the 5th Int. DAAAM Conference, 2006*, Tallinn, Estonia, p. 285-288.
- Mironovs V., Lapsa V.-A. (2006) *Mūra stiegrojuma karkass*. Latvijas patents Nr., LV13429B, Cl. E04C5/01, iesn. 18.10. 2004, iesn. Nr. P-04-126, publ 20.06.2006
- Mironovs V., Serdjuk D. (2003) Perforated Steel Bands as a Constructional Material. *Proceeding of Riga Technical University: Architecture and construction science*, p. 157 – 162.
- Mironov V., Serdjuk. D., Muktepavela F. (2003) Profiles from the wastes of stamping production. In *proceeding of the 13- th int. conf., „Eng.Materials and Tribology”*, 2003, Tallinn, Estonia, p. 46-50.
- Perforated tape rolls after punching in the factory SC „Ditton feed chain factory”. Internet resource of AS Ditton pievadķēžu rūpnīcas. Available: <http://www.dpr.lv>
- Pinkham M. (2003) *Manufacturing Slump Crimps Sales of ‘Metal With Holes*. Metal Center news.
- Steel reinforcement for FIBO blocks Available: <http://www.agande.net/lv/fibo-bi-armataara.html>
- Ермолов Е.Е. (1991) *Инженерные конструкции*. Москва: Стройиздат.. 450 стр.
- Герасименко А.А. (2001) *Некоторые особенности технологии нанесения порошковых полимерных покрытий. Электрохимическая защита оборудования и сооружений от коррозии*: Матер. Семинара. А.А. Герасименко (ред.). Москва: ЦРДЗ, стр. 32-34.
- ГОСТ 503 – 81 „Лента холоднокатаная из низкоуглеродистой стали. Технические условия”
- ГОСТ 2284 – 79 „Лента холоднокатаная из углеродистой конструкционной стали. Технические условия”
- Миронов В., Сердюк Д., Муктепавела Ф. (2004) Перфорированные стальные ленты и профили из промышленных отходов. Труды 3^{ей} межд. конференции «Материалы и покрытия в экстремальных условиях», Крым, Украина, сент. 2004, стр. 559-560.
- Тепиченко В.И., Лapidус А.А. (2001) *Технология строительных процессов*. Москва: Высшая школа.

II MATERIALS AND STRUCTURES

TOPOLOGY OPTIMIZATION OF MULTI-LAYERED COMPOSITE STRUCTURES

Janis Brauns*, Karlis Rocens**

* Latvia University of Agriculture, Department of Structural Engineering
Janis.Brauns@llu.lv

** Riga Technical University, Institute of Building and Reconstruction
rocensk@latnet.lv

ABSTRACT

Numerical analysis is performed in order to investigate deformation behavior and strength of antisymmetric laminates under tension caused by axial load. It is determined that antisymmetric orientation of external layers of in-plane balanced laminate can be used to ensure the necessary adaptive warping and strength of composite under action of tensile stresses. The efficiency of the use of carbon and glass epoxy laminates as well as wooden laminate (birch plywood) in wind rotor blades is analysed.

Key words: Laminates, Compliance, Stiffness, Force Stress, Couple Stress, Curvature, Strength

INTRODUCTION

The use of multilayered laminates with unidirectional fiber reinforced plies is well established for lightweight constructions and special applications (Hirano and Todoroki, 2005; Pagano and Soni, 1988)). Because of their high strength and stiffness characteristics, coupled with low weight, composite materials are more attractive for engineering applications than conventional isotropic materials. In addition, because of the highly anisotropic properties of single plies, composite materials allow tailoring of the laminate behavior to the structural needs.

In multilayered fibre-reinforced composites with variable fibre orientations, the directional expansion of the unidirectional single layers due to thermal effects, moisture absorption and chemical shrinkage leads to a discontinuous residual stress field over the laminate thickness. In the case of unsymmetrical laminate plates, these residual stresses can cause different multistable out-of-plane deformations (Brauns and Rocens, 1994; Diaconu and Sekine, 2003).

This study focuses on the purposeful adaptation of the residual stresses dependent on the stacking sequence of layered system in order to realise either laminates with defined multistable deformation states or to design adaptive structures. For the adjustment of laminate curvatures to technical requirements, methods are developed that can efficiently be applied to find an optimal laminate lay-up dependent on the material properties and loading conditions (Hansel and Becker, 2000). Furthermore, failure analysis is carried out in order to assess the resulting residual stress state with respect to first-ply failure.

In general, laminates can be designed to provide the desired strength and stiffness characteristics required for specific applications. The material anisotropy can be exploited to induce coupling between deformation modes. The use of fibre reinforced composite rotor blades enables a number of possible passive aerodynamic control options. By using adaptive wind rotor blades with twist coupling there is a possibility to keep good, steady power production and smooth out unwanted peaks in loading. The blades may be made wholly or partially from carbon fibre, which is a lighter, but costlier material with high strength. A numerical analysis is performed to investigate deformation behavior and strength of in-plane balanced antisymmetric laminates under tension caused by axial centrifugal load.

STRESS AND STRAIN RELATIONSHIPS OF LAYERED STRUCTURE

Composite materials can be constructed by bonding together several structural elements to form an integral structure. The properties and orientation of each element have to be chosen such that the composite is able to meet the design requirements of strength and stiffness. It is also necessary to know the behavior of the material under various environmental conditions, such as exposure to water, low and high temperature.

Within a layered composite of thickness h , deformation of one layer is constrained by the other ones of different orientations, and hence stresses arise in each layer. In general case, the stresses in the elementary layers are different and the stress state of the composite is inhomogeneous. By using a static equivalent system of average force stresses

σ_j and moment stresses μ_j acting on a unite volume of the composite material, the constitutive relations for the mid-plane strains ε_i^0 and the curvatures κ_i in matrix notations are given by

$$\begin{bmatrix} \varepsilon^0 \\ \kappa \end{bmatrix} = \begin{bmatrix} \alpha & \beta \\ \beta^T & \delta \end{bmatrix} \begin{bmatrix} \sigma \\ \mu \end{bmatrix}, \quad (1)$$

where α, β, δ are compliances of layered composite; superscript T denotes transposition operation.

The force stresses and moment stresses in layered composite are calculated by averaging

$$\sigma_j = \int_{-h/2}^{h/2} \tilde{\sigma}_j^{(k)} dx_3, \quad (2)$$

$$\mu_j = \int_{-h/2}^{h/2} \tilde{\sigma}_j^{(k)} x_3 dx_3. \quad (3)$$

The stresses $\tilde{\sigma}_j^{(k)}$ in the k th elementary layer in the coordinate of composite $\{x_i\}$ ($i = 1, 2, 3$) can be determined by using the layer stiffness A'_{ij} in the local coordinate system $\{x'_i\}$ and stress transformation matrix (Tsai and Hahn 1980). In the general case, the compliance matrices in (1) are represented in terms of composite stiffness:

$$\alpha = S + SBCBS; \quad (4)$$

$$\beta = -SBC; \quad (5)$$

$$\delta = C \quad (6)$$

with

$$C = [D - BSB]^{-1}. \quad (7)$$

The stresses in the elementary layers (Fig. 1) in the coordinates of composite $\{x_i\}$ can be determined by using the layer stiffness A'_{ij} in the local coordinate system $\{x'_i\}$ and stress transformation matrix. The stiffness components in (4)–(7) are evaluated by integrations:

$$[A_{ij}, B_{ij}, D_{ij}] = \int_{-h/2}^{h/2} \tilde{A}_{ij}^{(k)} [1, x_3, x_3^2] dx_3. \quad (8)$$

In (8) the stiffness matrix $[\tilde{A}_{ij}]^{(k)}$ of the elementary layer in the coordinate system $\{x_i\}$ can be

determined by using the transformation formula. The compliance matrix in (4), (5) and (7) is $[S_{ij}] = [A_{ij}]^{-1}$.

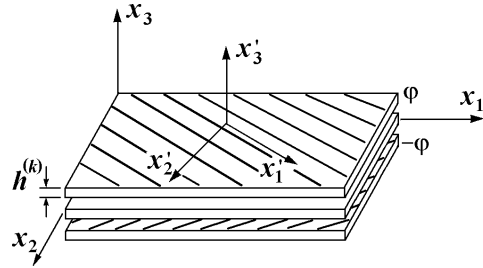


Figure 1. Multilayer model of antisymmetric laminated composite structure.

STRENGTH ANALYSIS OF DESIGNED LAMINATE

Predicting the failure of structural components is usually accomplished by comparing the stresses to the material strength limits. A number of failure criteria have been proposed, however, the main issue is whether there is any interaction between the modes of failure. Experimental observations for fiber-reinforced materials show interactions between the failure modes. For example, shear failure is expected to occur more easily if, in addition to the shear stress, there is also a normal tensile stress. The most frequently used failure criteria taking account of this effect are polynomial criteria advised by Malmeister (Malmeister, 1966) and Tsai and Wu (Tsai and Wu, 1971). This criterion is easy to apply because it does not distinguish between different failure modes. On the other hand, it takes into account the interaction between the in-plane stresses in different directions.

A more general form of the failure criterion for orthotropic materials, i.e., materials with two mutually perpendicular planes of symmetry in mechanical properties, under plane stress state is expressed as

$$\begin{aligned} f(\sigma_{ij}) = & F_{11}\sigma_{11} + F_{22}\sigma_{22} + 2F_{12}\sigma_{12} + \\ & + F_{1111}\sigma_{11}^2 + F_{2222}\sigma_{22}^2 + 4F_{1212}\sigma_{12}^2 + \\ & + 2F_{1122}\sigma_{11}\sigma_{22} + 4F_{1112}\sigma_{11}\sigma_{12} + \\ & + 4F_{2212}\sigma_{22}\sigma_{12} = 1. \end{aligned} \quad (9)$$

The coefficients in the stress function (9) are the components of tensors F_{ij} and F_{ijkl} . They are determined by means of the strength tensor $R_{\alpha\beta\gamma}$, where $\alpha = 0, 11, \bar{1}\bar{1}$; $\beta = 0, 22, \bar{2}\bar{2}$; $\gamma = 0, 12, \bar{1}\bar{2}$. The index 0 denotes that the given stress component is absent; the bar over the index is employed to indicate a compressive component. Using the strength values obtained experimentally, the coefficients are represented in the following form:

$$\begin{aligned}
 F_{11} &= \frac{R_{\overline{1100}} - R_{1100}}{R_{1100}R_{\overline{1100}}}; F_{22} = \frac{R_{\overline{0220}} - R_{0220}}{R_{0220}R_{\overline{0220}}}; \\
 F_{1111} &= \frac{1}{R_{1100}R_{\overline{1100}}}; F_{2222} = \frac{1}{R_{0220}R_{\overline{0220}}}; \\
 2F_{1122} &= \frac{F_{11} - F_{22}}{R_{11220}} + F_{1111} + F_{2222} - \frac{1}{R_{11220}^2}; \\
 4F_{1212} &= \frac{1}{R_{0012}R_{\overline{0012}}}.
 \end{aligned} \quad (10)$$

The axes 1 and 2 of the strength envelope (ellipsoid) are set in the plane defined by $\sigma_{11} \sim \sigma_{22}$ and axis 3 is parallel to the axis of shear stresses σ_{12} . The components of the tensor of the strength surface, F_{11} and F_{22} , express the displacement of the centre of the ellipsoid along the axes 1 and 2, respectively. The angle of rotation of the ellipsoid relative to axis 1 is a function of the component F_{1122} .

The mentioned criterion defines an envelope in stress space: if the stress state lies outside of this envelope, then failure is predicted. The failure mechanism is not specifically identified, although inspection of the relative magnitudes of the terms in (9) gives an indication of the likely contribution of the modes.

RESULTS AND ANALYSIS

Considering laminates with fixed total thickness, the objective function could be the effective elastic or strain characteristic, while constraints are imposed on other properties. The layer orientation design problem involves design of a laminate with a single orientation angle and the laminate can also be more complex, providing additional layers with fixed orientations. In practice, fibre-reinforced composite laminates for conventional stiff rotor blades incorporate a combination of unidirectional plies to support radial loads and provide sufficient bending stiffness, and 45° plies to restrict shear and torsion. Representing the pertinent characteristic as a function of undetermined face layer orientation angle $\pm\varphi$ and determining the optimum can be solved as optimisation problem.

Graphical procedure can be used for the design of laminates with prescribed in-plane properties (Miki, 1983). The procedure is suitable for in-plane balanced angle-ply laminates made up of stacks of layers with different orientation angles $\pm\varphi$. In addition to the balanced angle-ply groups, unidirectional layers with principal material axis aligned with the axes of the laminate, i.e. 0° and 90°, can be included in the stacking sequence.

For a in-plane balanced composite laminates elastic characteristics of the laminate can be determined by using lamination parameters that contain all the relevant information associated with the stacking

sequence. The lamination parameters can be determined in the following way

$$V_{1\{A,B,D\}} = \int_{-h/2}^{h/2} \cos 2\varphi \{1, x_3, x_3^2\} dx_3; \quad (11)$$

$$V_{2\{A,B,D\}} = \int_{-h/2}^{h/2} \sin 2\varphi \{1, x_3, x_3^2\} dx_3; \quad (12)$$

$$V_{3\{A,B,D\}} = \int_{-h/2}^{h/2} \cos 4\varphi \{1, x_3, x_3^2\} dx_3; \quad (13)$$

$$V_{4\{A,B,D\}} = \int_{-h/2}^{h/2} \sin 4\varphi \{1, x_3, x_3^2\} dx_3. \quad (14)$$

In general case, lamination parameters and material invariants (Tsai and Pagano, 1968) can be used for determination of the mentioned above stiffness characteristics A_{ij} , B_{ij} and D_{ij} . Two parameters V_{1A} and V_{3A} after normalizing were used to determine optimum design.

By using the lamination parameter diagram (Fig. 2), it is possible to determine the region of allowable combinations of lamination parameters. For a laminate of total thickness h , where the volume fraction of layers with $\pm\varphi_i$ orientation angles is v_i , normalized lamination parameters are given as

$$\overline{V}_1 = \frac{V_{1A}}{h} = \sum_{i=1}^N v_i \cos 2\varphi_i; \quad (15)$$

$$\overline{V}_3 = \frac{V_{3A}}{h} = \sum_{i=1}^N v_i \cos 4\varphi_i, \quad (16)$$

where N is the number of different $\pm\varphi$ groups. The values of the lamination parameters are always bounded, i.e., $-1 \leq (\overline{V}_1, \overline{V}_3) \leq 1$. For a laminate with one orientation angle the two parameters are related as

$$\overline{V}_3 = 2\overline{V}_1^2 - 1. \quad (17)$$

Values of all possible combinations of the lamination parameters are, therefore, located along the boundary line ABC (Fig. 2). The points A, B and C correspond to laminates with 0°, ±45°, and 90° orientation angles, respectively. Any point inside the boundary line corresponds to laminates with two or more fiber orientation.

Composite laminates for rotor blades incorporate a combination of unidirectional plies to support radial centrifugal loads and provide sufficient bending stiffness, and 45° plies to restrict shear and torsion. Using graphical procedure and representing the needed characteristic as a function of undetermined

external layer orientation angle φ the optimisation problem is solved. The procedure is suitable for in-plane balanced angle-ply laminates made up of stacks of layers with different orientation angles $\pm\varphi$. The analysed laminates consist of 9 layers that form an in-plane balanced antisymmetric system with stacking sequence $[\varphi, 45, -45, 90, 0, 90, -45, 45, -\varphi]$. In the lamination parameter diagram (Fig. 2) the point L corresponds to the orientation of external layers $\varphi = 0^\circ$ but the point N to $\varphi = 90^\circ$. The point M belongs to the laminate configuration with $\varphi = \pm 25^\circ$ when laminates indicate the maximum warping under action of axial load.

In Figures 3, 4 and 5 the curvature of the laminates determined by using relationship (1) and strength function determined according to (9) is shown. The warping of wooden laminate is greater in comparison with carbon epoxy and glass epoxy laminate, but in all cases there are allowable intervals, where the curvature changes from zero until maximum, but the stress level is allowable, i.e., $f(\sigma_{ij}) < 1$.

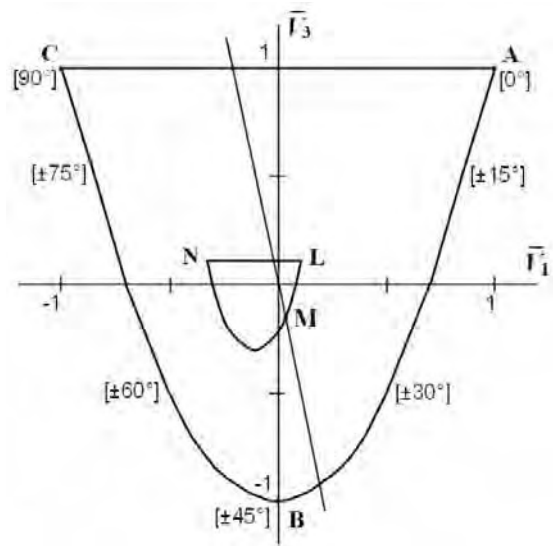


Figure 2. Design area for in-plane lamination parameters: ABC – defined stacks of layers; LMN – analysed laminates.

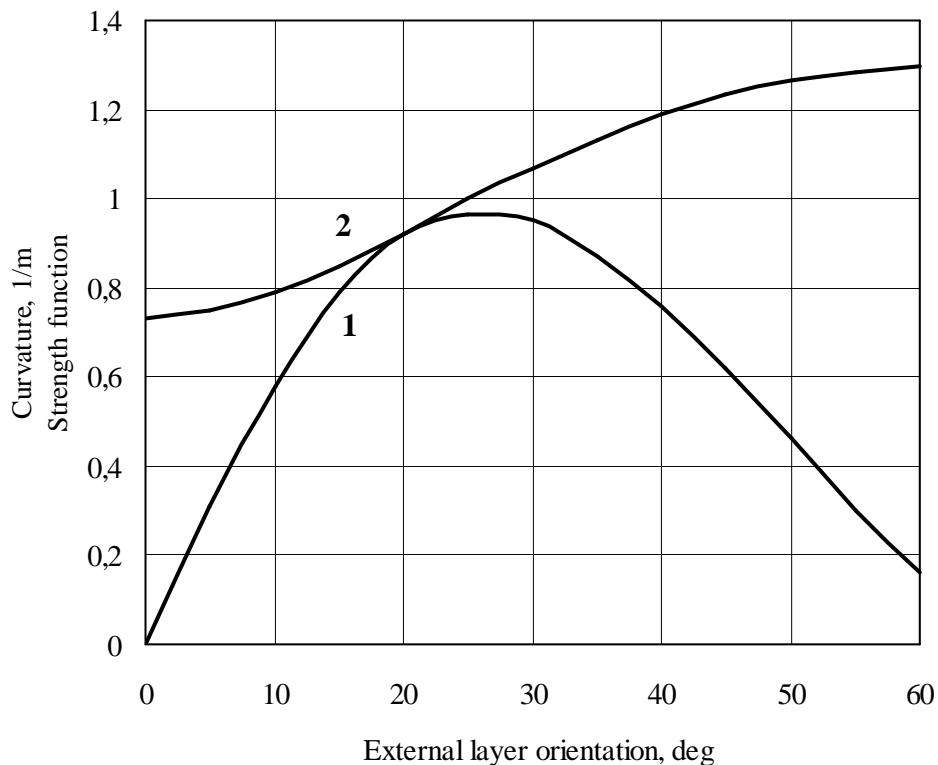


Figure 3. Curvature (1) and strength function (2) vs. external layer orientation for carbon epoxy laminate.

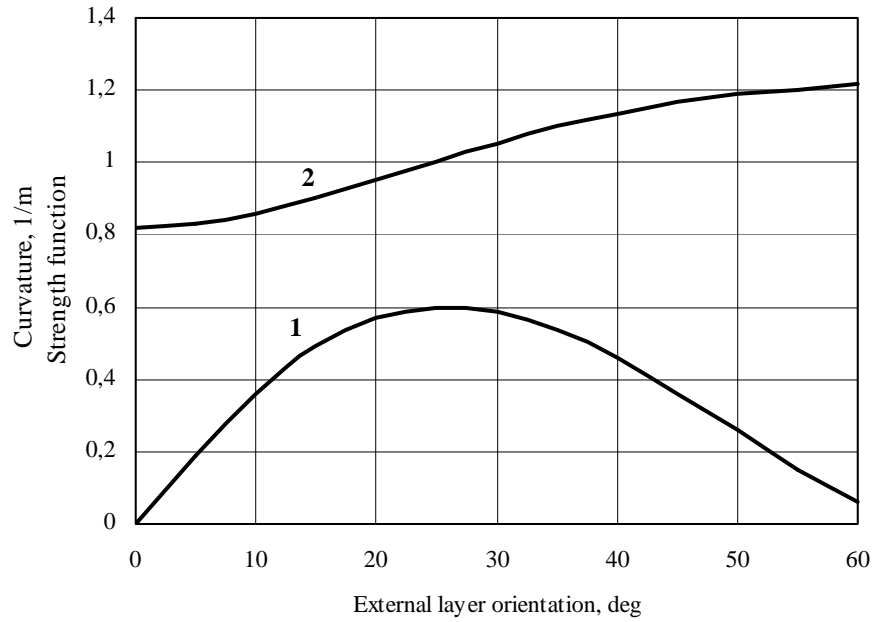


Figure 4. Curvature (1) and strength function (2) vs. external layer orientation for E-glass epoxy laminate.

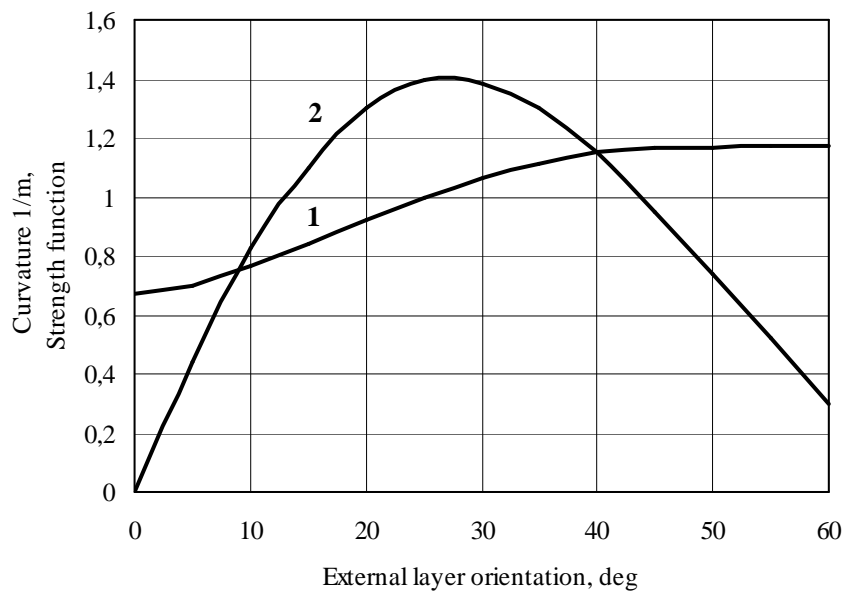


Figure 5. Curvature (1) and strength function (2) vs. external layer orientation for birch plywood.

Table 1

Strength and economical characteristics of laminates

Laminate	Carbon/epoxy	Glass/epoxy	Plywood
Average stresses at ultimate, MPa	270	80	45
Price, USD/m ²	46 700	22 000	33

CONCLUSIONS

Antisymmetric orientation of external layers of in-plane balanced laminate can be used to ensure the necessary adaptive warping and strength of the laminate under action of axial load.

The use of stretching-twisting coupling can be applied to provide a control mechanism of rotor blades which does not have any parts moving relative to each other, and which is therefore maintenance-free.

For in - plane balanced laminates with anti-

symmetric orientation of external layers under action of axial force adaptive warping and strength of the laminate can be ensured.

For the analysed laminates the allowable interval for external layer orientation is 0°–25°. Maximum twisting can be obtained in case of birch plywood but the price of this laminate is relatively low.

REFERENCES

- Brauns J. A. and Rocens K. A. (1994) Hygromechanics of composites with unsymmetric structure. *Mech. Compos. Mat.*, No. 30, p. 601–607.
- Diaconu C. G. and Sekine H. (2003) Flexural characteristics and layup optimization of laminated composite plates under hygrothermal conditions using lamination parameters. *J. Therm. Stresses*, No. 26, p. 905–922.
- Hansel W. and Becker W. (2000) An evolutionary algorithm for layerwise topology optimization of laminates. *Adv. Eng. Mat.*, Vol. 2, No. 7, p. 427–430.
- Hirano Y. and Todoroki A. (2005) Staking-sequence optimisation of composite delta wing to improve flutter limit using fractal branch and bond method. *Int. J. JSME*, No. 48, p. 65–72.
- Malmeister A. K. (1966) Geometry of strength theory. *Polymer Mech.*, No 4, p. 519 – 534.
- Miki M. (1983) A graphical method for designing fibrous laminated composites with required in-plane stiffness. *Trans. JSCM*, No. 9, p. 51–55.
- Pagano N. J. and Soni S. R. (1988) Strength analysis of composite turbine blades. *J. Reinf. Plast. and Compos.*, No. 7, p. 558–581.
- Tsai S. W. and Hahn H. T. (1980) *Introduction to Composite Materials*. Westport: Technomic Publ. Co.
- Tsai S. W. and Pagano N. J. (1968) Invariant properties of composite materials. In: *Composite Materials Workshop*. S.W. Tsai, J.C. Halpin, N.J. Pagano (eds.). Westport: Technomic Publ. Co., p. 233–253.
- Tsai S. W. and Wu E. M. (1971). A general theory of strength for anisotropic materials. *J. Compos. Mat.*, No. 5, p. 58–66.

MODELING OF FIBER BRIDGING BEHAVIOUR IN SFRC

Ulvis Skadins, Janis Brauns

Latvia University of Agriculture, Department of Structural Engineering
ulvis.skadins@llu.lv

ABSTRACT

By adding fibers to concrete mix the objective is to bridge discrete cracks providing for some control to the fracture process and increase the fracture energy. Fibers become active mainly when cracking starts and deformation of the fiber occurs. The pulley approach by Aveston and Kelly can be used to describe the bridging phenomena of a fiber crossing a cracked surface, where the bond-slip of the fiber is equal to the crack opening displacement. As the fiber is able to damage a part of the matrix, the bridging phenomena of a fiber crossing a cracked surface could be described by using the pulley that is attached to the matrix via a spring. In the modified model the crack opening is greater than the fiber slip. The displacement for which the fiber becomes effectively involved in the tension carrying mechanism is effective length which depends on the material parameters obtained from fiber pullout tests for varying angle and fiber types.

Keywords: effective crack width, fiber displacement, orientation angle, pullout test

INTRODUCTION

The low tensile strength of concrete is due to the propagation of internal micro cracks. The tensile strength of concrete could be improved by suitably arranged and closely spaced wire reinforcement. By adding fibers to concrete mix the objective is to bridge discrete cracks providing for some control to the fracture process and increase the fracture energy. For quasi-brittle materials, such as concrete, loaded in tension the behaviour beyond the peak load can be described by the crack opening displacement (w) depending on the applied load (F) (Fig. 1).

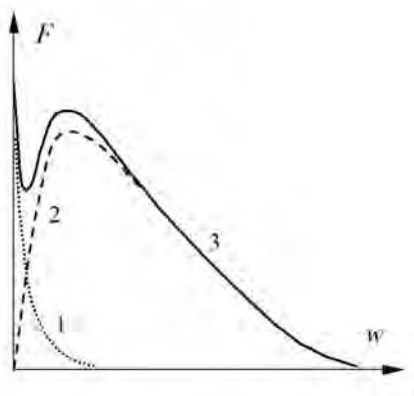


Figure 1. Crack opening for concrete (1), fibers (2) and SFRC (3).

As the principal benefits of the fibers are effective after concrete cracking, it is important to investigate the bridging phenomena in SFRC. There is a considerable residual strength of SFRC structures because the fibers guarantee a certain level of stress transfer between the faces of the crack.

Nevertheless, the nature of the stress transferring process at different fiber displacements needs to be studied. Is the effectiveness of fibers constant during the whole crack opening process? A numerical model, based on experimental data, needs to be developed, which will take into account the concrete strength, type of fiber, orientation angle and crack width. Part of this paper is allotted to represent the pullout tests performed to analyze the influence of the fiber type and orientation on the bridging process and to obtain the necessary material parameters for the numerical model.

Bridging models

To understand the bridging process in a FRC element, let us look at a small piece of concrete with a single arbitrary orientated steel fiber (see Figure 2). There is a micro crack in the matrix due to tensile stresses applied. The anchorage of the fiber is sufficient in both sides of the crack. The fiber has negligible reaction force until the bond-slip in the fiber-matrix interface has yet to be developed ($w = 0$).

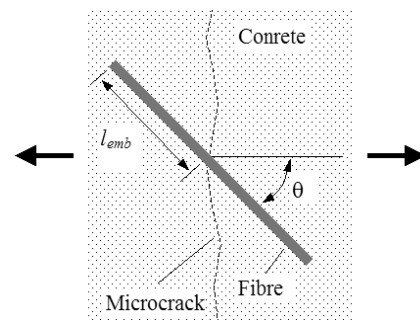


Figure 2. Bridging model at the beginning of crack formation.

When the crack width (w) increases, the fiber becomes active and deformation of the fiber occurs. The pulley approach (Aveston and Kelly, 1973) can be used to describe the bridging phenomena of a fiber crossing a cracked surface, with the assumption that the matrix at the exit point of the fiber is rigid. The model is shown in Figure 3. In this case the bond-slip of the fiber δ on the side of the shorter embedment is equal to the crack opening displacement ($\delta = w$).

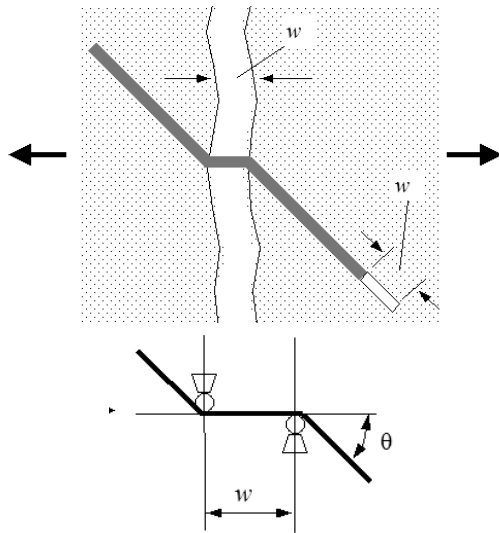


Figure 3. Bridging model based on pulley approach by Aveston and Kelly, 1973.

As the fiber-matrix interface has a negligible tensile strength, the fiber is able to damage a part of the matrix. In this case, the bridging phenomena of a fiber crossing a cracked surface could be described by using the pulley that is attached to the matrix via a spring (see Figure 4).

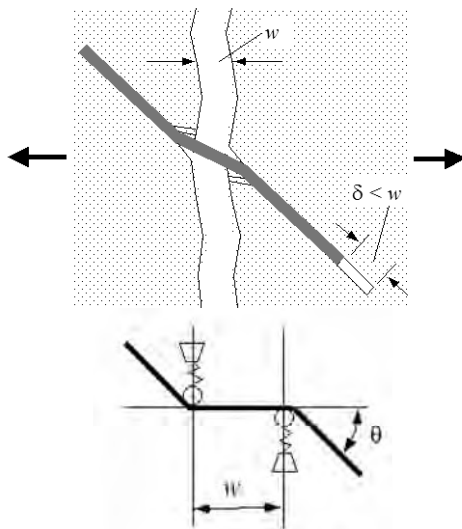


Figure 4. Modified bridging model – pulley attached to matrix via springs.

In the modified model the crack opening is greater than the fiber slip. The displacement for which the fiber becomes effectively involved in the tension carrying mechanism is the effective length w_{eff} which depends on the material parameters obtained from the fiber pullout tests for varying angle θ and fiber type (Brauns and Skadins, 2010; Fantilli et al., 2008).

The proposed model is based on the following basic assumptions.

The force, F_f , which can be taken by a single fiber is equal to zero when the crack width $w < w_{eff}$ and $w > l_{emb}$. Otherwise it can be found by the equation (1):

$$F_f = \pi d_f \tau_b (l_{emb} - w). \quad (1)$$

The effective length w_{eff} is determined at half of the maximum pullout force:

$$w_{eff} = w \quad \text{at} \quad F_{f,max} / 2. \quad (2)$$

The effective length or crack width at a certain orientation angle can be found by the equation (3):

$$w_{eff}(\theta) = K_1 + K_2 \tan \theta. \quad (3)$$

The fiber bond strength for $\theta = 0^\circ$ is described by the equation (4):

$$\tau_b = \frac{F_{f,max}}{\pi d_f l_{emb}}, \quad (4)$$

where in equations (1) to (4)

w – crack width or fiber displacement in pullout test;

$F_{f,max}$ – maximum single fiber pullout force;

K_1, K_2 – material parameters obtained from pullout tests;

θ – fiber orientation angle;

τ_b – fiber bond strength;

d_f – fiber diameter;

l_{emb} – fiber embedment length.

Pullout test

Short fibers act as a bridging mechanism over the crack. The behavior of fibers at the crack can be simulated by the single fiber pullout test (Figure 5). As the fiber orientation in FRC elements is random, the pullout test was performed for fibers with different orientation angles.

Specimen data

The tests were performed for four different types of fibers and four orientation angles. The fibers were concreted in small prisms with the dimensions of 40×40×60 mm.

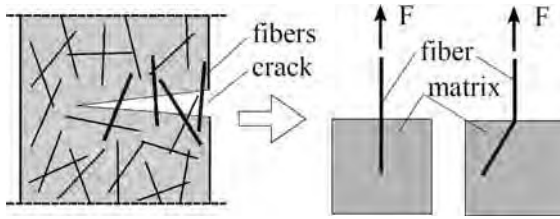


Figure 5. Pullout test as simulation of bridging process in cracked SFRC structure

The embedment length was 25 mm. The loosed part of the fibers was straightened. There were three specimens for each type and angle – all together 48 pieces. Concrete with very fine grains was used. The mean concrete strength was 55.1 MPa with the variation coefficient of 0.016.

Four different types of fibers were used, smooth (S), hooked (H), crimped (C) and flat ended (FE). The fiber diameter was 0.75 mm and length – 50 mm. The yield strength of the fiber steel was 1100 MPa.

Test setup

The tests were performed under closed looped conditions by controlling the position of the machine head and using the test speed 1 mm per minute. S9 type force transducer (max. load 50 kN) and three LVTD's (HBM WETA1/2 mm) were used to record the data for force-displacement curves. The test setup is shown in Figure 6.

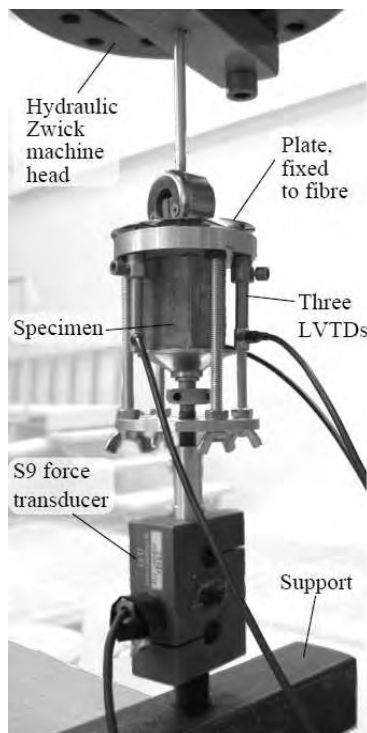


Figure 6. Pullout test setup.

Effective crack width

As it was mentioned before, the fibers become active after cracking. Nevertheless, not all of the fibers, crossing the developed crack, are effective at the very beginning of crack formation. From the test results it can be seen, that the fibers, which are more inclined, reach their maximal pullout force at a greater displacement (slip). That means that they will be involved in the bridging process when the crack is wide enough or when the width of the crack $w = w_{eff}$. It is assumed that the effective crack width (w_{eff}) can be found from the force-slip curves at the point $F_{f,max}/2$ (see equation (2)). For more inclined fibers the effective crack width is larger.

As the fibers at the angle of 90 degrees will have no effect in stress bridging, the tangent function is used to describe the relationship between the effective crack width and the fiber orientation angle. The agreement between the experimental results and theoretical function for each type of fibers is shown in Figure 7.

Critical value of the orientation angle

The fiber amount in concrete is one of the most important factors for post cracking behavior of a structure. There are several conditions that make a fiber effective if fulfilled:

- The fibers must be in the tension zone.
- They must be anchored enough (in both sides of the crack).
- The orientation of fibers cannot be parallel or close to parallel to the crack surface.
- The crack must be wide enough.

The SFRC structure design according to the crack width limit state requires ensuring comparatively small cracks in humid environment (0.3 mm). Although cracks can be wider in dry conditions and in the design of the ultimate limit state, they should be restricted to 3.5 mm (RILEM TC 162-TDF, 2003).

If the crack width is limited, then a certain portion of fibers, crossing the crack, will not be involved in the bridging process, for their orientation angle θ is too big. The angle θ_{crit} determining the boundary for the effective fibers can be found by the equation (5).

$$\theta_{crit} = \arctan\left(\frac{w - K_1}{K_2}\right) \quad (5)$$

At a certain crack width (w) only those fibers can be taken into account, which are inclined less than the critical angle (θ_{crit}).

The results of the equation (5) for different types of fibers and crack widths are given in Table 1.

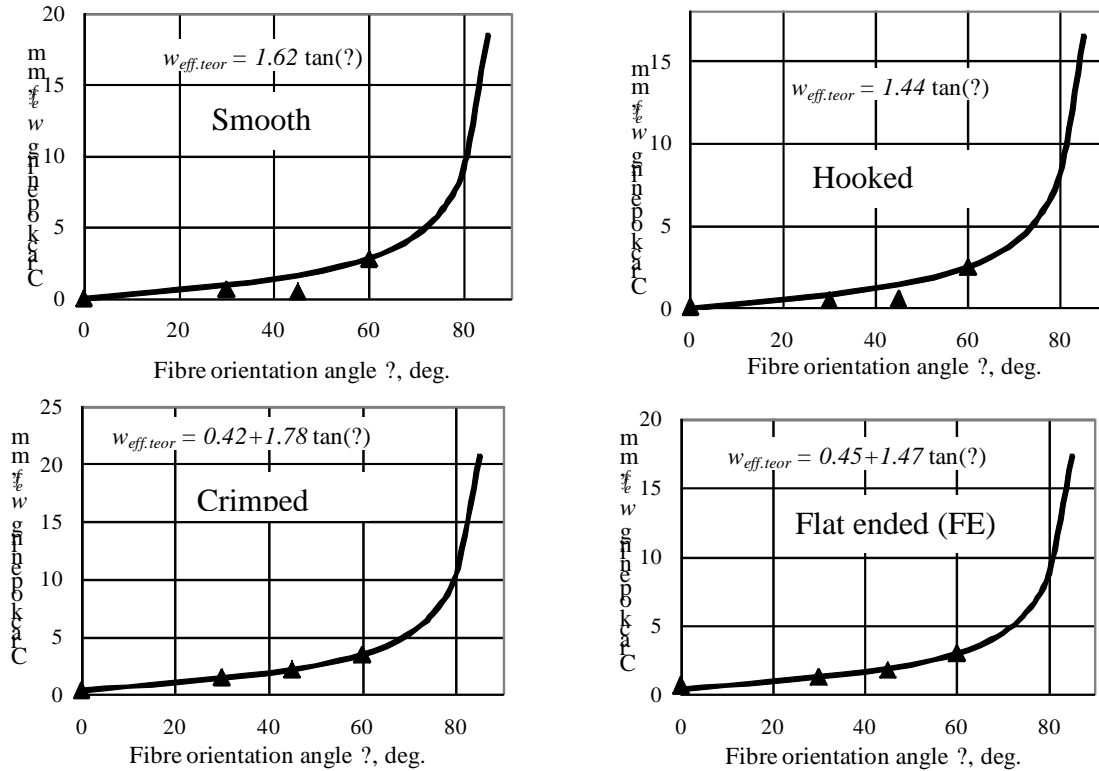


Figure 7. Effective crack width depending on fiber orientation angle.
▲ – experimental data; — – theoretical curve.

Table 1
Critical angle depending on crack width

Fiber type	Critical angle θ_{crit} (°) for crack width w (mm)			
	0.5	1.0	2.0	3.5
Smooth	17	32	51	65
Hooked-ended	19	35	54	68
Crimped-round	2	18	42	60
Flat-ended	2	20	46	64

CONCLUSIONS

The steel fiber interaction with concrete in the single pullout test characterizes the overall behaviour of FRC under tensile stresses.

The complete fiber pullout was investigated for smooth, hooked, headed and crimped fibers with different orientation.

A numerical model is developed to simulate steel fiber crack bridging behaviour for different types of fiber and orientations.

For small cracks only fibers with small orientation angle are involved in the load bearing capacity.

REFERENCES

- Aveston, J., Kelly, A. (1973) Theory of multiple fracture of fibrous composite. *Journal of Materials Science*, Vol. 8, No. 3, p. 352-362.
- Brauns, J., Skadins, U. (2010) Bond strength investigation and modelling in steel fiber concrete. In: *Abstracts of Intern. Conf. Mechanics of Composite Materials*, Riga, p.53-54.
- Fantilli, A. P., Mihashi, H., Vallini, P. (2008) Effect of bond-slip on the crack bridging capacity of steel fibers in cement-based composites. *Journal of Materials in Civil Engineering*, Vol. 2, No. 9, p. 588-598.
- RILEM TC 162-TDF (2003) σ - ϵ -design method. *Journal of Materials and Structures*, Vol. 36, p.560-567.

DETERMINATION OF SHRINKAGE OF FIBRE REINFORCED CONCRETE

Kauni Kiviste, Alexander Ryabchikov, Harri Lille

Estonian University of Life Sciences
Institute of Forestry and Rural Engineering
alexander.ryabchikov@emu.ee

ABSTRACT

During hardening of concrete, different chemical and physical processes occur. As a result, shrinkage of concrete develops causing cracking of construction elements. In order to reduce shrinkage, a variety of methods are used beginning from curing of concrete to using different shrinkage reducing admixtures. One possibility to reduce shrinkage is to add different types of fibres to concrete. The aim of this study was to explore the shrinkage of fibre reinforced concrete depending on the added types of fibre with different volume fractures. Altogether five series of experiments were carried out. Two series were carried out with steel fibre reinforced concrete with volume fractures of 0.32% (25 kg/m) and 0.51% (40 kg/m³), and two series with concrete reinforced by synthetic fibres with volume fractures of 0.44% (4 kg/m³) and 0.77% (7 kg/m³). One series of tests was performed with normal concrete. The shrinkage of the specimens was determined according to the standard ASTM C490. Steel fibre reinforced concrete with a volume fracture of 0.51% and concrete with synthetic fibres with a volume fracture of 0.77% displayed the smallest shrinkage. For concrete consisting less fibres, differences in shrinking were smaller. However, concrete without fibres showed the largest shrinkage.

Key words: concrete shrinkage, fibre reinforced concrete, steel fibres, synthetic fibres

INTRODUCTION

Drying shrinkage is probably the most deleterious property of portland cement concrete (Yazici, 2007). Shrinkage generally leads to cracking in concrete structures and further influences the service life of structures.

Shrinkage of concrete can be divided into two distinct stages: early and late age shrinkage. The early stage is commonly defined as the first 24 hours when the concrete is setting and starting to harden. Later ages, or long term, refers to concrete at an age of 24 hours and beyond (Holt, 2001).

Long term shrinkage can be divided into four types: drying, autogenous, thermal and carbonation. In case of drying shrinkage concrete loses water to the environment and undergoes a volumetric change. Early age drying shrinkage can be eliminated by proper handling and curing techniques to prevent moisture loss and to provide time for the material to strengthen.

Autogenous shrinkage is defined as a concrete volume change occurring without moisture transfer to the environment. It is merely the result of the internal chemical and structural reactions of concrete components. Thermal shrinkage refers to volume changes that occur when concrete undergoes temperature fluctuations. It is often referred to as thermal expansion, which is the portion resulting when the temperature of concrete is rising. Carbonation occurs when cement paste in hardened concrete reacts with moisture and carbon

dioxide in the air.

Hardened cement paste undergoes high drying shrinkage, whereas concrete shows significantly less shrinkage due to the restraint provided by more rigid aggregate particles. The restraint provided by aggregate particles to the shrinkage of concrete is well understood, and corresponding theoretical models have been successfully developed (Neville, 2003).

Introduction of different types of fibres also leads to reduction in the shrinkage of the cementations matrix (Illston, 2001). Fibre-reinforced concrete is currently used in a wide range of applications, including bridges, industrial floors, walls and structural slabs (Banthia, 1999). Fibres suited to reinforcing composites have been produced from steel, glass and organic polymers. Different fibres affect the properties of concrete differently. Adding of synthetic fibres prevents cracking caused by plastic shrinkage and plastic setting, and gives tensile strength in the initial phase of hardening. Adding of steel fibres gives to concrete higher flexural tensile strength, higher cracking resistance, higher impact resistance and higher resistance to volume shrinkage. Adding of fibres sufficiently improves the post-cracking process of the concrete (Banthia, 1999). In this study the shrinkage of fibre reinforced concrete, depending on the added types of fibre with different volume fractures, was investigated. Two types of fibres were used: steel crimped fibres and synthetic textured fibres. Later age shrinkage was investigated as well.

EXPERIMENTAL PROCEDURE AND METHOD

Measurements of the shrinkage of specimens were carried out according to the standard ASTM C490. According to the recommendation of the standard, the measurements of specimens were (75×75×285) mm. The cross-section of the specimens was related to the length of fibres, allowing them to take a random position in the mortar.

A special mold was designed and manufactured from plastic for casting specimens. Gauge studs were fixed to each end of a specimen for measurement of length change. Each mold was equipped by the end plate to hold the gauge studs properly in place during the setting period. The gauge length of the specimens was 250 mm, which was measured between the bottoms of the gauge studs.

The measuring equipment (Figure 1) was designed and manufactured for determining the length change of the specimens.

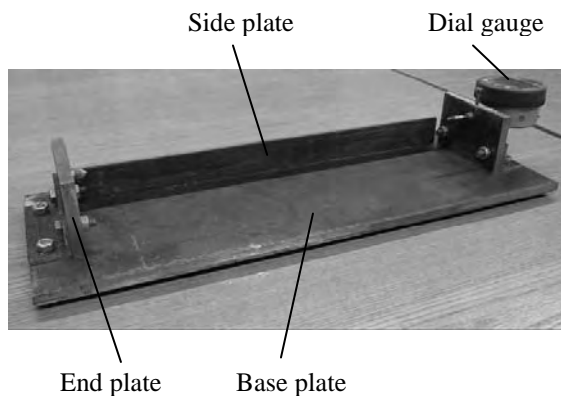


Figure 1. Equipment for measuring the length change of the specimens.

The length change was measured by the digital dial gauge Mitutoyo ID-C112B with an accuracy of 0.001 mm.

All test specimens were manufactured from industrial concrete class C25/30. The water/cement ratio was 0.65. The mix details of concrete are presented in Table 1. The unit weight of concrete was 2330 kg/m³.

Table 1

Mix details

Material	Quantity
Cement CEM II A-T 42.5 R	344.5 kg/m ³
Sand	1124.0 kg/m ³
Gravel, 4-12 mm	482.7 kg/m ³
Gravel, 8-16 mm	394.0 kg/m ³
Water	172.1 l

Two types of fibres were used for preparing the test specimens: steel crimped fibres TABIX 1/50

(length 50 mm, diameter of cross-section 1 mm) and synthetic textured fibers BARCHIP (length 50 mm, cross-section 0.65×1.3 mm).

The volume fractions of the fibers were chosen to correspond to fractures used in industrial floors. Specimens were prepared for five series of experiments. One series contained 12 specimens. The first and the second series were cast with steel fibres with a volume fraction of 0.32% and 0.51%, respectively. The third and the fourth series of specimens were cast with synthetic fibres with a volume fraction of 0.44% and 0.77%, respectively. The fifth series was prepared from plain concrete as the reference.

RESULTS AND DISCUSSION

As this study was carried out within a Master's course, the duration of the shrinkage measurements was limited to 60 days. During this time the ultimate shrinkage of concrete is 80% (Holt, 2001). The well-known equation (1) (Neville, 2003) can not be used for prediction of short term shrinkage of concrete, as is the case also in this study.

$$s(t) = \frac{t}{t + 35} \cdot s_{ult}, \quad (1)$$

where $s(t)$ is shrinkage after t days from the end of 7-day moist curing;

s_{ult} is ultimate shrinkage;

t is time in days from the end of moist curing.

Although the prediction of development of shrinkage by the above equation is subject to considerable variability, the equation can be used to estimate the ultimate shrinkage of a wide range of the moist-cured concretes. It can be seen that one half of ultimate shrinkage is expected to occur after 35-day drying. For steam-cured concrete, the value of 35 in the denominator is replaced by 55, and the time t is calculated at 1-3 days from the end of steam curing.

In the case of short term measurement the experimental data can be approximated by the following analytical equation

$$s(t) = \ln(1 + t^c), \quad (2)$$

where t is the number of days,

c is the dimensionless parameter.

The purpose was to find the unknown constants so that the measured displacements $s(t)$ are approximated in the best way. This problem was solved using the mathematical program *Mathcad 2001i Professional* regression function *genfit* (vx, vy, F) (Kir'yanov, 2001).

Test specimens from plain concrete were prepared for reference as the etalon. The results of the measurements and the approximation curve are presented in Figure 2.

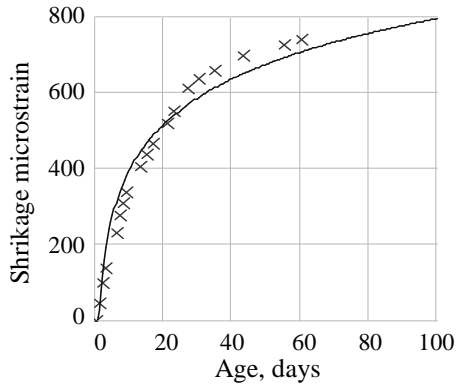


Figure 2. Experimental data and the curve of approximation of specimens cast from plain concrete.

Two series of experiments were carried out with specimens with a steel fibre content of 0.32% and 0.51% per volume, respectively. The experimental data and the curve of approximation for these series are shown in Figure 3.

The graphs presented in Figure 3 allow concluding that increasing the amount of fibres reduces the shrinkage of concrete.

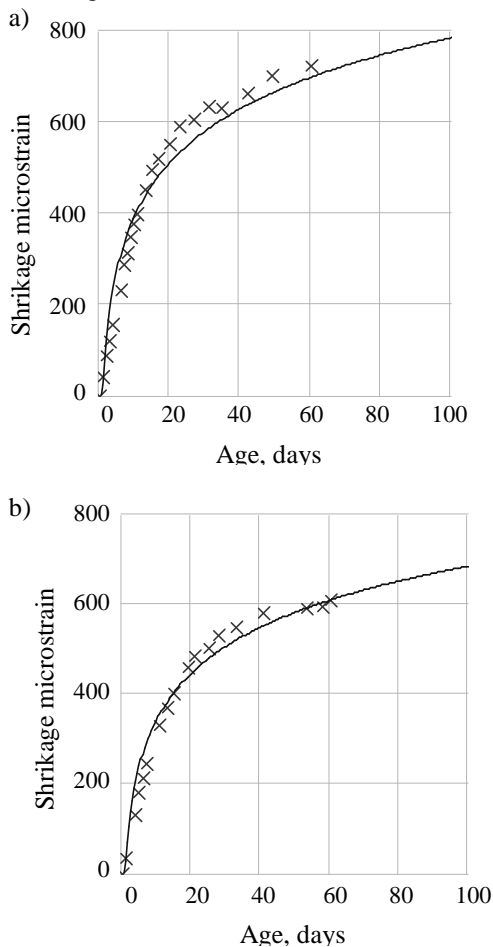


Figure 3. Experimental data and the curve of approximation of specimens containing steel crimped fibres 0.32% (a) and 0.51% (b).

The specimens with a fibre content of 0.32% did not practically reveal changes in shrinkage compared to the shrinkage of plain concrete (the difference is 1.3% at 60 days); however, the shrinkage of specimens with a fibre content of 0.51% was 13.8% lower at the same age. Higher fibre content weakens the mix and hence results in lower shrinkage (Neville, 2003).

Two series of experiments were carried out with specimens containing synthetic textured fibres with a volume fraction of 0.44% and 0.77%, respectively. The experimental data and the curve of approximation are shown in Figure 4. It is evident from the graphs, that the shrinkage of specimens with a fibre content of 0.77% was 7.8% lower at 60 days compared to the shrinkage of plain concrete. However, the shrinkage of specimens with a fibre content of 0.44% was 11% higher.

To verify the use of the proposed equation (2) for approximation of the experimental data, the data presented in (Bolander, 2004) were approximated using this equation. The data of two series of experiments were approximated: the data of the shrinkage of plane concrete and the data of the shrinkage of concrete with 2% steel crimped fibres per volume.

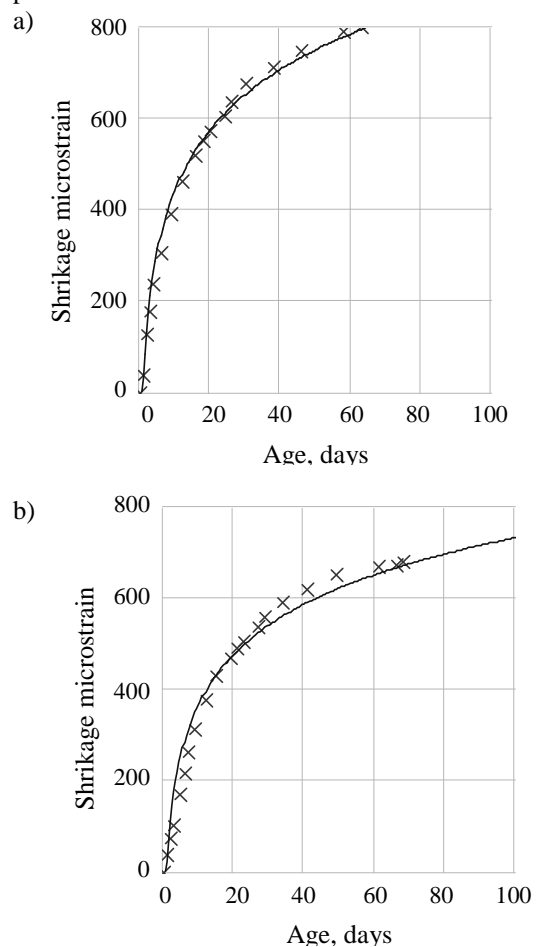


Figure 4. Experimental data and the curve of approximation of specimens containing synthetic textured fibres 0.44% (a) and 0.77% (b).

Measurement of shrinkage was carried out during up to 500 days. The results of approximation are presented in Figure 5 and in Table 2.

Table 2

Test specimens	Shrikage, microstrain		
	20 days	40 days	60 days
Plain concrete	518	638	708
Steel fibers 0.32%	511	630	699
Steel fibers 0.51%	446	549	610
Synth. fibers 0.44%	576	709	786
Synth. fibers 0.77%	477	588	653
Plain concrete (Bolander, 2004)	390	481	533
Steel fibers 2% (Bolander, 2004)	314	387	429

It is evident that the analytical equation approximated the experimental data satisfactorily also for long term measurements beginning from the 200th day. The highest mismatch occurred approximately between 50 and 160 days. There is no confirmation for the statement (Holt, 2001) that 80% of ultimate concrete shrinkage occurs during the first 60 days. According to the measurement results (Bolander, 2004), only 65% of ultimate shrinkage occurred during the first 60 days.

CONCLUSIONS

The experimental study showed that fibres with a small volume fracture did not affect significantly the shrinkage of concrete.

In the case of synthetic fibres shrinkage was slightly larger. Specimens with a higher volume fracture displayed smaller shrinkage compared to plain concrete in all cases.

The presented analytical expression proposed for short term experiments approximated the measured data satisfactorily, and can be used, with certain reliability, for prediction of shrinkage in long term experiments. According to the results of this study

REFERENCES

- Banthia N., MacDonald C., Tatnall P. (1999) *Structural Applications of Fiber Reinforced Concrete*. Farmington Hills: ACI International, SP-182. 256 p.
- Bolander E. (2004) Numerical modeling of fiber reinforced cement composites: linking material scales. In *Proc. of 6th International RILEM Symposium on Fibre Reinforced Concretes*. M. di Prisco, R. Felicetti and G.A. Plizzari (eds.). RILEM, p. 45-60.
- Holt E.E. (2001) *Early age autogenous shrinkage of concrete*. Espoo: Technical Research centre of Finland, VTT Publications 446.
- Illston J. M., Domone P. L. J. (2001). *Construction materials: their nature and behaviour*. 3rd ed. USA: Spon Press. 518 p.
- Kir'yanov D. (2001) *Mathcad 2001. Manual for self-tution*. Petersburg: BHV-Petersburg.
- Neville A.M. (2003) *Properties of concrete*. London: John Wiley & Sonc, Inc. 844 p.
- Yazici S. Inan G., Tabak V. (2007) Effect of aspect ratio and volume fraction of steel fiber on the mechanical properties of SFRC. *Construction and Building Materials*, No. 21, p. 1250-1253.

and basing on literature data, it can be supposed that at least half of ultimate shrinkage occurs during the first 35-40 days, and ultimate shrinkage can be measured 18 months after the preparation of specimens.

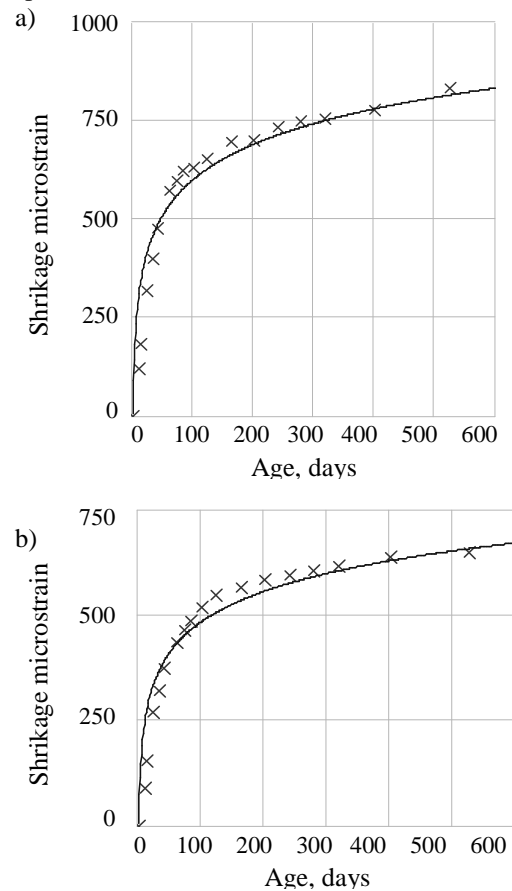


Figure 5. Experimental data and the curve of approximation of specimens of plane concrete (a) and with a steel fibre content of 2% (b).

This analysis was limited to the data obtained from the literature and from the experiments described above.

DEVELOPMENT OF A METHOD FOR MEASURING DESTRUCTION ENERGY AND GENERATED HEAT AT FATIGUE OF CONCRETE

R. Tepfers, G.O. Sjöström, J. I. Svensson, G. Herrmann

Chalmers University of Technology, Department of Civil and Environmental Engineering
Structural Engineering, Concrete Structures
ralejs.tepfers@chalmers.se

ABSTRACT

In fatigue of concrete, if the loads are not uniformly repeated and the dynamic load levels change, every particular load will contribute with certain portion to the fatigue deterioration of the concrete. For estimation of this destruction of concrete the Palmgren-Miner partial damage hypothesis has been used, but has turned out to give contradictory results. As the Palmgren-Miner hypothesis is not generally applicable to fatigue of concrete attempts have been made with volumetric, ultrasonic and acoustic emission measurements to interpret the damage accumulation in concrete. However, no acceptable relation between the measured values and the fatigue deterioration of concrete caused by different loads has been found. The present paper investigates a method for another parameter, which might be important for the deterioration process to be understood, when concrete is loaded by varying dynamic loads. The parameter is the energy absorbed by the concrete and is represented by the work in a form of load times of the deformation for each cycle of load. At each un-loading certain energy is regained, but not all. The load deformation relationship shows a hysteresis and the area within the hysteresis loop represents the absorbed energy used up in the material causing micro cracks, crushing material, redistributing stress and rising temperature due to internal friction. This research investigates methods to determine the energy for the fatigue destruction of concrete and for the rise of temperature within the concrete specimen. Different types of plates and Teflon layers are tested to avoid friction between cylinder ends and loading platens. An insulating material layer with thermocouples around the concrete cylinder is used for heat loss measurements. The paper presents the tests done and discusses problems with the measuring methods. A result is obtained which does not exclude the hypothesis that the destruction energy for concrete in compression is the same whether it is a static or dynamic fatigue failure.

Key words: Concrete, fatigue, absorbed energy, destruction energy, heat energy, measuring methods

INTRODUCTION

During 1970-ies the first concrete oil production platforms in North Sea were planned and erected. It was concluded that the platforms were loaded by different waves up to 30m in height. These varying waves caused fatigue to the structure. The influence of changing repeated loads on concrete was not investigated at that time.

In fatigue of concrete, if the loads are not uniformly repeated and the dynamic load levels change, every particular load will contribute with certain portion to the fatigue deterioration of the concrete. For estimation of this destruction of concrete the Palmgren-Miner, Palmgren (1924), Miner (1945), partial damage hypothesis has been used for steel, but for concrete has turned out to give contradictory results.

The Palmgren-Miner rule states that failure occurs when

$$\sum_{i=1}^I n_i / N_i = 1 \quad \dots \quad (1)$$

where n_i is the number of applied load cycles of type i , ;
 N_i is the pertinent fatigue life.

In codes the Palmgren-Miner sum for concrete has been altered down to 0.2 for reason of safety.

As the Palmgren-Miner hypothesis is not generally applicable to fatigue of concrete attempts have been made with volumetric, ultrasonic and acoustic emission measurements to interpret the damage accumulation in concrete. However, no acceptable relation between the measured values and the fatigue deterioration of concrete caused by different loads has been found.

The present paper investigates a method for another parameter, which might be important for the deterioration process to be understood, when concrete is loaded by varying dynamic loads. The parameter is the energy absorbed by the concrete and is represented by the work in a form of load times of the deformation for each cycle of load. At each un-loading certain energy is regained, but not all. The load deformation relationship shows a hysteresis and the area within the hysteresis loop represents the absorbed energy by the concrete used up in the material causing micro cracks, crushing material, redistributing stresses and rising temperature due to internal friction.

This research investigates the methods to determine the energy for the fatigue destruction of concrete and for the rise of temperature within the concrete

specimen. It is necessary to avoid friction between the loading platens and the concrete cylinders end surfaces to enable representative measurements of concrete deformations during loading cycles. Further the amount of energy used for temperature rise in the specimen and heat exchange with the loading machine plus losses to the surroundings have to be determined. Different types of plates and Teflon layers are tested to avoid friction between the cylinder ends and loading platens. An insulating mineral wool layer with thermocouples around the concrete cylinder is used for heat loss measurements from the concrete cylinder side surfaces. A wood fiber layer with thermocouples is used for heat exchange measurements between the cylinder end surfaces with two Teflon layers and the loading steel platens of the machine.

These types of measurements are difficult to perform especially at a fast load pulsating frequency of 2 Hz measuring at several levels of strain. The paper presents the tests done and discusses problems with the measuring methods, which unfortunately did not work satisfactory and have to be improved further. A result is obtained which does not exclude the hypothesis that the destruction energy for concrete in compression is the same whether it is a static or dynamic fatigue failure.

METHODS

Hypothesis

It can be assumed that for concrete static failure as well as fatigue failure the same amount of destruction energy is required. At static failure all supplied energy is used to destroy the concrete (a very slight rise of temperature is possible). At fatigue failure of the concrete specimen the supplied and absorbed energy generates internal friction heat and destruction of concrete. The idea with the tests is to measure the heat energy and to separate it from the destruction energy. The performed tests have a pilot character, because the necessary measuring methods have to be developed.

The supplied energy is represented by the areas A1, A2 etc. under the load-deformation curve as it is shown in Fig. 1.

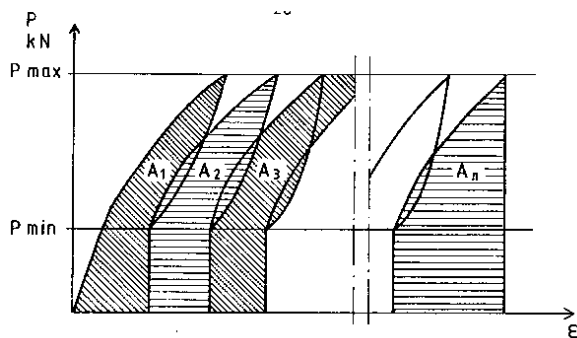


Figure 1. By the pulsating load machine supplied energy shown in load P – strain ε diagram.

The hysteresis loops represent the absorbed energy, which consist of destruction and the heat energy.

Energy balance

Energy balance of the in fatigue tested concrete specimen

$$\Delta W = \Delta E + \Delta Q; \quad \dots(2)$$

Where

ΔW is absorbed energy from loading machine

ΔE is generated heat from internal friction

ΔQ is destruction energy

Energy absorption measuring method

The energy supplied to and absorbed by the concrete cylinder is measured according to Fig. 2 and Fig. 3.

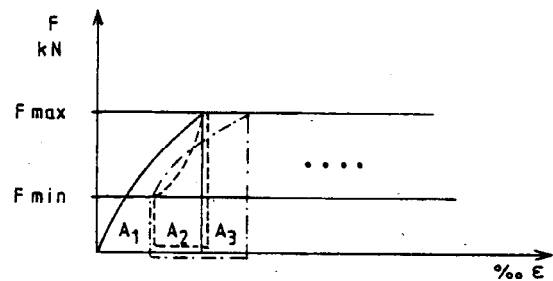


Figure 2. Load F – strain ε diagram showing absorbed energy measurement sequence. $W = A1 - A2 + A3 - \dots;$

The longitudinal strain gauges on opposite sides of the concrete cylinder were used for the registration of strain ε. The energy driven into the cylinder by the loading machine is calculated from the measurements according to formula (3).

$$W = F \cdot \Sigma \Delta \varepsilon_{//} \cdot H; \quad \dots(3)$$

Where W = energy, Nm or J

F = load N

$\Delta \varepsilon_{//}$ = incremented compressive strain %

H = height of cylinder m

The strain measurements were incremented in $\Delta \varepsilon_{//}$ according to Fig. 3 and the existing increments between the maximum and minimum load levels were used to register the measured load-deformation surfaces.

The strain gauge dummy is placed close to the cylinder surface under the insulating layer to have the same temperature as the strain gauges registering the vertical strain Fig. 4. It compensates for temperature changes.

The cylinders are loaded by sinusoidal load pulses with the frequency of 2 Hz. The recovery of concrete after each load cycle is connected with the applied rate of loading.

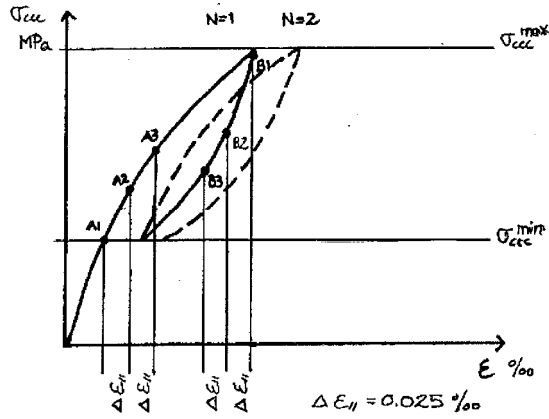


Figure 3. The principle for registration of $\Delta \epsilon_{||}$ values from stress-strain relation. Frequency is constant.

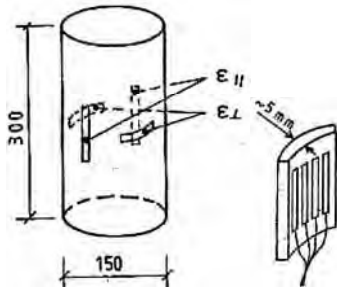


Figure 4. Strain gauges $\epsilon_{||}$ in longitudinal direction and ϵ_{\perp} in transverse direction on concrete cylinders and dummy for strain gauges.

A part of the absorbed energy, which is measured, is that which gives micro cracking and blocked deformations within the concrete. The blocked deformations have a time dependent recovery. This means that when taking the measurements with a constant rate of loading the measured absorbed energy will belong to just this certain rate of loading.

The measured absorbed energy is defined by the areas under the stress-strain relationship according to Fig. 1 and 2. In the measurements the strain is incremented according to Fig. 3

The strain increments were chosen to be 0.025‰ at on- and un-loading and this instead of load increments which due to a slight vibration in the machine caused a contact between the incremented load levels to make the system to believe that the top load level was reached and caused the system to change the registration direction. The absorbed energy was registered continuously and at specimen failure the complete absorbed energy was in the computer.

At the static tests obtained cylinder strength f_{ccc} was used to determine the minimum σ_{ccc}^{min} and maximum σ_{ccc}^{max} load levels at pulsation tests. The relation $R = \sigma_{ccc}^{min} / \sigma_{ccc}^{max}$, was chosen to be 0.20.

Friction reduction between concrete cylinder ends and loading platens

To be able to measure the absorbed energy it is necessary that the concrete cylinder is not restricted in transverse expansion by the loading platens, Fig. 5, because otherwise it is not possible to determine correctly the absorbed energy by the concrete cylinder.

The layers between the concrete cylinder end surfaces and loading platens should be without friction hindering concrete expansion. Tests were performed for this reason. Uneven changing shear stresses at the end surfaces will generate uncontrolled heat and have to be avoided.

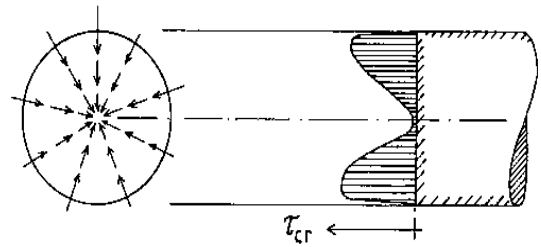


Figure 5. Fluctuating shear stresses τ_{cr} caused by friction, which also generate heat under load cycles.

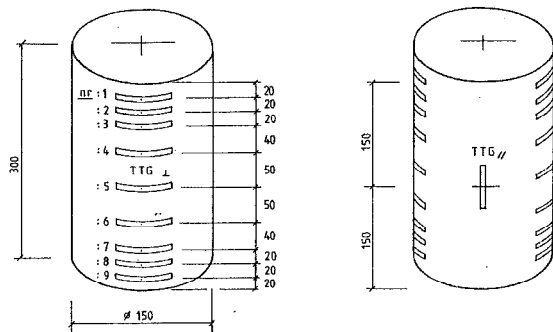


Figure 6. Arrangement of strain gauges $TTG_{||}$ in longitudinal direction and TTG_{\perp} in transverse direction on concrete cylinders.

The arrangement of strain gauges for measuring transverse expansion and longitudinal compressive strain is shown in Fig. 6.

Different layers consisting of wood fiber plates also cut in a form of a grid were tested. Long laboratory experience showed that wood fiber plates could be used instead of making a smooth layer on tested concrete objects surface exposed to compression. The best result was obtained with 2 layers of Teflon sheet between concrete and wood fiber plate giving uniform transverse deformation along the cylinder. The measured transverse expansion for 2 layers of Teflon sheet between concrete cylinder and wood fiber plate against loading platens of the machine are shown in Fig. 7. Two layers of Teflon sheet give

uniform expansion of the cylinder under load and should enable the determination of the supplied energy in absolute value.

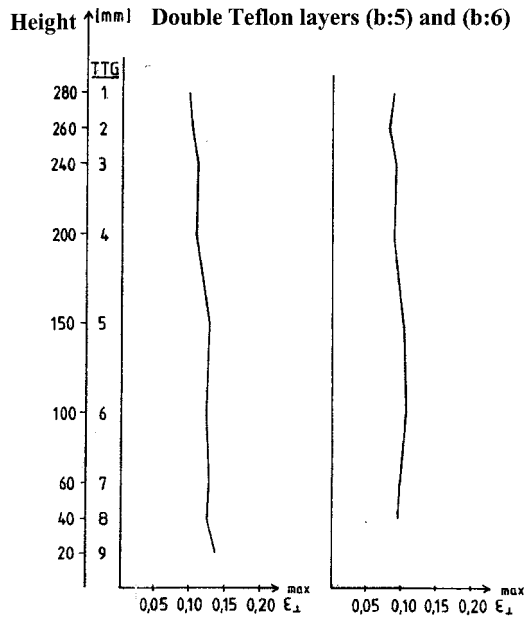


Figure 7. Along the height measured transverse cylinder expansion strain under load with two Teflon layers between cylinder and wood fiber plates against steel platens. TTG are strain gauges in transverse direction. Tests (b:5) and (b:6).



Figure 8. With two Teflon layers to reduce friction, the concrete cylinder completely disintegrates at compressive failure. Vertical cracks show up.

The concrete cylinders with two Teflon layers for friction reduction disintegrated completely at failure, Fig. 8. They did not form the usual friction caused conical concrete peaces at the ends of the failed concrete cylinder. The tensile cracks, due to exceeding ultimate tensile strain in transverse direction of the cylinder, were vertical along the

whole height of the cylinder. Double Teflon layers were chosen for tests.

Heat exchange of the concrete cylinder with surroundings

It is necessary to separate from the absorbed energy, the heat developed by internal concrete friction during the load cycles. This requires measurements of heat exchange with the surroundings and with the loading machine and also the heat stored by concrete. An insulating material layer (mineral wool) with thermocouples around the concrete cylinder is used for the heat loss measurements from the concrete cylinder side surfaces and a wood fiber plate with thermocouples is used for the heat exchange measurements from cylinder ends. The cylinder ends have 2 layers of Teflon, then wood fiber plate and then loading steel platens of the machine, Fig. 9 and 10.

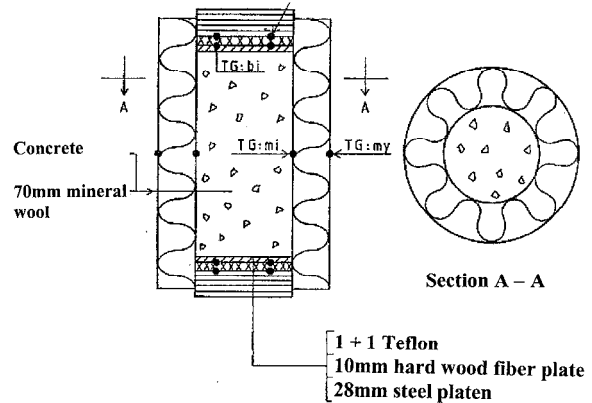


Figure 9. Thermocouples, TG:(location), attached on insulating layers.

A computer calculation program was prepared to register the heat exchange through the insulating jacket layer and the end insulating layers. During the test continuous heat flow from concrete cylinder was accumulated in the computer memory.

TEST PROGRAM

The test program is shown in Table 1. The used load frequency was 2Hz and $R = \sigma_{ccc}^{\min} / \sigma_{ccc}^{\max} = 0.20$. The number of load cycles N_c at failure in Table 1 has been calculated with equation (4) Aas-Jacobsen (1970) and Tefpers-Kutti (1979), Tefpers (1980 a, b).

$$\log_{10} N_c = (1 - \sigma_{ccc}^{\max} / f_{ccc}) / \{(0.685 (1 - R))\} \dots(4)$$

where:

N_c calculated number of load cycles at failure.

$\sigma_{ccc}^{\max} / f_{ccc}$ maximum pulsating stress related to static concrete compressive strength.

$R = \sigma_{ccc}^{\min} / \sigma_{ccc}^{\max} = 0.20$.

σ_{ccc}^{\min} minimum pulsating stress.

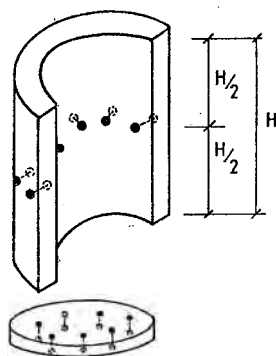


Figure 10. Concrete cylinder with insulating layers and wood fiber plates at cylinder ends with thermocouples.

Table 1

Test program of concrete cylinder fatigue tests with number of load cycles at failure N_c calculated with eq. (4)

Test No	$\sigma_{ccc}^{max}/f_{ccc}$	N_c	$\log N_c$
C: 6, 7	0.90	67	1.8248
C: 8, 9	0.85	546	2.7372
C: 10, 11	0.80	4463	3.6496
C: 12, 13	0.75	36475	4.5620
C: 14, 15	0.70	298194	5.4745

From the same batch of concrete 21 cylinders (height 300mm and diameter 150mm) and 12 cubes (side 150mm) were produced. 10 cylinders were tested in fatigue and three to determine static compressive strength. The rest was used for friction influence measurements and also in reserve.

CONCRETE

Composition of concrete was: cement 245 kg/m³, water 196 kg/m³, sand 1175 kg/m³ and crushed granite stone 694 kg/m³. For fresh concrete slump was 40mm, air content 1.0% and density 2365 kg/m³. The specimens were after remolding stored under water for 5 days followed by 3 days under wet feltings and then in laboratory at temperature 20° centigrade and RH 50% until the tests after 7

months, when the concrete strength was stable. The mean compressive cube strength determined on 6 cubes was 40.1 MPa and cylinder strength on 3 cylinders was 30.1 MPa at time of fatigue testing. The fatigue testing machine was Losenhausen 1000 kN servo pulsating machine with all sinus formed load pulses controlled.

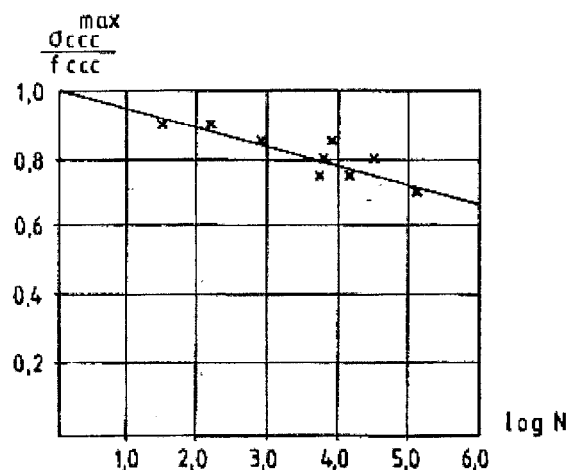


Figure 11. Wöhler or SN-relation of the performed fatigue tests. Line according to equation (4), Aas-Jacobsen (1970) and Tepfers-Kutti (1979).

The number of load cycles N at fatigue failure loads of the specimens in the test program, Table 1, are shown in Wöhler diagram Fig. 11 and put in relation to the fatigue line represented by eq. (4). The test results situated relative to this line shows normal agreement.

RESULTS AND DISCUSSION

Determination of static failure energy

The measured static failure energies determined according to eq. (3) on 3 cylinders was Test C:3 240 J; Test C:4 280 J and Test C:5 240 J with mean value 253 J are shown in Fig. 12.

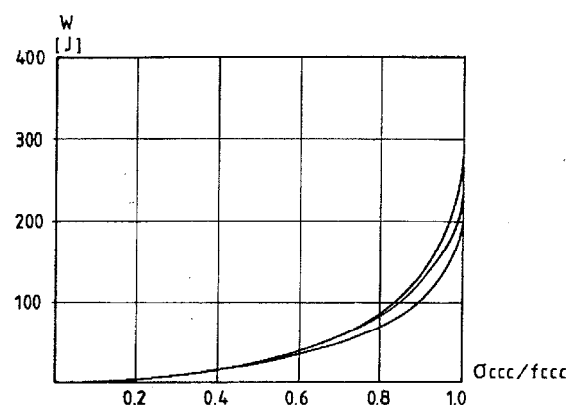


Figure 12. Absorbed static failure energy W at different related stress levels of concrete cylinders.

As the curve of the measured absorbed energy W close to the failure load is asymptotic, the values obtained are uncertain.

Measured absorbed energy

The measuring system for supplied and absorbed energy unfortunately did not work as expected. The absorbed energy measurements based on strain increments were registered unsatisfactory due to overflow in the computer system. Therefore, the results based on load increments of Bergquist (1984) are used in the evaluation instead, where this did not happen. The absorbed energy follows a straight line after a starting zone and is shown in Fig. 13. Bergquist did not measure the heat energy, so a separation of destruction energy and heat energy from his results is not possible.

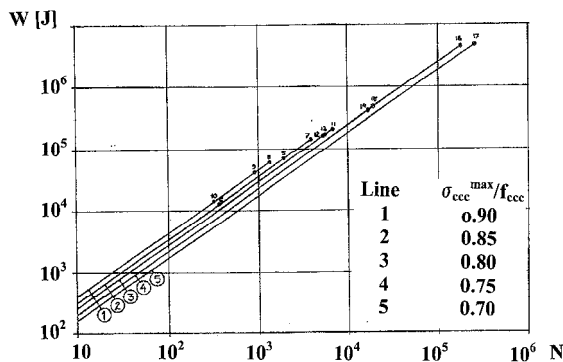


Figure 13. Absorbed energy W up to fatigue failure related to numbers of load cycles N . Bergquist (1984).

Average absorbed energy per load cycle at different stress levels is shown in Fig. 14, according to Bergquist (1984). It increases slightly with increasing the maximum pulsating stress level as it can be expected. The concrete cube strength of the present tests was 40.1 MPa and cylinder strength 30.1 MPa, while those of Bergquist (1984) 47.3 MPa respective 35.9 MPa.

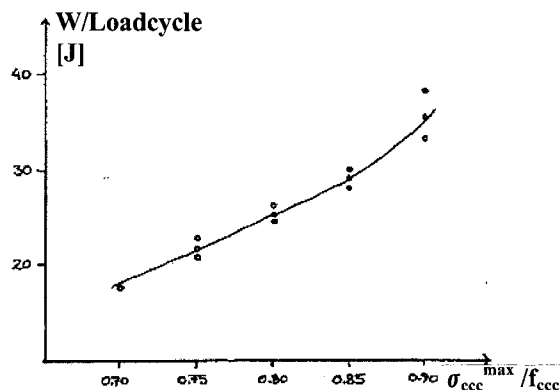


Figure 14. Average absorbed energy per load cycle at different related stress levels including destruction and heat energy, Bergquist (1984).

Measured heat energy

The development of heat energy in principle is shown in Fig. 15.

At the beginning of the measurements the temperature differences over the insulating layer are very small which makes the results very uncertain causing curves not starting at 0;0 point. The stored energy in the concrete cylinder and heat exchange with the loading machine platens dominates in the beginning phase, but the through insulating mineral wool measurement layer transmitted energy rose when temperature difference between the cylinder and air in the room increased.

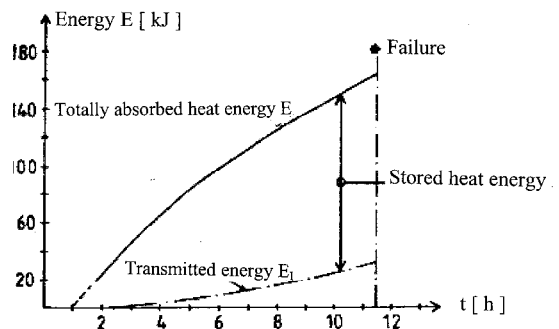


Figure 15. Relation in principle between stored heat energy and transmitted energy as function of time t is shown.

The thermocouples arranged in the wood fiber plate at cylinder ends however became destroyed by load pulses. The Teflon polymer layers experienced internal temperature increase due to pulsating load, and most likely did not function satisfactory.

Therefore energy exchange between the cylinder and loading platens went unfortunately out of control.

COMPARISON BETWEEN SUPPLIED AND ABSORBED ENERGY

Taking into considerations the shortcomings of the measurements a try to compare the absorbed energy and the energy in the form of heat and deterioration of concrete is done in the following.

It can be stated that temperature increase of the concrete cylinders was more for higher stress levels and could reach up to 10° centigrade and resulted in stored energy.

The transmitted energy was low due to the thickness of the cylinder side surface insulating layer for transmission energy measurements and due to this fact became uncertain, especially in the beginning phase of loadings, when the temperature difference over the insulating layer was small.

Improvements have to be done in placing thermocouples to avoid air slots between concrete and the insulating layer and also to better control surface heat resistance. Room temperature

development has also to be followed in detail. The energy transmission through the concrete cylinder ends to machine loading platens could not be determined, due to destruction of the measuring equipment by load pulses. It was therefore assumed to be the same as through side surfaces. The measuring technique has to be improved. Measurements for some specimens became however possible to use.

Fig. 16 shows heat energy measured for specimen C:14 compared with absorbed energy measured by Bergquist (1984). At the beginning the measurements, when registering smaller quantities, suffer from un-precision. In later phase an approach is observed between the absorbed energy and the measured heat energy consisting of the in the concrete cylinder stored and from concrete surfaces transmitted energy. The distance between these energies is the destruction energy. However the concrete in Bergquist's tests was 19% stronger than in the present tests and makes this distance wider.

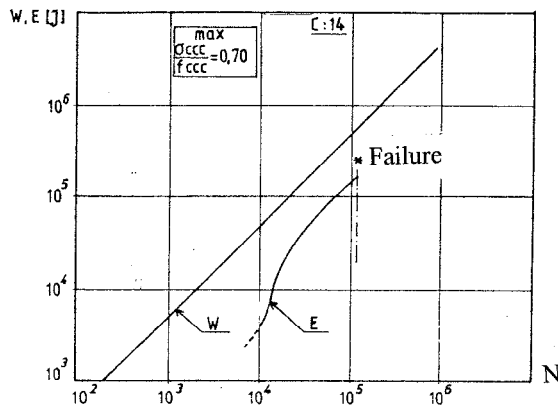


Figure16. Comparison between absorbed energy W (J) Bergquist (1984) and developed heat energy E (J) until fatigue failure of cylinder C:14.

In Fig. 17 a try is done to adapt the absorbed energy measurements performed by Bergquist (1984) to the concrete strength in present tests. The concrete compressive static cylinder strength f_{ccc} in Bergquist's tests was 19% higher and therefore comparison is done for Bergquist's tests with his $\sigma_{ccc}^{max} / f_{ccc} = 0.70$ adapted for present test C:12 with $\sigma_{ccc}^{max} / f_{ccc} = 0.75$ approaching somewhat the relative stress levels. It can be seen in Fig. 17 that the heat energy curve approaches the from machine load absorbed energy line according to Bergquist (1984) to a distance, which is of the size of the static destruction energy level 0.30 kJ.

It can be stated that measured absorbed energy and the measured developed heat energy are in region 100 kJ, while the destruction energy being the difference of absorbed and heat energies, is only about 0.3 kJ, as it was determined in static tests Fig. 12. The destruction energy is a small number obtained as the difference of two very big numbers.

As these are not very precise the destruction energy could not be determined with the necessary precision to confirm the hypothesis that the destruction energy is the same for static and fatigue types of concrete failures. But the hypothesis cannot be excluded either.

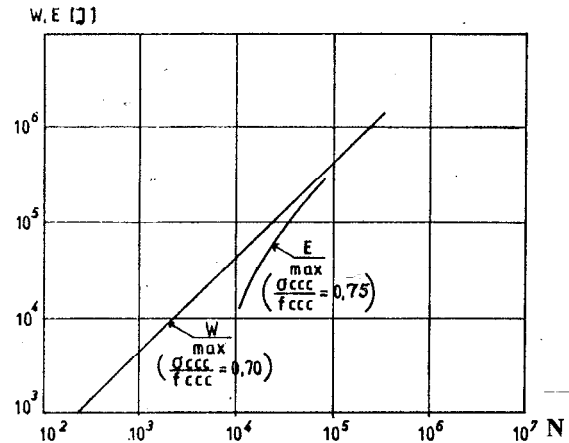


Figure17. Comparison between absorbed energy W (J), Bergquist (1984), with to these tests somewhat adapted concrete strength level, and developed heat energy E (J), test C:12, as function of load cycles N until fatigue failure.

As these tests, with these methods were performed for the first time a lot of complications turned up. To obtain better results repetition of the tests should be done with the necessary improvements in the measuring technique. However, the improvements could not be done due to certain reasons and in present paper are presented what the results became to be.

CONCLUSIONS

1. About friction between concrete cylinder and steel loading platens

Under static tests it is possible to avoid friction between concrete cylinder ends and steel loading platens with two Teflon layers.

Under pulsating load with frequency 2 Hz however the Teflon layers are deteriorated due to internal heat development in the polymer.

2. Temperature increase

Temperature increase was more for higher stress levels and could reach up to 10° centigrade in the concrete cylinder.

The transmitted energy was low due to thickness of the insulating layer for measurements and relatively small temperature gradient especially at the beginning of the tests, which made the results uncertain for transmission energy measurements.

Improvements have to be done in placing thermocouples to avoid air slots between concrete and the insulating layer and also to determine surface heat resistances.

Thermocouples placements possible to sustain the pressure between the concrete cylinder end surfaces and loading steel platens of the machine have to be developed.

Room temperature development has to be followed.

3. Developed heat energy and destruction energy

Both from the loading machine transmitted and by the concrete cylinder absorbed energy and developed heat energy, which is stored in concrete cylinder or transmitted to surroundings, is in region 100 kJ, while the destruction energy, being the

difference between absorbed and heat energies, might equal to that in the static tests 0.3 kJ.

The destruction energy in fatigue obviously is a small number obtained as the difference of two very big numbers. As these were not very precise, the destruction energy could not be determined with the necessary precision to confirm the hypothesis that the destruction energy is the same for static and fatigue types of concrete failures.

ACKNOWLEDGEMENT

The tests were done as students master thesis work with the aim to elaborate the systems for measuring of the absorbed and developed heat and destruction energies at fatigue of concrete, Sjöström G. O., Svensson J. I. (1985). A master thesis has a certain extent in work and the required limit was achieved. The measuring methods were developed, but new problems discovered. Here the results are documented of what was achieved and in further research the systems have to be improved. Unfortunately, a follow up of this investigation could not be performed due to unexpected passing away of responsible laboratory technician Gerald Herrmann.

The work was a follow up of earlier investigations in reference list, especially Tepfers et. al. (1977a), Tepfers et. al. (1977b), Tepfers et. al. (1984).

REFERENCES

- Aas-Jakobsen K. (1970) *Fatigue of concrete beams and columns*. Bulletin No.70-1, Institutt for betonkonstruksjoner, NTH Trondheim, September 1970, p. 148.
- Bergquist J. (1984) *Energiabsorption hos betong vid utmattande last (Energy absorption of concrete in fatigue)*. Department of Building Materials, Chalmers University of Technology, Work No. 396. Examination work 84:2. Göteborg, June 1984. p.48.
- Miner M. A. (1945) Cumulative damage in fatigue. *Trans. ASME*, Vol. 67.
- Palmgren A. (1924) Die lebensdauer von Kugellagern (The fatigue life of ball bearings). *Zeitschrift Verein Deutscher Ingenieure*, Vol 68, No. 1924, p. 339-341.
- Sjöström G. O., Svensson J. I. (1985) *Utveckling av metod för mätning av värme- och destruktions energi vid utmattning av betong (Development of method for measuring heat- and destruction energy at fatigue of concrete)*. Department of Building Materials, Chalmers University of Technology, Work No. 410. Examination work 85:3. Göteborg, June 1985. p. 60.
- Tepfers, R., Görilin, J., Samuelsson, T. (1977a) Concrete subjected to pulsating load and pulsating deformation of different wave forms. *Nordisk Betong* 4:1973. p. 27-36.
- Tepfers, R., Fridén, C., Georgsson, L. (1977b) A study of the applicability to the Palmgren-Miner partial damage hypothesis. *Magazine of Concrete Research*, Vol. 29, No 100, p. 123-130.
- Tepfers, R., Kutti, T.(1979) Fatigue Strength of Plain, Ordinary and Lightweight Concrete. *ACI Journal, Proceedings* Vol 76, No. 5, p. 635-652.
- Tepfers, R. (1980 a) Tensile Fatigue Strength of Plain Concrete. *ACI, Journal, Proceedings*, Vol 76, No. 8, p. 919-933.
- Tepfers, R. (1980 b) Fatigue of plain concrete subjected to stress reversals. *ACI Symposium at 1980 Fall Convention 23-26/9 1980, San Juan Puerto Rico*. American Concrete Institute Publication SP 75-9. p.195-215.
- Tepfers R., Hedberg B., Szczekocki G. (1984) Absorption of energy in fatigue loading of plain concrete. *Matériaux et Constructions*, Vol. 17, No 97. p. 59-64.

ENHANCED IMPACT ABSORPTION PROPERTIES OF PLYWOOD

Sanita Zike, Kaspars Kalnins

Riga Technical University, Institute of Materials and Structures
sanita.zike@rtu.lv, kaspars.kalnins@sigmanet.lv

ABSTRACT

Impact response of plywood laminate composites with imbedded glass and flax fibre fabrics utilising different adhesives were both experimentally produced and studied. Moreover the impact energy absorption of wood products as veneer, three and seven plies plywood and particle board were estimated. Therefore, laminate composites were subjected to drop-weight tests with initial energy of 150J and striker with diameter 20 mm in order to determine the impact force, energy absorption and deflection rate.

The experimental results approved poor impact absorption properties for both single veneer ply and particle board, the impact resistance was significantly higher in plywood products. In combination with thermoplastic polymer and textile fabrics the absorbed energy of laminates was considerably enhanced. The highest specific absorbed energy values have been observed for plywood laminate produced by polyethylene adhesive and incorporating the glass fibre fabrics. During the drop-weight impact tests all samples were punctured, showing local damage in the upper ply and much more extensive at the bottom ply. The damage extent was smaller in composite laminates reinforced with the fibre fabrics.

Keywords: drop-weight impact, bio-composite, veneer, flax fabric, plywood, laminates

INTRODUCTION

Plywood panels may be considered as the highest performance wood products frequently utilised by building and transportation industry as in concrete formwork systems, floors, walls and roofs in vehicles, container floors etc. Plywood production may be considered of particular interest because of inherent orthotropic nature of wood properties describing independent mechanical properties in the directions of three mutually perpendicular axes showing the highest load carrying performance in fibre direction taken as longitudinal. Therefore, manufacturing of plywood made of veneer sheets with varying fibre direction allows homogenising the strength properties of wood. It also significantly enhances the bending stiffness of the laminate structure, but still the strength properties in transverse direction are limited like poor impact resistance (Forest Products Laboratory, 2010).

The performance of wood and wood products can be improved incorporating it with other materials as fibre reinforced polymer (FRP) layers. The FRP layers can be used as outer layers of wood panels acting as protective and decorative coat enduring the stress from internal load abuse, damage from road debris, cracking caused by varying weather conditions. Therefore, FRP/plywood composite combines the structural properties of plywood – durability, bending strength and stiffness, dimensional stability and workability – with the long-wearing and weather-proof surface of a fiberglass-reinforced-plastic overlay, which also provides added strength and stiffness (www.apawood.org). Incorporation of FRP layers has been found useful in combination with glulam

and OSB panels (Gardner, 2011). In general, the largest increases in strength can be obtained with the lower grades of wood due to a larger difference in relative tension/compression strength values, which can be remedied by adding FRP tension reinforcement (Dagher et al., 1996). Implementation of glass fibre as reinforcement in FRP composites is more common whereas carbon fibre usage has not been found economical in terms of stiffness enhancement. Thus FRP materials allow increased utility of low-quality wood in construction; improved structural efficiency and reduced structural member size requirements and weight; to improve the serviceability; and to reduce the costs in some applications (Raftery, 2011; Pirvu et al., 2004).

Glass fibre fabrics are extensively used in polymer based laminate composites used in aerospace, transportation and marine industry especially for vehicle body production due to the highly specific mechanical properties. Polymer matrix based composites based on thermo set polymers with glass fibre reinforcement are brittle and subjected to extensive delamination while the impact response can be enhanced by implementation thermoplastic matrix and three dimensional textiles (Shyr and Pan, 2003; Zike et al., 2011; Reyes and Sharma, 2010).

Moreover, glass fibres are the class of synthetic fibres involving large energy sources in production and are hardly recyclable. Concern about environmental problems promoted by the steep increase of waste in disposals and high energy consumption is becoming more intensified. Consequently legislation has been set by the

European Directive 2005/64/EC devoted to decrease the environmental impact of vehicle waste; introducing recyclable materials in vehicle production thus implementation of natural products from renewable and biodegradable sources. Therefore, instead of synthetic fibre fabrics natural fibre textiles could be used providing biodegradability, low cost - natural fibres as flax and hemp fibres are up to 40% cheaper than standard glass fibres, nonabrasive nature, low energy consumption, high specific properties, low density, etc.

Main drawbacks are considered to be low thermal stability, low resistance to moisture and seasonal quality variations even between individual plants in the same cultivation (Ashori, 2008).

Commonly used adhesives are phenol- and urea-based formaldehyde resins which are toxic and sensitive to the external moisture. Therefore, replacing the existing adhesives with non-toxic, water resistant and good adhesion promoting materials may be considered beneficial (Forest Products Laboratory, 2010).

Formaldehyde is a toxic gas that can react with proteins of the body to cause irritation and, in some cases, inflammation of membranes of eyes, nose, and throat. However, formaldehyde is efficiently consumed in the curing reaction, and the highly durable phenol-formaldehyde, resorcinol-formaldehyde, and phenol-resorcinol-formaldehyde polymers do not chemically break down in service to release toxic gas. However, some emission of uncured components is observed in service life of products (Forest Products Laboratory, 2010). Additionally, manufacturing could be significantly enhanced and more efficient if instead of spreading glue between veneers, adhesive layer compatible with whole plywood lamination process could be used.

The walls and roofs in transport vehicles, also container floors can be subjected to the damage from road debris, tool drop and other small object impact under low velocity.

Thus, this research was focused on the development of plywood laminates with increased impact energy absorption capacity. In plywood laminates thermoplastic polymers as high density polyethylene (HDPE) and fibre fabrics made of glass and flax were incorporated. HDPE is preferred because the melting temperature is in range of 130-140°C compatible with plywood processing technology.

Furthermore, the impact properties as energy absorption, specific energy, impact load and damage extent were compared between composite laminates introducing woven and non-woven fabrics made of flax and glass fibre (GF) textiles, additionally laminates without textiles where experimentally produced to evaluate the influence on adhesive type bonding between plywood plies.

MATERIALS AND METHODS

Materials

Experimentally made laminated composites consisted of single veneer or three plies plywood as outer layers and GF/flax fabrics as inner layers. The fabrics used in this study were made of woven plain-wave structure and non-woven or stitched fibre fabrics (Fig.1). Commercially available non-woven stitched glass fibre fabrics made of four layers with fibre stacking 45/90/45/0°, flax fibre fabrics of two layers with stacking 0/90 ° and GF mat fabrics were used. Flax fabrics were prepared in the Institute of Textile Material Technologies and Design of the Riga Technical University (RTU) by Maris Manins.

In the experimental production of laminated composites two types of adhesives as traditionally utilized phenol-formaldehyde and high density polyethylene (HDPE) films and sheets representing class of thermoplastic polymers were employed. Moreover, once used HDPE film was employed being utilized for outdoor environmental exposure during the period of one year with thickness 80 µm. Composites with incorporated fabrics were made introducing HDPE sheets with thickness 1 mm.

Furthermore, the birch veneer plies, phenol-formaldehyde adhesive and also three and seven layer plywood which has been investigated in the present study was generously granted from the company A/S "Latvijas finieris".

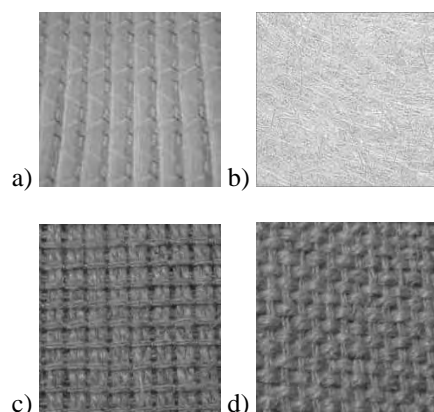


Figure 1. Fabrics implemented in this study:
a) stitched GF; b) GF mat; c) non-woven flax fibres;
d) woven plain-wave flax fibres.

Laminate manufacturing process

Experimental production of laminated composites involved stacking of separate sheets maintaining veneer plies as outer layers with overall dimensions 62 x 62 cm (Fig.1). Between veneer layers plies of thickness 1.4 mm each, HDPE and flax/glass fibre fabrics were incorporated. The processing of laminates was performed on laboratory equipment of the RTU, Institute of Materials and Structures –

handmade hot press (Fig.2). The laminates were hold for 10 minutes at the temperature of 150°C without pressure to ensure melting of thermoplastic adhesive and for 10 minutes under the pressure of 2bar. As the next step the composites were cooled down at the room temperature under pressure to avoid twisting or warping of the laminate specimens due to the thermal expansion and creep of separate layers. The obtained laminates were cut into specimens with dimensions of 10 x 10 cm according to the impact testing standard (ISO 6603-2).

Impact testing

For the impact tests a drop tower INSTRON Dynatup 9250HV has been utilised. During the test impact the machine was equipped with a hemispherical punch with a diameter of 20 mm. Specimens with dimensions of 100 × 100 mm were fixed in pneumatic clamping system with inner ring diameter of 76.2 mm.

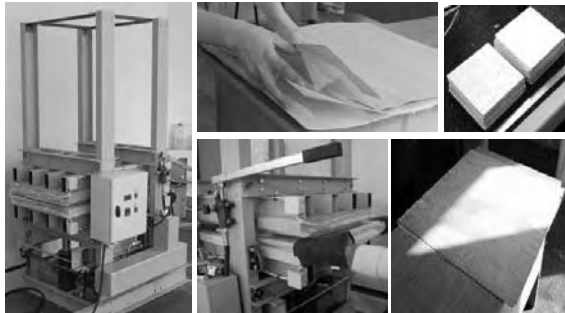


Figure 2. Experimental production of laminated composites.

The impact velocity was set to 3.4 m/s, height approximately 0.6 m and weight 26 kg in order to provide the resultant potential impact energy of 150 J.

RESULTS AND DISCUSSION

The impact response of any materials can be described by the amount of force and energy it can absorb. A typical impact response curve obtained in the tests may be subdivided in three following parts: ascending, peak force and descending part. The ascending part is related to the bending stiffness or material capability to resist the impact force in flexure. Maximum force shows the force needed to induce composite damage through the material fracture and delamination. The descending part depends on the material properties: brittle materials will show very sharp drop of load, laminated composites show gradual decrease because of delamination growth, in sandwich structured composites the load reached maximum peak can stay constant for a longer period if the resistance of the core material is sufficient, thus plateau can be

observed. The larger the area under the load-deflection curve the higher the level of energy is absorbed by the material (Shyr and Pan, 2003; Zike et al., 2011; Reyes and Sharma, 2010).

Impact properties between different laminate configurations were examined, thus the experimental part can be sectioned in several parts: impact resistance of different all-wood products; composite laminates with incorporated GF/flax fabrics and damage evaluation of different specimens after drop-weight impact tests.

Impact properties of all-wood products

Therefore, first of all the impact response to free-falling object impact of different wood products as veneer, particle board, three and seven plies plywood based on phenol-formaldehyde and HDPE film adhesive was compared (Fig.3). The best impact resistance was shown by laboratory manufactured plywood consisting of seven plies with reused HDPE film. The absorbed energy of similar plywood made with phenol-formaldehyde adhesive was approximately twice lower and the impact force one and a half times lower. The worst impact resistance was observed by single veneer and particle board. Even the mass and thickness of the particle board was twice larger than that of the seven plies plywood, the absorbed energy was about twice lower (Table 1).

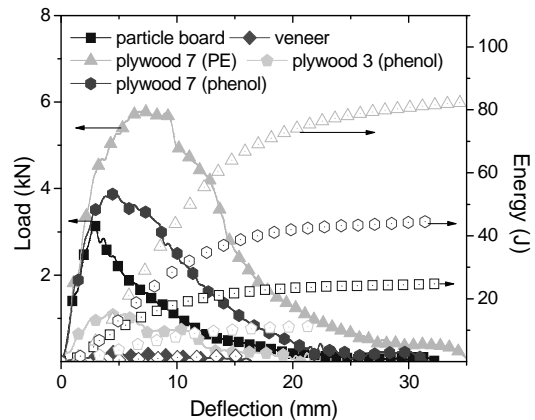


Figure 3. Impact force and absorbed energy of different wood products.

As the thicknesses of the tested specimens was different, specific absorbed impact energy was introduced showing the absorbed energy per unit weight. The highest specific energy was calculated for experimentally fabricated plywood with HDPE adhesive and the lowest for single veneer and particle board. Therefore, production of plywood and implementation of HDPE adhesive significantly increases the efficiency of impact resistance of wood products. The effect of adhesive could be explained by quite different properties between thermoplastic and thermo set polymers or HDPE

and phenol-formaldehyde, respectively. HDPE is a well-known thermoplastic material, because of the inherent molecular structure the thermoplastic polymers are more plastic and show higher toughness than thermo sets. The influence of adhesive toughness on overall performance on the composite impact properties in transverse direction is clearly evident by their higher performance. (Forest Products Laboratory, 2010).

Moreover, it can be observed that the impact response was highly dependent on the number of plies, for example, single veneer absorbs around 0.25J, three plies plywood four times more – 1J and seven plies plywood 4J, what is 16 times more comparing to single veneer ply (Fig. 3).

Impact properties of wood/GF & flax products

Implementation of fabric materials between veneer layers was expected to improve the plywood impact absorption properties more radically. In Fig.4 the impact response of composites made of different fabrics with phenol-formaldehyde adhesive was represented. The acquired results were compared with 3-ply plywood assuming the fabrics as the third ply (Fig.3). Therefore, incorporation of GF mat increased the impact force around 1.5 times, whereas non-woven flax and glass fibre fabrics increased the ultimate force values about 2 and 3.5 times.

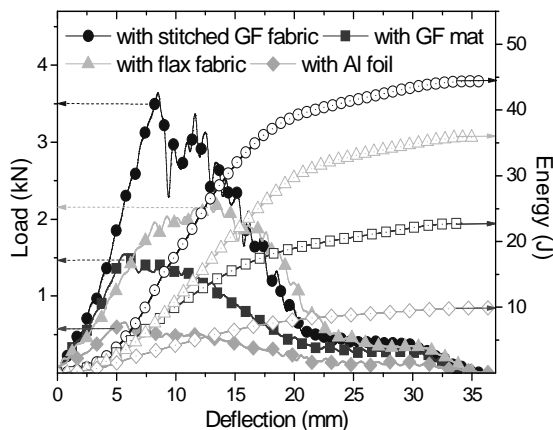


Figure 4. Impact force and absorbed energy of laminates with incorporated fabrics.

The energy absorption in composites increased more rapidly than the impact force, therefore, introduction of non-woven flax and GF fabrics can dissipate the impact energy 3.5 and 4.5 times more comparing with 3-ply plywood specimens. Laminated composite with stitched GF fabric showed similar impact strength properties as 7-ply plywood and had 1.3 times lower weight, consequently, the specific absorbed energy was 1.4 times higher than laminates with stitched GF fabric. Furthermore, correlation study has been done to

compare woven and non-woven GF fabrics laminate specimens made with single veneer and 3-ply plywood at the top plates. (Fig.5) An adhesive HDPE sheet was used to bond GF fabrics to the outer layers of veneer and plywood. However, the cover plate of 3 plies plywood was made of phenol-formaldehyde glue. The relation between the fabric type and impact response was more pronounced by laminates with outer layers made of single veneer ply. Laminate with woven GF fabric showed 2.5 times lower impact force and twice lower absorbed energy. Meanwhile the laminate made of 3-ply plywood in outer layers and woven GF fabrics showed 1.5 times lower impact force and 1.7 times lower impact energy absorption capacity. Therefore, larger enhancement was achieved employing less impact resisting sheets in outer layers.

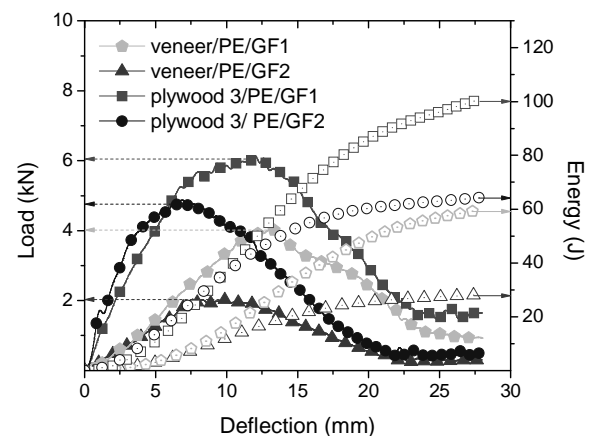


Figure 5. Impact force and absorbed energy of laminates with different GF fabrics and outer layers

Moreover, both GF composites made with 3-ply plywood in outer layers showed higher impact resistance (Fig.5) than 7-ply plywood made of phenol-formaldehyde (Fig.2). The impact force was increased 1.1-1.5 times and energy absorption 1.5-2.5 times. Although laminates with GF fabrics introduced between 3-ply plywood were heavier, the specific absorbed energy was still higher of GF composites. Comparing the specimens with single veneer layers as cover sides no significant changes in specific energy absorption have been observed (Table 1).

In addition, by comparing the results with 7-ply plywood made with HDPE film adhesive (Fig.3) it has been observed that only composites with 3-ply plywood at the outer layer with stitched GF fabric in the middle layer shows higher impact properties (Fig.5). Therefore, 7-ply plywood absorbs 53% (80J) from the initial energy 150J, whereas 3-ply plywood with incorporated stitched GF fabric 67% (100J). It may be assumed that incorporation of HDPE film also in outer layers between plywood plies could additionally increase the impact resistance in transverse direction.

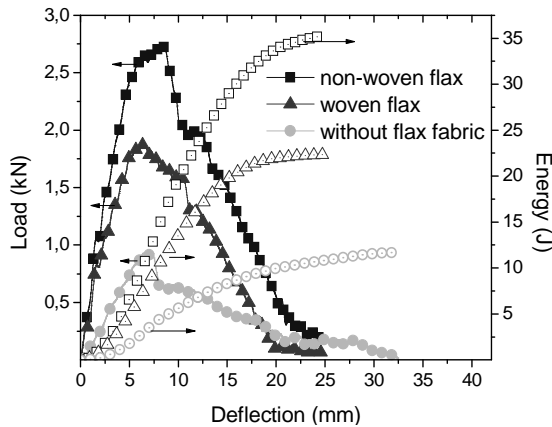


Figure 6. Comparison between composites made of different flax fabrics bonded between veneer sheets with HDPE adhesive.

Lower performance was observed by composites made of 3-ply plywood and woven plain-wave fabrics (Fig.5) showing 1.5 and 1.3 times lower impact force and absorbed energy rate comparing to composites with stitched GF fabric.

Additionally two types of flax fabrics incorporated between veneer layers bonded with HDPE adhesive were examined under the impact tests (Fig. 6). The drop-weight impact results showed the best performance of the laminate with non-woven fabric composed of two flax fabric layers. Therefore, non-woven flax fabric being twice heavier than the woven one showed about 1.5 times higher impact force and absorbed energy values. While two veneer sheets bonded with HDPE film show approximately 2-3 times lower impact force and absorbed energy values. In spite of enhancement composites made with flax fabrics showed lower energy dissipating capacity comparing to GF fabrics.

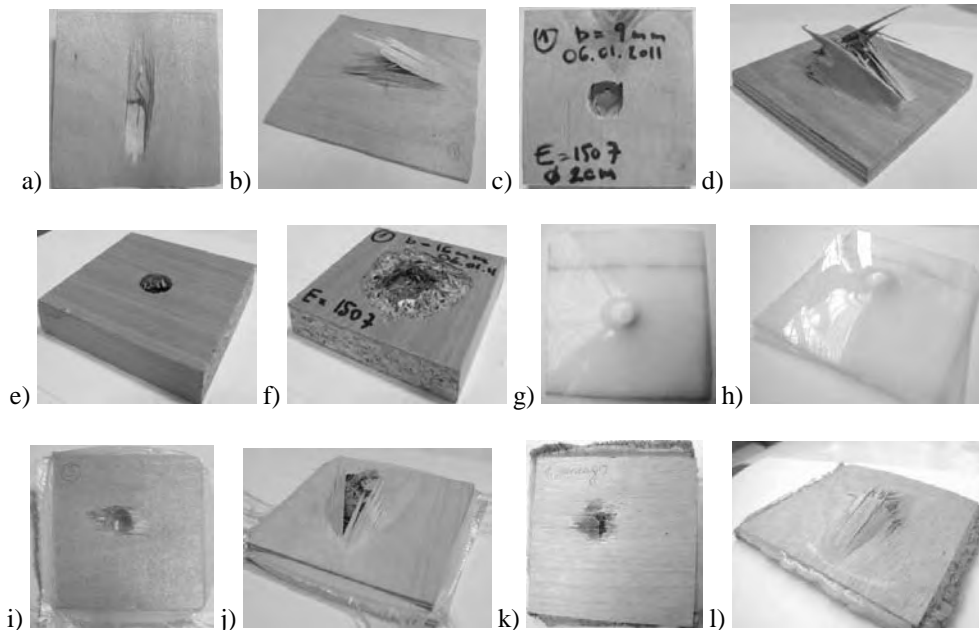


Figure 7. Specimens after the drop-weight impact tests: top (a) and bottom (b) of veneer; top (c) and bottom (d) of 7 plies plywood; top (e) and bottom (f) of particle board; top (g) and bottom (h) of HDPE; top (i) and bottom (j) of composite with GF fabric; top (k) and bottom (l) of composite with flax fabric.

Specific energy of specimens subjected to drop-weight impact

Table 1

Specimen	Thickness, mm	Impact force, kN	Absorbed energy, J	Mass, g	Specific energy, J/g
HDPE	1	1.3	18	9.7	1.86
Veneer	1.5	0.22	1.5	8	0.19
3-ply (phenol) plywood	4	1	12	27	0.45
7-ply (phenol) plywood	9	4	45	64	0.86
7-ply (PE) plywood	10	4	45	62	1.26
Particle board	16	3	23	111	0.21
Veneer/PE/GF/PE/veneer	4	2/3.8	30/ 60	43/50	0.7/1.22
3-ply plywood /PE/GF/PE/ 3-ply plywood	9	5 & 6	60 & 100	76.5/85	0.78/1.17
Veneer/PE/flax/PE/veneer	5	1.75/2.4	22/37.5	42/ 50	0.52/0.75

The specific absorbed energy by flax fabrics composites was within 0.5-0.75, whereas GF fabrics composites within 0.7-1.22 J/g (Table 1).

By graphical inspection of the tested specimens the damage in all specimens was more pronounced in wood fibre direction. (Fig.7) In the case of plywood and particle board the upper layer was damaged locally taking a circular form of striker head (Fig. 7c,e) more extensive damage was observed at the bottom layer also showing some pulled out middle plies (fig.7b,d,f). The amount of damage at the bottom of plywood samples could exceed the damage area at the specimen upper surface up to four times. Less extensive damage was observed in laminates with integrated HDPE film with both GF and flax fabrics (Fig.7j,l). The particle board due to drop-weight impact has disintegrated thus showing the most extensive damage among the tested samples (Fig. 7f). In plywood specimens fibre breakage, delamination between plies and crack growth has been observed both perpendicular and parallel to wood fibres. A plastic deformation of HDPE sheets may be noted explaining the better performance of plywood laminated with HDPE (Fig. 7g,h).

ACKNOWLEDGEMENTS

The authors would like to acknowledge the support of the company A/S "Latvijas finieris" by granting the testing specimens and to M.sc.ing. Māris Maniņš from the Institute of Textile Material Technologies and Design of the RTU for providing the flax fibre fabrics.

REFERENCES

- APAWOOD. FRP Plywood. Data file. [online] [accessed on 01.05.2011.]. Available: http://www.apawood.org/level_c.cfm?content=pub_ply_libmain
- Ashori A. (2008) Wood-plastic composites as promising green-composites for automotive industries! *Bioresource technology*, Vol. 99, p. 4661–4667.
- Dagher H., Kimball T., and Shaler S. (1996) Effect of FRP reinforcement on low grade eastern hemlock glulams. *Proceedings of National conference on wood transportation structures*, Forest Products Laboratory, p. 207-214.
- Directive 2005/64/EC of the European Parliament and of the Council of 26 October 2005 on the type-approval of motor vehicles with regard to their reusability, recyclability and recoverability
- Forest Products Laboratory (2010) *Wood handbook - Wood as an engineering material. General Technical Report FPL-GTR-190*. Madison, WI: U.S. Department of Agriculture, Forest Service, Forest Products Laboratory (chapters 2, 5, 10, 11).
- Gardner D. J. *Synthetic Fiber Reinforcement. Strategies for Glulam and Structural Wood Panels*. [online] [accessed on 01.05.2011.]. Available: www.forestprod.org/ec-nesection06mtggardner.pdf
- ISO 6603-2: 2000 Plastics – Determination of puncture impact behaviour of rigid plastics – Part 2: Instrumented impact testing.
- Pirvu A., Gardner D.J., and Lopez-Anido R. (2004) Carbon fiber-vinyl ester composite reinforcement of wood using the VARTM/SCRIMP fabrication process. *Composites Part A: Applied Science and Manufacturing*, Vol. 35, p. 1257–1265.
- Raftery G. (2011) Low-grade glued laminated timber reinforced with FRP plate. *Composites Part B: Engineering*, Vol. 42, p. 724-735.
- Reyes G., Sharma U. (2010) Modeling and damage repair of woven thermoplastic composites subjected to low velocity impact. *Composite Structures*, Vol. 92, p. 523–531.
- Shyr T.W., Pan Y.H. (2003) Impact resistance and damage characteristics of composite laminates. *Composite Structures*, Vol. 62, p. 193–203.
- Zike, S., Kalnins, K., Ozolins, O. (2011) Experimental Verification of Simulation Model of Impact Response Tests for Unsaturated Polyester/GF and PP/GF Composites. *Computer Methods in Materials Science*, Vol. 11, No.1, p. 88-94.

CONCLUSIONS

Different wood products have been subjected to drop-weight impact tests from which the lower impact resistance has been observed by particle board and single veneer whereas the highest energy absorption capacity of 7-ply plywood with HDPE film adhesive. Such laminate can dissipate twice higher impact energy than 7-ply plywood based on phenol-formaldehyde adhesive. Laboratory manufactured samples incorporating glass and flax fabric have been tested to assess the benefit of textile reinforcement. It has been proved that the largest amount of initial impact energy can be absorbed by plywood laminate with stitched GF fabric. The highest specific absorbed energy values among the test specimens have been obtained for plywood made of HDPE adhesive film and by incorporating GF fabrics. It was outlined that the GF shows more significant enhancement of transverse impact properties compared to flax fabric textiles integrated in plywood laminate. Moreover, once incorporating the textile fabrics a considerable reduction of damage propagation and laminates ply failure has been observed under the impact load.

INFLUENCE OF TECHNOLOGICAL AND STRUCTURE PROPERTIES ON SHAPE OF ASYMMETRIC PLYWOOD SHEET

Jānis Šliseris, Kārlis Rocēns

Riga Technical University, Department of Structural Engineering
janis.sliseris@gmail.com

ABSTRACT

The paper presents a numerical study of the technological process and plywood structure (veneer arrangement and thickness) influence on the shape of the sheet. The technological process after the gluing process, including the conditioning of the sheet in various moisture-temperature conditions is numerically modeled. Technological treatment- conditioning produces the stress-deformation field in the sheet. The behavior of wood material produce the stress-deformation field change in time. The standard linear solid model constitutive model of material is used in the analysis. The coupled moisture- temperature- stress analysis is done by using the Finite element method. The moisture- temperature conditions on the boundary of the sheet is defined by polynomial equations. The rational moisture-temperature conditioning parameters and plywood structure are proposed that provide the necessary shape of the sheet and its stability in time.

Key words: Technological process, plywood structure, standard linear solid model, stress-deformation field

INTRODUCTION

Rational structures with minimal material consumption and weight is one of the main research fields in today's structural engineering science. Wood resources could be rationally used (with small amount of sawdust and other less useful materials) by making plywood sheets. It is very popular to use flat plywood sheets in building as load bearing elements or covering elements. From the structural engineering point of view more effective it is to use curved plywood shells than flat sheets because of better cross section characteristic-second moment of area. The main obstacle for using curved shells is its difficult and expensive manufacturing. It could be significantly simplified by making the sheet with special asymmetrical structure and curved using veneer orthotropic moisture expansion properties. The curvature is obtained after gluing flat sheets with standard techniques and than conditioning in special moisture- temperature conditions (Šliseris, Rocēns 2010). The sheet with asymmetrical structure is more sensitive to moisture-temperature change and structure imperfections (Sliseris, Rocēns 2010). The special moisture-temperature conditioning has to be projected for the sheet to obtain the necessary shape. In many works the moisture diffusion problem is analyzed, for example (Olek, Weres 2007). The coupled moisture-temperature diffusion problem is considered in many works (Avramidis, Englezos, Papathanasiou 1992, Wook, Woo, Chang, etc. 2008). There are many works where the moisture-stress problem is solved in small, idealized wood samples (Fortino, Mirianon, Toratti 2009, Jönsson 2005). In many works composite structures are optimized including wood structures that are affected by

mechanical loading or moisture-temperature loadings (Sliseris, Rocens 2011, Goremikins, Rocēns 2010, Goremikins, Serdjuks 2010, Brauns, Rocens 2008). In very few works the temperature-moisture diffusion problem in modified wood (plywood) is solved. In the literature there is not any work dealing with the moisture-temperature-stress problem in plywood sheets with asymmetrical structure. This problem is numerically studied in this work.

NUMMERICAL METHOD OF MOISTURE-TEMPERATURE-STRESS ANALYSIS

Moisture analysis

The moisture analysis is done by using one dimensional moisture transfer model. It is assumed that moisture distribution through the thickness of the sheet is the same in any place of the sheet. Mathematically the moisture diffusion is modeled by the Fiks law (Liping 2005, Olek, Weres 2007):

$$\frac{\partial m}{\partial t} = \frac{\partial}{\partial z} \left(D \frac{\partial m}{\partial z} \right) \quad (1)$$
$$-a < z < a$$
$$t > 0$$

where m- moisture content (dimensionless), z- coordinate, on axis perpendicularly to the sheet surface, t- time, D- moisture diffusion coefficient ($\frac{m^2}{h}$), that is calculated by the following equation (Wook, Woo, Chang etc 2008):

$$D = 5.76 \exp \left(1.45m - \frac{5280}{T} \right) \quad (2)$$

where T- temperature (K).

The moisture diffusion coefficient depends on temperature T, therefore, the moisture diffusion process depends on temperature diffusion. The following initial and boundary conditions are used in the analysis:

$$m(z, t = 0) = m_0$$

$$D \frac{\partial m}{\partial t} = k_m (m - m_0), z = \pm a, t > 0 \quad (3)$$

where k_m – surface moisture emission coefficient.

Temperature analysis

Temperature analysis is done by using the classical Fourier law :

$$\rho(m)c(m,T) \frac{\partial T}{\partial t} = \nabla(\lambda(m,T)\nabla T) \quad (4)$$

where ρ – density of plywood (kg/m³), $c(m,T)$ – specific heat of plywood, $\lambda(m,T)$ – heat diffusivity coefficient, ∇ – Nabla operator (partial derivative with respect to coordinate).

The following initial and boundary conditions are used in simulation:

$$T(z, t = 0) = T_0$$

$$-\lambda(m,T) \frac{\partial T}{\partial t} = h(T - T_{sur}), z = \pm a, t > 0 \quad (5)$$

where h- surface temperature emission coefficient for plywood assumed it to be $h = 25 \frac{W}{m^2 K}$ (Fortino, Mirianon, Toratti 2009), T_{sur} – surrounding temperature (K).

Stress analysis

Typical plane stress shell element is used (Zienkiewicz, Taylor 2000). In the stress analysis the results from moisture and temperature analysis are used to calculate moisture caused stress (Ranta-Maunus 2003, Brauns, Rocens 2004). The total time is divided in small time steps and in each step the calculated stress value is corrected according to the standard linear solid model that consists of elastic spring in series of dashpot that is parallel to other spring elements. The constitutive equation is defined by the standard linear solid model, that could be used for solving technological problems of wood (Ugolev 1971, Rocens 1979):

$$n \frac{\partial \sigma}{\partial t} + \sigma = nH \frac{\partial \varepsilon}{\partial t} + E\varepsilon \quad (6)$$

where n- relaxation time (min), σ – stress component (MPa), ε – deformation component, H- instantaneous Jouns modulus (MPa), E- long term Jouns modulus (Mpa).

Using the mentioned constitutive equation in each time step the stress distribution curves that are obtained by the Finite element analysis are corrected. The stress values are corrected in particular points (in this case there are used 19 points) through the thickness of the sheet. Assumed that there is no shear deformation through the thickness of the sheet and deformation values through the thickness of the sheet could be approximated by linear equation. The stress-strain values are corrected in the direction of the main deformations without interactions to other directions. In addition two equations are used- the total internal force and moment should be zero, because there is no external moment of force. The final system of equation is the following:

$$\left\{ \begin{array}{l} n_1 \frac{\partial \sigma_1}{\partial t} + \sigma_1 = n_1 H_1 \frac{\partial \varepsilon_1}{\partial t} + E_1 \varepsilon_1 \\ \dots\dots\dots \\ n_{19} \frac{\partial \sigma_{19}}{\partial t} + \sigma_{19} = n_{19} H_{19} \frac{\partial \varepsilon_{19}}{\partial t} + E_{19} \varepsilon_{19} \\ \int_{-a}^a \sigma dz = 0 \\ \int_{-a}^a \sigma \cdot z dz = 0 \end{array} \right. \quad (7)$$

The system of equation (7) is used to correct the values of stress and deformations. The displacements, curvatures are obtained using the small deformation theory (Zienkiewicz, Taylor 2000). The rheological coefficients are dependent on temperature and moisture. It is assumed that only rheological coefficients in tangential direction of wood depend on temperature and moisture. The relationships are the following (Ugolev 1971) (when stress is under 85% of strength of wood):

$$H(m,T) = 2235.15 - 7007m - \dots \quad (8)$$

$$22.7T + 28.58mT + 5700m^2 + 0.079T^2$$

$$E(m,T) = 574 - 926m - \dots \quad (9)$$

$$3.76T - 9mT - 5460m^2 + 0.0026T^2$$

$$n(m,T) = 294.7 - 1236m - \dots \quad (10)$$

RESULTS OF MOISTURE-TEMPERATURE-STRESS ANALYSIS

In the numerical analysis a sheet with total thickness 20 mm was simulated. The total thickness of the layers that are orientated in longitudinal and shear direction are h_2, h_1 , respectively. The initial moisture content of the wood is 6% and final moisture content 12%.

Three different temperature conditioning regimes (TCR) are simulated. In each TCR there are different air temperature change relationships with respect to time. These relationships are shown in Fig. 4.

Before stress analysis moisture-temperature diffusion in the sheet transversal direction was simulated. The surface of temperature and moisture distribution in time through the thickness of the sheet is shown in Figure 1 and Figure 2.

The obtained moisture and temperature distribution curves were used in stress analysis. In all three TCR

the stress- deformation state of the plywood sheet was analysed. In Figure 3 the main curvature of the sheet depending on time for three temperature conditions is shown. The linear model indicates that there was used the linear relationship between stress and strain instead of rheological equations (6). It can be figured out that in this range of parameters used in the numerical experiment the difference in linear and nonlinear analysis is approximately 25%. The results for various TCR changes are in range of 5%.

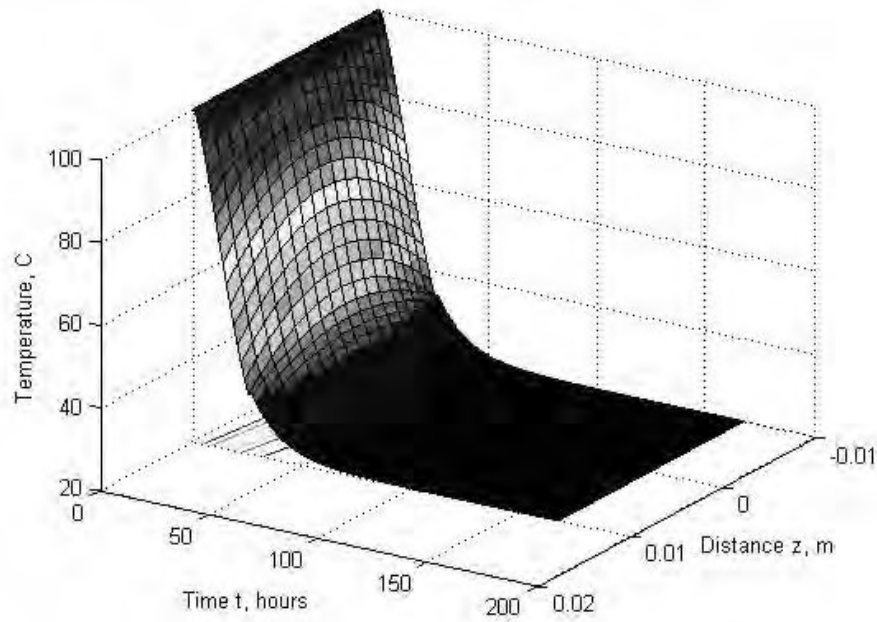


Figure 1. Temperature distribution through the thickness of the sheet in time in 1. TCR.

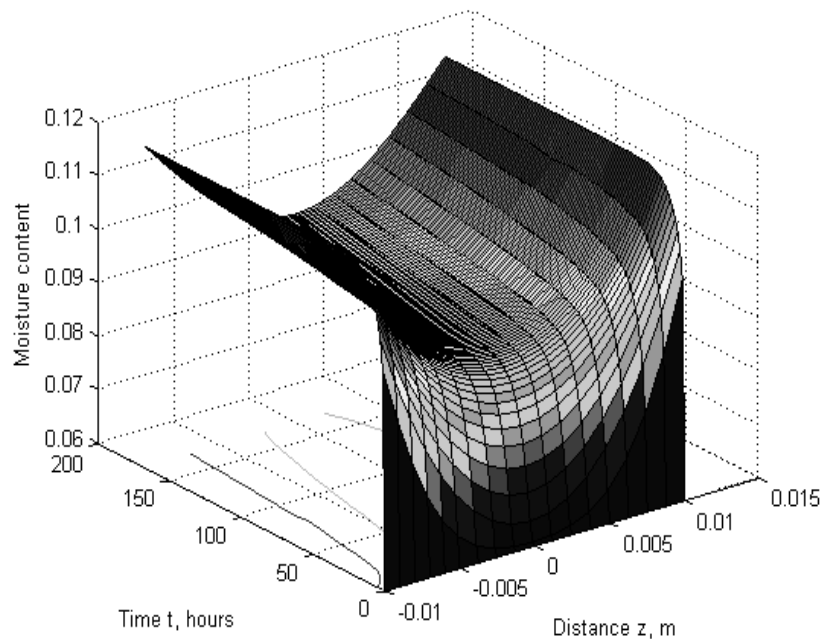


Figure 2. Moisture content distribution through the thickness of the sheet in time in 1. TCR.

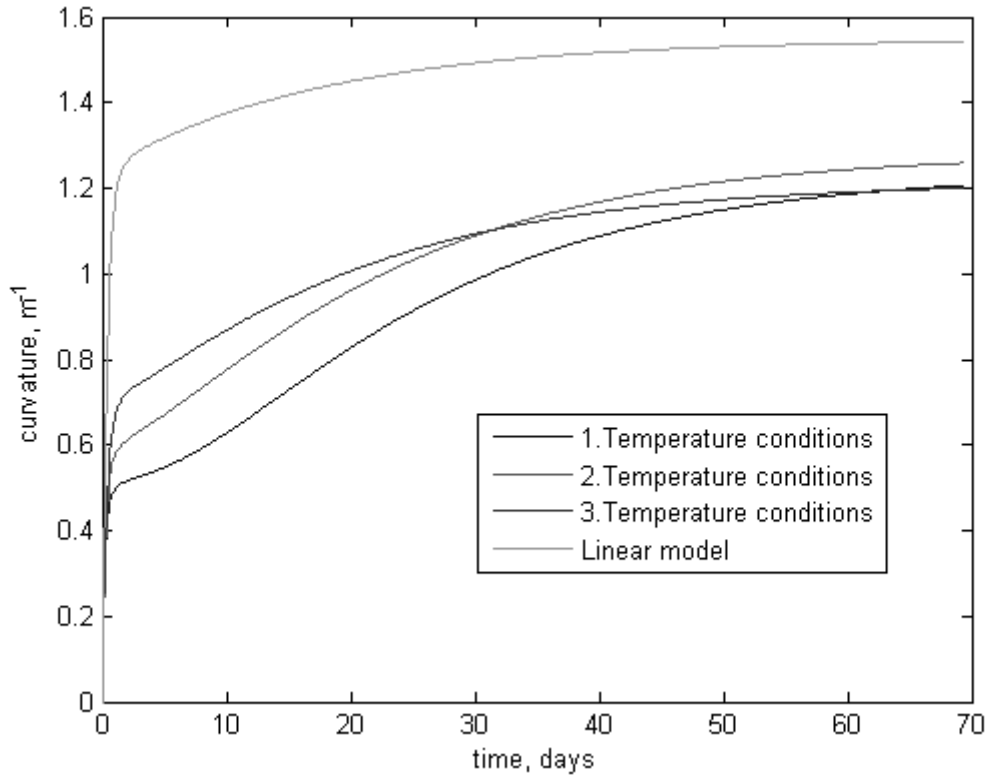


Figure 3. Curvature of the sheet depending on time for various TCR (see Fig. 4.).

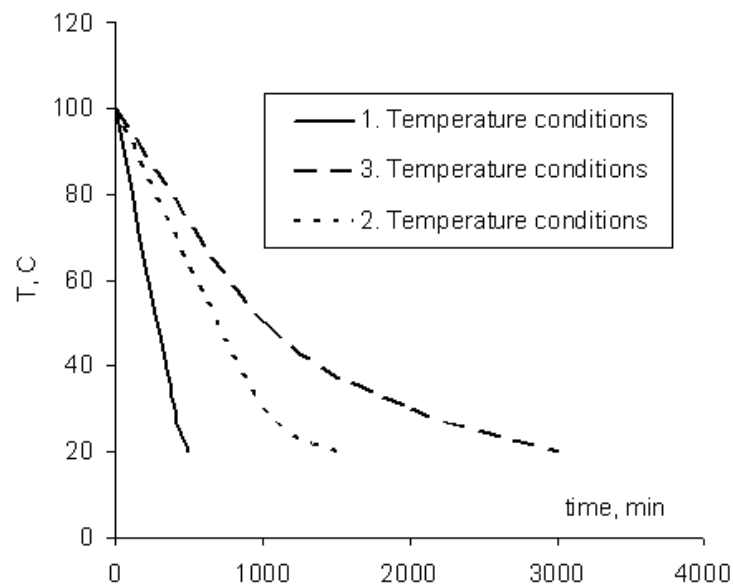


Figure 4. Temperature conditioning regimes (TCR).

In other numerical experiments the curvature of the sheet change in time for various ratios of shear and longitudinal layer thickness were analyzed. The obtained results are shown in Figure 5. It could be seen that in this range of ratios the curvature is increasing when the ratio is

increasing. Although there the ratio when the maximal curvature is obtained is between 5..7, depending on veneer properties and TCR and moisture regimes. In case if there are very large ratios then the shape stability is significantly decreased.

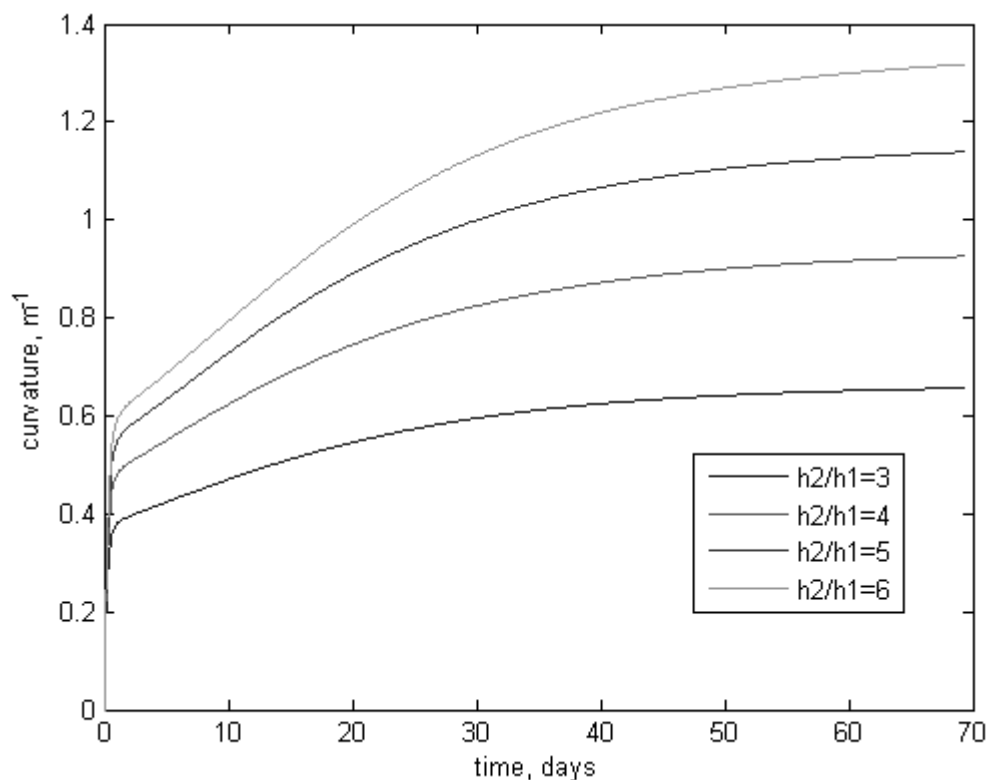


Figure 5. Curvature dependence of the structure of the sheet (ratio of shear and longitudinal layers thickness).

CONCLUSIONS

The influence of temperature conditioning regime and structure of asymmetrical with respect to mid surface plywood sheet are obtained by solving the coupled moisture-temperature-stress problem.

The temperature conditioning regime affects the final shape of the sheet in the range of 5 %. The maximal curvature of the sheet in the shortest time could be obtained by using the linear temperature conditioning regime with total time approximately 20..30 hours.

The results show that rational ratio of thickness of longitudinal and shear layers vary from 5..7 that gives maximal curvature of the sheet and provides shape stability in a long period of time.

The wood rheological properties inclusion in the analysis change the results in the range of 20..25% compared to the linear analysis.

In future the proposed model that takes into account rheological properties of plywood with experiments and other models should be verified.

REFERENCES

- Avramidis S., Englezos P., Papathanasiou T. (1992) Dynamic nonisothermal transport in hygroscopic porous media: moisture diffusion in wood. *AIChE J*, vol. 38, p. 1279–1287.
- Brauns J., Rocens K. (2008) Behaviour and Optimization of Environmental sensitive Layered systems. 8th *Nordic Symposium of Building Physics*. Copenhagen, Denmark, 16-18 June.
- Brauns J., Rocens K. (2004) Design of humidity sensitive wooden materials for multi-objective application. *Wood Sci. Technol.* vol. 38, p. 311-321.
- Goremikins V., Rocēns K. (2010) Rational Structure of Composite Trussed Beam. *Sixteenth International Conference Mechanics of Composite Materials*. Institute of Polymer Mechanics, University of Latvia, p. 75-75.
- Goremikins V., Serdjuks D. (2010) Rational Structure of Trussed Beam. *The 10th International Conference Modern Building Materials, Structures and Techniques*. Selected papers, Lithuania, Vilnius, 19.-21. May, p. 613-618.

- Fortino S., Mirianon F., Toratti T. (2009) A 3D moisture-stress FEM analysis for time dependent problems in timber structures. *Mechanics of time-dependent materials*, Vol. 13, p. 333-356.
- Jönsson, J. (2005) Moisture induced stresses in timber structures. *Technical Report TVBK-1031*, Dissertation, Division of Structural Engineering, Lund University of Technology.
- Liping C. (2005) Determination of diffusion coefficients for sub-alpine fir. *Wood science and technology*, Vol. 39, p. 153-162.
- Olek W., Weres J. (2007) Effects of the method of identification of the diffusion coefficient on accuracy of modeling bound water transfer in wood. *Transport in porous media*, Vol. 66, p. 135-144.
- Ranta-Maunus, A. (2003) *Effects of climate and climate variations on strength*. In: Thelandersson, S., Larsen, H.J. (eds.) *Timber Engineering*. Wiley, New York. 16 p.
- Rocens K.A. (1979) *Technological regulation of wood properties*. Riga: Zinatne. 220 p.
- Sliseris J., Rocens K. (2010) Curvature Analysis for Composite with Orthogonal, Asymmetrical Multi-Layer Structure. *Journal of Civil Engineering and Management*, Vol. 16, No. 2, p. 242-248.
- Sliseris J., Rocens K. (2010) Behavior of multilayer sheet with technological imperfection. In: *10th International Conference Modern Building Materials, Structures and Techniques*, Lithuania, p. 793-798.
- Sliseris J., Rocens K. (2011) Rational structure of panel with curved plywood ribs. *ICBSE 2011 : International Conference on Building Science and Engineering*, Venice, Italy, April 27-29.
- Ugolev B.N. (1971) *Deformations and stress in drying of wood*. Lesnaja promislenostj, Moscow. 174 p.
- Wook K., Woo Y., Chang D. E. etc. (2008) Some considerations in heterogeneous nonisothermal transport models for wood: a numerical study. *Journal of Wood Science*, Vol. 54, p. 267-277.
- Zienkiewicz O.C., Taylor R.L. (2000) *The Finite Element Method. Vol. 2. Solid Mechanics*. London: McGraw-Hill. 459 p.

OVERVIEW OF SOME NON-DESTRUCTIVE METHODS FOR IN SITU ASSESSMENT OF STRUCTURAL TIMBER

Marko Teder*, Kalle Pilt*, Matis Miljan*, Martti Lainurm*, Ragnar Kruuda*

*Estonian University of Life Sciences, Department of Rural Building
marko.teder@emu.ee

ABSTRACT

The need for structural health assessment of old buildings can emerge in order to assure or extend their service life. In renovating buildings it is essential to assess the condition of timber structures. Often there are situations where the wood structures need to be evaluated on site and visual assessment is confined. At this point the non-destructive methods can be used for evaluation. This research uses ultrasonic, resistance drilling and pilodyn methods for the assessment of timber samples taken from currently existing buildings of different ages. As bending being the most important loading mode and modulus of elasticity is a good indicator of strength in timber structures the results of non-destructive methods were compared with them. Individual arguments like ultrasound velocity, moisture content, drilling resistance and relative hardness used in the regression analysis did not give a correlation above average in prediction of the bending strength and modulus of elasticity of wood found in the standardized bending test. The correlation between the density of timber and the readings of the resistograph was the strongest, especially damaged by fungi and beetles. Thereby, when the age of wood increased, the strength of it decreased. The correlation between the readings of the resistograph and timber internal stresses was weak, meaning that the resistance of wood does not change significantly while loaded with longitudinal forces.

Key words: bending strength, modulus of elasticity, density, moisture content, acoustic measurement, resistance drilling, pilodyn

INTRODUCTION

In renovating buildings it is essential to assess the condition of timber structures. Historic timber structures must be preserved, in order to maintain their original structural purpose as much as possible, therewith taking into account the safety aspect for the inhabitants of the building. Therefore, an accurate condition assessment is needed to evaluate the serviceability of timber structures. The most accurate way of determining the mechanical properties of timber is destructive methods, the most relevant results of which are given by compression, tension and bending tests. But for the sake of preserving the historical value of buildings, the aforementioned methods are not an option.

Going further: although the importance of visual assessment of structure elements is highly decisive, the results can be very subjective and dependent on the observers' experiences and skills. And often there are situations on site where visual assessment is constrained, since the timber structural member has one or many sides covered and/or its geometry does not enable the inspection. Therefore, a need for other methods to gain reliable results based on scientific research is grounded. At this point non-destructive methods can be used for assessing the condition of wood structures.

There are several non-destructive methods that can be used in the assessment and determination of the quality and properties of timber (Niemz, 2009):

- mechanical (drilling resistance, hardness,

intrusion behaviour);

- electrical (correlation between electrical resistance and moisture, correlation between electrical resistance and fungal decay);
- acoustic (sound velocity, sound reflection, sound attenuation);
- thermal (heat radiation);
- electromagnetic waves (visible light, IR/NIR radiation, X-ray, neutron radiation, Synchrotron radiation).

The aim of this work was to investigate the non-destructive methods, the possibilities of using ultrasound, pilodyn and resistograph measurements to investigate the relationships of the physical-mechanical properties of timber. The comparable characteristics are the density and moisture content, because they have essential roles in the strength of wood.

NONDESTRUCTIVE METHODS AND TESTING

Ultrasound velocity method

In the assessment of the properties of wood, sound and ultrasound have been used rather widely. In general terms sound means an elastic wave that spreads in materials and its behaviour in various materials is different. For that reason we can give the acoustic properties for materials (Kettunen, 2006). If the distance of the wave transit is known,

we can measure the time and therefore calculate the speed. This is how the technical properties of a material can be measured. Consequently, the correlation between the speed of sound and a certain property of the material such as stiffness can be made (Lempriere, 2002).

The longitudinal measuring method of sound speed is the most widely used. In the assessment of the properties of a material the unit of speed of sound is a common parameter. In the evaluation of the properties of timber the usage of the ultrasound method is far-spread in sawmills, where the longitudinal measuring method has been used to sort lumber into classes of strength.

As there is a need to assess wood structures on site an obstacle occurs, because in most cases both ends of a member are covered and the measurement cannot be conducted. The measurement can only be done when placing the transducers parallel on one side or across facing each other. But the latter way of measuring is not always possible, because of the inaccessibility of both sides. This kind of measuring method also gives us only the local parameters of wood assessing the local properties.

The main advantage of using ultrasound is that the bar will be undamaged and it can be used further – no deformations or destructions occur. Tests can be made on the same member repeatedly without any substantial variation in the results (Bucur, 2006).

There have been several investigations conducted in that field. Ultrasound wave propagation is directly related to the elastic properties of the material through where it propagates. If the material is damaged, its stiffness decreases. The wave speed is a function of the square root of material stiffness. Lower speed or longer propagation times are generally indicative of worse conditions of wood. It is assumed that the ultrasound pulse velocity can be an index of the quality of wood as it can detect defects like cracks, knots, decay and deviation on grain orientation. In spite of the inhomogeneous nature and anisotropy of wood, it is possible to correlate the efficiency of wave propagation with physical and mechanical wood properties (Drdacky and Kloiber, 2006).

The density and modulus of elasticity (MOE) of a material strongly affect the acoustic properties of wood. Bucur and Chivers (1991) stated that velocity decreases with increased density. Thus the propagation of sound varies in different species of timber. But in other investigations the results have shown that velocity increases for larger density values (Haines et al., 1996). On the contrary, Mishiro (1996) found in his research that velocity was not affected by density.

As wood is an anisotropic material, the speed of sound varies in different directions due to the cell structure (Kettunen, 2006). Transverse waves are scattered at every cell wall. More impacts of waves on wood cells in the transversal direction make

them slower (Kotlina et al., 2008). Ultrasound velocity is influenced by the width of annual rings only in radial direction, due to the macroscopic structure of wood, proportion of early and latewood and cell orientation in the growth ring (Drdacky and Kloiber, 2006).

Kotlina et al. (2008) got the following results in measuring ultrasound velocity in wood members: in the longitudinal direction the velocity ranged from 3500 to 6500 m/s and 1000–2500 m/s across the grain. The ultrasound velocity decreases with increasing the moisture content (Drdacky and Kloiber, 2006). The velocity decreases dramatically with the moisture content up to the fibre saturation point, and thereafter the variation is very small (Bucur, 2006). It is also notable here that the moisture content over the fibre saturation point measured in the longitudinal direction does not have any significant effect on the ultrasound velocity (Machado et al., 2009).

Overall, the direct longitudinal measurement is fairly reliable method in the assessment of the strength of wood. However, according to the report of Machado et al. (2009) it is essential to note that an indirect measurement can give rather good results in determining the properties of stiffness and strength of wood. Furthermore, the results seem to indicate that as the distance (10 to 40 cm) between the transducers becomes larger the influence of deeper wood layers in the velocity of wave propagation increases. Therefore, in a situation where the wood structure is mostly covered and only one or two sides are accessible, it is possible to evaluate the strength of the member by the indirect measuring method. For wood the most favourable frequency range is between 20 kHz and 500 kHz because of the high attenuation of ultrasonic waves in wood at higher frequencies (ASTM 494-89, 1989; Tanasoiu et al., 2002).

Resistance drilling method

Resistance drilling (Resistograph) enables the inspection of timber through the depth of the member. Measurements are dependent on material resistance to drilling with the diameter of 1.5 to 3.0 mm. The resistograph has an electric motor and is battery-operated, which is very valuable for using in historic timber constructions. The drills are flexible and their length depends on type of the resistograph and manufacturer (Kotlina et al., 2008).

The output of resistance drilling is graphical, the tops on output characterise higher resistance or density and bottoms vice versa. Thus, the internal defects and damage of the timber member can be detected.

Different properties like hardness, density, strength classes, residual cross-section and also biodeterioration and natural defects can be determined with the analysis of the resistograph

graphs. Also the width of the annual rings and structure can be measured. The aforementioned strength indicators can be used to calculate residual strength properties of the timber structure based on Eurocode 5 (Pilt, 2009).

According to the report of Kasal and Anthony (2004) the relationship of resistance drilling to the density of the wooden member is variable, ranging between $r^2 = 0.21-0.69$.

The main disadvantage is the locality of inspection. In order to get a total overview of the member condition a numerous amount of drilling tests have to be made. But that is often limited for the sake of keeping the material authenticity. Another issue involves the drilling needle, because of the small diameter of the drill, it can bend easily during the process of drilling into the element. Thus we can receive inaccurate readings.

Pilodyn method

As the resistograph enables the examination through the cross-sectional area, pilodyn gives only superficial results of the element. The mode of operation consists in the penetration of a tongue in the wood element by means of dynamic impact. The result of this method is penetration depth. The diameter of the tongue is of 2.5 mm and maximum penetration is of 40 mm (Kotlinova et al., 2008).

The density is well related to the hardness of wood (Bonamini, 1995; Kasal and Antony 2004). Superficial values of density can be predicted with this kind of portable method. The results got by Görlacher (1987) demonstrated good correlation between the penetration depth and density. Also the extent estimation of damaged areas of the wooden member is shown by the penetration depth of the needle to the inner layers, deeper penetration refers to a more damaged timber.

Hereby, it should be also mentioned that the moisture content and the penetration directions have effect on the results. The penetration depth is higher in radial direction than in tangential direction. In tangential direction the needle has to penetrate through different earlywood and latewood layers, but in radial direction the penetration happens only in one part of the annual ring.

When operating with this device it is very important to hold it perpendicular to the element and another issue is the vibration evoked by the needle strike, which can result in misleading estimates.

METHODOLOGY

The objective of the experiment was to measure the ultrasound velocity in wood members with certain distances between ultrasound transducers and on two main sections—the end and tangential surfaces. The distances were chosen according to the suggestions of the manual of the testing device for the maximum and minimal parameters. For the

indirect measurements the distance was 0.1 to 0.6 m and for the direct measurements up to 1.5 m (Tico User Manual, 2008).

37 logs and beams dated from buildings with various uses were used for the present research. 124 members with dimensions of 50x50x1005–1100 mm were sawn out from the gathered. The chosen dimensions were based on the standard EN 408:2005, which means that the length of the member for the bending test should be at least 19 times the height of the cross-section. The specimens were graded into strength classes according to the Nordic standard of INSTA 142. Three strength classes were defined according to this standard: □C18, C18 and C24.

First of all a series of measurements with a *TICO Ultrasound Instrument* with 50 mm 54 kHz transducers were made with the number of 92 members.

Four different variants of measurements were conducted:

- 1) Five times with a spacing of 200 mm on the tangential surface at random early wood positions by using the indirect method (hereafter this characteristic is marked by “A”);
- 2) Three times with a spacing of 600 mm on the tangential surface at random early wood positions by using the indirect method (hereafter this characteristic is marked by “B”);
- 3) One time between the end surfaces in the longitudinal direction (hereafter this characteristic is marked by “C”);
- 4) Five times in the radial direction by random selection in the direct method (hereafter this characteristic is marked by “D”).

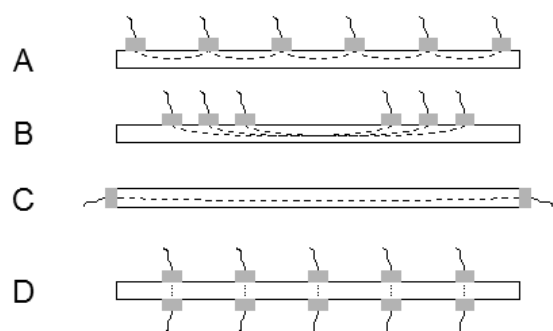


Figure 1. Schematic drawings of measurement methods applied with an ultrasound device: A - indirect measuring; B - indirect measuring; C - longitudinal direct measuring; D - transversal direct measuring.

The principle of this device is that it sends an ultrasound wave into the member by the transmitter probe and is picked up by the receiver probe with

the time of flight recorded in microseconds and also calculates the velocity when the length is entered. The bending strengths of the test pieces were determined by an Instron 3369 device and based on the standard EN 408:2005. Here it should be noted that the force was set in the radial direction with younger annual rings facing upwards. With this experiment the modulus of elasticity in addition to the bending strength was stored.

After the destructive tests a resistance drilling was made using the resistograph Sibtech DmP that measures the resistance minimally at every 0.1 mm. If the resistance of wood is relatively low the interval of the recording data is even ten times longer. The drilling was made in the same direction as in loading force in the bending tests. There were done 5 drilling holes with the distance of 10...15 cm from each other and the spots were designated randomly free from knots and gaps. The superficial hardness was measured with Pilodyn 6J after micro drilling.

The moisture content (MC) and the density of the specimens were found according to standardized tests. In addition the resistance of wood with the resistograph was measured under different compression loads. All data processing including diagrams, correlation and regression analysis was conducted by MS Excel and R software.

RESULTS AND DISCUSSION

The characteristics determined by the experiments are shown in Table 1. The variation of the values of the indicators of density, bending strength and modulus of elasticity were relatively symmetrical, thus revealing that the variation by the main physical-mechanical indicators of the specimen were regular.

To describe the linear relationship between the individual characters of wood by the correlation coefficient Table 2 is presented here. The one-to-

one correlation was between the maximum loading and bending strength, as this is a distinctive feature during the test causing the maximum bending strength with maximum force. That is why only the bending strength is taken into account hereafter.

Table 1
Characteristics of the statistical indicators

Main indicators / Characteristics	Max. bending strength, MPa	MOE, MPa	MC, %	Density, kg/m ³
Mean	42.98	10156.3	8.85	443.12
Median	43.36	10370.8	8.95	434.48
Standard error	13.87	2321.5	1.76	54.01
Minimum	9.06	6317.2	5.34	329.61
Maximum	80.12	17115.6	11.41	596.53

The relationship between the maximum bending strength and modulus of elasticity is remarkably strong ($r=0.72$), which proves the latter to be an important argument in assessment of wood structures. There is also a strong relationship between the density and modulus of elasticity ($r=0.8$), which is about 0.3 higher than between the density and maximum bending strength. The results verify the well-known fact that stiffness is a more global property than bending strength and thus more dependent on density. Thus density can also be a good estimator of wood strength. In analysing the relationships between the ultrasound measurements and other characteristics the general relationship is reliably linear and the results of the longitudinal measurements characterise the most important strength and stiffness properties of wood moderately well (in case of bending strength $r=0.42$ and modulus of elasticity $r=0.61$).

Correlation matrix of characteristics of specimens

Table 2

Characteristics	A, m/s	B, m/s	C, m/s	D, m/s	Max. force, N	Max. bending strength, MPa	MOE, MPa	MC, %	Density, kg/m ³
A, m/s	1								
B, m/s	0.63	1							
C, m/s	0.15	0.27	1						
D, m/s	0.32	0.05	-0.12	1					
Max. force, N	0.09	0.24	0.42	-0.29	1				
Max. bending strength, MPa	0.12	0.25	0.42	-0.25	1.00	1			
Modulus of elasticity, MPa	0.11	0.31	0.61	-0.38	0.72	0.72	1		
Moisture content, %	-0.23	-0.04	0.09	-0.78	0.35	0.31	0.30	1	
Density, kg/m ³	-0.09	0.07	0.40	-0.31	0.50	0.51	0.80	0.16	1

Notes: figures marked grey indicate a moderate relationship ($0.3 \leq |r| \leq 0.7$); figures marked dark grey indicate a strong relationship ($|r| \geq 0.7$).

According to the results of the indirect measurements (A and B) a moderate linear relationship to the modulus of elasticity occurs, the relationships with other characteristics are weak, except with each other, which was moderate ($r=0.63$). In investigating the relationships between the strength and ultrasound velocities Arriaga et al. (2006) found that a weak correlation between them was due to local defects having more influence on the strength than the general quality of the specimens. In that way the acquired results within this research are grounded.

A negative correlation occurs between the moisture content and ultrasound velocity (Bucur, 2006; Oliveira et al., 2005). In analysing the mentioned results within this paper the overall negative correlation is true, especially on the results of the transversal method (D), where there is a strong negative correlation ($r=-0.78$). As the measuring distances become bigger the moisture content also has a decreasing effect.

The correlations between the results of the density and the resistograph were found to be moderate and strong and statistically significant ($p\text{-value} \leq 0.05$) in all groups shown in Table 3. The strongest value was obtained among the group of specimens with fungal and beetle damage. Higher correlations can be explained by the low number on specimen within these groups. Fig. 2 illustrates a moderate, but statistically insignificant correlation ($r = 0,340$; $p = 0,071$) between the bending strength and the time of harvesting. However, it can be concluded, that the strength of wood decreases with increased age of wood. The significant variety of bending strength within the same age can be explained by the variety of damage, knots and location (sap- and heartwood) of specimens sawn out from the material. According to Fig. 3 the internal stress increases with decreasing resistance of wood under compression force. However, due to the low value of the coefficient of determination the internal stress has a weak influence on the resistance of wood. The relationships between the results of Pilodyn and physical-mechanical properties were moderately strong (see Fig. 4 to 5).

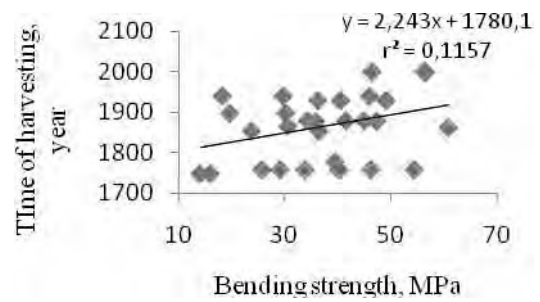


Figure 2. Relationship between bending strength and harvesting time.

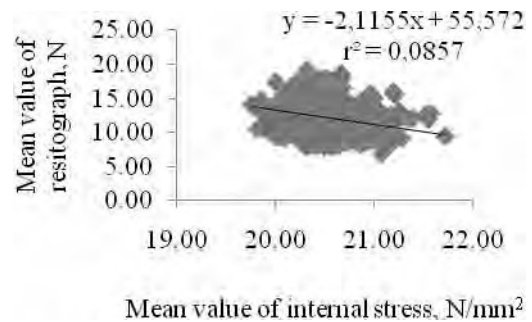


Figure 3. Relationship between resistance drilling and internal stresses.

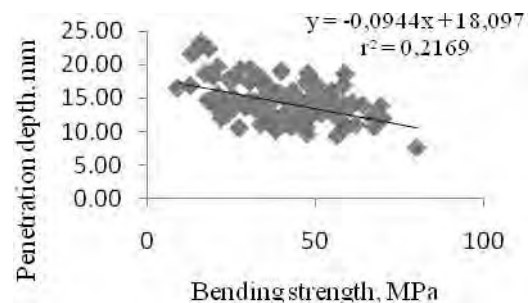


Figure 4. Relationship between penetration depth by Pilodyn and bending strength.

Results of regression analysis of resistograph and density

Table 3

Groups of specimens	Coefficient of correlation r	Coefficient of determination r^2	p-value	Number of specimens
All specimens	0,665	0,442	<0,001	124
Specimens in strength class of C24	0,568	0,322	<0,001	46
Specimens with knots of <250mm ²	0,805	0,649	<0,001	18
Specimens with knots of <1/4 and knot clusters of <1/3	0,614	0,378	<0,001	77
Specimens without cracks and fungal damage	0,733	0,537	<0,001	61
Specimens with fungal and beetle damage	0,850	0,722	<0,001	28

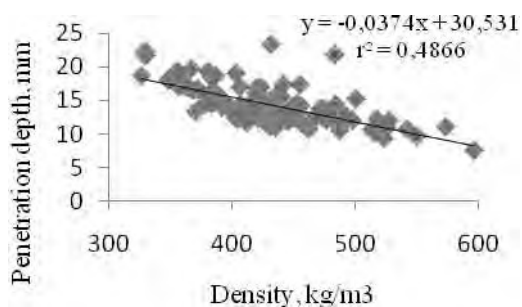


Figure 5. Relationship between penetration depth by Pilodyn and density.

The results concerning the relationship between the density and penetration depth obtained in this study confirm the findings of Görlacher (1987).

CONCLUSIONS

The main aim was to investigate the possibilities of applying some non-destructive measurements in assessment of the physical-mechanical properties of wood. For achieving this purpose series of measurements were done using the *TICO Ultrasound Instrument* with 54 kHz transducers, resistograph Sibtech DmP and Pilodyn devices to assess some characteristics in the wooden specimen. The analysis of ultrasound with different measurement techniques showed that the shorter the measured distance, the more local the evaluation for the wooden member. It turned out that the best arguments in prediction of the physical-mechanical

properties were longitudinal (C) and indirect measurements with a distance of 600 mm (B) within the literature as well as in this study.

The possibilities of using resistance drilling and needle penetration in prediction of the density of wooden members are remarkable. In spite of the low number of specimen the resistograph showed strong relationship within the group of fungi and beetle damage. In comparison of the aforementioned methods both described density with the same accuracy within the total number of specimen.

There can be found mixed results about the influence of the age on the mechanical properties of wood from literature. This study showed moderate, but statistically insignificant correlation between the time of harvesting and bending strength.

The correlation of the drill resistance to the compressive force of the wooden members is negatively weak. Thus, it can be concluded that the resistance of wood does not change significantly while loaded with longitudinal forces.

The assessment of the strength of individual members by the aforementioned methods can always be somewhat imprecise, because of the imperfection of the results of measuring on site. Also, it is essential to note that it is not always possible to measure ultrasound velocities in the longitudinal direction. Therefore, it is essential to continue with the investigation in this field and to search for stronger relationships between indirect and direct measuring methods.

REFERENCES

- Arriaga, F.; Iniguez, G.; Esteban, M.; Fernandez-Golfín, J. I. (2006) *Structural Tali timber: Assessment of strength and stiffness properties using visual and ultrasound methods*. Madrid: Springer-Verlag.
- ASTM 494-89. *Standard practice measuring velocity in materials* (1989).
- Bonamini G. (1995) Restoring timber structures – inspection and evaluation. *STEP/EUROFORTECH*, Vol. 2.
- Bucur, V. (2006) *Acoustics of Wood*. 2nd Edition. Germany: Springer-Verlag. 393 p.
- Bucur, V.; Chivers, R. C. (1991). Acoustic properties and anisotropy of some Australian wood species, *Acustica* 75.
- Drdacky, M. F.; Kloiber, M. (2006) *Non-destructive survey of historic timber*. NSF/MŠMT supported US-Czech project and RILEM Workshop. Czech Republic.
- EN 408 *Timber structures – Structural timber and glued laminated timber – Determination of some physical and mechanical properties*. European Committee for Standardization. Brussels (2005).
- Görlacher R. (1987) Non-destructive testing of wood: an in situ method for determination of density. *Holz as Roh-und Werkstoff*, Vol. 45, p. 273–278.
- Hahnijärvi, A.; Ranta-Manus, A.; Turk, G. (2005) *Potential of strength grading of timber with combined measurement techniques*. Espoo, Finland.
- Haines, D. W.; Leban, J. M.; Herbe, C. (1996) Determination of Young's modulus for spruce, fir and isotropic materials by resonance flexure method with comparison to static flexure and other dynamic methods. *Wood Science and Technology* 30.

ISO 3130:1975 Wood – Determination of moisture content for physical and mechanical tests. International Organization for Standardization. Switzerland, 1975. ISO 3131:1975. Wood – Determination of density for physical and mechanical tests. International Organization for Standardization. Switzerland (1975).

Kasal A., Anthony R. (2004) Advances in situ evaluation of timber structures. *Progress in Structural Engineering and Materials*, Vol. 6, No. 2, p. 94-103.

Kettunen, O. P. (2006). *Wood structure and properties*. Switzerland: Trans Tech Publications Ltd. 401 p.

Kotlina, M.; Kloiber, M.; Vasconcelos, G.; Lourenco, P. J. B. B.; Branco, J. M. G. (2008) *Non-destructive testing of wood*. Portugal.

Lempriere, B. M. (2002) *Ultrasound and elastic waves*. USA: Academic Press. 241 p.

Machado, J.; Palma, P.; Simoes, S. (2009) *Ultrasound indirect method for evaluating clear wood strength and stiffness*. France.

Mishiro, A. (1996) Effect of density on ultrasound velocity in wood. *Mokuzai Gakkaishi*, Vol. 49, No. 9.

Niemz, P. (2009) *Methods of non-destructive wood testing*. Zurich: Institute for Building Materials.

Oliveira, F. G. R.; Candian, M.; Lucchette, F. F.; Salgon, J. L.; Sales, A. (2005) Moisture content effect on ultrasound velocity in *Goupia Glabra*. *Materials Research*.

Pilt K. (2009) Mittepurustavad meetodid puitkonstruktsioonide kestvuse uurimiseks kultuuriväärtuslikes hoonetes. In: *Muinsuskaitse aastaraamat*. Tallinn: Muinsuskaitseamet, p. 78-81.

Tanasoiu, V.; Miclea, C.; Tanasoiu, C. (2002) Non-destructive testing techniques and piezoelectric ultrasounds transducers for wood and built in wooden structures. *Journal of Optoelectronics and Advanced Materials*, Vol. 4.

Tico User Manual. (2008). Proceq SA, Schwerzenbach, Switzerland.

TIME DEPENDING SERVICE LOAD INFLUENCE ON STEEL TOWER VIBRATIONS

Līga Gaile*, Ivars Radinsh**

Rīga Technical University, *Department of Structural Engineering,

Rīga Technical University, *Department of Structural Analysis

liga.gaile_1@bf.rtu.lv, ivarsr@bf.rtu.lv

ABSTRACT

Usually typical steel towers are mainly subject to wind loads. In the case of sightseeing towers with lattice steel structure core and low natural frequency of the structure human and structure interaction could play a role in the tower design. This paper analyses the response of the tower structure to excitation caused by a human movement to assure safe exploitation and acceptable human comfort levels during the exploitation. There are adopted different levels of the structure and human behavior synchronization and its effect on the structure. This phenomenon (synchronization) should be taken into account because people respond naturally to a structure oscillation when the structure has a frequency close to people natural movement frequency. In this paper there are possible mode shapes of the existing 34m high steel core sightseeing tower structure analyzed. The paper gives recommendations of the maximum number of people allowed on the existing structure to ensure safe tower exploitation. The dynamic performance is established through finite element modeling of the tower structure.

Key words: frequency, mode shapes, sightseeing tower, steel tower, synchronization

INTRODUCTION

Lattice steel structures are remarkably flexible, low in damping and light in weight. Traditionally for such type of structures dynamic analyses are performed and dynamic parameters such as fundamental frequencies, mode shapes and damping ratios are found to evaluate wind induced vibrations and effects on the structure. Even most advanced and comprehensive codes concentrate mainly on these issues, including the Eurocodes.

In case of the steel lattice sightseeing towers with low natural frequency of the structure human and structure interaction could play a role in the tower design. Human walking induces dynamic and time varying forces. These forces have components in vertical, lateral and longitudinal directions. The lateral forces are a consequence of the sideway oscillation of the gravity centre of a human's body while stepping alternatively with the right or left foot forwards (Franck, 2009).

The published data on dynamics loads quote that pedestrian vertical and longitudinal walking on stationary pavements fundamental frequency is 2.0 Hz for normal walk, 1.7 Hz for slow walk and 2.3 for fast walk. Horizontal fundamental frequency is 1.0 Hz for normal walk, 0.85 Hz for slow walk and 1.15 for fast walk (Bachman, 1987). In a case of the tower structure there is an interest in the horizontal and longitudinal component of the pacing frequency. Recently, there has been a growing tendency to construct light weight foot bridges. Due to the experienced problems in some of these structures with lateral vibrations there have been

performed studies about phenomenon of synchronous lateral excitation.

It is noted that humans are much more sensitive to lateral vibration than vertical one. Even if horizontal vibration is only 2-3 millimeters lateral motion affects balance and pedestrians tend to walk with their feet further apart which increases the lateral force imparted by individuals. In order to maintain balance, pedestrians tend to synchronize their footsteps with the motion of the structure. This instinctive behavior ensures that dynamic forces are applied at the resonant frequency of the structure and increase the motion even more. As the motion increases also the synchronization between pedestrians increases. It will not go infinitely but reaches a steady state by people stopping when motion becomes too uncomfortable (Fujino et al. 1993). It is presumed that the same processes will take place on sightseeing towers. Wind forces will promote initiation of the lateral motion and because of adaptive nature of the human beings the lateral vibration will have a self excited nature until some point.

Expected lattice sightseeing tower vibrations require limitation to meet the human comfort criteria. The limit values for acceleration in the international codes are directly linked to pedestrian comfort. International standards and sources in literature propose different acceleration limit values for different reasons but most of these values coincide within a certain bandwidth.

Guideline (Heinemeyer, 2009) recommended bandwidths for different comfort levels are presented in Table 1.

Table 1

Acceleration limits	
Degree of comfort	Lateral acceleration limit a_{limit}
Maximum	$<0.1 \text{ m/s}^2$
Medium	$0.1-0.3 \text{ m/s}^2$
Minimum	$0.3-0.8 \text{ m/s}^2$
Unacceptable discomfort	$>0.8 \text{ m/s}^2$

MATERIALS AND METHODS

The present study focuses on the identification whether the particular structure - sightseeing steel lattice tower is at the risk of the harmonic human induced excitation in resonance with natural frequency of the structure. The study looks at the allowable static live load bandwidth to meet the acceleration limits and takes into account possible human and structure synchronization. There are possible mode shapes and corresponding fundamental frequencies of the existing steel core sightseeing tower analyzed. The studied steel core sightseeing tower is located in Dzintari, Jurmala city, Latvia. It is open for public since the 15th of May 2010. The total height of the tower is 36.48m. All elements – the inner and outer core, platforms, and stairs are made of steel except the wooden cladding on the facades of the steel cores. The structural configuration of the tower and its picture is provided in Figure 1. and Figure 2.

The structure consists of a braced inner core with dimensions 1500x1500mm made of tubes with the cross section 200x200x8 and the outer core with dimensions 4240x4240mm made of tubes with the cross section 140x140x5. The outer core does not have any vertical bracing as this was requested by the architectural concept. The inner and outer cores are connected only with steel stairs.

Since the tower was opened for public there have been complaints about tower excessive vibration. The human perception of vibration is very sensitive and the reaction is substantially psychological. Therefore it should be analyzed whether these vibrations are realistic or just perceived by the human visual stimuli. The literature (Heinemeyer, 2009) provides a recommendation whenever fundamental frequencies are close to a critical range (from the point of view of the pedestrian excitation) to use a more precise numerical model, because hand formulas and simplified methods are not enough for assessment of fundamental frequencies. The finite element software is widely spread and accepted as a more precise numerical model. To evaluate the degree of vibration there were fundamental frequencies and critical mode shapes of the existing tower established using three dimensional finite element models created by structural analysis software STRAP 12.5.



Figure 1. Sightseeing tower in Dzintari.

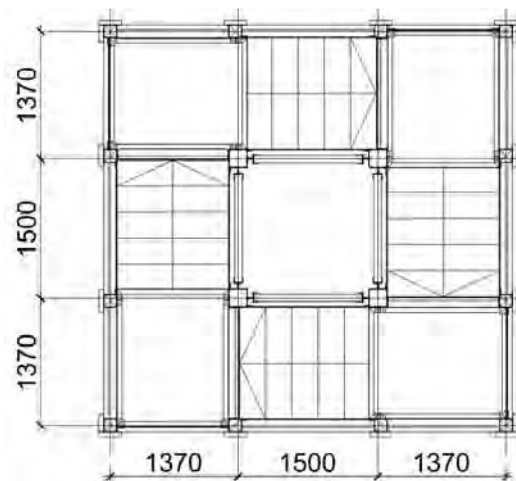


Figure 2. Plan of the sightseeing tower in Dzintari

The fundamental frequency and mode shapes of the structural system can be determined by solving undamped free vibration equation (1) (MacLeod I., 2005):

$$K \phi = M \phi \Omega^2 \quad (1)$$

where K – stiffness matrix;

M – mass matrix;

Φ – corresponding eigenvector matrix;

Ω – eigenvalue matrix.

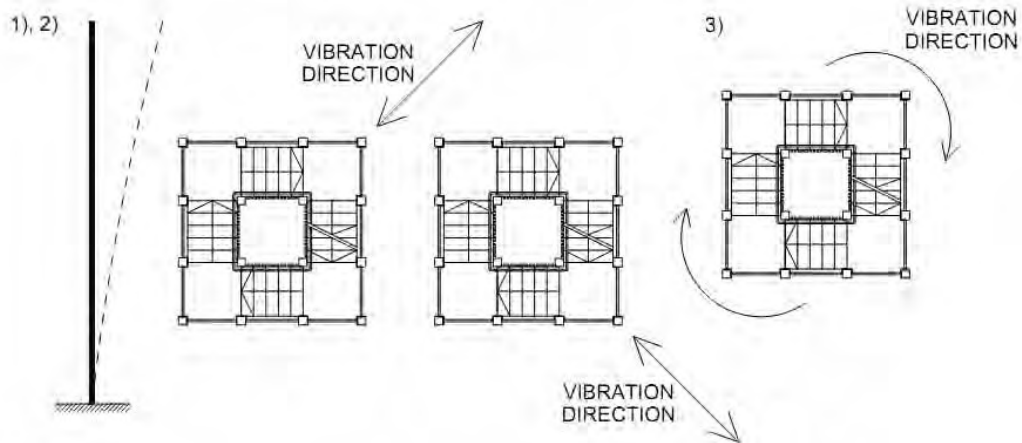


Figure 4. Mode shapes,
where 1), 2) first and second mode shape and vibration directions accordingly;
3) third mode shape vibration direction.

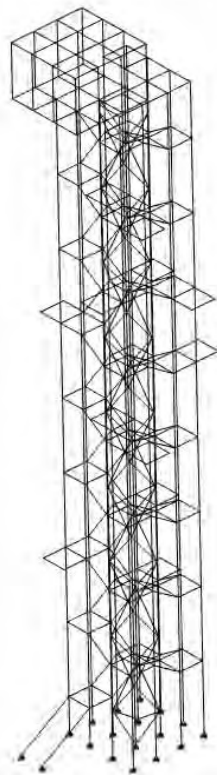


Figure 3. FE model of the tower.

For extraction of eigenvalues the structural analysis software uses the subspace iteration technique. The created finite element (FE) model is presented in Figure 3. and the first three critical mode shapes for the structure are presented in Figure 4.

There is a necessity to evaluate the influence of the static sightseers' mass on the tower natural frequency because natural frequencies of the structure decrease due to a live load and could shift into the critical frequency range or could leave it.

In literature (Heinemeyer, 2009) it can be found that the critical interval of $0,5\text{Hz} \leq f_i \leq 1,2\text{Hz}$ for the lateral vibrations and critical range for longitudinal ones is $0,5\text{Hz} \leq f_i \leq 1,2\text{Hz}$, where f_i is natural frequency of the structure. In the tower case the longitudinal component corresponds to the tower torsional mode. The critical range of natural frequencies is based on empirical pedestrians on the flat surface. In this paper it is assumed that similar range will be present for the pedestrian movement on the stairs. But more careful investigation is required as this matter has not been found in literature.

To evaluate acceleration of the tower there is adapted a recommended method in literature (Heinemeyer, 2009) and adjusted to suite the tower case. If harmonic load ($F_0 \sin(2\pi f_0 t)$) is applied to a damped single degree of freedom system, the response of the system would be:

$$x(t) = \frac{F_0/4\pi^2 M}{\sqrt{(f^2 - f_0^2)^2 + 4\xi^2 f^2 f_0^2}} \sin(2\pi f_0 t - \varphi) \quad (1)$$

where F_0 – amplitude of the lateral load, N;
 M – system mass, kg;
 f – system natural frequency, Hz;
 f_0 – load frequency, Hz;
 ξ – structural damping ratio;

$$\varphi = \arctan\left(\frac{2\xi f f_0}{f^2 - f_0^2}\right)$$

From the results obtained by Arup Partnership in the experiment with a shaking table (Newland, 2003) and given by Dallard, 2001 and Fitzpatrick, 2001 amplitude of the lateral load is taken as

percentage of the vertical live load and depending on the lateral amplitude of the tower vibration (3). It is observed that the fundamental component of the lateral force increases with the platform amplitude but remains insensitive to the lateral frequency of the structure:

$$H_0 = 0,2A + 4 \quad (3)$$

where H_0 – lateral force/vertical force, %;
 A – tower vibration amplitude, mm.

Let us model a lattice tower as a cantilever with one degree of freedom and apply amplitude of the horizontal load at the cantilever tip. The equivalent mass applied at the cantilever tip from the tower mass and pedestrian live load uniformly distributed over the height of tower can be obtained by taking approximately one fourth of the total mass of the beam at the free end (Thompson, 2007). Then by approximate methods such as the Rayleigh's method or the Dunkerley's formula approximate equivalent mass of cantilever is found applying formula:

$$m = \frac{33m_b}{140} \quad (4)$$

where m_b – uniformly distributed mass, kg.

To analyze the effect on the structure from the pedestrian synchronization there is considered the first translational mode shape. There is analyzed one of the critical directions of the tower vibration. Applied horizontal live load component is taken as a half of the total equivalent horizontal force taking into account the degree of the synchronization effect. In this paper it is assumed that the sightseers' stream is up and down the same. There is considered only lateral force component influence on the tower vibration.

The loading created by pedestrians' is much more complex in the sightseeing towers than in the case of the bridges. Not only transverse loading should be considered but also longitudinal loading. Horizontal and vertical load component value should be determined as well for pedestrian movement on stairs. This issue will be addressed in a separate study, but for now the Eurocode approach is used for the tower vibration calculations.

During the synchronization process pedestrians adopt the same pacing frequency as natural frequency of the tower. The response of the system (1) becomes:

$$x(t) = \frac{F_0}{8\pi^2 M \xi f^2} \sin(2\pi f t - \frac{\pi}{2}) \quad (5)$$

where F_0 – amplitude of the lateral load, N;
 M – system mass, kg;
 f – system natural frequency, Hz;
 ξ – structural damping ratio.

According to the recommendations of the Eurocode (Eurocode, 2005) the damping ratio ξ for the steel lattice tower with ordinary bolts is 0.05.

Displacement of the tower tip can be found from equation (5):

$$y(t) = x(t)\Phi \quad (6)$$

where $y(t)$ – vector of the movement of concentrated mass;

$x(t)$ – response of the system;

Φ – vector of modal displacement at the tip of the cantilever.

Then human comfort criteria – acceleration at the tip of the tower for the first translational mode shape can be found from equation (7):

$$y''(t) = -\frac{F_0}{2M\xi} \sin(2\pi f t - \frac{\pi}{2}) \quad (7)$$

where F_0 – amplitude of the lateral load, N;

M – system mass, kg;

f – system natural frequency, Hz;

ξ – structural damping ratio.

RESULTS AND DISCUSSION

The determined natural frequencies of the sightseeing tower for the first two mode shapes were just outside the critical frequency range of $0.5\text{Hz} \leq f_i \leq 1.2\text{Hz}$ and equal to 1.26Hz and 1.3Hz for translational mode shapes.

For the torsional mode shape the tower is already in the critical range of $1.25\text{Hz} \leq f_i \leq 2.3\text{Hz}$. This means that the sightseers' live load should be taken into account for the tower natural frequency determination. In Figure 5 the natural frequency dependence on the additional sightseers' live load is presented.

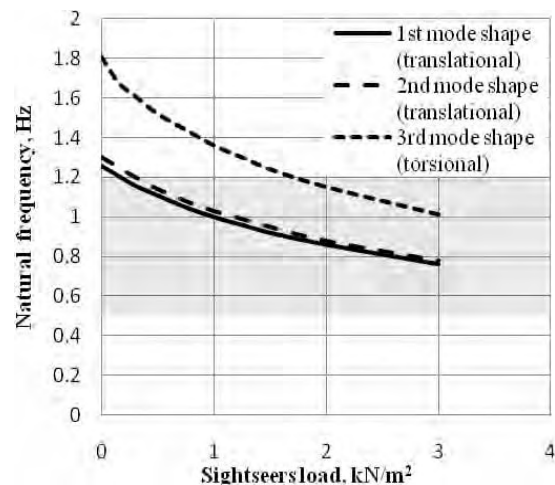


Figure 5. Calculated natural frequencies of the tower as a function of the applied live load.

The chart shows that the visitors' movement up and down the tower may induce vibration combined in torsional and translational directions. When the live load increases torsional vibration gets less frequent and leaves critical range when the live load is around 1.7Hz, which is a significant amount of people on the tower.

It should be mentioned that the accidental situation - intentional tower swaying was not analysed.

"Fujino et al. (1993) estimated from the video recordings of crowd movement that some 20% or more of pedestrians on the bridge were walking in synchronism with the bridge's lateral vibration which had a frequency of about 0.9Hz and amplitude of 10mm" (Newland, 2003).

A similar process of tower sightseers' synchronization is assumed to happen, because it is natural for humans to compensate additional lateral movement of their centre of gravity by swaying with the structure displacement. The initial amplitude of 10mm is 1/3350 of the sightseeing tower deflection and can be easily initiated by wind forces.

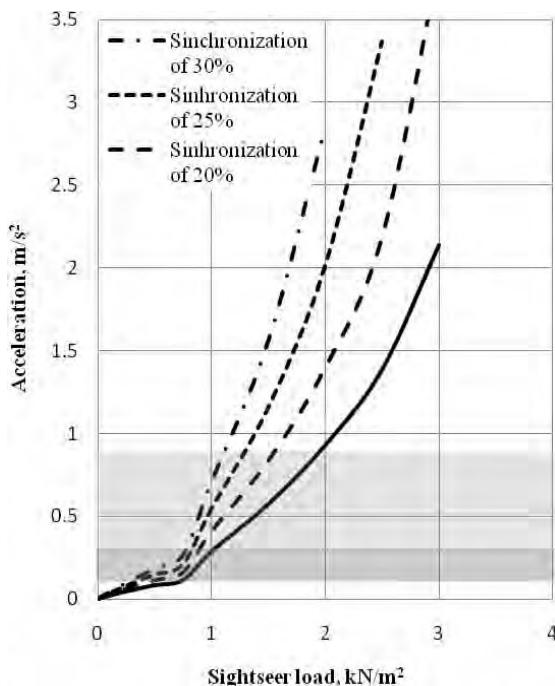


Figure 6. Maximum resonance acceleration.

In this study the range of sightseers' synchronisation has been taken from 15% to 30%. Initiated acceleration from this phenomenon is presented in Figure 6.

During sightseers' synchronization with the structure their step frequency matches to the tower natural frequency. The calculated resonance maximum acceleration is presented in Figure 6, and shows that the medium comfort level for tower visitors is when the sightseers' stream does not exceed 0.75kN/m^2 . It corresponds to 180 sightseers with mean weight of 75kg.

When higher live load and degree of synchronization is presented the acceleration increases to unacceptable level. If 15% of synchronization occurs the allowable live load will be almost 2kN/m^2 till unacceptable level is reached in comparison with synchronization level of 30% when unacceptable level will be reached with $1,2\text{kN/m}^2$ live load.

CONCLUSIONS

According to analytical calculations of the existing 34m high steel lattice sightseeing tower dynamic performance is susceptible to the human induced vibrations. It is concluded that for steel lattice tower type structures with natural frequencies close to the lateral pacing frequency it is important to take into account the potential live load in the tower modal mass calculations. The existing sightseeing tower in Dzintari has critical natural frequency for the torsional mode shape. Therefore, even a relatively light live load induces tower vibrations created by the sightseers' pacing force longitudinal component. More increase of live load adds transversional vibrations created by the sightseers' pacing force horizontal component and depends on the degree of sightseers' synchronization. There is a necessity for further research to evaluate the degree of human synchronization effect during the tower type structure exploitation. The recommended maximum allowable live load to meet medium degree of the comfort level for the tower visitors is 135kN in respect to tower transversional vibrations. In this study there have not the resonance accelerations for the torsional vibration mode been calculated which could further limit the maximum live load.

REFERENCES

- Bachman H., Ammann W. (1987). Vibration in Structures Induced by Man and Machines. Structural Engineering Document 3e. *International Association for Bridge and Structural Engineering (IABSE)*, ch. 2: Man Induced Vibrations, Appendix A: Case Reports.
- Dallard P., Fitzpatrick T. Flint A., Low A., Smith R. R., Willford M., Roche M. (2001). London Millenium Bridge: Pedestrian – Induced Lateral Vibration. *Journal of Bridge Engineering*, No. 6, p. 412-417.
- Franck L. (2009) *Synchronous Lateral Excitation of Footbridges*. Swiss: Swiss Federal Institute of Technology. 5 p.

Fujino Y., Pacheco B., Nakamura S., Warnitchai P.(1993). Synchronization of human walking observed during lateral vibration of human walking observed during lateral vibration of a congested pedestrian bridge. *Earthquake Engineering and Structural Dynamic* , No. 22, p. 741-758.

Heinemeyer C., Butz C., Keil A. et al., (2009) *Design of Lightweight Footbridges for Human Induced Vibrations*. Luxembourg: *Office for Official Publications of the European Communities*. 15 p.

MacLeod I. A. (2005). *Modern Structural analysis. Modeling Process and Guidance*, p. 138-139.

Newland D. E. (2003). Pedestrian Excitation of Bridges recent Results. *Tenth International Congress on Sound and Vibration*. p. 4-5.

Research Fund for Coal and Steel. Human induced Vibrations of Steel Structures. Design of Footbridges. Background Document. RFS2-CT-2007-00033, 2007, p. 5-6, 12.

IMPLEMENTATION OF EUROCODE STANDARDS IN LATVIA

Andris Steinerts*, Leonids Pakrastinsh, Liga Gaile****

*Latvia University of Agriculture, Department of Architecture and Building

**Riga Technical University, Department of Structural Engineering

andris.steinerts@llu.lv; leonids.pakrastins@rtu.lv; smgprojects@inbox.lv

ABSTRACT

History and the current situation of implementation of Eurocode in Latvia is analyzed. Short information regarding collaboration with Deutsches Institut für Bautechnik (German Institute of Construction Technology) and about the results of the Twinning project LV/2005-IB/EC/01 financed by the European Transition facilities funds is given. On examples of application of Eurocode 0 and Eurocode 6 some essential differences are analyzed which have to be considered by the responsible Technical committees for standardization when discussing the values of Nationally determined parameters (NDP).

Key words: Implementation of Eurocode, partial factors, verification of Eurocode and Latvian Building codes and SNiP

INTRODUCTION

Despite of the difficult economic situation in Latvia, the implementation of Eurocode standards according to the Recommendations 2003/887/EEC of the EU Commission from December the 12th of 2003 is proceeding. The Latvian Eurocode National Implementation plan for 2008-2011 was accepted by the Cabinet of Ministers in July, 2008 (Decree No.455 from July the 29th, 2008). Having regard of European Harmonization trends, as well as the fact, that for Latvia it would be not easy or even impossible to develop its own and independent National Building Regulation system, Latvia should be interested in the development of harmonized Normative Base of European Economic area, such as it is developed in the standardization area.

PROGRESS IN IMPLEMENTATION

Transition period

It was planned, that till the end of 2009 there will be withdrawn or amended Latvian Building codes (LBN), which regulate the procedure of structural design and are based on the principles taken from the former Soviet SNiP system, wherewith construction design in Latvia will be allowed only according to the requirements of Eurocode standards. It is a serious task not only for the state governmental institutions – the Building department of the Ministry of Economics and the Latvian standardization system in the person of the Technical Committee for Standardization LVS/STK 30 “Construction” as well as for the structural designers and both universities – the Riga Technical University and the Latvia University of Agriculture that are training civil engineers and structural designers.

The transition to application of the Eurocode standard system in Latvia is effected in two phases.

The first step was already taken by adopting LNB 214-03 “Geotechnics. Pile foundations and sub base” and by adoption of amendments to LNB 207-01 “Geotechnics. Construction foundations and sub base” and LNB 003-01 “Building climatology”.

According to the first phase of the National Implementation plan, amendments were made to the Latvian Building codes, by which the transition period of structural design of relevant structures started. During this transition period dual approach is on place - it is allowed for structural designers to apply either approved in the end of the nineties of the last century LBNs or apply the Eurocode standards. Referring to steel structures the new Building codes should replace the former Soviet SNiP codes. At the end of the transition period the Eurocode system as the only method should be used for the structural design of buildings and bridges in Latvia. The amendments for the following Latvian Building codes LBN 203-97; LBN 205-97; LBN 206-99, LBN 207-01 and LBN 214-03 were announced at the end of 2007 and beginning of 2008.

Current situation

Currently all Eurocode basic standards have been adapted as Latvian National standards. 26 of them are translated in Latvian. To 16 Eurocodes Latvian National annexes are elaborated. For other Eurocode standards Latvian Building codes prescribe to use the recommended values of Nationally determined parameters.

Due to emergency with the state budget and lack of financing on September the 30th, 2009 the Decree of the Cabinet of Ministers No.455 was amended and some activities of implementation were reduced. Nevertheless, in October of 2010 the subcommittee of the “Eurocodes” was established at the LVS/TC 30 “Construction”. The main tasks for this

subcommittee are drafting of National annexes to the Eurocode standards as well as revision of Latvian texts of some translated earlier Eurocode standards.

Problems

Serious problems shall be encountered preparing the National Annexes to EN 1993 "Design of steel structures" and EN 1997 group of standards "Geotechnical design".

Eurocode 7 standards are general and in numerous cases allow application of national design and testing methods. The national annexes to the above standards shall be drafted in parallel with the amendments to the Latvian Building codes LNB 207-01 and LNB 214-03 that shall remain in force with slight amendments after implementation of the Eurocode standards. It means that the Geotechnical Eurocode (EN 1997) shall be used together with the National Annex and the above mentioned LBN.

The problem with Eurocode 3 and Eurocode 9 is in consideration that there are not acting Latvian Building codes on design of steel and alumina structures. There are still former Soviet SNiPs in use parallel to the relevant Eurocode standards. Due to lack of financing the planned LBN 204 "Design of steel structures" is not elaborated.

COMPARISON OF LBN AND EUROCODE APPROACH

Transition from the national building codes LBN to the Eurocode will cause no conceptual problems in Latvia as both are based on the limit state method. The difference is in more detailed partial factors method and reference period of loads. In LBN system and in SNiP system being used in the former Soviet Union the reference period is 5 or 10 years but in the Eurocode – 50 years.

Therefore, the nationally determined parameters (NDP) shall be adjusted. For the determination of NDP EU Member States may consider their existing design practice and design rules in order to maintain their traditional level of safety.

Latvia as a Member State has the advantage that the partial safety factor system for the design of structures was already in use since many years by using SNiPs during the Soviet occupation time and inherited after in LBNs.

The disadvantage, however, is that the existing LBN system is not exactly fitting to the Eurocode partial factor system what makes the adoption of the LBN system to the new one somewhat difficult. In the following there are given some essential differences which have to be considered in the process of adaption of Eurocodes when discussing the values of NDPs at the responsible technical committees.

Examples

According to formula (6.10) of EN 1990:21002 the design value of the effect of actions is to be determined by the expression for the load combination for permanent and accompanying variable situations:

$$E_d = E \left\{ \sum_{j \geq 1} \gamma_{G,j} \cdot G_{k,j} + \gamma_{Q,1} \cdot Q_{k,1} + \sum_{i \geq 1} \gamma_{Q,i} \cdot \psi_{0,i} Q_{k,i} \right\}$$

If the recommended values for ψ_0 are taken from table A1.1, e.g.: $\psi_0 = 0,7$ (for non storage areas) and the recommended values for γ_G and γ_Q from table A1.2(A), NOTE 2: $\gamma_G = 1,35$; $\gamma_Q = 1,5$

The equation reads:

$$E_d = E \left\{ \sum_{j \geq 1} 1,35 G_{k,j} + 1,5 \cdot Q_{k,1} + \sum_{i \geq 1} 1,5 \cdot 0,7 \cdot Q_{k,i} \right\} \quad (1)$$

Verification

Since the design value of the effect of actions must be less than or equal to the design value of the resistance which is the characteristic value of the resistance divided by the partial factor for material properties γ_M

$$E_d \leq R_d ; \quad R_d = \frac{R_k}{\gamma_M}$$

the verification equation can be expressed as

$$E_d \leq \frac{R_k}{\gamma_M}$$

where:

E_d - design value of the effect of actions such as internal force, moment or a vector representing several internal forces or moments;

R_d - design value of the corresponding resistance.

R_k - characteristic value of the corresponding resistance.

According to EN 1996-1-1:

The factor γ_M is taken from the table in paragraph 2.4.3 of EN 1996-1-1 (the lowest value is: $\gamma_M = 1.5$ for material A and class 1, the highest one is: $\gamma_M = 3.0$ for material C and class 5)

The verification equation then reads:

$$E_d \leq \frac{R_k}{1,5 - > 3} \quad (2)$$

According to LBN or SNiP 2.01.07-85, paragraphs 1.10 to 1.13 there are verification equations for four cases.

Basic combination - load combination for permanent and accompanying variable situations

$$E_d = E \left\{ \psi_G \cdot \sum_{j \geq 1} \gamma_{G,j} \cdot G_{k,j} + \sum_{i > 1} \gamma_{Q,i} \cdot \psi_{Q,i} \cdot Q_{k,i} \right\} \quad (3)$$

$\psi_G = 1,0$ for permanent loads;

$\psi_{Q,i} = 0,9$ (0,95) for continuous (transient) imposed loads.

If only one life load is acting:

$$E_d = E \left\{ \psi_G \sum_{j \geq 1} \gamma_{G,j} \cdot G_{k,j} + \psi_{Q,1} \cdot \gamma_{Q,1} \cdot Q_{k,1} \right\} \quad (4)$$

$\psi_G = 1,0$ for permanent loads;

$\psi_{Q,1} = 1,0$ for imposed loads.

In case of additional load combination when three and more imposed loads will be considered:

$$E_d = E \left\{ \psi_G \sum_{j \geq 1} \gamma_{G,j} \cdot G_{k,j} + \sum_{i > 1} \gamma_{Q,i} \cdot \psi_{Q,i} \cdot Q_{k,i} \right\} \quad (5)$$

$\psi_G = 1,0$ for permanent loads;

$\psi_{Q,1} = 1,0$ for the first imposed load;

$\psi_{Q,2} = 0,8$ for the second load;

$\psi_{Q,j} = 0,6$ for all other loads.

In case of specific load combination:

$$E_d = E \left\{ \psi_G \sum_{j \geq 1} \gamma_{G,j} \cdot G_{k,j} + \sum_{i > 1} \gamma_{Q,i} \cdot \psi_{Q,i} \cdot Q_{k,i} \right\} \quad (6)$$

$\psi_G = 1,0$ for permanent loads;

$\psi_{Q,1} = 0,95$ (0,8) for continuous (transient) imposed loads.

The verification equation is based on SNiP II-22-81 table 14, $\gamma_M = 2,0$:

$$E_d \leq \frac{R_u}{2,0} \quad (7)$$

R_u in SNiP corresponds to R_k in Eurocode 0.

Recommendations for partial factors in National annex to LVS EN 1990

For comparison of safety levels both sides of the verification equation, loads and actions as well as the resistance, have to be considered.

The Eurocode en 1990 for actions distinguishes only between permanent actions: dead loads and variable actions: life loads. The Latvian Building code (SNiP) sets also different partial factors for different materials and the way of production: on site or prefabricated.

In the following tables the recommended partial combination and safety factors of EN 1990 for actions are compared with the Latvian code.

Table 1
National choice Design values of actions

Latvian code/former Soviet code SNiP 2.01.07-85 (Table 1)		EN 1990 Recommended values	
Permanent actions			
Dead load	γ_f	Dead load	1,35
Metal (steel)	1,05		
Concrete, masonry, wood etc.	1,1		
Layers, pre fabricated	1,2		
Layers, made on site	1,3		
Accompanying Variable actions			
Life load	γ_f	Life load incl. snow, wind etc.	1,5
< 2,0 kN/m ²	1,3		
≥ 2,0 kN/m ²	1,2		
Snow loads	1,4		
Return period 10 years			
Wind load	1,4		
Return period 5 years	(1,6)		

$$E_d = E \left\{ \sum_{j \geq 1} \gamma_{G,j} \cdot G_{k,j} + \gamma_{Q,1} \cdot Q_{k,1} + \sum_{i > 1} \gamma_{Q,i} \cdot \psi_{0,i} \cdot Q_{k,i} \right\}$$

Table 2
Basic load combination factors for permanent and accompanying variable situation according to EN 1990 (Table A1.1)

Action	ψ_0
Imposed loads in buildings	0,7
Snow loads on buildings (see EN 1991-1-3)	0,7(-0,5)
Wind loads on buildings (see EN 1991-1-4)	0,6
Temperature (non-fire) in buildings (see EN 1991-1-5)	0,6

The table is not complete (excerpt).

Comparison of both methods

The given situation is to design the same building with the same loads (LBN 003 /LBN 004) by using loads according to SNiP and EC 0.

For a qualitative comparison the expressions for only one life load (< 2,0 kN/m² for LBN) are

chosen:

$$E_d = E \left\{ \sum_{j \geq 1} \gamma_{G,j} \cdot G_{k,j} + \gamma_{Q,1} \cdot Q_{k,1} \right\} \quad (4)$$

with $\gamma_G = 1,1$ and $\gamma_Q = 1,3$ according to LBN (SNIp).

$$E_d = E \left\{ \sum_{j \geq 1} 1,1 \cdot G_{k,j} + 1,3 \cdot Q_{k,1} \right\} \quad (4a)$$

and

$$E_d = E \left\{ \sum_{j \geq 1} 1,35 \cdot G_{k,j} + 1,5 \cdot Q_{k,1} \right\} \quad (1a)$$

according to EN 1990.

By comparison of expression (7) with (2) the resistance is for LBN (SNIp):

$$R_d = \frac{R_u}{2,0} \leq E \left\{ \sum_{j \geq 1} 1,1 \cdot G_{k,j} + 1,3 \cdot Q_{k,1} \right\}$$

for EN 1990.

$$R_d = \frac{R_k}{(1,5 \div 3,0)} \leq E \left\{ \sum_{j \geq 1} 1,35 \cdot G_{k,j} + 1,5 \cdot Q_{k,1} \right\}$$

or for LBN (SNIp)

$$R_u \geq E \left\{ \sum_{j \geq 1} 2,2 \cdot G_{k,j} + 2,6 \cdot Q_{k,1} \right\}$$

for EC 1990.

$$R_k \geq E \left\{ \sum_{j \geq 1} 2,03 \cdot G_{k,j} + 2,25 \cdot Q_{k,1} \right\} \quad \text{with}$$

$$\gamma_M = 1.5.$$

That means that even for this simple case and for the same loads it is not possible to state in general that the one or the other verification is safer or more or less economic because the result depends on the ratio of life load and dead load. For this purpose the design has to be performed in any case.

Taking into account that in the case of SNIp the basic information on the statistical evaluation is not

available and that the return period for snow loads is 10 years instead of 50 years in the Eurocode design and for wind loads 5 years instead of also 50 years it is proposed to take the recommended values for ψ and γ from EC 0 and EC 6 for the National Annex of Latvia.

INTERNATIONAL COOPERATION

A serious step in implementation of Eurocodes was the Twinning project LV/2005-IB/EC/01 financed by the European Transition facilities funds. The Project was put into effect in June 2006 and carried out by one of the leading European applied research institutions – Deutsches Institut für Bautechnik (German Institute of Construction Technology). The project included training of Latvian experts by the leading German experts, preparation of methodical booklets and drafting of the first national annexes to the Eurocode standards.

The next step was training of the Latvian structural designers by the Latvian experts trained by the German experts. Next practical trainings built on lectures prepared by the Latvian experts for Latvian structural designers took place. Detailed information about results of this Project is available on www.em.gov.lv → Darbības jomas → Būvniecība → Noderīgi → Eirokodeksa standartu ieviešana.

CONCLUSIONS

Despite of the difficult economic situation in Latvia, the implementation of Eurocode standards according to the Latvian Eurocode National Implementation plan and the Recommendations 2003/887/EEC of the EU Commission form December the 12th of 2003 with some delay is proceeding.

A serious step in implementation of Eurocodes was the Twinning project LV/2005-IB/EC/01 financed by the European Transition facilities funds.

The Latvian Building codes of structural design (and SNIp) are not exactly fitting to the Eurocode partial factor system what makes the adoption of the Eurocode somewhat difficult in sense of designation of NDP and elaboration of National annexes.

REFERENCES

- SNIp 2.01.07-85 – Нагрузки и воздействия [Construction norms and regulations “Loads and actions”] (1988), Москва.
- SNIp II-22-81 – Каменные и армокаменные конструкции [Construction norms and regulations “Masonry and reinforced masonry structures”] (1983) Москва.
- Eirokodeksa standartu nacionālais ieviešanas plāns, Ministru kabineta 2008.gada 2008.gada 29.jūlija rīkojums Nr.455 Available: <http://www.em.gov.lv>
- Eirokodeksa standartu ieviešana būvkonstrukciju projektēšanas praksē Latvijā – Presentations of the results of the Twinning project LV/2005-IB/EC/01 “Implementation of Eurocode standards in structural design practice in Latvia”. Available: <http://www.em.gov.lv>

BEHAVIOUR OF COLD-FORMED Z-SHAPED STEEL PURLIN IN FIRE

Wei Lu*, Pentti Mäkeläinen*, Jyri Outinen**

*Department of Civil and Structural Engineering
Aalto University, Espoo, Finland

Wei.Lu@tkk.fi, Pentti.Makelainen@aalto.fi

**Ruukki Construction

Rautaruukki Oyj., Vantaa, Finland

Jyri.Outinen@ruukki.com

ABSTRACT

Great deals of researches on steel beams in steel framed structures have indicated that a steel beam can have a substantial fire resistance in catenary action at large deformation. However, few researches are available for investigating the behaviour of cold-formed steel purlin in fire. A 3D finite element model incorporating both geometric and material non-linearity is created to investigate the behaviour of cold-formed Z-shaped steel purlin in fire. It has been shown that due to the thinness of the material and degradation of the material properties at elevated temperature, the profile buckles locally under restrained thermal expansion in early stage. In the large deformation, tensile forces developed in steel purlins to resist the transversely applied load. The steel purlin can survive in fire via catenary action. Comparing to one-span purlin, two-span purlins have less in-web-plane deformation due to the capability of mid-support but with larger out-of-web-plane deformation due to the sudden lateral-torsional buckling. The earlier inelastic buckling at two end supports in one-span purlin actually helps reduce the compressive forces developed due to restrained thermal expansion. However, the maximum axial tension forces developed at the supports are the same for both one-span and two-span purlins.

Key words: cold-formed steel, Z-shaped purlin, structural fire design, catenary action, FE modelling

INTRODUCTION

Traditionally, the resistance of steel beam in fire is calculated according to flexural bending behaviour with small deflection and without considering the effects of end axial restraints. This practice of evaluating fire resistance of the beam is based on standard fire tests on a simply supported individual beam. In real structure, the surrounding members restrain the beam both axially and rotationally. With the presence of axial constraints, the beam will behave in catenary action at large deflection stage. The catenary action is a load carrying mechanism where the bending moment capacity of the beam is negligible but the beam will still be able to resist the applied transversal load with the tension force developed in the beam via further deflection even with reduced material strength (Usmari et al., 2001, Yin and Wang, 2004, Wong, 2005, Wang and Yin, 2006). If large deflection is acceptable in practice, the fire protection might be unnecessary or reduced. Cold-formed steel purlins have been widely used in industrial buildings to act both as a secondary beam to support the roof sheeting and as the bracing member to stabilize the main frame structure. Currently, few researches have been available on the investigation of the behaviour of cold-formed steel purlin in fire. In this paper, a 3D finite element model incorporating both geometric and material non-linearities is created to investigate the behaviour of cold-formed Z-shaped steel purlin in

fire. The model has been used to understand the failure mechanism of the purlin and further to investigate the effect of the number of spans on the behaviour of the purlin.

FINITE ELEMENT MODELLING

Geometry

The roof construction with a lightweight purlin in this research is composed of a Z-shaped purlin and a sandwich panel. The sandwich panel is connected to the top flange of the purlin with a roof screw at panel crest. The purlin is bolted to U-shaped steel consoles, which are in turn welded to the supporting members. The structural details of sandwich-purlin systems and its connections to the supporting truss are shown in Fig. 1. The dimensions of Z-shaped steel purlin and U-shaped steel console are shown in Fig. 2.

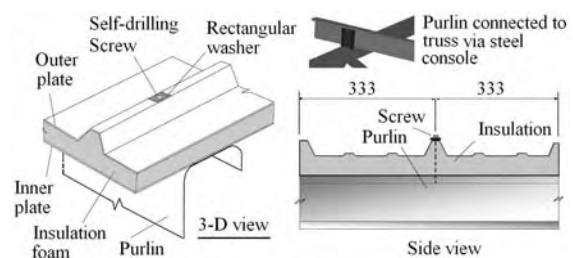


Figure 1. Crest-fixed sandwich-purlin systems.

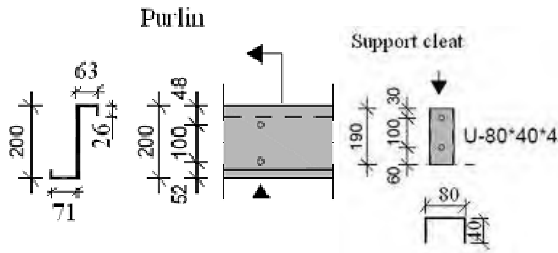


Figure 2. Dimensions of purlin and steel console.

The thickness of purlin is 2 mm and the span length of the purlin is 6 m. The distance between the screw connectors is 333 mm.

Three FE models have been created according to the number of span and heating conditions as shown in Table 1. Model 1Span is the model for one span purlin exposed to fire; Model 2Span2Heat is the model for two-span purlin and both spans exposed to fire; and Model 2Span1Heat is the model for two-span purlin but with only one span exposed to fire.

Table 1

Models	FE models	
	Heating span	Span no.
1Span	1	
2Span2Heat	2	
2Span1Heat	1	

FE meshes

Fig. 3 shows the FE model of a single span sandwich purlin system. The model is composed of steel purlin, steel console and steel sheeting, which is used to simulate the inner plate of the sandwich panel. Commercial FE software, ABAQUS/Explicit (2009), is used as an analysis tool. The quasi-static analysis procedure was adopted. Thin shell elements with reduced integration S4R are used to model purlin, steel sheeting and steel consoles. Three dimensional connector elements with 2 nodes (CONN3D2) are used to simulate the connections between the sheeting and purlin, and between the purlin and steel consoles. The connection-type of the connector elements according to ABAQUS is a BEAM, which provides a rigid beam connection between two connected nodes, and imposes kinematic constraints. The general contacts have been defined among the contact surfaces in the whole FE models.

Material properties

The steel grades of steel purlin and steel sheeting are both S350GD+Z. The stress-strain curves at elevated temperatures without strain hardening given in EN 1993-1-2 (2005) have been used and

have been transformed to true stress and true strain curves. The reduction factors for yield strength at elevated temperature are taken from EN 1993-1-2 Annex E and reduction factors for modulus of elasticity are taken from the main text of EN 1993-1-2. It is assumed that the material properties of the console steel are not affected by the increasing of temperature. The steel grade of the steel console is S355. Thermal elongation of steel at high temperature is defined as stated in EN 1993-1-2. Density of steel is 7850 kg/m³ and modulus of elasticity is 210 000 N/mm².

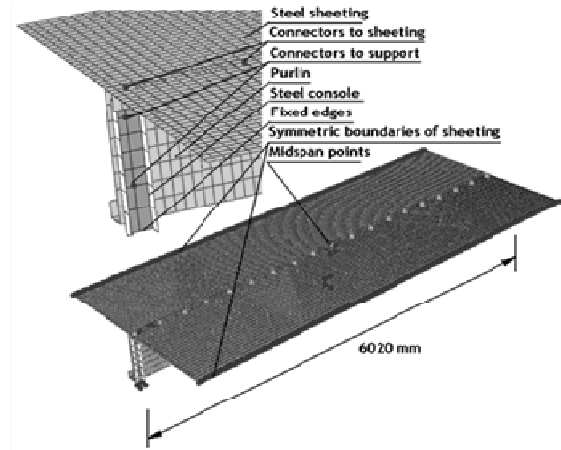


Figure 3. FE-modelling of single span purlin.

Loading and boundary conditions

The two-step analysis is carried out, in which the mechanical loading (0.73 kN/m²) was applied first (step 1) and then the temperatures were increased according to the nominal fire curve (step 2). It is assumed that in the models, the temperatures are uniform in steel purlin and steel sheeting. In FE models two steel consoles are clamped along the welded edges, and along span length the symmetric boundary conditions are defined for steel sheeting (Fig.3). Two types of outputs are required from FE models, i.e., the displacements of the given nodes of the cross-section at mid span, and the reaction forces at the fixed edges of the steel consoles (Fig.4).

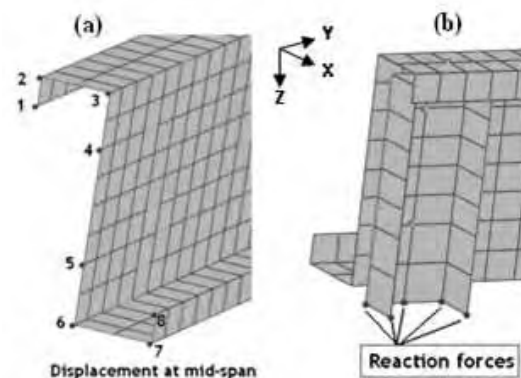


Figure 4. Output details in FE model.

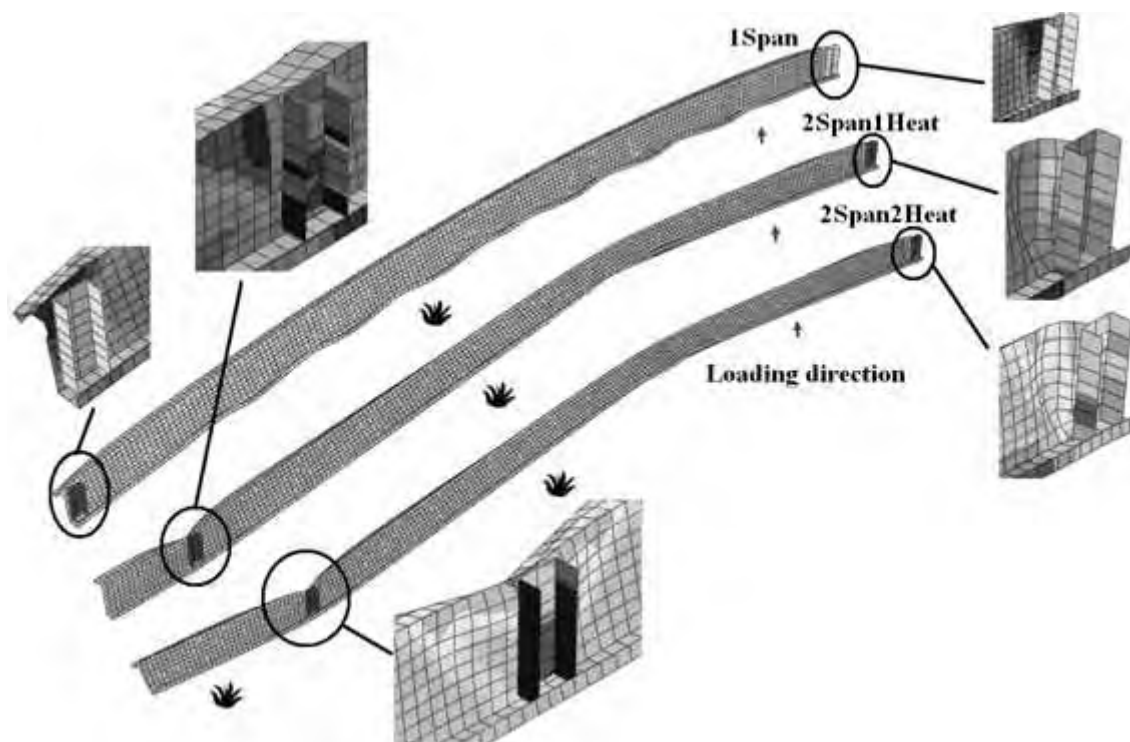


Figure 5. Deformed shapes of purlin systems.

ANALYSES OF FE RESULTS

Deformed shape

Fig. 5 shows the deformed shapes of purlin systems at 603 °C for three models respectively. For Model 1Span, multiple-wave local buckling of the purlin lip located at the loading side has been observed. This is the result of the joint influences of both the compression forces coming from the restrained thermal expansion and the mechanical loading applied to purlin via steel sheeting. For Model 2Span1Heat, local buckling of the purlin lip is first observed at the place with the maximum sagging bending moment. Then the inelastic buckling at mid support occurred at free flange of the purlin near the support. Finally, the sudden lateral-torsional buckling of the purlin happened when the temperature is at 490 °C. When comparing to model 2Span1Heat, the Model 2Span2Heat has the similar deformed shape. However, the lateral-torsional buckling occurred at 480 °C. Besides, the deformation of the Model 2Span2Heat happened at both spans whereas the deformation of the Model 2Span1Heat occurred only in the span exposed to fire.

Out-of-web plane displacements

Fig.6 shows the comparisons of out-of-web-plane deformation of the point 6 of the cross-section at mid-span for three models. Due to the similar deformed shapes at right supports (Fig. 5) for three models, the initial out-of-web-plane deformations have been observed at temperature of 184 °C for the

Model 1Span and 123 °C for both the Model 2Span1Heat and Model 2Span2Heat. Because of the different deformed shapes at left/mid supports (Fig. 5) and different heating conditions, the Model 2Span1Heat has sudden out-of-web-plane deformation at around 490 °C while the Model 2Span2Heat at around 480 °C. However, no sudden out-of-plane deformation has been observed for the Model 1Span. The out-of-web-plane deformation for the Model 1Span increases further after the inelastic buckling at the end supports and multiple-wave local buckling of the restrained flange and lip. Therefore, the Model 1Span has a smaller out-of-web-plane deformation comparing to two-span models after their sudden out-of-web-plane deformation.

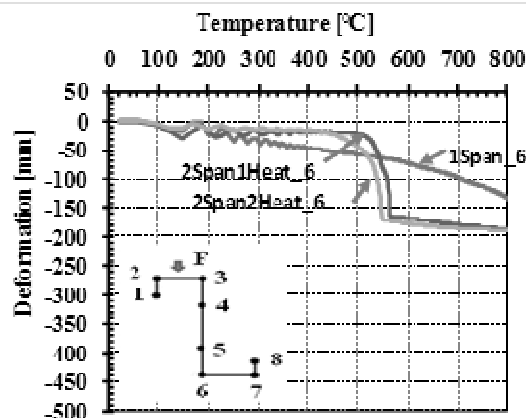


Figure 6. Displacement temperature curves (out-of-web plane).

In-web plane displacements

Fig. 7 shows the comparisons of in-web-plane deformation of the point 3 and point 6 of the cross-section at mid-span for the above-mentioned three models, respectively.

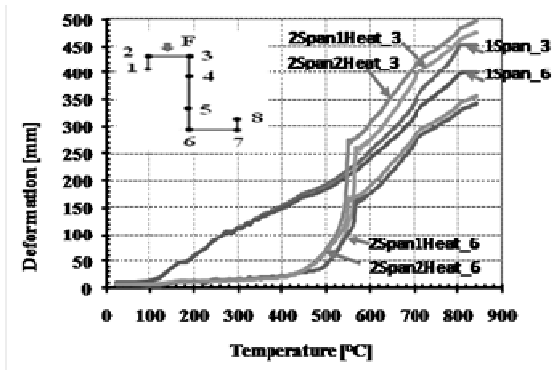


Figure 7. Displacement temperature curves (in-web plane).

It can be seen that the in-web-plane deformation is increased at around 184 °C for the Model 1Span due to the early inelastic buckling of both end supports. However, no big increases were observed in the deformations for two-span models before sudden lateral-torsional buckling at around 490 °C for the Model 2Span2Heat and at around 480 °C for the Model 2Span1Heat because of mid-supports. At the same time, the original Z-shaped cross-sections fall down and bend in minor axis. For the Model 1Span, due to local buckling of the flange restrained by steel sheeting, the point 3 and 6 deformed separately at already 200 °C.

Reaction forces developed at supports

Fig. 8 and Fig. 9 show the developed axial forces at the fixed edges of the steel consoles at right and left/mid supports for three models. It can be seen that for all models, the axial forces developed at the right end supports are initially compressive due to the restrained thermal expansion; then transferred to tensile forces when the purlins are in catenary actions. It can be seen that the maximum compressive forces occurred at the temperature of 123 °C for two-span models and 184 °C for the one-span model, and then the forces decreased. This decreasing is caused by the inelastic buckling at the right end supports. For the Model 2Span1Heat and Model 2Span2Heat the second force decreasing occurred at the temperature a little less than 500 °C. The second decreasing is due to the inelastic local buckling at mid supports and lateral-torsional buckling of purlin. In addition, the compressive forces are transferred to tensile forces at around 511 °C for the one-span model, at 561 °C for the Model 2Span2Heat and at 544 °C for the Model 2Span1Heat.

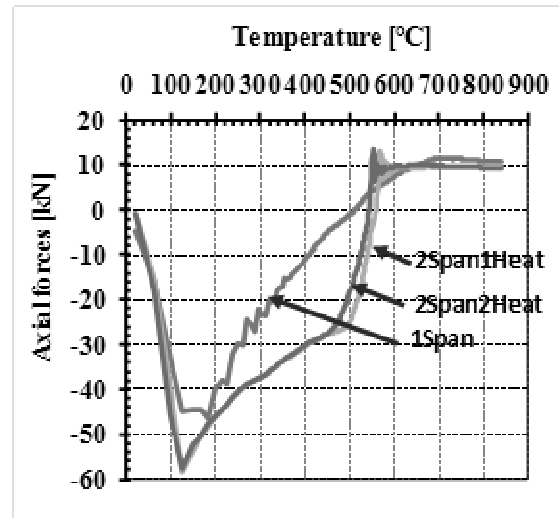


Figure 8. Axial forces developed at right support.

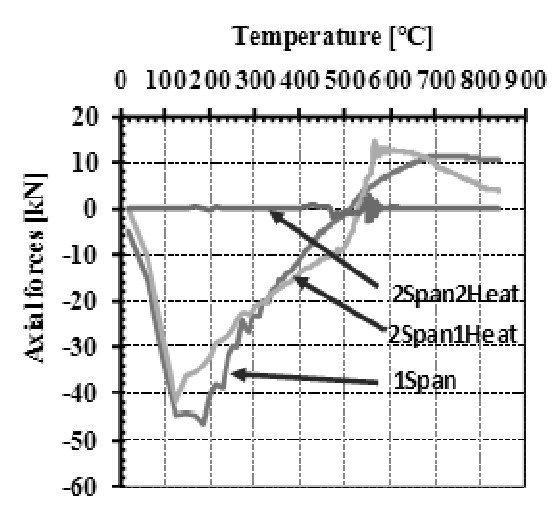


Figure 9. Axial forces developed at left support.

CONCLUSIONS

The compressive forces developed initially at the supports due to the restrained thermal expansion. The maximum value has been reached at about 184 °C for the one-span model and 123 °C for two-span models. Due to inelastic buckling of the purlin at the end supports, the compressive force was decreased. At 511 °C for the Model 1Span, at 544 °C for the Model 2Span2Heat and at 561 °C for the Model 2Span1Heat, the axial forces changed from compression to tension, the purlins were in catenary action. This behaviour was observed for all models. The purlin heated from two spans behaves similarly to the purlin heated from only one span. The sudden out-of-web-plane deformation occurred at about 10 °C earlier for the purlin heated from both spans. In addition, the axial reaction forces at the mid-support are zero for the purlin heated from two spans

because of the symmetry of structures.

When comparing to one-span purlins, two-span purlins have smaller in-web-plane deformation due to the mid-support. However, two-span purlins have larger out-of-web-plane deformation due to sudden lateral-torsional buckling. As far as the reaction forces at support are concerned, the earlier inelastic

buckling at two end supports in one-span purlin actually helps reduce the compressive forces developed at the end supports. However, when the purlins are in catenary action, the maximum axial tension forces developed at the supports are the same for both one-span and two-span purlins.

ACKNOWLEDGEMENT

This research has been financially supported by Rautaruukki Oyj. Mr. Reijo Lindgren from CSC-IT Centre for Science Ltd has been helping for creating the finite element model using ABAQUS. The authors gratefully acknowledge for the supports.

REFERENCES

ABAQUS on-line documentations (2009). Version 6.9.

Eurocode 3 (2005) Design of Steel Structures. *Part 1.2: General rules. Structural fire design.*

Usmani A.S, Rotter J.M, Lamont S., Sanad A.M., and Gillie M.(2001) Fundamental principles of structural behaviour under thermal effects. *Fire Safety Journal*, Vol. 36, No. 8, p. 721-744.

Wang Y.C. and Yin Y.Z. (2006) A simplified analysis of catenary action in steel beam in fire and implications on fire resistant design. *Steel and Composite Structures*, Vol. 6, No. 5, p. 367-386.

Wong M.B.(2005) Modelling of axial restraints for limiting temperature calculation of steel members in fire. *Journal of Constructional Steel Research*, Vol. 61, No. 5, p. 675-687.

NUMERICAL VERSUS EXPERIMENTAL INVESTIGATION OF PLYWOOD SANDWICH PANELS WITH CORRUGATED CORE

Edgars Labans*, Kaspars Kalniņš*

*Riga Technical University, Institute of Materials and Structures
edgars.labans@rtu.lv, kaspars.kalnins@sigmanet.lv

ABSTRACT

In the present research, an investigation of the mechanical behaviour of plywood sandwich panels, consisting of plywood surfaces and corrugated plywood core, has been performed using the finite element analysis in ANSYS code. For evaluation purposes, the results from finite element simulations were verified with experimental strain and deflection measurements performed using actual sandwich panels in 4-point bending test set-up. A good correlation between numerical and experimental results has been achieved. Using the validated finite element model of sandwich panel an optimization procedure has been developed to identify the best combinations for cross section parameters leading to optimal weight/ stiffness designs. A number of design guidelines have been drawn to establish the optimal panel configurations for given span length and corresponding load carrying abilities.

Key words: finite element analysis, 3D sandwich structures, metamodeling, optimizations

INTRODUCTION

The Nordic and the Eastern European countries have one of the largest territories of forests where export of sawn timber and wood products like plywood and various chipboards take a significant part in the national export structure. Also bearing in mind the historical wood research traditions in Latvia it makes a good background for new wood based product development. One of the promising directions in new products research and development may be considered lightweight sandwich structures with reduced structural weight and load bearing capacities close to the traditional engineering materials like plywood. Such solution offers material with high specific strength - strength/ density ratio is much higher than in solid wood case. Plywood sandwich panels consisting of plywood surfaces and corrugated plywood core may become an adequate alternative for thick traditional plywood boards in several fields like surface and maritime transport demanding reduced weight and sufficient load bearing capacity. Moreover, considerable wood resource savings, thus solving environment issues, also could be reached using such solutions. However, some scientific effort is required to develop a functional product with optimal cross-section parameters.

Traditionally wood products have been analyzed with simple analytical assumptions and approved with extensive experimental testing. Such assumption restricts the variety of structural applications and imposes restraints on structural weight saving. In contrary numerical simulations based on the finite element method (FEM) can deliver time saving tailored plywood structural solutions with potential of easy change design

requirements. To simulate the plywood behaviour and to optimize the complicated multilayer material structure FEM commercial code ANSYS (2009) has been utilized. FEM analysis using commercial codes has been considered as industrial standard for aerospace and car industry in order to reduce the required physical experiments in prototype development process. Employing of parametrical the model in the development process allows saving time in design optimisation using the metamodeling technique and elaboration of design guidelines to tailor the customer requirements.

To use this design method a detailed parametrical model validated with physical tests is needed. Considering that plywood is modelled as multilayer material consisting of veneers composed in several layers with different orientation of fibres, the mechanical and physical behaviour of laminate is largely dependant upon the performance of each individual material layer and its bonding (Wu et al, 2005). This is why it is important to determine the material unidirectional properties to create an accurate parametrical model for structural plywood boards.

A governing mechanics of corrugated structures has been described and methods compared in source (Luo et al., 192). More recent publications describe the analysis of corrugated structures by FEM (Mackerle, 2005; Gilchrist et al., 1999) and computer codes based on FEM usage (Hudson et al., 2010), good correlation between experimental and numerical results was found approving the efficiency of FEM for structural design. FEM analysis and experimental tests on wood based panels with corrugated core (wood fibreboard) were performed by (Hunt, 2004) to show the potential of 3D wood fibreboards. Sandwich plywood panels

with rib-stiffened and corrugated core have been investigated by (Zudrags et al., 2009) with the aim to increase plywood specific stiffness. Optimisation procedures using stiffness and weight ratio for plywood sandwich panels with rib-stiffened core were described in (Kalnins et al., 2009).

The aim of this paper is to validate the numerical model of plywood sandwich panel with experimental results and applying metamodeling methodology to develop the optimisation procedure.

MATERIALS AND METHODS

FEM modelling

For numerical simulation of the bending tests a FEM commercial code ANSYS v.11 (2009) has been applied. A parametrical model of the panel was created with variable cross section parameters and bending loading set up options. Corrugate V-core plywood sandwich panel has been modelled according to the EN 789 (2004) test set-up by using ANSYS 4-node shell element SHELL 181. It has been assumed that each ply has thickness of 1.3 mm and transversal isotropic material properties (Figure 1, 2).

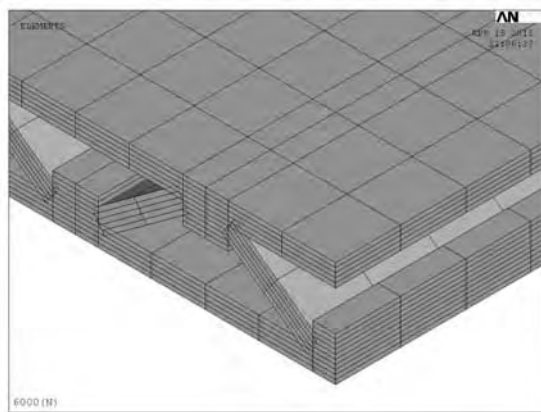


Figure 1. Finite element laminate mesh through the panel cross section.

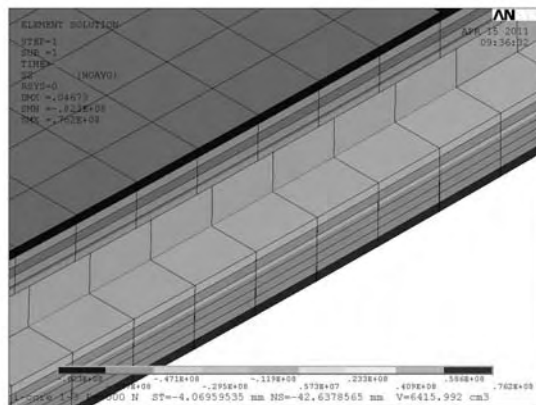


Figure 2. Stress distribution in sandwich structure.

Numerical model geometry was created to match the panel dimensions according to the manufacturing tolerance where the thickness of outer plies has been reduced by 20%.

The mechanical properties used in the numerical model were obtained in the previous study (Labans et al, 2010) and summarized in Table 1.

Table 1
Veneer mechanical properties

Name of the elastic property	Symbol	Optimal values
Modulus of elasticity in fibre direction	E_x	17 GPa
Modulus of elasticity perpendicular to fibre direction	E_y	0.5 GPa
Poisson ratio in fibre direction	P_{xy}	0.35
Poisson ratio perpendicular to fibre direction	P_{yx}	0.03
Shear modulus	G	0.7 GPa
Density	R_o	600 kg/m ³

Corrugate core roundups are required in the manufacturing process; however, including them in the numerical model is not reasonable (Figure 3).

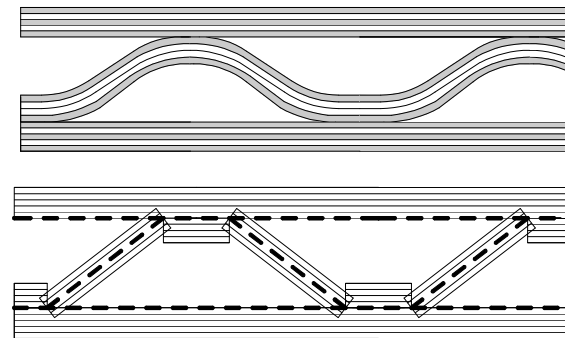


Figure 3. Manufactured cross section of sandwich panel (upper); numerical ANSYS model (lower).

Metamodelling procedure

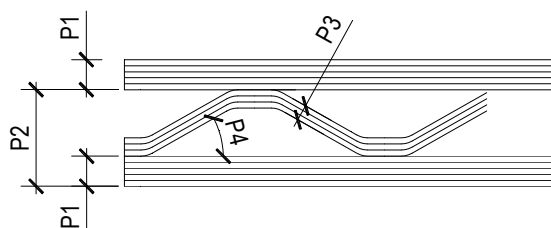
In industrial applications, in order to reduce the development time involving the high precision simulations, the metamodels also called surrogate models can be constructed to replace the original response with the approximation functions (Kalnins et al., 2009). The design optimization process using metamodels usually consists of three major steps: 1) design of computer experiments 2) construction of approximation functions that best describe the behaviour of the problem 3) employing developed metamodels in the optimization task or derivation of the design guidelines.

Table 2

Cross section design variables

Parameter	Nomenclature	Lower limit	Upper limit	Increment step	Units
Number of cover plate plies	P1	3	7	2	-
Total section height	P2	30	50	5	mm
Number of plies in corrugate section	P3	3	5	1	-
Corrugated ply angle	P4	30	60	-	deg

In the current research a sequential design based on the Means Square error criterion has been evaluated by EdaOpt software (Auziņš et.al 2007). A total of 125 points for four design variables have been evaluated. Four design variables have been used to describe different cross section parameters, in particular number of plies in upper **P1** and corrugate plates **P4**, the total section height **P2** and the angle between the upper plate and the corrugate core **P3** as displayed in Figure 4. The design boundaries for the variables are given in Table 2. As response parameters acquired during the numeric calculations are maximum deflection at the midspan U , normal stress at the midspan σ and the tension strain in outer ply ϵ .

**Figure 4.** Variable cross section parameters.

The span length of the four point loading model was kept constant; however, the width of the panel has been linked with the corrugated ply angle parameter **P4**. This constraint assures that the acquired results for different topology models would be comparable, as the width parameter and corrugate topology have linear dependency. This means that the acquired response values were multiplied with the coefficient k_r characterizing relation of the actual panel width against the standard width of the panel of 300 mm.

Experimental investigation

Three sandwich panels with corrugated core have been tested in 4-point bending set up according to EN-789 (Figure 5) at the Riga Technical University, Institute of Materials and Structures (IMS). The average length of the panels is 1200 mm, width – 300 mm, and thickness 30 mm, width of one corrugate wave – 75 mm. Surfaces plate manufactured of 5-layer plywood and corrugate core from corrugated 4-layer symmetrical plywood sheet where the outer plies are parallel to the cover

plate longitudinal axis. All panels have been tested up to 22 mm deflection which corresponds to approximately 40 % of the critical load for this type of specimens. Deflections under the symmetrical loading conditions have been recorded with extensometer at the midspan, strains on outer surfaces measured using strain-gauges (produced by HBM).

**Figure 5.** Sandwich panel in 4-point bending test set-up on INSTRON 8802.

For two panels strains were measured on both sides of the outer surfaces and also in several positions on the corrugate core panel surfaces. In total 14 strain-gauges were used to cover one panel. On the other hand, for the third panel strain measurements were taken only on the cover plate outer surfaces with 6 strain-gauges.

RESULTS AND DISCUSSION

Validation of the numerical model

To validate the numerical model of the plywood sandwich panel, experimental strain and deflection measurements have been compared with the response values extracted from the numerical simulations. The numerical and experimental deflection curves are compared in Figure 6.

One can note that the load deflection curves have linear behaviour, indicating the elastic deformation of the panels. The numerical results practically match the experimental load/deflection values. The vertical line is added to the graph in order to identify the deflection limit state (5% of span length) prescribed by structural safety codes.

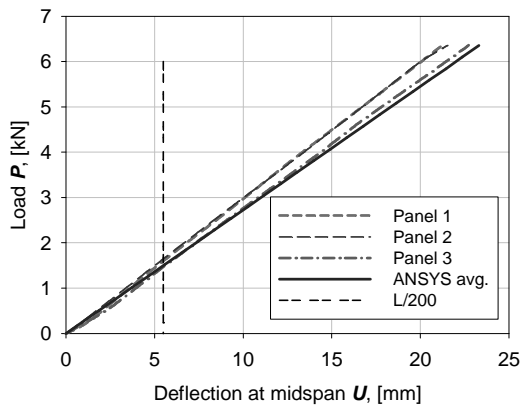


Figure 6. Load/deflection curves of sandwich panels.

The load/ strain curves are shown in Figure 7. Curves with negative strain values are obtained from strain-gauges attached to the upper surfaces of the cover panels or in the compressed zone. In the same way the curves with the positive strain values are obtained from sandwich panel bottom surfaces. Likewise to the previous figure, the numerical values are close to the experimentally obtained ones. The load/ strain curves derived from the strain gauges attached at the corrugated core surface are summarized in Figure 8. The shear strain values obtained by numerical modelling are higher than the experimental values in average by 10-15 %. This could be explained by inaccurate positioning of the strain values, because strains should be measured in 45 degrees angle toward the panel longitudinal axis. Precise measuring angle probably was not reached or maximal strains were positioned at a different angle because of not precise veneers orientation in plywood sandwich production.

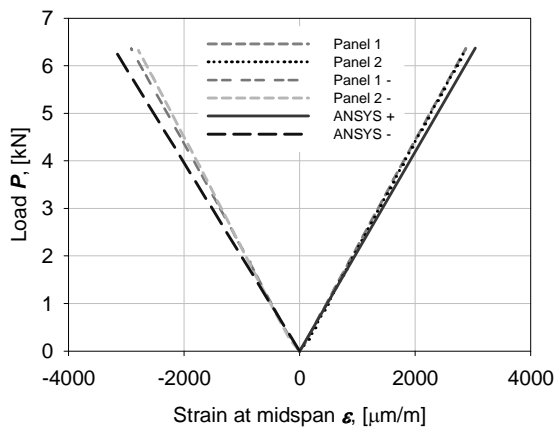


Figure 7. Load/ strain curves on the sandwich panel outer plates.

It has been concluded from the verification study that the parametrical model elaborated in ANSYS code matches the mechanical behaviour of the sandwich panel observed in the experimental tests.

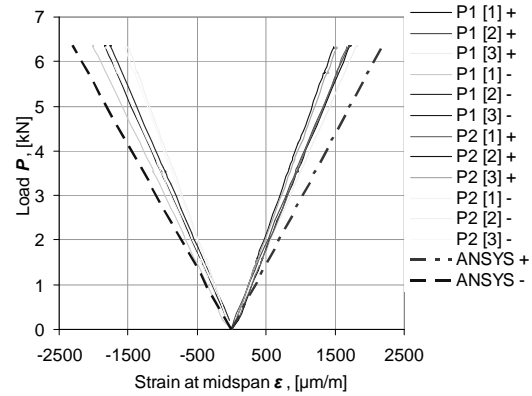


Figure 8. Load/ strain curves on sandwich panels corrugated core surface.

It may be recommended to utilize such model for metamodelling based optimisation procedure.

Optimisation results

During the optimization procedure the maximum stiffness and volume ratio combinations have been obtained for the given parametrical variables and normalized versus homogeneous plywood panel (Table 3).

Table 3

Optimal plywood sandwich parameters sorted according to homogeneous panel geometry

Variable	Set1	Set 2	Set 3	Set 4	Set 5
P1	3	5	5	3	3
P2	0.03	0.035	0.04	0.045	0.05
P3	5	5	3	5	5
P4	60	60	60	60	60
V_s,cm³	3966	6600	5580	5300	5360
V_s-V_p,%	55	37	53	61	64
U_s-U_p, %	22	14	30	35	42
Total, %	33	23	23	26	22

The sandwich panel volume parameter has been marked as V_s in contrary to the homogenous plywood volume as V_p . Respectively U_s and U_p – deflections for sandwich panels and plywood panels of the same thickness. To estimate the efficiency of the cross section parameters deflections and volumes of the sandwich panels were compared with the homogenous plywood values. The difference between the sandwich panel and pure plywood volume has been divided by the sandwich panel volume to acquire volume reduction (%) using sandwich structure. A similar action has been used to assess the deflection values for both structural types. The parameter **Total** stands for the difference between the volume gain and deflection loss (%). In average a total gain value in

comparison with homogenous plywood is 25 %.

In order to graphically assess the influence between the parametrical variables, the 3-D influence graphs have been constructed to show the dependencies with the deflection and strain response values (Figures 9, 10, 11). It may be evident that the cross section height parameter has the most sensitivity to decrease both the global and local deflection of the sandwich panel.

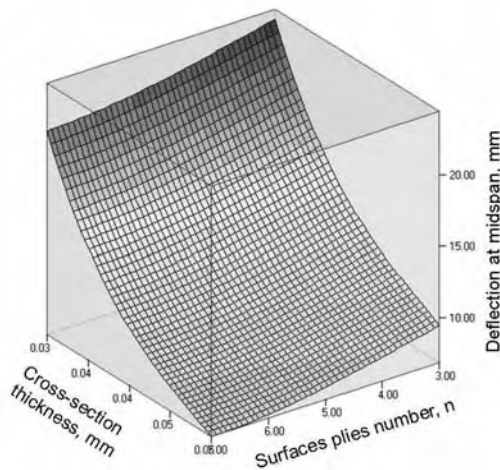


Figure 9. Panel thickness/ outer plies number versus panel deflection at the midspan graph.

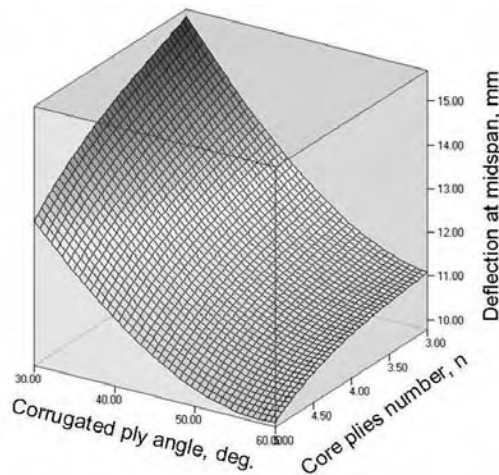


Figure 10. Number of plies in corrugate section / corrugated ply angle versus panel deflection at the midspan graph.

A general trend could be estimated from Figure 10 that panel deflection is largely dependent on the corrugated ply angle parameter *P4*. The panel stiffness is more sensitive towards the change of the angle than the core plywood thickness. However, some combinations with a smaller angle also should be considered in case of manufacturing difficulties of plywood structures with small bend radius.

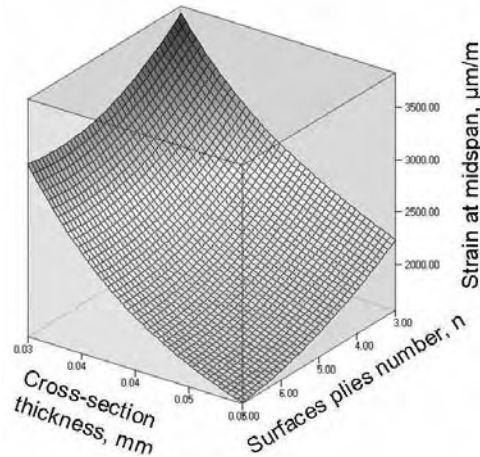


Figure 11. Panel thickness/ outer plies number influence graph on elastic strain.

For the sandwich panel of each thickness with optimal cross section parameters design guidelines were evaluated for better demonstration of the load bearing capacity at different span length (Figure 12).

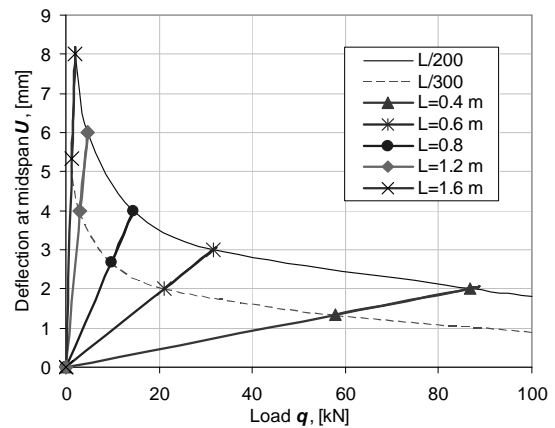


Figure 12. Acceptable load / deflection graph for panels with 30 mm thickness, 3-layer surfaces and corrugated ply angle 60°.

One may notice that the load bearing capacity decreases exponentially by increment of the span length. For other panels the span/ limit load graphs have been constructed as well to assess the load carrying possibilities for panels with different cross-section parameters.

The ultimate load values for sandwich panels could range up to large plastic strain limit state –in this particular case strain up to 5000µm/m. This may be stated as the current strain limit determined analysing the material properties and physical tests for similar type panels. The limit load values largely depend on the span length parameter, thus for every sandwich panel thickness a separate graph has been drawn.

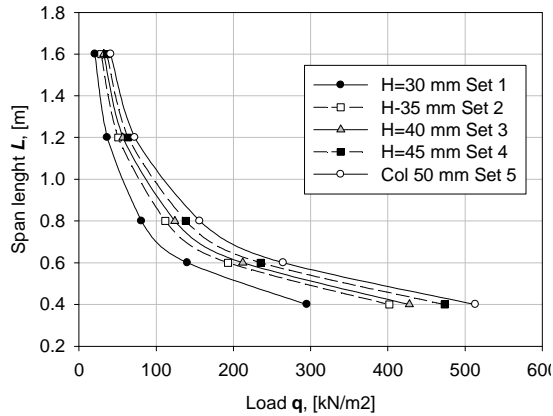


Figure 13. Ultimate load/span graph. Restriction-load values causing major plastic strains leading to material destruction ($\epsilon_{\max}=0.005$).

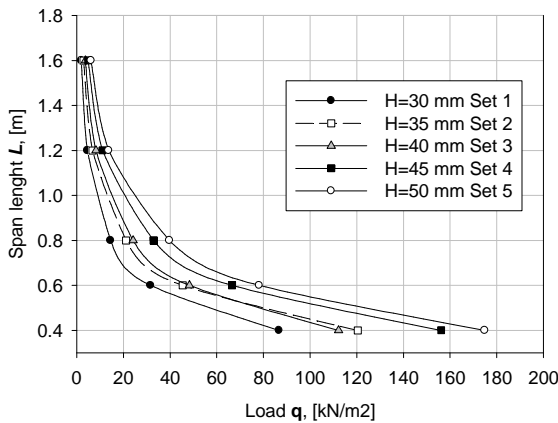


Figure 14. Load /span length graph for deflection limit 5 % of span length.

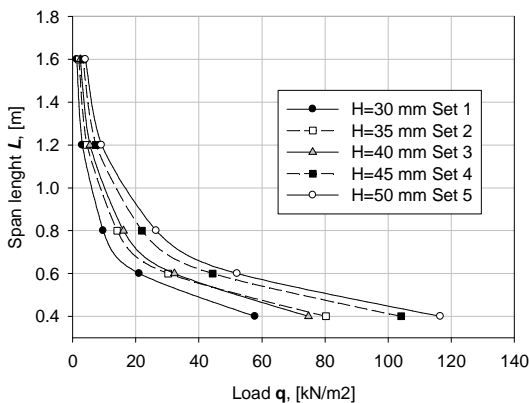


Figure 15. Load /span length graph for deflection limit 3.3 % of span length.

ACKNOWLEDGEMENTS

The authors acknowledge support from the company A/S “Latvijas finieris” for providing the specimens for the veneer property tests.

REFERENCES

Auziņš J., Januševskis A. (2007) *Eksperimentu plānošana un analīze*. Riga: RTU publishing. p. 208.

Similar load/span curves have also been constructed to determine the sandwich panel load bearing capacity up to the specific deflection limit (Figure 14, 15). The deflection limit has been set to 5 % which correspond to 1/200 of the span length, in same manner 3.3 % correspond to ratio of 1/300 of the span length.

Using the acquired design guidelines it is possible to easily assess the efficiency of sandwich structures comparing them with homogenous plywood and foresee deformation values at various loading and span length. For example, it is clearly seen that a sandwich panel with 40 mm total thickness is not as economically efficient as a panel with 30 mm total thickness at small span lengths (0.4-0.6 m).

CONCLUSIONS

During the present investigation of plywood sandwich panels with corrugated core, multilayer numerical models with variable cross section parameters have been evaluated and verified with the experimental results. The acquired numerical results were compared with the experimental results acquired by testing of three manufactured panel prototypes in 4-point bending set up according to EN-789 and a good agreement between the experimental and the numerical results has been acquired.

It has been concluded that the corrugated panel stiffness is largely dependent on the corrugated ply angle. The best results acquired from the optimisation procedure indicated the 60° corrugate plate angle, however, this value may not be possible to achieve by manufacturing restraints.

The optimisation results demonstrate that in some combinations of design variables the sandwich panels could be up to 40 % weight effective comparing with homogeneous plywood panels with the corresponding height, by losing only 10-20 % of the load carrying capacity.

Based on the optimisation results the design guidelines were constructed for a limited amount of considered panel configurations delivering the optimal cross section parameters, within the given deflection and maximal strain limits.

ANSYS Version 11. (2009) *User Manual*. USA, Papenburg.

EN 789:2004. *Timber structures. Test methods*. Determination of mechanical properties of wood based panels. Brussels: European Committee for Standardization (CEN).

Gilchrist A. C., Suhling J. C., Urbanik T. J. (1999) Nonlinear finite element modelling of corrugated board. AMD-Vol. 231/MD-Vol. 85. *Mechanics of Cellulosic Materials*, ASME, p. 101-106.

Hudson C. W., Carruthers J.J., Robinson A.M. (2010) Multiple objective optimisation of composite sandwich structures for rail vehicle floor panels. *Composite Structures*, No. 92, p. 2077–2082.

Hunt J.F. (2004) 3D Engineered Fiberboard: Finite Element Analysis of a New Building Product. 2004 *International ANSYS Conference*. Pittsburg, PA, May, p. 24-26.

Jekabsons G. (2010) VariReg: A software tool for regression modelling using various modelling methods, available at <http://www.cs.rtu.lv/jekabsons/> [online] [accessed on 04.05.2011.].

Kalnins K., Jekabsons G., Zudrags K., Beitlers R. (2009) Metamodels in optimisation of plywood sandwich panels. *Shell Structures: Theory and Applications*, Vol. 2. Pietraszkiewicz W. and Kreja I. (eds.), CRC press /Taylor & Francis Group, London, UK, p. 291-294.

Labans E., Kalniņš K., Ozoliņš O.(2010) Experimental and Numerical Identification of Veneers Mechanical Properties. *RTU Construction science*, Vol. 11, p. 38.-43.

Luo S., Suhling J. C., Considine J. M., Laufenberg T. L. (1992) The bending stiffness of corrugated board. AMD-Vol. 145/MD-Vol. 36, *Mechanics of Cellulosic Materials*, ASME, p. 15-26.

Mackerle J. (2005) Finite element analyses in wood research: a bibliography. *Wood science and technology* , No. 39, p. 579-600.

Zudrags K., Kalnins K., Jekabsons G., Ozolins O. (2009) Bending properties of plywood I-core sandwich panel. *Proceedings of the 5th Nordic-Baltic Network in Wood Material Science and Engineering*. Meeting, Copenhagen, p. 169-175.

Wu Q, Cai Z, Lee JN. (2005) Tensile and dimensional properties of wood strands made from plantation southern pine lumber. *For Prod J* , Vol. 55, No. 2, p. 87–92.

PROPERTIES OF COLD-FORMED STEEL SECTIONS

Atis Dandens, Janis Kreilis, Guntis Andersons

Latvia University of Agriculture, Department of Structural Engineering

Janis.Kreilis@llu.lv; Guntis.Andersons@llu.lv

ABSTRACT

There is great flexibility in the design using cold-formed steel. The low cost, ease of manufacture and controlled quality can encourage the development of innovative uses. In spite of the advantages, the range of application is limited in Latvia, especially for load bearing structures. The resistance of thin-walled cold-formed steel sections should be determined according to EN 1993-1-3 (2006) and 1993-1-5 (2006) by the effective width method. As a first step, in this paper the resistance to local buckling of cold-formed sections in compression and bending is analysed taking into account geometrical proportions, influence of rounded corners and stiffeners. By numerical analysis there is given the estimation of effective U and C-section properties in the range of width-to-thickness (b/t) and width-to-height (b/h) in concordance with EN 1993-1-3, Section 5. In addition to the numerical analysis there are presented and assessed results of experimental research with natural beams in bending.

Key words: cold-formed steel; effective section properties; numerical analysis; experimental method; assessment of results

INTRODUCTION

Cold-formed steel offers many advantages, including: ease of prefabrication and mass production, increase of strength in fabrication process, uniformity of quality, low weight, economy of transportation and handling, and quick and simple erection or installation.

Thin-walled cold-formed steel sections (CFSS) are produced by bending and shaping flat sheets at room temperature. Material is easily workable and many possible shapes can be produced.

The structural behaviour of CFSS can be distinguished from typical hot rolled sections with the tendency to be more sensitive to buckling effects. The tendency to buckle increases as the width to thickness ratio of the plated elements increases. It is obvious, that design standards were needed to establishing requirements and laws to control the buckling and strength characteristics.

The use of CFSS members in building construction began more than 150 years ago in the United States and Great Britain. The first edition of specifications for design (in 1946) was followed by many revisions and developments finished in 2007. The European Union has adopted Eurocode EN 1993-1-3 in 2006 and it has been mandated that all member states adopt these codes in 2010. Further directions in reviewing of plate buckling rules are given in (Johansson and Veljkovic, 2009).

CFSS can be used widely in building applications (e.g., www.lysaght.com) and can be specially shaped to suit the particular application. The most common sections are the U, C and Z shapes. However, a whole range of variants of these basic shapes, including geometrical proportions, edge lips and internal stiffeners can be produced.

MATERIALS AND METHODS

Theoretical modelling

For practical design of CFSS designers normally refer to the manufacturers' data or use software in case of non-standard shapes. For this purpose there MathCad programme is used and numerical analysis performed to estimate the effective U and C-section properties in compression and bending in accordance with EN 1993-1-3, Section 5 by the effective width method. For comparison, for outstand compressed elements an alternative mixed method given in the Annex D is used. The resistance of compressed flanges with edge stiffeners was determined using iterations. Initially the data from the numerical tests were compared with those from the worked examples (ECCS TC7 TWG 7.5 (2008)).

The summarized results, showing the influence of the geometric characteristics (in cm) on the properties of CFSS are given in some examples:

1) U-section formed from a steel sheet 300x4 mm in the available range of width-to-thickness (b/t) and width-to-height (b/h) ratios subjected to compression and bending. The results of the numerical analysis are shown as X-Y plots (Fig.1, Fig.2), where $\text{ratio}_i = b / h$. The gross section and effective section modulus W_z , W_{efz} were calculated according to the free edge (outstand compressed element). For comparison, the curve for the effective area of the compressed U-section (A_{efc}) is added (see Fig.1, a).

2) Double C-section arranged back-to-back, subjected to compression (Fig.3), made from steel sheets 300x1,5 mm with variable ratio (b/h) and edge stiffener width $c = 0,4 b$ (Fig.4). For comparison, the curve for the effective area of the compressed double-C (A_{efc}) section is added (Fig.4).

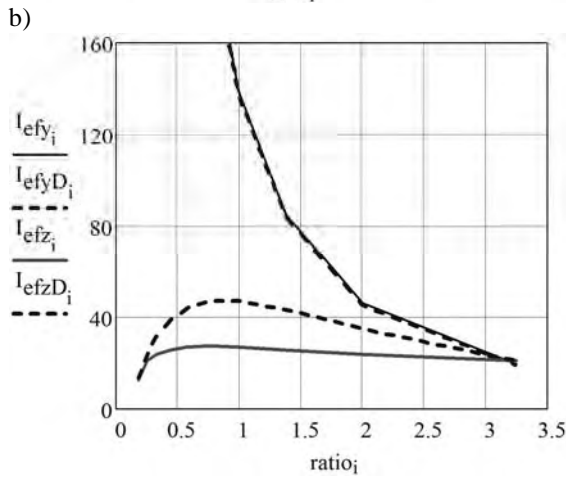
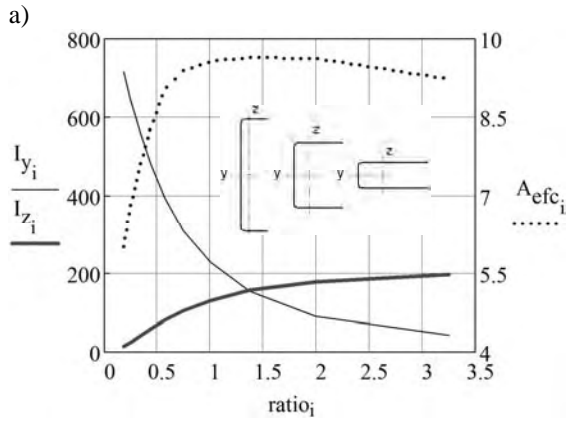


Figure 1. Properties of U-section in compression, where I_y , I_z and I_{efy} , I_{efz} – second moment of area for gross and effective section; I_{efD} – by mixed method.

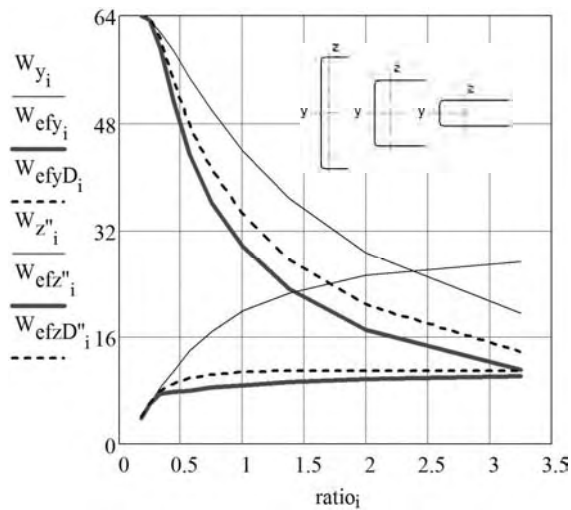


Figure 2. U-section in bending, where W_y , W_z'' and W_{efy} , W_{efz}'' – section modulus for gross and effective section; W_{efD} – by mixed method.

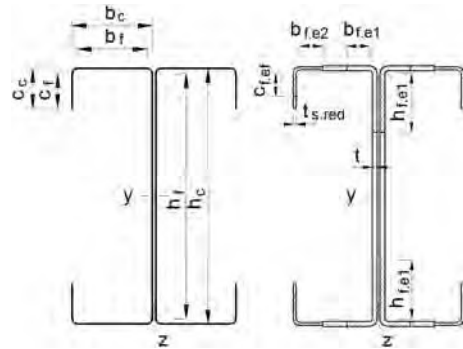


Figure 3. Double C-section.

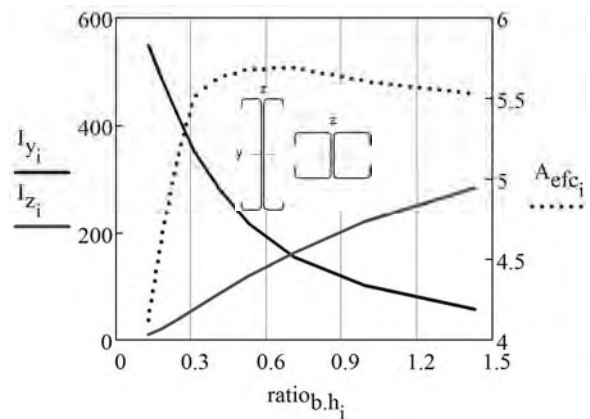


Figure 4. Properties of double C-section in compression

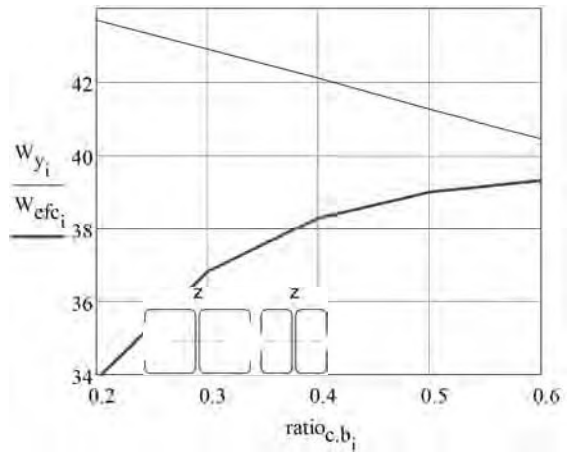


Figure 5. Double C-section in bending, where W_y and W_{efc} – section modulus for gross and effective section (for fibres in compression)

3) Double C-section arranged back-to-back, subjected to bending, made from steel sheets 300x1,5 mm with constant $h = 150$ mm and variable ratio (c/b) , where edge stiffeners $c = (0,2 \dots 0,6)$ (Fig.5).

Experimental research

The test specimens (from RUUKKI standard sections) were taken as simply supported double-C beams (Fig.6), arranged back-to-back and loaded in bending at three points of the span (i.e., the four-point bending tests). Loads are applied only about y-y axis of the cross-section. Lateral restraints were added at the supports and load points to avoid torsional buckling. The tests were carried out by loading equipment Zwick-Roell using operating program TestXpertII:

a) “short beam” tests. Beams with span $L = 1430$ mm (it is less than $15h$) were tested for verification of the experimental method. One test with the beam from double-C 200 ($t=2$ mm) and one test with double-C 150 ($t=1$ mm) was performed and the moment resistance was determined;

b) “long beam” tests with beams according to EN 1993-1-3, Annex A:

- series of three specimens from double-C150 ($t=1$ mm) with span $L=15h = 2250$ mm;

- series of three specimens from double-C120 ($t=1$ mm) with span $L=15h = 1800$ mm.

The webs of beams are connected by pairs of bolts (see Fig.6 and Fig.7); as the webs can locally buckle independently of each other, the slenderness is considered equal to the width divided by the thickness.

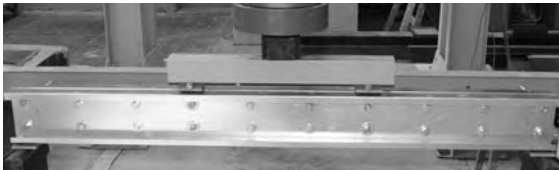


Figure 6. Experimental research of beams.

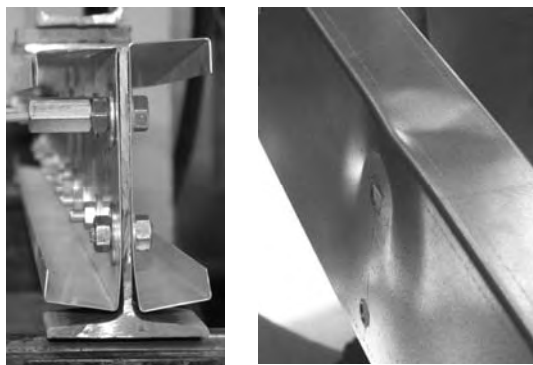


Figure 7. Supporting of beams and local buckling of compressed flange and web.

The experimental results are illustrated in Fig.8, Fig.9 and Fig.10; deflections are shown relative to span of the beams (w / L). The tests for series of beams leads to practically equal graphs. All specimens were collapsed due to local buckling of compressed cross-section elements.

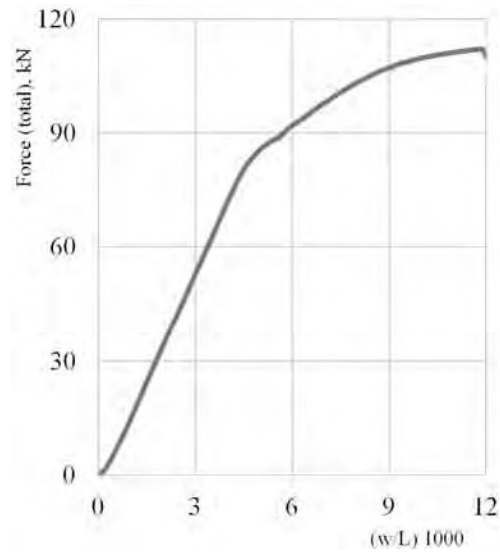


Figure 8. Double-C 200 “short beam” test.

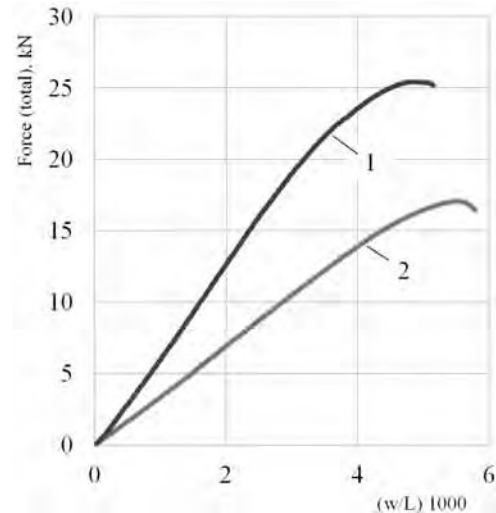


Figure 9. Double-C 150 beams tests, where 1 – “short beam”; 2 – series results.

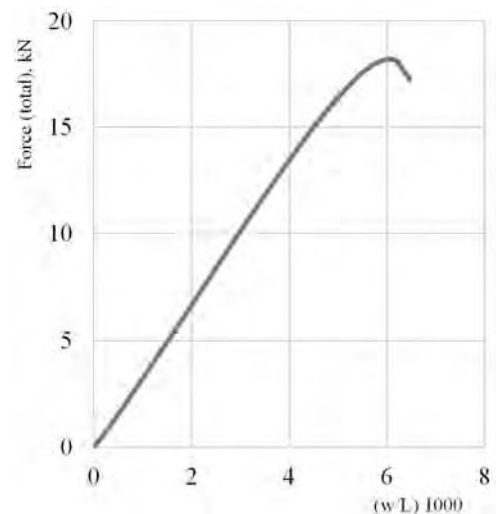


Figure 10. Double-C 120 beams tests.

The “short beam” tests validate the experimental method; in comparison with “long beam” tests the limit value of loading up to which direct proportionality exists is more explicit. The following nonlinear stage indicates that effective properties of cross-sections progressively become determinative and the effective section modulus W_{eff} is lesser than the gross elastic modulus W_{el} . The relationship “force-deflection” for beam from the double-C200 section differs from other experimental curves due to greater thickness ($t = 2$ mm) and due to interaction with lateral restraints at the loading points prevented global torsional buckling. Prior to local buckling effects there was observed waving of the compressed flanges in the central part of the span.

RESULTS AND DISCUSSION

Evaluation of theoretical modelling

Estimation of correct CFSS properties is of essential importance. The presented examples illustrate the necessity of using the effective properties of CFSS and eliminate the possibilities of using the gross section properties. Modelling the different U-shapes by varying of the ratio $=b/h$ leads to the conclusion, that determination of the section properties about z-z axis is of primary importance. Using for outstand elements (flanges) the mixed effective width/effective thickness method, given in the Annex D of EN 1993-1-3, shows evident differences (see Fig.2), thereby in some cases the mentioned mixed method must be used warily. Normally the influence of rounded corners on CFSS resistance may be neglected; the section modulus with increasing of the internal radius decreases under 3%. For determination of the stiffness properties the influence should always be taken into account. On the other hand, there is a well-known change in the mechanical properties of steel by virtue of cold forming. It is supposed, that the yield strength is increased in the bends of the section up to 15%.

Modelling the double C-sections in compression (see Fig.4) by varying of the ratio width-to-height of the section elements shows up the rational proportions (where $I_y \approx I_z$ and the effectiveness of the compressed area) for the initial calculations. The curves for double C-section in bending (see Fig.5) reflect the meaning of the width of the edge stiffeners – the effective section modulus increases only with the width up to $\sim 0,6 b$.

Resistance of cross-sections

Generally design assisted by testing is recommended for determination of the resistance of CFSS at ultimate limit states. It is firmly applied for sections with relatively high b_p / t ratios. In connection with the performed experimental

research the properties of the used cross-sections are analysed in accordance with EN 1993-1-3, Sect.6.1, and summarized in Table1:

- bending resistance M_{cRd} is determined assuming yielding at the compressed flange and section modulus $W_{eff} < W_{el}$;
- shear lag shall be taken into account to 1993-1-5, Sect.3. As the ratio - compressed flange width-to-length between the points of zero moments for the beams (b_0/L_e) is relatively small, the effect of shear lag is considered having no influence on the bending resistance of the section;
- shear resistance V_{bRd} is determined depending on the shear buckling strength and web slenderness;
- local transverse resistance. As the local load (support reaction) is applied through a cleat (see Fig.7), distortion of the web is eliminated and the local resistance of the web to the transverse force needs not be considered (EN 1993-1-3, Sect.6.1.7.1);

Table 1

Evaluation of tests results

Cross section	Span, mm	W_{eff} , cm ³	M_{cRd} , kNm	V_{bRd} , kN	$\frac{V_{Ed}}{V_{bRd}}$	$\frac{M_{Ed}}{M_{cRd}}$
C15 0	1430	17,1 7	6,01	25,2	0,50	1,01
C20 0	1430	69,1 2	24,1 9	94,8	0,59	1,10
C12 0	1800	13,5 2	4,73	24,0	0,37	1,13
(series)					0,38	1,16
C15 0	2250	16,9 3	5,93	25,2	0,33	1,06
(series)					0,34	1,09

- combined shear and bending resistance. As for the beam from double-C200 the shear force V_{Ed} is larger than a half of the shear force resistance $0,5 V_{bRd}$ (web resistance), interaction between the shear force and bending moment have to be taken into account, because shear buckling may reduce the bending resistance of the cross-section.

The resistance needs not be reduced if the following equation should be satisfied (EN 1993-1-5, Sect.7.1):

$$\frac{M_{y,Ed}}{M_{y,Rd}} + \left(1 - \frac{M_{f,Rd}}{M_{pl,Rd}}\right) \left(\frac{2 V_{Ed}}{V_{pl,Rd}} - 1\right)^2 \leq 1,0,$$

In this case, the moment resistance of the cross-section consisting of the effective area of the flanges only - $M_{f,Rd} = f_y h A_f = 33,8$ kNm is larger than the design plastic resistance of the cross-section consisting of the effective area of the flanges and the fully effective web - $M_{pl,Rd} = M_{cRd}$ (see Table1).

It is evident, that for this class of beams there is no interaction, because the flanges only can carry the bending moment and the web is resisting the shear. These results consistent with notations (Johansson and Veljkovic, 2009), accented the necessity to check the moment and shear resistances without interaction. By the numerical analysis it is clarified, that the provided height of the cross-section for the discussed beam should be above 300 mm, when reduction of the bending resistance starts.

CONCLUSIONS

The use of CFSS members in building can develop the diversity in steel design. The lack of discussion, explanation and worked examples delays to take advantages of CFSS in comparison with hot rolled sections in Latvia. It is caused also by slow implementation of the Eurocodes (including EC3). The numerical analysis of the CFSS properties and plotted data for the sections subjected to compression and bending illustrates the influence of

variable geometrical proportions. Knowing the preferable section properties, these data can help make a choice for the shape of the section or to improve the properties for non-standard sections. For example, for U-sections the ratio $b/h = 0,75...1,5$ is recommended in compression as well in bending. Without doubt, edge and intermediate stiffeners of flanges and webs increase the resistance to compression, but a highly stiffened section is less easy to manufacture and often less practicable from the point of connections. Thereby, a compromise between the section efficiency and practicability is often necessary and needs to be studied in further research.

The experimental research approved the method of testing and showed the stability of the acquired parameters, as well that keeping of precision in the tests with CFSS (e.g., symmetry of loading) is of great importance. Comparing with the numerical data shows good agreement.

ACKNOWLEDGEMENTS

The authors are much obliged to the company SIA Ruukki Latvija for providing the specimens for the tests.

REFERENCES

- Eurocode 3 (2006). Design of steel structures. Part 1-3: *General rules – Supplementary rules for cold-formed members and sheeting*. ENV 1993-1-3.
- Eurocode 3 (2006). Design of steel structures. Part 1-5: *Plated structural elements*. ENV 1993-1-5.
- B.Johansson, Milan Veljkovic (2009) Review of plate buckling rules in EN 1993-1-5. Ernst & Sohn Verlag fur Architektur und technische Wissenschaften GmbH & Co.KG, Berlin. *Steel Construction*, Vol. 2, No. 4.
- Cold Formed Sections*. Available: <http://www.lysaght.com>
- ECCS TC7 TWG 7.5. Practical Improvement of Design Procedures. Worked Examples According to EN 1993-1-3 Eurocode 3, Part 1.3 (2008).

III LANDSCAPE AND ENVIRONMENT

“CLIMATE- ENERGY- AND CULTURAL LANDSCAPE MODEL SAUWALD DONAUTAL” – EXPERIENCES WITH A PILOT PROJECT ON INTEGRATED REGIONAL RESOURCE MANAGEMENT BASED ON A NEW BIOGAS TECHNOLOGY

Peter Kurz

Vienna University of Technology, Faculty of Architecture and Planning,
Institute of Urban Design and Landscape Architecture
peter.kurz@tuwien.ac.at

ABSTRACT

This paper presents a model project where cultural landscape management and the production of “green” energy are combined to an integrated project on sustainable regional development. The project is based on a newly developed, small-scaled and mobile biomass-system, the 3A-biogas®-technology. 3A-biogas® uses a three-step composting-process to generate methane for the production of electric and thermal energy. The advantages compared to well known systems refer to a) low energy density required for the manipulated biogenic materials, b) a small and mobile plant, which generates low investment costs and c) possibility to combine biogenic waste, lop and hay of heterogeneous quality. These characteristics make the technology highly suitable for adoption in landscape-management of less-favoured rural regions.

The focus of the paper is set on the process of creating a regional programme interlinking landscape-, waste- and energy management based on implementation of the 3A-biogas®-technology. Therefore, two scopes are highlighted: cross-links between landscape-planning, energy- and composting-technology in the field of engineering are sketched in the first part of the paper. The 3A-biogas®-technology is briefly introduced, followed by an overview on how the technology is “translated” to fit the questions of regional landscape-, waste- and energy management. In the concluding section some important questions on calculation of costs for landscape management based on 3A-biogas® are discussed, regarding the experiences from our pilot study.

Key words: cultural landscape management, 3A-biogas®-technology, rural development, grassland vegetation

INTRODUCTION

Maintenance of traditional cultural landscapes and efforts on creating decentralised, CO₂-neutral energy systems are both outstanding issues in the current Austrian rural and regional policies. Ongoing abandonment of traditional agricultural farming systems raises increasing interest in alternative strategies in the management of – frequently touristy employed – rural landscapes. One possible alternative to livestock breeding may be the use of landscape-management hay for production of bio-energy. However, earlier experiences in trying to link production of bio-energy with landscape management issues for ecological, but also for social reasons did not end up with satisfying results: large scale projects advanced processes of intensification, concentration of land-tenure, displacement of regionally grown structures of land-use and external grasp on regional resource base (Graß, 2008; Kruska, Emmerling, 2008; Schöne, 2008; Schulze, Köppel 2007). Thus, demands for technologies better adaptable for the

specific needs of landscape management and conservation issues were raised (Hasselmann, Bergmann, 2007). The crucial questions appear to be a) abilities to dispose low-energy materials in rather small capacities b) varying capacity utilization and c) low costs in investment, maintenance and management (Prochnow et al., 2007). Those framework conditions do not necessarily go hand in hand with profit maximising entrepreneurship strategies. This is why – apart from technological issues – further considerations focus on how to organise a system fitting the different needs of land-owners, communities, land managers and conservationists. As important as the technology itself seem the modes of its implementation and the embedding in regional structures within a “co-evolutionary process” (Schulz-Schaeffer, 2002).

This paper explores experiences with introduction and implementation of a small-scale technology – the 3A-biogas® system – for the use in landscape management and decentralised energy production in

a regional pilot project. Choosing a bottom up approach – cooperation between experts, communities and stakeholders – the first part of the paper describes the pathway of integrating the technology into the regional environmental, economic and social structures. The second part of the paper outlines a few figures on financial calculation of grassland management based on 3A-biogas[®], as they can be deduced from our case-study experiences so far.

Methodological remark

The inquiry is methodologically grounded in the principles of action research, as described by Altrichter (2007). Action research is an experience-based approach to generating knowledge by investigating praxis. In action research the researcher is part of the (cooperative, team-conducted) process he or she explores, running through a circle of acting and reflecting. The reflected experience forms the foundation for practical, professional theory (Altrichter, 2007). The action research approach was developed in teachers' research, by teachers exploring their class. Lately it has been extended and transformed to investigate several areas of social processes (Kurz, 2010). The empirical facts and data presented in the paper are an outcome of the conducted feasibility study and were gradually elaborated further in the following participatory discussions.

3A-BIOGAS[®] TECHNOLOGY

3A-biogas[®] is a technology developed for the treatment of organic material containing high dry matter percentage to produce electric and thermal energy. The technology combines biogas- and compost- production including sanitation of the compost. Using a batch-process, the biological decomposition in 3A-biogas[®] takes place during 3 operating phases (aerobic, anaerobic, aerobic) in a closed domain without intermediate movement of substrates (Müller et al., 2006):

- In the initial aerobic phase (up to 6 days, reaching temperatures up to 70° C) the input material is ventilated, the substrate is aerated and the aerobic microbiological activity causes an increase of temperature. Within this phase lightly degradable substances are reduced (decrease of acid formation), the substrates are sanitized (reduction of pathogen) and the material is heated for the second phase. Carbon dioxide and water is the output of the initial phase.
- The second phase of the process (25-40 days, 35-45° C) is carried out under mesophile anaerobic conditions, starting the methane production. Digestion takes place, biogas is produced and the volume of the input substrate is gradually reduced.

- The third phase starts (about 10 days, up to 60° C) with anew aeration of the substrate. Organic materials are stabilised and become quite inodorous. The output of the phase is compost, which can be further composted outside the fermentation reactors to reach a further stage of maturity.

While treating such substrates in conventional liquid biogas plants high volumes of water would be necessary (which remain in most cases as wastewater subsequently), the 3A-biogas batch-process for solid state bio-waste can reach the best available synergies of composting and fermentation technology. The 3A-biogas[®]-process was developed by A. Steffen and patented in 1988.

Technology	Process	Substrate	Outputs
Composting	aerobic	solid state	Compost
3A-biogas	aerobic / anaerobic	solid state	Energy & Compost
Liquid fermentation	anaerobic	liquid	Energy & liquid Digestate

Source: Müller et al., 2006

Figure 1. 3A-biogas[®]-technology.

The technology is integrated in a container system. The minimum load of the organic material should not go below 500 t/year, optimized use of capacity can be reached up to 2000 t/year. Average gain of biogas is 120 m³/t, containing 60% of methane. The energy output is 3 kW (electric) and 6 kW (thermal) per m³ CH₄ (Müller et al., 2006).

CLIMATE-, ENERGY- AND CULTURAL LANDSCAPE MODEL SAUWALD DONAUTAL

Several 3A-biogas[®] facilities have been employed successfully in the treatment of organic waste in earlier projects (see Müller et al., 2006). The experiences indicated that well structured materials such as lop and grass contribute to an improved process. The outcomes of those test runs justified considerations on application of the technology under “field conditions” in landscape management, where high amounts of dry organic materials emerge (Prochnow et al., 2007). The 3A-biogas[®] technology – so the assumption – therefore could provide a tool which not only allows reintegration of those materials in regional material flows, but also contributes – to a minor degree – to regional energy autonomy. These were the considerations which ended up in the development of the pilot

project “Climate-, Energy- and Cultural Landscape Model Sauwald-Donautal”. Involving a team of experts in waste management, energy management and landscape planning the project was initiated by the regional LEADER- management. The basic conception behind the project was to link issues of cultural landscape management, organic waste management and decentralised, regional energy support. The core of the project should be the 3A-biogas[®] technology. However, according to the philosophy of endogenous regional development (Van der Ploeg, 2009), broad integration into the existing regional (environmental, economic and social) structures was defined as a central goal of the project by the regional LEADER management. Therefore, a cooperative, participatory approach to implementation should be designed. As a particular – non-commercial – objective of the project the stabilisation of the open landscape and its diverse grassland types was drafted (Kurz, 2010).

The chosen model-region, the Donautal (Danube Valley) is a mountainous area, characterised by small scale agriculture. Grassland- and forestry are the predominant categories of land use. While soft tourism forms one of the major sources of income, land abandonment and reforestation create massive problems in regional development of the touristy used region (Kurz, 2011). Decline of tiny structured open landscapes not only implies losses of diversity and splendid views.



Figure 2. Model region Sauwald-Donautal.

It also induces negative influences on the micro-climate and quality of life of the narrow valley landscape as a whole. For these reasons several efforts on finding practical alternatives to ongoing reforestation had been undertaken in the past.

Design of the pilot project

Fig. 3 visualises the workflow of the pilot-project: around the 3A-biogas[®] technology a model bottom-up process was designed, structured in a four stage setting. Starting with general information on the technical performance (Stage 1) a feasibility study regarding regional framework conditions was assigned (Stage 2). This formed the foundation for participatory development of an integrated concept in the fields of landscape management, organic waste management and regional energy production/support (Stage 3). Stage 4 should contain the elaboration of the definite plan for the implementation of the project. Each stage should be characterised by interaction between the experts` inputs (analysis), followed by discussion and further elaboration in teamwork. These processes should help identify the possible conflicts and problems, commonly elaborate solutions and – by the way – form a regional network pushing the project forward.

Assessment of feasibility in landscape conservation and landscape management

In the case of landscape- and grassland management basically two questions were considered significant:

- a) how much organic material can be allocated, when does the material occur – according to time and frequency of harvesting – and which are the expectable costs for harvesting and transport?
- b) how has management to be organised so that the ecological quality and diversity of the regional grasslands can be sustained or even improved?

To answer these questions comprehensive analyses of regional grassland vegetation was conducted. According to the method of Braun-Blanquet (1964), grasslands were typologically described and vegetation dynamics were analysed focussing on different management techniques. Potential yields were evaluated, regarding optimized dates and frequencies of mowing (Kurz, 2011). By mapping grassland types, structural data as plot structure, land tenure and allotment could be integrated in the examination. Founded on the analyses of the field data several maps and GIS-based analysis were generated (see Fig. 4). The technical analyses lead to the modelling of three scenarios, which functioned as a tool for communication in the following participatory process:

- minimum scenario: implementation of grassland areas currently managed by

- nature conservationists;
- optimum scenario: currently managed additionally including abandoned areas;
- maximum scenario: optimisation of energy output by including all areas regionally available.

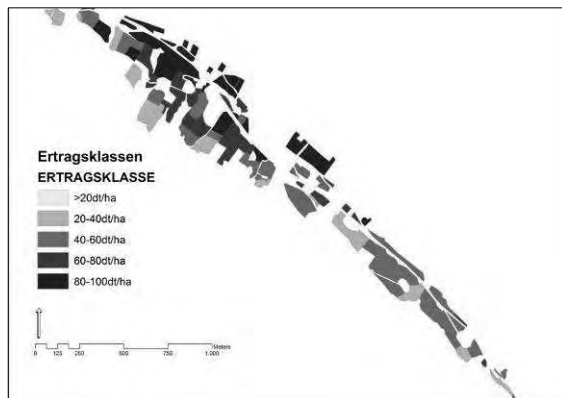


Figure 4. Potential yields of grassland types.

While scenarios 1 and 2 should estimate the economic impacts of proceeding under ecologically favoured conditions, the goal of scenario 3 was to assess environmental effects within an income-orientated setting.

Further steps in project development

Comparison of these alternatives formed the starting point for a discourse process, in which the pressure groups (landowners, community representatives, landscape managers, the team of experts etc.), elaborated the operational framework for possible implementation. Collaterally, more detailed information and data were organised. For a management concept on landscape issues for example

- hot spots of land abandonment were identified;
- measures for maintenance and management were defined;
- organisational questions of logistics were discussed and possible arrangements in the processing (legal frameworks and social organisation of cooperation, contracting between the involved actors etc.) were weighed.

These processes took place in small group settings, accompanied by the expert team, moderating the working groups and operating them by providing the data, tools and working papers. The results of these workshops were presented and discussed in another plenary session, which was eventually followed by elaboration of a definite plan for implementation. This contained the formation of a regional landscape management association, founding of a cooperation operating the 3A-plant and contractually agreements with regional waste managers on supply with organic waste (see Fig. 3).

LANDSCAPE MANAGEMENT BASED ON 3A-BIOGAS – SOME REMARKS ON THE CALCULATION OF COSTS AND RETURNS

A central issue in application of the 3A-biogas[®]-technology in landscape maintenance and –management actually concerned economic questions of cost effectiveness. At best, so the general assumption at the starting point of the project, landscape management and expected energy outputs should form a self supporting system. To estimate the economic feasibility of the tested technology, a cost calculation for the pilot region was elaborated. The model was based on balancing between the harvesting costs and expected yields out of the composting. Our cost modelling regarded the factors *potential yield/ha*, *plot size/allotment* and *mowing frequency* on the input side. For calculation of labour- and machinery costs we could access cost schedules from regional landscape management associations (using a compensation key of 30€/plot+5 Eurocent/m²). The calculation of outputs is based on the experiences from the previous test runs of 3A-biogas[®]-assets: Taking in account a yield of biogas of 120 m³/t (60% of methane), an output of 3 kW and an electricity tariff of 18 Eurocent/kWh, we can estimate a yield of 50 €/t organic material. Additionally, already the gained subsidies out of agro-environmental- and nature conservation schemes were taken into account for calculation. Based on these data we could calculate the expected costs and earning for each single plot. Table 1 gives calculation examples for three regionally “typical” field plots: the examples demonstrate that for large size fields (>1 ha) with intensive grassland types the yields of biomass are the central factor allowing a positive financial balance. With poor grasslands, on the other hand, a positive balancing is achieved due to the nature protection subsidies. In contrast, from an economic perspective the so called “average” grasslands generating medium yields on middle sized plots (0,5-0,8 ha) appear problematic. These types usually do neither hold high potentials of organic material, nor are they currently favoured as ecologically notably valuable by nature protection schemes. However, as highlighted by our vegetation analyses, these typical hay meadows not only cover considerable parts of the project area. They actually also suffer the highest pressure of abandonment and reforestation, so that measures for maintenance in their cases are badly needed (Kurz, 2011).

Transforming the computation to the level of the region of inquiry as a whole (about 70 ha of grassland to be managed, estimated 470t of organic material from hay, ca. 24.000 €/year earnings, 37.500 € costs, ca. 10.000 € from subsidies), our calculation saw a deficit of 3.500 €/year. This was almost exactly the amount that could be gained of charges for deposal and composting of organic waste.

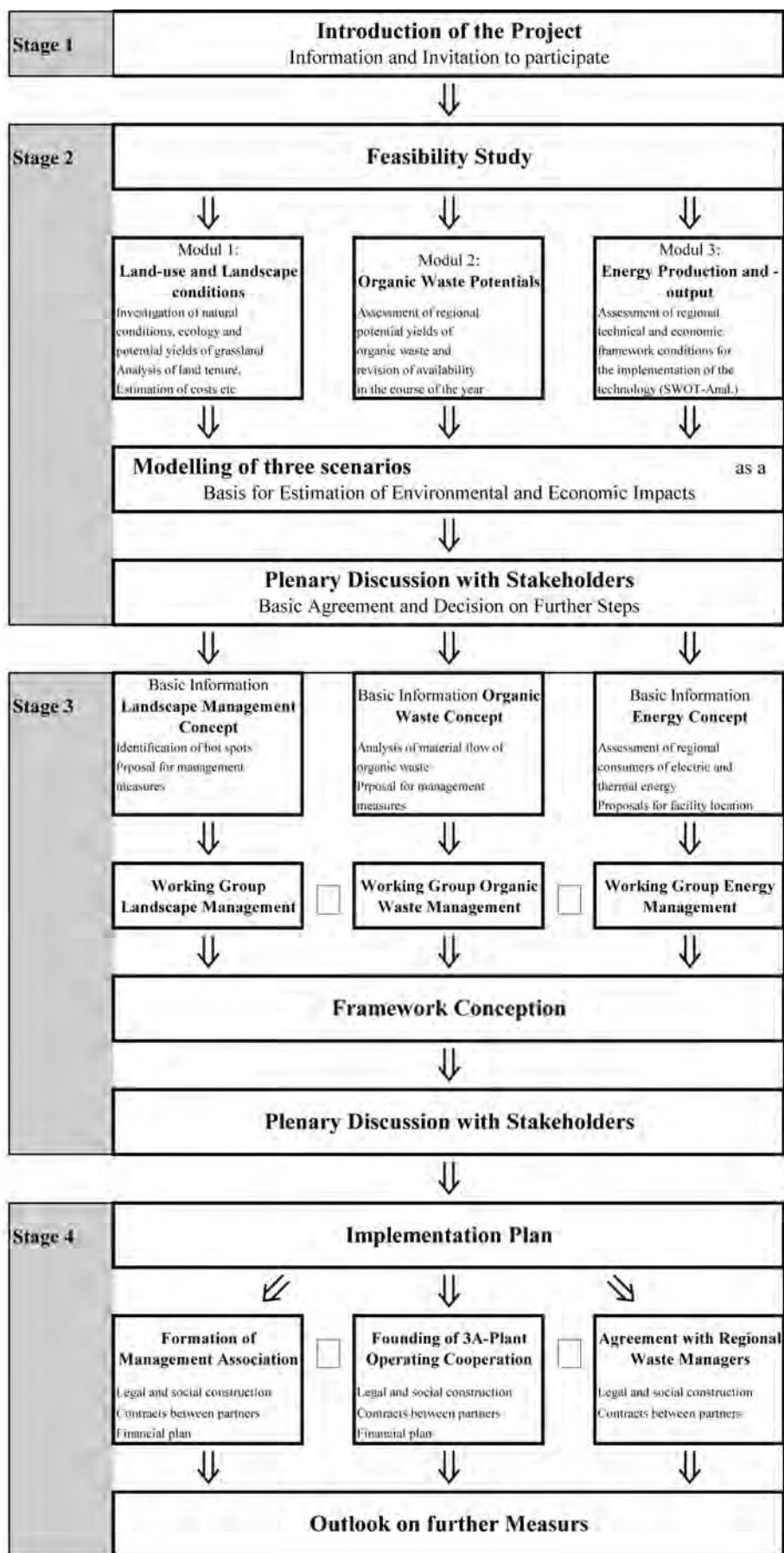


Figure 3. Project design.

Table 1

Example calculation for three plots with typical regional grassland types

Vegetation Type	Intensive grassland Alopecurus Type	Hay meadow Arrhenatherum Type	Extensive grassland Festuca rubra Type
Potential yield (t/ha)	10	7	3
Plot size (ha)	1,2	0,6	0,3
Yield (t/ha)	10,8	4,2	1
Mowing frequency/year	3	2	1
Harvest costs in €*	630	330	180
Subsidies in €**	120	60	130
Netto costs in €	510	270	50
Yield earnings from 3A biogas in €***	540	210	50
Difference in €	30	-60	0

* Calculation basis: 30 €/plot + 5ct/m² (compensation key of regional management associations)

** Calculation basis: Austrian Environmental Scheme ÖPUL, Nature protection schemes

*** Calculation basis: 50 €/t of organic material with an calculated price of 5ct/kWh

Therefore – as a result from combining the proceeding of organic waste and hay – the project could achieve an equated “raw” balance. However, neither the investment cost, nor maintenance and manpower are considered in the calculation yet. These expenses have to be funded from additional sources. In the case of our project these contain landowners’ contributions to maintenance, sponsoring and – in the long run – hopefully contributions by regional touristy as a beneficiary of cultural landscape maintenance.

CONCLUSIONS

Summarizing our experiences we can state that the 3A-biogas[®] technology offers a practical tool for combined, integrated management of landscape, organic waste and energy on a small scaled regional level. In our case study the system proved adaptable to local framework conditions and needs. The central importance for our project was achieved by the combination of the different sources: organic waste, lop and hay from landscape management. This results from the technical issues – achievement of well balanced relations between the energy

density and composting performance – as well as from the economic point of view. While the material from landscape management is only seasonally available and expenses for harvesting and bringing of allocated materials cannot be fully covered by 3A-biogas[®], organic waste material may balance and compensate those shortcomings to a certain degree.

However, a cost-effective processing of landscape management products turned out to be impossible through 3A-biogas[®], so that additional financial sources (nature protection schemes, sponsoring, tourism as a beneficiary of landscape management) have to be funded. Retrospective, for these purposes the chosen bottom-up approach proved viable: it helped creating a network of regional actors who gradually identified with the project and took on responsibility for it. From this perspective we could observe not only broader regional awareness for cultural landscape issues, promoted by the project. It subsequently also increased the willingness to financially support landscape management as a regional concern, especially with some regional non-agrarian great landowners.

ACKNOWLEDGEMENTS

We want to thank the Austrian Climate- and Energy Fund and the LEADER-Region Sauwald for funding the project.

REFERENCES

- Altrichter H. (2007) *Lehrerinnen und Lehrer erforschen ihren Unterricht*. Bad Heilbrunn. 288 p.
- Braun-Blanquet J. (1964) *Die Pflanzensoziologie*. Wien, New York. 865 p.
- Graß R. (2008) Energie aus Biomasse – ein Beitrag zum Klimaschutz? *Ökologie und Landbau*, Vol. 145, No. 1, p. 26-28.
- Hasselmann H., Bergmann H. (2007) Vom Land- zum Energiewirt: Überlegungen zur Rentabilität von Biogasanlagen auf der Grundlage unterschiedlicher Substrate und Voraussetzungen in Deutschland. *Zeitschrift für Agrarwirtschaft und Agrarsoziologie* 1/07, p. 91-100.

- Kruska V., Emmerling C. (2008) Flächennutzungswandel durch Biogaserzeugung. *Regionale und lokale Erhebungen in Rheinland-Pfalz*. In: *Naturschutz und Landschaftsplanung*, Vol. 40, No. 3, p. 69-72.
- Kurz P. (2010) Alternatives to Reforestation. Introducing a Problem-based approach to Education in Cultural Landscape Planning. In: *Cultural Landscapes. ECLAS Conference Proceedings*. p. 875-884.
- Kurz P. (2011) *Klima-, Energie und Kulturlandschaftsmodell Sawwald Donautal*. Teilbericht Kulturlandschaft. 67 p.
- Müller H., Schmitdt O., Hinterberger S. (2006) *3A-biogas. Three step fermentation of solid state biowaste for biogas production and sanitation* [online] [accessed on 30.4.2010.].
Available <http://askeu.com/Default.asp?Menu=20&Bereich=6&SubBereich=25&KW=0&ArtikelPPV=8043>
- Prochnow A., Heiermann M., Drenckhahn A., Schelle H. (2007) Biomethanisierung von Landschaftspflegeaufwuchs. Jahresverlauf der Biogaserträge. *Naturschutz und Landschaftsplanung*, Vol. 39, No. 1, p. 19-24.
- Schöne F. (2008) Anbau von Energiepflanzen: Chancen und Gefahren für die Umwelt. *Ökologie und Landbau*, Vol. 116, No. 4, p. 29-30.
- Schulze C., Köppel J. (2007) Gebietskulissen für den Energiepflanzenanbau? Steuerungsmöglichkeiten in der Planung. *Naturschutz und Landschaftsplanung*, Vol. 39, No. 9, p. 269-272.
- Schulz-Schaeffer I. *Akteur-Netzwerk-Theorie: Zur Koevolution von Gesellschaft, Natur und Technik* [online] [accessed on 30.4.2010.].
Available: <http://www.unidue.de/imperia/md/content/soziologie/akteurnetzwerktheorie.pdf>
- Van der Ploeg J.D. (2009) *The new peasantries. Struggles for Autonomy and Sustainability in an Era of Empire and Globalisation*. London. 356 p.

THE PRESERVATIONS PROBLEMS OF CULTURAL HISTORICAL HERITAGE AND LANDSCAPE IN LATVIA

Aija Ziemeļniece

Latvia University of Agriculture, Faculty of Rural Engineering
aija@k-projekts.lv

ABSTRACT

Exaggerated scale and proportions destroy the historical spatial context of the buildings of estates and their landscape. Little by little the national identity and intimacy of Latvian rural landscape having an essential role for attaching the tourism infrastructure toward rural cultural landscape have been lost. The method of industrial management creates the process of the scale transformation. The attachment of tourism infrastructure is too less for studying a separate historical object without taking into consideration the context of the historical landscape. A purposeful preservation of the cultural landscape valuable both artistically and architectonically may provide the creation of long time commercial activity of rural tourism in Latvia.

Key words: Cultural historical landscape, restoration, context, sight lines, landscape space of estate parks

INTRODUCTION

The old estate parks in Latvia are often developed in such a way that their oblong axis or some of their cross axis melt with the forest landscape in their more distant composition or pass over with the field landscape in a slow connection, too. A particularly pictorial compositional solution of Zemgale estate parks is the inclusion of the relief or river flow-as the moments of surprise in distant sight lines, or as a culmination element while (*Old Jelgava...*, 2010) estimating the landscape of the river banks.

The perception of rural landscape relating to the history of civilization in the principal sight lines or sight points is often from the roads. The expression of the visually esthetic quality of the landscape space is influenced by the length of the sight line, the width of the sight angle and the side wings of a specific sight point. The sight lines or the perspectives are visually very susceptible and fragile where this expressiveness may be lost particularly quickly by including new building scales and proportions in the landscape or by developing new groups of tree and bush plantations (Janelis, 2010).

Although in the territorial planning of rural municipalities there are defined the places of the monuments relating to the cultural history as well as their protection zones it is often only a formal presumption. The formulated length of the protection zone in the law (100m or 500m) is often too small. This problem is discussed for a rather long time and it is found that the value of an architectural monument must not be divided from the total context of the landscape space. Often a situation is created when the historical landscape may soon be covered up by new buildings usually connected with the production load of agriculture or industry in the territories of rural municipalities.



Figure 1. In the main sight points from the park not the elements of the building architecture, but the romanticism of the park is dominant



Figure 2. The house of the farm – hands of the estate with the coach house. The coach house with a splendid window of palladio type.

MATERIAL AND METHODS

The methods of the industrial management create the transformation process of the landscape scale. Particularly it may be referred to the attachment of international finances to the intensification of

agriculture. Its fast use in building has created a new scale sight lines and conclusion in the landscape space, so that some changes should be done in the territorial planning of the municipalities as regards the protection zones around the cultural historical space. In order to attach the tourism infrastructure the investigation of a separate historical object is not ensonce if it is not connected with the context of the historical landscape. The large scale of the agrolandscape and in contrast to it the compositionally fragile historical environment having the fragility of scale and forms of the building of parks and estates, often create the disharmony in the main sight points from the roads. An example is the locations of the building ensembles of Zemgale historical estate, where next to them the fertile arable lands of Latvia are concentrated.

The main axis of Grosswurzau estate is marked by a long lane of oaks which is to end at the parade courtyard of the master house (Brūģis, 1997). In some years new grain bunkers and a drying - kiln located next to the existing one have been built at the end of the lane. Next to the part of the park – huge metal hangars for storage of agricultural production.

One of the summer residences of Kurland dukedom (Lancmanis, 2003) - Swethof estate palace has been compositionally disarranged, the same way it can be said about the part of its park divided by the motor road, but in the park zone not only production of a building firm, but also building of new detached houses have been formed.

The park and the planting zone of its old trees having a historical land dam and a small water canal along the perimeter-even today mark the territory of the old park. Altaz estate palace may be perceived in a spacially wider scale where in the sight lines from the side of the Tukums road the expressive of panorama has been lost as regards the landscape, because the production building of biogas having a huge cattle stand has covered up the main sight points. The ensemble of Wilzenhof estate having the old road bed, lane, a little bridge, ponds, front courtyard and a picturesque park may be perceived approximately in the distance of half kilometer. But the southern and eastern part of the park and the estate building in the dense building zone is covered up by the living block, kinder garden and a sport hall. The regulations about the protection zone of 500 m around the cultural historical monuments adopted prove again that the condition given may not be used in all cases equally. It may be used not only as regards the historical buildings, but also to the cultural landscape space in total, where the distance of the sight lines is not larges than 500m in the territories of plains. In the territorial planning of municipalities a clear zone of building regulation and protection of landscape is not found for each of the cultural historical locations.



Figure 3. Sweythof palace in the sight line from the old road. The main facade with the stage bank of the river.



Figure 4. Sight from the palace to the river and the water meadow location of the historical road and bridge.



Figure 5. Friedrichlust palace. Architect Severin Jensen.1780. The park and place of the old pond.

It is particularly important as regards the elaboration of the tourism routes in which the main sight points from the roads characterize the identity marks of Latvian cultural landscape. The so-called “golden circle” is around Jelgava (Mitau), the former capital of Kurland dukedom. There are several summer residences of the dukedom around Jelgava – the place of the winter palace. The circle begins with the ensemble of Swethof palace making its way along the right bank of Swete river.

At present the old road bed has been forgotten and is not used, but the sight points towards the historical building ensemble with the former place of the bridge have remained. The sight lines are longer than 1 km and such protection zone is not included in the municipal territorial planning. If in such a zone the transformation of the land used in agriculture has been foreseen as a building territory, it will cover up the historical landscape.

The next place of the summer residence of the golden circle is situated 10 km from the building ensemble of Swethof – Grunhof palace having an expressive play of the relief and the road bed. Already at present the protective zone there is a dense village building with many-storied dwelling houses and detached houses breaking the expressive sight lines.

The territorial planning does not mention the possibilities of transformation of the competing building or those of regulation of the building in sides to clear the sight lines to the historical space. Quite contrary, the investments are being attached to the infrastructure in order to reconstruct the building of the after war period.

In the opposite side of the park farm labourers' and servants' house as well as their landscape space with courtyards and farm buildings are located. At present the after war detached buildings have broken in a mixed structure. While privatizing the land, the detailed planning did not take into consideration the protection line even in the distance of 100m.

After the calamity of two world wars one of the 5 summer residences of the dukedom – the splendid Lust castle has been lost completely. But Ruhental – as the most splendid of them has regained its glitter. It is nice too, that for the tourists stream coming from Riga direction to Ruhental the square of the old Bauska town council and the town council house are being restored (Lancmanis, 2001).

The historical zone of Wurzau palace is the the last one of the circle of summer residences around Jelgava (Janelis, 2010).



Figure 6. Friedrichlust palace. Old trees of the park gradually vanish and the new ones appear in their place.

The old estate road in the northern part has kept its bed and today it is encircled by the detached houses of the village which do not suppress the scale of the historical building on the left bank of Wurzau river.

The estate park is situated on the right bank of the river and its marks of altitude are lower than the left bank of the river where the palace is situated. The different mark altitude of the river banks made the sight lines of the landscape more expressive from the windows of the palace. The perimeters of the parks end with a dam and canal. In the western side next to the canal and dam the historical road with the bridge is located. The dam and canal as the last elements of the park are similar in their development to the development line of the Swethof estate park which may be seen even today in the south-west side.

The compositional building of the Wurzau estate park is disarranged by the bed of the new road, crossing the longitudinal axis of the park. The historical road and the bridge of the estate were dismantled in the 20- and 30-ties of the 20th century. Now in the southern part of the park there is agrolandscape with arable lands.

The municipal territorial planning does not mention prohibition about the possible transformation of agricultural lands for the building territory. The protection zone is necessary to be approximately 2 km long from the southern side of the park including the picturesque sight of the landscape in the direction from Oglaine estate road. From this road in the western direction on cloudless days the steeple of Wurzau church may be seen.



Figure 7. The ruin of the Wurzau palace. Architect Severin Jensen.1781. Composition axis of the palace ensemble with the park and river.

The inclusion of the cultural landscape protection zones in the territorial planning is rather difficult because the immovable properties are registered in the land book in which the protection lines are not mentioned.

Therefore, the information is to be included in the architectural planning task for every land plot separately.

RESULTS AND DISCUSION

The cultural heritage is made of the resources accumulated in total and taken as the heritage from the past and which there is a value for the whole society independently from the possession of the property (Bruģis, 2005). During the last years the main values in Europe are the human ones in the conception of cultural heritage.

In the continuous development of the society and the special environment, the cultural heritage is not used enough as the potential for a long term development as well as for the preservation of the identity of the landscape space. Everybody must take into consideration the mutual regulations of game creating and preserving the quality of the space.



Figure 8. The park of Wurzau palace. The old road as a dam and a borderline of the park.

The owners would not be allowed to obtain the land in a valuable cultural historical environment if they do not wish to take part in the preservation of the cultural landscape. The protection zone of the cultural heritage does not belong only to its owner but to the whole society.

A qualitative historical landscape space is a well-cultivated and restored cultural heritage the preservation policy of which should be included in the development conception of the rural municipal territory. It influences the possibilities of tourism infrastructure development.

CONCLUSIONS

Separate buildings cannot be loved upon from the mutual landscape space or the green grass concept included in the beginning of the formation of the historical building (relief, sight lines, old road bed etc.).

It is true that in the new socio economical conditions, the fragile historical landscape space structure meets significant changes of the property relations carrying different interests of property management which sometimes obtains the character of an elemental development in the rural municipal territories. The transformation processes of the cultural landscape should be detailed evaluating them by the specialists of the state cultural monument protection.

While searching the synthesis and harmony for the historical and modern things one must try to restore the identity of the landscape space characteristic to the cultural historical environment.

REFERENCES

- Bruģis D. (1997) *The Bornsmunde estate*. Rīga: AGB, 24.p.
- Bruģis D. (2005) *The Jungfernhof*. Rīga: Citrons, p. 3-47.
- Janelis I.M. (2010) *The gardens and parks in Latvia*. Rīga: Neputns, p. 22.-29.
- Lancmanis I. (2003) *The Schwitten and Gross-Bersteln estate*. Rīga: Citrons, p. 3-24.
- Lancmanis I. (2001) *The Garrsen and Lambertshof*. Rīga: Tipo-Print, p. 5-24; 43-48.
- Old Jelgava* (2010). LMA Mākslas vēstures institūts. Rīga: Neputns, p. 17-33.
- The Palast Ruhental. Ernsts Johans Bīrons* (1992 a). Rīga:Rīgas paraugtipogrāfija, p. 67-73, 115, 124.
- The Palast Ruhental..The Gross-Elley palast* (1992 b). Rīga: Preses nams, 82-108.
- Szoego baron Leon von Manteuffel. *Im Gotteslandchen Kurland*. Verlag-Limburg an der Lahn (2002), p. 7-18, 99 -146.
- Thimm G.,Modrow B.,Schelter A. *Historische (2000) Garten in Deutschland. Denkmalgerechte Parkpflege . Herausgegeben von der Deutschen Gesellschaft fur Gartenkunst und Landschaftskultur*. Berlin, p. 5-74.

THE FORMING ELEMENTS OF THE BALTIC SEA COASTAL LANDSCAPE IDENTITY FROM THE TOWN OF AINAŽI TO THE ESTUARY OF THE RIVER SALACA

Daiga Zigmunde, Natalija Nitavska, Raimonda Lineja

Latvia University of Agriculture, Department of Architecture and Construction
natalija.nitavska@llu.lv; daiga.zigmunde@llu.lv

ABSTRACT

The research was carried out in 2010-2011 to investigate the elements involved in forming the landscape identity of the Baltic Sea coast from the town of Ainaži to the estuary of the river Salaca covering a 14 km long coastal area in Latvia. Three aspects were distinguished in the research: visual aspects – visually recognized existing elements; historical aspects – elements existed in the past, at present have disappeared or have been destroyed; and cognitive aspects – memories, association of the place etc. Historical assessment included the study of the transformation processes of the place by using the data of scientific literature and historical materials. The case study method was used in the identification and evaluation of visual elements of the landscape by using photography, mapping and an evaluation matrix. An inquiry of experts and public was performed to highlight the existing features representing the identity of the place. The grouping of the landscape identity elements was accomplished according to their importance and meaning determined in the inquiry. The main conclusions of the research showed that there is an importance to provide landscape identity as a continuing process where the existing landscape elements interact with already disappeared features recognized in people's memories.

Key words: landscape identity, landscape elements, landscape perception, Baltic Sea coast

INTRODUCTION

This research addresses the landscape identity of the Baltic Sea coastal area in Latvia. Historically and nowadays the Baltic Sea and its coastal areas are economically essential and visually recognizable parts of Latvia. The coastal landscape of the Baltic Sea in Latvia is especially sensitive because of its attractiveness for living and recreation (*Piekrastes telpiskās...*, 2010). Sandy beaches, pine woods, healthy environment, as well as traditions and economic activities are making this place magnetic, and the area is becoming more populated and developed. At the same time the coastal area of the Baltic Sea is unique with rare biotopes, naturalness, historical heritage and diversity of landscape elements (*Kultūrvēstures avoti...*, 2008). Thus the coastal area has great potential for development based on the integration of natural, living and recreational resources (Hohlovska, Trusinš, 2009; Hohlovska, Trusinš, 2010).

However, marginalization, loss of natural and inherited values caused by the rapid development, the globalization processes and climate change have affected the pattern of this area. Therefore the coastal landscape of the Baltic Sea has changed substantially during the last hundred years. Its sensitive ecosystems and the recognizability of the places have been threatened.

The changes of the pattern and elements of the Baltic Sea coastal landscape are significant also in the context of the Latvian landscape identity. The

Baltic Sea coastal area has always been and still is a part of the Latvian landscape identity. Therefore identification, evaluation and protection of specific coastal landscape elements forming the identity of this area are essential.

The research on the landscape identity of the Baltic Sea coastal area can be divided into two multidisciplinary research fields. One addresses the issue of landscape identity, the second – the Baltic Sea coastal area.

Landscape Identity

Identity is a complicated concept because of the different interpretations of it. Under the influence of globalization the concept of identity has become very popular. It is acknowledged that no country can exist without its own identity, which covers traditions, heritage, language and the environment, and also the inner world of each individual and the country as a whole.

The word “identity” has its roots in Latin – *identificare, identifico* - to identify, means to correlate the object with oneself and being in close connection with the ongoing variability of self, proving the independent existence of self and separation of self from other persons (*Новеііууіі филозофскіі...*, 2003). On the other hand, the other word used in Latin is - *identificus* – meaning identity, absolute matching or coincidence of two objects. Scientist S. Kruks (2004) in his research has found that there are two aspects of identity,

which are often mutually mixed. "Oneness" (*memete*) is a self-similarity in the course of time, "self" (*ipseite*) is a separation of self from each other (Kruks, 2004).

The various interpretations of the concept of identity is the reason for different approaches to scientific research. Currently, the Latvian identity is mostly investigated from an economical, sociological, philosophical, political, linguistic and pedagogical aspects. But at the same time the concept of identity is closely related to the definition of landscape, where landscape is an objective reality, section of the land surface, encompassed by natural components and formations, as well as the combination of man-made elements (Ramans, 1967). Thus the concept of landscape identity is widely used by geographers, architects and landscape architects.

The research on the pedagogical aspects was carried out by M. Dirba (2003). It concerns the layered structure of the Latvian identity including ethnic, national, supranational (Latvian and / or minorities, Latvian, European and global) levels (Dirba, 2003). We can find similarity in modeling landscape identity, where a single element of landscape fits into a definite landscape, which in turn fits into the type of the landscape, region and further - into the image of Latvia.

The sociology researches cover symbolic expression of identity, for example, symbols, habits and rituals which may help to identify the nation from the outside, as well as identify it inwardly (Kruks, 2004). The symbolic meaning of separate landscape elements becomes more important when defining the identity of a specific place. The use of elements with symbolic meaning have been widely discussed in economy in connection with brands, which are most often used in the context of regional identity.

The history and culture of a specific place take great part in establishing of the identity of this territory. The historic and cultural exploration explains the existence and location of landscape structures, individual landscape elements and their groups, as well as sequentially reflects all of man's relationship with nature. Landscape identity researches have basically been focused on the exploration of regional transformation processes, sense of place and impact of urbanization processes on the landscape identity (Carter et al., 2007; Stewart et al., 2004).

Landscape researchers note the multidisciplinary and multidimensional structure of the concept of identity, where the importance of the landscape's social aspect and nature is closely connected with the level of perception, and their role in human daily activities (Massey, 1995). Researchers emphasize the importance of the political and economic processes, as well as the influence of mutual relationships of social and ethnic groups.

The assessment of historic structural elements of landscape identity is based on a comprehensive study of the history of the place - from the beginning of landscape formation, where morphological and climatic factors are of great importance, and finally to the place of each man-made element, where the changes of landscape structure and the changes of individual elements of the landscape is the result of human activities, reflecting the country's political, social and economic situation (Nikodemus, Rasa, 2005; *Piekrastes telpiskās...*, 2010). The concepts of landscape biography, landscape reading and consecutiveness of the place development have been used more often in recent years to describe interaction between man, historical events and changes in nature (Zariņa, 2010). Different matrixes have been used in landscape researches for describing historical events, where the stages of development have been shown in the context of political and economic systems, the dominant ethnic and social groups, functional changes and the appearance of new symbols in the landscape (Murzyn-Kupisz, Gwosdz, 2011).

The most important conclusion found in the works of many landscape researchers is that the identity of the landscape is changing because the landscape is a product containing natural and human elements that continuously change due to natural processes and human activities.

The Baltic Sea Coastal area

The development of the landscape identity of the Baltic Sea coastal area includes a close interconnection between natural, historical, cultural, social, political and emotional factors.

Latvian geographers A.Melluma, O.Nikodemus (Melluma, 2003; *Ainavu aizsardzība...*, 2000) and geologists G.Eberhards, J.Lapinskis, I.Grīne etc. (Eberhards et al., 2009; Eberhards, Lapinskis, 2008; Lapinskis, 2010) have investigated transformations of the Baltic Sea coastline affected by natural processes (erosion etc.). They have used topographic maps from 1935-2007, as well field surveys to evaluate these changes.

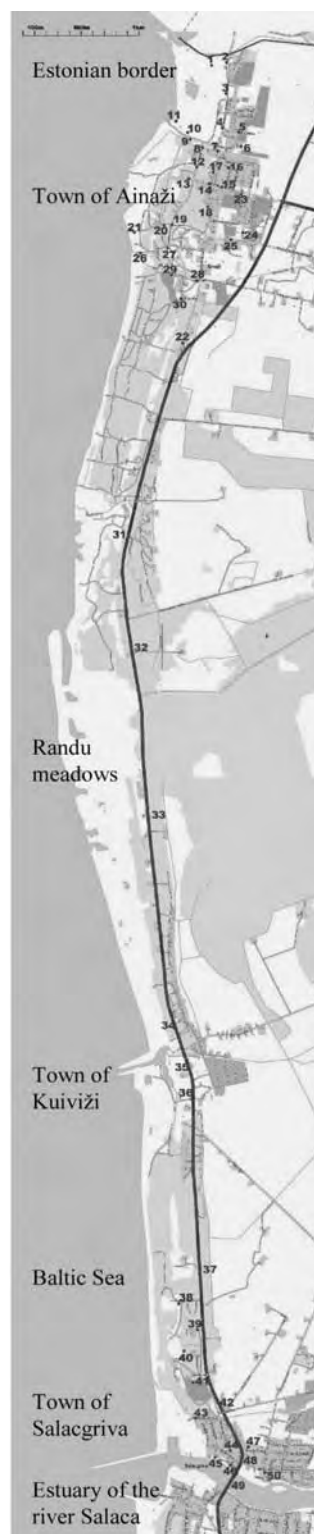
The biologists and geographers from the Latvia University have carried out scientific work to identify and preserve the Latvian seacoast biotopes and species protected on a European scale (areas of Natura 2000). This is one of the problematic issues because of the location of unique coastal biotopes in a wide range of the Baltic Sea coastal area. In the framework of this survey it is planned to establish a system of balanced conservation and management of these areas, to map biotopes, to investigate the expansion of foreign plant species, to develop individual nature protection and management plans for especially protected nature territories, and to inform the public (*Piekrastes biotopu...*, 2008). Also

the European Environment Agency addresses the public, scientists and politicians the question of importance of preserving coastal ecosystems. They point out the continuous degradation of the European seacoast which is influencing the quality of life in Europe. The recent tendencies show an increasing number of artificial and built-up territories in the seacoast areas in Europe (*Eiropas piekrastes...*, 2006).

Therefore, nowadays the possibilities of using, planning and management of the Baltic Sea coastal area is becoming more and more of a significant question. Latvian geographers A. Pužulis and K.Jansone have researched this issue in the Latvian case by pointing out the role of legislative and regulative documentation in usage, planning and management of the Baltic Sea coastal area. In their research the scientists concluded that different territories of the coastal areas should have individual development plans based on specific particularities, as well as changeability and sensitivity of the whole coastal area (Pužulis, 2010). Similar activities have been done by architects and spatial planners from Riga Technical University. The scientists J.Trušīņš and I.Hohlovskā have investigated the problems and possibilities connected with the use of the Baltic Sea coastal area for recreation. They have emphasized the role of sea coastal resorts in the historical development of specific cultural environment and heritage, as well as a necessity of sustainable development methods in the planning system of the Baltic Sea coastal areas. J.Trušīņš and I.Hohlovskā proposed a planning approach which includes control of the anthropogenic load, balanced consumption of nature resources by zoning the areas into active and passive recreation territories (Hohlovskā, Trušīņš, 2009, Hohlovskā, Trušīņš, 2010). Architects and scientists J.Briņķis, I.Strautmanis, E.Bērziņš have worked on the architectural heritage in the Baltic Sea coastal area. Those are historical buildings (resorts, summer houses etc.). Most of them are abandoned and are rarely used (Briņķis et al., 2009). The architectural heritage is one of the most important factors influencing local singularity of the sea coastal towns. Scientists have similar experiences and proposals as A.Pužulis. They pertain to the improvement of the existing legislative and regulative documentation in Latvia. Researchers J.Briņķis, I.Strautmanis, E.Bērziņš have worked out models of the development of the Baltic Sea coastal area. Those models have made it possible to interpret a development of permitted planned situations and variations in the context of definite territories (Briņķis et al., 2009).

The Baltic Sea coastal area has also been attractive for some individuals – photographers, artists, scientists etc. (Ziedonis, 2009) who have crossed the whole Baltic Sea coast from the Lithuanian/Latvian to the Latvian/Estonian border

to explore the sense of the place and natural beauty of this area. At this point it is possible to investigate the role of human perception of the place in the context of understanding of landscape identity of the Baltic Sea coastal area.



Source: maps from Google Earth's sources

Figure 1. The research object - the Baltic Sea coastal area from the estuary of the river Salaca to the town of Ainaži.

The importance of human perception and associations in landscape planning has also been pointed out in several researches of landscape scientists (Bell, 2009).

In conclusion it can be noted that researches on the Baltic Sea coastal area have mostly been carried out in the research fields of geomorphologic transformations of the sea coastal line, nature protection, spatial planning and recreation. Thus so far no extensive research has been carried out on the landscape identity of the Baltic Sea coastal area as a multifaceted and important part of the Latvian national identity.

The research of the landscape identity of the Baltic Sea coastal area was conducted in 2010-2011. The aim of the study was to investigate and determine the visual elements of different landscapes of the Baltic Sea coast involved in forming the landscape identity of this area. The research was based on a multilayered approach which included historical and field surveys, as well as human perception studies by using questionnaires of experts and inhabitants.

MATERIALS AND METHODS

Research object

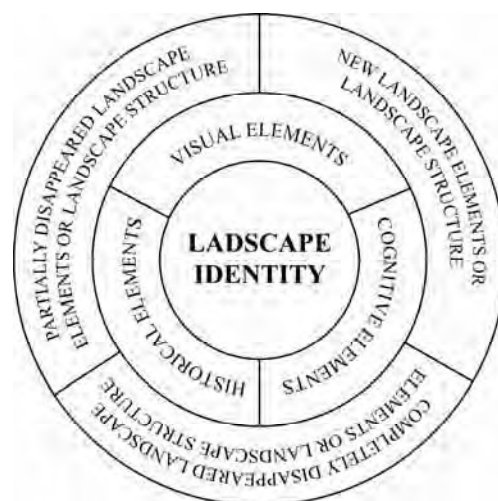
The research object is the Baltic Sea coastal area from the town of Ainaži to the estuary of the river Salaca. The research area is 14 km long and 11.3 km² large and is located in Latvia, Vidzeme region, in the North-Eastern part of the Gulf of Riga (Figure 1). The whole area belongs to the landscape protection zone of the North Vidzeme Biosphere Reserve which is the only one of its kind a special area of conservation in Latvia. The reason for selecting this territory as a research object was – a high landscape diversity of the area which includes natural landscapes, rural landscape, small and bigger towns.

The Baltic Sea coastal area from the river Salaca to the town of Ainaži is a part of Salacgrīva county. The area includes the following urban territories – the town of Ainaži, Kuiviži village and part of the town of Salacgrīva located on the right bank of the Salaca river. The town of Ainaži was founded on the place of the ancient Libyan fishermen's village near the Estonian border. Kuiviži is the fishermen's village developed on the place where the river Krišupīte flows into the Gulf of Riga. The town of Salaca is the center of the Salacgrīva county, and it was established on the estuary of the river Salaca.

Approach of landscape identity assessment

Approach of the landscape identity assessment of the Baltic Sea coastal area was based on the exploration of landscape elements which are the key to the perception of identity and which play one of the important roles in the formation of landscape

identity. The elements forming the landscape identity were divided into three groups by following criteria: visual aspects – visually recognized existing nature and man made elements; historical aspects – nature and man-made elements that existed in the past, and have disappeared or have been destroyed at present; and cognitive aspects – human memories, association of the place, traditions, symbols, emotional experiences, etc. (Figure 2).



Source: N.Īitavska

Figure 2. The groups of the forming elements of the landscape identity – visual, historical and cognitive.

The approach included the sequential investigations in all three groups and was based on determination and evaluation of the forming elements of the landscape identity. The combining of cartographical and descriptive methods, as well as questionnaires from experts and public were used in the study. According to this the research was carried out from the October 2010 till March 2011 in several stages.

Historical assessment

The historical assessment of the research area was worked out in October and November of 2010. The historical assessment included the study of the genesis of the place and transformation processes through times by using the data from scientific literature and historical materials – maps, photos and essays. In the historical assessment of the forming elements of the landscape identity the following stages were accomplished:

1. *A defining historic development stages.* The data from literature sources and archive materials (*Ainažu pilsētas...*, 2003; *Baltijas valstu...*, 2010; *Latvijas padomju...*, 1985; *Latvijas pilsētas*, 1999; *Maldavs, Melluma, Seile*, 1981; *Salacgrīvai 80*, 2008; *Salacgrīvas pilsētas...*, 2004; *Renemanis*, 2006) were used for exploring the transformation processes and events of the historical development of the research area.

Table 1

Historically important development stages of landscape

Landscape historic development			Landscape nowadays			
time period	actions, events, processes, etc.	landscape changes	completely disappeared	or landscape	partially elements	remaining landscape elements or landscape structure
1. Events or natural processes arising from natural factors						
2. Events or natural processes arising from anthropogenic factors						

According to these data, the content of the events, action or process and their changes in the landscape were described in the matrix shown in Table 1.

In the landscape historical development matrix the events and changes in the landscape were described by the following criteria: historical development period and the appropriate actions, events, processes and corresponding changes in the landscape. The collected historical data were grouped into characteristic historic development stages according to the significance/importance of the historical events or processes in the landscape changes, and the events were also divided into two groups – the natural or/and anthropogenic.

Here, it was important to mark whether the historical events can still be seen in the landscape as individual elements or as landscape structure. Thus the matrix contained information about the current situation - landscape elements, which have completely disappeared, wholly or partially remaining landscape elements or a landscape structure. These marks of the existing situation were drawn in the field surveys following in the next stage of the research – visual assessment.

2. *The research on spatial development* was based on the comparative evaluation of cartographic and photo material (*Baltijas valstu...*, 2010; *Latvijas pilsētas...*, 1999; *Latvijas padomju...*, 1985; *Salacgrīvai 80*, 2008; Renemanis, 2006) of different time periods (Eetvelde, Antrop, 2009). The data from this investigation were attached to the appropriate historical stage in the landscape historical development matrix. In the cartographical and photo survey it was important to mark the landscape elements of the long-term existence as forming elements of a definite landscape structure (Carter et al., 2007; Stewart et al., 2004), because these elements are often the key of the landscape identity. The landscape elements detected in the historical assessment were divided into two groups: fully or partially preserved and completely disappeared. They were used in the next stages of the research. The completely disappeared landscape elements or landscape structure were included in questionnaires of the cognitive assessment (the last stage of the landscape identity assessment), in order to determine whether these landscape elements form the identity of the invisible (which is not less important) landscape. Fully or partially preserved landscape elements were included into the visual assessment.

Visual assessment

The case study method (field survey) was used in the visual assessment of the landscape from December till February 2011. The method included the identification and evaluation of visual elements of the landscape by using background information from historical assessment and literature, aerial photography, maps, photos taken by digital camera and an evaluation matrix. Visual assessment of the elements forming the landscape identity of the Baltic Sea coastal area was carried out in the following stages:

1. *Developing an evaluation matrix of the visible elements of the landscape.* The evaluation matrix was developed to characterize and evaluate existing landscape elements of the area by different criteria. The matrix had three parts. The first part of the matrix gives general information of the place (view) chosen for the detecting visual elements of the landscape, as well as characterizes the visual perception of the place (view). The general information contains number and geographic coordinates of the view point, investigation time, and short annotation of the place, investigation point marked in the map and shown in the photo. The second part of the evaluation matrix describes the characterizing of a visual perception of the view. The following criteria were included into the second part of the evaluation matrix: the visual accessibility, scale, terrain, color, materials, textures, diversity, rarity, naturalism, movement, sensations (Ode et al., 2008; *Landscape character...*, 2002; *Ainavu aizsardzība...*, 2000). Different values were attached to each criterion (Table 2). The third part of the matrix included all groups of elements recognized in existing landscape (buildings, individual architectural elements, roads and paths, land surface, greenery, water) to detect the dominating landscape element of the place (Table 3).

2. *Field survey.* The obtaining of the required data for the assessment of landscape visual elements was performed in nature by using the evaluation matrix developed previously. Firstly, different landscape types were identified by subjective approach to choose different characteristic and unique landscapes for visual assessment. Fifty view points were detected and numbered. The geographic coordinates were added to each view point by using GPS navigation system (Becker Traffic Assisst 7926).

Table 2

Characterization of the visual perception

Criteria of the visual perception	Characterization of criteria
Visual accessibility	unavailable, a narrow, limited, partly accessible, open, fully accessible
Scale	intimate, close, small, medium, large, wide
Terrain	smooth, flat with some hills, gently wavy, hilly, dunes, hill, cliff, steep slope, valley, gully, gorge
Color	neutral, monochrome, nuanced, vivid, colorful, checkered, with some bright elements
Materials	natural landscape, wood, stone, plaster, concrete, bricks, glass, metal, synthetic materials, other materials
Texture	smooth, soft, fine, rough, sharp, fragmented
Diversity	uniform, simple, various, complex
Rarity	common, typical, unique, rare, unique
Movement	dead, quiet, lively, uproarious
Naturalism	natural, natural with some man-made elements, anthropogenic environment with some natural elements, an urban
Sensations	boring, neutral, pleasant, safe, calming, interesting, inspiring, provocative, intrusive, unpleasant, unsafe

Table 3

Characterization of dominating landscape elements

Groups of landscape elements	Dominating landscape elements
Buildings	ruins, separate buildings, farmstead, building groups, urban settlement, village, outskirts of a town, small town, residential area, heritage buildings, industrial buildings, military buildings, harbor, railway station, other buildings, no building
Individual architectural elements	poles, electricity and other forms of communication towers, fences, walls, monuments, bridge, elevated road, observation tower, a lighthouse, wind generators, other elements, no element
Roads and paths	trampled down paths, crisp surface pedestrian trail, a hard surface pedestrian trail, footbridge, earth road, loose surface road, hard surface road, highway, railway, other roads, no road
Land surface	rocky bank, sandy bank, coastal grassland, bogged up area, moss, agricultural land, lawn, meadow, loose surfaces - playgrounds, solid surfaces - playgrounds, other types of land surface
Greenery	grass clusters, individual shrubs, groups of bushes, individual trees, tree clusters, groves, forests, allotment, alleys, squares, parks, gardens, orchards, buffer plantings, other greenery, no greenery
Water elements	marsh, ditch, stream, river, pond, lake, quarry, swimming pool, water, sea, other water elements, no water element

Each point was mapped and photographed by digital camera in panoramic view (360°). Short description of view was presented, including key words. The evaluation matrix was filled in for each view point by choosing appropriate value of the criteria of visual perception in the first part of the matrix, and by marking the dominating landscape element in the second part of the matrix. The election of values was based on subjective approach and performed by three researchers in landscape architecture.

3. *Data processing and analysis of results.* According to the collected data, a map of landscape spatial structure and view points was created. The map contained geographic coordinates of each view point (Figure 1).

The data of the evaluation matrix were aggregated and processed by SPSS. The measurement for aggregated data was their nominal value. All matrix questions were of closed question type. For the questions which had only one response option, the data were coded and marked with numbers. But for the questions which had several response options, a dichotomous analytical method was used - each response option provided a separate variable with a column, option codes: 1 – there is an answer, 0 – no answer.

For the analysis of the results both primary and

secondary data analysis were used. Primary data analysis - empirical distribution, shows the feature under investigation at a repetition rate (the number of times the version is found in the study). Secondary data analysis - analysis of contingency, determines whether there are correlations between the presences of different nominal data. The data were summarized in Table $r \times c$, where r was the number of rows, but c was the number of columns. Set the significance level of 5% error probability (confidence level 95%). For decision making X^2 and Kramer's coefficient were used.

Cognitive assessment – associative part of the research

After identification of existing landscape elements, a survey of experts and public was performed by using data, collected and analyzed in the field survey, to highlight the elements representing the identity of the place. The questionnaires were performed in March 2011. Cognitive assessment was performed in the following stages:

1. *Developing questionnaires* were based on the data collected in two previous stages of the research. The potential forming elements of the Baltic Sea landscape identity was selected: from the historical assessment - the completely disappeared landscape elements or landscape structure that

could still remain in people's memories, elements with high heritage value; from visual assessment - dominating and specific landscape elements.

The layout of the questionnaire had three parts. The first part represented personal data of a respondent from inhabitant group – place of residence, period of living in the research area (Salacgrīva county). In the expert questionnaire this information was replaced by questions about professional experience of the respondent. Both groups were asked to mark the age and gender of the respondent.

The second part of the questionnaire was created without images to determine an associative aspect of the landscape identity of the research area. The aim of this part was to clarify the associations of a place based on people's memories, traditions, songs, beliefs, etc. The respondents were asked: to highlight the most appropriate statement about the research area (the place is unique in the world/Latvian scale, similar only to a few places or looks like many other places); to mark 3 elements most vividly characterizing the research area; to describe emotions/memories about the research area.

The third part of the questionnaire addressed the emotional evaluation of definite landscape elements/landscape structure of the research area. Images of 10 different places were selected from the visual assessment part (representatives of typical landscapes; unique landscapes) and included in the questionnaire. Specific criteria were enclosed for describing an emotional impression of each place showed in the image. They were sensations of the place: boring, neutral, pleasant, interesting, inspiring, unpleasant, unsafe; and type of the landscape: common, typical, unique, rare, unique. The questionnaires were developed on the individually created base on the web site www.visidati.lv.

2. *Questionnaires* were performed electronically and in paper format. Invitation to take part into electronically available questionnaire was send individually to each participant. Paper forms of the questionnaire were distributed and filled in the town of Salacgrīva. 326 inhabitants of the research area and 61 experts took part in the survey. The selection of the inhabitant group was based on their place of residence. They were living or had lived in Ainaži, Kuiviži or Salacgrīva before. In the expert group the professionals from the fields of landscape architecture, horticulture, environment, geography, architecture and civil engineering and art participated.

3. *Data processing and analysis of results.* The data from the questionnaire were collected and processed in the SPSS. The measurement for aggregated data was their nominal value.

The questionnaire included both - closed and partially closed and open questions. Closed and partially closed questions with a multiple-choice

data were coded and marked with numbers. But for the questions which have several response options, a dichotomous analytical method was used - each response option provided a separate variable with a column, option codes: 1 – there is an answer, 0 – no answer. For open questions the data were grouped by similar characteristics and then encoded. For open questions there was no need to be grouped together, the data were unencoded; the more specific and interesting responses were described separately.

For the analysis of the results both primary and secondary data analysis were used. Primary data analysis - empirical distribution, shows the feature under investigation at a repetition rate (the number of times the version is found in the study). Secondary data analysis - analysis of contingency, determines whether there exist correlations between the presences of different nominal data.

The data were summarized in Table $r \times c$, where r is the number of rows, but c is the number of columns. Set the significance level of 5% error probability (confidence level 95%). For decision making X^2 and Kramer's coefficient were used.

RESULTS AND DISCUSSION

The results were obtained in three stages of the landscape identity assessment of the Baltic Sea coastal area from the town of Ainaži to the estuary of the river Salaca. These were historical, visual and cognitive assessments. The obtained data and results of each stage were selectively included in the assessment process of the following stages.

The results of the historical assessment showed that there are two groups of landscape elements – still exiting or partly destroyed historical elements; and those which have already disappeared (Table 3). From historical events influencing the forming of the landscape identity of Ainaži-Salacgrīva; the historical existence of the Baltic Sea is most significant. This promoted a development of the first settlements, as well as the harbor and naval school which according to the public and expert surveys (Figure 4) were the most recognizable landscape elements of the place.

The legacy of the soviet period – the fishing industry has mainly influenced the associations of the place. These are connected with people's memories about buying fish, such as lampreys, seeing fishermen working on fishing boats. But the other aspect of this industry is associated with multi-storey houses built for workers during the Soviet period. Those buildings have created a different pattern and image of the town of Salacgrīva.

The historically developed landscape identity of this place has been disturbed, because the scale of those buildings conflicts with small churches and old wooden houses.

Table 4

Results of the historical assessment

Characteristic historical development period	Historical events	Already disappeared landscape elements	Still existing or partly destroyed historical elements
~ 6 500 years ago	Post- Litorina Sea	Some of elements located under water	Terrain of the coast
5th, 6th c.	First settlements of the Livs	Buildings and historical structure of the town	Place of the historical settlement
till 19th c.	The Great Northern War; under Russia	Castle, road network, buildings	Some manor houses; ruins of warehouse
19th c.	Development of the shipping; harbor; structure of the town	Railway, part of the infrastructure, buildings	Spatial Structure of the town, buildings (partly)
20th c.	World Wore I ; World Wore II; Soviet period; collectivization, industrialization	Harbor, other buildings and objects destroyed during World Wore II, later - without managing	Buildings, greenery

Table 5

Results of visual assessment

Characterization of the visual perception of the research area			Characterization of dominating landscape elements of the research area	
Criteria of the visual perception	Most referred characterization of criteria		Groups of landscape elements	Dominating landscape elements
Visual accessibility	limited 46%		Buildings	heritage buildings 21% small town 11%
Scale	medium 40%		Individual architectural elements	poles 33,6% fences 21,5%
Terrain	smooth 68%		Roads and paths	no value because of winter time
Color	neutral 30% monochrome 28%		Land surface	no value because of winter time
Materials	wood, stone, bricks, plaster 15-17%		Greenery	groups of bushes 19,2% wood 26% individual trees 16,3%
Texture Diversity	rough 72% simple 40% complex 38%		Water elements	no water elements 67,3%
Rarity	common 50%			
Movement	dead 44%			
Naturalism	natural with some man made elements 38%			
Sensations	neutral 30%			

This was proved by a survey where 33 % of the experts marked the view with a church inside the multi-storey building area as unpleasant.

Still existing or partly destroyed historical elements were involved in the visual and cognitive assessment to detect their importance in the forming of the landscape identity of the research area. The results of the visual assessment are presented in Table 4. In characterization of dominating landscape elements the results showed that historical buildings were perceived as dominating buildings of the research area in 21 % of cases. And this was the highest result in this group. In the materials group the most widely used in historical buildings were wood, stone and brick. These were stated as dominant materials within 15-17% of cases. In the cognitive assessment (associative part

of the research) the inhabitants' first impressions about the landscape of Ainaži-Salacgrīva and landscape elements in it were linked with the seacoast; home, family and childhood, a quiet and peaceful life.

At the same time in both survey groups (experts and public), the meaning of local activities and traditions, like Sea celebrations, festivals: Free Wave and Pozitivus etc., were pointed out as important aspects in forming the present-day landscape identity of Ainaži-Salacgrīva.

Most of the experts (61%) and inhabitants (41%) noted that the landscape of Ainaži-Salacgrīva has a specific image not found in many other places. Also the singularity of the research area in the world scale (33%) was marked in the survey of inhabitants (Figure 3).

The sensation of the landscape of Ainaži-Salacgrīva was characterized with positive feelings – pleasant (58%), inspiring (17%), and interesting (15%). Negative sensations of the place did not exceed 1.5% (Figure 4).

The harbour of Salacgrīva, jetty of Ainaži, museum of Ainaži naval school, Fishermen’s park and the river Salaca were detected as more referred landscape elements in the survey from the experts and public (Figure 5). Fish (e.g. lampreys), fishermen, sun, summer and wind were pointed out as being more popular associations of the place. As it can be seen in Figure 5, the natural elements - coastal meadows, the river Salaca and Fishermen’s park are of great importance in forming the landscape identity of Ainaži-Salacgrīva.

According to the results of the landscape identity assessment it is possible to distinguish the main forming elements and whole image of the landscape identity of Ainaži-Salacgrīva. It is a landscape with narrow spaces in it, on a small and medium scale. This landscape has a smooth terrain, seldom - hilly relief on the seacoast shaped during the period of the Litorina Sea. The landscape of Ainaži-Salacgrīva has a rough texture determined by architecture and old individual trees. It is sometimes intercepted with some brighter elements, but most frequently it is monochrome or neutral in colours which are reflected by the building materials – wood, stone and brick. In some parts of Ainaži-Salacgrīva area the landscape is complex, but mostly simple in its diversity.

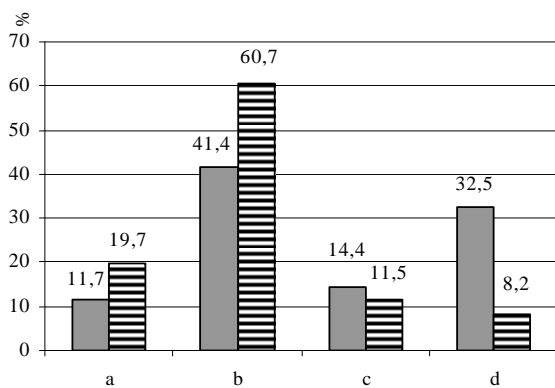


Figure 3. Landscape singularity of Ainaži-Salacgrīva, where:

■ - answers of public survey; ▨ - answers of expert survey;

a – there are several landscapes in Latvia similar to the landscape of the Ainaži-Salacgrīva; b – the landscape of Ainaži-Salacgrīva has specific image, similar only with few other towns; c – this kind of landscape is only one in Latvia; d - .no similar landscape exists in the world.

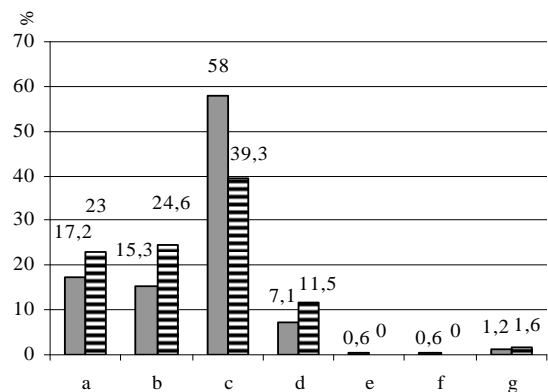


Figure 4. Emotions and memories of Ainaži-Salacgrīva, where:

■ - answers of public survey; ▨ - answers of expert survey;

a – inspiring; b – interesting; c – pleasurable; d - neutral; e – boring; f – unpleasant; g – unsafe.

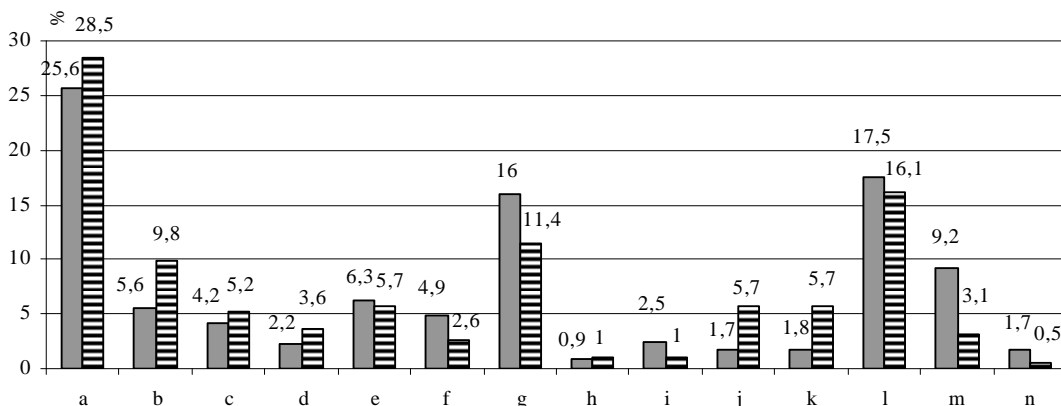


Figure 5. Elements characterizing the landscape of Ainaži-Salacgrīva, where:

■ - answers of public survey; ▨ - answers of expert survey;

a - sea coast, Randu meadows (coastal meadows); b – harbour; c – wind generators; d – old warehouse; e – Northern jetty; f – White Sun; g - museum of Ainaži naval school; h – fishermen’s cemetery; i – memorial site of soldiers killed in World War II (monument in Salacgrīva); j – stone buildings; k – lighthouse of Ainaži; l – the river of Salaca; m – Fishermen’s park; n – other.

The landscape is characterized as common or typical, in some places – unique (coastal meadows). Overall, the area of Ainaži – Salacgrīva could be described as a natural landscape with some human made elements, less – anthropogenic environment with some separate nature elements. This aspect is reflected within the movement of the landscape - dead or silent. It is alive only in places with intensive traffic and town centers.

The buildings of the research area have mostly been formed by one or two-storey heritage buildings. Fences and utility poles are the most common elements in the area. Greenery is represented by woods, individual trees or bushes, as well as alleys and allotments in the towns. Irrespective of the invisibility of the sea in the towns, it is the first element referred to as a symbol and recognizable element of the place and it plays an important role in creating the sense and identity of the place.

CONCLUSIONS

The research confirms that landscape identity has tripartite nature formed from historical, visual and cognitive aspects. Thus it is important to link all of them into one research method.

The historical assessment combined with cognitive (associative) assessment helps to understand the role of already disappeared historical landscape elements in creating the landscape identity of the place. The research results showed that still existing historical elements were more significant in the context of recognizability and visual identity of the place than the elements which had already disappeared. But those are no less important in creating a sensation and background information of the place. The visual assessment makes it possible to acknowledge the role of the existing historical elements in forming of the landscape, as well as being an important part for elaborating the

questionnaire form for the public and expert surveys. The cognitive assessment with questionnaires is the last part of the research and they are substantial in defining of the landscape identity. The research showed that the cognitive aspect was of particular importance. It is proved by the perception of water elements in Ainaži-Salacgrīva case. The respondents' answers showed a significance of the sea, while the water's surface is not visible from the town.

Thus the conclusion of the research is that there is an importance to provide the landscape identity as a complex and continuing process where the existing landscape elements interact with those which have already disappeared and are recognized in people's memories and traditions, still creating a sensation of the place. Those could be re-established in a contemporary way as symbols, art works or as traditions but they should still remain as historical landmarks of the place.

There is seasonal limitation in using this method of identity assessment, because some elements are not visible or are visually different (nature elements) in the winter time. Thus it is necessary to repeat the visual assessment during different seasons.

Sometimes legislative rules and regulations influence the landscape identity more than it is considered in the method of the landscape identity assessment. This aspect should be taken into consideration for further research. For better results interviews with experts who are working in the field of sea coastal landscape research should be conducted.

The method of the landscape identity assessment can be used to monitor the changes of the landscape identity. The results obtained can be used for working out guidelines for landscape design and development.

REFERENCES

- Ainavu aizsardzība*. Nozares pārskats rajona plānojuma izstrādāšanai (2000). Rīga: Vides aizsardzības un reģionālās attīstības ministrija. 92 lpp.
- Ainažu pilsētas ar lauku teritoriju teritorijas plānojums*. I. Daļa. Paskaidrojuma raksts [online] (2003). [Accessed on 2.05.2011.]. Available: http://www.rpr.gov.lv/uploads/filedir/Ter_planojumi/Pilsetas/Ainazi/I.dala-Ainazi-Paskaidrojuma-raksts.pdf
- Baltijas valstu kartes un aerofotogrāfijas* [online] (2010). [Accessed on 1.05.2011.]. Available: <http://www.balticmaps.eu/>
- Bell S. (2009) Social Exclusion, Rural Poverty and Landscape Change in Latvia [online] [accessed on 17.03.2011.]. Available at: www.openspace.eca.ac.uk/conference/proceedings/PDF/Bell.pdf
- Briņķis J., Strautmanis I., Bērziņš E. (2009) Development of the Baltic Seacoast as One of the Essential Factors in Preservation of Unique Qualities of the Local Scenery. *Scientific Journal of Riga Technical University*, Vol.3, p. 161 – 170.
- Carter J., Dyer P., Sharma B. (2007) Dis-placed voices: sense of place and place-identity on the Sunshine Coast. *Social and Cultural Geography*, Vol. 8, No. 5, p. 755-773.
- Landscape character assessment*. Guidance for England and Scotland (2002). UK, Gloucestershire: John Dower House, 84 p.

- Dirba M. (2003) *Latvijas identitāte: pedagoģiskais aspekts*. Rīga: RaKa. 130 lpp.
- Eberhards G., Grīne I., Lapinskis J., Purgalis I., Saltupe B., Torklere A. (2009) Changes in Latvia's seacoast (1935-2007). *Baltica*, Vol. 22, No. 1, p. 11-22.
- Eberhards G., Lapinskis J. (2008). *Baltijas jūras Latvijas krasta procesi. Atlants*. Rīga: LU Akademiskais apgads. 64 lpp.
- Eetvelde V., Antrop M. (2009) Indicators for assessing changing landscape character of cultural landscapes in Flanders (Belgium). *Land Use Policy*, Vol. 26, p. 901-910.
- Eiropas piekrastes pastāvīga degradācija apdraud dzīves līmeni Eiropā* [online] (2006). [Accessed on 2.05.2011]. Available: http://www.eea.europa.eu/lv/publications/briefing_2006_3/
- Hohlovska I., Trusins J. (2009) Development of recreation of Vidzeme coastal zone. Issues and solutions., *Scientific Journal of Riga Technical University*, Vol. 3, p. 181 – 191.
- Hohlovska I., Trusins J. (2010) Ilgtspējības principi piekrastes rekreācijas plānošanā. *Scientific Journal of Riga Technical University*, Vol. 4, p.21-24.
- Kruks S. (2004) *Kolektīva identitāte: nācijas un grupas*. Rīga: Latvijas Universitāte, 7.-24. lpp.
- Kultūrvēstures avoti un Latvijas piekraste* (2008). Letonika, otrais kongress: rakstu krājums. Rīga: Latvijas Zinātņu Akadēmijas Vēstis. 381 lpp.
- Lapinskis J. (2010) *Baltijas jūras Kurzemes krasta dinamika: promocijas darba kopsavilkums*. Rīga: Latvijas Universitāte. 65 lpp.
- Latvijas padomju enciklopēdija. 6.sējums* (1985). P.Jērāns (red.). Rīga: Cīņa. 784 lpp.
- Latvijas pilsētas. Enciklopēdija* (1999). A.Iltne, U.Placēns (red.). Rīga: Preses nams. 592 lpp.
- Maldavs Z., Melluma A., Seile A. (1981) *Ģeomorfoloģijas pamati*. Rīga: Zvaigzne. 210 lpp.
- Massey D. (1995) The conceptualization of place. In: *A place in the world? Places, cultures and globalization*. D. Massey, P. Jess (ed.). Oxford: Oxford University Press, p. 45–77.
- Melluma A. (2003) *Piekrastes ilgtspējīga attīstība* [online] [accessed on 2.04.2011.]. Available: http://piekraste.daba.lv/LV/izdale/Latvijas_piekrastes_ilgtspējīga_attistiba.pdf
- Murzyn-Kupisz M., Gwosdz K. (2011) The changing identity of the Central European city: the case of Katowice. *Journal of Historical Geography*, Vol.37, p.113-126.
- Nikodemus O., Rasa I. (2005) *Gaujas Nacionālā parka ainavu estētiskais vērtējums* [online] [accessed on 10.03.2010]. Available: http://www.daba.gov.lv/upload/File/Publikācijas/ZIN_P_GNP_Ainavu_est-vert.pdf
- Ode A., Tveit M.S., Fry G. (2008) Capturing Landscape Visual Character Using Indicators: Touching base with Landscape Aesthetic Theory. *Landscape Research*, No. 33, p. 89-117.
- Piekrastes biotopu aizsardzība un apsaimniekošana Latvijā* [online] (2008). [Accessed on 1.05.2011.]. Available: http://piekraste.daba.lv/LV/projekts/par_projektu.shtml
- Piekrastes telpiskās attīstības pamatnostādnes 2011.-2017.gadam*. Stratēģiskais ietekmes uz vidi novērtējums [online] (2010). [Accessed on 2.05.2011.]. Available: http://www.mk.gov.lv/doc/2005/RAPLMpamn_230410_piekr.502.doc
- Pužulis A. (2010) The Baltic coastal area management issues in Latvia. *Tiltai/Bridges/Bruken*, Vol.1, p. 89-100.
- Ramans K. (1967) *Ģeogrāfiskās ainavas*. Rīga: Liesma. 615 lpp.
- Renemanis V. (2006) *Ainažu pilsētai 80*. Rīga: Pērse. 171 lpp.
- Salacgrīvai 80* (2008). G. Šīmanis (red.). Rīga: Jūras Vēstis. 303 lpp.
- Salacgrīvas pilsētas ar lauku teritoriju attīstības plāns*. Esošās situācijas apraksts. II.sējums [online] (2004). [Accessed on 2.05.2011.]. Available: http://www.rpr.gov.lv/uploads/filedir/Ter_plaanojumi/Pilsetas/Salacgriva/esoshaa_situācijas_apraksts.pdf
- Stewart W.P., Liebert D., Larkin K.W. (2004) Community identities as visions for landscape change. *Landscape and Urban Planning*, Vol.69, p. 315-334.
- Zariņa A. (2010) *Ainavas pēctecīgums: ainavu veidošanās vēsturiskie un biogrāfiskie aspekti Latgalē*: promocijas darba kopsavilkums. Rīga: Latvijas Universitāte. 96 lpp.
- Ziedonis R. (2009) *Jūras zemē Latvijā*. Rīga: Zvaigzne. 287 lpp.
- Новейший философский словарь* (Original philosophy glossary) (2003). А. Грицанов (ред). Москва: Книжный Дом. 1280 с.

DEVELOPMENT TENDENCIES OF LANDSCAPE COMPOSITION IN URBAN RESIDENTIAL AREAS OF LATVIA

Una Īle

Latvia University of Agriculture,
Department of Architecture and Building
unaile@inbox.lv

ABSTRACT

Large-scale residential areas are an important part of urban environment. The present condition of the outdoor territory in Latvia in the 21st century has both positive and negative characteristics. These characteristics greatly affect further development of these multi-storey residential area courtyards. Consequently, the chosen theme on the multi-storey residential area courtyards in Latvia is topical and essential for development of any urban environment. Multi-storey residential area courtyards in Latvia can be divided into two major groups that differ from each other with the period of construction. One group comprises those courtyards built in the second half of the 20th century, and the other group – courtyards planned and constructed in the 21st century. The method chosen and applied in the research helped define the current condition of multi-storey residential area courtyards. The examples chosen and analysed by the author of the present paper provide information on typical development tendencies of residential outdoor territories in multi-storey residential area courtyards in Latvia. The results obtained in the research are essential and topical, and can be considered in development plans for any other municipality of Latvia, especially for planning, landscaping and renovating the living environment in multi-storey residential area courtyards. The quality of living environment in courtyards greatly affects its exploitation intensity for everyday and recreation necessities for every resident of the area.

Key words: development tendencies, urban residential areas of Latvia

INTRODUCTION

Modern multi-storey residential area courtyards in most cities of Latvia have been neglected. The major part of the city is occupied by large residential areas built in the second half of the 20th century. Such multi-storey residential areas and their courtyards have not experienced any transformation or renovation over the recent years. The present condition of courtyards does not correspond to modern requirements, which results in multiple problems with territorial planning, which, as a result, are not able to provide functional exploitation possibilities for residents; thus, the planning can be characterized as unsuccessful. Fewer amounts of problems can be observed in 21st century projects and landscaped residential area courtyards. Their visual appearance greatly contrasts with those built in the 20th century. The major part of these courtyards is characterized as successful and with positive development tendencies.

The aim of this article is to analyse the present condition in urban multi-storey residential area courtyards in Latvia, and to determine the typical development tendencies in these territories.

MATERIALS AND METHODS

The term 'quality of living environment' in Latvia is well known. Prior to regaining the independence

in 1991, in the Soviet Union period, Latvian architects were intensively working on such issues as healthy environment, environment aesthetics, and environment space organization. The economic situation of that period and ideological aptitude towards better future allowed thinking of environment quality and aesthetics. Nevertheless, today this great housing period has left considerable serious problems for the further development of urban residential areas. These areas typically have uncountable landscape composition problems that affect every resident of the territory. The neglectful attitude of residents towards the living environment, non-functional spatial planning that causes irreversible negative consequences, is only a small part of greater problems in large-scale residential areas. Consequently, to determine the present condition the empirical method was applied and statistic data (survey) were gathered from 100 respondents. The empirical method comprised the definition of the present condition, its observation and analysis of legal framework materials in Riga, Jelgava, Ventspils and Liepaja cities in the summer of 2010. The data collected from the survey group of 100 respondents presented information that precisely evaluated the present condition in multi-storey residential area courtyards. The group of the respondents comprised residents from the territories analysed from the age 20 – 65, in Riga and Jelgava multi-storey residential areas. The questions

prepared cover the following topics: resettling from one multi-storey residential area to another residential area; residents' knowledge on infrastructure modernization projects proposed by the municipalities in their residential areas; the most successfully planned modern courtyards, and the processes affecting courtyards, according to the residents (Karpova, 2008; Īle, 2010).

RESULTS AND DISCUSSION

A modern multi-storey residential area courtyard – it is a sophisticated multi-functional space in the environment that is used by thousands of people daily. Unfortunately, in Latvia, the major part of these territories has unsuccessful planning that greatly affects the present condition in these territories. For example, see Figure 1 and 2. The projects constructed in the Soviet Period today are no longer able to bear the great load because many aspects of residential outdoors have changed. There are multiple problems that also affect the requirements of the building regulations LBN100 for planning and organising territory.



Source: (Пучин et al., 1977)

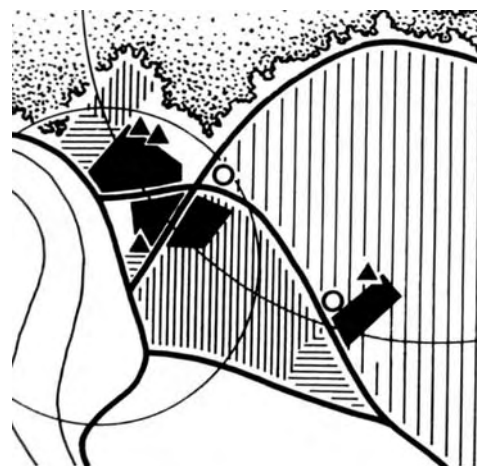
Figure 1. Liepāja city housing example.



Source: (Пучин et al., 1977)

Figure 2. Liepāja city quarter housing plan, where 1–in-built servicing institutions (canteen, bread shop, cafe); 2–public utilities (washhouse, garages, steamshop and fuel storehouse).

These regulations for urban housing have not been in force since restoration of independence. Nevertheless; it defines requirements that concern, for example, the amount of parking lots, the distance of new buildings from residential buildings, and insulation requirements and usage that is important in the context of urban planning. Urbanization gradually takes over more new territories. The deeper the process, the more complex the emerging problems are. Having regained the property rights for several free housing land territories, they are freely sold to different investors who propose to project and build new residential buildings, ignoring the common housing principles of the area. Without a unified area development plan, where detailed humanization propositions are foreseen, it is easy to imagine the chaos that arises in the course of such actions in the residential areas of Riga. Therefore, it is essential to ensure that area detail plan projects are prerequisite also in large-scale residential areas. To stop the technical progress in housing is practically impossible and it is not necessary to do so. It is important to find ways how to improve, enrich, and make the architecture that defines the image of cities and countries in the whole world more diverse. If only the building itself is considered in planning, then the city can face great problems. There will be very few comfortable and open spaces. It is especially necessary to accentuate that in general and detail plans of national, regional, urban and municipal development, spatial structure composition, and its visual landscape image has to be granted a special important place, see Figure 3.



Source: (Пучин et al., 1977)

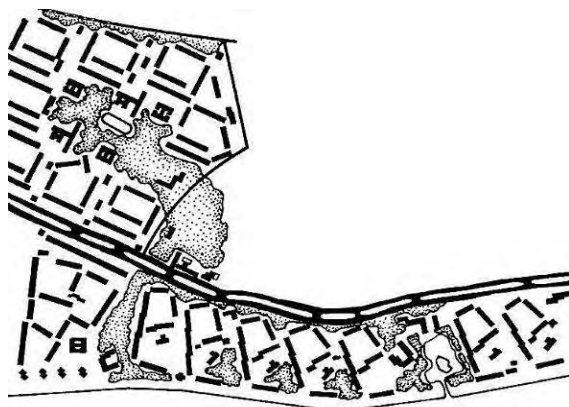
Figure 3. Ventspils city north-eastern area residential zone location, where 1–new residential areas; 2–large-scale residential housing area; 3–estate housing; 4–reserve territories for residential area building; 5–children institutions; 6–schools.

It can be noted that landscape architecture, as one of the most important parts of territorial environment planning, emerges on the basis of progressive functional, economic, and aesthetic factors. It improves the development quality of living environment in the broadest urban housing aspect. Landscape architecture projects are an essential and guiding part of territorial environment planning. Strictly observing these regulations, landscape composition in multi-storey residential areas in Latvia in this situation would gradually improve and prevent further development of negative tendencies. It would be unfortunate, if the projecting, housing and Latvia climate-appropriate residential home programmatic experience would lapse and the quiet period in housing sphere would linger.

Excluding some very unsuccessful examples, the first housing boom of the 21st century has enriched the stock of residential buildings in Riga with interesting and user-friendly examples of architecture. With few exceptions, buildings of this period are not geographically located in chronologically closed large territories like witnesses of earlier housing period – Bulvāru loks (semi-circle of boulevards) built a century ago, Āgenskalna priedes and Ķengarags areas, or Purvciems area – built forty to fifty years ago, or Mežciems, Zolitūde, and Ziepniekkalns areas – last decade of the Soviet industrialization. See Ķengarags residential area housing scheme in Figure 4.

The region of Riga is developing faster than other regions of Latvia, therefore, unwanted phenomena and perilousness caused by uncoordinated development are more frequent than in other regions. Consequently, the residents of these territories want something to be changed. See the respondent opinions in Table 1.

At present, multi-storey residential areas develop unevenly, and there is a danger of stratification of several multi-storey residential areas.



Source: (Buka et al., 1987)

Figure 4. Ķengarags residential area planning and housing scheme in Riga.

Table 1
Respondent opinions about moving from multi-storey residential area

Nr.	Respondent opinions	%
1.	Would like to move to another residential area that is more functional and suitable for everyday needs.	30
2.	Do not want to move to another area, it is not necessary, because everything is satisfying.	12
3.	Have thought about moving to another residential areas, but the financial condition is not safe enough to move.	58

The main part of multi-storey residential areas does not correspond to the modern requirements of multi-functionality, and the residential fund is worn out.

Another considerable problem is that the area is overcrowded by residents of nearby residential areas, which disturbs well-being of inhabitants, and does not allow the area to function as intended. The respondents find that the main reasons for this problem are as follows: the areas are constantly unattended and unmaintained; the infrastructure is of low quality; the roads are only mended temporarily; financial difficulties (municipal and private); the increasing car amount causes disorder in car parking near the residential houses, the wear of housing and surrounding landscape; culture, attitude, and behavior of inhabitants, their indifference and neglectful attitude; activities and decisions made by the municipalities; teenage vandalism; property management inconsistencies and unwillingness to maintain the area; poorly planned and non-functional territory plans; location of multi-storey residential areas; residential areas are often located on private land properties; therefore, the municipalities cannot invest in private properties, for example, in order to reconstruct the roads. Aside of the above mentioned facts, an important aspect is the residents' competency as regards the present development processes in multi-storey residential areas, see Table 2.

By providing in due time the constructed surface and underground street infrastructure that includes complex infrastructure development – reconstruction and renovation of street surface and roads, construction of sidewalks and car parking lots, bikeways, water and sewerage network, storm water maintenance systems, electricity and lighting, electronic communication, etc., it helps developing attractive and qualitative urban environment that is one of the main prerequisites for creating qualitative and aesthetic living environment.

Table 2
 Residents' competence about municipality
 organized infrastructure modernization project
 realization over the last year

Nr.	Resident's opinion	%
1.	Yes, the project has been carried out	28
2.	No, the project has not been carried out	56
3.	Lack of information	16

Source: (Afaņaševa, 2009; Briņķis, 2004; Economic and Ecological Factors..., 2006; Īle, 2010; Karpova, 2008; Krēģers, 2009; Liepa-Zemeša et al., 2009; Planning Region..., 2007; Strautmanis, 1982; Strautmanis et al., 2003; Widarsson, 2005; Ерохина et al., 1987).



Source: from author's personal archive

Figure 5. Outdoor territory landscape for adult activity in Ventspils.

Multi-storey residential areas present multiple possibilities for applying physical changes and transformations that should be done in many multi-storey residential area courtyards. For example, see Figure 5. The development of these objects can critically affect the social structure of the property. The decisions made can affect the way how buildings are used and their maintenance process. It is an essential criterion for successful regeneration. These days transformation of old factories into residential or office buildings is not an innovation, it is, instead, a logical development – industrialization of the city centre or its neighborhood is neither economically, nor ecologically substantiated, see Figure 6.

Unfortunately, by constantly relying on the proximity of parks and multiple recreational possibilities they provide, it is now common that the idea of creating children playgrounds in the courtyard territory is often neglected, and instead, many car parking areas are constructed. It is unfortunate; because well planned and landscaped private courtyards facilitate the unification of micro-communities, improve relationships among the residents, which is an irreplaceable quality in the modern stressful and rapid lifestyle to establish new communications.



Source: (Rukšāne, 2009)

Figure 6. Former flour storehouse 'Druva' transformed into residential building.



Source: from author's personal archive

Figure 7. Courtyard design in „Dienvidu pakavs”.

Another important issue is the use of the composition elements: colour, shape, rhythm, dynamics, flexibility and material (glass, concrete). One successful example of residential area landscape composition can be found in Riga – “Dienvidu pakavs” residential building complex in Ziepniekkalna area, see Figure 7.

Another successful example is “Iecavkrasti” in Jelgava. The respondents find that the area courtyard is functional, aesthetically pleasant, harmonious, tidy and well planned. In case if the first random development visions are realized, the 119 series nine-storey and twelve-storey residential building landscape would be supplemented by impersonal residential and office towers. Nevertheless; good ideas, if presented in the right light to the right person, tend to be fulfilled, as it was in the case of “Dienvidu pakavs”. The “Sarma & Norde” architects were successful enough to convince the owner of the project to consider the benefits of a perimetrical or horseshoe-like shape housing, the need to renovate Ziepniekkalna area, and the human factor and successful landscape, maintaining the initial owner's economy based and urban building regulations approved requirements, such as the amount of the square meters, cost of a square meter, selling possibilities and housing density, insulation etc. The horseshoe-like shape

ensures that the public space quality is not merely a toll paid by the owner to the city, but also a well-planned functionally aesthetic part of the courtyard. The courtyard territory is also available to the nearby area residents – pedestrians, and its two-level planning creates a special feeling of being in a private territory, where the outdoor image can be observed only in close-up, see Figure 8. The colour segments logically divide two play areas – for younger children and older. They are adapted almost for all children’s needs: crawling, climbing, sliding, drawing and shaping, but it lacks such an important item as swings. The modern idea of planting berry bushes and fruit trees near the playground is a ‘tasty’ and successful solution. Along with falling leaves of autumn, a topical issue might become the terrace maintenance. The courtyard plan ensures that there are no parking spaces on the territory, instead – parking lots are constructed underground, which is a modern and ecological solution that takes into consideration the safety of children. In both courtyard territories the central elements of the territory are trees - the oak tree and lime-tree - which were maintained before the area was even built, see Figure 9 and 10 (Rukšāne, 2009; Towers, 2000; Ventpils city development..., 2007).



Source: from author’s private archive

Figure 8. Playground constructions in „Dienvidu pakavs”.

Today the initiative of residential building owners and residents has become more important not only as regards the energy efficiency, but also the issue of courtyard maintenance. There are courtyards that are initially planned to be maintained by the municipality, but there are such exceptions where, after privatization, the resident becomes the owner of the apartment, and the shared area of the residential building, as well as its surrounding territory. Consequently, the responsibility over the courtyard lies on every resident of the area; therefore, its maintenance and renovation is to be performed by the residents themselves. Unfortunately, the residents are poorly informed about how these issues are to be resolved and how to properly organize the courtyard territory. A typical example of this problem is a courtyard project in Jelgava city large-scale residential area, see Figure 11. Planning the first environmental education territory in the city, the municipality has proposed the top level aim for reorganization of the infrastructure in public space environment – to make people aware of nature’s processes by allowing observing and comparing.



Source: from author’s private archive

Figure 10. Central element – lime-tree in „Dienvidu pakavs”.



Source: from author’s private archive

Figure 9. Central elements – oak trees in „Dienvidu pakavs”.



Source: from author’s private archive

Figure 11. Example of courtyard plan in Jelgava.

In this educational territory children and teenagers will have the opportunity to study nature through feelings by coming into contact with natural materials, actively playing in specially made constructions, and by observing and applying informative elements in their activities. The environmental education square is constructed in the shape of a spider web, with multiple pathways for acquiring nature, for example, Lauku taka (Country path), Zvēru taka (Animal path), and Putnu taka (Bird path), where several elements of nature are located, such as an ant heap, sun clock, and spider's nest. All constructions and the relief are made of natural materials – wood, stone, sand, and gravel. In the centre of the square there are swings, slides, and other playground constructions, and there are benches placed around the square. The equipment of the square is appropriate for children from the age 2-15 years, and the total area of the territory is around three thousand square meters (Bartaševics, 2009; Čepanone, 2009; Jerošenko, 2009).

A significant difference from the earlier residential housing territories and those built at the beginning of the 21st century is that now it is required that the area provides at least one parking space for every apartment, and this space has to be within the territory of the residential housing. If the building construction takes place in the whole quarter:

- car parking lots can be constructed in the underground, on the territory surface, and in another multi-storey building;
- if only one building is constructed, then the amount of its apartments depends on the amount of the parking spaces;
- in case of underground parking lots, the cost of building becomes significantly higher and the landscape is planned without trees.
- courtyards can function as car parking lots with an obligatory children playground squeezed into the corner. This type of planning can often be observed in Riga, and it emphasizes negative development tendencies of the courtyard, see Figure 12.



Source: from author's private archive

Figure 12. Children playground near underground parking lots.

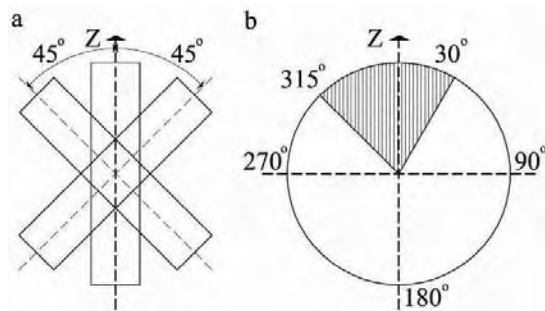
Table 2
 Residential environment aims for rehabilitation and humanization

No	Desirable requirements
1.	Disposition of auxiliary buildings and low quality residential buildings that do not correspond to the modern housing sanitary and hygienic requirements in perimetrical building quarter indoors.
2.	Vertical and horizontal zoning of the quarter indoor territory for creating areas for car parking in one or several levels and resting areas for people from different age groups, and creation of new well-planned pathways for pedestrians.
3.	Improvement and development of greenery system using both quarter indoor terraces and roof terraces.
4.	Improvement of the existing houses, eliminating communal and replanning low quality apartments.
5.	If necessary, eliminate apartments from building's first and second floors to build rooms for trade, offices and other public functions.
6.	Exploitation of the roof territory for building apartments and art workshops.
7.	Construction of new houses, using spaces in between perimetrical buildings, or in separate cases, building new groups of buildings inside the quarter indoor territory.
8.	Improvement of the building facade visual quality using colours and modern decorative techniques, considering also the roof coverage as a view both from the street and higher levels.

Along with the above mentioned solutions to be performed, another important issue that would provide comfortable living environment for residents is the improvement of the sanitary and hygienic conditions in the areas considered. It is important to diminish the density in residential areas to ensure good insolation, noise isolation and aeration, see Figure 13 - Insolation scheme for residential buildings.

The noise level in residential complexes depends on the type of planning and housing. The transport noise level in residential territory depends on the location of the residential buildings. Optimal space should be foreseen already in the project – on the one hand – the housing area should be minimal, and – on the other hand – it is necessary that the area of free territory is as large as possible.

The climate of the area is defined not only by the size of the greenery area, but also by its quality.



Source: (Briņķis et al., 2009)

Figure 13. Residential building insulation scheme, where a–building location; b–favourable and unfavourable areas.

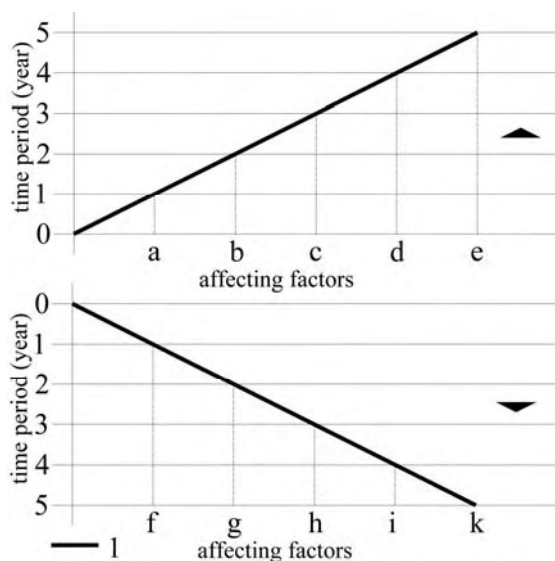
In multi-storey residential housing areas it is necessary to provide recreational zones and children playground areas.

These must also be a detached area for garbage disposal bins, which could be one for several buildings, because it is really difficult to find a place 20 meters from windows, but no farther than 100 meters from building exits. In many cases the solution for this problem is even better, because garbage disposal bins are integrated in the first floor of the building or under a separate lean-to. New housing projects lack simple everyday necessity constructions – sheds. There are often problems for residents to find a place to store seasonal equipment, such as boats, skis, bicycles, which are often stored on the balcony. An irreplaceable part of the new housing project is a transformer. It is built with a reserve for future neighborhood with the developer's money and given to the electric power supplier. Storm water maintenance has been performed neither during the Soviet period, nor since the restoration of independence of Latvia. There is no well-defined responsibility system (it is unclear which institution is responsible for storm water maintenance and the corresponding institution). Storm water sewerage systems are joined with other economic sewerage systems or vice versa. No inventory of storm water maintenance systems has been performed, the systems are outworn and they cannot perform as intended. There is no storm water maintenance models projected in Latvian cities. Even worse – the technical infrastructure and their provided public and social service do not correspond to the European standards. The philosophy of storm water maintenance has changed over the last two decades. An ideal storm water maintenance system is a system that allows absorbing and storing the water in the place of origination. Today the main idea is to incorporate building systems with urban and landscape planning, providing that the quality of area where storm water is collected would not significantly change. According to the regulations regarding LBN (The Latvian Building Code)

223–99 the storm water maintenance systems are to ensure qualitative disposal of water where the frequency is around 0.33 – 20 years (usually 0.5 – 2 years) depending on the type of building, the size of the catchment area and the land surface slope. Overflow of land is allowed in case of intense rain, where its frequency is around 10 – 100 years (usually 50 years), preventing the building basements from overflowing (Buka et al., 1987; Economic and Ecologic Factors ... , 2006; Krēgers, 2009; Kruše et al., 1995; Saistošie noteikumi Nr. 09–11 ... , 2009; Strautmanis et al., 2003; Vides aizsardzības un reģionālās ..., 2001).

The economy of urban housing is greatly affected by rational territory exploitation. The length of all engineering network (underground and surface) and the width of the territory for landscaping are planned according to the height of the buildings and their density. Further course of residential housing development in this period is connected with finding free territories in new and old cities, as well as with transition to wide urban reconstruction. Only with strict planning the sustainability and durability can be achieved, at the same time, with the responsibly considering what happens on the ground level. When planning new residential areas or cities on a flat relief (Riga and its surrounding area), the most attention is to be paid to the housing silhouette as a whole, and the relation between separate objects as one of the most important ground rules for harmonization of the relation between the environment and the newly created system. The aim for further development of environment is a creation of multi-functional and intensively exploitable urban environment, as well as maintenance of the identity of the area, its improvement, and harmonization of the environment.

Looking from a broader perspective of urban environment, a priority should be the renovation and modernization of already existing densely populated residential areas, as well as their humanization, improving the public transport accessibility. This action might prevent people from moving away from their present residences, and the city from expanding. The problem lies in the fact that not always the needs and requirements of inhabitants can be satisfied and fulfilled in the area of their residence, because it is often hindered by external factors that cannot always be affected. Looking at the present situation in courtyards of large-scale residential areas from the aesthetic quality perspective, the general image of environment is rather monotonous, boring and dilapidated. There are several factors that affect the aesthetic quality of residential areas in the territories analysed, see Figure 14. According to the authors' observations, such negative factors found in these areas make the residential outdoor environment unpleasant, degraded, and depressing.



Source: author's construction

Figure 14. Factors affecting aesthetic quality, where l—aesthetic quality curve; a—good social conditions; b—safe environment; c—harmonious environment; d—functionality; e—high quality landscape and greenery; f—bad social conditions; g—degraded environment; h—disharmonious environment; i—non-functional environment; k—low quality landscape and greenery.

The issue of the aesthetic quality in courtyards is an essential aspect of public outdoor environment which needs to be considered more often in the future, and it is necessary to find more solutions for more successful development of these territories (Buka et al., 1987; Liepa–Zemeša et al., 2009; Strautmanis, 1977; Treija, 2008; Environment

sciences, 2008).

CONCLUSIONS

The data obtained in the research process have provided essential and important information about the present condition of multi-storey residential area courtyards in Latvia that were built both in the Soviet period and in the last decade. Consequently, the housing period is one of the main aspects that presently determine further development of courtyards in Latvia. Having analysed the territories selected, it has become obvious that the development process of these territories at present is uneven. The negative features that degrade the present condition of multi-storey residential area courtyards need to be prevented, considering the opinions of the residents of these areas, and encouraging them to join in residential area maintenance activities. Such actions might prevent the area from degrading and would change the residents' negative attitude towards residential environment, where they spend the major part of their lives. There are not enough multi-storey residential area courtyards in Latvia to characterize them as functional, aesthetically pleasant for pleasant recreation, and as harmonious and tidy. The problems enlisted were analysed, which led to the conclusions that should be considered by any municipality and private owner for further investment in outdoor territory development, in order to create and renovate the courtyards of these multi-storey residential areas, providing safe and pleasant environment for every resident of the territory.

ACKNOWLEDGEMENTS

The work was supported by the European Social Fund project „Realization assistance of LLU doctoral studies”. Contract No. 2009/0180/1DP/1.1.2.1.2/09/IPIA/VIAA/017.

REFERENCES

- Afanasjeva A. (2009) Main Motifs: the change of zoning and the red lines. *Jelgavas Vēstnesis*, No.12, p. 6–7.
- Bartaševics R. (2009) Children Playground Area Found in RAF Community [online] [accessed on 12.11.2009.]. Available: <http://www.jelgavnieki.lv/?act=10&art=14201>
- Briņķis J. (2004) The Main focuses of functional and architectonically spatial structure transformation in the residential areas of Latvia. *Architecture and Urban Planning, Scientific writings by Riga Technical University*, Vol. 2, No. 5, p. 26–29.
- Briņķis J., Buka O. (2009) Urban Planning Aspects for Housing Complexes. Riga: *Riga Technical University*. p. 96.
- Buka O., Volrāts U. (1987) Sanitary Hygienic Conditions In: *Urban Planning*. Riga: Zvaigzne, p. 215–217.
- Čepanone S. (2009) Environmental Education Square Opened. *Jelgavas Vēstnesis*, No. 44, p. 3.
- Economic and Ecologic Factors for Sustainable Storm water Maintenance in Residential Areas* (2006). Phare 2003. Jelgava: Jelgavas Tipogrāfija. p. 56.

- Īle U. (2010) Guideline for development of landscape spatial composition of the residential areas. *Annual 16th International Scientific Conference Proceedings. Research for Rural Development 2010*, p. 169–173.
- Jerošenko V. (2009) New Solutions needed for Improving Apartment Houses [online] [accessed on 18.07.2010.]. Available: http://www.managimene.lv/bizness/nepiecesami_jauni_risinajumi_daudzdzivoklu_namu_sakartosanai
- Karpova Z. (2008) The quality of living space in Latvia. The present state. *Architecture and Urban Planning, Scientific writings by Riga Technical University*, Vol. 10, No. 2, p.180–192.
- Krēgers I. (2009) Solid Residual of Wonder. *Latvijas Architektūra*, No. 84, p. 76–78.
- Kruše M., P., Althaus D., Gabriēls I. (1995) *Ecologic housing*. Riga: VAK, Bundstift, Bildungswerk Umwelt und Kultur, Preses nams, p. 30–80.
- Liepa–Zemeša M., Treija S. (2009) High-rise Building Development in Urban Environment. *Architecture and Urban Planning, Scientific writings by Riga Technical University*, Vol. 10, No. 3, p. 52–66.
- Riga Planning Region Spatial (Territorial) Planning. Part I Present Condition. Appendix. Data for Present Condition Analysis (2007) [online] [accessed on 22.09.2010.]. Available: <http://www.rigaregion.lv/pub/main.php?lapa=271&oid=274>
- Rukšāne I. (2009) „Park Side” on Rūpniecības street. *Latvijas Architektūra*, No. 85, p. 40–44.
- Strautmanis I. (1977) *Dialogue with Space*. Riga: Liesma, p. 25–127.
- Strautmanis I. (1982) *Art in Architecture*. Riga: Liesma, p. 71–86.
- Strautmanis I., Briņķis J. (2003) The rehabilitation of living environment in the mixed-housing areas of Riga. *Architecture and Urban Planning, Scientific writings by Riga Technical University*, Vol. 2, No. 4, p. 58–63.
- Towers G. (2000) *Shelter is not enough* [online] [accessed on 16.01.2010.]. Available:http://www.google.com/books?id=L8iVNk7RVuYC&printsec=frontcover&hl=lv&source=gbs_slider_thumb#v=onepage&q=&f=false
- Treija S. (2008) Riga Large-scale Residential Area Structural Development Affecting Factors. *Architecture and Urban Planning, Scientific writings by Riga Technical University*, Vol. 10, No. 2, p. 154–170.
- Ventspils city development programme 2007 -2013. Present Condition and SWOT analysis.* (2007) Ventspils City Council. 139 p.
- Ministry of Environmental Protection and Regional Development (2001) Perspective Structure of Population Structure. In: *Development of Population Structure*. Riga: Jumava, p.71–80.
- M.Ķļaviņš, O.Nikodemus, V.Segliņš, V.Melecis, M.Vircavs, K.Āboliņa(2008) *Environmental science*. Riga: Academic Staff of the University of Latvia 600 p.
- Widarsson L. (2005) Stormwater and accessibility. In: *Sustainable city of tomorrow*. Stockholm: Vasteras. 142 p.
- Ерохина В.И., Жеребцова Г.П., Вольфтруб Т.И., Покалов О.Н., Щурова Г.В. (1987) *Озеленение населенных мест*. Москва: Стройиздат, с.45.–83.
- Пучин Э., Пиешиньш Я., Лусе М. (1977) *Жилой комплекс малого города*. Рига: Зинатне. 268 с.

POSSIBILITIES OF UNIFIED LANDSCAPE DEVELOPMENT IN TRANSNATIONAL BORDERLAND VALKA-VALGA EXAMPLE

Maija Jankevica

Latvia University of Agriculture, Faculty of Rural Engineering,
Department of Architecture and Building Construction
maija.jankevica@inbox.lv

ABSTRACT

There are only few border cities over the world and one of them is located at the northern border of Latvia. The purpose of the research was to assess the possibilities of single development of common borderspace areas and a historical centre in Valka – Valga. In the research qualitative research methods: cartographic, descriptive, comparative and analytical methods were used. In the research the green structures in Valka and Valga cities were analyzed, common areas identified and directions for a positive impact on the overall landscape of the border town were determined. Examples of architectural practice in other European border towns were used to provide landscape improvements. Development of the city character is influenced by the architectural infrastructure and esthetical resources. Border towns have experienced different historical processes. Each European border town has different landscape values that sometimes include diversity and contrast.

Key words: border towns, urban landscape, divided cities, architectural and landscape quality, border areas

INTRODUCTION

A border town is a town close to the boundary between two countries, states or regions. Usually the term implies that it is one of the things the town is most famous for (The Free Encyclopedia...).

A pair of border cities consists of two separate but almost adjacent cities on a national border. A major distinction, to be made in relation to such cities, is between duplicated and partitioned border cities. Duplication refers to situations where the establishment of one border settlement sooner or later was followed by the rise of a second settlement on the other side of the border. This type of development could be found along the borders of Mexico and the USA, and Canada and the USA. Partition occurred mainly in the Central Europe after the World War 2, when previously united cities were divided into two different entities by drawing new boundaries.

A new type of paired border cities is connected cities – border cities that have been paired by new infrastructure, for example, Calais and Dover are connected by the Channel tunnel, and Copenhagen and Malmo by the Oresund Bridge (Buursink, 2001).

For many decades while Valka has been developing into the jurisdiction of two states, the quality of the townscape and the condition of the urban structure has significantly decreased (Bratuškis, 2008). Some authors point out that border towns are unique places with historical, national and social interaction between two different countries. Inter borderspace as a unique urban phenomenon in the historical development is not an obstacle, but an

overall quality of the property for citizens (Bratuškis, 2008).

To find solutions for Valka – Valga urban problems, it is necessary to set the main goal and tasks to achieve the goal.

The main goal of the research is to assess the possibilities of single development of common borderspace areas and the historical centre in Valka – Valga, which is divided by the current situation.

The main tasks are to describe frontier settlements, their types and inherent properties, to characterize the Valka – Valga physiographic features and their cultural and historical processes, to research territorial planning documents, to inventor the current situation of the green areas and urban territories in Valka - Valga, to compare the architectural and landscape values in six European border towns and to find solutions to challenged landscape and urban problems in Valka – Valga.

So far no one has acted on a theoretical level in the landscape adaptation field, especially in the environment of the border town. Currently, the landscape formation occurs within the same country. It is not so popular to promote united development for several countries sharing a common site. The main objective of all projects is to further the developments of both towns planning together, then the boundary will become merely symbolic. After the Schengen agreement there are many border towns in Europe, which try to go beyond nationalism and create a common cross border identity, for example, Kerkrade – Herzogenrath on the Dutch – German border, which is recognisable with its particular city centre: New Street (Ehlers, 2001).

MATERIALS AND METHODS

The area of the research is Valka – Valga border town between Latvia and Estonia. The subject of the research is architectural and landscape environment in the Latvian and Estonian border town.

In the research Valka – Valga is discussed through different ways of investigation: regional, historical, landscape spatial, territorial planning and Europe border towns context.

The basis of the research was Valka – Valga border town. Landscape survey, photo fixation and inventory were managed in the spot of this Latvian and Estonian town. Historical information about Valka and Valga development in time was found in holdings of the Local History Museum of Valka. At the research territorial plans and programmes of development were analyzed and compared. Information about other border towns in Europe was found on the Internet and in special literature of landscape design. Pictures from border towns abroad were received from people who live in Gubin, Gerlitz and Nova Gorica.

In the research qualitative research methods were used. *The descriptive method* was used for literature studies of Valka – Valga regional characteristics and history. *The cartographic method* was used to illustrate the location and current situation of six chosen border towns, for analysis of the territorial plans and the historical situation of Valka – Valga. Aerial photographs for the cartographic method were used (Google Maps...). *The analytical method* was used for survey of the current situation in Valka – Valga border town, Kevin's Lynch "city image" and "city building" analysis (Lynch, 1960), study of the territorial plans. *The comparative method* was used for literature studies of border towns abroad, green areas, architecture, historical development and territorial plans of Valka and Valga.

The six European border towns were compared with architectural, landscape and historic properties also using geographical, social and economical characteristics. In the present study the following border towns were analyzed: Tornio – Haparanda (Finland, Sweden), Narva – Ivangorod (Estonia, Russia), Guben – Gubin (Germany, Poland), Gorizia – Nova Gorica (Italy, Slovenia), Gorlitz – Zgorzelec (Germany, Poland) and Valka – Valga (Latvia, Estonia).

RESULTS AND DISCUSSION

Regional characters of Valka and Valga

Valka is a Latvian town on the northern national border with the Estonian city Valga. The border town is located on the banks of Pedele river. The length of Pedele river is 31 km. The river crosses the border perpendicular and creates a high quality natural landscape and green recreational area.

The area of Valga is 16.5 km² and that of Valka is 14.2 km². Their population are respectively 14153 and 6164 inhabitants (The Free Encyclopedia...). The general characteristics are shown in Table 1.

Valka and Valga are located in the node of rail and auto traffic roads. The area of the town is similar in both towns, however, the population is disparity. The nearest town of Valga is Tartu, which is the second largest city in Estonia and a notable Estonian education centre. Closeness of Tartu gives a wide scope to Valga.

Table 1
General characteristics of Valka and Valga

	Valka	Valga
Area (km ²)	14,36	16,50
Population	6164	14153
Distance from cities (km)	Riga – 160; Valmiera – 45; Cesis – 70; Aluksne – 75	Tallinn – 210; Tartu – 75; Otepa – 45; Parnu – 120
Water courses	Pedele, Varzupite	
Common border (km)	4,9	

The border of Valka and Valga has different nature – it goes along streets, nature pavement territories, the river, cemetery, private houses and railway. Varzupite river acts like a border in the centre of the border town. There are public and private spaces on the border.

Historical development of the territory

The Livonian town Valka (Walk) at first was under the government of Poland – Lithuania common state and acquired a status of a town in 1584 (The Free Encyclopedia...). Up to the 20th century the town was ruled by Sweden and Russian. The first division of Valka occurred in 1920 between the newly – born Latvian and Estonian states. The old town centre got into the Estonian town Valga. Latvian Valka had to start new development of the town in earlier suburbs.

In 1941 Valka – Valga was occupied by the German military forces. In 1944 Valka and Valga are released from the German army. The town got into the Soviet Union occupation. (The Free Encyclopedia ...) There occurred destruction of old wooden houses and massive building constructions of blockhouses. The image of Valka – Valga town was modified and disarranged.

The second division of Valka and Valga was in 1990, when the border was restored by the decay of the Soviet Union. On January 1, 2009 all border – crossing points were removed and roads and fences opened between the two countries because of both countries joining the Schengen Agreement.

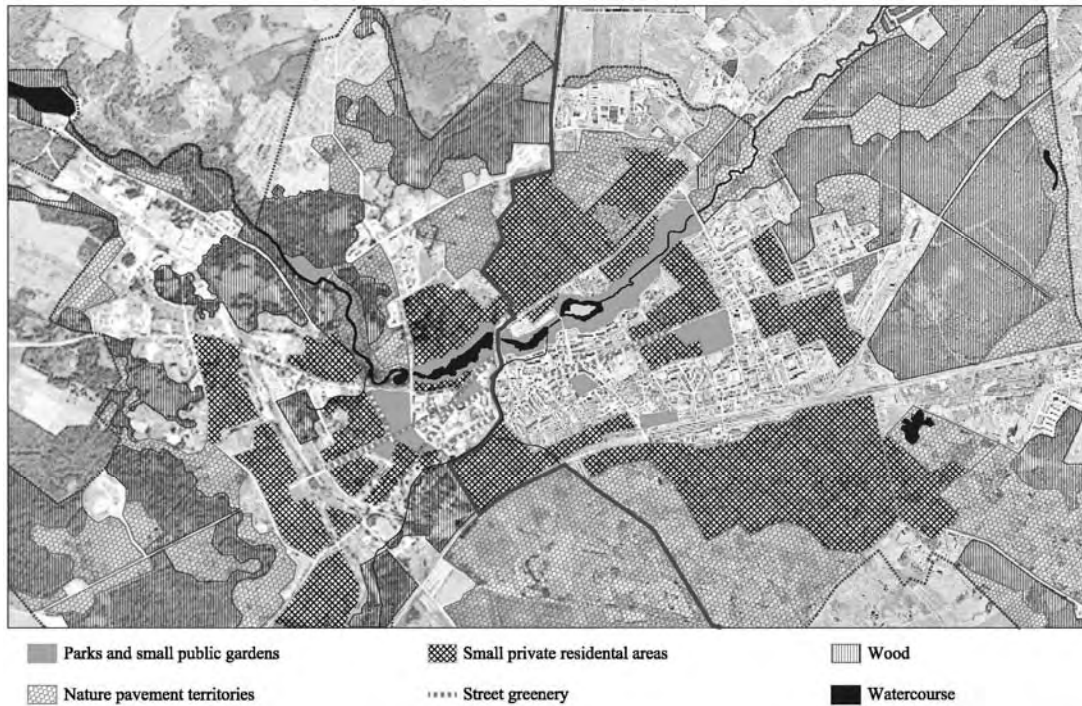


Figure 1. Green structure of Valka and Valga.

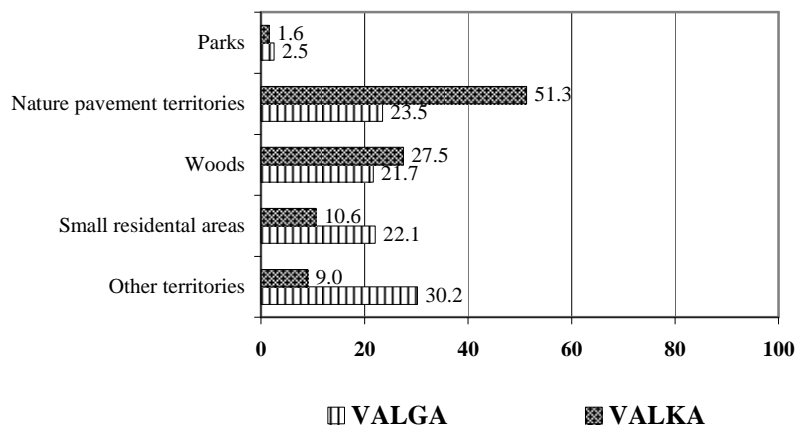


Figure 2. Comparison of green structure in Valka and Valga
 where Y – types of areas;
 X – amount, %.

Landscape spatial structure of Valka – Valga

The urban landscape structure of Valka – Valga is formed by nature pavement territories, public spaces, watercourses (Fig. 1), street network and links between two separate administrative town centres. Each town has unique objects that attract inhabitants of the neighbour town. Valka – Valga is a town of a dynamical open or linear designing structure, where industrial and residential areas are located parallel. The migration of inhabitants is determined by the placement of the transport roads. The green structure of Valka – Valga is formed by untouched nature pavement territories, woods, parks

and public spaces, watercourses and small private residential areas with cultivated gardens. The majority of green recreational areas are located near Pedele river and in the south of the border town. Most of the artificial green territories parks and squares are situated in Valga town (Fig. 2). Small residential areas dominate in the building structure of Valka (10.6 %). These areas look like green territories because of the low – rise houses and their small gardens around. There are many parks in the centre of Valka: Lugazu plaza, Eidemana square and Culture – recreation park with the amphitheatre near Pedele river.

In the administrative centre of Valga there are orderly public building greenery and green spaces. Street greenery is shaped where the road is wider. There are two main parks in Valga: Town (*Linna*) park and Sade park. Both parks have watercourses. The historical development of Valka and Valga border towns are analogical. There are differences between the national statuses of both towns. Valka is a small provincial town but Valga is near the top ten largest towns in Estonia. It reflects in the

architectural environment and quality in the common border town.

There are small residential areas in Valka and many multi storey buildings in Valga (Fig. 3).

There are unarranged and unattractive residential areas near Varzupite river on the national border. Clusters of shops and commercial buildings are focused near the border on the Valga side to attract consumers from Latvia.

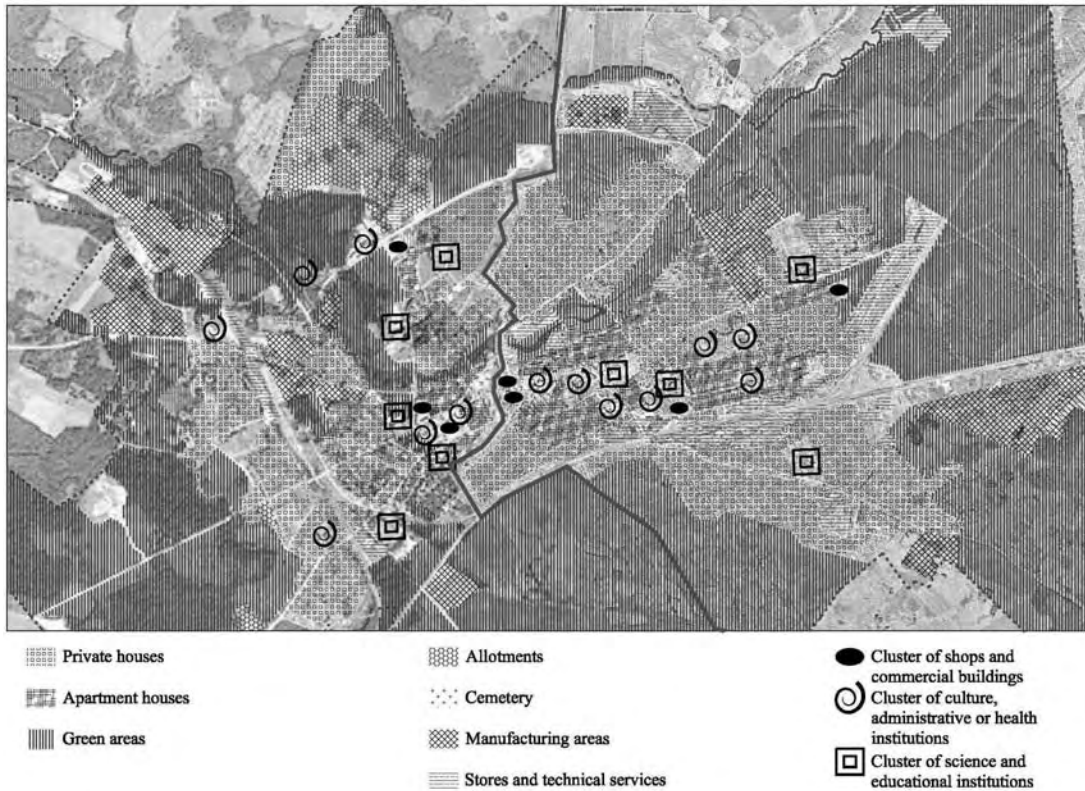


Figure 3. City building of Valka and Valga after K. Lynch.

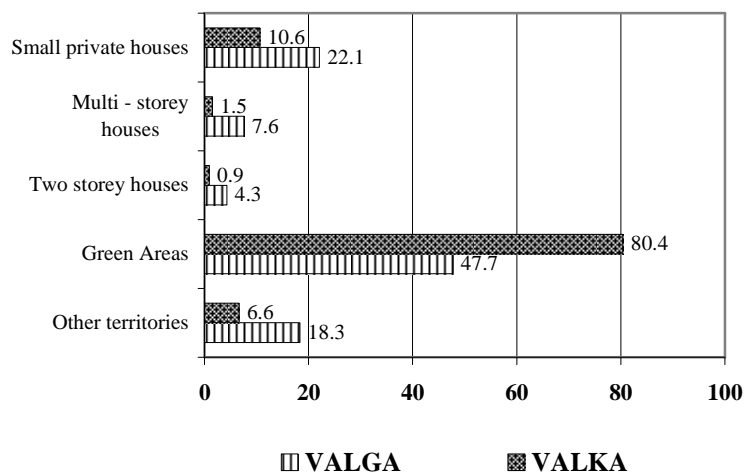


Figure 4. Comparison of building structure in Valka and Valga where Y – types of areas; X – amount, %.

Clusters of culture, administrative or health institutions and science and educational institutions are located near the town centers. If the location is far from the center, institutions become few.

Manufacturing areas and stores, technical services are located along the main roads and railway outside the town centers. There are few industrial areas in the centre of Valga. Green areas in Valga are almost two times less (47.7%) and built up areas are approximately three times more than in Valka (52.3% and 19.6%). There are maintained historical buildings in the centre of Valga town. Three heritage valued ensembles are in Valka: Teraudskola, Valka high school, Culture house. The towers of the churches serve as vertical domains in both towns. Although there are many high objects in both towns, mostly industrial facilities: water towers, electrical – poles, the silhouette of Valka - Valga border town are wide and low.

Expansion of the border town is limited by the banks of the river, railway and national border. The building structure of the town is influenced by the natural topography, which is diverse on the Valka side. This is the reason why there is an orthogonal street network system in Valga and free planning street network system in Valka.

A visual space is created by Varzupite and Pedele rivers flowing together (Fig. 5). Varzupite river acts like a border in the centre of Valka – Valga frontier town. It is possible to develop a green territory near Varzupite river as recreational area. There are many different sights in the borderland. Some views contain harmonic natural landscapes, some views uncover misbalanced household buildings and industrial areas. There is a landscaped territory on the river banks of the Pedele.



Figure 5. Scheme of Valka – Valga borderland in the centre of frontier town.

The landscape quality is reduced by unattractive private houses and allotment areas. The majority of these areas are neglected and opened to recreational parks. There are also unfinished and tumbledown buildings in the borderland.

The borderland of Valka – Valga is made by landscape elements of high and low visual aesthetic quality. Different unattractive elements are detected at full length of the border.

Landscape architectonic space in context of territorial planning

In comparison between the both towns territorial planning, which occurs separately, the main purpose of Valga is the development and growth of the town in the scale of all Estonia (Territorial plan of Valga...). The main purpose of Valka is becoming an important educational and tourism centre in Vidzeme region of Latvia (Territorial plan of Valka...). International collaboration with Valga is highlighted in the program of development of Valka. There are discussed questions about nature protection and development of green networks in the territorial plan of Valga. As green territories are less in the Valga side, the local authorities started to think about nature conservation problems.

Valga town is more guided to arrangement of green areas. There are listed - formation of street greenery, protective plantation, usage of perennial flowers and shrubs instead of trees.

The central action of landscaping in Valka is adjustment of Pedele river. Lugazu plaza – the central square of the town will be projected and landscaped within the framework of the Via Haensatica project. There is no information about the arrangement of the Varzupite river green area in both regional plans.

Development of the transport infrastructure is provided in the Via Haensatica project. Both towns participate in the project, which provides a ring road construction along the both towns to reduce traffic in the centre of the border town, a new system of bikeways along the border, through recreational areas and in the town centres.

Development of small residential areas is provided in both maps of the planned allowed functional use of the territory. Areas of multi – storey buildings are not provided in Valka and Valga. Many recreational and tourism areas are provided in Valka territory.

The ensembles of cultural heritage in Valga old town have one wide protection zone in the map of the protection zones of Valga. There are many separated protection zones of historical objects in the map of Valka.

The comparison between the regional plans brought out problems, what appear when Valka and Valga are planned and designed separately. The cartographic material, nomenclature of legends and

applied language in the regional plans also disagree. There were discussed issues about a common process of regional planning in both Valka and Valga programmes of development.

Architectural and landscape quality in European border towns

Valka is one of the cities in the world where the border crosses the city centre and divides it into two parts, creating a twin city Valga and Valka. A similar situation is Tornio in Finland and Haparanda in Sweden, Guben in Germany and Gubin in Poland, Gorizia in Italy and Nova Gorica in Slovenia, Gorlitz in Germany and Zgorzelec in Poland, as well as Narva and Ivangoroda in Estonia and Russia. These six border towns have common and different landscape values that are shown in Table 2. All border towns have a river which has an important aesthetic quality. The important recreational role played by the river channels reflects both their ecology and appearance (Richards, 1982). In five border towns the river or its fragments act as a border. Pedele river flows through the centre of the town, a part of Varzupite river flows on the border. Soča river flows near the border around Gorizia – Nova Gorica.

In some border towns the cultural heritage is maintained that appears in forms of buildings. Tornio – Haparanda has recognizable Finish and Sweedish architecture, also in Gorizia we can find houses from Italian architecture samples. Germany – Poland has a balance between architecture. Architecture in Germany and Poland is similar. Different architecture styles are in Valka – Valga and Narva – Ivanogorod. Most of the buildings in the Latvian side are low-rise residential buildings but in the Estonian side near the town centre there are low-rise and also multi-storey buildings. As Narva is one of the largest cities in Estonia, it has a skyline with many multi-storey buildings and old Baroque houses. There are old soviet style buildings on the Russia side.

Most border towns have public green spaces. There are natural green structures as mountains, woods and islands in these border towns. Guben – Gubin has a very harmonious urban greenery system. Valka – Valga has a nice open-air stage that includes Pedele river. Sometimes the parks would require improvements, for example, in Latvia, Estonia, Poland and Russia.

CONCLUSIONS

Based on the research results:

1) Valka and Valga towns have similar historical development. At the beginning it was a Livonian town Walk, where Latvians and Estonians lived together. After 1920 Walk was divided. The division affected Latvian Valka, it has to start over again the development of the town.

Table 2

Landscape values in European border towns		
	Architecture	Landscape
Tornio – Haparanda	T: 4-5 storey buildings; wooden buildings from 19 th Century; memorials; commemorative sites; churches, chimneys – vertical domains H: red brick houses; 2-3 storey buildings; modern 21 st Century houses; wooden architecture; churches, chimneys – vertical domains	T: location on Suensaari Island; stone retaining walls – parks are created in levels; golf-course; Tornio river H: orderly system of street greenery – birches, perennials, annuals; golf-course; walking path of 5 km; Tornio river
Narva – Ivangorod	N: Herman fortress; 3-5 storey soviet period buildings; 12 storey block houses; coloured buildings from Baroque; churches I: fortress; grey faded 3-5 storey soviet buildings; private houses; monuments; block houses – vertical domains	N: ordered street greenery in town centre – annuals; new small garden architecture forms; Narva river I: watermill; amphitheatre; undeveloped street greenery; Narva river
Guben – Gubin	Maintained cultural heritage; modern multi-storey building and semidetached housing; 3-5 storey soviet style buildings; churches, chimneys as vertical domains	Orderly system of street greenery, landscaped parks with cultivated plantation, new small architecture forms; fountains; renewed historical parks; Lusatian Neise river.
Gorizia – Nova Gorica	G: Italian architecture with red roofs and shutters; stones in facades; 3-4 storey buildings; churches – vertical domains NG: low Italian houses 1-3 storey; 3-9 storey modern buildings with colourful facades; churches, multi-storey houses – vertical domains	G: mountains; geometrical parks; landscape parks; monastery gardens; fountains; narrow streets; Soča river NG: mountains; wild nature territories; valley; vineyards; Soča river
Gorlitz – Zgorzelec	Maintained cultural heritage with colourful facades; 4-9 storey modern houses; 3-5 storey soviet style buildings; churches, towers – vertical domains	Landscaped parks; orderly system of street greenery; hard groundcover usage instead of grass; Lusatian Neise river
Valka – Valga	VK: low residential houses; few 5 storey soviet period buildings; churches, towers - vertical domains VG: low residential areas far from centre; 5 storey buildings with colourful facades; churches, chimneys – vertical domains	VK: wooden paths on river shores of Pedele; open air stage; Pedele, Varzupite rivers VG: asphalt paths on river shores of Pedele; few greenery in parks; orderly street greenery in centre

2) Analyzing the image of the town, there were many vertical domains found in Valka – Valga, mostly industrial objects. The structure of Valka – Valga is influenced by separate town centres. Tieback works between both town public spaces.

3) Green structure of Valka towns can be developed, because of many untouched nature pavement territories (51.3 %) – meadows, green areas, alluvial lands. The most part of Valga is occupied by buildings. There are contrasts between private houses in Valka and multi-storey buildings in Valga.

4) The visual aesthetic quality of the common borderland is negatively influenced by industrial objects, neglected private houses and household areas. Both towns are participating in landscaping the river banks of the Pedele, but there are many mistakes and no tieback in the Pedele park projecting process.

5) Valka and Valga towns have to participate in common planning, to eliminate the problems that appear when areas are planned separately.

6) Different connections can be found in the comparison between European border towns. When there is no border in the town, usually the border town is divided by a river. There is architectural diversity in duplicated border towns (Tornio – Haparanda, Narva – Ivangorod). There is architectural and landscape unity maintained in partitioned border cities, which were owned by one

country at the beginning (Guben – Gubin, Gorizia – Nova Gorica, Gorlitz – Nova Gorica). Valka – Valga is a partitioned city where both nations live together, there are architecture diversity and contrast in this situation.

7) There are many unique potentialities how to use the borderland of Valka – Valga. The nature pavement territory in the south of the border town can be used as a border – crossing park, where visitors could travel by bike, horse or on foot. In the places, where the border crosses the street, the border could be drawn in the road surfacing like in Baarle Nassau – Baarle Hertog settlement in the Netherlands – Belgium. Drawing the borderline serves as an attractive and interesting sideshow for the town visitors. The next step is landscaping the green area near Varzupite river. In many border towns of Europe, divided by the river, the area near the river is created as promenade or esplanade, where the neighbouring town can be seen over the water. The borderland of Valka – Valga is miscellaneously usable for active and passive recreation with visual and functional objects.

ACKNOWLEDGEMENTS

This research is supported by the European Social Fund under the project „Atbalsts LLU maģistra studiju īstenošanai” in the programme „Atbalsts maģistra studiju programmu īstenošanai”. Contract No. 2009/0165/1DP/1.1.2.1.1/09/IPIA/VIAA/008.

REFERENCES

- Buursink J. (2001) The binational reality of border-crossing cities. *GeoJournal*, No. 54, p. 7-19.
- Bratuškins U. (2008) Problematic development aspects of common urban townscape in the border area of Valka-Valga. *RTU raksti*, No. ..., p. 98-107.
- Ehlers N. (2001) The Utopia of a binational city. *GeoJournal*, No. 54, p. 21-32.
- Google Maps. [online] [accessed on 24.09.2010.]. Available: <http://maps.google.com/>
- Lynch K. (1960) *Image of the city*. Cambridge: MIT Press. 194 p.
- Richards K. (1982) *Rivers form and process in alluvial channels*. Cambridge, 286 p.
- Territorial plan of Valga. Valga linna ūldplaneering. [online] [accessed on 07.12.2010.]. Available: <http://www.valgalv.ee/et/Linnakodanikule/Ehitus-ja-planeerimine/Uldplaneering>
- Territorial plan of Valka. Valkas pilsētas teritoriālpilnoģums. [online] [accessed on 07.12.2010.]. Available: <http://www.valka.lv/Valkas-pilsetas-teritorijas-planojums/>
- The Free Encyclopedia Wikipedia. Border Towns [online] [accessed on 17.11.2009.]. Available: <http://www.wikipedia.com/bordertowns>

IV ENGINEERING OF ENVIRONMENTAL ENERGY

ANALYSIS OF GHG REDUCTION POSSIBILITIES IN LATVIA BY IMPLEMENTING LED STREET LIGHTING TECHNOLOGIES

Ansis Avotins, Leonids Ribickis

Riga Technical University,
Institute of Industrial Electronics and Electrotechnics
ansis.avotins@rtu.lv

ABSTRACT

This manuscript deals with the EU policy in energy efficiency and CO₂ emission reduction from the perspective of possible improvements in Latvia street lighting system. The paper also shows the results of examination of the existing situation, estimation of further street lighting development possibilities, and experimental measurements in real conditions.

Key words: street lighting, GHG emissions, solid-state lighting, energy efficiency

INTRODUCTION

Nowadays a demand for more energy efficient devices also in lighting industry is increasing, as there is a great potential for energy savings and CO₂ emission reduction to contribute to the European Union (EU) Action Plan for energy efficiency, where the EU in 2008 adopted an integrated energy and climate change limitation policies to be implemented by 2020. With this policy it is intended to develop the sustainable and energy efficient economy of Europe with low carbon emissions, by implementing such events as greenhouse gas reduction by 20%, energy consumption reduction by 20% (or improving energy efficiency), 20% of the EU energy obtained from renewable sources. Street lighting systems have a high potential for improving the energy efficiency, which are identified as significant energy consumers, but they are needed for traffic and citizen safety and security.

Solid-state lighting still is a new technology for street lighting application and its main advantage is the ability to regulate light output in full range - from 0% to 100% with no photometric parameter changes, where conventional lighting with high intensity discharge (HID) lamps, could be regulated just from 50% to 100%, and can cause color shift and color rendering index (CRI), as well as significant drop of luminous efficiency (lm/W).

As a new technology LEDs still are in the development process, and the main obstacle for wider application of LED luminaries is the initial cost of LEDs, which tend to be much higher than HID sources. According to a DOE study, LED technology has been experiencing steady rates of improvement not only in efficiency (approximately 35% annually) but also in cost (approximately 20% annually). When looking at some economic aspects from the engineering - economic analysis done in (Azevedo et al., 2009), which indicates that white

solid-state lighting already has a lower levelized annual cost (LAC) than incandescent bulbs, and will be lower than that of the most efficient fluorescent bulbs by the end of this decade.

To compare different illumination technologies with different lifetimes by economical means, a LAC should be compared rather than just the net present value.

$$LAC = I \frac{d}{(1 - (1 + d)^{-n})} + O \& M$$

where I is the initial capital investment in the lighting system, d is the discount rate, n is the number of the years of lifetime, and O&M is the expected annualized cost of operation and maintenance.

It indicates that countries with limited budget should be careful by planning investment in retrofitting the existing street lighting lanterns with high pressure sodium vapor (HPS) lamps to new solid-state lighting with light emitting diode (LED) technology, unless the retrofitting is technically and economically justified or subsidized with additional investments.

MATERIALS AND METHODS

Description of LED luminary

It is important to understand the main characteristics of LEDs in order to understand how to drive them properly. One of the LED characteristics is their colour, with very narrow band of wavelength, which determines the voltage drop across the LED, while it is operating. The current level determines the light output level, the higher the current, the higher the luminosity of a LED, and also the temperature. Due to production variations, the LED wavelength and thus also the voltage drop has variations, typically $\pm 10\%$

(Winder, 2008). As the temperature rises, the voltage drop reduces by ~2mV per degree. When operating LED at maximal parameters, small changes in voltage can make significant changes in the current value and possibly damage the LED, thus appropriate power supply must be used. To obtain a correct value of CO₂ emissions for street luminary, which is mainly obtained from the consumed electrical energy value, not only the light source efficacy (lm/W), but also the ballast and fixture efficiency (lm/W) should be taken into account, as they can significantly influence the total efficacy (lm/W). Also electromagnetic ballasts typically consume 10-15% more electrical energy than similar electronic ballasts.

Table 1

Efficacy of lighting devices and fixtures			
Light source efficacy [lm/W]	Ballast efficiency [%]	Fixture efficiency [%]	Total efficacy [lm/W]
Incandescent 4 to 18 lm/W	100	40 - 90	2 - 16 lm/W
Halogen 15 to 33 lm/W	100	40 - 90	6 - 30 lm/W
Fluorescent tubes 60 to 105 lm/W	65 - 95	40 - 90	16 - 90 lm/W
CFL 35 to 80 lm/W	65 - 95	40 - 90	9 - 68 lm/W
HID 14 to 140 lm/W	70 - 95	40 - 90	4 - 120 lm/W
White LED 60 to 188* lm/W	75 - 95	40 - 95	18 - 170 lm/W

*188 lm/W is a target for white LED at 2015 of US DOE

Table 1 shows a comparison of different light source luminaries, thus the total efficacy ranges differ from the light source efficacy (Azevedo et al., 2009).

Standards

Another important topic for public and street lighting luminaries is compliance with different local and EU standards, which help municipalities to avoid low quality products and ensure sustainable lighting. The compliance of LED luminaries to lighting class is very important for municipalities which manage the city lighting system. For LED luminaries there is no special standard of their performance, the parameters and norms defined in the existing standard EN 13201-2:2004, which includes recommendations from CEN and CIE, can be applied to choose an appropriate LED luminary. These standards are recommendations, but some other standards or government rules can be mandatory for the municipalities in Latvia, like the road maintenance class. If, the road maintenance class defined by traffic intensity, is used for the choice of the lighting class, then combining it with EN 13201-2:2004 classes, Table 2 can be made.

Table 2

Lighting class vs road maintenance class in Latvia

Average traffic intensity (cars per day)	Municipality road class	Lighting class
above 5000	A	M1, M2, M3
from 1000 to 5000	A1	M1, M2, M3
from 500 to 1000	B	M1, M2, M3
from 100 to 500	C	M2, M3, M4, M5
below 100	D	M4, M5

Table 3

Lighting class, minimal luminance and recommended illuminance of road class

Lighting class	Minimal luminance, L_{min} (cd/m ²)	Minimal illuminance amount, E (lx)
M1	2,0	30
M2	1,5	20
M3	1,0	15
M4	0,75	10
M5	0,5	7,5

Most of the small municipalities are able to measure illuminance with a standard lux meter, and chose the appropriate values from Table 3.

Any LED driver circuit using the MOSFET switch connected to AC mains should meet the limited radiated, emitted and harmonic current emissions specified by the standard IEC/EN 61000-3-2. Within this standard the Class C corresponds to the lighting.

The conducted emission limits in the 150kHz to 30MHz frequency range are specified in the standard IEC/EN 61000-6-3 (covers 20MHz to 1GHz). The emission levels to meet the EN55022/CISPR22 Class B are 30dB μ V/m in the frequency range 30MHz to 200MHz.

RESULTS AND DISCUSSION

Survey of lighting systems in Latvia

To obtain data about the existing situation in the lighting systems in Latvia, an intensive survey of 44 public lighting managing companies, agencies and Latvian municipalities was done by help of the Latvian Ministry of Environment.

The survey indicates that most lighting systems in Latvia have not been reconstructed since their installation date (some of them are more than 30 years old), most of the street lighting managing institutions (municipalities, agencies, private companies) in the survey admit that some part of their lighting system is in bad technical condition. Mostly it deals with old poles for luminaries, that have reached the end or are very close of their depreciation period, for materials like reinforced concrete, steel, wood, in average 35% of the system (see Fig.1.).

Also lots of cables are very old (see Fig.1.) and in bad condition, due to damaged isolations during road reconstructions and repairs.

Technical condition evaluation results

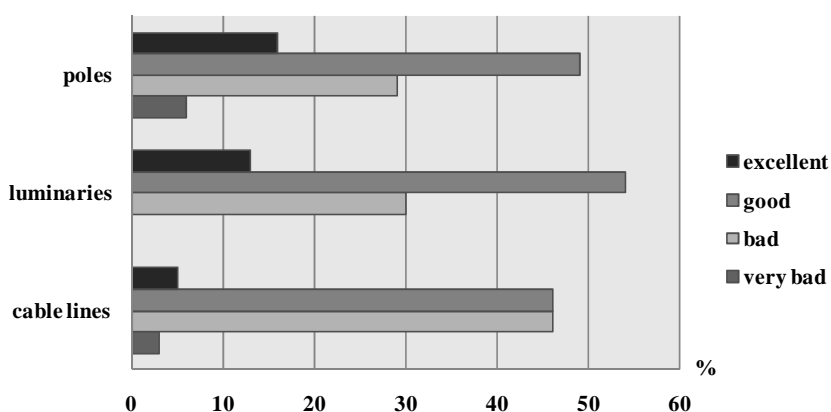


Figure 1. Overall technical condition of poles, luminaries and cable lines of lighting systems.

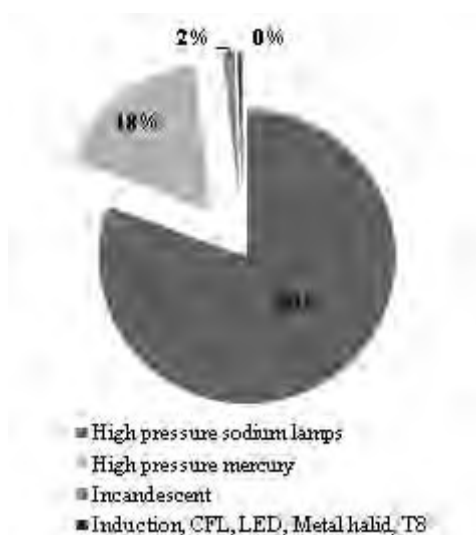


Figure 2. Total rated power versus light source used.

Implementation of power line communication for dimmable LED luminaries would be a challenge in this situation.

As the change of luminaries is the easiest way to reduce the energy consumption, most of the managing institutions of lighting systems, are in the process to change or already have changed old luminaries with mercury vapour lamps to luminaries with High Pressure Sodium (HPS) vapour lamps, thus admitting in the survey, 33% (see Fig.1.) of the luminaries to be in a bad technical condition in an average lighting system. The payoff of investment (change to HPS) will be reached in the next 2-4 years, depending on the system operating hours per year, giving the time and opportunity to develop intelligent power LED luminary. From the survey data the total rated power of luminaries installed at the lighting systems in Latvia is 12,148 MW, which is calculated from the indicated light source technology, capacity and

number at the survey questionnaires. Fig.2. shows the percentage of the total rated power of the installed light source technologies. It is obvious that the HPS lamps dominate at street lighting systems, as it is still one of the most efficient light sources, but surprising is that there still are 18% of mercury vapour lamps and even incandescent lamp light sources, and that gives a great opportunity to change these 19% to LED technology luminaries, as the retrofitting investment payoff would be more cost-effective, than retrofitting HPS lamps with LEDs.

As it can be seen from Table 4, the total costs and energy consumption from 2008 to 2009 has decreased, despite the continuously growing electricity rates.

Table 4

Total power of lighting installations and costs

		Latvia Total	Riga	Other cities
Power of lighting installations		MW	MW	MW
Total power of light installations	2008	13,543	7,3	6,243
	2009	13,757	7,2	6,557
Consumption of electrical energy		MWh per year	MWh per year	MWh per year
Electrical energy consumed	2008	46 228	28 203	18 025
	2009	36 497	21 966	14 532
Costs		10 ⁶ LVL per year	10 ⁶ LVL per year	10 ⁶ LVL per year
Consumed electrical energy	2008	2,706	1,410	1,055
	2009	2,136	1,286	0,851
Annual O&M excluding energy consumption	LVL	1,958	1,014	0,944
Annual O&M costs including energy consumption	LVL**	4,095	2,300	1,795

Table 5

Results of calculation of CO₂ savings

Retrofitting Scenario Description	Average rated power per lamp	lamp count	Electrical energy savings	CO ₂ savings per year (0,397)	Electrical energy savings per lifetime	CO ₂ savings per lifetime (0,397)
	W	pc.	MWh/year	t/year	MWh/life	t/life
Incandescent	133	1 196	0	0	0	0
LED w/o dimming	27	1 196	534	212	10 626	4 218
LED + dimming	27	1 196	590	234	11 734	4 658
HME	239	9 069	0	0	0	0
LED w/o dimming	70	9 069	6 478	2 572	128 915	51 179
LED + dimming	70	9 069	7 573	3 006	150 702	59 829
HPS	137	72 568	0	0	0	0
LED w/o dimming	70	72 568	20 363	8 084	405 216	160 871
LED + dimming	70	72 568	29 123	11 562	579 553	230 083
Total possible savings w/o dimming			27 375	10 868	544 756	216 268
Total possible savings with dimming			37 286	14 803	741 990	294 570

It was possible due to the implemented “light saving” measures, like turning off the lighting at night hours due to mechanical timer, turning off two phases, where both methods are not preferable as no light would be available, or changing to more effective lamps or luminaries, where the survey indicates that it was the best method for most of the managing institutions of the lighting systems.

Calculation of possible CO₂ savings

The Latvian lighting systems have present luminaries with incandescent lamps, high pressure mercury lamps (HME), high pressure sodium lamps with very wide range of rated power of lamps, so more than one retrofitting scenario is possible.

To calculate the potential CO₂ savings of retrofitting the existing light sources to LEDs, an average rated power per lamp light source type is calculated, and according to the survey data, totally 1196 incandescent lamps are installed with the average rated power 132,9W per lamp, and the total rated power 158,94kW, as these lamps are mainly installed in parks and decorative lighting, where the pole height is around 6m, an appropriate average LED lamp of 27W can be used to reach similar luminous output. Also 9069 HME lamps, with the average rated power of 239,44W per lamp, are available and the total rated power is 2171,5kW and an appropriate LED lamp would be 70W (average value).

The total number of HPS lamps is 72568, with the average rated power of 136,56W and the total rated power of 9909kW and an appropriate LED lamp would be 70W (average value). For calculations it is assumed, that the lighting system is working 11 hours daily, but when using dimming 4 hours have 100% of light output, 1 hour - 70% and 6 hours - 30% of light output.

According to the method for calculation of GHG emissions from the Latvian Ministry of Environment, 1MWh = 0.397 t CO₂ GHG emissions, when saving electrical energy.

On-site optical measurements of LED luminaries

Nowadays at the market lots of simple LED (without embedded dimming capability) luminaries are already available, but the technical data about the optical and electrical properties are mostly not full, or little technical info, as it is the result of aggressive marketing strategy. To compare production variations and specified optical parameters of several LED luminaries available on the market, on-site testing was done with the method, which can be repeated by every municipality with an ordinary luxmeter.

In order to evaluate the illumination level of the street more accurately, LED luminaries were placed in series, as shown in Fig.3, where HPS luminary is equipped with a 250 W high-pressure sodium vapor bulb. The selected layout allows switching off HPS luminaries, thus the illumination measurements are not affected by adjacent luminaries. The measurements are performed by Hagner "EC-1" luxmeter, (lx 0.1-200000 range, and accuracy +/- 3% (+/- digit).

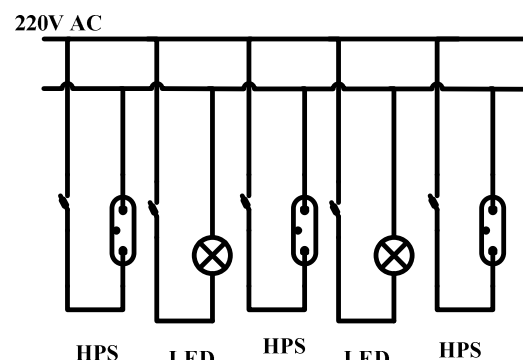


Figure 3. On-site luminary layout..

The experimental street lane is typical M3-M4 class, with the width of 12 m, pole height of 8-10 m. The distance between the poles typically is around 30-35m. Thus according to the measurement method described in the CIE standards, a

measurement point of 2x2m intersection was selected, and accordingly the lux value measured. The obtained data are shown in Figure 4, where the darkest color represents the value close to 0 lux and lighter color – closer to 20 lux, an exception is LED 2, LED 7 and LED 8, where the central grey dots represent 40-50 lux. From the obtained graphs the optical properties can be evaluated and compared with HPS luminary. As it can be seen, LED 1, LED 3-5 does not meet the requirements to replace the HPS 150W luminary, but it shows better uniformity, thus it allows to place these luminaries in parks or places where the poles are less than 6 m high. LED 6-8 are supposed for different distances

between the poles and lane widths, so to get better uniformity, a careful selection must be done.

Electrical parameter measurements of LED luminaries

Also electrical properties are mostly unclearly described in the LED luminary technical datasheet, not telling if the active power value includes the power supply consumption and losses. To evaluate the electrical properties of LED luminaries, LED1-8 was tested, where LED9 is floodlight, which optical performance is not comparable with HPS streetlamps.

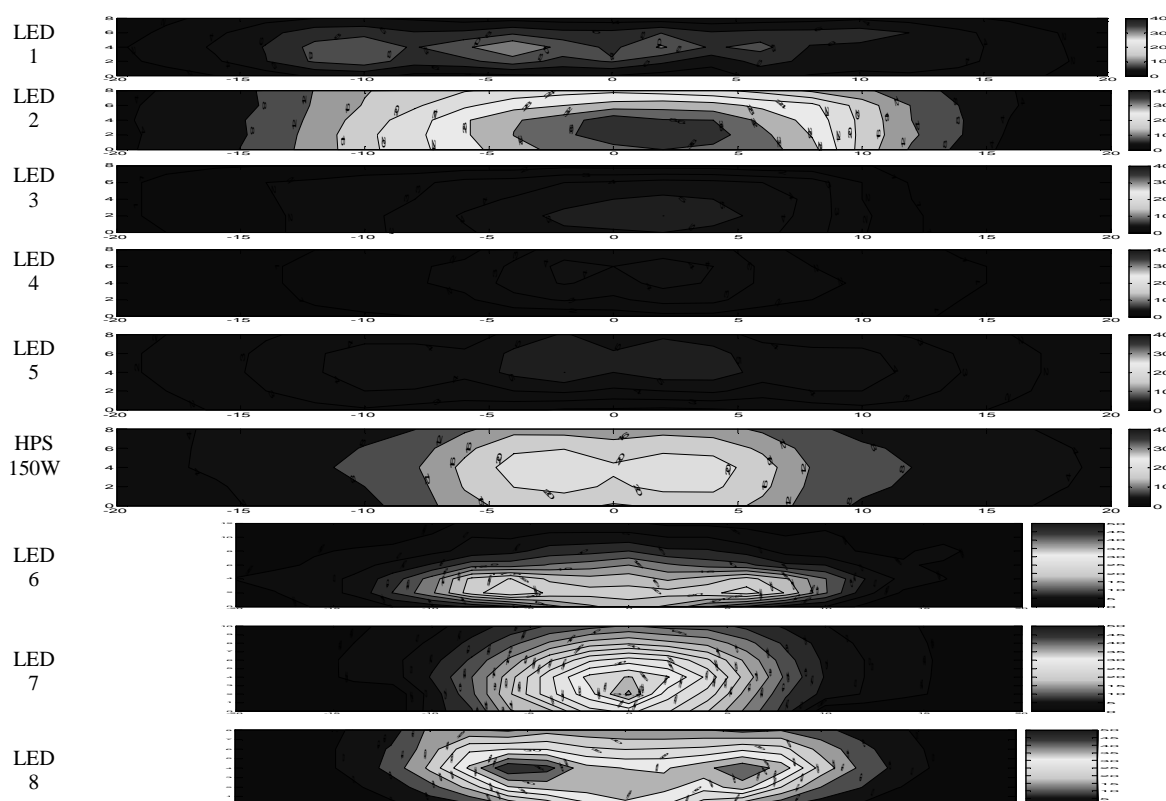


Figure 4. Comparison of different LED luminary photometrical performance at ~45 lux scale.

Table 6

Comparison of different LED luminary electrical parameters

Parameter Luminary	U [V]	I [mA]	P [W]	$\phi 1$	$\cos(\phi 1)$	I1 [mA]	THDi [%]	S [VA]	Q [var]
LED1 50W	225	390	51	19	0.95	240	128	87.2	70.7
LED2 225W	224	1020	221	12	0.98	1010	16	228.4	57.6
LED3 35W	225	170	35	21	0.93	160	17	38.2	15.2
LED4 25W	225	110	25	-3	1.00	110	29	26	7
LED5 50W	228	210	47	14	0.97	210	26	50	17
LED6 140W	221	683	150	3.7	0.998	679	11.2	151.3	19.5
LED7 112W	222	564	124	0.75	0.999	561	10.9	125.3	13.7
LED8 84W	221	489	107	2.59	0.999	486	11.9	108.3	13.7
LED9 24W	216	114	24	11.3	0.98	112	15.3	24.6	6.1
HPS 400W	225	1730	369	-14	0.97	1670	28	395	141
HPS 150W	226	780	165	-18	0.95	770	20	176	63

$$Q = U_{\text{rms}} \times I_{\text{rms}} \times \sin(\varphi_1) \quad (1)$$

$$S^2 = P^2 + Q^2 \quad (2)$$

$$S = \frac{P\sqrt{1 + \text{THD}^2}}{\cos \varphi_1} \quad (3)$$

The TrueRMS or instantaneous current and voltage values were measured experimentally, and other electrical parameters were calculated in MATLAB using formulas 1-3, and as the supply voltage distortion is negligible, it was considered that the voltage waveform is sinusoidal. Thus the results are shown in Table 6.

REFERENCES

- Azevedo Lima I., Morgan Granger M., Morgan F. (2009) The Transition to Solid-State Lighting. *Proceedings of the IEEE*, Vol. 97, No. 3, p. 481-510.
- Winder S. (2008) *Power supplies for LED driving*. Elsevier.

CONCLUSIONS

The survey also shows that a simple HME luminary change can be economically justified also changing them directly to LED luminary, thus increasing the CO₂ emission savings.

All of the tested LED luminaries have passed the electrical quality requirements for $\cos \phi$, but one of them has efficiency problems with THD, reactive power, and two - compliance with the optical performance requirements for ME2-ME3 class streets. The measurement results show that LED luminaries can replace the existing HPS and HME, but due to the high price, it needs additional political or financial support.

PECULIARITIES OF HEAT FLOW OF INSULATION CONSTRUCTIONS IN BUILDINGS WITH COLD UNDERGROUND SILTUMA PLŪSMU ĪPATNĪBAS ĒKU AR AUKSTO PAGRĪDI NOROBĒŽOJŠĀS KONSTRUKCIJĀS

Uldis Iljins*, Uldis Gross*, Juris Skujans**

Latvia University of Agriculture

*Department of Physics

uldis.iljins@llu.lv ; uldis.gross@llu.lv

**Department of Architecture and Building

juris.skujans@llu.lv

ABSTRACT

A popular solution in construction is an unheated garage or storehouse premises on the first or the socle floor of a building. Monolith concrete is the most common material for the first or the socle floor constructions in such cases. All surfaces of the construction disposed to outside air are insulated, and seemingly no cold bridges are developed. But the cold bridge can appear at places where the heat flow is not homogeneous. In this construction it is a place where the floor covering collides with the external wall. The thermal coefficient of linear thermal bridge has been calculated analytically with approximation and using the computer program ANSYS. Comparing both solutions, it can be stated that approximation of such types in analytical calculations does not show significant mistakes, and the obtained results are precise both qualitatively and quantitatively. The authors have offered a solution to prevent the heat loss caused by cold bridge, and it has been calculated using the ANSYS program.

Key words: cold bridge, insulation constructions of buildings, thermal coefficient

INTRODUCTION

The construction (see Fig.1.) consists of a monolith concrete wall and a covering with FIBO block wall above. All surfaces disposed to outside air are insulated.

The technical parameters used in calculation of insulated construction are presented in Tab.1.

MATERIALS AND METHODS

Without going into the root of heat flow physics, there might be an impression that there are no relevant thermal cold bridges in the presented insulated construction, because all surfaces disposed to outside air are insulated. But it is not quite true – it has to be considered that the heat flow quantity is influenced not only by thermal conductivity of the material, but also by squares through which heat flows run. In case of non homogeneous flows the latter condition may have a conclusive meaning, and it is so at the presented insulation construction. The heat flows from the covering Q_3 and FIBO blocks Q_2 through surface CB (0,2m) (Fig.1.) go into the underground wall, where the outflow conditional square consists of $2H=6m$. Along with this, the thermal resistance decreases accordingly, and thermal cold bridge develops in the square ABCD.

The thermal coefficient of the cold bridge can be calculated using analytical and numeral methods. Each method has its strengths and weaknesses. The

advantage of the analytical method is its relatively low calculation costs (only the specialist's wage), a possibility to use unlimited numbers and variations of physical parameters (thicknesses, conductivities, etc.) and quick calculation results.

The weakness of this method is the fact that analytical methods cannot be used for complicated constructions. Numeral methods can be used for any constructions, but calculations have to be supported by complicated and expensive computer programs. Other weaknesses - long calculation time, difficulties to vary geometrical parameters of the constructions, because each change of geometrical parameters requires redefining parameters of mathematical grid.

In order to calculate the thermal coefficient of the presented linear thermal cold bridge, we will use both analytical and numeral methods. The results from both methods will be compared.

The described insulated construction cannot be directly calculated using analytical methods. It can be done by approximation, conditionally dividing the construction into four parts:

1. Underground wall
2. Covering
3. FIBO wall
4. Cold bridge (square ABCD Fig.1.).

We will formulate mathematical physics problems for the first three objects, but for the whole cold bridge volume it will be assumed that its temperature is constant T_1 .

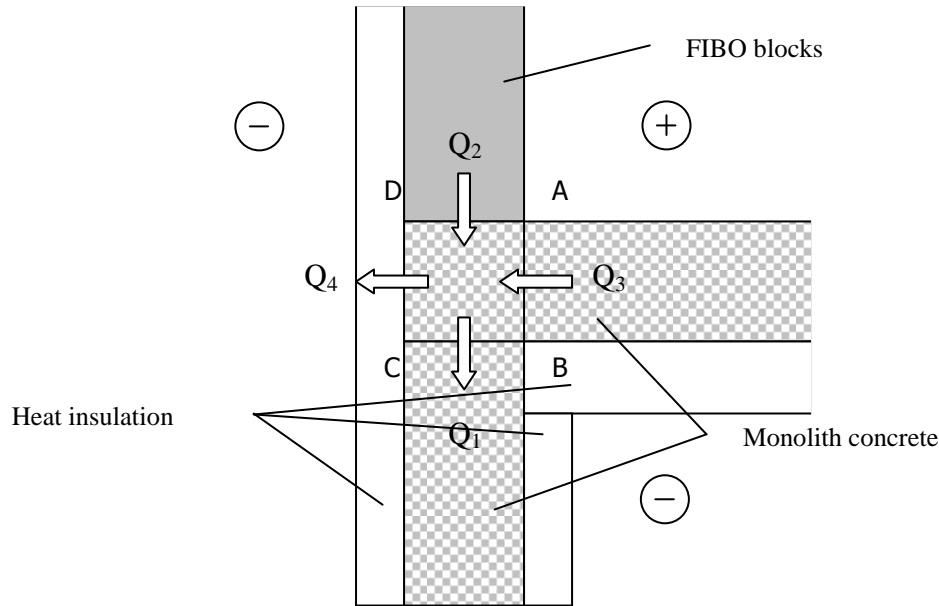


Figure 1. Insulation construction.

Table 1

Physical parameters of construction					
No	Name	Thickness d, m	Thermal conductivity λ , W/(m·K)	Water steam resistance factor μ	Surface thermal resistance R_{si} or R_{se} , m^2K/W
1.	Monolith concrete	0,2	2,0	100	
2.	FIBO blocks	0,2	0,24	6	
3.	Outside wall heat insulation (mineral cotton)	0,1	0,04	1	
4.	Heat insulation under the covering (mineral cotton)	0,15	0,04	1	
5.	Foam polystyrene (used to weaken the influence of cold bridge)	0,05	0,04	60	
6.	Outside wall surface thermal resistance R_{se}				0,04
7.	FIBO blocks wall surface thermal resistance R_{si}				0,13
8.	Covering surface thermal resistance R_{si}				0,17
9.	Calculation elements: underground wall, FIBO wall height, lengths of covering assumed $H=3$ m.				

This temperature T_1 is not known, and the heat balance equation will be used to calculate it at the end:

$$Q_2 + Q_3 = Q_1 + Q_4, \quad (1)$$

where Q_2, Q_3 – cold bridge heat inflow from FIBO wall and monolith concrete covering, W/m.

Q_1, Q_4 – cold bridge heat outflow through underground and outside walls, W/m.

1. Calculation of underground wall temperature and heat flow

We will formulate mathematical physics problems, consisting of the heat conductivity (Laplace) equation in order to calculate the heat flow in the underground wall.

$$\frac{\partial^2 T}{\partial x^2} + \frac{\partial^2 T}{\partial y^2} = 0, \quad (2)$$

where T – temperature $^{\circ}C$,
 x, y – coordinates (Fig.2.), m.

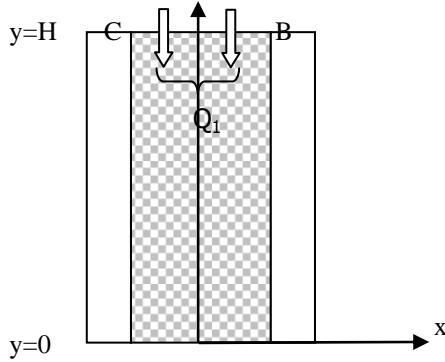


Figure 2. Underground wall calculation scheme.

The border conditions have to be defined. From the above analysis, it is known that on the line CB (Fig.1., 2.) the temperature is constant T_1 , the 1th kind of border conditions is developed:

$$T|_{y=H} = T_1. \quad (3)$$

At coordinate $y = 0$ the underground wall collides with the ground, thus it can be assumed that the underground wall will have a strength border condition:

$$T|_{y=0} = T_z, \quad (4)$$

where T_z – earth temperature, °C (in calculations assumed -18 °C).

If the border conditions (3) and (4) are stands, the solution is symmetrical in relation to y axis, and it is possible to find the solution only for the positive y values (solution is symmetrical for the negative coordinates) $y > 0$, but on the border $x = 0$

$$\left. \frac{\partial T}{\partial x} \right|_{x=0} = 0 \quad (5)$$

will stand.

On the border $x = d/2$, where d is the ground wall thickness, the monolith concrete construction collides with the heat insulation layer. In order to simplify the calculations (temperature division in the heat insulation layer will not be calculated – it is not relevant) we will include the heat insulation layer into the surface thermal return coefficient, at the corresponding 3rd kind border condition on the line $x = d/2$

$$-\lambda \left. \frac{\partial T}{\partial x} \right|_{x=d/2} = \alpha_1 (T|_{x=d/2} - T_0), \quad (6)$$

where λ – heat conductivity, W/(m·K);

$$\alpha_1 = \frac{1}{R_{se} + d_i / \lambda_i}, \text{ where } R_{se} = 0,04 \text{ m}^2 \text{ K/W};$$

d_i – thickness of the heat insulation layer, m;
 λ_i – thermal conductivity of heat insulation, W/(m·K);

T_0 – open air temperature (in calculations assumed -20 °C).

Solving the mathematical physics problem (2 -6) with the variables separation method

$$T(x, y) = T_z + (T_1 - T_z) \frac{y}{H} + \sum_{k=1}^{\infty} A_k \text{ch} \mu_k x \sin \mu_k y, \quad (7)$$

$$\text{where } \mu_k = \frac{\pi k}{H};$$

$$A_k = -\frac{2}{\pi k} \cdot \frac{(-1)^k (T_1 - T_z) + (1 - \cos \pi k) (T_z - T_0)}{\lambda \mu_k / \alpha_1 \cdot \text{sh} \mu_k d / 2 + \text{ch} \mu_k d / 2}$$

The heat flow Q_1 through the surface CB (Fig.1.) can be found

$$Q_1 = 2 \int_0^{d/2} \lambda \left. \frac{\partial T}{\partial y} \right|_{y=H} dx = \lambda \frac{(T_1 - T_z) d}{H} + 2 \lambda \sum_{k=1}^{\infty} (-1)^k A_k \text{sh} \mu_k \frac{d}{2}. \quad (8)$$

2. Calculation of FIBO wall, covering temperature and heat flow

The same expressions can be used for FIBO walls and the covering temperature distribution calculations. Thus, we will show it for the covering. (Fig. 3.)

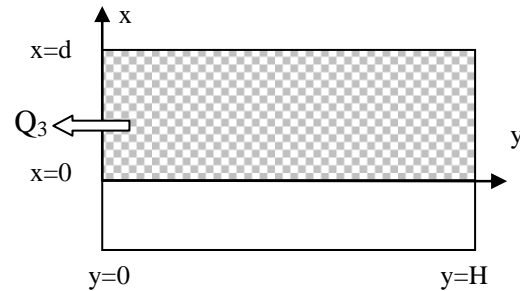


Figure 3. Covering calculation scheme

The mathematical physics problem will be made by equation (2) and border conditions:

$$T|_{y=0} = T_1, \quad (9)$$

$$\left. \frac{\partial T}{\partial y} \right|_{y=H} = 0, \quad (10)$$

It is assumed, that enough far from the cold bridge ($y = H = 3$ m) the heat flow is homogenous. On the covering upper ($x = d$) and bottom ($x = 0$) surfaces, there will be the 3rd kind of border conditions:

$$\lambda \left. \frac{\partial T}{\partial x} \right|_{x=d} = \alpha_2 (T_i - T|_{x=d}), \quad (11)$$

where T_i – inside temperature (in calculations assumed 20 °C);

$$\alpha_2 = \alpha_i = 1/R_{si} = 1/0,17, \text{ W/(m}^2 \cdot \text{K)};$$

$$\lambda \left. \frac{\partial T}{\partial x} \right|_{x=0} = \alpha_1 (T|_{x=0} - T_0), \quad (12)$$

where in the coefficient α_1 , the heat insulation layer under the covering is included

$$\alpha_1 = \frac{1}{R_{se} + d_i / \lambda_i}.$$

Solving the mathematical physics problem (2, 9 – 12) with the variables separation method

$$T(x, y) = T_1 + \sum_{k=0}^{\infty} (C_k \text{sh} \mu_k x + D_k \text{ch} \mu_k x) \sin \mu_k y, \quad (13)$$

where $\mu_k = \frac{\pi(k+0,5)}{H}$, $k=0, 1, 2, \dots$

$$C_k = \frac{2}{\pi(k+0,5)} x \frac{(T_1 - T_0)(\lambda \mu_k / \alpha_2 \cdot \text{sh} \mu_k d + \text{ch} \mu_k d) + (T_1 - T_1)}{(1 + \lambda^2 \mu_k^2 / (\alpha_1 \alpha_2)) \cdot \text{sh} \mu_k d + \lambda \mu_k (1 / \alpha_1 + 1 / \alpha_2) \text{ch} \mu_k d}$$

$$D_k = \frac{2}{\pi(k+0,5)} x \frac{(T_1 - T_0) \lambda \mu_k / \alpha_1 - (T_1 - T_0)(\lambda \mu_k / \alpha_2 \cdot \text{ch} \mu_k d + \text{sh} \mu_k d)}{(1 + \lambda^2 \mu_k^2 / (\alpha_1 \alpha_2)) \cdot \text{sh} \mu_k d + \lambda \mu_k (1 / \alpha_1 + 1 / \alpha_2) \text{ch} \mu_k d}$$

Accordingly - Q_2 and Q_3 will be found in the form

$$Q_{2,3} = - \int_0^d \lambda \left. \frac{\partial T}{\partial y} \right|_{y=0} dx = - \lambda \sum_{k=0}^{\infty} C_k (\text{ch} \mu_k d - 1) + D_k \text{sh} \mu_k d. \quad (14)$$

In order to find the heat flow Q_4 through the outside wall, homogenous solution formulas will be used

$$Q_4 = \frac{T_1 - T_0}{R_{se} + d_i / \lambda_i}. \quad (15)$$

Including the found heat flows (8, 14, 15) in expression (1), we get transcendent equation in relation to unknown cold bridge temperature T_1 . This equation can be easily solved numerically, using Microsoft Excel tool Solver.

The heat flow through the covering and FIBO wall is not homogenous, especially close to the place where they collide. These can be calculated using temperature distribution (13)

$$Q_{gr, FIBO} = \int_0^H \lambda \left. \frac{\partial T}{\partial x} \right|_{x=d} dy = \lambda \sum_{k=0}^{\infty} C_k \text{ch} \mu_k d + D_k \text{sh} \mu_k d. \quad (16)$$

If the heat flow is homogenous, the analogical value of expression (16) can be calculated using the formula

$$Q_{hom} = \frac{(T_1 - T_0)H}{R_{si} + R_{se} + d / \lambda + d_i / \lambda_i}. \quad (17)$$

In expressions (16, 17) it needs to be considered, that the covering and FIBO wall calculations have different R_{si} and insulation layer thickness d_i . Then the linear cold bridge thermal coefficient Ψ W/(m·K), which is calculated on 1 K temperature difference between the outside and inside air, can be found as the following:

$$\Psi_{gr, FIBO} = \frac{\lambda}{T_1 - T_0} \sum_{k=0}^{\infty} C_k \text{ch} \mu_k d + D_k \text{sh} \mu_k d - \frac{H}{R_{si} + R_{se} + d / \lambda + d_i / \lambda_i}, \quad (18)$$

But the thermal coefficient of the common linear cold bridge:

$$\Psi = \Psi_{gr} + \Psi_{FIBO}. \quad (19)$$

In order to assess the analytical solution approximation (formula 1 – cold bridge has constant temperature T_1) accurately, this task was solved numerically using the program ANSYS.

RESULTS AND DISCUSSION

The influence of the cold bridge in the building construction expresses as significant decrease of temperature of the FIBO wall and covering (Fig.1.) close to the point A. This temperature distribution can be calculated by expression (13), and it is presented in Fig. 4., 5. The curves 1 and 2 accordingly – temperature on inner and outer surfaces where they collide with the heat insulation layer (Fig.3. $x=d$ and $x=0$).

As it is seen from the calculations, Fig.1 point A forecasted temperature is 7,7 °C, which on the FIBO wall reaches the balanced temperature 18,5 °C approx. 30 cm distance, but on monolith concrete covering 18,3 °C 1 m distance. Thus, the micro climate of the premises is significantly worsened. Fig.4. curve 2 – the existing minimum does not have physical basis. That is reached by approximations used in calculations, that all cold bridges have the same temperature.

The temperature distribution in the underground wall on y axis (Fig.2.) is shown in Fig.6. It can be seen that temperature distribution is not linear in nature. At $y=0$ $T=T_z=-18$ °C, but at the wall upper part $y=H=3$ m $T=7,7$ °C.

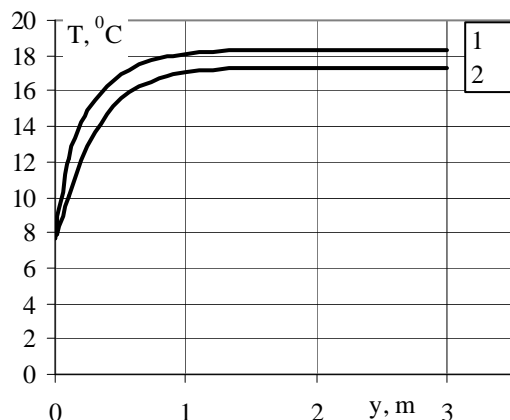


Figure 4. Temperature distribution in FIBO wall. 1 – on the inner surface of the wall; 2 – on the outer surface under heat insulation

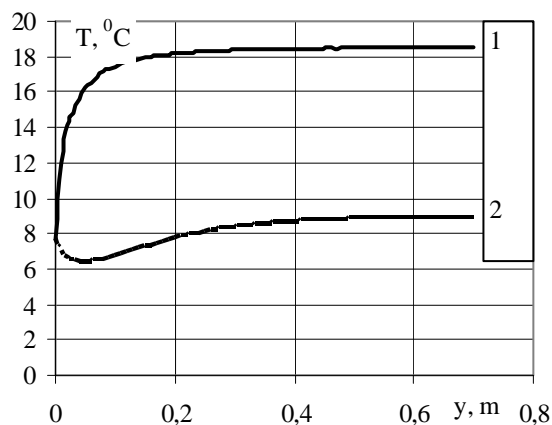


Figure 5. Temperature distribution in covering. 1 – on the inner surface of the covering; 2 – on the outer surface of the covering above heat insulation

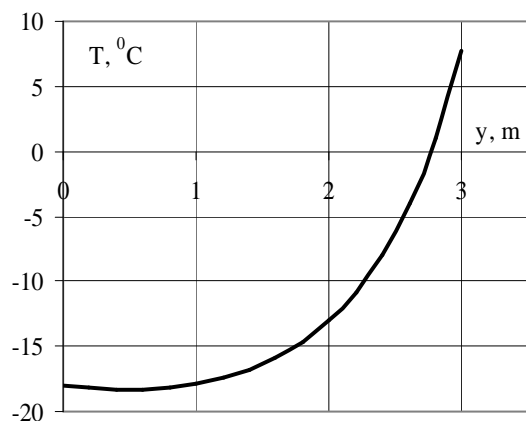


Figure 6. Temperature distribution on underground wall axis line.

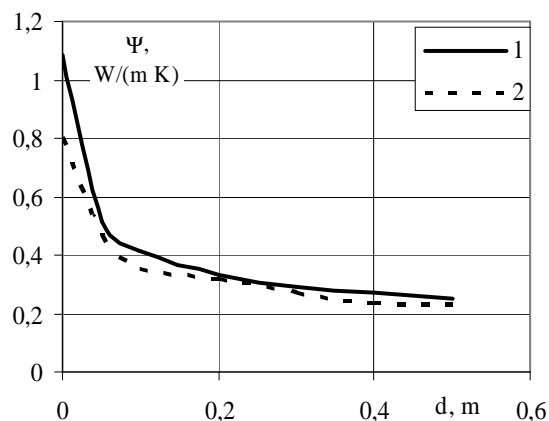


Figure 7. Linear cold bridge thermal coefficient Ψ depending on underground wall heat insulation thickness. Curve 1 has been obtained analytically, 2 – numerically by program ANSYS.

The Building Regulation LBN 002-01 defines the normative Ψ_R and maximal values Ψ_{RM} for the linear cold bridge thermal coefficient Ψ . For example, for dwelling-houses at the temperature factor $k=1$ the values are the following: $\Psi_R=0,2W/(m K)$; $\Psi_{RM}=0,25W/(m K)$. When using Tab.1. physical values, the thermal coefficient of the linear cold bridge of dwelling-houses, depending on the underground wall heat insulation thickness, is presented in Fig.7.

As it is seen, the thermal coefficient of the cold bridge increases the normative value even at heat insulation layer thickness of 0,5 m. Thus, the increase of the heat insulation layer of underground does not avert significantly the influence of cold bridge and it cannot be suggested as problem solution. At the same time when comparing the analytical and numerical solutions, it is seen that approximation of the analytical methods on average gives 10% higher value of the thermal coefficient.

Another possibility is to increase the heat insulation thickness under the monolith concrete covering. Fig.8. shows the cold bridge thermal coefficient dependence on the thickness of the heat insulation layer of the covering.

From the graph it is visible that when increasing the heat insulation layer thickness under monolith concrete covering, the thermal coefficient of cold bridge even increases. It is understandable from physical considerations, because heat flow goes into the direction of lower thermal resistance, and the flow goes through the cold bridge when the resistance of the covering becomes stronger. Thus, additional heat insulation under monolith concrete covering will not solve the problem but even intensify it. The problem solution is a heat insulation layer of 15 cm under the monolith concrete covering, which (Fig.1.) collides with the point B, dividing into two parts.

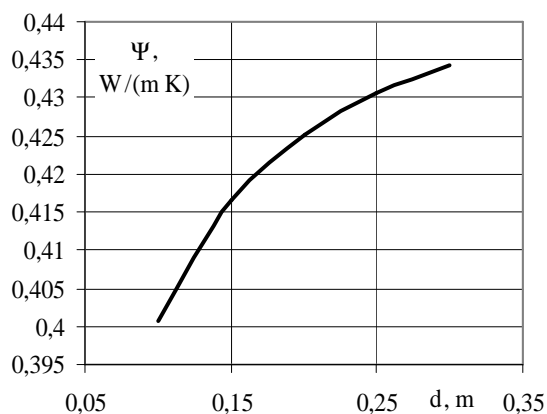


Figure 8. Linear cold bridge thermal coefficient Ψ depending on thickness of heat insulation under monolith concrete covering.

The first part of 10 cm thickness is the mineral cotton under the monolith concrete covering, but the second part of 5 cm thickness of foam polystyrene has to be placed inside the premise above the covering. The thermal coefficient of the covering $U=0,246 \text{ W}/(\text{m}^2\cdot\text{K})$ will not be changed, but the thermal coefficient of cold bridge will be decreased to $\Psi =0,237 \text{ W}/(\text{m K})$. The value is calculated analytically, and it is expected that the real Ψ value will be even 10% less, what coincides with the LBN 002-01 requirements.

The temperature distribution depending on the thickness of the heat insulation layer on y axis (analogical to Fig.5.) is presented in Fig. 9. The trend line No.1 is temperature inside the premises above the foam polystyrene heat insulation layer, the trend line No.2 – under it, at the level where foam polystyrene and monolith concrete collide, the trend line No.3 – under monolith concrete, at the level where it collides with the mineral cotton heat insulation layer.

As it is seen from the curve 1, the problems raised by the cold bridge in the premises have been eliminated.

REFERENCES

Borodiņecs A., Krēliņš A. (2007) *Riga Technical University recommendations for construction regulation LBN 002-01 usage in building design and construction* (in Latvian) editor: RTU, Riga, 131 p.

Latvian Building Regulation LBN 002-01, "Heat Engineering of Insulation Constructions of Buildings", (in Latvian) Approved by the Cabinet of Minister, Republic of Latvia, November 27, 2001, regulation Nr 495.

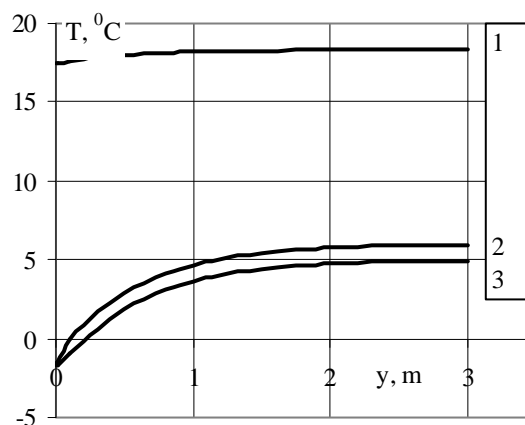


Figure 9. Temperature distribution in covering after cold bridge heat insulation.

Additionally, the risk of condensate development has to be assessed. The calculation shows that at outside temperature above $-10 \text{ }^\circ\text{C}$, the condensate risk does not exist. If the outside temperature is under $-10 \text{ }^\circ\text{C}$ for a long time, little condensate can develop on the surface where monolith concrete and polystyrene collide. The condensate dries up during the drying period. The condensate risk possibility is eliminated if a steam barrier above the polystyrene layer is used in the premise.

CONCLUSIONS

1. A cold bridge develops in the analysed construction, in spite of heat insulation of all surfaces which are disposed to outside air.
2. The cold bridge thermal coefficient can be decreased to the Building Regulation LBN 002-01 requirements, by dividing the covering heat insulation layer into two parts:
 - Mineral cotton layer of 10 cm under the covering;
 - Polystyrene layer of 5 cm above the covering.

THERMAL ANALYSIS OF OVERGROUND BOUND CONSTRUCTIONS

Sandris Liepins, Silvija Strausa, Uldis Iljins*, Uldis Gross*
Latvia University of Agriculture, Faculty of Rural Engineering,
*Latvia University of Agriculture, Faculty of Information Technologies
e-mail: sandris.liepins@inbox.lv, silvija.strausa@llu.lv,
uldis.iljins@llu.lv, uldis.gross@llu.lv

ABSTRACT

Thermographic cameras are widely used for inspecting and analyzing surfaces of overground bound constructions. The method demonstrates a complete image of thermal spots and is suitable for giving limited conclusions about the whole surface temperature of the bound construction. The main problem of infrared analysis is exact temperature layout, because different heat transmission areas can be seen on the screen, but heat radiation levels are not so reliable. Such temperature differences can exceed even 50% of the real surface temperature. To explore more accurate surface point temperatures special thermal sensors and sensor types were applied. By point type infrared and thermo-couple device temperature distribution points on building material surface were gathered, compared and calibrated with the infrared camera output image. With heat flow and attachable temperature sensors, the material surface and surrounding temperatures were analyzed in an extended period. Also mathematical temperature curves were calculated to prove the temperature distribution on the surface. All samples for practical research were made at the Tenax factory, located in Dobeles, Latvia. The manufacturer of these samples gave heat properties to compare with the experimental data. By using the above mentioned methods, exact temperature loads can be defined and calculated; these methods are also suitable for analyzing heat transmission of overground bound constructions.

Key words: bound constructions, heat transmission, infrared method.

INTRODUCTION

There is a need for thermographic calculations regarding bound constructions to design energy saving buildings with good indoor climatic conditions, in combination with efficient and highly durable materials, as well as environmentally friendly technologies.

Building bound constructions generally consist of foundations, walls and roofs, but this study analyzes only the above-ground parts of those structures. In every type of construction, intra-thermal processes take place. They depend on the properties of the applied materials and exterior environment. Thermal processes in structures can be identified and quantified in cases where one or more structural surfaces are in different heat and moisture (environmental) conditions. The order of thermal designing of bound constructions is regulated by the Latvian building regulation LBN 002-01 "Heat transfer in building envelopes".

The aim of the research was to combine analytical and experimental methods of thermal analysis and carry out experimental thermal analysis of bound constructions (exterior composite panels).

Using thermal imaging cameras with contact measuring devices, and setting the surface temperature proxies in a wide area, bound construction heat transmission can be calculated by means of a three-temperature method, which includes the point and linear thermal bridges and

other places of heat loss in constructions. The method provides an opportunity to expand the experimental use of the thermal image camera for determining heat transfer of bound constructions.

MATERIALS AND METHODS

Technical devices used in the research

1. Electronic measuring system of heat flows and temperatures MBox RF1.

Wireless measuring device of heat flows and temperatures MBox RF1 is designed to measure long term temperatures and heat flows with time step and storing the measured data in a computer.

Technical data:

- Sensors: Thermocouple (K), flow sensors;
- Number of measurement channels: 8 for temperature, 2 for flows;
- Measurement range: temperature -50°C to +120°C, flows -150 to +150W/m²;
- Accuracy: temperature ±0.2 °C, flows ±0.5W/m²;
- Resolution: temperature: 0.01 °C, flows 0.01Wm².

2. Testo 845. A thermometer which works in the spectrum of infrared waves in a narrow area (points), equipped with a thermocouple probe for contact measuring surface temperature:

- Measurement range: -35°C to +950°C;
- Accuracy of the infrared device and thermocouple at room temperature: ±0.75°C.

3. ThermoPro TP8. Camera of thermal picture, works in the spectrum of infrared waves (thermographic camera):

- Measurement range: -20°C to $+800^{\circ}\text{C}$;
- Resolution: 384×288 thermal pixels (sensors);
- Accuracy: $\pm 1^{\circ}\text{C}$ or 1% of the result.

4. Elektrolux ECN 2658/BNI 280. A cooling chamber (Figure 1):

- Class: SN/T;
- Volume: 260 L;
- Cover size: 540 x 845 mm;
- Temperature: -33 to -38°C (measured in an experiment).

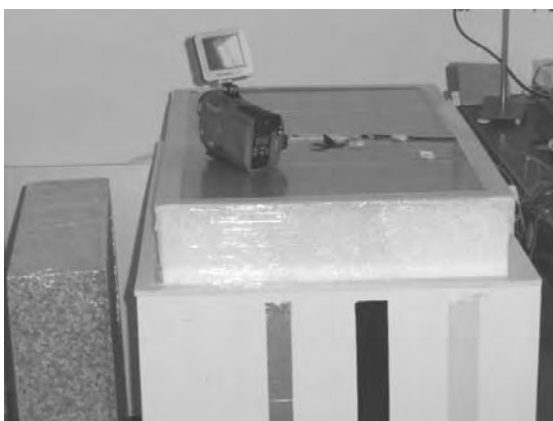


Figure 1. Cooling chamber Elektrolux ECN 2658/BNI 280, laboratory sample, TP8, etc.

Description of the sample

The sample for laboratory measurements was produced at the factory of company Tenax in Dobele, Latvia.

Specifications of the experimental sample:

- Size: width – 540mm, length – 845mm, height – 150mm;
- Type of sample: composite facade panel consisting of two painted metal sheets and thermoinsulation layer;
- Stuffing: expanded polystyrene EPS with graphite foam particles ('Neopor', Tenax), type EPS 150;

The book 'Sendvičpaneļi Tenax. Metodiskie norādījumi projektētājiem un būvniekiem' (SIA Tenax, 2004) gives a coefficient of permeability U ($\text{W}/\text{m}^2\text{K}$): type EPS 150, thickness 150mm, $U=0.224 \text{ W}/\text{m}^2\text{K}$.

Description of laboratory research method

The experimental research methods had several parts.

Setting up samples and connecting sensors. Each wireless transmitters' thermocouples were divided into groups, two in each. There were eight thermocouples and four groups.

After fixing the thermocouples, heat flow measuring devices q_1 and q_2 were fixed. The scheme of the mounted thermocouples and heat flow measuring devices is shown in Figure 2.

Figure 3 shows the fixation of thermocouples. For about 48 hours the sample was loaded with the *temperature difference* where room temperature was $+18..+24^{\circ}\text{C}$, but in the cooling chamber $-33..-38^{\circ}\text{C}$, and $\Delta T \sim 56^{\circ}\text{C}$ (within $\Delta=50$ to 62°C).

Parallel to the period when heat processes were normalized (reaching a balance) and the heat process can be described as homogeneous and heat flows are almost constant, data registration programm *UmeasRF* registered incoming signals with an hour interval (40 measurements were registered, 7 and 8 were chosen for data analysis).

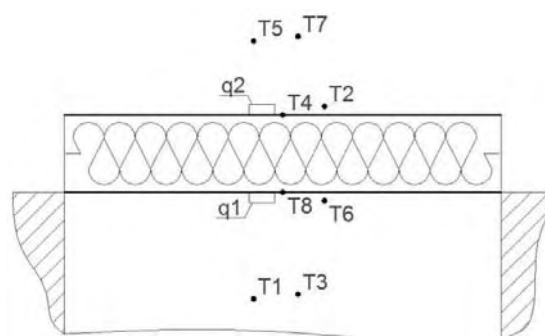


Figure 2. Scheme of the fixation of thermocouples and heat flow measuring devices.

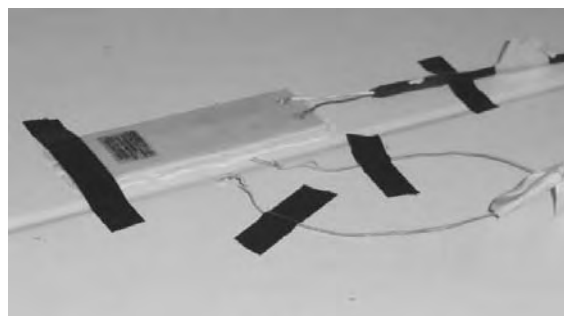


Figure 3. Fixed state of two thermocouples and heat flow measuring device.

When temperatures were stable, *the sample was turned around 180°* on the condition that the side of the sample which was in the room was placed into the cooling chamber's cold zone and the cold zone sample surface was turned to the warm zone of the room. Thermal blow of the opposite surfaces in this case was ΔT reaching $\sim 60^{\circ}\text{C}$ (from $+23^{\circ}\text{C}$ to -37°C).

This conception was presumed because quality and general data were needed for analysis of sensors ($T_1 \dots T_8, q_1, q_2$). That excludes error in case if one of the sensors transmits incorrect information (Figure 4).

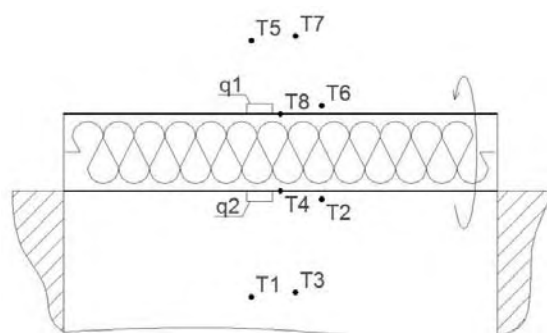


Figure 4. Scheme of mounting of thermocouples and heat flow measuring device in reversed position.

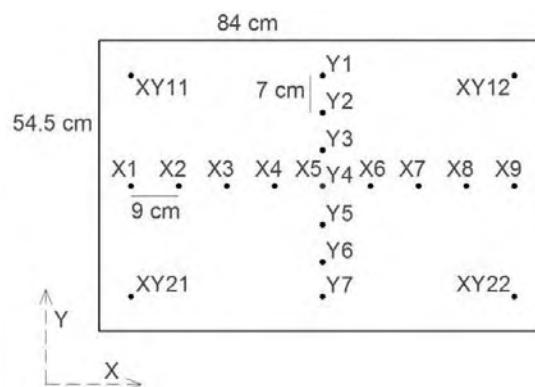


Figure 5. Scheme of measurement points of the sample surface.

Measurements of the laboratory sample, °C

Table 1

Reading at point	Testo 845, I.R., $\epsilon=0.99$	Testo 845, T.C.	ThermoPro TP8, $\epsilon=0.99$	ThermoPro TP8, $\epsilon=0.90$
X1	23.4	23.7	25.1	24.6
X2	23.1	23.6	24.3	24.0
X3	23.0	23.6	23.9	23.5
X4	22.9	23.5	23.8	23.4
X5	22.9	23.3	23.6	23.3
X6	23.0	23.4	23.8	23.4
X7	23.0	23.5	24.0	23.6
X8	23.2	23.9	24.3	24.1
X9	23.4	24.2	25.2	24.7
Y1	23.4	23.8	24.6	24.2
Y2	23.2	23.7	24.2	23.9
Y3	23.1	23.6	23.8	23.5
Y4	23.1	23.5	23.6	23.3
Y5	23.4	23.7	23.8	23.5
Y6	23.6	24.1	24.2	23.7
Y7	23.7	24.6	24.7	24.4
XY11	23.3	24.2	25.3	25.3
XY12	23.5	24.4	25.4	25.4
XY21	23.3	24.4	25.3	25.3
XY22	23.5	24.7	25.4	25.4

where

Testo 845 I.R. – temperatures in the infrared spectrum acquired from the Testo 845,

Testo 845, T.C. – temperatures at points read from the Testo 845 thermocouples probe,

ThermoPro TP8, $\epsilon=0.99$ – results from the programme treating pictures in the infrared spectrum where the coefficient of the surface emission is $\epsilon=0.99$,

ThermoPro TP8, $\epsilon=0.90$ – results from the programme treating pictures in the infrared spectrum where the coefficient of the surface emission is calibrated by trial and error method $\epsilon=0.90$ and corresponds to the result on X-axis at point X₅.

When the second stabilization process was over, the surface of the sample was divided into parts over the midfield in the area of 72 x 42 cm, where the step on X-axis was 9 cm, but the step on Y-axis was 7 cm. Measurement points on X-axis were marked

as X₁ .. X₉; on Y-axis: Y₁ .. Y₇. (Figure 5).

According to the matrix principle measurement points XY₁₁ (upper left corner), XY₁₂, XY₂₁ un XY₂₂ (lower right corner) were marked in the corners of the sample.

In the marked points, surface temperatures were measured using the device Testo 845 with a surface thermometer which works in the spectrum of infrared waves and thermocouple probe. The data gathered are shown in Table 1.

After reading the surface temperature with Testo 845, thermography of the sample was carried out with ThermoPro TP8.

Calibrating emission coefficient ϵ of the picture in the infrared spectrum real temperature division on the sample surface was obtained which corresponded to the measurements of thermocouple in characteristic points on X-axis and Y-axis.

From the results of the recorder MBox RF1 measurements $T_1 \dots T_8$ were chosen; resistance of surface air layers and coefficient of heat permeability U (W/m^2K) were calculated according to civil physics formulas.

RESULTS AND DISCUSSION

Measurements of laboratory samples

Measurements of the surface temperatures show that measurements from the Testo 845 I.R. (infrared spectrum) with emissivity $\epsilon=0.99$ contain lower temperatures than the Testo 845 T.C. and ThermoPro TP8. Figures show error of the device because the value of surface emissivity ϵ cannot be higher than 1. Electronic measuring device of heat flows and temperatures MBox RF1 fixed temperature on the surface $T_4 = 19.55$ °C; couples $T_5; T_7$ (environmental temperature) = 20.31 °C; couples $T_1; T_3$ (temperature in cold area) = -36.70 °C (First case, see Figure 2). After flipping, the temperature on surface $T_8 = 20.00$ °C; couples $T_5; T_7$ (environmental temperature) = 20.73 °C; couples $T_1; T_3$ (temperature in cold area) = -36.63 °C (Second case, see Figure 4).



Figure 6. Measurements of the surface temperature with ThermoPro TP8 ($\epsilon=0.90$). Analysis made in the programme Guide IrAnalyser.

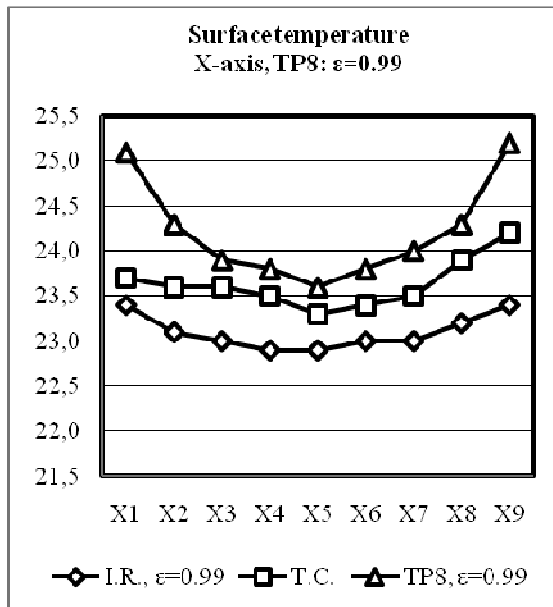


Figure 7. Measurements of the surface temperature on X-axis (ThermoPro TP8: $\epsilon=0.99$).

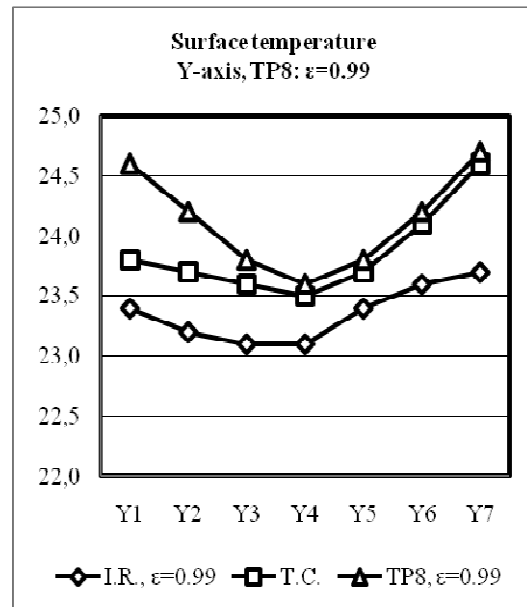


Figure 8. Measurements of the surface temperatures on Y-axis (ThermoPro TP8: $\epsilon=0.99$).

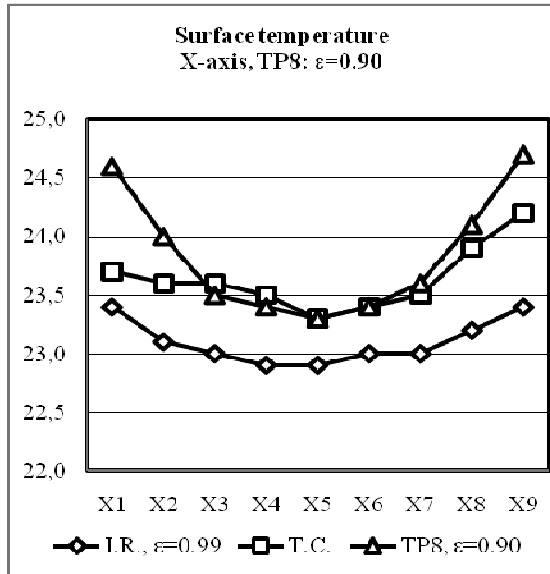


Figure 9. Measurements of the surface temperature on X-axis (ThermoPro TP8: ε=0.90).

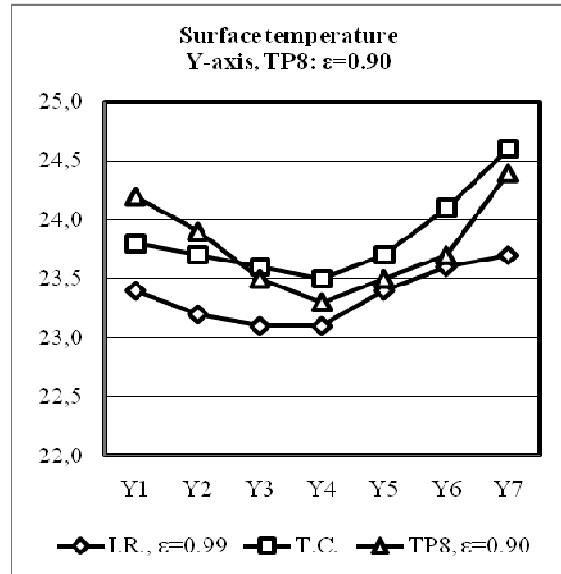


Figure 10. Measurements of the surface temperature on Y-axis (ThermoPro TP8: pie ε=0.90).

Heat flows q and heat permeability coefficient U can be defined:

$$q = \alpha_i (T_i - T_e) = U (T_i - T_e) \quad \text{um} \quad (1)$$

$$U = \alpha_i \frac{T_i - T_1}{T_i - T_e} \quad (2)$$

where

α_i – coefficient of heat transmission on inner surface, W/m^2K

T_i – temperature in room, °C

T_e – outer temperature in air, °C

T_1 – temperature on the first surface of the bound construction, °C

Respectively,

$$q = \alpha \Delta T \quad \text{um} \quad \alpha = \frac{q}{\Delta T} \quad (3)$$

Heat transmission coefficients of the border layer $\alpha_{i,1}$; $\alpha_{i,2}$ (for the first and second cases):

$$\alpha_{i,1} = \frac{16.11_{(q1,q2)}}{20.31_{(T5,T7)} - 19.55_{(T4)}} = 21.20 \frac{W}{m^2K} \quad (4)$$

$$\alpha_{i,2} = \frac{18.99_{(q1,q2)}}{20.73_{(T5,T7)} - 20.00_{(T8)}} = 26.01 \frac{W}{m^2K} \quad (5)$$

Knowing heat transmission coefficients of border air layer α , according to equation (2) it is possible to calculate the heat transmission of the bound construction $U_{1-1, 1-2}$ (W/m^2K) In the first case:

$$U_{1-1} = \alpha_i \frac{T_i - T_1}{T_i - T_e} = 21.20 \frac{20.31_{(T5,T7)} - 19.55_{(T4)}}{20.31_{(T5,T7)} - (-36.70_{(T1,T3)})} = 0.283 \frac{W}{m^2K} \quad (6)$$

Equation (6) is called 'equation of heat transmission coefficient by method of three temperatures'.

Verification of the equation (6) by expression (1), marking as U_{1-2} (calculation No 2 for the first case):

$$U_{1-2} = \frac{q}{(T_i - T_e)} = \frac{16.11_{(q1,q2)}}{20.31_{(T5,T7)} - (-36.70_{(T1,T3)})} = 0.283 \frac{W}{m^2K} \quad (7)$$

Observation (1): Verification of the first calculation is correct.
Heat permeability $U_{2-1, 2-2}$ (W/m²K) of bound construction in the second case:

$$U_{2-1} = \alpha_i \frac{T_i - T_1}{T_i - T_e} = 26.01 \frac{20.73_{(T_5, T_7)} - 20.00_{(T_9)}}{20.73_{(T_5, T_7)} - (-36.63_{(T_1, T_3)})} = 0.331 \frac{W}{m^2 K} \quad (8)$$

Verification of the equation (8):

$$U_{2-2} = \frac{q}{(T_i - T_e)} = \frac{18.99_{(q_1, q_2)}}{20.73_{(T_5, T_7)} - (-36.63_{(T_1, T_3)})} = 0.331 \frac{W}{m^2 K} \quad (9)$$

Observation (2): Verification of the second calculation is correct.

Standardized coefficient of heat permeability given by the manufacturer to the construction $U=0.224$ W/m²K. After calculations, mismatches in both cases: $\Delta_1 = 20.8\%$; $\Delta_2 = 32.3\%$.

Mismatches (2) $\Delta_2 = 32.3\%$ can be explained by 'thermal blow' what the construction gets after flipping and it is not clear how the insulation layer between heat flow measuring device and surface of the sample behaves. It can be possible that the attracted air moisture creates ice crystals in the insulator interfering with the reading of accurate data.

CONCLUSIONS

Camera of thermal imaging, which shows surface temperatures in the infrared spectrum alone without

other devices indicates only the general temperature of the surface, which can differ from real temperatures >50%, because of an incorrect assumptive coefficient of the surface emission ($\epsilon=0.01..0.99$);

When using the thermographic camera together with other measuring devices and defining surface temperatures in a wide area, it is possible to calculate the heat permeability of the bound construction, also pointed and linear thermal bridges and other spots of heat loss in the construction. We used the method of three temperatures in the calculations;

A set of several precise devices allows us to objectively evaluate the obtained results and avoid serious failures in measurements.

REFERENCES

- Akmens P., Krēsliņš A. (1995) *Ēku apkure un ventilācija* 1.daļa. Rīga: Zvaigzne ABC. 168 lpp.
- Ministru kabineta noteikumi Nr.495, LBN 002-01 'Ēku norobežojošo konstrukciju siltumtehnika', Rīga, 27.11.2001.
- PAIC (Procesu izpētes un analīzes centrs), Siltuma plūsmu un temperatūras elektroniskās sistēmas MBox RF1 lietotāja instrukcija, Rīga: PAIC, 2007. – 7 lpp.
- Sendvičpaneļi Tenax*. Metodiskie norādījumi projektētājiem un būvniekiem (2004) SIA Tenax, LLU. Jelgava. 122 lpp.
- Valters A., Apinis A., Ogrīņš M., Danebergs A., Lūsis Dz., Okmanis A., Čudars J. (1992) *Fizika*. Rīga: Zvaigzne. 735 lpp.

HEAT ENERGY CONSUMPTION IN UNRENOVATED BUILDINGS AND IN BUILDINGS AFTER PARTIAL RENOVATION

Ēriks Krūmiņš

Latvia University of Agriculture, Department of Architecture and Building
eriks.krumins@riga.lv

Ilze Dimdiņa, Arturs Lešinskis

Riga Technical University, Institute of Heat, Gas and Water Technology
ilze@epakavs.lv; Arturs.Lesinskis@rtu.lv

ABSTRACT

The aim of the present study was to analyse the heat energy consumption in public buildings. Our data contained information about more than 400 public buildings, including the data of the heat energy consumption depending on the use of the building, electric energy consumption and the data about the quantity and quality of windows in these buildings in 2008. The data were analysed dividing all public buildings into twelve groups: schools, special status education schools, day-care centres, hospitals, libraries, cult buildings, recreation centres, local government buildings, museums, sport centres, academy of music, and shelters. The largest groups are schools and day-care centres /kindergartens/. These two groups we analysed particularly. Our analysis focused on the heat energy consumption in buildings with new double-pane windows and frames from polyvinylchloride (PVC) with heat transmittance $U \leq 1,8 \text{ W}/(\text{m}^2 \cdot \text{K})$ and in buildings with simple windows divided into two-panes with two separate wooden frames (heat transmittance $U \geq 2,5 \text{ W}/(\text{m}^2 \cdot \text{K})$). We analysed the data of the indoor air quality (IAQ) in three day-care centre buildings from March 11 to 16, 2011. The data analysis showed that partial renovation – change of the windows, doors etc. with and without heat insulation of the buildings - does not provide the heat energy consumption economy required by the Ministry of Economics by the year 2020, and in the majority of cases made consumption even bigger.

Keywords: heat, consumption, day-care centres, renovation, public buildings

INTRODUCTION

Energy consumption economy and optimisation lead to less carbon dioxide emission. Significant decisions of the European Parliament and of the Council are:

- Directive 2002/91/EC of the European Parliament and the Council of 16 December 2002 – on the energy performance of buildings,
- Directive 2004/8/EC of the European Parliament and the Council of 11 February 2004 – on the promotion of cogeneration based on a useful heat demand in the internal energy market and amending Directive 92/42/EEC,
- Directive 2006/32/EC of the European Parliament and the Council of 5 April 2006 on energy end-use efficiency and energy services and repealing Council Directive 93/76/EEC (Text with EEA relevance).

On the basis of these documents the Latvian Cabinet of Ministers made laws for local use: Latvian Construction Standard LBN 002-01 “Building Envelope Calorific”,

- Latvian Law on The Energy Performance of Buildings,
- Latvian Construction Standard LBN 208-08 “Public Buildings and Structures”.

The main ministry for energy issues is the Ministry of Economics. The Latvian Energy Development Guidelines for the years 2007- 2016 define that the heat energy consumption should decrease by approximately 28%. In the time period up to the year 2020 the heat energy consumption should decrease by 40%. Is it possible to achieve this with the previous renovation methods? We researched it and give an answer in this study.

Buildings that have very high heat energy demands are part of Latvia’s heritage from the Soviet times. The great majority of public buildings do not have mechanical ventilation systems.

Heat energy consumption in public buildings has been explored in very few Latvian scientific researches. We did not find a similar study in Latvian scientific publications. Building renovation was made under conditions of inadequate information. The IAQ started to worsen after the end of the time period. This unpleasantness is omitted. Outdoor air infiltration had stopped and people need to open windows to make the IAQ better. Our study shows that we need to change something in the building process in Latvia. This time we presented day-care centres and school buildings heat consumption on average in the year 2008 and a part of the data processing results from IAQ parameters in the six day-care centre buildings which were obtained in February and March 2011.

MATERIALS AND METHODS

Total obtained data

Aggregate information contained data about 420 public buildings which were divided into 12 groups: special status education schools – 43 060m² ; shelters – 9 993m²; local government buildings – 44 077m²; recreation centres – 59 994m²; museums - 369m²; hospitals – 15 232m²; sport centres – 18 435m²; libraries – 8 324m²; academy of music – 5 368m²; day-care centres – 248 923m²; schools – 841 395m²; cult buildings – 6 067m².

Our analysis focused on heat energy consumption in unrenovated day-care centres and school buildings and in day-care centres and school buildings after a partial renovation (data contained and analysis included also some new ones that were built as a control group). The data of these two groups had to be analysed particularly. At last before the analysis was finished we compared heat consumption in unrenovated buildings and in buildings after a partial renovation. The methods of analysis were based on (E.Krumins et al., 2010) software. Our analysis showed that there was a big difference after renovation in heat consumption in buildings with similar total floor areas.

IAQ measurements

In the winter season (from 11 March to 16 March) 2011 we continued the research in the six day-care centre buildings with the aim to attain data from the IAQ parameters. In this research, we used: in unrenovated day-care centre building – MINILOG GSOFT 40K V7.80 (air temperature logger), EASYLOG 40RF GSOFT 40K V7.80 (air relative humidity logger) from 11 February to 17 March. Two Wöhler CDL 210 version 1.1.6. (air temperature, relative humidity and carbon dioxide quantity) loggers in partially renovated and new day-care centre buildings with different time of building. After attaining the measurement data, we analysed and compared these data.

RESULTS AND DISCUSSION

Heat consumption

Now we present the heat consumption per annum in correlation with the building floor areas in school buildings Fig.1, Fig.2 and day-care centre buildings Fig.3 and Fig.4 in 2008.

In Fig.2 we clearly see that in partially renovated school buildings something was done incorrectly. The school buildings with similar total floor areas have different heat consumption per annum. For example, comparing the building total floor areas (m²) and heat consumption (MWh) per annum in:

- school building no.1: 3607m² – 412,97MWh;
- school building no.2: 3675m² –

- 459,00MWh;
- school building no.3: 3570m² – 517,61MWh;
- school building no.4: 3484m² – 645,82MWh;
- school building no.5: 3224m² – 723,15MWh.

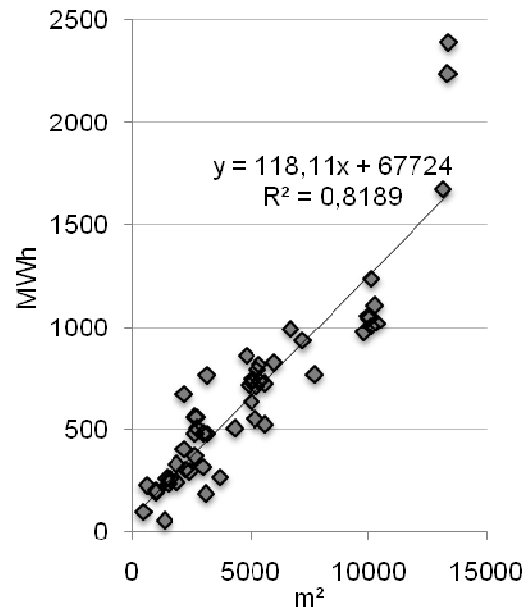


Figure 1. Unrenovated school buildings. Total heat energy consumption (MWh) per annum correlation with building floor areas (m²).

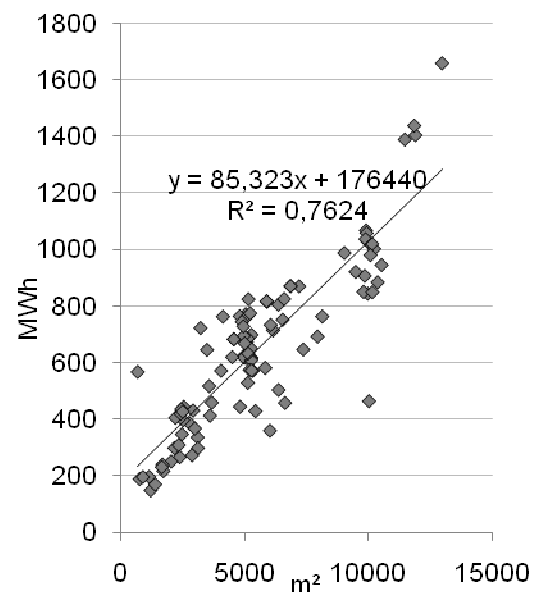


Figure 2. Partially renovated school buildings. Total heat energy consumption (MWh) per annum correlation with building floor areas (m²).

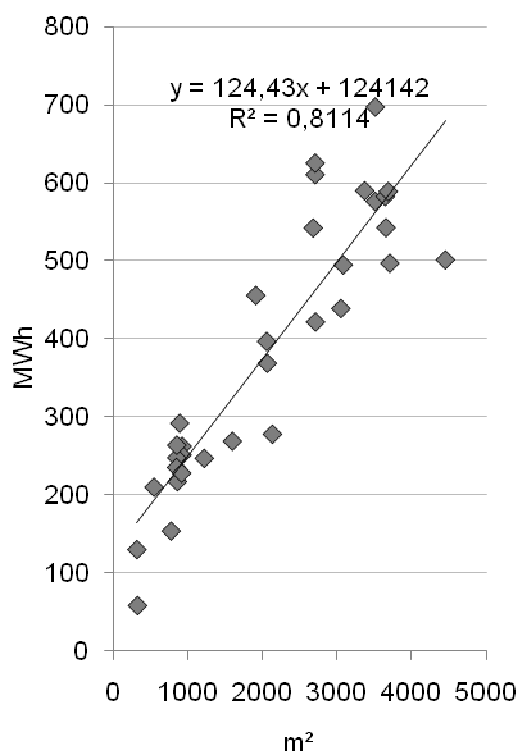


Figure 3. Unrenovated day-care centre buildings. Total heat energy consumption (MWh) per annum correlation with building floor areas (m²).

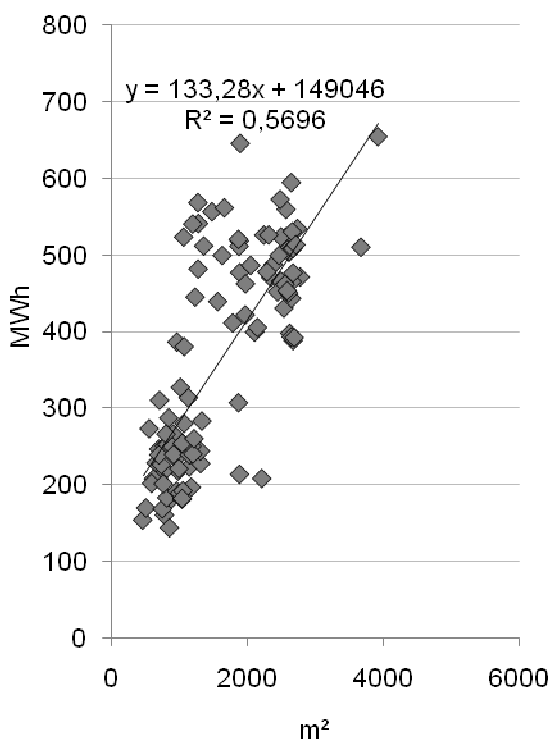


Figure 4. Partially renovated day-care centre buildings. Total heat energy consumption (MWh) per annum correlation with building floor areas (m²).

In Fig.4 we clearly see that in the partially renovated day-care centre buildings also something was done incorrectly. As in the school buildings in the day-care centre buildings with similar total floor areas also there is different heat consumption per annum. For example, comparing the building total floor areas (m²) and heat consumption (MWh) per annum in:

- day-care centre building no.1: 2217m² – 208,00MWh;
- day-care centre building no.2: 1890m² – 213,53MWh;
- day-care centre building no.3: 2142m² – 278,02MWh;
- day-care centre building no.4: 1875m² – 306,82MWh;
- day-care centre building no.5: 1976m² – 421,39MWh;
- day-care centre building no.6: 1893m² – 476,61MWh;
- day-care centre building no.7: 2054m² – 486,00MWh;
- day-care centre building no.8: 1886m² – 517,69MWh;
- day-care centre building no.9: 1901m² – 645,00MWh.

Fig.5 demonstrates four trendlines: 1. abstract – trendline made under the Latvian Energy Development Guidelines for the years 2007- 2016 and by the year 2020 the heat energy consumption must be decreased by 40% (from 250kWh/m² per annum to 150kWh/m² per annum on average in Latvia); 2. unrenovated buildings trendline; 3. Partially renovated buildings trendline; 4. Normative – trendline that demonstrates right renovation under the Latvian Energy Development Guidelines for the years 2007- 2016 and till the year 2020 from school buildings. It is evident that only three unrenovated school buildings and three school buildings after a partial renovation are located under the normative trendline. We analyzed 101 partially renovated school buildings and 55 unrenovated school buildings. That spells out a necessity as four buildings were not renovated and in only five (!!!) school buildings (5% from all partially renovated school buildings) partial renovation was done properly this time.

Fig.6 also demonstrates four trendlines: 1. abstract – trendline made under the Latvian Energy Development Guidelines for the years 2007- 2016 and by the year 2020 the heat energy consumption must be decreased by 40% (from 250kWh/m² per annum to 150kWh/m² per annum on average in Latvia); 2. unrenovated buildings trendline; 3. partially renovated buildings trendline; 4. normative – trendline that shows proper renovation under the Latvian Energy Development Guidelines for the years 2007- 2016 and to the year 2020 for day-care centre buildings.

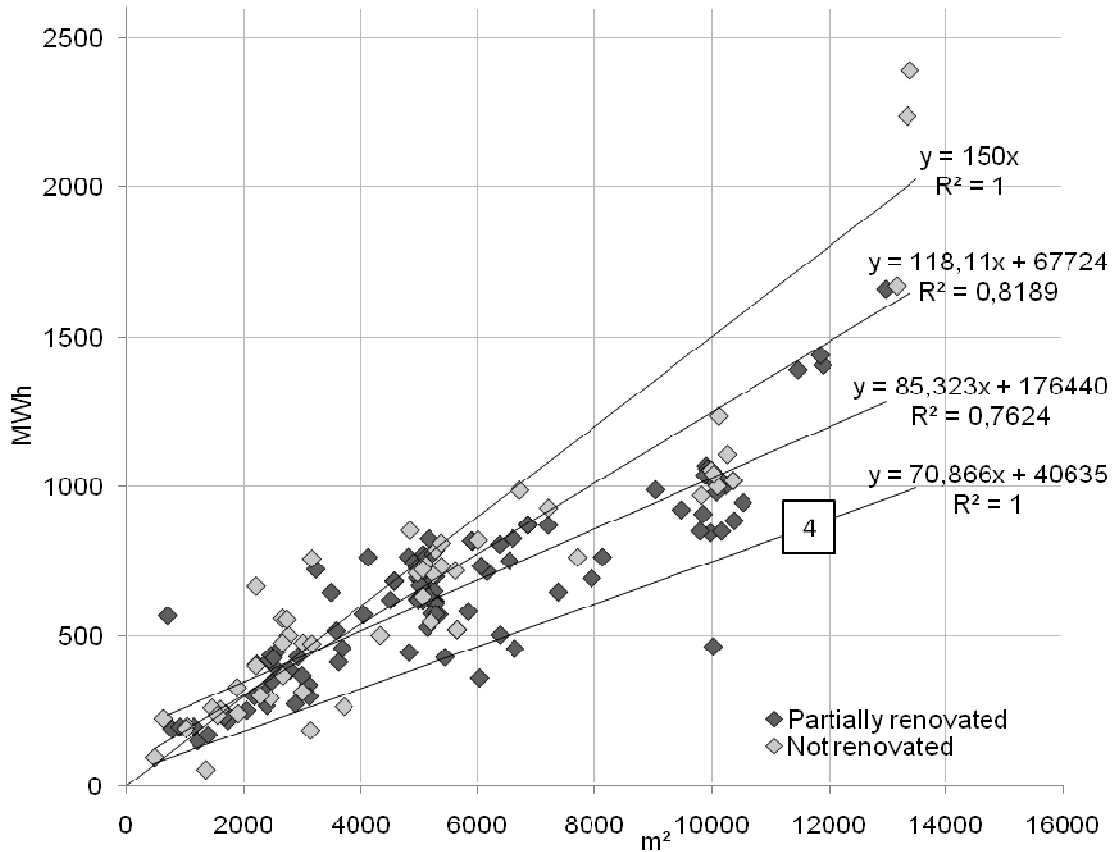


Figure 5. Unrenovated and partially renovated school buildings.

Total heat energy consumption (MWh) per annum correlation with building floor areas (m²) with trendlines:
 1. abstract; 2. unrenovated buildings; 3. partially renovated buildings; 4. normative.

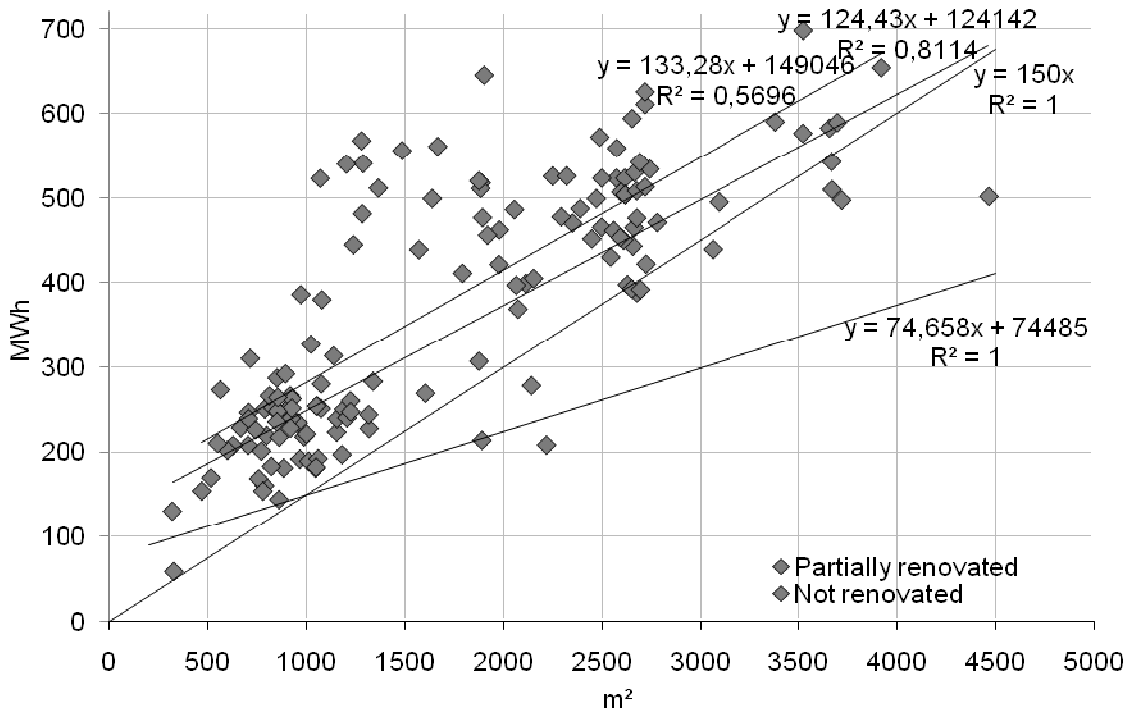


Figure 6. Unrenovated and partially renovated day-care centre buildings.

Total heat energy consumption (MWh) per annum correlation with building floor areas (m²) with trendlines:
 1. abstract; 2. unrenovated buildings; 3. partially renovated buildings; 4. normative.

It is evident that only one unrenovated day-care centre building and three day-care centre buildings after a partial renovation are located under (on) the normative trend line.

We had to analyse 111 partially renovated day-care centre buildings and 32 unrenovated day-care centre buildings. That spells out a necessity as one day-care centre building was not renovated and in only three (!!!) day-care centre buildings (2,7% from all partially renovated day-care centre buildings) partial renovation was done correctly this time.

IAQ measurements

This time we present the data from the IAQ measurements in three day-care centre buildings from 11 March to 16 March 2011 in:

1. unrenovated day-care centre building (total floor area – 2142m², heat consumption per annum – 278 020kWh;
2. partially renovated (in the year 2007) day-care centre building (total floor area – 1901m², heat consumption per annum – 645 000kWh;
3. new (was built in 2005) day-care centre building (total floor area – 2217m², heat consumption per annum – 208 000kWh).

The average outdoor air relative humidity and temperature are presented in Fig.7 and Fig.8. This was made from information data bases from the state limited liability company "Latvian Environment, Geology and Meteorology Centre" homepage.

They did not have information about the outdoor carbon dioxide (CO₂) quantity. Our measurements show the CO₂ quantity from 400ppm (parts per million, 10⁻⁶) to 450ppm in Riga city.

Fig.9 presents the outdoor air and indoor air relative humidity in per cents in day-care centre buildings. The horizontal axis presents the data of times and date. Minor gridlines disclose time:

- first 2:00;
- second 5:00;
- third 8:00;
- fourth 11:00 etc..

Major gridlines, for example from:

- zero to eight are the first data, achieved on 11March;
- nine to sixteen are the second data achieved on 12March
- seventeen to twenty four are the third data achieved on 13 March, etc..

(12 March - Saturday and 13 March - Sunday)

The following figure clearly shows that the indoor air relative humidity is very low. The recommended IAQ minimum is 30% (maximum is 70%) as was written in the Labour Protection Requirements in Workplaces as prescribed in the Regulation no. 359 from 28 April, 2009 of the Cabinet of Ministers of the Republic of Latvia.

Renovation and new building of day-care centre

buildings did not guarantee this requirement. In the partially renovated day-care centre building, the indoor air humidity was insignificantly lower than in the unrenovated building and in the new one.

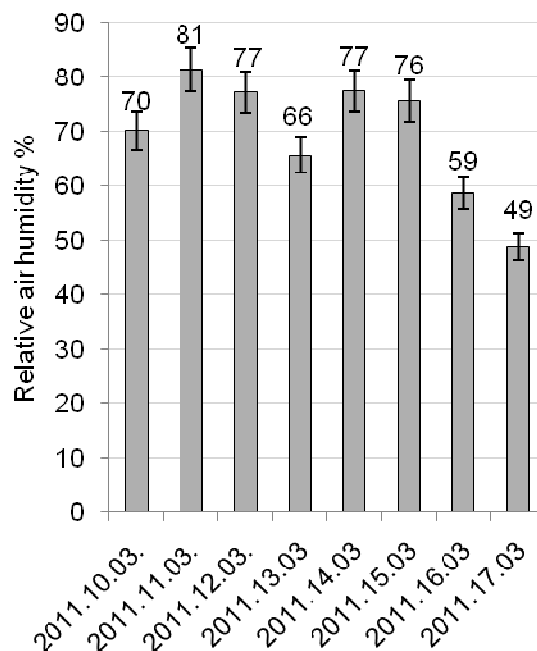


Figure 7. Average outdoor air relative humidity from 10 March till 17march 2011 with error bars.

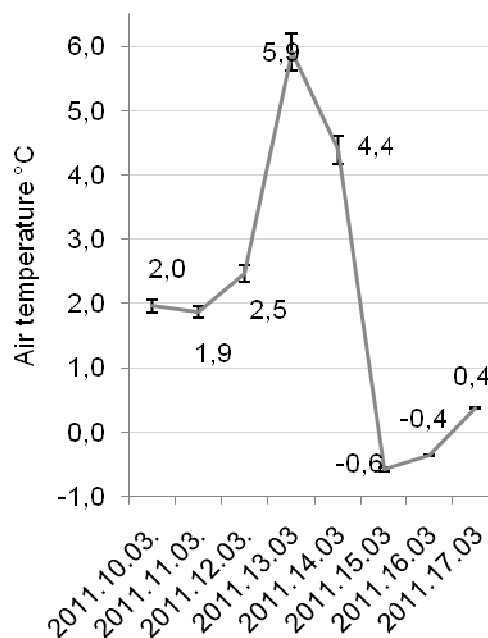


Figure 8. Average outdoor air temperature from 10 March to 17march 2011 with error bars with 5% value.

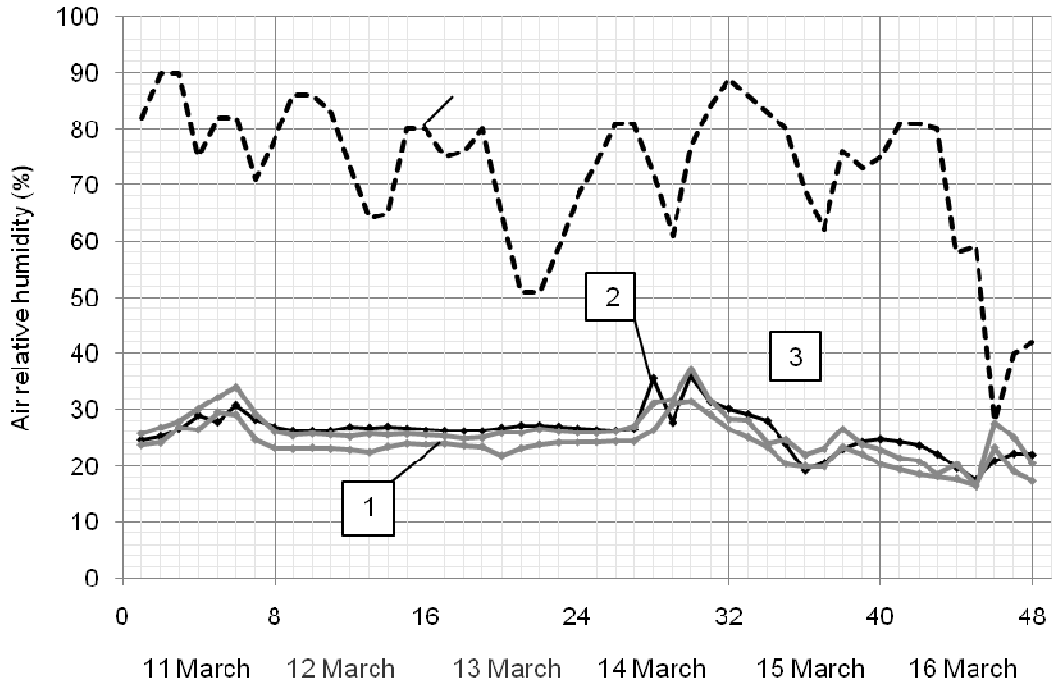


Figure 9. Air relative humidity in:
 1 – partially renovated building (2007, average heat consumption 339kWh/m² per annum);
 2 – newly erected building (built in 2005, average heat consumption 94kWh/m² per annum);
 3 – unrenovated (average heat consumption 130kWh/m² per annum); 4 – outdoor.

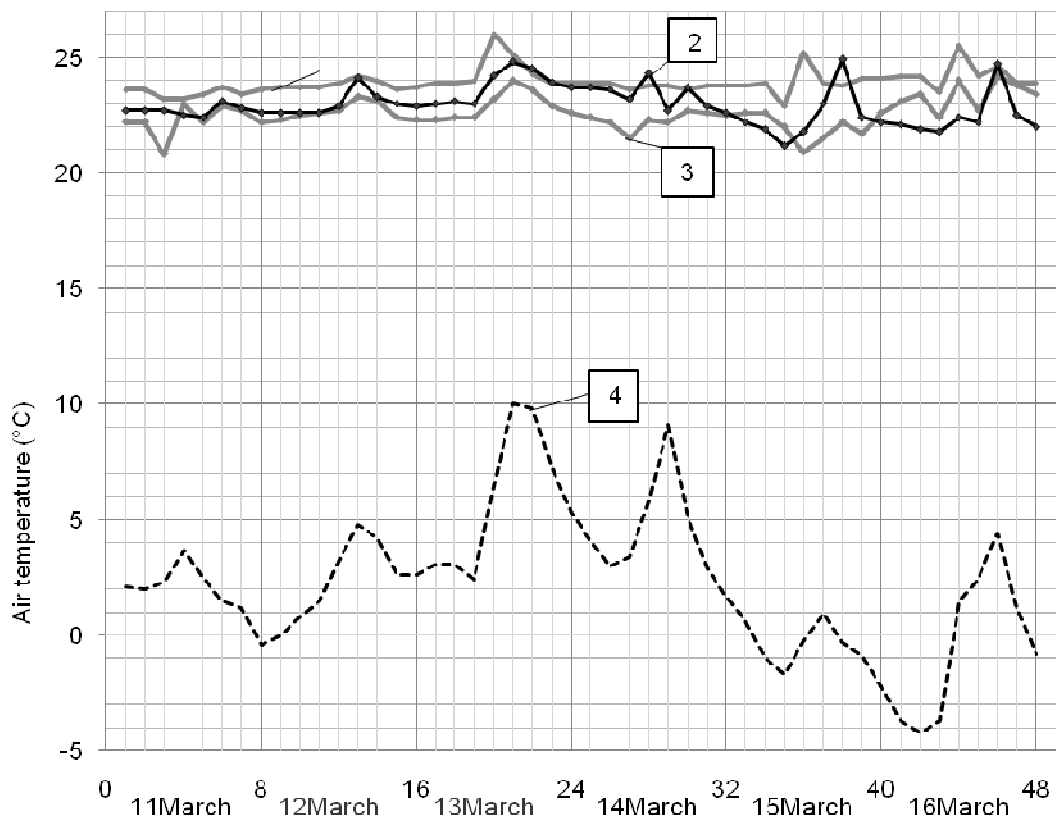


Figure 10. Air temperature in:
 1 – partially renovated building (2007, average heat consumption 339kWh/m² per annum)
 2 – newly erected building (built in 2005, average heat consumption 94kWh/m² per annum)
 3 – unrenovated (average heat consumption 130kWh/m² per annum); 4 – outdoor.

Fig.10 presents the indoor and outdoor air temperature in Riga city in the time period from 11 March to 16 March 2011 (12 March - Saturday and 13 March - Sunday). The horizontal axis presents the data of times and date. Minor gridlines disclose time:

- first 2:00;
- second 5:00;
- third 8:00;
- fourth 11:00 etc..

Major gridlines from:

- zero to eight are the first data achieved on 11 March;
- nine to sixteen are the second data achieved on 12 March;
- seventeen to twenty four are the third data achieved on 13 March, etc..

The highest indoor air temperature was in the partially renovated day-care centre building, medium indoor air temperature was in the newly erected building and the lowest was in the unrenovated building. In the partially renovated and in the newly erected buildings it was higher and just 1-2 degrees lower than +25°C. This temperature is the maximum from the recommended optimum in the Labour Protection Requirements in Workplaces as prescribed in the Regulation no. 359 from 28 April 2009 of the Cabinet of Ministers of the Republic of Latvia. The recommended air temperature is from +19 to +25°C if the outdoor average air temperature is +10°C or lower. In our case, better and more economical indoor air temperature from +21 to

+24°C was in the unrenovated day-care centre building.

As we see in Fig.10, the outdoor air temperature was from minus four degrees to plus ten degrees Celsius. The indoor air temperature in all types of the buildings changed in accordance with the outdoor air temperature changes. This indicates that in thermal energy consumption it is possible to realize optimization. The first step is to change the established heat demand for each day-care centre building. It is necessary to make the day-night conditions and workday and holiday conditions with a temperature difference. Our study justified this. Fig. 11 presents the change in the carbon dioxide level in the indoor environment in our study period in two day-care centre buildings. They are a partially renovated day-care centre building and a new one.

Fig.11 presents the carbon dioxide (CO₂) level in ppm in the indoor environment. In Latvia we did not find an institution or structure which had a fixed CO₂ level outdoors. The state limited liability company "Latvian Environment, Geology and Meteorology Centre" has information about the outdoor air quality, but not included information about CO₂ in the outdoor environment.

We find a similar study in the Minnesota Department of the Health Fact Sheet from April 2010: "Carbon dioxide is a colourless, odourless gas. It is produced both naturally and through human activities, such as burning gasoline, coal, oil, and wood. In the indoor environment, people exhale CO₂, which contributes to CO₂ levels in the air.

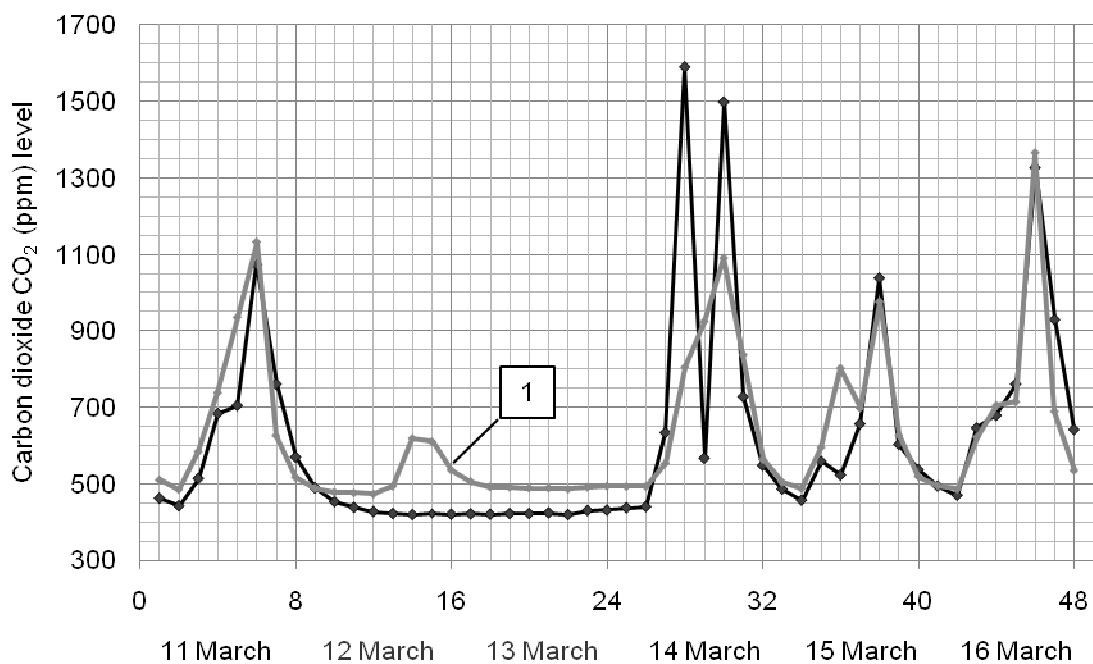


Figure 11. Carbon dioxide in the indoor environment in:

- 1 – partially renovated building (2007, average heat consumption 339kWh/m² per annum)
- 2 – newly erected building (built in 2005, average heat consumption 94kWh/m² per annum)

The outdoor concentration of carbon dioxide can vary from 350-400 ppm or higher in areas with high traffic or industrial activity.” Our fixed CO₂ level varied from 410 till 440 ppm in February and March 2011. The Minnesota Department of Health had written: “the level of CO₂ indoors depends upon:

1. the number of people present;
2. how long an area has been occupied;
3. the amount of outdoor fresh air entering the area;
4. the size of the room or area;
5. whether combustion by-products are contaminating the indoor air (e.g., idling vehicles near air intakes, leaky furnaces, tobacco smoke), the outdoor concentration.

Carbon dioxide concentrations indoors can vary from several hundred ppm to over 1000 ppm in areas with many occupants present for an extended period of time and where outdoor air ventilation is limited.” In Fig.11 the horizontal axis presents the data of times and date. Minor gridlines disclose time:

- first 2:00;
- second 5:00;
- third 8:00;
- fourth 11:00 etc..

Major gridlines from:

- zero to eight are the first data achieved on 11March;
- nine to sixteen are the second data achieved on 12March;
- seventeen till twenty four are the third data achieved on 13 March, etc..

Our fixed occupancies (floor area and existence of the ventilation system) are:

1. in a partially renovated day-care centre building (3 – 4 years old children/adults), floor area 64m², there is no mechanical ventilation system:
 - 11 March – 17/2
 - 12 March – 0/0
 - 13 March – 0/0
 - 14 March – 17/2

- 15 March – 17/2
 - 16 March – 16/2
2. in the new one (4-5 years old children/adults), floor area 45m², there is a mechanical ventilation system:
 - 11 March – 14/2
 - 12 March – 0/0
 - 13 March – 0/0
 - 14 March – 18/2
 - 16 March – 15/2
 - 15 March – 16/2

Fig.11 displays that in the newly erected day-care centre building with a mechanical ventilation system, the CO₂ concentrations in the indoor air in many cases are larger than in a partially renovated day-care building without a mechanical ventilation system. This indicates a necessity to analyse and optimise the ventilation system operation .

CONCLUSIONS

Our presented study of the heat consumption and IAQ measurements in different types (unrenovated, partially renovated and newly erected buildings) of existent day-care centre buildings has affirmed:

1. Partial renovation does not decrease heat energy in most cases. Buildings with similar total floor areas after a partial renovation had big heat consumption differences.
2. Partial renovation was done incorrectly in the majority of cases in school buildings and in day-care centre buildings. This was confirmed by the IAQ measurements in the day-care centre buildings and heat consumption analysis on building per one square metre per annum.
3. After a partial renovation in day-care centre buildings it is necessary to set correct heat demands on the control panel in each heat exchanger.

In each day-care centre building and renovation project it is necessary to include a mechanical ventilation system which can attain the building requirements for correct IAQ as defined in the Latvian Building Laws.

ACKNOWLEDGEMENTS

The work was supported by the European Social Fund project. Contract no. 2009/0180/1DP/1.1.2.1.2/09/IPIA/VIAA/017

REFERENCES

Krūmiņš, Ē., Dimdiņa, I., Lešinskis, A. (2010) Heat Consumption Analysis In Riga City Public Buildings. Proceedings of the SSTP-7th International Conference on Indoor Climate Of Buildings, November 28 – December 1, 2010, High Tatras, Slovakia, p.217-223.

Directive 2002/91/EC of the European Parliament and the Council of 16 December 2002 – on the energy performance of buildings. [online] [accessed on 12.11.2010]. Available: <http://eur-lex.europa.eu/LexUriServ/LexUriServ.do?uri=OJ:L:2003:001:0065:0065:EN:PDF>

Directive 2006/32/EC of the European Parliament and the Council of 5 April 2006 on energy end-use efficiency and energy services and repealing Council Directive 93/76/EEC (Text with EEA relevance). [online] [accessed on 12.11.2010]. Available: <http://eur-lex.europa.eu/LexUriServ/LexUriServ.do?uri=OJ:L:2006:114:0064:0064:en:pdf>

Directive 2004/8/EC of the European Parliament and the Council of 11 February 2004 – on the promotion of cogeneration based on a useful heat demand in the internal energy market and amending Directive 92/42/EEC [online] [accessed on 12.10.2010]. Available: http://www.energy.eu/directives/1_05220040221en00500060.pdf

Labour Protection Requirements in Workplaces [online] [accessed on 12.02.2011]. Available: <http://www.likumi.lv/doc.php?id=191430&from=off>

Latvian Construction Standard LBN 002-01 “Building Envelope Calorific” [online] [accessed on 31.01.2011]. Available: <http://www.likumi.lv/doc.php?id=56049>

Latvian Construction Standard LBN 208-00 “Public Buildings and Structures” [online] [accessed on 31.01.2011]. Available: <http://www.likumi.lv/doc.php?id=178746&from=off>

Latvian Environment, Geology and Meteorology Centre [online] [accessed on 19.02.2011]. Available: http://www.meteo.lv/pdf_base/meteor_2008.html

Latvian Law on The Energy Performance of Buildings [online] [accessed on 31.01.2011]. Available: <http://www.likumi.lv/doc.php?id=173237>

Ministry of Economics of Republic of Latvia [online] [accessed on 31.01.2011]. Available: <http://www.em.gov.lv/em/2nd/?lng=lv&cat=30173>

Minnesota Department of Health Fact Sheet April 2010 [online] [accessed on 22.02.2011]. Available: <http://www.health.state.mn.us/divs/eh/indoorair/co2/carbondioxide.pdf>

INDOOR AIR QUALITY AND ENERGY EFFICIENCY IN MULTI-APARTMENT BUILDINGS BEFORE AND AFTER RENOVATION: A CASE STUDY OF TWO BUILDINGS IN RIGA

Ilze Dimdiņa*, Arturs Lešinskis*, Ēriks Krūmiņš**,
Vilis Krūmiņš***, Laimdota Šnīdere***, Viktors Zagorskis****

*Riga Technical University, Institute of Heat, Gas and Water Technology
ilze.dimdina@gmail.com ; Arturs.Lesinskis@rtu.lv

**Latvia University of Agriculture, Department of Architecture and Building
eriks.krumins@riga.lv

***Ltd Kaimiņiem.lv

vilis.krumins@gmail.com ; Laimdota.Snidere@urban-art.lv

****Riga Technical University,

Computing Centre at Faculty of Electronics and Telecommunications

Viktors.Zagorskis@rtu.lv

ABSTRACT

We present an ongoing project which aims at monitoring IAQ in multi-apartment buildings (MABs) before and after renovation. We collected measures of indoor air microclimate parameters in 6 apartments of 3 MABs of standard construction buildings (type 464) in Riga, during the heating season of 2010/2011. In 3 apartments of one renovated building and in 3 apartments of two unrenovated buildings (on the first, middle and top floor), sensors of air temperature, relative humidity, CO₂ concentration level, and air flow velocity are located to find the average value of IAQ parameters, and to make calculations of indoor air exchange in each apartment. At the same time, the outdoor air temperature and relative humidity are measured. The measurements are made every minute, and the paper presents the data for duration of several months.

In general, the results show that the ventilation system must be updated in all apartments. The thermal energy for heating is reduced by about 50% in renovated MAB. The heat energy consumption in different apartments of the renovated building and temperature measures in all the project apartments demonstrate the necessity to change the heat consumption according to individual financial possibilities and comfort demands.

Key words: CO₂ concentration level, energy efficiency, heat energy consumption, indoor air quality, multi-apartment buildings

INTRODUCTION

Previous experience shows that renovation of ventilation systems is not a typical component of renovation of MABs in Latvia. As a consequence, rooms are not ventilated enough and the indoor air quality (IAQ) is reduced. This, in turn, leads to progression of the so called sick building syndrome (SBS). IAQ measures in 13 unrenovated MABs shows that the CO₂ concentration level in 19 of the examined 30 apartments was ≥ 1000 , indicating insufficient ventilation (Dimdina et al., 2010).

The study was carried out in the frameworks of the Baltic Sea Transnational Cooperation Programme 2007-2013, within the project "Energy Efficient and Integrated Urban Planning (UrbEnergy)", which involved development of an internet portal for on-line monitoring of the indoor climate and consumption parameters of renovated and not renovated buildings in Latvia.

The project objective was to identify the microclimate problems in residential buildings before and after renovation, develop

recommendations for residential indoor climate and energy efficiency, to test the practical effect of upgrades aimed at indoor air quality improvement, to draw public attention to residential indoor climate problems, to promote civic education and the progress of high-quality renovation of residential buildings.

MATERIALS AND METHODS

Project buildings and apartments

For the project, 5 (five) MABs in Riga were selected, in two types of standard residential buildings: three of the buildings were of the so called project type 464 (5 floors, 3 staircases, 45 apartments in each building), and two were of the so called project type 602 (9 floors, 2 staircases, 72 apartments in each building). Because the ownership of MAB apartments in Latvia is typically individual (each apartment has a separate owner), the measurements in all the selected apartments had to be agreed with the apartment owners. Because such agreement was not reached in some cases, the

planned microclimate monitoring was not implemented in three apartments in one of the non-renovated 464-series building, but identical apartments were used in two nearby buildings. In addition, the total number of the planned measurements (98 measurement points in 12 apartments) was not achieved because of various technical problems (for example, sealed exhaust ducts) and human factors. As a result, not all monitoring data were fully secured from all measurement points, and in some cases the missing data have been imputed by using indicators from the corresponding measurement point in another, equivalent building within the project. In such cases, the methodology of calculations is explained in the notes to the corresponding results table (see Table 1).

IAQ parameters are measured in 3 apartments (on the first, middle and top floor) of two non-renovated MABs of the type 464 (464-N1 and 464-N2), and in 3 apartments (on the first, middle and top floor) of one renovated MAB of the type 464 (464-R), and in 2 apartments (on the top floor) of one renovated (602-R) and one non-renovated (602-N) MAB of the type 602. In this paper just the MABs of the type 464 are reviewed.

Standard 464-series MAB description (Pasaules bankas tehniskā vienība, 2002): construction year starting from 1961, five (5) floors, sectional type (with a staircase in the middle of each section), with basements and technical space on the attic level, with loggias or balconies; outer wall: 300 mm thick lightweight concrete panels, on outer corners of the balcony and stair area up to 420 mm thick lightweight concrete panels; windows and balcony doors: double glazing in wooden frames.

Renovation upgrades of the 464-series building in year 2008 (Jermaka, 2010): attic insulation with ecowool (200 mm); facade insulation with rock wool (100 mm); basement insulation with extruded foam (100 mm), common areas window and door replacement to double-glazed windows in PVC frames, installation of thermostats and heat meters (allocators) on each radiator.

The two unrenovated MABs 464-N1 and 464-N2 had the North oriented end-walls insulated, correspondingly in 2007 and 2005.

The schematic layout and photo (S end-wall, W facade with loggias) of the renovated 464-series building (464-R) and the two non-renovated buildings (464-N1 and 464-N2) are depicted in Figure 1.

The apartments for the IAQ parameter measurements were chosen, taking into account their location within the building. Individual upgrades in the apartments are:

- 464-R/middle (3) floor - extractor fan in the kitchen and in the combined sanitary facility;
- 464-R/top (5) floor - extractor hood in the kitchen, glassed loggia, combined sanitary facility;



Figure 1. 464-series MABs photo and schematic location (renovated: 464-R; not renovated: 464-N1 and 464-N2).

- 464-N2/first (1) floor - recirculating hood in the kitchen;
- 464-N2/middle (4) floor - double-glazed windows in PVC frames, glassed loggia;
- 464-N1/top (5) floor - S end-wall insulated from inside (2004), new radiators (2009), extractor fan in the kitchen and in the combined sanitary facility.

Measuring equipment and measurements

For the indoor air parameter measurements, a complex measuring equipment was used, which was set up, in coordination with the apartment owner, in the owner's bedroom (about 1 m above the floor - the working area) or in the kitchen area (about 1 to 1,8 m above the floor). The equipment measurement accuracy (at 25⁰C) is the following: for temperature $\pm 0,5^{\circ}\text{C}$, for relative humidity $\pm 3\%$ of reading value; for CO₂ concentration to ± 40 ppm + 3% of reading value.

For the indoor corner temperature measurements a sensor with an accuracy of $\pm 0,3$ K (at 25⁰C) was used. For the measurements of exhaust ventilation ducts of the kitchen and lavatory, the measuring equipment with an accuracy of: air flow rate $<0,5$ m/s $\pm 7\%$ of reading value (at 25⁰C); temperature $< 0,5^{\circ}\text{C}$ (at 25⁰C, $> 0,5$ m/s) was used.

The outdoor air temperature and relative humidity were measured approximately 1 m above the ground with an accuracy (at 25⁰C) of $\pm 0,3$ K, relative humidity $\pm 3\%$ of reading value (at 30 ... 70% r.m.), $\pm 5\%$ of reading value (at 10 ... 30% r.m. and 70 ... 90% r.m.), $\pm 10\%$ of reading value (at 5 ... 10% r.m. and 90 ... 95% r.m.).

The planned reading period was 1 minute. If a reading was not made due to the technical reasons, the point value in the chart did not appear for the respective period. If the reading is performed, but the measuring equipment "has not provided an answer", the value is recorded outside of the measuring range, allowing it to be ignored during the data processing (details of data collection - see below).

At the present time, the total number of

simultaneously measured parameters in MABs of the type 464 is 45. In each of 6 project apartments the air temperature, relative humidity and CO₂ concentration level in the bedroom or kitchen (Table 1) are measured; air temperature and air flow velocity in two exhaust ventilation ducts (from the kitchen and lavatory) are measured; in 1 project apartment the air temperature at the exterior corner is measured; outdoor air temperature and relative humidity are measured.

Data extraction, processing

The equipment that participated in the course of the data collection (Dimdiņa et al., 2010):

- controller - provides instantaneous measurements of temperature, relative humidity, carbon dioxide concentration and air flow rate of the object and object points;

- server (hardware and software) for data acquisition and processing - set up as a real physical IBM PC-type device which operates based on the Linux type environment, the server regularly communicates with the existing controllers, surveying the current (instantaneous) data values (data collected at 1 min intervals);

There are regular communication sessions taking place between the server and the controllers, during which the data are obtained from the controllers and transferred to the data processing module. Physical or transport-level disturbances are recorded in files. Program modules ensure the data analysis by performing the following functions:

- separate the controller data from possible interference, which does not include physical or transport-level disturbance categories;

- make the data format adjustment and rounding of the data values: temperature - accuracy of 0,1⁰C, relative humidity - accuracy of 1%, CO₂ concentration - 0,001%, air flow rate - 0,1 m/s.

Thermal energy consumption calculation

The input of the district heating system of each MAB is equipped with an individual building heating substation enabled to count the total heat consumption for heating and hot water heating. The methodologies used to calculate the data on the building heat consumption and distribution of heating and hot water among the apartments depended on the building maintenance manager. In one building (464-series renovated building 464-R) the apartment owners had created their own association, and all the other buildings (464-N1, 464-N2, 602-R, 602-N) were managed by a municipality-owned maintenance company. In the building managed by the apartment owners association, the methodology was approved by the apartment owners meeting in accordance with the procedure prescribed by law. The methodology used by the municipality maintenance company has

been determined by the Riga City Council (Riga City Council, 2010). Calculations are carried out once a month. The accounting policies and calculations described below are based on the information received from the particular building manager.

The methodology for calculating of thermal heating in the renovated 464-series MAB (464-R) (1):

$$Q_H = Q - Q_{hw} = Q - (V_{hw} * T_{hw} / T) \quad (1)$$

where Q_H - heat consumption for heating the buildings [MWh];

Q - total thermal energy consumption for heating and hot water delivered to the building [MWh];

Q_{hw} - heat consumption for hot water heating in the building [MWh];

V_{hw} - total hot water consumption in the building (the sum of the individual monthly hot water meter reading amount; the study calculations assumed a constant average of 145 m³ of hot water consumption per building per month) [m³];

T_{hw} - hot water heating rate (the operator's calculations assumed a constant amount of 2,75 LVL/m³ in the 2010/2011 heating season, according to the actual average costs in the summer of 2010) [LVL/m³];

T - heating rate (variable depending on the primary fuel (in the particular case - natural gas) prices and tax changes, heat supply in Riga in all project buildings is provided by the JSC "Rīgas Siltums") [LVL/MWh].

The buildings total heat consumption Q_H is calculated and distributed between the apartments according to the following scheme: 60% based on the heating square meters S_H and 40% based on individual heating (allocator) readings. All the allocator reading data processing and calculations are performed by a service company in accordance with the approved methodology, and taking into account the housing situation and other factors.

In the non-renovated 464-series (464-N1, 464-N2) MABs thermal heating calculations are performed on the basis of the Riga municipality building regulations (Riga City Council, 2010), under which (2):

$$Q'_H = Q - Q'_{hw} - Q_c = Q - (V_{hw} * T'_{hw} / T) - q_c * n \quad (2)$$

where Q'_H - heat consumption for heating buildings [MWh];

Q'_{hw} - heat consumption for hot water heating in the building [MWh];

Q_c - heat consumption for hot water circulation within the building [MWh];

T'_{hw} - hot water heating rate [LVL/m³];

$q_c = 0,1$ MWh/apartments - heat consumption for ensuring the hot water circulation per apartment [MWh];

n - number of apartments in MAB.

In the non-renovated buildings, where individual heat metering in apartments is not provided, the buildings total heat consumption Q'_H is calculated and distributed among the apartments on the basis of heating square meters S_H .

This study uses the data about building and apartment thermal energy consumption for heating and hot water in accordance with the information provided by the maintenance manager and heat supplier.

Calculation of air exchange

In accordance with the laws (LR Ministru cabinets, 2009), the normative exchange of air L_{norm} in an apartment is calculated as:

- minimally secured air vent from the apartment, the sum of all the facilities required airflows: at least 50 m³/h from a combined sanitary facility, at least 25 m³/h from toilet facilities, at least 25 m³/h from a bathroom, at least 60 to 90 m³/h from a kitchen (from a kitchen with an electric oven or with a 2-ring gas stove - minimum of 60 m³/h, from a kitchen with 3-ring gas stove - minimum of 75 m³/h, from a kitchen with 4-ring gas cooker - at least 90 m³/h);
- minimum air supply to be provided in the apartment, the sum of all the facilities required airflows: at least 3 m³/m² per hour flow to the living areas and bedrooms.

In this study the IAQ measurements and calculations have been made in apartments with more than one living room or bedroom, so the exhaust airflow is assumed to be at least 90 m³/h from the cooking area; the actual data about the type of the cooking stove were not collected. The bedroom and living room areas have been assumed to be average, according to the standard project plans; in all building types the apartment ceiling height is assumed to be 2,5 m, whereas the actual measurement or comparison with the data from the inventory file has not been done. In the calculations, the largest amount obtained by comparing the required exhaust and supply air quantity for an apartment is assumed to be the air exchange in the apartment. The air exchange L_{mes} , in accordance with the measurements of the airflow speed in the exhaust ventilation channels from the kitchen and toilet facilities, has been calculated in the following way (3):

$$L_s = s * 0,9 * v * 3600 \quad (3)$$

where L_s – airflow through the exhaust ventilation channel [m³/h];

s – area of the exhaust ventilation channel, in all calculations assumed equal to 0,10* 0,15=0,015 m²;

0,9 – applied correction coefficient for the distribution of the airflow speed within the cross-section of the ventilation channel;

v – measurement of the airflow speed [m/s]; 3600 – coefficient for transition from seconds to hours.

RESULTS AND DISCUSSION

Separately the results of IAQ measures are presented in Figures 2-6. On abscissa there is the period of the measures – date or time.

To reach the normative level of the air exchange L_{norm} in the apartments with the defined exhaust ventilation channel parameters (see *Calculation of air exchange*) and to provide the airflow exchange of $L_{norm} = 140$ m³/h in the apartments (with 2 exhaust ventilation channels) of the type 464 MAB, the necessary airflow speed is 1,44 m/s. Typical results of the measures show that the air velocity in exhaust ventilation channels does not exceed 1 m/s, and the ventilation problems increase in the upper floors and in renovated MAB without organized supply ventilation – see Fig.2.

The relative humidity level increases in the upper floors and in renovated MAB without organized supply ventilation – see Fig.3. Under specific outdoor climate conditions, excessively dry indoor air there is a problem with good ventilation without humidifying.

The CO₂ concentration level in the apartments is mostly dependent on the habits of the inhabitants. The CO₂ concentration level increases in the upper floors and in renovated MAB without organized supply ventilation - see Fig.4. Problems are most often created by blocked exhaust ventilation channels.

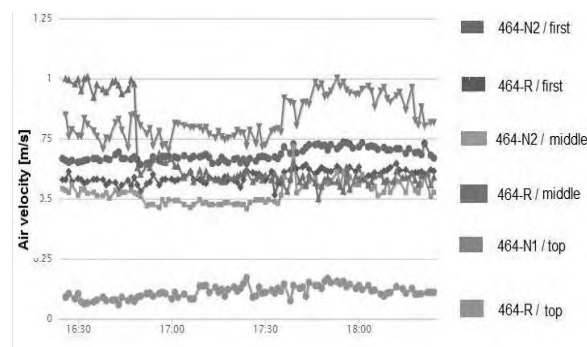


Figure 2. Air velocity in exhaust ventilation channel in kitchen (outdoor temperature about -10⁰C).

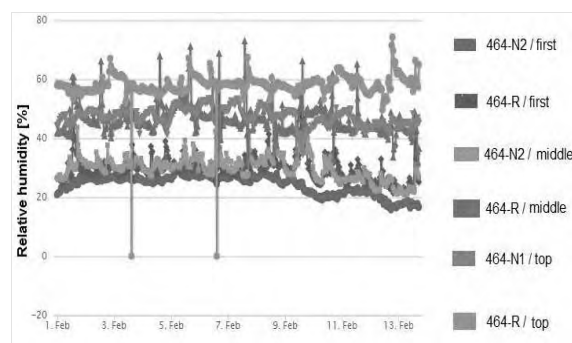


Figure 3. Relative humidity in apartments.

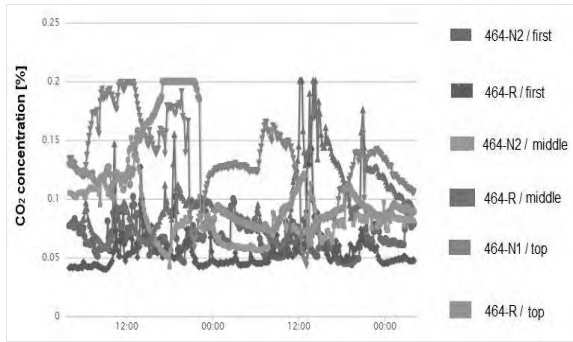


Figure 4. CO₂ concentration level in apartments (outdoor temperature -5...-10 °C).

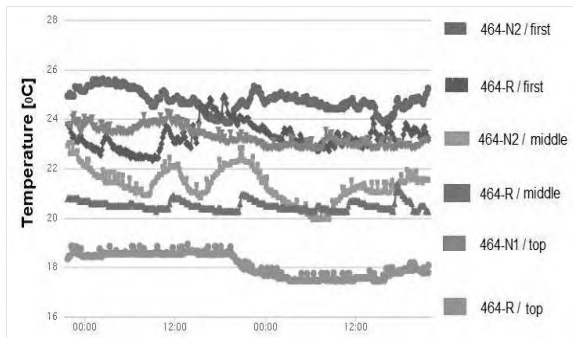


Figure 5. Temperature in apartments.

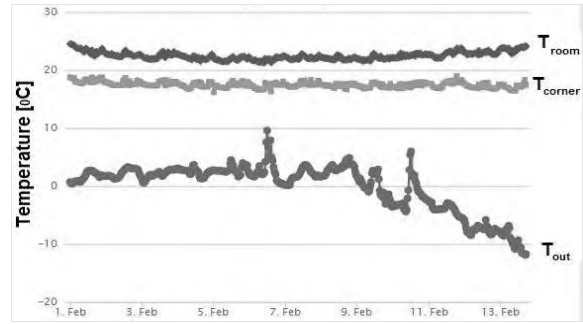


Figure 6. Temperature difference (464-N2/first floor)

The temperature measures in different apartments demonstrate the necessity to change the heat consumption in accordance with individual financial capabilities and comfort demands – see Fig.5. The temperature difference between the corner and the middle of a room in a typical unrenovated MAB exceed 5°C – see Fig.6.

The average outdoor temperatures in Riga in 2010: October +6,05°C (average by legislation +7,2⁰C); November +3,32°C (+2,1⁰C); December -5,70°C (-2,3⁰C) – data of the Latvian Environment, Geology and Meteorology Centre. Table 1 presents location of the complex measurement equipment in the apartments and thermal energy consumption of MABs and individual heat consumption of apartments.

Table 1
Thermal energy consumption of MABs and apartments and location of complex measuring equipment

MAB/apartment floor	S _H , m ²	Location of compl.meas.eq.	Parameter, Dimension	X, 2010	XI, 2010	XII, 2010	Total
464-R	2342,91		Q, MWh	17,28	23,06	36,39	76,73
			Q*1000/S _H , kWh/m ²	7	10	16	33
464-R/first	65,01	kitchen, E facade		11	19	23	53
464-R/middle	38,44	kitchen, W facade		3	5	11	19
464-R/top	67,90	bedroom, N end-wall and W fasade with glassed loggia	Q _H *1000/ S _H , kWh/m ²	2	5	11	18
464-N2	2342,91*		Q, MWh	30,3	46,51	73,13	149,94
			Q*1000/S _H , kWh/m ²	13	20	31	64
464-N2/first	65,65	bedroom, S end-wall and W fasade with loggia	Q _H *1000/ S _H , kWh/m ²	6	13	24	43
464-N2/middle	48,13	bedroom, W fasade with glassed loggia		6	13	24	43
464-N1	2342,91*		Q, MWh	37,1	51,66	80,22	168,98
			Q*1000/S _H , kWh/m ²	16	22	34	72
464-N1/top	64,59	bedroom, S end-wall and W fasade with loggia	Q _H *1000/ S _H , kWh/m ²	9	15	27	51

* comparison of the data from the inventory file is not done

CONCLUSIONS

The results of the indoor air quality measurements confirmed ventilation problems and indicated a reduced level of comfort. To improve the microclimate in MAB, the ventilation system must be updated in all apartments (Dimdiņa et al., 2010). The air permeability difference between a typical blocked duct (with a plastic bottle) is 100% before the dismantling of barriers and 400% after the dismantling of barriers (Caune et al., 2010).

In the upper floors, the observed accumulated moisture in the building constructions is 20...35% higher compared to the lower floors, as well as condensate can be observed in the exterior wall corners. These are consequences resulting from the air exchange level that is 2 to 4 times below the normative.

The average bedroom temperature in the renovated buildings is 22...24 °C, at the outdoor temperature range between -5 °C and +5° C. The average temperature in the non-renovated buildings is 22...24 °C, with 15 °C observed in the corners. But lowering of the temperature is precluded by the risk

of creating condensate in the corners. It is not possible to reach the temperature of 25 °C in the bathroom at apartment dwellers' preferred time; the actual temperature is 21...22 °C (Caune et al., 2010).

The temperature measures in different apartments demonstrate the necessity to change the heat consumption according to individual financial capabilities and comfort demands. The thermal energy for heating is reduced by about 50% in the renovated MAB.

Activities that can increase the energy efficiency of buildings, for example, heat insulation of buildings, must be carried out in a complex with all of the engineering system restoration, improvement, or modernization.

ACKNOWLEDGMENTS

The authors would like to thank the apartment owners of the Project buildings for allowing to perform measurements.

Research is realized with financial support to I.Dimdiņa from JSC Latvijas gāze.

REFERENCES

- Caune O.; Dimdiņa I.; Krūmiņš V.; Kupča L.; Stirna G.; Šnīdere L. (2010) Portāla izveide, datu pieejamība, iekštelpu klimata parametru un patēriņa datu mērījumu veikšana, uzkrāto datu veida un apjoma apraksts, portāla uzturēšanas apraksts. „Development of an internet portal for on-line monitoring of indoor climate and consumption parameters of renovated and not renovated buildings in Latvia” Project report.
- Dimdiņa I., Krūmiņš Ē., Krūmiņš V., Lešinskis A., Šnīdere L. (2010) Results of living-room microclimate parameter measures in multi-apartment buildings before renovation. The 7th International Conference „Indoor climate of buildings 2010”, pp. 33-40.
- Jermaka V. (2010) Veiksmīgas renovācijas paraugs Rīgā, Discussion „Daudzdzīvokļu dzīvojamo ēku renovācijas gaita Rīgā 2010.gadā”, Power Point Presentation. Available: http://www.rea.riga.lv/files/Veiksmigas_renovacijas_paraugs_Riga.pdf
- LR Ministru kabinets. (2009) Noteikumi Nr.102 no 03.02.2009., Noteikumi par Latvijas būvnormatīvu LBN 211-08 "Daudzstāvu daudzdzīvokļu dzīvojamie nami", Latvian Construction Norms.
- Pasaules Bankas tehniskā vienība. (2002) Mājokļu energoefektivitātes pasākumu sagatavošana Latvijā, Project report.
- Rīga City Council. (2010) Instrukcija Nr.9 "Rīgas pašvaldības īpašumā vai pārvaldīšanā esošajās daudzdzīvokļu dzīvojamās mājās patērētās siltumenerģijas sadales un maksas aprēķināšanas kārtība", Latvian Legislation Norms. Available: http://www.rs.lv/lv/htmls/norm_dok/dokuments.php?id=44

INDOOR AIR QUALITY AND THERMAL COMFORT EVALUATION IN LATVIAN DAYCARE CENTERS WITH CARBON DIOXIDE, TEMPERATURE AND HUMIDITY AS INDICATORS

Galina Stankevica

Riga Technical University, Department of Heat and Gas Technology
galina.stankevica@rtu.lv

ABSTRACT

Latvian children under the age of 7 can spend up to 60 hours per week in daycare centers and therefore it is very important to establish a healthy and comfortable daycare environment that children will find pleasant and stimulating to stay in. This study investigates the indoor air quality and thermal comfort within six daycare centers (old, renovated and new-built) in moderate climate zone of Latvia. The measurements of carbon dioxide, air temperature and relative humidity were carried out, and the data regarding daycare center characteristics and maintenance activities were collected via combination of field visits, record analysis and interviews. It was found that the carbon dioxide concentrations exceeded 1000 ppm in 75% of the daycare centers studied, with the highest (1356 ppm) measured in a renovated facility with the natural ventilation system. Thus, installation of a more efficient ventilation system (mechanical) is recommended to provide acceptable indoor air quality, since opening of windows itself cannot provide the optimal conditions indoors. In all facilities the temperature was kept above 20°C and the average relative humidity was 40 ± 5%, creating comfortable thermal environment for children.

Key words: daycare center, indoor air quality, thermal comfort

INTRODUCTION

About 75% of all children under the age of 7 living in the capital of Latvia Riga spend about 30-60 hours per week in daycare centers. However, research studies indicate that daycare facilities due to the improper indoor air quality (IAQ) may actually be hazardous to children's health. (Hagerhed-Engman et al., 2006; Haby et al., 2000) have reported increased risks of asthma and allergies for children spending their time in daycare environments compared to the care obtained at home. Therefore, for the last few decades an increased attention has been directed towards creation of appropriate indoor environment in daycare centers.

Carbon dioxide (CO₂) is one of the most commonly used indicators of IAQ in spaces, where people are the main pollution source, and it also serves as the determiner for adequate ventilation. CO₂ itself is normally not harmful, however its excessive exposure is found to cause headaches, fatigue, increases the risk of sick leave (Erdmann, 2002; Milton et al., 2000), and even risks for sudden infant death (Corbyn, 1993). The maximum recommended CO₂ concentration in a space is 800 ppm (parts per million) above the outdoor according to the European standard (EN 13779, 2005). The upper limit for the CO₂ concentration in the ASHRAE standard 62.1 (ASHRAE, 2004) should not exceed 2500 ppm, while 1000 ppm is the recommended value. The majority of indoor climate studies in daycare environments were conducted in

Nordic countries. The mean CO₂ levels reported in Scandinavian countries were as follows: 810 ppm in Finnish daycare centers (Ruotsalainen and Jaakkola, 1993), about 1400 ppm in Denmark (Pejtersen, 1991), and as low as 640 ppm in Sweden (Cars et al. 1992). (Borodinecs and Budjko, 2009) investigated IAQ in two Latvian daycare centers and reported the maximum CO₂ concentration as high as 1700 and 1450 ppm in rooms with PVC and wooden frame windows respectively.

While CO₂ describes IAQ, temperature and relative humidity are usually used to determine the thermal comfort level in indoor environments. According to the Latvian building norms No. 596 (MK, 2002) the minimum acceptable air temperature in daycare centers is at least 20.0°C or 18.0°C for children younger and older than 3 years respectively. The ASHRAE standard 62.1 (ASHRAE, 2004) recommends keeping the temperature in the range of 23-26°C and relative humidity between 30 and 60%.

The majority of Latvian daycare centers were constructed in accordance to the old Soviet building codes which stated that ventilation should be achieved by natural means, i.e., fresh air supplied through the window construction and exhausted through the vents (stack effect). It was presumed that such solution would result in sufficient air exchange. Lately the majority of daycare centers in Riga were reconstructed: the external walls insulated and wooden frame windows were changed to PVC (polyvinyl chloride) ones. However, these actions alone possess great risk of IAQ problems,

since the buildings became more airtight leading to insufficient air exchange indoors.

Since very limited data are available regarding the indoor air quality in Latvian daycare centers, and being concerned about IAQ children are exposed to in the present construction buildings, the author of this study evaluated the current IAQ and the thermal comfort status in six daycare centers in Riga Region.

MATERIALS AND METHODS

Daycare center selection

Six daycare centers (4%) from a total of 153 were randomly selected from the Education, Youth and Sports Department database of the Riga Council. The facilities differ in the type of construction, i.e., whether the building is old, renovated or new-built (two buildings per each category). All daycare centers were inspected and details of their characteristics were noted, including the type of heating and ventilation system, occupant density, building materials etc. In addition, the daycare center personnel were inquired about the frequency of window opening, cleaning routines and day regime at the facilities.

Field measurements

The CO₂ concentration, temperature and relative humidity are convenient and reliable indicators of the indoor air quality and comfort level. The measurements of these parameters were carried out simultaneously during the period of one week in October 2010 at all daycare facilities, with the exception of CO₂ concentration that was measured only in renovated and new-built daycare centers. Indoor sampling locations were determined prior the measurements through a walkthrough assessment. Since the placement of the measuring devices close to the breathing zone of children, i.e., at the height of 0.5-0.7 m, was restricted, the indoor samplings were performed at the height of 1.5-1.8 m close to the internal perimeter wall. All measurements were conducted continuously from 7 am on Monday to 5 pm on Friday at 5 min intervals. The indoor air temperature and humidity data were collected by the HOBO U12 Family data loggers with the following parameters: temperature -20°C to 70°C (±0.35°C) and relative humidity 10% to 90% with the accuracy (±2.5%). The HOBO loggers were interfaced with the CO₂ monitors Telaire 7001 measuring in the range of 0 to 10000 ppm (±50 ppm). In addition to the HOBO loggers, Testo 175-H2 measuring devices were used, having the following parameters: measurement range -20°C to 70°C with resolution 0.1°C, and relative humidity 0 to 100% with resolution of 0.1%.

Since only two measurement sets of HOBO and Telaire were available it was decided to measure simultaneously in one renovated and new built

daycare center couple for the first three days and during the last two days at the second couple of renovated and new-built facilities.

The daycare centers in this paper are designated by their type, i.e., new-built, renovated or old, and corresponding number. Three daycare centers (New 2, Renovated 1, Old 2) have a single room for nap and playing; in other daycare centers nap activity and playing are carried out in separate spaces. In the latter case sampling was performed in the playing room, where children consequently spend more time.

Data analysis

The measured IAQ and thermal environment parameters among three categories of daycare centers were compared. The means and ± standard deviation (SD) of CO₂, room temperature and relative humidity levels were calculated. Results and Discussion.

Daycare center characteristics

The basic data of the daycare centers and the selected spaces investigated are given in Table 1.

Table 1

Daycare center details

Daycare center	Area [m ²]	Ventilation system [-]	Heating system [-]	Floor area per person [m ² /pers]*
Old 1	742	Natural	Radiators	3.2
Old 2	1078	Natural	Radiators	3.2
Ren. 1	2152	Mechanical	Radiators	3.3
Ren. 2	2112	Natural	Radiators	3.3
New 1	3472	Mechanical	Underfloor	5.7
New 2	2024	Mechanical	Underfloor	3.8

* In the measured space

The number of children in one group ranged from 15 to 22 children. The age of children in the rooms investigated varied from 3-6 years. The typical daytime regime in the daycare centers was as follows: from 7 am to 10:30 am indoor activities in the playing room, 10:30 to 12 am promenade, 12:30 to 15:00 nap-time, and the rest of the time is spent indoors.

All daycare facilities have double glazed windows in PVC frames. The maintenance personnel in all daycare centers still relies on natural ventilation for achieving acceptable indoor air quality, and opens the windows every time the children are outside.

Carbon dioxide

In this study the average indoor CO₂ concentration during the daytime for all daycare facilities was 730 ± 170 ppm (Table 2).

In the majority of the daycare centers (75%) CO₂

levels exceeded the ASHRAE recommended value of 1000 ppm. However, this increase was not substantial and the maximum values measured were halved ASHRAE's tolerance maximum of 2500 ppm.

Table 2

Summary statistics of measured carbon dioxide concentration expressed in parts per million (ppm)

Daycare c.	Mean (95% CI)	Median	Min	Max
New 1	707 (603-811)	732	450	1123
New 2	609 (470-748)	601	421	945
Ren. 1	743 (604-882)	775	462	1140
Ren. 2	864 (651-1077)	843	500	1356
Overall	731 (561-901)	734	421	1356

It was also observed that in multipurpose rooms (for general activities and nap), the nap-time average CO₂ level was about 60 ppm higher compared to the non-nap time average CO₂ level. This can be explained by the fact, that children were placed in a closed space without adequate air exchange. Even though in the present study the CO₂ concentration was not measured in sleeping-only rooms, the study conducted in the US daycare centers (Feng and Lee, 2002) showed 24.3% CO₂ increment from non-nap time to nap-time in this type of rooms. Thus, it can be expected that Latvian daycare centers might follow the similar tendency, but this should be confirmed by further experiments in sleeping-only rooms. The highest CO₂ concentration was obtained in the Renovated 2 daycare center, which has a natural ventilation system as opposed to the other three daycare centers with a mechanical system

installed. Even though opening of windows does lower the CO₂ concentration, it is still not enough to achieve the optimal level since low outdoor air temperature limits the airing period.

Thus, better indoor air quality is achieved in mechanically ventilated spaces with constant supply of fresh air.

Temperature

The outdoor air parameters for October 26, which was a typical mid-week, cold day, are presented in Figure 1.

The outdoor air temperature varied from 2.0°C to 8.8°C and the relative humidity was in a range of 44% to 100%.

The variation of the daytime room temperature across the daycare centers on the 26th October is shown in Figure 2.

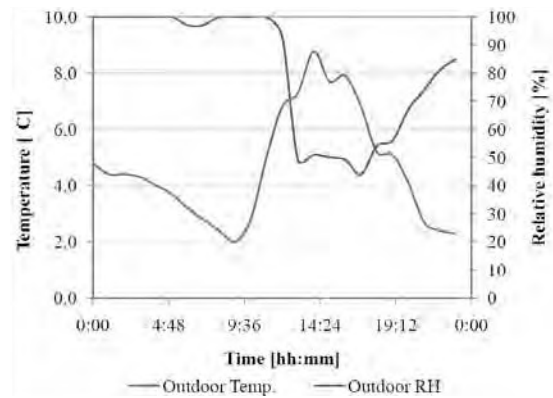


Figure 1. Atmospheric conditions on 26th October.

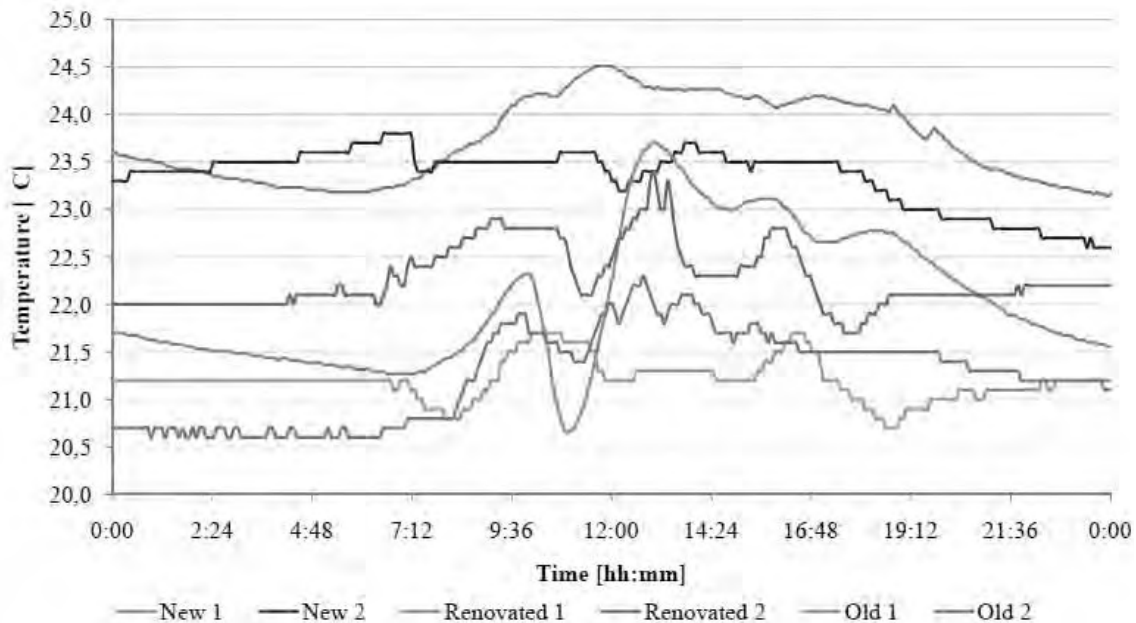


Figure 2. Temperature variation in six daycare centers on 26th October.

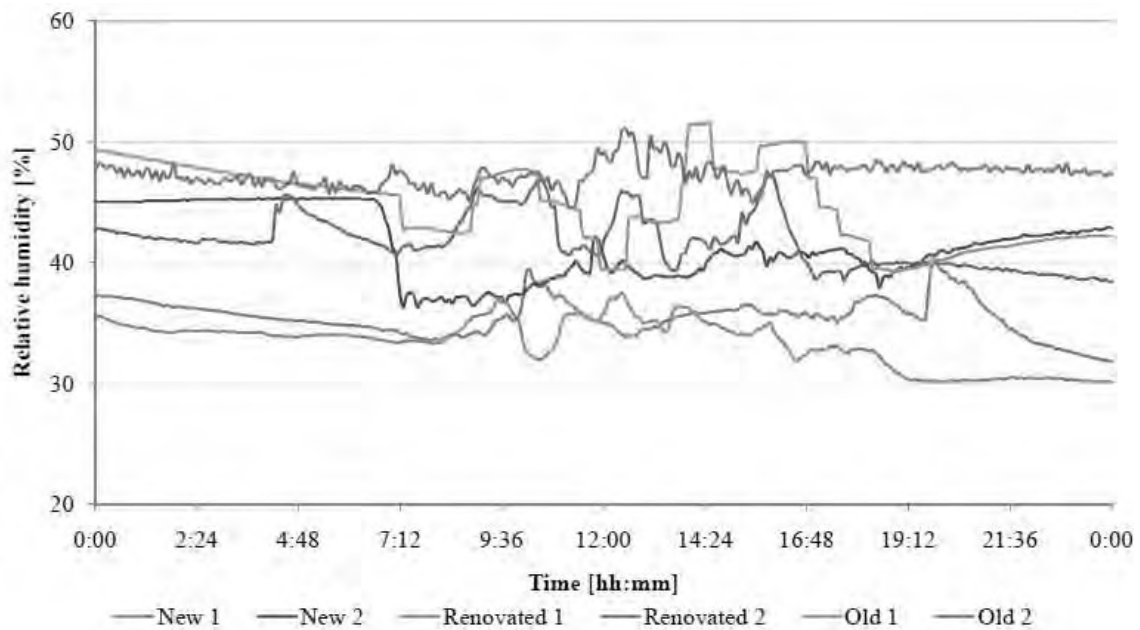


Figure 1. Relative humidity variation in six daycare centers on 26th October

The average room temperature in all six daycare centers during the daytime was $22.5 \pm 1.1^\circ\text{C}$. In all facilities the temperature was kept above 18°C , which is the minimum acceptable stipulated by the Latvian building norms No. 596 (MK, 2002) for children older the age of three. 67% of the daycare facilities were outside the ASHRAE recommended comfort range of $23\text{--}26^\circ\text{C}$, having temperatures lower than 23°C . The temperatures were highest in the new-built daycare centers, that both have the underfloor heating system and mechanical ventilation system that explains also not very large temperature fluctuations, i.e., $24.1 \pm 0.3^\circ\text{C}$ and $23.5 \pm 0.1^\circ\text{C}$ for the New 1 and New 2 daycare center, respectively. The greatest temperature fluctuations occurred in the renovated facilities, especially in the Renovated 1 ($\sigma = 0.8^\circ\text{C}$), where the temperature ranged from 20.7°C to 23.7°C . The temperature drops are a result of extensive airing by opening the windows and consequent creation of draft. However, the indoor temperature does not drop rapidly due to the relatively short time of windows being opened. In all of the facilities there is a potential for saving energy by using the night-time temperature setback of up to 3°C .

Relative humidity

The variation in the relative humidity across the six daycare centers is shown in Figure 3. The average relative humidity of the six daycare centers was $40 \pm 5\%$ and did not vary to a great extent during the day. All of the facilities had the relative humidity in a range of 30 to 60% that is recommended by the ASHRAE standard 62.1 (ASHRAE, 2004). The relative humidity slightly decreased every time the windows were opened. The largest decrement was

observed in the first half of the working day. This also corresponds to the rapid outdoor humidity decrease by almost 50% after 12 pm (Figure 1).

The relatively low humidity levels in the spaces also correspond to no visible signs of any moisture damage or mold growth on the indoor surfaces that were examined during the building visits.

CONCLUSIONS

This study provides assessment of the indoor air quality and thermal comfort in Latvian daycare centers with carbon dioxide, temperature and relative humidity as indicators. The CO_2 concentrations exceeded 1000 ppm in 75% of the daycare centers studied, with the highest (1356 ppm) measured in the Renovated 2 daycare facility with the natural ventilation system. Thus, the installation of more efficient ventilation system (mechanical) is recommended for improving the indoor air quality, since opening of the windows cannot provide the optimal conditions indoors. In all facilities the temperature was kept above 20°C and the average relative humidity was $40 \pm 5\%$, creating comfortable thermal environment for children. The greatest temperature fluctuations were observed in the renovated daycare centers and this is another indicator that the daycare center personnel still rely entirely on natural ventilation for proper indoor air quality. Therefore, Riga Municipality must take actions to educate the personnel, and carry out regular inspection and maintenance of the ventilation system to ensure its proper operation. In all of the facilities there is a potential for saving energy by using the night-time temperature setback of up to 3°C .

REFERENCES

- ASHRAE Standard 62.1. (2004) Ventilation for acceptable indoor air quality. American Society of Heating, Refrigerating and Air Conditioning Engineers, Atlanta.
- Borodinecs A., Budjko Z. (2009) Indoor air quality in nursery schools in Latvia. In: Proceedings of Healthy Buildings 2009, Healthy Buildings 2009, Syracuse, NY, USA, p. 1-4.
- Cars H., Petersson C., Hakansson A. (1992) Infectious diseases and day-care center environment. *Scandinavian Journal of Infectious Diseases*, Vol. 24, No. 4, p. 525-528.
- Corbyn J.A. (1993) Sudden infant death due to carbon dioxide and other pollutant accumulation at the face of a sleeping baby. *Medical hypothesis*, Vol. 41, No. 6, p. 483-494.
- Erdmann C.A., Steiner K.C., Apte M.G. (2002) Indoor carbon dioxide concentrations and SBS symptoms in office buildings revisited analyses of the 100 building BASE study dataset. In: Proceedings of Indoor Air 2002, Indoor Air 2002, Santa Cruz, CA, USA, p. 443-448.
- European Standard EN 13779 (2005) Ventilation for non-residential buildings - Performance requirements for ventilation and room-conditioning systems. European Committee for Standardization, Brussels.
- Ferng S.F., Lee L.W. (2002) Indoor air quality assessment of daycare facilities with carbon dioxide, temperature, and humidity as indicators. *Journal of Environmental Health*, Vol. 65, p. 14-18.
- Haby M.M., Marks G.B., Peat J.K., Leeder S.R. (2000) Daycare attendance before the age of two protects against atopy in preschool age children. *Pediatric Pulmonology*, Vol. 30, No. 5, p. 377-384.
- Hagerhed-Engman L., Bornehag C.G., Sundell J., Aberg N. (2006) Day-care attendance and increased risk for respiratory and allergic symptoms in pre-school age. *Allergy*, Vol. 61, No. 4, p. 447-453.
- Milton D.K., Glencross P.M., Walters M.D. (2000) Risk of sick leave associated with outdoor ventilation level, humidification, and building-related complaints, *Indoor Air*, No. 10, p. 212-221.
- Ministru kabineta noteikumi Nr.596. (2002) Higiēnas prasības izglītības iestādēm, kas īsteno pirmsskolas izglītības programmas. Latvijas Vēstnesis, Rīga.
- Pejtersen J., Clausen G., Sorensen D., Quistgaard D., Iwashita G., Zhang Y., Fanger P.O. (1991) Air pollution sources in kindergartens. In: Proceedings of IAQ 1991, Healthy Buildings 1991, Washington DC, Atlanta, USA, p. 221-224.
- Ruotsalainen R., Jaakkola J.J. (1993) Ventilation and indoor air quality in Finnish daycare centers. *Environment International*, Vol. 19, No. 2, p. 109-119.

V ENVIRONMENTAL ENGINEERING

ANTI-SEEPAGE MEANS FOR PROTECTIVE EMBANKMENT OF KARIOTIŠKĖS SEWAGE SLUDGE DUMP

Zydrunas Vycius, Tatjana Sankauskienė, Petras Milius

Lithuanian University of Agriculture, Water and Land Management Faculty,
Department of Building Constructions

zydrunas.vycius@lzuu.lt; tatjana.sankauskiene@gmail.com; miliusp@gmail.com

ABSTRACT

The seepage through the protective embankment of the Kariotiškės sewage sludge dump and anti-seepage means for the stopping of seepage are analysed in the article. It was determined that during the closure works of the dump of Kariotiškės it is necessary to ensure (due to the environmental protection requirements) that sludge filtrate should not filtrate through the protective embankment and should not gain access into the surroundings. Having viewed all possible anti-seepage means (drainage, changing of permeable soils into impermeable ones, etc.) as well as the geological situation we came to the conclusion that one of the most effective, economic and simplest ways was the arrangement of hermetic sheet piling.

Keywords: seepage, modelling, Kariotiškės sewage sludge dump, filtration coefficient, sludge filtrate, protective embankment, impermeable shield.

INTRODUCTION

The aim of the Directive is, by way of stringent operational and technical requirements on the sewage dumps (COUNCIL DIRECTIVE..., 2011), to provide for measures, which should help prevent or reduce negative impact on the environment, in particular the pollution of surface water, ground water, soil and air. Whereas it is necessary to indicate clearly the requirements with which sewage dumps must comply as regards location, conditioning, management, control, closure and preventive and protective measures to be taken against any threat to the environment in the short as well as in the long-term perspective, and more especially against the pollution of groundwater by the leaking of the filtrate into the soil.

The object of this article is one of the largest dumps in Lithuania, i.e., the Kariotiškės sewage sludge dump. The dump covers the area of 5.48 ha, the area of mirror surface is 4.80 ha, the maximum depth – 12.0 m, the perimeter of protective embankments – 394 m. It was calculated that approx. 389840 m³ of sludge were accumulated in the storage.

The objective of this article was to analyse seepage through the protective embankment of the Kariotiškės sewage sludge dump. As the basis for this work, geotechnical investigations over the protective embankment of the Kariotiškės sewage sludge dump (carried out by CJSC “Geotechniniai tyrimai”) were used as well as geotechnical cross-sections of the protective embankment were created.

The altitudes of the crest of the protective embankment of the Kariotiškės sewage sludge dump are 172.6...172.9, and those of the base of the

embankment – 167.4...169.3. The crest width of the protective embankment is approx. 2.5 m, and its slope sinks at a 32° angle on the average (in some cross sections the slope sinks even at a 45° angle on the average). Landslides have formed in some places of the protective embankment of the Kariotiškės sewage sludge dump. Cracks have formed on the top of the embankment (along the embankment). One can observe water seepage, slope wash and landslides in some places of the protective embankment.

The protective embankment of the Kariotiškės sewage sludge dump consists of technogenical soil (bulk soil – dusty clay and sand with additives consisting of demolition waste, domestic rubbish and organic materials). The bottom of the Kariotiškės sewage sludge dump consists of glacial and fluvioglacial landforms (moraine sandy, dusty clay, gravelly sand and dusty sand) and swamp sediments (peat).

The thickness of the bulk soil is 5.4...7.0 m above the centre of the embankment and it decreases up to 2.1...3.8 m at the foot of the embankment. The major part of the embankment consists of medium-hard and hard dusty clays interstratifying with the weaker ones – soft plastic or hard plastic dusty clays, mellow and medium dense sands. Clay soils naturally lie under the embankment of the bulk soil, which stratify from 164.5 up to 167.4 altitudes. The thickness of the soil layers of the base of the embankment was not determined.

In the analysed primary data it was not fixed that the ground water was in the depth of 1.8...7.0 m from the ground surface (altitude 165.5...168.8). The water occurs in the seams of the bulk sand, peat layers as well as in the aquiferous sand streaks situated in moraine sandy and dusty clays. In some

places of the protective embankment one can observe water seepage, slope wash and landslides. The most important seepage parameter – filtration coefficient – was not defined for the singled out geological soil layers.

METHOD

The available data show (UAB „Geotechniniai tyrimai“, Kariotiškių nuotekų dumblo sąvartyno uždarymas. Nuotekų ..., 2009; UAB „Geotechniniai tyrimai“, Kariotiškių nuotekų dumblo sąvartyno uždarymas. Dumblo ..., 2009) that the seepage (through the protective embankment of the Kariotiškės sewage sludge dump) can occur from the sewage sludge into the swamp situated below. According to the environment protection requirements, the filtrate from the sludge dump should not gain access into the surroundings. The waste sludge filtrate can gain access into the surroundings, when the protective sheet is not arranged (or is damaged) in the slopes and (or) the bottom of the Kariotiškės sewage sludge dump. There are no data on the arrangement and functioning of the protective sheet. There is no any available design documentation over the arrangement of the protective sheet while arranging the Kariotiškės sewage sludge dump.

At present, closure works of the Kariotiškės sewage sludge dump are being carried out. It should be ensured that the waste sludge filtrate should not gain access into the surroundings and should not pollute it. The project of the Kariotiškės dump was prepared in 1981-1983, the dump was built in 1984-1986 and the exploitation of the dump started in 1987. Not much attention was paid to the

environment protection and job fulfilment quality then, therefore, the protective sheet for the sewage sludge dump could not be arranged at all.

The seepage through the protective embankment was analysed when carrying out the numerical modelling of the seepage. The numerical modelling of the seepage was carried out in the cross sections I-I, II-II, III-III and IV-IV (made by CJSC “Geotechniniai tyrimai”) of the protective embankment (Fig. 1), in which the soil layers were singled out and the geotechnical characteristics of some soils were defined. The modelling was carried out using the computer seepage modelling program Geostudio Seep/W 2007 (Geostudio ..., 2011).

The seepage modelling consists of four interconnected parts: the creation of the numerical model, the mathematical solution of this model, the analysis of the results and the calibration of the mathematical model. Creating the numerical model of the analysed territory the schematised environment of the seepage as well as the geological, hydrogeological, topographical and some other factors influencing the process of the seepage are being expressed in numbers. Since the modelled territory is not borderless and has boundaries, it is very important to correctly define and depict the marginal conditions. The mathematical solution of the created numerical modelling is being carried out while solving differential equations (depicting mathematical groundwater movement model) by mathematical methods. The received results are compared with natural investigations or data and, if necessary, the calibration of the created numerical model is being carried out.

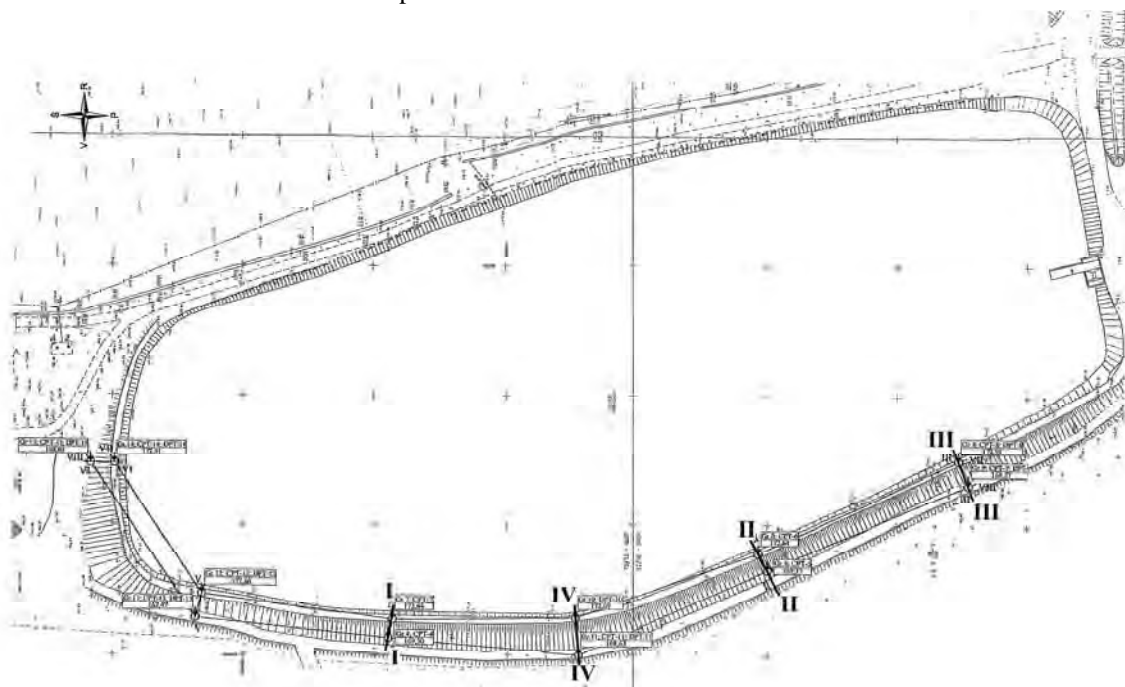


Fig. 1. Places of the geotechnical cross-sections in the protective embankment of the Kariotiškės sewage sludge dump.

The creation of the seepage model of the analysed territory is the stage of modelling requiring much work, time and professional knowledge. The more precisely the numerical model will correspond to the real situation, the more precise and reliable modelling results will be. The precision of the calculated seepage parameters depends upon the precision of the primary data and their correspondence to the real situation, therefore, reliable primary data (which are determined by natural investigations) are necessary for the modelling of the seepage tasks. The permeability of soils is depicted by the filtration coefficient k (Craig, 1995; Todd et al., 2005; Ухов et al., 2004) when analysing and modelling seepage. When there are no determined filtration coefficients of soils, they are chosen considering the known geological characteristics of soils (Dobkevičius, 2001; Verrujit, 2006; Далматов, 1988) and generalized filtration coefficients (presented in literature) of different types of soils (LST 1445, 1996; STR 1.04.02:2004, 2004). The filtration coefficients are presented in Table 1.

It should be noted that only possible limits of variation of the filtration coefficients of different types of soils are presented in literature, therefore, the chosen particular values of the filtration coefficient can differ from the ones existing in nature (Pocius, 1996; Šimkus et al., 1973; Морарекул et al., 1979). The values of the filtration coefficients of soils depend upon many factors, such as the granulometric and mineral composition of soils, density, structure and texture, amount of additives as well as upon the chemical composition and temperature of ground water, therefore, the chosen filtration coefficients of soils can differ from the natural ones (Pranaitis et al., 1979; Šimkus, 1984; Тер-Мартirosян, 1990). The boreholes, according to which the soils were singled out and their geotechnical parameters were defined, were bored on top of the protective embankment and at the foot of the dry slope. It

gives a sufficiently comprehensive view on the soils forming the protective embankment, but it does not provide us with comprehensive information over the natural soils existing under the protective embankment, especially those existing under the wet slope of the embankment and the bottom of the dump. Without the sufficient primary simulation data the seepage is modelled only through the protective embankment of the Kariotiškės sewage sludge dump.

It should be noted that according to the data received from the CJSC “Geotechniniai tyrimai”, naturally stratified layers of moraine clay predominantly lie under the protective embankment (above its dry slope). According to the literature data, clay soils are considered less permeable or practically impermeable soils. The permeability of moraine clay soils is even up to 10^{10} less than the one of permeable sandy soils. Moraine clay soils are used when arranging impermeable insulating substrata (sheets), therefore, seepage of the sludge filtrate from the sludge dump through the layers of moraine clay is practically impossible.

ANALYSES OF MODELLING RESULTS

Four seepage numerical models were made in the cross-sections I-I, II-II, III-III and IV-IV of the protective embankment (Fig. 1).

The aim of the modelling was the final results of the stable seepage, the main seepage parameters used in the modelling did not vary, and, therefore, the unconfined stable seepage was modelled. Besides, the possible errors of choosing of the filtration coefficients of soils when modelling stable seepage (when the coefficients of seepage of soils were not defined by field and laboratory experiments, they were chosen according to the literature data) had less impact upon the accuracy of the modelling results than when modelling unstable seepage.

Table 1

Filtration coefficients of soils

Nr.	Types of soil	Soil consistency and density	The coefficient of filtration k of soil <i>m/day</i>
1	Bulk soil: dusty clay	Soft plastic	0.01
2	Bulk soil: dusty clay	Hard plastic	0.01
3	Bulk soil: dusty clay	Medium hard	0,01
4	Bulk soil: dusty clay	Hard	0.01
5	Bulk soil: sand	Mellow	30
6	Bulk soil: sand	Medium dense	15
7	Peat	Medium and well decomposed	1.0
8	Dusty sand	Dense	5
9	Moraine sandy dusty clay	Dense plastic – soft plastic	0.0001
10	Moraine sandy dusty clay	Hard plastic	0.0001
11	Moraine sandy dusty clay	Medium hard	0.0001
12	Moraine sandy dusty clay	Hard	0.0001
13	Gravelly sand	Dense	50
14	Dusty sand	Dense	5

When creating the numerical models of seepage the level of sludge in the dump and the potential limits of the seepage of the sludge filtrate, the dry slope of the protective embankment and the swamp at the foot of the embankment, were defined by boundary conditions. According to the presented primary data, the altitude of the dump filling with sludge was accepted as 171.6 and set as the first boundary condition – the fixed water level H ($H=171.6$). The dry slope of the protective embankment and the swamp at the foot of the embankment were accepted as the second boundary condition – discharge flowing through the boundaries Q ($Q=0$ m^3/s). Such a creation of the model and the acceptance of the boundary conditions allowed modelling and analysing seepage from the sludge dump. The coefficients of seepage of the geological layers of the created models were set according to the accepted values (Table 1). In default of the presented data, precipitation and evaporation were not estimated in the process of seepage modelling.

As it was mentioned before, the seepage of the filtrate from the sludge dump into the swamp situated behind the protective embankment can occur if the protective sheet of the sludge dump is not arranged or is damaged. Since there are no data concerning the protective sheet and there is no available design documentation over the arrangement of the protective sheet (during the arrangement of the Kariotiškės sewage sludge dump), the potentially worst possible variant was chosen – the protective sheet was not arranged at all and did not limit the seepage from the sludge dump. Calculations of the created seepage models are being carried out using the finite element method. For achievement of the modelling accuracy, irregular elements, such as quadrangulans and triangles ensuring the correspondence of the model to nature, are chosen. The size of the boundary of the elements is accepted not larger than 0.3 m

during the seepage modelling, thus partitioning the numeric models into more or less 9000-10000 finite elements and ensuring the accuracy of the modelling.

The curve of depression, isolines of hydrostatic pressure, vectors and flow lines of the ground water flow are the modelling results. The curve of depression shows the surface of ground aquifer. In this surface, the hydrostatic pressure (rejecting the atmospheric pressure) is equal to zero. Going deeper, this pressure increases. The lines of hydrostatic pressure above the curve of depression can be explained in the following way: aeration zones were estimated during the modelling. The ground water flow vectors show the intensity of the water flow. The velocity of the ground water flow is the largest in such places, where the vector arrows are the longest and, vice versa, the velocity of the ground water flow is the smallest, where the vector arrows are the shortest. The number of the vector arrows of the velocity of the ground water flow shows the intensity of the ground water flow. The flow lines show the directions and lines of the separate ground water flows (separate water particles) in the common seepage flow. The example of the modelling results is presented in Fig. 2.

Analysing the modelling results we see that with the absence or damage of the sheet seepage occurs (through the protective embankment of the Kariotiškės sewage sludge dump) from the sewage sludge into the swamp situated below. Following the modelling results we see that most intensively the seepage occurs through permeable sandy soils.

The seepage modelling results of the protective embankment show that the curve of depression (ground water level) will match the ground surface at the foot of the embankment when seepage is stable.

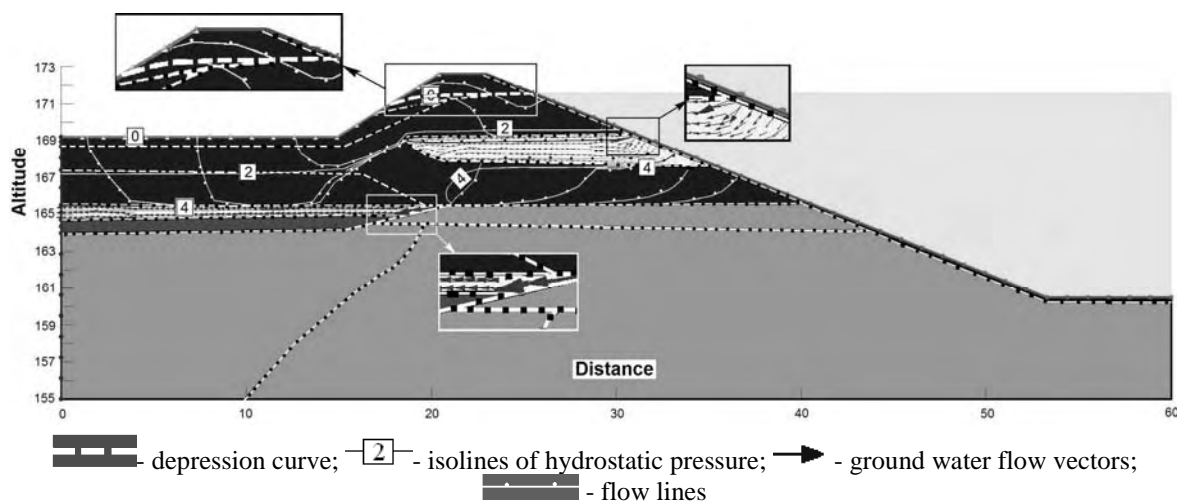


Fig. 2. Seepage modelling results of the section I-I in the protective embankment of the Kariotiškės sewage sludge dump.

In three of four cross-sections (II-II, III-III and IV-IV) the depression curve comes up into the ground surface in the dry slope of the embankment and can be the reason for water seepages and landslides in the slope. Following the environmental protection requirements the filtrate from the sludge dump should not gain access into the surroundings, therefore, means for stopping the seepage are necessary.

Having viewed all the possible anti-seepage means (drainage, changing of permeable soils into impermeable ones, etc.) as well as the geological situation we came to the conclusion that one of the most effective, economic and simplest ways was the arrangement of hermetic sheet piling (Ruplys, 1988; Ренгач, 1970). Following the report over the soil geotechnical investigations of the protective embankment and the foot of the embankment of the Kariotiškės sewage sludge dump one can see that in some places the protective embankment is arranged on permeable soils, through which seepage of sludge filtrate from the sludge dump can occur. In order to prevent the seepage through the protective embankment and permeable layers, especially during the closure works of the sludge storage, when the distributed load will be put and the filtration velocity will increase, it is purposeful to arrange hermetic sheet piling (when sinking it through permeable soils up to practically impermeable moraine clay soils). Thus the arrangement of the hermetic sheet piling will double the effect, i.e., will stop the seepage through the protective embankment and block up (lock) permeable layers of the natural soil.

In order to evaluate the influence of the hermetic sheet piling upon the seepage from the Kariotiškės sewage sludge dump, the numerical models of the four cross-sections I-I, II-II, III-III and IV-IV were created. The geotechnical characteristics of soils in the created seepage models are analogical to the

earlier created models. The altitude of the dump filled with sludge is accepted as the first boundary condition – the fixed water level H ($H=171.6$), the dry slope of the protective embankment and the swamp situated at the foot of the slope are accepted as the second boundary condition – discharge flowing through the boundary Q ($Q=0 \text{ m}^3/\text{s}$), precipitation and evaporation were not estimated in default of the data.

The modelling of the seepage was carried out when accepting potentially the worst variant, i.e., when the protective shield was not arranged. The seepage calculations were carried out using the finite difference method when partitioning the numeric models into more or less 9000-10000 finite elements and thus ensuring accuracy of the modelling results.

The modelling results consist of the curve of depression, isolines of hydrostatic pressure, vectors and flow lines of the ground water flow. The example of the modelling results is presented in Figure 3.

Analysing the results of the seepage modelling (when the hermetic sheet piling is arranged) we see that the seepage through the protective embankment of the Kariotiškės sewage sludge dump will be stopped and the sludge filtrate should not gain access into the swamp situated at the foot of the embankment. The arrangement of the hermetic sheet piling (when sinking it through permeable soils up to practically impermeable moraine clay soils) stops the seepage through the protective embankment of the Kariotiškės sewage sludge dump and locks the natural layers of the permeable soil situated beneath the embankment.

The arrangement of the hermetic sheet piling is the most efficient and optimal anti-seepage means due to the blocking of permeable layers. Hermetic sheet piling increases the stability of the protective embankment as well and is easy to arrange.

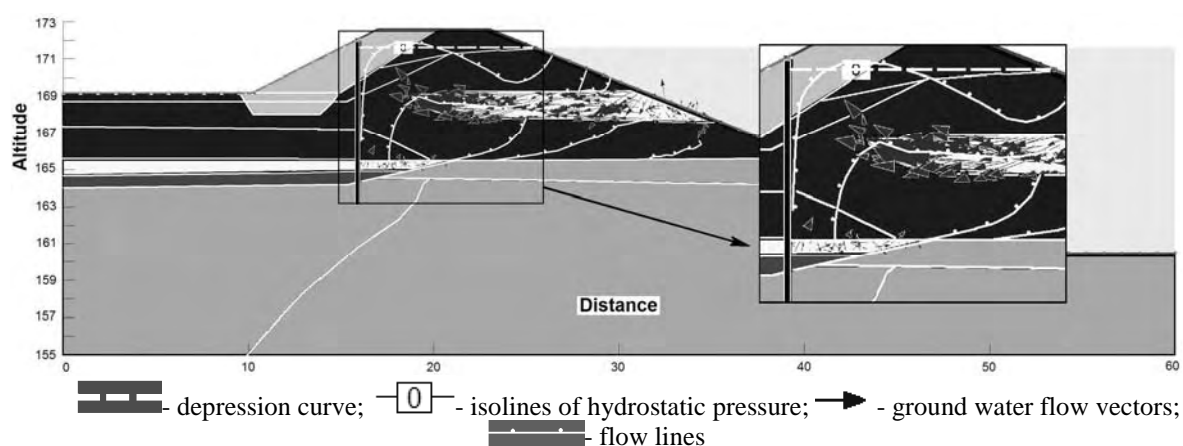


Fig. 3. Seepage modelling results with hermetic sheet piling of the section I-I in the protective embankment of the Kariotiškės sewage sludge dump.

The bottom of the sheet piling should be sunk into hard and medium hard plastic moraine clay soils occurring beneath permeable soils. It should ensure its static stability.

CONCLUSIONS

1. In order to ensure the environment protection requirements when carrying out the closure works of the Kariotiškės dump, the geological situation and possible anti-seepage means blocking sludge seepage through the protective embankment were analysed. It was defined that in default of the damaged protective sheet the filtrate from the sludge dump can gain access into the surroundings, i.e., can filtrate into the swamp situated at the foot of the embankment.

2. The modelling of the seepage of the Kariotiškės sewage sludge dump was carried out. Following the analysis of the received results it was defined that:

- seepage most intensively occurs through

permeable sandy soils; through less permeable clay soils it is much more slower;

- in three of four cross-sections (I-II, III-III and IV-IV) the depression curve comes up into the ground surface in the dry slope of the embankment and can be the reason for water seepages and landslides in the slope.

3. The suggested arrangement of hermetic sheet pilings (deepened into the naturally stratified impermeable layers of moraine clay) is one of the most efficient, economic and simplest ways stopping the seepage of the sludge dump filtrate through the protective embankment as well as through the blocked layers of the protective embankment.

4. The analysis of the carried out modelling results showed that the hermetic sheet piling showed the best result as anti-seepage means. Besides, it increases the stability of the protective embankment.

REFERENCES

COUNCIL DIRECTIVE 1999/31/EC of 26 April 1999 on the landfill of waste THE COUNCIL OF THE EUROPEAN UNION [online] [accessed on January 6, 2011]. Available: <http://eur-lex.europa.eu/LexUriServ>

Craig. R. F. (1995) *Soil mechanics*. London: Chapman and Hall. 425 p.

Dobkevičius M. (2001) *Hidrogeodinamika*. Vilnius: Enciklopedija. 345 p.

Geostudio program [online] [accessed on February 24, 2011.]. Available: <http://www.geo-slope.com>

LST 1445. (1996) *Geotechnika: gruntų klasifikacija ir identifikacija*.

Pocius A. (1996) *Geologija (konspektas)*. Kaunas: LŽŪU. 104 p.

Pranaitis V., Sidauga B. (1979) *Inžinerinė geologija*. Vilnius: Mokslas. 283 p.

Ruplys B. (1988) *Hidrotechniniai statiniai*. Vilnius: Mokslas. 343 p.

STR 1.04.02:2004. (2004) *Inžineriniai geologiniai (geotechniniai) tyrimai*.

Šimkus J. (1984) *Gruntų mechanika, pagrindai ir pamatai*. Vilnius: Mokslas. 270 p.

Šimkus J., Alikonis A., Sidauga B. (1973) *Lietuvos TSR gruntų statybinės savybės*. Vilnius: Mintis. 92 p.

Todd D. K., Mays L. W. (2005) *Groundwater hydrology*. Third edition. Wiley, New York. 636 p.

UAB „Geotechniniai tyrimai“. (2009) *Kariotiškių nuotekų dumblo sąvartyno uždarymas. Nuotekų dumblo sąvartyno apsauginio pylimo geotechniniai tyrimai*. Vilnius. 22 p.

UAB „Geotechniniai tyrimai“. (2009) *Kariotiškių nuotekų dumblo sąvartyno uždarymas. Dumblo geotechniniai tyrimai*. Vilnius. 14 p.

Verrujit A. (2006) *Soil mechanics*. Netherlands: Delft University of Technology. 315 p.

Далматов Б. И. (1988) *Механика грунтов, основания и фундаменты*. Ленинград: Стройиздат. 415 с.

Морарескул Н. Н. (1979) *Основания и фундаменты в торфяных грунтах*. Ленинград: Стройиздат. 80 с.

Ренгач В. Н. (1970) *Шпунтовые стенки (расчет и проектирование)*. Ленинград: Стройиздат. 113 сс.

Тер-Мартиросян З. Г. (1990) *Геологические параметры грунтов и расчеты оснований сооружений*. Москва: Стройиздат. 200 с.

Ухов С. В., Семенов В.И., Знаменский В. И., Тер-Мартиросян З. Г., Чернышов С.Н. (2004) *Механика грунтов, основания и фундаменты*. Москва: Высшая школа. 566 с.

THERMAL CONDUCTIVITY OF THATCHED (REED) ROOF IN COMPOSITE CEILING

Uku Vigel, Meeli Kams

Estonian University of Life Sciences, Institute of Forestry and Rural Engineering
eizo@hotmail.ee; meeli.kams@mail.ee

ABSTRACT

The aim of the study is to determine the thermal conductivity of reed roof in composite ceilings of civil houses, which are in use. The thermal conductivity of houses in use depends on the inside microclimate conditions and outdoor climate (cover of snow on the roof, blast of wind, radiation of frost, solar energy etc). Up to now the thermal conductivity of reed was identified in laboratory conditions without consideration of the outdoor climate conditions for roofs. Measuring thermal flow and temperature inside and outside of the reed roof in composite ceiling allows calculating the coefficient of heat conductivity (λ , W / mK), what is necessary for thermal calculations of the named buildings. Analysis of measuring thermal conductivity of reed roofs of six living houses during the heating period gives medium arithmetic for λ 0,11 W/mK for reed in composite ceiling with snow-cover (thickness 150 ... 300 mm).

Key words: thermal conductivity, reed roof, composite ceiling, climatic conditions, radiation of frost

INTRODUCTION

The thermal conductivity of reed is determined and the coefficient of thermal conductivity (λ , W / mK) is calculated depending on water consistent 0,050 ... 0,058 W/mK (Rekomendatsii po primeneniju..., 1988) p.9,10 and for reed mats 0,059 ... 0,078 W/mK. For reed mats another reference material is present (SNiP II-3-79..., 1982) p. 27 0,06 ... 0,07 W/mK. But the submitted coefficients do not consider the outdoor climate conditions (especially radiation of frost) and specificity of composite ceiling with reed roof. Consequently, it is necessary to determine the coefficient of thermal conductivity for reed in composite ceiling for houses in use experimentally. It is needed for calculating the heat cost to engineer and reconstruct the buildings with composite reed roofs in similar climate conditions as the Estonian Republic. Up to now there are 2982 buildings with thatched roofs in use (Konks, 2011). On Figure 1 there are two of them as examples.

EXPERIMENTAL INVESTIGATION

The study was carried out in six houses, where people lived year-round.

In five houses the measurements were done during one winter day with a thermo gauge sonde probe and thermovisor thermovisor because these houses are too far from the research centre in Tartu. In one house near Tartu the study was carried out during the heating period. Figure 1. The house is built using ecological building materials: wood, stone, saw-dust and reed. The composite ceiling consists of the following layers:

- reed 300 mm
- paper
- saw-dust between the rafter 50x150 mm, in the distance 1000mm
- boarding 18 mm.

The following methods for the determination of the thermal conductivity of composite reed roof were used:

- measuring with thermo-camera Therma CAM B2 inside rooms
- measuring with temperature gages TMC 1-HD, TMC 6 – HD, TMC 20 – HD and TMC 50 – HD in connection with the data carrier logger HOBU U12 – 006 and HOBU U12 [4] in all layers of insulated roof;
- measuring with heat flow plates FQ90119 in two positions in the house near Tartu;
- measuring with a thermo-gauge in all layers of insulated roof-ceiling on five buildings;
- calculation method, equation 1 [4]

$$\lambda = \frac{qd}{T_1 - T_2} \quad (1)$$

q – thermal conductivity, W/m²

d – ply (thickness) of the material, m

T₁ – temperature of the warm side layer, °K

T₂ – temperature of the cold side layer, °K

The thermal conductivity of reed roof was determined under various climate conditions outside:

- cover of snow on the roof;
- blast of wind
- radiation of frost (sky radiation temperature - 70°C)
- solar energy etc.



Figure 1. Houses with thatched roof in the Estonian Republic.



Figure 2. The house nearby Tartu in Ihaste built of ecological building materials.

The microclimate inside the house was investigated in the same living house where people were living all the year round.

The analysis of measuring gives the following coefficient of heat conductivity

- near Tartu – $\lambda=0,10$ W/mK
- Hiiu I – $\lambda=0,12$ W/mK
- Hiiu II – $\lambda=0,106$ W/mK
- Hiiu III – $\lambda=0,118$ W/mK
- Otepää – $\lambda=0,115$ W/mK
- Puhja – $\lambda=0,107$ W/mK

Medium arithmetic for λ is 0,111 W/mK.

The investigation of using air-barrier in the layer between saw-dust and reed shows that air-barrier is useful, Figure 3. The radiation of frost during the night decreases the temperature of snow on the roof, Figure 4. The frost radiation is especially harmful when the snow is in ice, then the capacity of frost is considerable in snow.

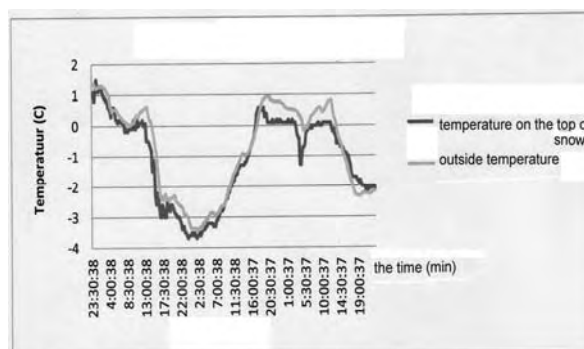


Figure 4. Radiation of frost decreases the temperature on the top of snow on the roof (11.01.2011 ... 13.01.2011).

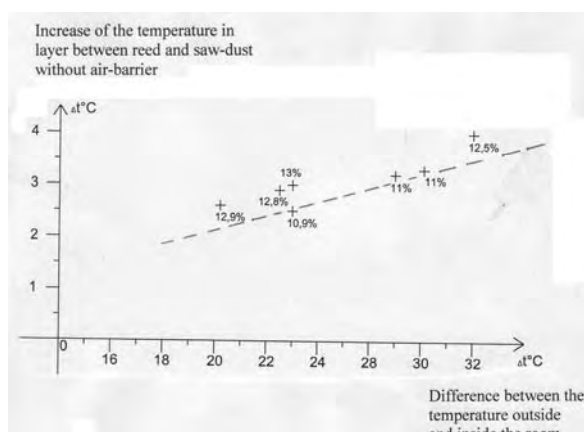


Figure 3. Decrease of thermal resistance of saw-dust without air-barrier (10,9 % ... 13 %).

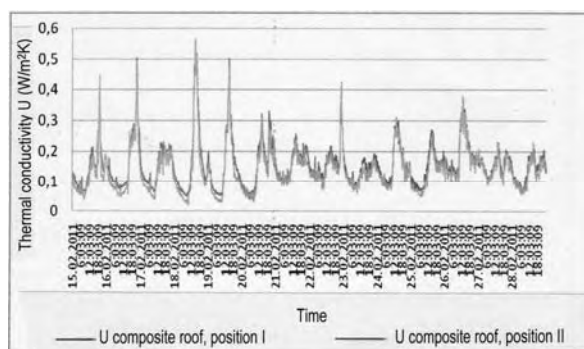


Figure 5. Thermal conductivity of reed in composite ceiling with snow-cover is changing quite a lot.

The thermal conductivity of reed in composite ceiling is increasing up to five times in clear up (cloudless) nights when it is influenced by frost radiation from the sky, Figure 5.

CONCLUSIONS

Based on the test results and numerical analysis:

- the thermal conductivity of reed in composite ceiling is increasing up to five times in cloudless night by the reason of frost radiation from the sky.
- the coefficient of thermal conductivity λ (W/mK) for reed in composite ceiling with a

snow cover for houses in use in the climate conditions of the Estonian Republic is 0,11 W/mK.

REFERENCES

Rekomendatsii po primeneniju mestnõh teploizoljatsionnõh materialov pri stroitelstbe životnobotšeskih zdanii (1988). Moskva. 36 p.

SNiP II-3-79*. Stroitelnoje normõ i pravila. Normõ projektirovanija. Stroitel'naja teplotehnika. (1982). Moskva: Stroiizdat. 40 p.

Konks, V. (2011) Answer to request for information from Register of Buildings of Estonian Republic. E-mail from 03.08.2011. List of buildings with thatched roof in Estonia, all together 2982 buildings.

Standard of Estonian Republic. EVS-EN-ISO 7345 (2006)

BUILDING AS LONG-TERM ENVIRONMENTAL DEVELOPMENT AND PRESERVATION CONDITION

Sandra Gusta,
Latvia University of Agriculture,
Department of Architecture and Building
sandra.gusta@llu.lv

ABSTRACT

Long-term building ideas developed in other countries known as sustainable building are becoming more popular also in Latvia. That is stimulated with the help of many conditions: economic (necessity for saving resources and energy), social (market - dictated by the consumers, high demands for the quality and accommodations), as well as activation of the environmental issues (taking responsibility for the diminishing of the climate changes and pollution). The paper describes International agreements on climate change reduction. Latvian national policy documents, main energy design and livability criteria of the Model Home 2020 experiments, BREEAM (Building Research Establishment's Environmental Assessment Method), there are analyzed current economic situations in the building evaluation in Latvia. In this paper sustainable building and management basic principles are inspected and technical criteria are analyzed. Also characteristic building economic analysis is given. The paper gives recommendations for the improvement of the situation.

Key words: long-term environmental development, sustainable building, BREEAM

INTRODUCTION

In the times of climate changes and globalization researches involving security of long-term environment, saving of the resources, as well as the preservation of the identity and singularity of the place are activating. The concept long-term involves balancing of the economic and social issues of the environment, maintaining balanced development.

The aim of long-term development is to secure continuous improvements of the quality of life and welfare for the existing and future generations. It is an essential goal of the European Union. However, rapid global changes, from the melting of glaciers to the growing demand for the energy and resources, are making it difficult to reach the goal mentioned.

Also in the field of building, the task is to create a continuous cycle: to improve the general ecological characteristic quantity of building products in the whole turnover cycle, to popularize and stimulate the demand for building products and technologies and to help consumers make the best choice with the help of more coordinated and more simple labelling.

Long-term building ideas developed in other countries known as sustainable building are becoming more popular also in Latvia. That is stimulated with the help of many conditions: economic (necessity for saving resources and energy), social (market - dictated by the consumers, high demands for the quality and accommodations), as well as activation of the environmental issues (taking responsibility for the diminishing of the climate changes and pollution).

Table 1

Benefits of long-term building		
Environmental benefits	Economic benefits	Social benefits
preservation of the ecosystem and biodiversity;	diminished building expenses;	improved air quality;
raised air and water quality;	raised value added;	raised comfort level and healthy living conditions;
less solid fuel;	support to the local manufacturers and economic;	diminished spare load to the infrastructure;
saving and non-exhausting natural resources.	raised working productivity and employee satisfaction;	higher quality of life.
	improved economic (economy in the whole usage time) showings of the building life cycle.	

There are many advantages of the long-term building securing long-term development. (J. Brizga: Creating qualitative, environment-

friendly, and health-friendly living space, ecologic, economic, and social sustainability is facilitated. It is a way of living environment and health friendlier, without giving up nowadays so common accommodations and quality standards, though at the same time thinking of the future of our children and grandchildren and rights living in clean, resources non-exhaust environment.

Long-term building involves complex solutions and practice, that increases the efficiency of houses, diminishing consumption of the energy, water and other natural resources, diminishing houses, their building and management processes material input per unit, power-intensity and negative impact to the people's health and environment. It can be achieved choosing appropriate architectonic and constructive solutions, proper building location to optimize in the planning of the buildings, building, exploitation and demolition, consumed and exploited resources, evaluating their complexly in the whole life (building, management, and demolition) cycle. (www.zalasmajas.lv)

INTERNATIONAL AGREEMENTS ON CLIMATE CHANGE REDUCTION

At the United Nations Conference in Rio de Janeiro, 1992, sustainable development was announced as the way of social-economic questions balanced solution and environment protection.

The UN climate change conference in Mexico, Cancun, was on 29 Nov.-10 Dec. 2010. The Member States have agreed to fight global warming and developing countries to provide funds for a compromise in the fight against the climate change. A new document was adapted to combat global warming, which also includes the Green Climate Fund for the developing countries, where a significant proportion of the funding will go to fight the climate change.

Latvia has undertaken to fulfill its international commitment to global climate change by signing the UN Framework Convention on Climate Change (the Convention) in 1992 in Rio de Janeiro and ratification of the Saeima in 1995.

The Convention aims are to achieve greenhouse gas (GHG) concentration in the stabilization of the atmosphere at a level that would prevent dangerous anthropogenic interference with the climate system. On January 23, 2008, the European Commission published the Climate Energy Package and the related documents. The package includes the following laws and regulations:

1. Emissions Trading Scheme (ETS) Directive Statement;
2. The decision to reduce emissions in sectors not covered by the ETS;
3. Renewables project;
4. The draft directive carbon capture and storage and impact assessment.

The future of construction is facing serious challenges – resource supply, energy efficiency and unhealthy buildings to name but three. The real challenge facing us is essentially a dual challenge – energy and livability.

The EU has adopted a comprehensive package for European energy policy up to 2020. It entails that EU member states are to reduce their total energy consumption and CO₂ emissions by 20%. Moreover, all EU member states must document that 20% of their total energy consumption comes from renewable energy sources.

The Latvian national policy documents are:

1. Latvian National Development Plan 2007-2013. Sustainable development is defined as the social, environmental and economic factors of employment;
2. Construction industry guidelines for 2011-2015: "The main task of the Guidelines is to establish policies for sustainable and competitive construction industry development";
3. Construction sector policy framework; one of the six principles of environmentally sound, competitive and sustainable construction principles;
4. Construction Law Project. One of the four fundamental principles of sustainable construction principles;
5. Recommendations for the promotion of environmentally friendly construction, approved by the Cabinet, 22.12.2008;
6. Environmentally-friendly procurement manual;
7. European Parliament and Council Directive 2008/98/EC of 19.11.2008, on waste and repealing certain Directives;
8. European Parliament and Council Directive 2010/31/EK 19/05/2010, on buildings;
9. Energy management system EFT EN ISO 16001, from 2011;
10. Founded a new association - the Latvian Council of sustainable construction. "

MODEL HOME 2020

In order to find solutions to the challenges of climate change and livability, we need to examine a future model that addresses them as a holistic solution.

The ultimate objective of future construction and subsequent use of a building is taken into account in the design phase; it should employ modern technology and visionary design to create an efficient building envelope without compromising the highest standards of comfort and health; and it should have the lowest possible impact on the climate by using renewable energy sources and adopting the concept of climate payback.

In the EU today, we spend 90 % of our time indoors, in buildings that consume over 40 % of the total energy consumption. Up to 30% of the building stock does not contribute to nor provide a

healthy indoor climate. Looking into a future perspective of how we construct and renovate buildings, it is necessary to consider climate changes, resource supply and human health.

Energy challenge. Buildings consume approximately 40% of all the energy we use (European figures).

Considering the total energy consumption throughout the whole life cycle of a building, the energy performance and energy supply is an important issue in the concern about climate changes, security of supply and reduced global energy consumption.



Figure 1 Energy, environment and indoor climate challenge.

Environment challenge. Although the challenges we face are global, the local environment, which always has unique features, must be considered carefully. An open-minded approach to flexible solutions that take into account local cultural and infrastructural differences creates a cleaner environment with less pollution and waste, each time reflected in the best solution for the specific context.

Indoor climate challenge. People spend 90 % of their time indoors, but less than 30% of the building stock contributes to or provides a healthy indoor climate. Humans need comfortable conditions including thermal conditions, fresh air and daylight when they are indoors. These factors have a positive effect on our health and well-being as well as our ability to perform.

The real challenge facing us is essentially a dual challenge – the energy challenge and the livability challenge. Seven main criteria have been identified as the most important for the energy design and livability criteria of the project Model Home 2020 experiments by specialists of WELUX Group. The main energy design and livability criteria of the

Model Home 2020 experiments are:

1. Energy consumption targets.
2. Low-energy standards.
3. Optimized design.
4. Highest energy marking.
5. Intelligent energy performance control.
6. Documentation of embodied energy.

It means: maximized daylight availability, highest daylight levels, strategic window positions, healthy indoor climate, automatic control of natural ventilation, stack effect/chimney effect, sound materials.

BREEAM (Building Research Establishment's Environmental Assessment Method)

BREEAM is the world's leading and most widely used environmental assessment method for buildings. At the time of writing, BREEAM has certified over 200,000 buildings since it was first launched in 1990.

- Developed in the British Research Establishment (BRE), UK;
- The method is an adaptation process in Latvia, Russia, Sweden, Norway, Spain, France, the Netherlands, Turkey, United Arab Emirates;
- Buildings with a certificate of higher market value;
- BREEAM: more than 70 objectively measurable criteria for evaluation of sustainable building nine categories of 'energy', 'material', 'process of construction / building management', 'health / well-being', 'transport', 'water', 'waste', 'pollution'

Aims of BREEAM:

- To mitigate the life cycle impacts of buildings on the environment
- To enable buildings to be recognised according to their environmental benefits
- To provide a credible, environmental label for buildings
- To stimulate demand for sustainable buildings

Objectives of BREEAM:

1. To provide market recognition of buildings with a low environmental impact
2. To ensure best environmental practice it is incorporated in building planning, design, construction and operation.
3. To define a robust, cost-effective performance standard surpassing that required by regulations.
4. To challenge the market to provide innovative, cost effective solutions that minimise the environmental impact of buildings.
5. To raise the awareness amongst owners, occupants, designers and operators of the benefits of buildings with a reduced life cycle impact on the environment.
6. To allow organisations to demonstrate progress towards corporate environmental objectives.

BREEAM has been developed to meet the following underlying principles:

1. Ensure **environmental quality** through an accessible, holistic and balanced measure of environmental impacts.
2. Use **quantified measures** for determining environmental quality.
3. Adopt a **flexible approach**, avoiding prescriptive specification and design solutions.
4. Use **best available science** and **best practice** as the basis for quantifying and calibrating a cost effective performance standard for defining environmental quality.
5. Reflect the **social and economic benefits** of meeting the environmental objectives covered.
6. Provide a **common framework** of assessment that is tailored to meet the 'local' context including regulation, climate and sector.
7. **Integrate construction professionals** in the development and operational processes to ensure wide understanding and accessibility.
8. Adopt **third party certification** to ensure independence, credibility and consistency of the label.
9. Adopt the **existing industry** tools, practices and other standards wherever possible to support developments in policy and technology, build on the existing skills and understanding and minimise costs.
10. **Stakeholder consultation** to inform ongoing development in accordance with the underlying principles and the pace of change in the performance standards (accounting for policy, regulation and market capability).

BREEAM (*British Environmental Assessment Method*):

It sets the standards for the best practice in sustainable development and demonstrates a level of achievement.

It has become the vocabulary used to describe the environmental performance of a building;

BREEAM sets the standard for the best practice in sustainable building design, construction and operation and has become one of the most comprehensive and widely recognized measures of a building environmental performance.

A BREEAM assessment uses recognized measures of performance, which are set against established benchmarks, to evaluate the specification, design, construction and use of a building. The measures used represent a broad range of categories and criteria from energy to ecology. They include aspects related to energy and water use, the internal environment (health and well-being), pollution, transport, materials, waste, ecology and management processes.

A Certificated BREEAM assessment is delivered by a licensed organization, using assessors trained under a UKAS accredited competent person scheme, at various stages in a building life

cycle. This provides clients, developers, designers and others with:

market recognition for low environmental impact buildings;
confidence that is tried and tested environmental practice incorporated in the building;
inspiration to find innovative solutions that minimize the environmental impact;
a benchmark that is higher than regulation;
a system to help reduce running costs, improve working and living environments;
a standard that demonstrates progress towards corporate and organizational environmental objectives.

What does BREEAM do?

- BREEAM addresses wide-ranging environmental and sustainability issues and enables developers, designers and building managers to demonstrate the environmental credentials of their buildings to clients, planners and other initial parties, BREEAM:
- uses a straightforward scoring system that is transparent, flexible, easy to understand and supported by evidence-based science and research;
- has a positive influence on the design, construction and management of buildings;
- defines and maintains a robust technical standard with rigorous quality assurance and certification.

Who uses BREEAM?

Clients, planners development agencies, funders and developers use BREEAM to specify the sustainability performance of their buildings in a way that is quick, comprehensive, highly visible in the marketplace and provides a level playing field.

Property agents use it to promote the environmental credentials and benefits of a building to potential purchasers and tenants.

Design teams use it as a method to improve the performance of their buildings and their own experience and knowledge of environmental aspects of sustainability.

Managers use it to reduce running costs, measure and improve the performance of buildings, empower staff, develop action plans, monitor and report performance at both the single building and portfolio level.

BREEAM NEW CONSTRUCTION

BREEAM New Construction is a performance based assessment method and certification scheme for new buildings. The primary aim of BREEAM New Construction is to mitigate the life cycle impacts of new buildings on the environment in a robust and cost effective manner. This is achieved

through integration and use of the scheme by clients and their project teams at key stages in the design and procurement process. This enables the client, through the BREEAM Assessor and the BRE Global certification process, to measure, evaluate and reflect the performance of their building against best practice in an independent and robust manner. This performance is quantified by a number of individual measures and associated criteria stretching across a range of environmental issues see Table 3, which is ultimately expressed as a single certified BREEAM rating, i.e., the label (section 3 describes how a BREEAM rating is calculated). When to engage with the BREEAM NC scheme, timing the engagement with and use of BREEAM via the BREEAM Assessor is essential for ensuring seamless integration of the methodology in the procurement process. Without this, the ability to cost effectively optimise the building environmental performance and achieve the desired rating will be compromised. Appointing a BREEAM Assessor or Accredited Professional early in the project will help in achieving the target rating without undue impacts on the flexibility of design decisions, budgets and potential solutions.

BREEAM-LV

BREEAM-LV is an official at the Bree "family" owned, localized version of the assessment of buildings in the Latvian situation. It means:

1. Economic benefits (higher value and market demand, lower operating costs, support local producers),
2. Social benefits (healthier and more comfortable indoor climate, balanced integration of the surrounding infrastructure,
3. Environmental benefits (less CO₂ emissions and other pollution, conserves energy, water and other resources, respect for ecology and biodiversity).

PROBLEMS OF BUILDING SECTOR OF LATVIA

Compared to 2009, the construction volume at constant prices in 2010 has reduced by 23.6%. Of which construction of buildings has decreased by 24.9% and the volume of civil engineering structures constructed – by 22.3%.

Compared to the 3rd quarter of 2010, the construction volume in the 4th quarter of 2010 decreased by 5.5%, according to seasonally adjusted data at constant prices. Of which the construction of buildings diminished by 6.6% and the volume of civil engineering structures constructed have grown by 1.5%.

In 2010 the construction volume (at current prices) comprised LVL 757.5 million, of which in the 4th quarter – LVL 228.9 million, according to the data of the Central Statistical Bureau.

Table 3
BREEAM 2011 New Construction environmental sections and assessment issues

Energy	Water
Reduction of CO ₂ emissions	Water consumption
Energy monitoring	Water monitoring
Energy efficient external lighting	Water leak detection and prevention
Low or zero carbon technologies	Water efficient equipment (process)
Energy efficient cold storage	Waste
Energy efficient transportation systems	Construction waste management
Energy efficient laboratory systems	Recycled aggregate
Energy efficient equipment (process)	Operational waste
Drying space	Speculative floor and ceiling finishes
Transport	Materials
Public transport accessibility	Life cycle impacts
Proximity to amenities	Hard landscaping and boundary protection
Cyclist amenities	Responsible sourcing of materials
Maximum car parking capacity	Insulation
Travel plan	Designing for robustness
Land use and ecology	Pollution
Site selection	Impact of refrigerants
Ecological value of site / protection of ecological features	NO _x emissions from heating/cooling source
Mitigating ecological impact	Surface water run-off
Enhancing site ecology	Reduction of night time light pollution
Long term impact on biodiversity	Noise attenuation
Health and wellbeing	Management
Visual comfort	Sustainable procurement
Indoor air quality	Responsible construction practices
Thermal comfort	Construction site impacts
Water quality	Stakeholder participation
Acoustic performance	Service life planning and costing
Safety and security	Innovation
	New technology, process and practices

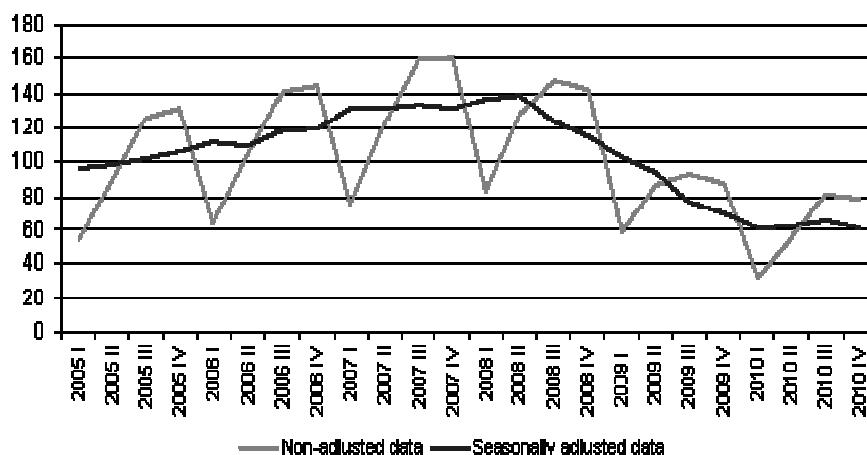


Figure 3. Construction volume index (2005 = 100).

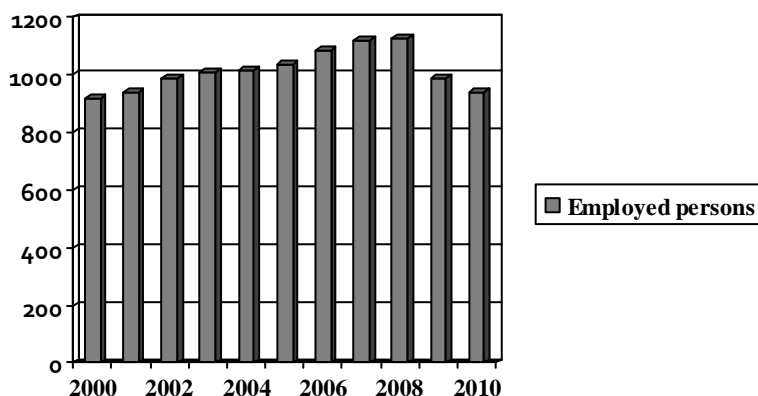


Figure 4 Employed persons in Latvia

Table 4
Construction volume Thsd lats (at current prices)

Year	1st quarter	2nd quarter	3rd quarter	4th quarter	Total
2008	300141	460419	532716	475199	1768475
2009	203514	277839	288112	249457	1018922
2010	107145	173991	247502	228904	757442

Compared to the 4th quarter of 2009, the construction volume in the 4th quarter of 2010 has decreased by 9.6%, according to working day adjusted data at constant prices.

Of which construction of buildings reduced by 6.1% and the volume of civil engineering structures constructed – by 11.9%

If compared to the corresponding period a year before, the most notable reduction of construction and repairs was observed in construction of office buildings and in construction of bridges – by 63.4% and 47.6%, respectively.

Table 5
Completed residential buildings by quarter, thsd m²

	1st quarter	2 nd quarter	3rd quarter	4th quarter	Year
Total					
2008	258.9	235.0	336.0	323.3	1153.2
2009	200.0	228.6	118.0	125.4	672.0
2010	102.1	121.9	83.6	74.2	381.8
..investors	-	-	-	-	-
private persons					
2008	112.2	90.6	109.5	166.7	479.0
2009	123.0	118.0	95.1	90.9	427.0
2010	89.5	91.3	75.5	64.9	321.2

But growth of the construction volume, in turn, was recorded in construction of wholesale and retail trade buildings and in construction of industrial buildings and warehouses – by 123.6% and 56.4%, respectively.

In 2010 construction management authorities granted 1725 building permits for construction, capital repairs, reconstruction and restoration of single dwelling buildings with total floor space 378.6 thousand m² (in 2009 – 2110 and 427.7 thousand m², respectively). 295 building permits were granted for construction of production buildings and warehouses with total floor space 536.5 thousand m² (in 2009 - 198 permits and 299.0 thousand m², respectively).

In the 4th quarter of 2010 326 building permits were granted for construction of single dwelling buildings with total floor space 75.9 thousand m² (in the 4th quarter of 2009 – 405 and 83.1 thousand m², respectively). 105 building permits were granted for construction of production buildings and warehouses with total floor space 153.1 thousand m² (in the 4th quarter of 2009 - 56 permits and 77.0 thousand m², respectively).

In 2010 1095 building permits were granted for construction of new single dwelling buildings with total floor space 244.2 thousand m² (in the 4th quarter of 2010 – 197 and 47.7 thousand m², respectively) and 179 permits were issued for construction of new industrial buildings and warehouses with total floor space 332.5 thousand m² (in the 4th quarter of 2010 – 69 and 100.7 thousand m², respectively).

RESULTS AND DISCUSSION

Results of the housing demand qualitative changes are:

1. In the short-term period – a rise of prices for houses in the sector with new standards, after them a rise of prices in all housing sectors. Stopping replenishment and construct of small-sized and social housings.
2. In the long-time period – surplus of housing, including houses not corresponding to the market demand. Falling of the prices in the sector with new

REFERENCES

- 6th Environmental Action Programme (2002-2012) [online] [accessed on January 24, 2011.]. Available: <http://www.ec.europa.eu/environment/newprg/index.htm>
- Brizga J. (2006) *Zaļā iepirkuma rokasgrāmata*. Celtniecības un būvniecības darbi. Rīga: Biedrība Zaļā brīvība. 18.-30. lpp.
- Proposal for a Community Lisbon Programme 2008-2010 – COM (2007) 804. [online] [accessed on January 24, 2011.] Available: http://www.ec.europa.eu/legislation_summaries/employment_and_social_policy/growth_and_jobs/c11804_en.htm
- Renewed EU Sustainable Development Strategy, Council of the EU 10917/06 [online] [accessed on January 24, 2011.]. Available: http://www.ec.europa.eu/sustainable/docs/renewed_eu_sds_en.pdf
- Velux production. [online] [accessed on June 24, 2011.]. Available: http://www.velux.com/sustainable_living/model_home_2020/newsletter/default.aspx
- LR CSB data base [online] [accessed on May 12, 2011.]. Available: <http://www.csb.gov.lv/>

standards and, further, in all sector of housing.

CONCLUSIONS

Suggestions for proximate period in the building sector to reduce problems which have caused competition in Latvia:

1. Reducing bureaucracy caused barriers in the building sector.
2. To arrange the legislation basis, especially in relation to the building standards.
- 3 Further simplifying of the EU funds and procurement procedures for the state or local government that paid for constructive advices during the project;
4. Continue the BEEAM-LV adaptation and implementation process in Latvia;
5. Provide with the strong level of the building competition process and the control results as well as the change of the fundamental principles of competition, so it does not leave the construction cost as the only evaluation criterion.
6. Carrying out public procurement in accordance with the Public Procurement Law or public service provider procurement law, competition regulations to incorporate sustainable building assessment criteria;
7. To accomplish a very skilled expertise in the documentation preparation stage, provide clients with high quality regulation of competition;
8. To develop very precise technical specifications and contract documentation: included into project as construction materials and construction specifications as detailed work organization and cost calculations (estimate). Without specifying the names and parameters of used materials and mechanisms in the work description; contractor's offer generates distrust, as well as gives a serious effect on project evaluation;
9. Choose the most economically advantageous tender selection criteria;
10. Raise the level of competence of the tender evaluation commission in the construction industry, as well as in the related laws, the Cabinet of Ministers and other standards.

ENERGY-EFFICIENT WASTEWATER TREATMENT TECHNOLOGIES IN CONSTRUCTED WETLANDS

Eriks Tilgalis, Linda Grinberga*

Latvia University of Agriculture

Department of Architecture and Building Construction

eriks.tilgalis@llu.lv

*Department of Environmental Engineering and Water Management

linda.grinberga@llu.lv

ABSTRACT

Usually in wastewater treatment plants the removal of organic matter is ensured in aerotanks in biochemical reactions where activated sludge in presence of oxygen transforms the organic matter. The quantity of organic matter in water can be determined as the biochemical oxygen demand in five days (BOD). BOD in village municipal sewage is around 250 mg l⁻¹ or 65 g per day from each resident. It means that 1.7 kg of oxygen is needed for mineralizing one kg of organic matter. Therefore, it can be concluded that high oxygen demand is required to mineralize organic matter using aerotanks. With a compressor and aeration discs or tubes the oxygen in the form of air is provided to aerotank. To reduce electricity consumption in wastewater treatment, we present to adapt natural conditions. Mineralization of organic matter in constructed wetlands performs basing on bacteria activity in presence of oxygen. The main difference is the method for oxygen supply. In constructed wetlands oxygen demand provides the plants growing above the filter material and it consumes no electricity. Constructed wetlands can be designed with different water flow in filter material – horizontal flow wetlands, vertical flow wetlands and shallow ponds with plants.

Keywords: Constructed wetland, wastewater treatment

INTRODUCTION

Nowadays, people tend to focus on nature and environment protection, as far as possible giving up excessive use of chemicals in everyday life. A sustainable use and development of natural resources is one of the environmental retention initiatives. Wastewater generation is an integral part of human life processes, including both domestic waste water and industrial waste water and rainwater drainage, if they contain anthropogenic pollutants - dust, oil, soil particles. The level of waste water pollution depends on the concentration of pollutants and waste water composition. Natural processes are the most environmentally friendly way to treat man-made waste. However, not necessarily the natural treatment methods give the desired degree of extraction and are able to treat waste water fast enough. Treatment plant adaptation to the situation is often associated with the use of additional mechanical plant or electrical energy use, which increases the maintenance costs.

In Latvia for wastewater treatment mostly biological wastewater treatment plants are used – aerotanks with activated sludge as the main organic matter reducer. Activated sludge requires solid air or pure oxygen supply to support the living and usually we ensure it with compressors or oxygenating pumps. About 15 - 20 m³ of air per 1 m³ of wastewater is used in this mineralization process. Consequently, treating 1 m³ of typical wastewater with coercive aeration consumes 15 –

20 m³ of air, what means 0.264 – 0.352 kW per each m³ of wastewater depending on the power of the air compressor.

In further points an opportunity to purify municipal wastewater close to natural processes, not using additional machinery or electrical energy is described. In order to make more sustainable wastewater treatment and to save electricity, it is possible to choose a wastewater treatment method that works due natural processes and does not require special operation. These requirements meet the worldwide known and widely used extensive method to different quality wastewater treatment in constructed wetland. If there is an additional territory it is possible to change the present energy-intensive wastewater treatment plants to constructed wetlands, adjusting the wetland area, flow direction and other parameters to the actual situation. The operating principle of constructed wetland is using the natural degradation processes and nutrient uptake. (Langergraber, 2006) Several factors affect the ability of constructed wetlands to retain nutrients including alternate dry (aerobic) and wet (anaerobic) conditions, hydraulic retention time (HRT), influent nutrient concentration, water depth, hydraulic loading rate, emergent vegetation, water chemistry, and soil type (Chavan, 2008). As shown by studies, for subsurface flow wetlands primary treatment, at a minimum, it is required to remove settle able and floating solids prior to the wetland bed. This is typically provided through the use of

settling tanks (Kadlec, 2008; Reddy, 2008). As defined by Vymazal (2003) wetlands are known to act as biofilters through a complex of physical, chemical and biological factors which all participate in the reduction of the number of bacteria.

MATERIALS AND METHODS

Site description

Using constructed wetlands as municipal wastewater treatment is a new discipline in Latvia. Four constructed wetlands (Tinuzi, Tervete, Birzi, Pedvale) implemented in Latvia from 2003 to 2005 work properly and effectively. For the referred years data are available on BOD, COD and suspended solids, also phosphorus and nitrogen concentration in the wastewater before and after treatment in constructed wetlands. The major design parameters are presented in Table 1. All these constructed wetlands were designed to treat mechanically prepared municipal wastewater. The mechanical pretreatment is provided by the settling cameras with volume for 3 day effluent discharge. As the monitoring data show, at the outlet of constructed wetlands wastewater is purified in accordance with the existing legal requirements of Latvia, i.e., BOD does not exceed 25 mg/l, COD does not exceed 125 mg/l, and suspended solids are less than 35 mg/l.

Table 1

Major design parameters

Location	Start of operation (year)	Population equivalent (PE)	Wetland area (m ²)
Tinuzi	2003	190	960
Tervere	2004	240	1200
Birzi	2005	400	2000
Pedvale	2003	45	160

Flow regime

To improve the performance of constructed wetland as a wastewater treatment plant Bavor H. J. (2010) offers to change the flow regimes, for example, for agriculture and agroforestry runoff treatment design several individual wetland cells with different flow regimes. It means alternately using surface and subsurface wetlands. To make water move inconsistent with the natural terrain requires the use of forced pumping that means additional electricity consumption throughout the entire period of wetland use. Besides, treating municipal wastewater in the Latvian climate the cold season of the year should be taken into account. November till March the air temperature continuously is below 0°C and creates a snow cover. Choosing surface flow constructed wetland for municipal wastewater treatment makes a risk of freezing that can impair the functioning of the wetland or stop it completely. Therefore, in the climate conditions of Latvia the

municipal wastewater treatment is suitable in subsurface flow constructed wetlands.

In subsurface flow constructed wetlands (in horizontal or vertical direction) the wastewater is fed in at the inlet and flows slowly through the porous medium under the surface of the bed until it reaches the outlet zone where it is collected before leaving via level control arrangement at the outlet. As Vymazal (2008) presents during this passage the wastewater will come into contact with a network of aerobic, anoxic and anaerobic zones. In the aerobic zones roots and rhizomes occur that leak oxygen into the substrate (Vymazal, 2008). Wetland plants are morphologically and anatomically adapted to growing in a water saturated substrate by the presence of internal gas spaces called aerenchymas throughout the plant tissue. (Hondulas, 1994) Three constructed wetlands mentioned in Table 1 - Tervete, Birzi and Pedvale are all horizontal subsurface flow municipal wastewater treatment plants. The water flow direction is in a more or less horizontal path. Constructed wetland in Tinuzi is a vertical subsurface flow municipal wastewater treatment plant.

Determination of the area

The horizontal subsurface flow constructed wetlands for municipal wastewater treatment are installed with the calculation that water flow in the filter layer is directed horizontally 5 – 8 meters from the inlet infiltration pipes to the outlet drain pipes. Reeds on the top layer of the filter not only enrich the filter with oxygen, but also garnet the gravel and create an aesthetic view. The wetland area required for optimal wastewater treatment should be adopted 7 m² per PE. Wetlands can be successfully used in industrial wastewater treatment, assuming in calculations a PE equal to 60 g per day BOD₅. The optimal limit of BOD₅ at the inlet of constructed wetland is less than 150 mg/l. To get that limit, prior to inlet in wetland the effluent is treated mechanically 3 days in the septic tank. The wetland size depends on the time period, that wastewater is necessary to spend in wetland filter to purify to legal regulation requirements. The water subsistence time in the filter is around 7 - 8 hours, which provide wastewater treatment. The time is determined by the speed with which waste water flows through the filter. The filter material shall be selected from coarse sand or gravel with a particle size diameter 0.5 – 5 mm. The water flow speed v (m/s) through the filter is assumed 20 m per day or 0.00023 m/s. The distance L (m), that water makes from the inlet pipe to the drainage tube in time T (hours) is calculated by formula below.

$$L = T * v = (7*3600) * 0.00023 = 5.8 \text{ m.}$$

In vertical subsurface flow constructed wetlands water filtrates through 1 m thick layer of coarse sand. The time of filtration is about 1 hour.

RESULTS AND DISCUSSION

As defined by Acharya G. (2005) wetlands have several advantages, like direct benefits: include the raw materials and physical products that are used directly for production, consumption, and sale including those providing energy, shelter, foods, water supply, transport, and recreation. Indirect benefits: these include ecological functions which maintain, protect, and support natural and human systems through services such as maintenance of water quality, flow and storage, flood control and storm protection, nutrient retention, and micro-climate stabilization, and other productive and consumptive activities. (Acharya, 2005)

A comparison was made between the two wastewater treatment plants mentioned above - aerotanks with forced aeration and subsurface flow constructed wetlands with the reed plantation on the surface of the filter. As the average capacity is presented 100 PE, that is approximately 15 m³ per day.

As the main indicators, which compile the total operative costs of the wastewater treatment plant, equipment costs, construction costs, consumption of electricity during operation and maintenance are presented. These indicators are presented in Figure 1. In total costs the wastewater pumping station is not included, because the installation of it depends on the relief of the area. Besides the costs in both treatments plant kinds would be similar. Similarly the energy deletion well behind the pumping station is necessary in both cases.

The equipment costs of the aerotank comprise the cost of a metallic or polymer container with typical equipment that is usually offered by the company. The equipment also includes the air compressor and air inlet wheels. These equipment costs are mostly fixed and independent on the site conditions and location. Whereas the equipment costs of constructed wetland are variable, they vary depending on the filter material obtaining place distance, transport costs etc.

The construction costs as well as the equipment costs are lump sum payment when starting the operation of the treatment plant. Duration of the action and quality does not affect the costs. The companies that offer standard wastewater treatment plants with aeration are tended to include construction costs in the plant amount price or equipment costs.

In Figure 1 reflected construction costs are calculated according to the average offered construction costs in Latvia. Ground work and technique are taken into account.

The consumption of electricity during operation in Figure 1 is calculated according to the quantity of wastewater within 5 years.

Five years is a minimal warranty period for a wastewater treatment plant. Whereas the constructed wetland activity is required to meet the electricity, electric energy amount to be zero. Electricity consumption for the aerotank is drawn up of the air compressor.

The maintenance during the plant exploitation is complex to express in monetary. The more mechanical parts the equipment has the more necessary it is to closely monitor these facilities on regular basis, and it requires a specially educated person.

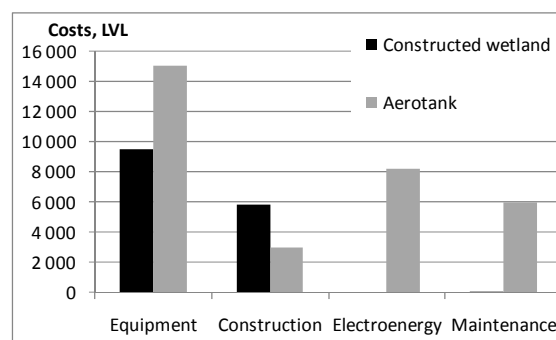


Figure 1. Cost comparison between constructed wetland and aerotank.

As Figure 1 shows constructed wetland has lower equipment costs than the biological treatment plant with aeration and activated sludge called aerotank. The occasion is non mechanical and natural materials are used as a filter to mineralize organic matter and nutrients with natural aeration. As the wetland takes greater area than a compact aerotank, also the construction draws up in higher costs. The wetland long-term operating costs are lower or even close to zero.

CONCLUSION

Latvian non-city residents are living in farmsteads as well as in the city outskirts areas where the occupied area of the property is sufficient to include open artificial or natural waters, such as a pond. Therefore, the installation of constructed wetlands is territorially suitable for Latvia.

In Latvia constructed wetlands are economically beneficial in small objects, i.e., separate households, villages up to 300 inhabitants, sanatoriums, because their operating costs are low.

Benefits of some wetlands will always be difficult to quantify and measure primarily because the required scientific, technical, or economic data are difficult to obtain and also that certain intrinsic values are not measurable by the existing economic valuation methods.

REFERENCES

- Acharya G. (2005) *Wetland: Economic Value*. Encyclopedia of Soil Science: Second Edition. R. Lal (ed.) p. 1895 – 1899.
- Bavor H.J. (2010) Application of Costructed Wetlands in Recycling, Agriculture and Agroforestry: Water Management for Changing Flow Regimes. *Water and Nutrient Management in Natural and Constructed Wetlands*. J. Vymazal (ed.). Chapter 1, p.1 – 7.
- Chavan P.V., Dennett K.E., Marchand E.A. (2008) Behavior of Pilot-Scale Constructed Wetlands in Removing Nutrients and Sediments Under Varying Environmental Conditions. *Water Air Soil Pollut.* p. 192 – 239.
- Hondulas J. L. (1994) *Treatment of polluted water using wetland plants in a floating habitat*. United States [online]. Available: <http://www.freepatentsonline.com/5337516.html>
- Jorgensen S.E. (2010) *Application of Ecological Indicators for the Assessment of Wetland Ecosystem Health*. Handbook of Ecological Indicators for Assessment of Ecosystem Health, Second Edition. S.E. Jorgensen, F. Xu, R. Costanza (ed.), p. 201 – 210.
- Kadlec R.H., Wallace S.D. (2008) *Treatment Wetlands, Second Edition*. USA: Taylor & Francis Group. 1000 p.
- Langergraber G. (2006) *Constructed Wetlands – Introduction and Principles*. Palestine: Ramallah. 123 p.
- Maehlum T., Jenssen P.D. (2003) Design and Performance of Intergrated Subsurface Flow Wetlands in a Cold Climate. *Constructed Wetlands for Wastewater Treatment in Cold Climates*. Chapter 4, p. 69 – 86.
- Reddy K.R., DeLaune R.D (2008) *Biogeochemistry of Wetlands. Science and Applications*. USA: Taylor & Francis Group. 757 p.
- Vymazal J., Ottova V., Balcarova J., Dousova H. (2003) Seasonal Variation in Fecal Indicators Removal in Constructed Wetlands with Horizontal Subsurface flow. *Constructed Wetlands for Wastewater Treatment in Cold Climates*. Chapter 13. p. 229 – 250.
- Vymazal J. (2008) Constructed Wetlands for Wastewater Treatment: A Review. *Proceedings of Taal 2007*. p. 965 – 980.

CALCULATION METHOD OF RAINWATER DISCHARGE

Reinis Ziemelnieks, Eriks Tilgalis
Latvia University of Agriculture.
Department of Architecture and Building
reinis.ziemelnieks@llu.lv

ABSTRACT

A method for calculating rain flow probability of different recurrence was developed in 2010 thesis for the city Riga (R.Ziemelnieks). The aim of this paper is to develop a method for determining the rain flow for other major Latvian cities and populated areas. The data were collected over an extended period of maximum rainfall and the surface runoff coefficients were specified for different types of covering materials. The improvement of the existing rainwater flow calculation method is given in the Latvian Building Normative LBN 223-99, which is partly borrowed from the Soviet Union improved building standards and regulations CHuП 2.04.03-85 (SNIP)(Строительные нормы...,1985), which are based on the promotion work thesis by Soviet scientist Kurganov (Курганов) in 1978(Курганов, 1984). The paper gives the coefficient of Ψ values for different surfaces and the estimated k-values of Latvian towns, depending on the desirable flow of rainwater probability in 200-1% range. The method developed enables the calculation of the maximum rate flow of rainwater in urban areas with different probability.

Key words: rainwater, rain flow, k-coefficient, surface runoff, co-system.

INTRODUCTION

Data of research studies carried out as well as media news show that heavy downpours in Riga and other Latvian cities become more intensive year after year (Negaisa sekas., Bauska piedzīvo..). Rain or co-system sewerage systems are not able to carry away all surface waters quickly from the squares and streets having the heavy impermeable cover (Ziemelnieks, Tilgalis, Juhna, 2008). At present parking places, pavements and roads having the impermeable hard cover increase fastly in towns (Ziemelnieks, Tilgalis, 2009). The problems caused by rain waters in the city territories have become actual recently beginning more and more to feel the presence of rain and snow melting waters in the sewerage systems. The situation becomes worse by the connection of rainwater sewerage collectors to the sewerage networks, which creates an additional load to the sewerage networks of the co-systems and pumping stations during the rain. Pumping and purification of rain waters create additional costs of electro energy for the service establishments. Coming of insufficient unpurified rainwater in the water reservoirs creates serious environmental pollutions.

MATERIALS AND METHODS

Processing of rain data

This study makes use of the rain observation data from different inhabited locations and towns using the publicly asseccible information of the agency of Latvia environment, geology and meteorology (LVGMA) (Tables of Meterological Observations..., Meterological and hydrological..). The rain observation data rows were summed up and supplemented in order to improve the existing

calculation method of maximum rainwater discharge in the town of Latvia by means of the new k-coefficient. The data of rain intensity during the warm period from April till September were chosen and used when the downpours with the maximum intensity are observed in Latvia causing the flooding of territories and streets. The precipitation model groups were drawn up selecting the maximum empirical data quantities, in addition by taking into consideration the air temperature regime, the period of warm weather, thus the hard kind of precipitation – snow, ice was not estimated and was excluded from the investigation. The results of the measurements reflecting as „0” have been discarded because then the precipitation has been possibly very small, the system was not able to fix this amount or the precipitation has not been at all.

Rainwater discharge calculation methods

In order to be able to calculate the rain water discharge according to the data obtained with a larger possibility, some improvements of the existing adopted calculations were carried out, thus by improving the drawn up formula with k-coefficient of the rainwater maximum discharge by A.Ziverts (Ziverts, 1997):

$$Q_{\max} = \Psi \cdot q \cdot k \cdot F \quad [l \cdot s^{-1}] \quad (1)$$

in which

Q_{\max} – max 20 minutes rainfall discharge, $l \cdot s^{-1}$;

Ψ – coefficient of surface runoff (Table 1);

q – runoff module $l \cdot (s \cdot ha)^{-1}$ (Table 2);

k – coefficient depending on the calculation probability % (Table 2);

F – size of the surface area, ha.

The calculation simplified expression of the existing discharge module by E.Tilgalis (Tilgalis, 2004) was used as the calculation basis (2) presuming the length of the specific downpour up to 20 min and its average rain intensity 1 mm min⁻¹.

$$q = 0.13 \cdot \alpha \quad [l \text{ (s} \cdot \text{ha)}^{-1}] \quad (2)$$

in which

α - rainfall amount in millimeters(mm), e.g., in Riga during the period without frost according to the summed up date by A. Zīverts, in Table 2 is 368mm, 71 years of observation.

The kind of material use of the surface cover may be different in the location of use of a conformable area, therefore the rainwater discharges change. In Latvia the coefficients of surface discharge have not been summed up in literature. The coefficients of rainwater discharge surface for the present surface cover areas have been studied in the world and their values are shown in Table 1.

The data of the table show clearly that it is possible to reduce the rainwater discharge several times by using the surface covering materials not dense enough of a conformable way.

RESULTS AND DISCUSSION

By determining the values of the precipitation intensity of maximum minutes and by specifying the coefficients of surface runoff for different kinds of covering materials, the calculation method of the existing discharge has been improved. The existing calculations in the Latvian building normative LBN 223-99 envisage the precipitation discharge having the repetition period once a year (100%), twice (200%) or thrice in a year (300%). Moreover the calculation given by LBN and recommendations partly adopted and improved from the building norms and regulations of the USSR СНиП 2.04.03-85 (СниП) are based on the basis of Kurganov, USSR scientist promotion paper worked out in 1978 and which have been improved during the course of time and later shown in the handbooks of different kind and number table materials (Kurganov, 1984). The calculations have been specified and about in 1986 Snip projecting materials are officially accessible (Metodiskie norādījumi lietus..., 1983).

The existing method of rainwater calculation amount according to MK Latvian building normative „MK regulations No.214” „Regulations about Latvian building normative LBN 223-99”Outer networks and buildings of sewerage” (“LV”, 198/199 (1658/1659), 18.06.1999.) that came into force on 01.10.1999 with the alterations (regulations on LBN 223-99., 2010), is complicated. In order to obtain the rain amount (l s⁻¹) it is necessary to use 7 different parameters.

The second popular method used in Latvia for calculation of the discharge amount is a simplified method worked out by A.Zīverts and Ē.Tilgalis (Tilgalis, 2004).

Table 1

Runoff coefficients	
Use of areas or type of covering material of surface area	Coefficient, φ
Use of areas	
Town office	0.70 - 0.95
Commercial premises	0.50 - 0.70
Populated areas	
Detached house	0.30 - 0.50
Flat in a dwelling house	0.40 - 0.60
Flat (apartments)	0.60 - 0.80
Inhabited suburb district	0.25 - 0.40
Industrial district	
Light industry	0.50- 0.80
Heavy industry	0.60 - 0.90
Parks, green areas, cemeteries	0.10 - 0.30
Railway carriage park, playground	0.20 - 0.40
Meadows for pastures	0.10 - 0.30
Surface area covering material	
Street, pavement covering by asphalt or concrete	0.70-0.95
Concrete area	0.80-0.95
Concrete cobble stone covering	0.70-0.80
Pedestrian pavements and part for transport	0.75-0.85
House roof covering material (depending on material)	0.75-0.95
Grassland having sandy soil composition	
Sandy soil with 2% decline or less	0.05-0.10
Sandy soil with 2%-8% decline	0.10-0.16
Sandy soil with 8% decline or more (precipice, slope)	0.16-0.20
Grassland having clayey soil composition	
Decline 2% or less	0.10 - 0.16
Decline 2%-8%	0.17 - 0.25
Decline 8% and more (precipice, slope)	0.26 - 0.36

Source: Computer applications in hydraulic engineering (basic hydrology-rainfall) (translation report by R.Ziemelnieks)

Using this method it is possible to calculate the discharges with the possibility up to 200%. In addition, the determined k-coefficient dependent on the calculation possibility was determined basing on the previous carried out investigations in the promotion work (R.Ziemelnieks). The method elaborated provides for the possibility to calculate the maximum rainwater discharges in inhabited locations with a different possibility. In the result of the investigation it is possible to conclude that in Latvia it is advisable to use the calculations with the repetition possibility 50 or 25% (frequency of repetition once in 2 or 4 years). According to the

table drawn up by A.Zīverts (Zīverts, 1997) several improvements were carried out, values of k-coefficients were determined and the runoff module

was calculated at different provisions for the inhabited locations of Latvia. The numerical results are summarized in Table 2.

Table 2

Values of k-coefficients

No.	City, populated place	Dura-tion of observation, years	Size of the alpha value (rainfall April-September)	Values	200%	100%	50%	25%	10%	5%	1%
1	Cīrava	33	272	q, l (s ha) ⁻¹	35	59	72	89	109	122	154
				k-coefficient	0,75	1,25	1,54	1,92	2,37	2,67	3,35
2	Dagda	27	268	q, l (s ha) ⁻¹	35	58	71	87	107	120	151
				k-coefficient	0,75	1,23	1,50	1,84	2,33	2,60	3,30
3	Daugavpils	42	276	q, l (s ha) ⁻¹	36	60	73	90	110	124	156
				k-coefficient	0,77	1,27	1,58	1,95	2,40	2,70	3,40
4	Dzērbene	33	428	q, l (s ha) ⁻¹	56	92	113	139	171	192	242
				k-coefficient	1,17	2,00	2,47	3,00	3,70	4,12	6,10
5	Gulbene	39	391	q, l (s ha) ⁻¹	51	84	103	127	156	175	221
				k-coefficient	1,05	1,77	2,23	2,74	3,40	3,80	4,75
6	Gureļi	37	447	q, l (s ha) ⁻¹	58	96	118	146	178	200	252
				k-coefficient	1,23	2,07	2,54	3,15	3,85	4,35	6,65
7	Ieriķi	35	391	q, l (s ha) ⁻¹	51	84	103	127	156	175	221
				k-coefficient	1,05	1,77	2,23	2,74	3,40	3,80	4,75
8	Jelgava	50	335	q, l (s ha) ⁻¹	44	72	88	109	134	150	189
				k-coefficient	0,93	1,54	1,86	2,37	2,90	3,25	4,00
9	Kabile	41	291	q, l (s ha) ⁻¹	38	63	77	95	116	130	164
				k-coefficient	0,80	1,33	1,63	2,05	2,50	2,80	3,57
10	Kolka	57	250	q, l (s ha) ⁻¹	33	54	66	81	100	112	141
				k-coefficient	0,71	1,15	1,37	1,73	2,15	2,45	3,10
11	Kosa	25	428	q, l (s ha) ⁻¹	56	92	113	139	171	192	242
				k-coefficient	1,17	2,00	2,47	3,00	3,70	4,12	6,10
12	Kuldīga	42	291	q, l (s ha) ⁻¹	38	63	77	95	116	130	164
				k-coefficient	0,80	1,33	1,63	2,05	2,50	2,80	3,57
13	Lejasciems	29	484	q, l (s ha) ⁻¹	63	104	127	158	193	217	273
				k-coefficient	1,33	2,27	2,74	3,45	4,24	4,63	7,90
14	Liepāja	63	235	q, l (s ha) ⁻¹	31	51	62	77	94	105	133
				k-coefficient	0,68	1,05	1,30	1,63	2,03	2,30	2,85
15	Mālpils	38	409	q, l (s ha) ⁻¹	53	88	108	133	163	183	231
				k-coefficient	1,12	1,86	2,35	2,85	3,55	3,95	5,60
16	Ogre	31	335	q, l (s ha) ⁻¹	44	72	88	109	134	150	189
				k-coefficient	0,93	1,54	1,86	2,37	2,90	3,25	4,00
17	Pilskalne	35	277	q, l (s ha) ⁻¹	36	60	73	90	111	124	156
				k-coefficient	0,77	1,27	1,58	1,95	2,43	2,70	3,40
18	Priekuļi	47	409	q, l (s ha) ⁻¹	53	88	108	133	163	183	231
				k-coefficient	1,12	1,86	2,35	2,85	3,55	3,95	5,60
19	Ranka	34	391	q, l (s ha) ⁻¹	51	84	103	127	156	175	221
				k-coefficient	1,05	1,77	2,23	2,74	3,40	3,80	4,75
20	Rēzekne	37	264	q, l (s ha) ⁻¹	34	57	69	86	105	118	149

				k-coefficient	0,73	1,20	2,10	1,82	3,13	2,54	3,22
21	Rīga	71	368	q, l (s ha) ⁻¹	48	79	97	120	147	165	208
				k-coefficient	1,00	1,68	2,10	2,60	3,12	3,60	4,50
22	Saldus	27	263	q, l (s ha) ⁻¹	34	57	69	86	105	118	148
				k-coefficient	0,73	1,20	1,45	1,82	2,30	2,54	3,18
23	Stāmeriene	38	447	q, l (s ha) ⁻¹	58	96	118	146	178	200	252
				k-coefficient	1,23	2,07	2,54	3,15	3,85	4,35	6,65
24	Stende	46	304	q, l (s ha) ⁻¹	40	66	80	99	121	136	172
				k-coefficient	0,85	1,37	1,70	2,12	2,64	2,95	3,75
25	Subate	37	228	q, l (s ha) ⁻¹	30	49	60	74	91	102	129
				k-coefficient	0,65	1,03	1,27	1,60	1,97	2,19	2,77
26	Užava	25	272	q, l (s ha) ⁻¹	35	59	72	89	109	122	154
				k-coefficient	0,75	1,25	1,54	1,92	2,37	2,67	3,35
27	Ventspils	59	298	q, l (s ha) ⁻¹	39	64	78	97	119	133	168
				k-coefficient	0,83	1,35	1,65	2,10	2,57	2,85	3,65

Source: Calculated and created by R.Ziemeļnieks

In order to envisage the statistic indicators for at least the next 10-15 years, the data rows should be supplemented with new observations in order to calculate the forecast of the possibility and to determine the long-time average value of the duration curves. Approximately at least 5-year number rows are to be selected to envisage the precipitation amount minimally. At least registration data of 25 years measurements are to be used for a more accurate forecast possibility. The value of the error or the inaccuracy of the forecast are determined by the length of the number rows, the less the row, the larger – the inaccuracy. Tables and figures should be inserted in the width of one or two columns and should not exceed the margins of the document.

CONCLUSIONS

1. The newly formed formula and the values given offer an accurate calculation of the rainwater discharge.
2. According to the values of k-coefficient numbers obtained, it is possible to conclude, that one may take into consideration larger possibilities of the consequences of the flood, while choosing the surface covering material with a less repetition possibility.

3. The elaborated calculation method of maximum rainwater discharge shows that LBN 223-99 method is imperfect and gives incorrect results in the rainwater system calculation, it is proved by the fact that during heavy downpours many Latvian streets are flooded.
4. In future the work must be continued at the improvement of the calculation methods of more accurate maximum rain water discharges as well as at different kinds of calculation methods in the territory of Latvia
5. By carrying out the calculations of rainwater discharges one is to take into consideration the given kinds of the use of squares and the covering type which may influence the amount of the discharge.
6. It is possible to regulate the discharge most effectively by rainwater infiltration locally using not dense enough surface covering materials.
7. According to the calculation results obtained, one is to conclude that it is more useful to invert the means in building the sewerage of separate system, because it is influenced by the electroenergy rise in price.

REFERENCES

Metodiskie norādījumi lietuvu kanalizācijas projektēšanā (1983) Komunālās saimniecības pārvaldes ministrija LPSRS projektēšanas institūts „Latkomunālprojekts”, izlaidums HBK -3-83. Rīga: institūts „Latkomunālprojekts”, 66 lpp.

Meteoroloģisko novērojumu tabulas TMS, Rīga, I-XII, stacijas Nr. 5692410. Laika josla Griničas. \Reģions Zemgale, Stacija: Rīga. Kods: RIAS99PA. Latvijas Republikas hidrometeoroloģijas pārvaldes dabas vides stāvokļa valsts datu fonds jeb LVGMA.

Ziemeļnieks R., Tilgalis E. (2009) Calculation method of rainfall flow rate. *LUA Annual 15th International Scientific Conference Proceedings, Research for Rural Development 2009*. Jelgava: Latvia University of Agriculture, p. 315-319.

Ziemeļnieks R., Tilgalis E., Juhna V. (2008) Rainfall effect on sewage co-system activity in Riga. *LUA Annual 14th International Scientific Conference Proceedings, Research for Rural Development 2008*. Jelgava: Latvia University of Agriculture, p. 194-199.

Tilgalis Ē. (2004) *Noteikūdeņu savākšana un attīrīšana: mācību grāmata*. Jelgava: LLU, LVAF. 239 lpp.

Zīverts A. (1997) *Ievads hidroloģijā: mācību palīglīdzeklis*. Jelgava: LLU. 111 lpp.

Bauska piedzīvo sen neredzētus plūdus [online] [accessed on 16.07.2009.]. Available: http://www.bauskaszive.lv/portals/vide/raksts.html?xml_id=8943

Meteoroloģisko un hidroloģisko novērojumu dati [online] [accessed on 04.01.2010.]. Available: http://www.meteo.lv/public/hidrometeo_dati.html

Negaisa sekas Jelgavā [online] [accessed on 18.07.2010.]. Available: <http://www.jelgavnieki.lv/?act=4&art=17640>

Noteikumi par LBN 223-99 Kanalizācijas ārējie tīkli un būves: MK noteikumi Nr.214 [online] [accessed on 07.05.2010.]. Available: <http://www.likumi.lv/doc.php?id=19996>

Строительные нормы и правила (1985) *СНиП 2.04.03-85 "Канализация. Наружные сети и сооружения"* (утв. постановлением Госстроя СССР от 21 мая 1985 г. N 71)(с изменениями от 20 мая 1986 г.). Москва: Госстрой СССР. 129 с.

Курганов А.М. (1984) *Таблицы параметров предельной интенсивности дождя для определения расходов в системах водоотведения: толковый справочник*. Москва: Стройиздат. 108 с.